UNIVERSITY OF PAVIA

DEPARTMENT OF DRUG SCIENCES

PHD SCHOOL IN CHEMICAL AND PHARMACEUTICAL

SCIENCES (XXXI CYCLE)

DESIGN AND SYNTHESIS OF LSRK KINASE INHIBITORS AS QUORUM SENSING MODULATORS

Silvia Stotani

Tutor: Simona Collina
Co-tutor: Fabrizio Giordanetto

Academic year 2017/2018

To Fabrizio,

who made everything possible…

THE RESEARCH

Resistance to antibiotics is posing a continuous threat to public health and significant health care costs are associated to its management. Validating new antibacterial targets against antimicrobial resistance (AMR) remains highly challenging. In the last decades, modulation/inhibition of bacterial cell-to-cell communication (i.e., Quorum Sensing, QS) mechanisms has become an appealing therapeutic approach against bacterial resistance. It is already well known that interference with bacterial QS affects biofilm properties (e.g., thickness, mass) as well as biofilm formation. QS is mediated by production and release of small signaling molecules called autoinducers (AIs). Autoinducer-2 (AI-2) is a well-known class of QS signals produced by several bacterial species and responsible for inter- and intra-species communication and, as a consequence, it has been termed "universal autoinducer". The development of small molecules able to modulate the AI-2-mediated signaling would thus result in broad spectrum antimicrobial activity. 4,5-dihydroxy-2,3-pentanedione (DPD) is the key compound in the biosynthesis of AI-2 and modulates QS in both Gram-negative and Gram-positive bacteria. DPD-analogues would therefore have great potential as Quorum Sensing Inhibitors (QSI) and as antimicrobial drugs. Remarkably, two DPD-analogues (i.e., isobutyl-DPD and phenyl-DPD) have already shown that, in combination with gentamicin, they are able to almost completely clear pre-existing biofilms in *E. coli* and *P. aeruginosa*, respectively. In enteric bacteria (e.g., *E. coli* and *S. typhimurium*), DPD is phosphorylated by LsrK kinase resulting in phospho-DPD which activates QS upon interaction with the transcriptional regulator LsrR .

The research performed during my PhD is a part of the program of the INTEGRATE consortium, a multidisciplinary Marie Curie Educational Training Network (ETN) funded by the EU Horizon 2020 Programme focused on the validation of new Gram-negative antibacterial targets. As part of the INTEGRATE research program, the main goal of my research activity was to assess the relevance of LsrK kinase inhibition in the context of QS.

Following a ligand-based approach where DPD was the starting point of the whole research, small series of DPD-related compounds were designed and synthesized. To do so, the first task in my three-years project was the development of a new synthetic strategy towards DPD. A novel, robust and short protocol (that requires only one purification step) was planned and executed and, in order to show its applicability to the production of different C_1-DPD analogues, phenyl-DPD was also synthesized. The new strategy inspired the synthesis of eight small libraries of DPD-inspired heterocycles (DPD-Ihs) where the diketo moiety of DPD was embedded in heteroaromatic rings. All the synthesized compounds were purified and characterized by proton and carbon nuclear magnetic resonance (i.e., ^{1}H NMR, ^{13}C NMR, respectively) and ultra-high pressure liquid chromatography-mass spectrometry (i.e., UHPLC-MS, purity > 90%). The majority of the DPD-analogues reported in the literature suffer from instability/volatility and the absence of ultraviolet (UV)-active substituents renders their detection as well as their purification very challenging. In the compounds I've synthesized during my PhD, the open/closed equilibrium typical of such compounds is not

possible. Furthermore, the compounds are stable, easy to purify by column chromatography and to detect by classical analytical methods (e.g., UHPLC-MS) due to the presence of heteroaromatic groups that increase molecular weight (MW) and UV absorbance.

All the synthesized compounds were evaluated (by our INTEGRATE collaborators at the University of Helsinki, Finland) against LsrK in a D-luciferin-based bioluminescence assay. Remarkably, four compounds displayed IC$_{50}$ values comprised between 100 μM and 500 μM and molecular modeling studies (performed by our INTEGRATE collaborators at the University of Kuopio, Finland) supported the medicinal chemistry research. The results reached so far, led to two research papers: the first one published in *Molecules* on October 6th 2018 and entitled "*A Versatile Strategy for the Synthesis of 4,5-Dihydroxy-2,3-Pentanedione (DPD) and Related Compounds as Potential Modulators of Bacterial Quorum Sensing*" (Stotani S. *et al*., Molecules **2018**, *23(10)*, 2545) and the second (submitted to *Journal of Medicinal Chemistry* on January 5th) entitled "*DPD-inspired discovery of novel LsrK kinase inhibitors: an opportunity to fight antimicrobial resistance*".

The PhD thesis is organized as follow:

Chapter 1 introduces the concepts of antibiotic and antibiotic resistance and describes some strategies to circumvent the latter. A brief description of QS, its mechanism and inhibition strategies are also provided, together with a detailed account of AI-2-mediated QS.

Chapter 2 provides an introduction to kinases and kinase inhibition, particularly focusing on the role of LsrK kinase in QS. The chapter also details the building of a LsrK homology model and the analysis of the binding site. Cloning, over-expression, purification and crystallization of LsrK are also reported.

Chapter 3 summarizes the enantioselective and racemic synthesis of DPD reported in the literature.

Chapter 4 discusses the newly-developed synthesis of racemic DPD.

Chapter 5 summarizes the synthesis and biological evaluation of all the DPD-analogues reported in the literature.

Chapter 6 discusses the design and synthesis of eight new libraries of DPD-IHs.

Chapter 7 describes the assays to evaluate QS inhibition reported in the literature and the D-luciferin-based bioluminescence assay developed by our collaborators at the University of Helsinki. The chapter also illustrates the biological activities of the compounds presented in Chapters 4 and 6.

Chapter 8 is a collection of all the experimental procedures and experimental data.

Appendix is the paper published in *Molecules* on October 6th 2018 and entitled "*A Versatile Strategy for the Synthesis of 4,5-Dihydroxy-2,3-Pentanedione (DPD) and Related Compounds as Potential Modulators of Bacterial Quorum Sensing*" (Stotani S. *et al*., *Molecules* **2018**, *23(10)*, 2545).

A manuscript entitled "*DPD-inspired discovery of novel LsrK kinase inhibitors: an opportunity to fight antimicrobial resistance*" (Stotani S. *et al*.) submitted to *Journal of Medicinal Chemistry* on January 5th.

TABLE OF CONTENTS

LIST OF ABBREVIATIONS

(2,2,6,6-tetramethylpiperidin-1-yl)oxidanyl	TEMPO
(2R,4S)-2,4-dihydroxy-2-methyldihydrofuran-3-one	R-DHMF
(2R,4S)-2-methyl-2,3,3,4-tetrahydroxytetrahydrofuran	R-THMF
(2S,4S)-2,4-dihydroxy-2-methyldihydrofuran-3-one	S-DHMF
(2S,4S)-2-methyl-2,3,3,4-tetrahydroxytetrahydrofuran	S-THMF
(2S,4S)-2-methyl-2,3,3,4-tetrahydroxytetrahydrofuranborate	S-THMF-borate
1,2,3-trihydroxy-1-methylpentane	TriHMP
1,3-bis-(2,6-diisopropylphenyl)imidazolium chloride	HIPrCl
1,4-diazabicyclo[2.2.2]octane	DABCO
1,8-diazabicyclo(5.4.0)undec-7-ene	DBU
1-deoxy-D-erythro-hexo-2,3-diulose	DEHD
1-hydroxybenzotriazole	HOBt
1-methylimidazole	NMI
2,3-dichloro-5,6-dicyano-1,4-benzoquinone	DDQ
2-amino acetophenone	2-AA
2-chloro-4,6-dimethoxy-1,3,5-triazine	CDMT
2-dicyclohexylphosphino-2′,6′-dimethoxybiphenyl	Sphos
2-nitro-5-thiobenzoate	TNB^-
3,4,4-trihydroxy-2-pentanone-5-phosphate	P-TPO
4,5-dihydroxy-2,3-pentanedione	DPD
4-dimethylaminopyridine	DMAP
4-hydroxy-5-methyl-3(2H)-furanone	HMF
4-toluenesulfonyl chloride	TosCl
5,5'-dithiobis-(2-nitrobenzoic acid)	DTNB
5'-methyl-thioadenosine	MTA
5'-methylthioadenosine nucleosidase	MTAN
6-aminopenicillanic acid	6-APA
Absorbance at 280 nm	A_{280}
Acetic acid	AcOH
Acetic anhydride	Ac_2O
Acetonitrile	CAN
Activated methyl cycle	AMC
Acylated-acyl carrier protein	Acyl-ACP
Adenosine diphosphate	ADP
Adenosine triphosphate	ATP

Aluminium trichloride	$AlCl_3$
Aminoglycoside-modifying enzymes	AMEs
Aminoglycoside-*O*-phosphotransferases	APHs
Ammonium acetate	NH_4OAc
Ammonium fluoride	NH_4F
Ampere	A
Ångström	Å
Antimicrobial peptides	AMPs
Antimicrobial resistance	AMR
Arginine	Arg
Aspartic acid	Asp
Autoinducer-2	AI-2
Autoinducers	AIs
Autoinducing peptide I	AIP-I
Autoinducing peptides	AIPs
Basic Local Alignment Search Tool	BLAST
Benzyl bromide	BnBr
Bis(acetonitrile)dichloropalladium(II)	$PdCl_2(CH_3CN)_2$
Bis(triphenylphosphine)palladium(II) dichloride	$PdCl_2(PPh_3)_2$
Broad	Br
C_4-alkoxy-5-hydroxy-2,3-pentanediones	C_4-alkoxy-HDPs
Calculated extinction coefficient	ε_{calc}
Carbon nuclear magnetic resonance	^{13}C NMR
Carbon tetrabromide	CBr_4
Carbon tetrachloride	CCl_4
Centimeter	cm
Central nervous system	CNS
Cerium chloride heptahydrate	$CeCl_3*7H_2O$
Cesium carbonate	Cs_2CO_3
Cesium fluoride	CsF
Chloramphenicol acetyltransferases	CATs
Chloroform	$CHCl_3$
Chloro(pentamethylcyclopentadienyl)(cyclooctadiene)ruthenium(II)	Cp*Ru(COD)
cis-2,5-dihydroxy-2-methylcyclopentanone	*cis*-DHMP
Copper (I)-catalyzed Azide-Alkyne Cycloaddition	CuAAC
Copper iodide	CuI
Copper sulfate (pentahydrate)	$CuSO_4*5H_2O$

Density functional theory	DFT
Deoxyribonucleic acid	DNA
Deuterated acetic acid	ACOD-d_3
Deuterated acetone	Acetone-d_6
Deuterated acetonitrile	CD_3CN
Deuterated chloroform	$CDCl_3$
Deuterated dimethyl sulfoxide	d_6-DMSO
Deuterated methanol	MeOD
Deuterated sulfuric acid	D_2SO_4
Deuterated water	D_2O
Dichloromethane	DCM
(Diethylamino)difluorosulfonium tetrafluoroborate	Xtal-Fluor-E
Diethyl ether	Et_2O
Diffusible signal factor	DSF
Dihydrofolic acid	DHF A
Dihydroxyacetone phosphate	DHAP
Diisopropylamine	DIPA
Dimethylformamide	DMF
Dimethyl sulfide	DMS
Dimethyl sulfoxide	DMSO
Disodium deuterium phosphate	Na_2DPO_4
DPD-inspired heterocycles	DPD-Ihs
D-ribulose-5-phosphate	Ru5P
Doublet	d
Doublet of doublets	dd
Doublet of triplets	dt
Educational Training Network	ETN
Ethylenediaminetetraacetic acid	EDTA
Electron-withdrawing	EWG
Electron Spray Ionization	ESI
Ethanol	EtOH
Exempli gratia	e.g.
Fluorescence resonance energy transfer	FRET
Food and Drug Administration	FDA
Gas chromatography-mass spectrometry	GC-MS
Glycerol	GOL
Glycine	Gly

Gravitational acceleration	g
Guanosine triphosphate	GTP
Half-life	$t_{1/2}$
Heteronuclear Multiple Bond Correlation	HMBC
High performance liquid chromatography	HPLC
High performance liquid chromatography-electrospray ionization tandem mass spectrometry	HPLC-ESI-MS/MS
High resolution electrospray ionization-mass spectra	ESI-FTMS
High-throughput screening	HTS
Holo-acyl carrier protein	Holo-ACP
Homocysteine	Hcys
Homoserine lactone	HSL
Hydrochloric acid	HCl
Hydroxylamine hydrochloride	$NH_2OH*HCl$
Kinetic isotope effects	KIEs
Id est	i.e.
Immucillin	ImmA
Isopropyl-β-D-1-thiogalactopyranoside	IPTG
Lactate dehydrogenase	LDH
L-fructose	LFR
Limit of detection	LOD
Liquid chromatography tandem mass spectrometry	LC-MS/MS
Lithium bromide	LiBr
Lithium hydroxide	LiOH
Luria Broth	LB
LuxS regulated	Lsr
Magnesium sulphate	$MgSO_4$
Maltose-binding protein	MBP
Messenger RNA	mRNA
meta-chloroperoxybenzoic acid	*m*-CPBA
Methanol	MeOH
Methylhydrazine	$MeNHNH_2$
Methyl iodide	MeI
Microliter	μL
Micrometer	μm
Micromolar	μM
Microwave	MW

Milligram	mg
Milliliter	mL
Millimolar	mM
Mode of action	MOA
Molar	M
Molecular weight	MW
Molecular weight cut-off	MWCO
Multi-drug resistant	MDR
Multiplet	m
N-acetyltransferases	AACs
N-Acyl homoserine lactones	AHLs
Nanomolar	nM
National Center for Biotechnology Information	NCBI
N-chlorosuccinimide	NCS
Nickel-nitrilotriacetic acid	Ni-NTA
Nicotinamide adenine dinucleotide (reduced form)	NADH
N'-ethylcarbodiimide hydrochloride	EDC*HCl
N-methylmorpholine	NMM
N-methylmorpholine *N*-oxide	NMO
N-methyl-*N*-(trimethylsilyl)trifluoroacetamide	MSTFA
N,N'-dicicloesilcarbodiimmide	DCC
N,N-diisopropylethylamine	DIPEA
N,O-dimethylhydroxylamine hydrochloride	CH_3NHOCH_3*HCl
normal-butyllithium	*n*-BuLi
O-adenyltransferases	ANTs
Optical density at 600 nm	OD_{600}
Osmium tetroxide	OsO_4
Oxidative pentose phosphate	OPP
Ozone	O_3
Palladium acetate	$Pd(OAc)_2$
Palladium hydroxide on carbon	$Pd(OH)_2/C$
para-aminobenzoic acid	PABA
para-toluen sulfonic acid	*p*-TSA
Parts per million	Ppm
Penicillin-binding protein	PBP
Pentamethylcyclopentadienylbis(triphenylphosphine)ruthenium(II) chloride	$Cp^*RuCl(PPh_3)_2$
Pentamethylcyclopentadienyl ruthenium dichloride dimer	$Cp^*[RuCl_4]$

Phenylalanine	Phe
Phenyl-DPD	Ph-DPD
Phenyl isocyanate	PhNCO
Phosphoenolpyruvate	PEP
Phosphorus nuclear magnetic resonance	^{31}P NMR
Platinum on carbon	Pt/C
Polymerase chain reaction	PCR
Position-Specific Iterative BLAST	PSI-BLAST
Potassium acetate	KOAc
Potassium bicarbonate	$KHCO_3$
Potassium bromide	KBr
Potassium carbonate	K_2CO_3
Potassium periodate	KIO_4
Potassium permanganate	$KMnO_4$
Potassium *tert*-butoxide	*t*-BuOK
Potassium thioacetate	KSAc
Protein Data Bank	PDB
Proton nuclear meagnetic resonance	^{1}H NMR
Pseudomonas quinolone signal	PQS
Pyridinium chlorochromate	PCC
Pyruvate kinase	PK
Quartet	q
Quorum Sensing	QS
Quorum Sensing Inhibitors	QSI
Ribonucleic acid	RNA
Rotations per minute	rpm
Ruthenium-catalyzed Azide-Alkyne Cycloaddition	RuAAC
Ruthenium oxide (hydrated)	RuO_2*H_2O
S-3,3,4,5-tetrahydroxy-2-pentanone	*S*-THP
S-3,3,4,5-tetrahydroxy-2-pentanone-5-phosphate	P-DPD
S-4,5-dihydroxy-2,3-pentanedione	*S*-DPD
S-adenosylmethionine	SAM
S-adenosylhomocysteine	SAH
Serine	Ser
Singlet	s
Small molecules kinase inhibitors	SMKIs
Sodium ascorbate	Na ascorbate

Sodium bicarbonate	$NaHCO_3$
Sodium borohydride	$NaBH_4$
Sodium carbonate decahydrate	$Na_2CO_3*10H_2O$
Sodium chloride	$NaCl$
Sodium deuteroxide	$NaOD$
Sodium dideuterium phosphate	NaD_2PO_4
Sodium Dodecyl Sulphate - PolyAcrylamide Gel Electrophoresis	SDS-PAGE
Sodium hydride	NaH
Sodium hydroxide	$NaOH$
Sodium hypochlorite	$NaOCl$
S-ribosylhomocisteine	SRH
Sulfuric acid	H_2SO_4
Tandem mass spectrometry	MS/MS
tert-butyl alcohol	*t*-BuOH
tert-butyldimethylsilyl	TBDMS
tert-butyldimethylsilyl chloride	TBDMSCl
tert-butyldiphenylsilyl	TBDPS
tert-butyldiphenylsilyl chloride	TBDPSCl
Tetrabromomethane	CBr_4
Tetrabutylammonium fluoride	TBAF
Tetrahydrofolic acid	THF A
Tetrahydrofuran	THF
Thin layer chromatography	TLC
Threonine	Thr
Tobacco Etch Virus nuclear-inclusion-a endopeptidase	TEV protease
Toluene	PhMe
trans-2,5-dihydroxy-2-methylcyclopentanone	*trans*-DHMP
Transfer-RNA	*t*RNA
Trifluoromethyltrimethylsilane	$TMSCF_3$
Triethylamine	Et_3N
Triethylamine trihydrofluoride	Et_3N*3HF
Trimethyl orthoformate	$CH(OMe)_3$
Trimethylsilyl azide	$TMSN_3$
Trimethylsilyl	TMS
Trimethylsilyl chloride	TMSCl
Trimethylsilyldiazomethane	$TMSCHN_2$
Triplet	t

Triplet of doublet	td
Triphenylphosphine	PPh_3
Tris(hydroxymethyl)aminomethane hydrochloride	Tris*HCl
Ultra-high pressure liquid chromatography-mass spectrometry	UHPLC-MS
Ultraviolet	UV
Volume/volume	v/v
Water	H_2O
Wild type	WT
World Health Organization	WHO
Yet Another Scientific Artificial Reality Application	YASARA
Zinc (metallic)	Zn^0

1. INTRODUCTION

1.1 Antibiotics and antibacterial targets

Antibiotics are drugs used for the prevention and/or treatment of bacterial infections and they can either kill bacteria (i.e., bactericidal) or inhibit their growth (i.e., bacteriostatic). Most of the antibiotics currently in use target a limited number of essential cellular processes and can be classified in (Figure 1.1):

- Cell wall synthesis inhibitors: carbapenems, cephalosporines, glycopeptides, monobactams, penicillins and polypeptides inhibit the synthesis or the cross-linking of peptidoglycan (a component of bacterial cell wall) resulting in osmotic lysis; lipopetides and polypeptides alter and disrupt the cell-membrane causing cellular leakage;

- Protein synthesis inhibitors: aminoglycosides and tetracyclines bind to the 30S ribosomal subunit preventing translation, initiation and transfer RNA (*t*RNA) binding; macrolides, oxazolidinones, phenicols and streptogramins instead bind to the 50S ribosomal subunit and disrupt peptidyl transferase activity as well as translocation;

- Nucleic acid synthesis inhibitors: rifampin binds to deoxyribonucleic acid (DNA)-directed ribonucleic acid (RNA) polymerase and inhibit messenger RNA (mRNA) synthesis; quinolones bind to the DNA gyrase or to the topoisomerase IV and prevent DNA replication;

- Folate metabolism inhibitors: sulfonamides and trimethoprim inhibit the synthesis of nucleic acids by blocking, respectively, the conversion of para-aminobenzoic acid (PABA) to dihydropteroate (a precursor of tetrahydrofolic acid, THF A) and the reduction of dihydrofolic acid (DHF A) to THF A.

Some of them (e.g., glycopeptides) have a narrow spectrum of activity while others (e.g., β-lactams) are considered broad-spectrum antibacterial agents since they target processes that are common across different bacterial species.[1]
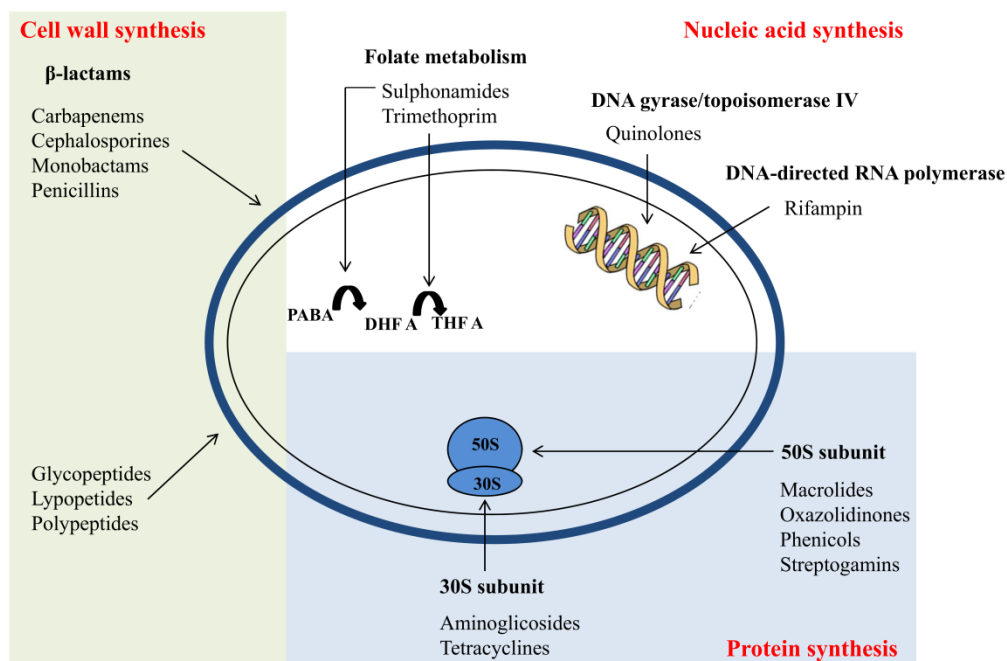

Figure 1.1: Mechanisms of action of antibiotics

With the introduction of β-lactams (1928) and sulfonamides (1932) in the market, the "modern age of antibacterial treatment" began. The majority of the drugs currently in use were discovered between the 1940s and the 1960s, in the so called "golden age" of antibiotic discovery. This time lapse was followed by a deep "innovation gap" where isolation of the 6-aminopenicillanic acid (6-APA) core and advances in synthetic chemistry allowed the production of new semi-synthetic derivatives that were modified versions of the existing ones (with the sole exception of the carbapenems) but no new chemical entities were brought into clinical use (Figure 1.2).[2,3]
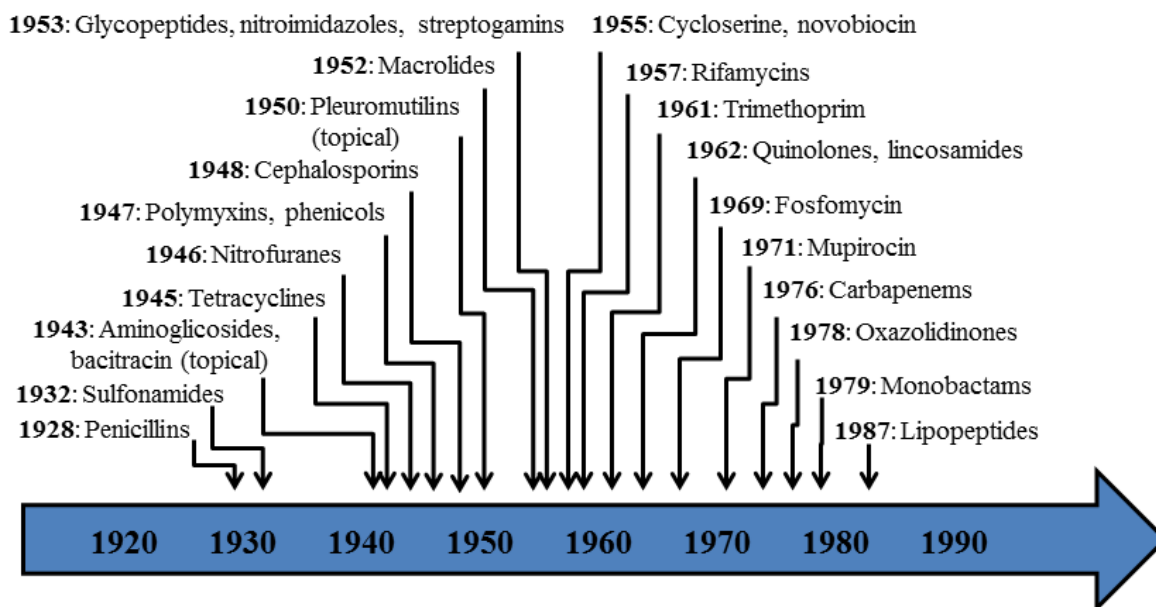

Figure 1.2: Antibiotic discovery timeline (1920 – 1990)

Forty years had to pass before a new scaffold (i.e., the oxazolidinone drug linezolid) was introduced into clinical practice in 2000. Modification of already approved drugs, despite increasing the number of products launched, had a huge cost in terms of the spreading of resistance: drugs with the same scaffold act with the same mode of action (MOA) and resistance to one antibiotic is rapidly followed by cross-resistance to the whole class.[4–6]

Stringent government regulations as well as the significant investments required to discover and develop new antibiotics pushed big pharmaceutical companies to partially/completely abandon antibacterial research in the mid-1990s. For a long time, antibiotic discovery has been considered a target-poor therapeutic area and industries have preferred to invest in more profitable sectors (e.g., cancer, chronic diseases).[7–14] At the beginning of the new century, completion of bacterial and human genome opened the door to the study of hundreds of novel potential targets for antibacterial drugs. Together with new advances in combinatorial chemistry, high-throughput screening (HTS) and molecular biology, a new era of genomic-derived antibiotics could potentially begin but, unfortunately, this kind of approach failed to identify tractable new targets and Food and Drug Administration (FDA) antibiotics' approvals dropped from 29 in the 1980s to only 9 in the 2000s.[15–20] From 2000 onwards, five new classes of antibiotics have been developed: (i) oxazolidinone (linezolid, 2000, Figure 1.3); (ii) lipopeptide (daptomycin, 2003, Figure 1.3); (iii)

pleuromutilin (retapamulin, 2007, Figure 1.3); (iv) macrolactone (fidaxomicin, 2011, Figure 1.3) and (v) diarylquinoline (bedaquiline, 2012, Figure 1.3).
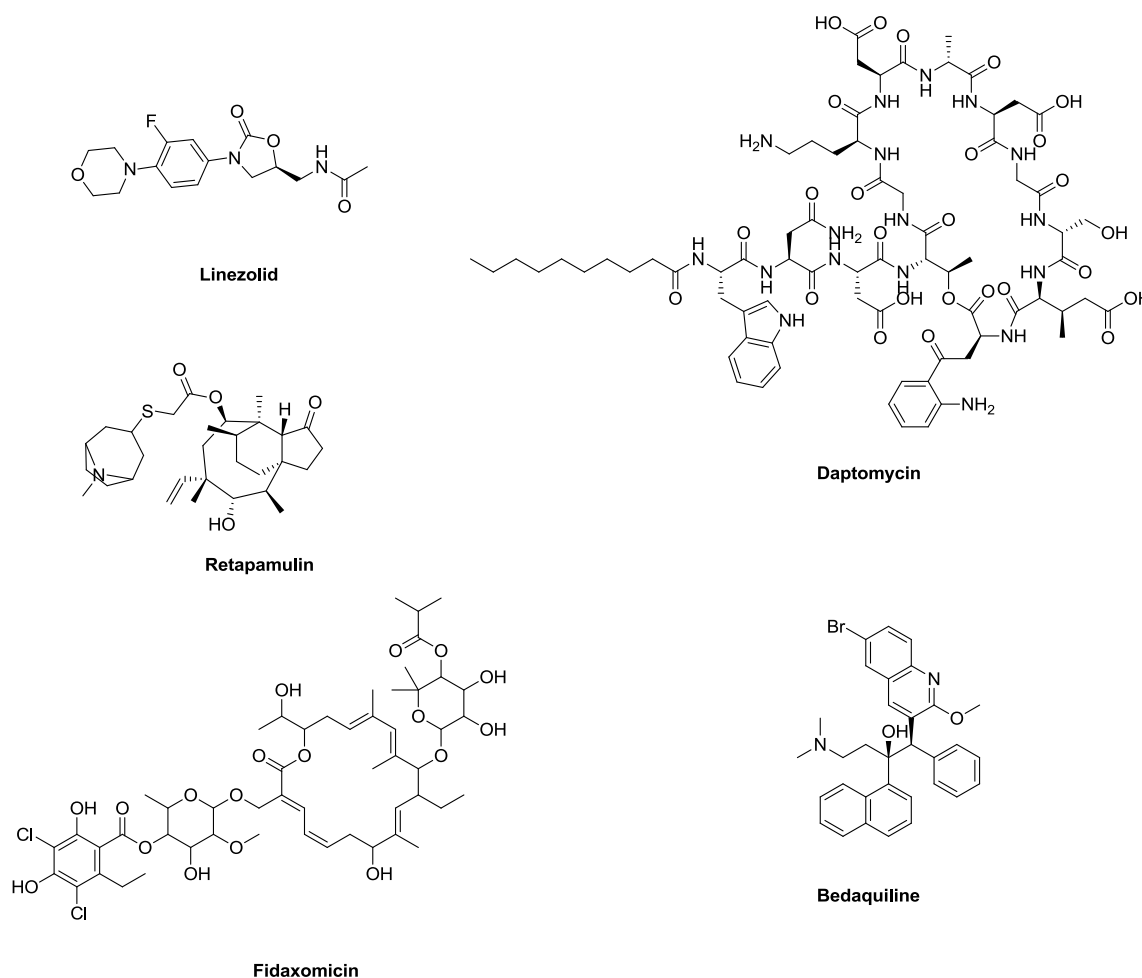
Figure 1.3: Structure of the five novel classes of antibiotics developed since 2000

The recent discoveries are the result of growing antimicrobial stewardship programs and increased government investments[21–23] to tackle multi-drug resistant (MDR) bacteria and discover new non-essential targets (see further) before going back to the "pre-antibiotic era".[24–33]

1.2 Antibiotic resistance and its mechanisms

Antibiotic resistance is an increasingly serious threat to global public health and represents a huge burden for health care costs. It is dangerously rising to high levels all over the world and it is estimated that, by 2050, "*drug resistant infections will kill an extra 10 million people a year worldwide*".[34] Inappropriate prescribing of antibiotics, poor compliance with treatment regimes, the use of antibiotics in agriculture, poor hygiene and infection control in hospitals are just some of the reasons that contribute to the spread of resistance.[35–42] Antibiotics are routinely used to grow animal's food thus facilitating the diffusion of resistance to humans through ingestion. Pharmaceutical's waste released in the environment exacerbate even more the problem and we now live in an era where a growing number of infections (e.g., gonorrhea, pneumonia, tuberculosis) are hard to treat as antibiotics are becoming less and less effective.[43–49]

Resistance is not a modern phenomenon: a recent study of Beringian permafrost sediments containing 30.000 years-old DNA identified genes encoding resistance to β-lactams, glycopeptides and tetracyclines. However, at that time, the selection pressure necessary to confer them an evolutionary advantage for their expression was still missing. The beginning of the modern antibiotic era has provided the selection pressure necessary for the recapture of resistance elements from the resistome (i.e., the global reservoir of resistance elements) and contributed to the development of multi-drug resistant pathogens.[50–52] Resistance can arise through genetic mutations or can be acquired from other bacteria via mobile plasmids or transposons (i.e., horizontal gene transfer).[53–59] Over the centuries, bacteria have evolved several protective mechanisms to inactivate, remove and, in general, circumvent antibiotics' toxicity. Here we report the most studied (Figure 1.4):

- Efflux pumps: they are membrane proteins that export antibiotics outside the bacterial cell and maintain their intracellular level low. They can be specific to a certain class of antibiotics but most of them are multidrug transporters, thus contributing to the development of multi-drug resistance;[60–62]

- Target site alterations: variations of the target sites of antibiotics prevent their binding therefore limiting their efficacy. Modifications in the 30S and 50S ribosomal subunit confer resistance to macrolides, tetracyclines and all the other drugs that affect protein synthesis; mutations of the penicillin-binding protein (PBP) reduces the affinity for β-lactams; alterations of the cell wall precursors (e.g., D-alanyl-D-alanine is changed to D-alanyl-D-lactate) cause resistance to glycopeptides while mutated DNA-gyrase and topoisomerase IV originate fluoroquinolones resistance;[52]

- Enzymatic inactivation: the three main enzymes responsible for antibiotics inactivation are β-lactamases, aminoglycoside-modifying enzymes (AMEs) and chloramphenicol acetyltransferases (CATs). About 300 β-lactamases are known and they hydrolyze nearly all β-lactams that have amide and ester bonds (e.g., cephalosporins, carbapenems, monobactams, penicillins); AMEs inactivate aminoglycoside through kinases (aminoglycoside-O-phosphotransferases, APHs), O-adenyltransferases (ANTs) and N-acetyltransferases (AACs) thus impeding the binding to the 30S ribosomal subunit; AACs acetylate hydroxyl groups of chloramphenicol disrupting its binding to the 50S ribosomal subunit;[41]
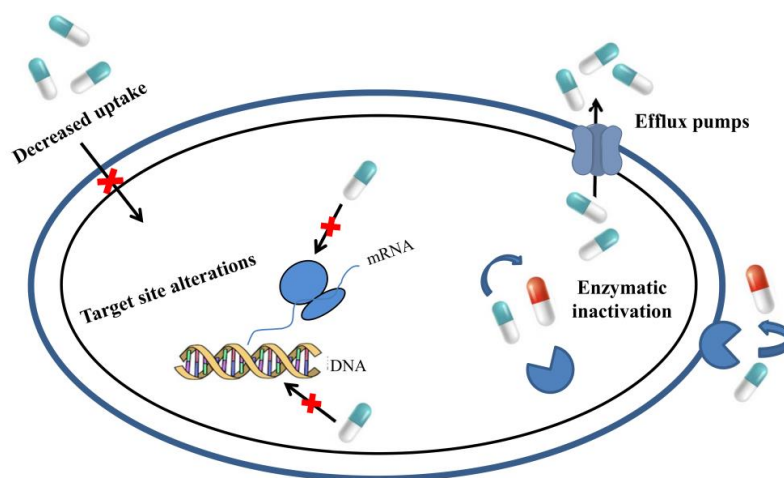
Figure 1.4: Mechanisms of antibiotic resistance

- <u>Decreased uptake</u>: is a common phenomenon in Gram-negative bacteria who are able to modify the composition of their outer cell membrane in order to reduce antibiotics' uptake. Changes in the selectivity and/or concentration of porin channels (i.e., transmembrane proteins that act as cellular pores) also diminish intracellular antibiotic concentration. If coupled with an increased activity of efflux pumps, the amount of drug available inside the cell drastically reduces.[60,62,63]

1.3   Action plans and new strategies to fight antibacterial resistance

The increasing economic and healthcare concerns generated by antibiotic resistance have prompted the organization of global collective actions to address the threat. The World Health Organization (WHO) developed a global action plan to tackle this growing problem at the 68th World Health Assembly in May 2015.[64] The main goal of the plan was to ensure prevention and successful treatments to all who need them, using effective and safe medicines for as long as possible. Five strategic objectives were set out:

1   Raise the awareness about AMR through trainings, education and communication;

2   Optimize the use of antibiotics in both human and animal health;

3   Increase the knowledge on incidence, prevalence and spreading of resistance in order to develop new tools, policies and regulations;

4   Apply preventive measures to reduce the incidence of infections;

5   Potentiate investments in vaccines, new diagnostic tools or medicines.

The more effective long-term solutions to address AMR are based on the discovery of (i) novel drugs (e.g., antimicrobial peptides and bacteriophages); (ii) "smart" delivery systems (e.g., antimicrobial polymers, nanoparticles, liposomes) and (iii) innovative combination approaches (e.g., multidrug cocktails). I will briefly describe below such solutions.

- <u>Antimicrobial peptides (AMPs):</u> are 12 to 50 amino acids peptides displaying potent (i.e., micromolar (µM) range) and broad spectrum antibacterial activity. AMPs include (i) anionic peptides (rich in glutamic acid and aspartic acid); (ii) cationic peptides (rich in arginine, glycine, proline, phenylalanine and tryptophan); (iii) anionic and cationic peptides that contain cysteine and form disulfide bonds and (iv) linear cationic α-helical peptides. AMPs act through different mechanisms including inhibition of cell wall synthesis, formation of pores, alteration of the cell membrane, activation of autolysin, inhibition of DNA, RNA, and protein synthesis. They are able to kill Gram-negative and Gram-positive bacteria, enveloped viruses and fungi (just to cite a few) and they also have immunomodulatory functions including the ability to alter host gene expression, to induce chemokine production and/or act as chemokines, to inhibit lipopolysaccharide induced pro-inflammatory cytokine production, to promote wound healing and modulate the responses of dendritic cells and cells of the adaptive immune response. Their use is generally limited to topical or intravenous administration due to their short half-lives ($t_{1/2}$);[65–72]

- <u>Bacteriophages:</u> are viruses specifically designed to recognize bacteria through a cell surface receptor and infect them. They have been reported to be effective against several Gram-negative (e.g., *E. coli*, *P.*

aeruginosa) as well as Gram-positive bacteria (e.g., *E. faecium*, *S. aureus*). As they lack in selectivity, resistance can arise due to alteration of the bacterial cell surface receptors. They can be used as cocktails with traditional antibiotics. Alternatively, bacteriophage components (e.g., virolysis) can serve as sources of potent new antimicrobials;[73–77]

- Antimicrobial polymers: are produced by insertion of an active antimicrobial onto a polymer via an alkyl or an acetyl linker. This structure increases antibiotics stability, $t_{1/2}$, efficacy and selectivity, minimizing at the same time their toxicity;[78,79]

- Nanoparticles: improve intracellular delivery and the therapeutic index of antibiotics thus reducing the dose and frequency of administration. Metal ion nanoparticles, especially silver compounds, have been recently explored as carriers for antibiotic delivery. Despite their potential, these kind of delivery systems are not yet well established due to their complicate characterization and short $t_{1/2}$;[80–82]

- Liposomes: have a membrane-like structure that facilitates drug release in the cytoplasm, potentially saturating efflux pumps and reducing the emergence of resistance. Unfortunately, they have a short $t_{1/2}$, limited encapsulation efficiency and temperature sensitivity that can lead to inadequate delivery;[83–86]

- Multidrug cocktails (e.g., the combination of antibiotics targeting different pathways) are very successful tools to combat AMR. Often, antibacterial drugs can also be combined with non-antibiotic adjuvants (i.e., compounds used to prevent or assist in the amelioration of a disease). Common adjuvants that had clinical success include antiseptics (e.g., chlorhexidine) and natural (e.g., biosurfactants) or biological (e.g., bacteriophages) moieties. Antiseptics are thought to permeate and disrupt the cell wall as well as inactivate ATPases. Despite their success, resistance can arise locally due to selective pressure and it has been observed *in vitro* with combinations of chlorhexidine and minocycline (or rifampicin). Recent combination therapies couple antibiotics with natural and biological adjuvants. Bacteriophages paired with antibiotics proved to be more effective than either components delivered individually. Plant-derived compounds (e.g., thymol), biosurfactants (e.g., sophorolipid) and antibodies (IgG classes) can also be used as adjuvants to enhance antimicrobial efficacy.[87–93]

An emerging innovative approach to fight AMR is the modulation/inhibition of QS. In the following paragraphs I will describe the QS systems in bacteria, the enzymes and molecules involved and all the recent advances reported in the literature particularly focusing on AI-2-mediated QS.

1.4 Quorum Sensing (QS)

QS is a cell-to-cell communication mechanism that allows bacteria to coordinate their gene expression and act as a population.[94–98] This phenomenon is detrimental for humans as QS regulates pathogenic processes such as virulence factor production,[99,100] susceptibility to antibiotics[101] and biofilm formation.[102–104] In the last decades, the modulation of QS has emerged as a potential therapeutic target to fight AMR: a treatment that doesn't inhibit bacterial growth will not generate selective pressure and, therefore, the chance for resistance to arise can be significantly reduced.[105–108] QS is mediated by production, release and response to AIs. Conventionally, AIs have been divided into three main categories: (i) *N*-Acyl homoserine lactones

(AHLs)[109,110] used by Gram-negative bacteria; (ii) oligopeptides, used by Gram-positive bacteria and (iii) AI-2 used by both Gram-positive and Gram-negative bacteria. Other QS signals include (iv) *Pseudomonas* quinolone signal (PQS),[111–113] (v) diffusible signal factor (DSF),[114,115] (vi) γ-butyrolactone,[116] (vii) 2-amino acetophenone (2-AA),[117] (viii) bradyoxetin.[118]

I will briefly describe AHLs- and oligopeptides-based QS and, more in details, AI-2-mediated QS.

1.4.1 *N*-Acyl homoserine lactone (AHL)-based Quorum Sensing

AHLs are formed by a homoserine lactone (HSL) ring attached to an acyl chain (4 to 18 carbon long). AHLs differ in the length of the acyl chain, in the oxidation state at position 3 and in the saturation of the chain itself (Figure 1.5).

$R_1 = H, =O, OH$
$R_2 = 1-17C$
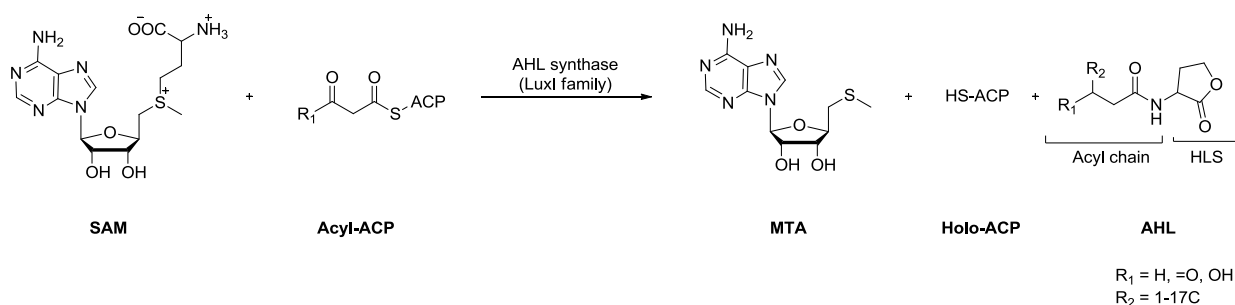
Figure 1.5: Biosynthesis of AHLs

AHLs are biosynthesized from an acylated-acyl carrier protein (acyl-ACP) and *S*-adenosylmethionine (SAM) by members of the LuxI family of AHLs synthases after release of holo-acyl carrier protein (holo-ACP) and 5'-methyl-thioadenosine (MTA) (Figure 1.5). After being biosynthesized, AHLs passively diffuse the bacterial cell and accumulate in the extracellular medium. There are also evidences of actively transported AHLs in certain bacteria. Once a threshold concentration is reached, AHLs bind to a cytoplasmic LuxR-type receptor activating the expression of QS-regulated genes. The AHLs receptor have some degree of specificity based on the length, oxidation state and saturation of the acyl chain and each bacterial species has his own pair of synthase/receptor to produce and respond to specific AHLs.[119]

1.4.2 Oligopeptides-based Quorum Sensing

Oligopepetides are used as autoinducer molecules by Gram-positive bacteria. They are produced intracellularly and actively transported outside the cell. Between translation, export and detection, they undergo several modifications, including cyclization. Some linear oligopeptides are actively transported in the cell where they interact with specific regulators (e.g., PrgX in *E. faecalis* and NprR in *B. thuringiensis*) but the majority of the autoinducing peptides (AIPs) are detected extracellularly by a membrane-bound sensor kinase activating or repressing QS gene expression.[120,121]

1.4.3 AI-2-based Quorum Sensing

AI-2-mediated QS exists in both Gram-negative and Gram-positive bacteria. Since the synthase responsible for AI-2 biosynthesis (i.e., LuxS, see further) is present in more than 70 bacterial species, AI-2 is also defined as the "universal autoinducer". The first evidence of AI-2-mediated signal date back to 1994 when Bassler *et al.* observed QS activity in *V. harveyi* mutant strains lacking the AHL synthase and proposed the existence of an alternative QS system.[122] A few years later, AI-2 activity was detected in a wide range of LuxS-containing species suggesting that bacteria use AI-2 to communicate with each other.[123] This prompted several research groups to investigate more in details AI-2 production and by 2002 two *in vitro* biosyntheses were reported.[124,125] The term AI-2 refers to a group of molecules all having DPD as a common precursor. This small chemical entity spontaneously rearranges to yield different structures in equilibrium with each other. In aqueous solution, linear DPD is in equilibrium with its two cyclic isomers *S*-DHMF and *R*-DHMF (Figure 1.6). Their hydration at C_3 forms the two cyclic tetrahydrated isomers *S*-THMF and *R*-THMF (Figure 1.6). X-ray crystallography revealed that *R*-THMF is the isomer recognized by the plant symbiont *S. melioti* (Protein Data Bank ID, PDB ID: 3EJW[126]) and by the two human pathogens *S. typhimurium* (PDB ID: 1TJY[127]) and *Y. pestis* (PDB ID: 3T95[128]) while isomer *S*-THMF, in the form of the borate ester *S*-THMF-borate, is the active species in *V. harveyi* and it has been co-crystallized in complex with LuxP (PDB ID: 1JX6[129]).

To complicate even more the picture, the hydrated form of linear DPD (i.e., *S*-THP, Figure 1.6) is phosphorylated at position 5 by LsrK (to generate phospho-DPD, P-DPD, Figure 1.6) in the members of the Enterobacteriacee family (e.g., *E.coli* and *S. typhimurium*).
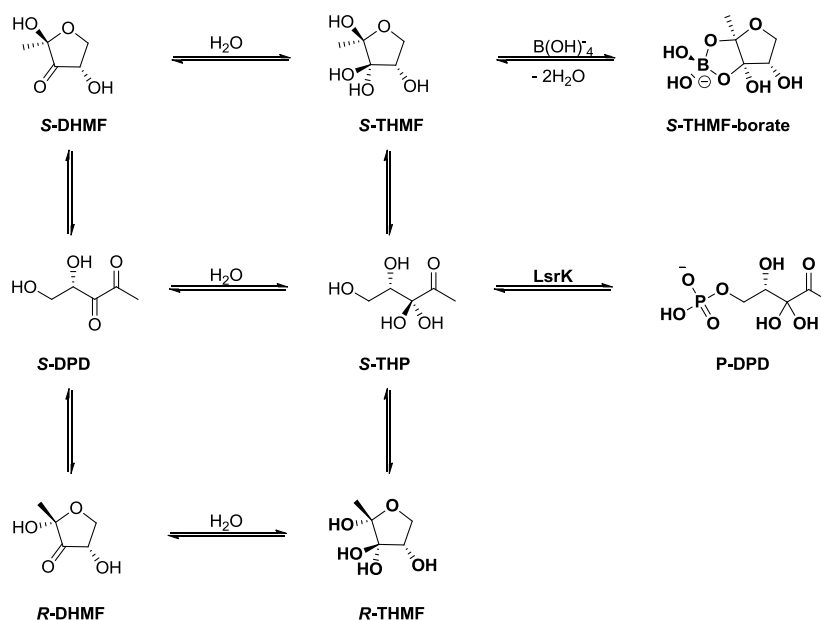

Figure 1.6: AI-2 species in equilibrium in aqueous medium: (2*S*,4*S*)-2,4-dihydroxy-2-methyldihydrofuran-3-one (*S*-DHMF); *S*-4,5-dihydroxy-2,3-pentanedione (*S*-DPD); (2*R*,4*S*)-2,4-dihydroxy-2-methyldihydrofuran-3-one (*R*-DHMF); (2*S*,4*S*)-2-methyl-2,3,3,4-tetrahydroxytetrahydrofuran (*S*-THMF); *S*-3,3,4,5-tetrahydroxy-2-pentanone (*S*-THP); (2*R*,4*S*)-2-methyl-2,3,3,4-tetrahydroxytetrahydrofuran (*R*-THMF); (2*S*,4*S*)-2-methyl-2,3,3,4-tetrahydroxytetrahydrofuranborate (*S*-THMF-borate); *S*-3,3,4,5-tetrahydroxy-2-pentanone-5-phosphate (**P-DPD**)

AI-2 is biosynthesized in the intracellular medium in a three steps pathway: (i) SAM is demethylated by a methyltransferase to generate *S*-adenosylhomocysteine (SAH); (ii) 5'-methylthioadenosine nucleosidase (MTAN, also known as Pfs) removes the adenine from SAH to produce *S*-ribosylhomocysteine (SRH); (iii) LuxS catalyzes the displacement of homocysteine (Hcys) from SRH to form AI-2 (Figure 1.7).
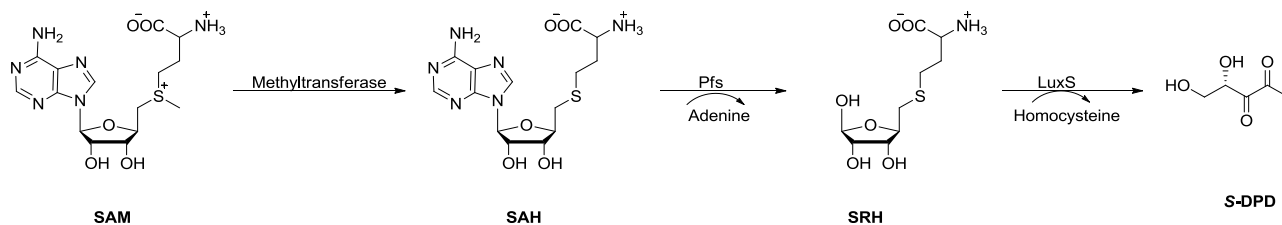

Figure 1.7: Biosynthesis of AI-2

An alternative pathway for the formation of AI-2 is the isomerization (by ribulosephosphateisomerase) of D-ribulose-5-phosphate (Ru5P), formed during the catabolism of glucose via the oxidative pentose phosphate (OPP) pathway (Figure 1.8). This isomerization allows for the production of 4-hydroxy-5-methyl-3(2*H*)-furanone (HMF), which has been shown to have moderate bioluminescence activity in *V. harveyi*. The production of DPD via this pathway was confirmed by incubation of Ru5P with ribulosephosphateisomerase in the presence of *o*-phenylendiamine as carbonyl-trapping reagent and analysis of the corresponding quinoxaline derivative by high-performance liquid chromatography-electrospray ionization tandem mass spectrometry (HPLC-ESI-MS/MS, Figure 1.8).[130]
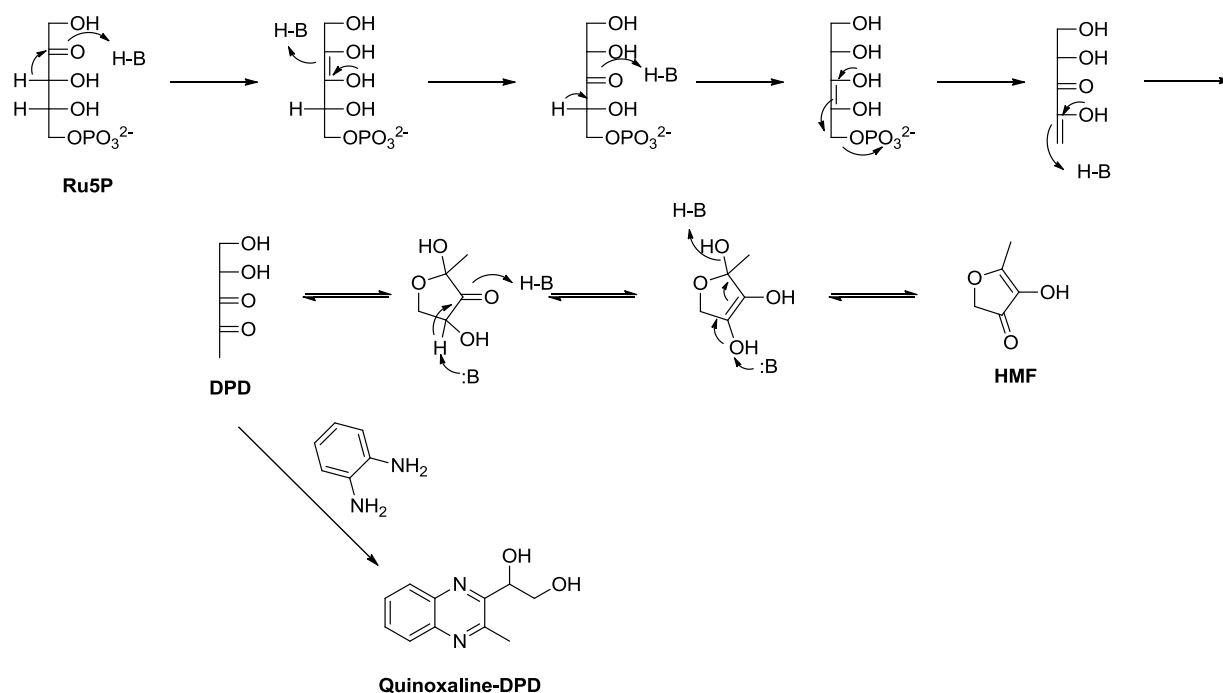
Figure 1.8: Isomerization of Ru5P to DPD and HMF

After being biosynthesized inside bacterial cells, AI-2 is exported in the extracellular medium but it is still unclear how. Due to its hydrophilic nature, it is unlikely that it can passively cross the cell membrane so the YdgG protein has been proposed as a potential transporter.[131,132] Deletion of *ydgG* resulted in a 6-fold increase in cell motility as well as in a 7000-fold increase in biofilm thickness in *E. coli*. However, under conditions where AI-2 uptake was inhibited, the AI-2 extracellular level was only 2-fold lower compared to the wild type (WT) suggesting that there should be other mechanism(s) to export AI-2. AI-2 accumulates in the extracellular medium but, once a threshold concentration is reached, it is internalized through the Lsr (LuxS regulated) transporter system. In enteric bacteria (e.g., *S. typhimurium* and *E. coli*), P-DPD binds to the repressor LsrR (PDB ID: 4L4Z[133]) that dissociates from the promoter region of the *lsr* operon thus starting operon transcription. As a result, the expression of the transporter on the cell surface is increased as well as the internalization of AI-2 and the expression of LsrK.[134] P-DPD is then processed by LsrG and LsrF: LsrG catalyzes its isomerization to 3,4,4-trihydroxy-2-pentanone-5-phosphate (P-TPO, Figure 1.9). Studies have shown that *lsr* expression is increased in LsrG mutants as a result of phospho-AI-2 accumulation.[135] LsrF instead acts as a thyolase that catalyzes the transfer of an acetyl group from the hydrated form of P-TPO to coenzyme A forming dihydroxyacetone phosphate (DHAP, Figure 1.9) and acetyl-CoA (Figure 1.9). As for LsrG, LsrF mutants show increased *lsr* expression and phospho-AI-2 accumulation. With the degradation of phospo-AI-2 by LsrG and LsrF, the AI-2 signaling cycle closes.[136]
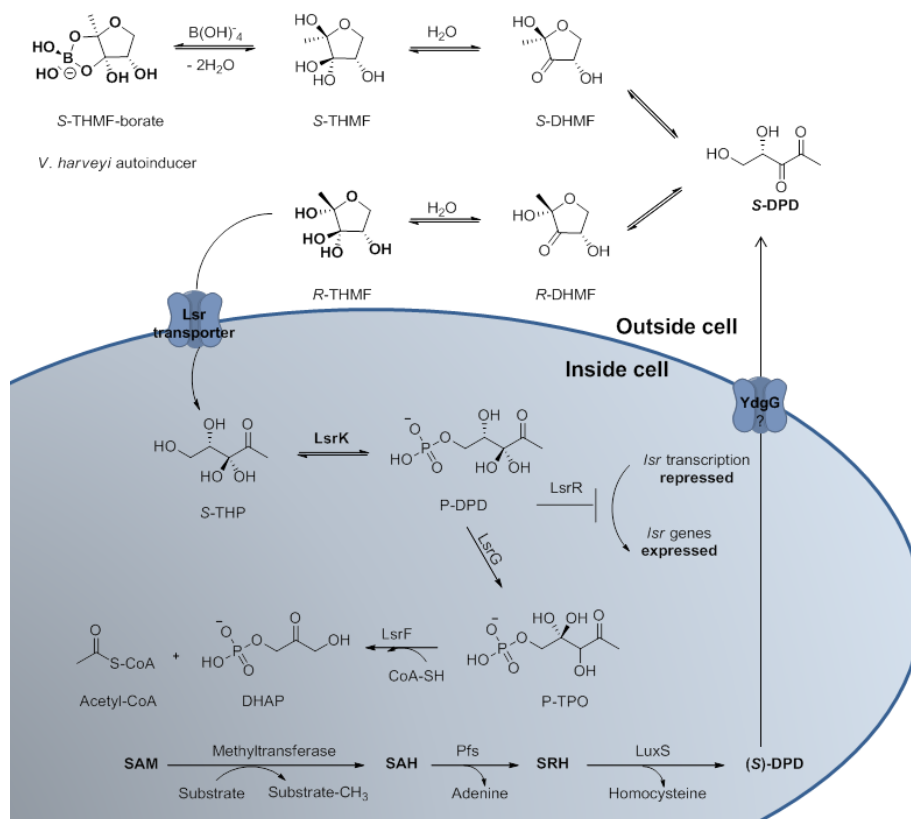
Figure 1.9: AI-2 production and internalization (at high cell density) in enteric bacteria (e.g., *S. typhimurium* and *E. coli*)
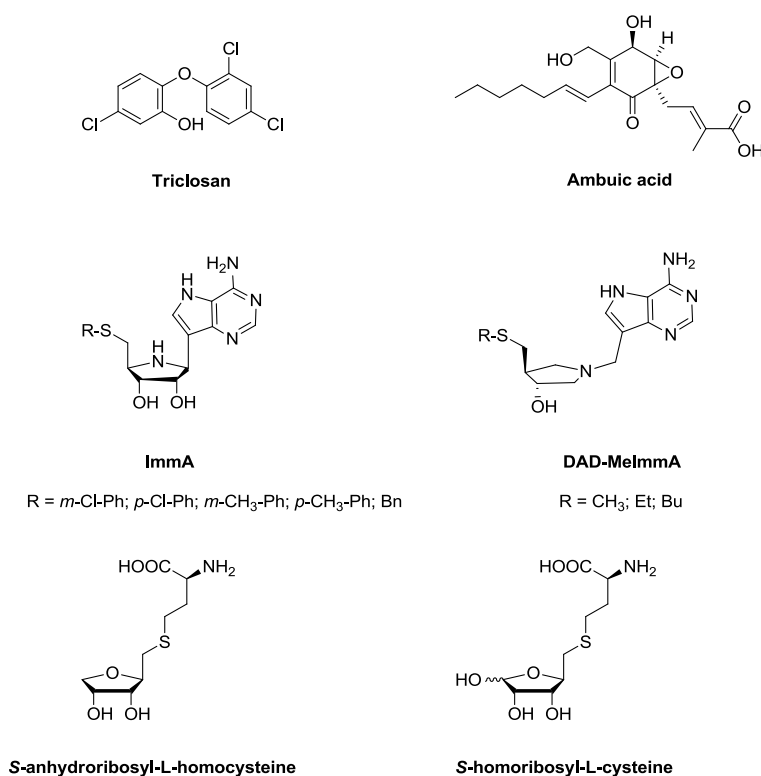
1.5   Inhibition of Quorum Sensing

In the last decades, inhibition of QS has become an appealing strategy to fight AMR. Targeting non-essential genes for bacterial survival reduces in fact the selective pressure responsible for the rise of resistance. Through modulation/inhibition of QS, several bacterial virulence factors that facilitate human infections can be controlled and their negative effects, including mortality, can be reduced.[137] Together with resistance at cellular level, bacteria can live in biofilm communities gaining additional resistance often defined as "community resistance". It is estimated that 80% of human bacterial infections are complicated by the formation of biofilms where bacteria have 1000-fold higher tolerance to antibiotics compared to the same organisms in a planktonic state. Biofilms are microbial communities of cells attached to each other (or to a surface) embedded within an extracellular polymeric matrix. Biofilms are enriched in oxygen and nutrients that help cell differentiation. Cells in deeper layers need to adapt to the limited nutrients and oxygen availability (compared to cells on the surface) and have slower metabolism, creating therefore different subpopulations that respond differently to antibiotic treatment.[138,139] Components of the biofilm matrix form a shield that protects against antibiotics and the negative charge of the extracellular DNA that forms the matrix has been shown to be involved in resistance towards cationic peptides.[140] Exposure to sub-inhibitory concentration of drugs, due to the protection offered by the extracellular matrix, creates favorable conditions for selection of resistant phenotypes and increases mutation rates. Cells in biofilm can also adopt a slow or non-growing phenotype (i.e., persister cells) in response to stressful conditions and antibiotics that are specifically active against dividing cells (e.g., β-lactams) will have limited effects. Furthermore, persister cells can survive antibiotic treatment and cause relapses.[141–143] Biofilms also promote the development of resistance at a cellular level: they display a mutation rate 100-fold higher than planktonic cells and the presence of extracellular DNA in the matrix can facilitate horizontal gene transfer and spread resistance across different microbial organisms.[144–146] Several studies have shown that interference with QS affects biofilm formation and biofilm properties: addition of synthetic AI-2 (6.4 μM) to WT *E. coli* K-12 MG 1655 increased biofilm mass by 30-fold.[147] Two AI-2-analogues (i.e., isobutyl-DPD and phenyl-DPD, see Chapter 5) in combination with gentamicin have made almost complete the clearance of pre-existing biofilms in *E. coli* and *P. aeruginosa*, respectively and *lsrK* and *lsrR* mutants were found to form biofilms with altered architecture and significantly thinner.[148] QSIs represent therefore interesting tools to be used, in combination with "conventional" antibiotic therapies, against AMR.[149,150] The development of QSIs has mostly focused on AHLs- and oligopeptides-based QS as they are species-specific QS systems and can be directly associated to particular pathogenesis.[151,152] In the last decades, inhibition of AI-2-mediated QS also started to attract the attention of the scientific community as it would result in broad spectrum antimicrobial activity. Three main points of QS interception are possible: (i) signal generation, (ii) signal degradation and (iii) signal detection/transduction and they will be briefly described below.

1.5.1 Inhibition of Quorum Sensing signal generation

This kind of approach limits signal accumulation and there are evidences of its efficacy both *in vitro* and in *vivo*. Inhibition of AHLs production can be achieved by (i) inhibition of SAM synthesis; (ii) inhibition of acyl-ACP production or (iii) inactivation of AHL synthase (Figure 1.5). So far, only triclosan[153] and diazobroines[154] (Figure 1.10) are known as inhibitors of FabI (NADH-dependent enoyl-ACP reductase), an alcohol dehydrogenase that catalyzes the last step of acyl-ACP biosynthesis.

The synthesis of AIPs is mediated by essential bacterial enzymes such as ribosomes and peptidases so the inhibition of such kind of enzymes will have an impact on bacterial growth more than an anti-QS effect. Therefore, only a few studies focused on the inhibition of the biosynthesis of AIPs. Recently, ambuic acid (Figure 1.10) was found to inhibit (although its target is still unclear) the biosynthesis of cyclic peptides in several Gram-positive bacteria, including *E. faecalis* and *S. aureus*.[155]

MTAN catalyzes the hydrolytic depurination of SAH to produce SRH. Additionally, MTAN depurinates MTA in the biosynthesis of AHLs. Together with the disruption of the synthesis of both AHLs and AI-2, MTAN inhibition interferes also with polyamine biosynthesis, methionine salvage and other important metabolic pathways. Kinetic isotope effects (KIEs) studies, together with co-crystal structures of MTANs with several transition state analogues enabled the identification of a transition state model of MTAN of different bacterial species (e.g., *S. aureus*, *E. coli*, *S. pneumoniae*) facilitating the rational design of new inhibitors.[156–161] Here are reported some examples of (i) immucillin (ImmA) derivatives (Figure 1.10) and the DADMe-ImmA derivatives which mimic, respectively, the early and the late dissociative transition state of MTAN.[162–165]

Triclosan

Ambuic acid

ImmA

R = *m*-Cl-Ph; *p*-Cl-Ph; *m*-CH₃-Ph; *p*-CH₃-Ph; Bn

DAD-MeImmA

R = CH₃; Et; Bu

S-anhydroribosyl-L-homocysteine

S-homoribosyl-L-cysteine

Figure 1.10: Structures of the signal generation inhibitors of AHL-, oligopeptides- and AI-2-mediated QS

Most of the analogues developed have been assayed *in vitro* on purified MTANs and only some of them have been tested *in vivo* to assess their effects on QS and biofilm formation. Several MTAN inhibitors inhibited AHL production in *V. cholera* and both AI-2 and AHL production in *E. coli* and, to a different extent, biofilm formation.[166–170]

LuxS is a synthase that generates DPD upon removal of Hcys from SRH. It is present in a wide range of bacterial species where it is not only involved in AI-2 biosynthesis but also in the activated methyl cycle (AMC).[171,172] LuxS is a homodimer with two identic (highly conserved) active sites at the dimer interface. Each active site contains a tetrahedrally coordinated divalent ion, usually Fe^{+2} (although only minimal effects on its activity could be observed by replacement of Fe^{+2} with Co^{+2}). LuxS is not present in mammals and its inhibition should limit unwanted off-target effects. To date, no potent inhibitors of LuxS have been identified. The first compounds reported by Alfaro *et al.* were the two substrate analogues *S*-anhydroribosyl-L-homocysteine and *S*-homoribosyl-L-cysteine (Figure 1.10) that inhibited, respectively, the first and the last step of the catalytic mechanism.[173] Several substrate analogues bear modifications at C_3 or on the furanose ring (e.g., oxygen is replaced by nitrogen) but they do not display high activity.[174,175]

1.5.2 Degradation of Quorum Sensing signaling molecules

Enzymatic degradation of oligopeptides-based QS is almost completely unexplored due to the broad substrate specificity of proteases while degradation of AHLs has extensively been studied as an interesting QS inhibition strategy. Three classes of enzymes target AHL signals:

- Acylases: irreversibly cleave the bond between the lactone ring and the acyl tail with the release of the homoserine lactone moiety and the fatty acid chain. They exhibit specificity based on the length of the acyl chain and its substitution at position 3 because the binding pocket is constrained and needs to adjust upon ligand binding;[176–178]

- Lactonases: are metalloproteins that reversibly hydrolize the esteric bond of the lactone ring to yield the corresponding acyl homoserine molecule. The cleavage can spontaneously occur at basic pH and be restored in acidic conditions. Lactonases are usually not substrate-specific since the lactone ring is highly conserved among the AHLs and the variable acyl chain interacts non-specifically with the binding site;[179–181]

- Oxidoreductases: are not very well known enzymes able to oxidize/reduce (and therefore inactivate) the AHLs acyl side chain.[182–184]

1.5.3 Inhibition of Quorum Sensing signal detection/transduction

The generation of analogues of native signals is the most intuitive way to design QSIs that are still able to interact with the receptor while disrupting the downstream signaling process. An alternative is to modify the structure of known inhibitors in order to increase their potency.

Numerous natural and non-natural AHL molecules have been evaluated on multiple LuxR-type receptors exhibiting a wide range (e.g., agonistic, antagonistic) of activity. The general structures of some examples of

non-natural AHLs (i.e., thiolactones,[185] triazolyldihydrofuranones[186] and urea analogues[187]) are reported in Figure 1.11. Elucidation of several crystal structures (e.g., TraR,[188,189] SdiA,[190] LasR[191,192]) together with molecular docking/modeling programs have enormously helped scientists in the design of compounds that would potentially bind the ligand binding pocket of AHL proteins. The studies indicated that favorable hydrogen bonds as well as hydrophobic van der Walls interactions between the ligand and the binding site are essential for activity. Changes in the length and/or substitution of the acyl chain together with alteration of all/part of the lactone ring and of its chirality can also have a huge impact on the activity and selectivity of a given compound. Unfortunately, most of the studies published so far have focused on the *in vitro* evaluation of the potential agonistic/antagonistic activity of AHLs analogues and their *in vivo* effects on QS, as well as *in vivo* studies on their stability have been neglected.

In *S. aureus*, cyclic AIPs belonging to four different groups (i.e., I – IV) interact with specific AgrC sensor kinases and regulate biofilm and exotoxin production.[193] Several SAR studies focused on the identification of critical amino acids for each AIP group revealed how small substitutions can have significant impact on AIP role. Following this strategy, many research group have generated, mutating native AIPs, sets of molecules with higher/lower activity, no activity, changes from self-activation to self-inhibition activity.[194–196]

Of note, in 2008, Fowler *et al.* produced a library of analogues of autoinducing peptide I (AIP-I) from *S. aureus* where the 14 macrocyclic peptide-peptoid hybrids (peptomers) were lacking the thioester linkage. One of the macrocyles was found, although with an unknown mechanism, to alter biofilm formation *in vitro* (Figure 1.11).[197]

Thiolactones   **Triazolyldihydrofuranones**   **Urea analogues**

AIP-I analogue   **Phenylboronic acid derivatives**   **Pyrogallol derivatives**
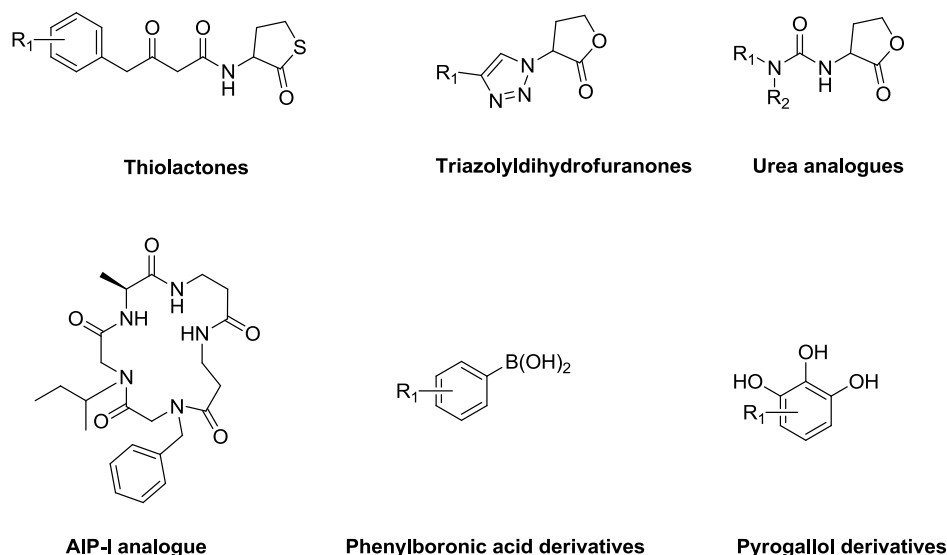
Figure 1.11: Structures of the signal detection/transduction inhibitors of AHL-, oligopeptides- and AI-2-mediated QS

AI-2-based QS is undoubtedly well known but the number of papers focused on the development of small molecules able to modulate AI-2-based QS is way lower when compared to the extensive amount of data on LuxR type receptors and AHL-based QS modulation. Furthermore, the rational design of AI-2 modulators has been thwarted by the lack of structural information as well as by the unstable nature of the AI-2 precursor DPD (see Chapter 3). The studies reported are mostly focused on the discovery of analogues of

known signaling molecules (e.g., *R*-THMF, *S*-THMF). In 2008, Ni *et al*. screened a small library of boronic acids envisioning that, due to the similar structure of the boronic acid functional group to *S*-THMF-borate, they could bind to LuxP and inhibit QS in *V. harveyi*. Five phenylboronic acids (the general structure is shown in Figure 1.11) displayed single-digit micromolar IC_{50} values. The excellent results prompted the group to further screen a second library of 30 *para*-subsituted arylboronic acids and additional eleven molecules were found to exhibit similar IC_{50} values (for additional details, see[198]).

The same research group tested also a small set of pyrogallol-derivatives reasoning that, once complexed with boric acid, they could act as molecular mimic of *S*-THMF-borate. Five compounds showed IC_{50} values in the single-digit micromolar range and none of them was cytotoxic (see Figure 1.11 for the general structure and [198] for more details).[198]

In the last decade, a large number of papers focusing on the synthesis of DPD-derivatives has been reported. This manuscript contains a section dedicated to the DPD-analogues reported in the literature (see Chapter 5) and a chapter (Chapter 6) that describes my work focused on the synthesis of DPD-Ihs.

2.   LSRK KINASE AS TARGET

Phosphorylation of the linear form of the "universal autoinducer" *S*-DPD is mediated by the bacterial kinase LsrK and results in the activation of QS in both in *E. coli* and *S. typhimurium*.[94,95] In this chapter, I will describe LsrK from a biological and computational point of view and explain its catalytic mechanism. When I started my PhD in 2015, no crystal structure was available for LsrK and I therefore built a LsrK homology model to guide the design of novel compounds. Furthermore, I've also spent four months (March – June 2017) at the University of Cambridge attempting LsrK crystallization. In June 2018, three crystal structures of LsrK/HPr (a phosphocarrier protein) alone or in complex with adenosine triphosphate (ATP) and adenosine diphosphate (ADP) (PDB ID: 5YA0, 5YA1, 5YA2, respectively) were published.[199]

2.1   Kinase binding site and kinase inhibitors

Kinases are defined as enzymes that transfer a phosphate group (from ATP or guanosine triphosphate, GTP) to a substrate that contains an alcohol, an amino, a carboxyl or a phosphate group as acceptor. Kinases represent one of the largest protein family in eukaryotes having 518 members encoded in the human genome. Kinases play an important role in the regulation of a variety of cellular processes such as apoptosis, differentiation, proliferation, survival, transcription and their dysregulation often results in diseases like cancer, inflammation, central nervous system (CNS) disorders, cardiovascular diseases. Kinase phosphorylation has been identified also in prokaryotic organisms and associated to biofilm formation and virulence. A variety of small molecules kinase inhibitors (SMKIs) targeting bacterial and/or prokaryotic kinases has been reported but, so far, no inhibitor has been approved as antimicrobial agent.[200–208]

Despite having different aminoacidic sequences, human kinases have similar 3D structures especially at the binding site: two domains (N- and C-terminal, β-stranded and α-helical, respectively) and a connecting hinge region. ATP binds in the cleft between the two domains and its adenine ring forms hydrogen bonds with the residues in the hinge region. All the kinases have a flexible activation loop starting with the conserved tripeptide aspartic acid-phenylanaline-glycine (Asp-Phe-Gly, DFG motif) that controls access to the binding site and it is also called "magnesium positioning loop" as Asp coordinates a Mg^{+2} ion. A conserved region is also the P-loop (or Walker A motif), a Gly-rich loop between the $β_1$ and $β_2$ strands of the N-domain important for phosphate binding and coordination with the $β\text{-}PO_4^{-2}$. Deep in the ATP pocket is the "gatekeeper", an important residue that controls the access to the back part of the binding site and it is often mutated in case of resistance. The Phe of the DFG motif makes hydrophobic contacts with one residue from the C-terminal and one from the N-terminal creating what is called a "DFG-in" conformation. When the Phe moves out from the hydrophobic pocket, the orientation of the DFG-Asp changes and it is no longer able to coordinate Mg^{+2} thus resulting in an inactive conformation defined "DFG-out" (Figure 2.1).[209–213]
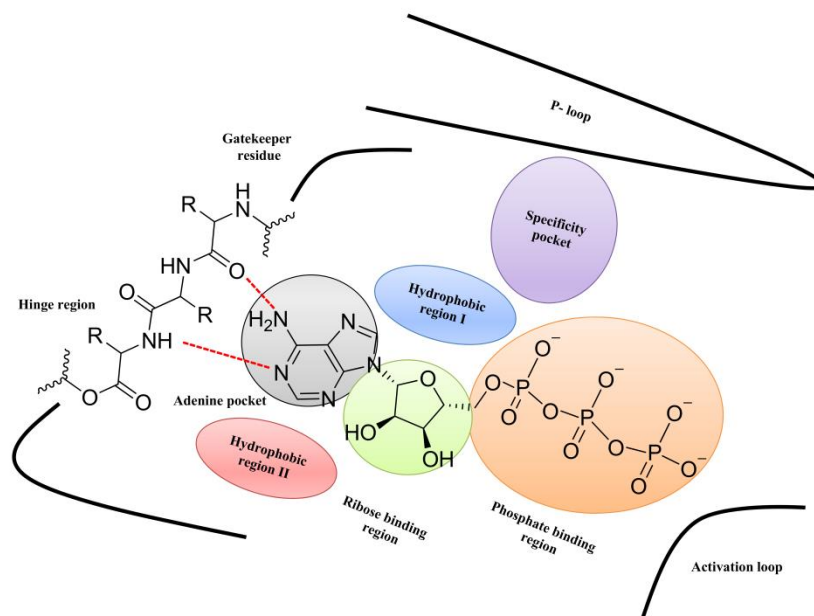
Figure 2.1: Schematic representation of kinases' ATP binding site. Hydrogen bonds are represented in red broken lines

Kinase inhibitors can be divided into two classes, based on their binding modes: (i) irreversible inhibitors covalently bind to a cysteine residue close to the ATP-binding site thus irreversibly blocking ATP binding; (ii) reversible inhibitors can be further classified into four different types. Type I inhibitors are ATP-competitive inhibitors and bind to the active form of kinases ("DFG-in" conformation); type II inhibitors bind and stabilize the inactive form ("DFG-out" conformation) with the DFG-Asp oriented outside the ATP binding site; type III inhibitors bind in an allosteric pocket close to the ATP binding site while type IV bind in an allosteric pocket far from the ATP binding site. Bivalent and bisubstrate inhibitors (type V) display more than one of such binding modes (Figure 2.2). The majority of the SMKIs are interacting with the ATP binding site which is structurally and functionally conserved. Therefore, a poly-pharmacological effect (i.e., a drug that act on multiple targets) is often observed.[214]

Selectivity is a very controversial topic when talking about kinases: target promiscuity may lead to off-target toxicity and drug's withdrawal from the market but, for the treatment of certain diseases (e.g., cancer), a multitarget drug may be advantageous. Most of the type I and type II inhibitors approved by the FDA are valuable and effective multitarget anticancer drugs (e.g., pazopanib, ponatinib, sorafenib). Multitarget inhibitors are more suitable in oncology, where the signal cascade responsible for tumorigenesis is very complex, while selective SMKIs are used to overcome off-target toxicity and side effects outside the oncology area.[215–217] High selectivity can be achieved with the development of allosteric inhibitors that do not bind to the ATP binding site.
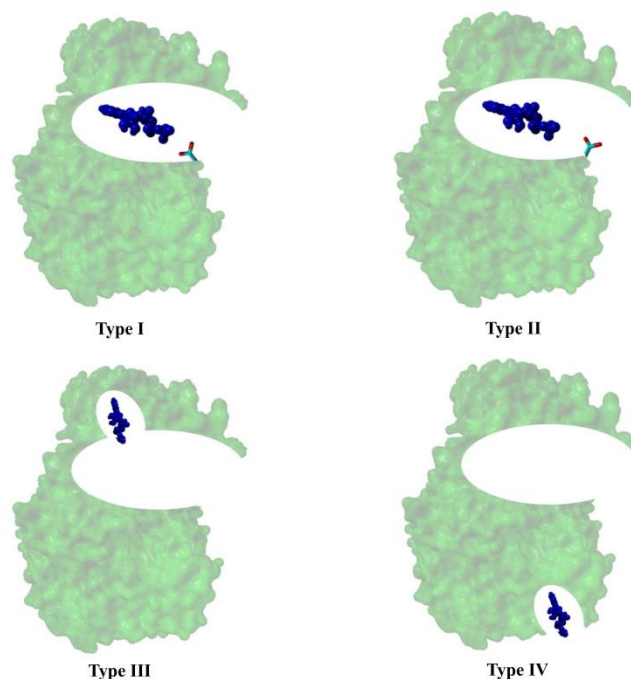
Figure 2.2: Type I – IV reversible binding mode for kinase inhibitors. For the figure was used the co-crystal structure of PDK1 with ATP (PDB ID: 4RRV[218]) manipulated with YASARA (version 16.4.6.L.32)[219]

2.2 LsrK and the FGGY carbohydrate kinase family

LsrK belongs to a family of carbohydrate kinases called FGGY family. Over 4000 family members have been identified in the National Center for Biotechnology Information (NCBI) non-redundant sequence database[220] and at least 44 crystal structures have been solved. Members of this family transfer a phosphate group from ATP to several sugars ranging from trioses to heptoses. Representatives of the FGGY family can be found in several bacterial genomes where they are involved in the catabolic pathway of carbohydrates.

From a structural point of view, all the described members are constituted by two actin-like ATPase domains called, respectively, FGGY_N and FGGY_C. The substrate (i.e., the sugar) and ATP bind in the catalytic cleft between the two domains: the sugar binds deeply in the cleft and interacts mostly with the residues in the N-domain while the ATP binds near the opening of the cleft and interacts with residues in both the N- and C-terminal domains. Upon binding of the sugar, the cleft closes to prevent the entrance of solvent and the phosphorylation takes place (Figure 2.3).[221]

In 2011, Zhang *et al.* analyzed, at both the phylogenetic and the molecular level, a set of 446 FGGY kinases. The analysis revealed that glycerol kinase (GlpK), L-ribulokinase (AraB) and xylulo kinase (XylB) are present in the majority of the bacterial species. GlpK's molecular mechanism and specificity remained unchanged throughout evolution since glycerol plays a unique role in both carbohydrate and lipid metabolism and, as it is the smallest sugar substrate in the FGGY family, its specificity has been preserved.
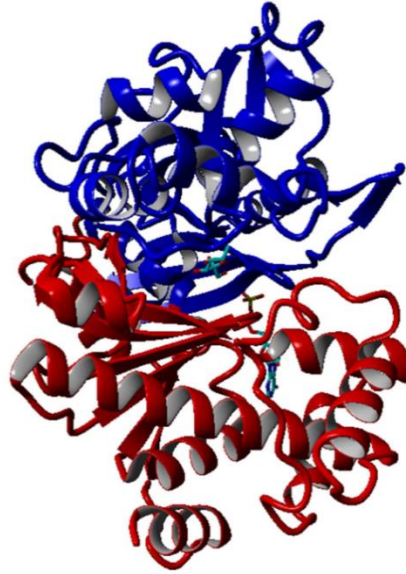
Figure 2.3: 3D structure of L-rhamnulose kinase from *E. coli* (PDB ID: 2UYT). The FGGY_N and FGGY_C domains are colored, respectively, in blue and red. Figure created with YASARA (version 16.4.6.L.32)[219]

AraB and XylB instead branched into new functions or into different biochemical mechanisms within the same function still maintaining their specificity through a small set of specificity-determining residues. In this evolutionary model, LsrK is predicted to branch from XylB and, more specifically, it sits between LyxK, FucK I, II and RhaB I, II (Figure 2.4).
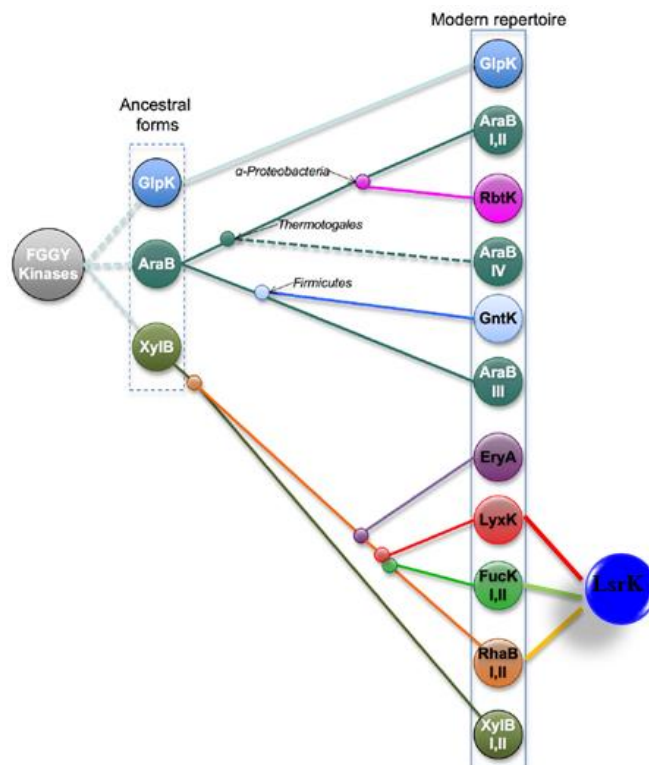
Figure 2.4: Proposed evolutionary model for the members of the FGGY kinase family from Zhang *et al.*[221] Figure adapted from *PLOS Comput Biol* **2011**, *7* (12), e1002318. Copyright © 2011 Zhang *et al.*[221]

2.3 LsrK and its role in QS

Several studies have been performed to better understand LsrK's activity and its importance in bacterial QS. In 2007, Xavier *et al*. demonstrated [with isotope labeling thin layer chromatography (TLC) studies] that LrsK phosphorylates DPD to produce P-DPD. Tandem mass spectrometry (MS/MS) scanning and phosphorus nuclear magnetic resonance (^{31}P NMR) revealed that the phosphorylation occurs at position C_5 and further experiments on the repressor LsrR showed that P-DPD binds to it and regulates *lsr* expression in enteric bacteria.[222] LsrK mutants do not activate *lsr* transcription because of the lack of phospho-AI-2 and, as a consequence, the reduced expression of the Lsr transporter results in extracellular AI-2 accumulation.[223] Furthermore, when LsrK and ATP were added *ex vivo* (i.e., in the extracellular medium) to *E. coli*, *S. typhimurium* and *V. harveyi* (both in pure cultures and in a synthetic ecosystem), the phosphorylation of AI-2 outside the cells impeded the transport of phospho-AI-2 through the Lsr transporter due to its negative charge. As a result, a reduction in *lsr* expression and attenuation of QS were observed (both in the single cultures and in the three species ecosystem).[224] It is clear why LsrK represents a really attractive anti-infective target and how its selective modulation could attenuate AI-2 related pathogenesis. As a first step towards a better understanding of LsrK's kinetic mechanisms, in 2013 Zhu *et al*. developed an accurate UV-visible assay that allowed for steady-state kinetic analysis. In the assay, ADP production (as a consequence of LsrK-mediated phosphorylation) was coupled with the oxidation of nicotinamide adenine dinucleotide (reduced form, NADH) by pyruvate kinase (PK) and lactate dehydrogenase (LDH, Figure 2.5) using phosphoenolpyruvate (PEP) as starting material. The initial velocity of LsrK catalysis was calculated by measuring the consumption of NADH at 340 nm. The resulting data were consistent with a model where ATP is the first substrate and DPD cannot bind without ATP binding first. Important kinetic parameters such as k_{cat} (7.4 ± 0.6 s^{-1}), $K_{m,\ ATP}$ (150 ± 30 µM) and $K_{m(app),\ DPD}$ (1.0 ± 0.2 mM) were measured to further understand the critical role of LsrK in QS and to help the rational design of molecules targeting AI-2-based QS.
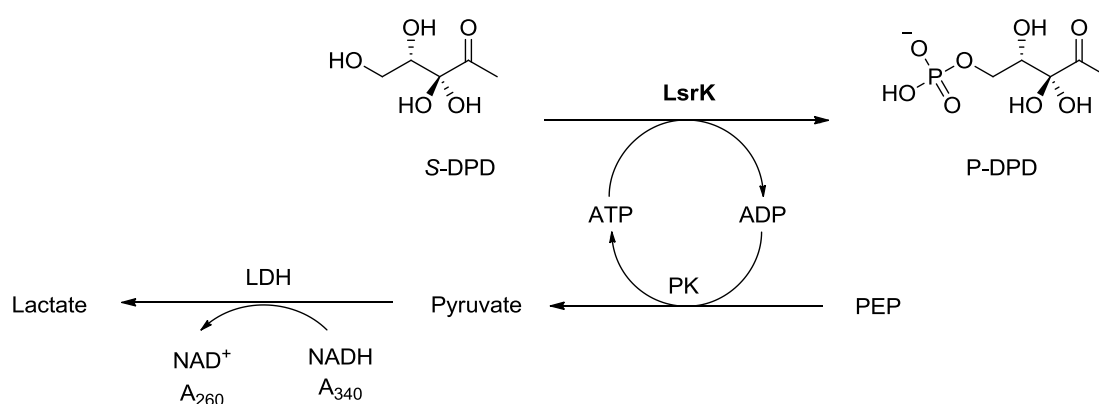
Figure 2.5: Phosphorylation of *S*-DPD by LsrK and PK/LDH reaction coupled to it

2.4 Homology model of LsrK and analysis of the binding site

As the goal of my project was the investigation of the effect(s) of LsrK's inhibition on QS through design and synthesis of potential inhibitors, knowing LsrK's catalytic mechanism and the residues involved in the catalytic activity was fundamental but impeded by the absence of a 3D structure (not available when I started my research activity in 2015). In order to have a better understanding of LsrK 3D conformation and of its binding site, I built a homology model. Since the binding site closes upon binding of the ligand, both an open and a closed homology model were built.

The first and critical step when building a homology model is to choose a related homologous protein to use as a template. The easiest method is to run serial pairwise sequence alignments using database search techniques such as BLAST (Basic Local Alignment Search Tool). After inserting in the software YASARA (Yet Another Scientific Artificial Reality Application) the sequence of LsrK from *S. typhimurium* (uniprot code: Q8ZKQ6, 530 residues, see Chapter 8.2.1 for full sequence), three PSI-BLAST (Position-Specific Iterative BLAST) iterations (see Chapter 8.2.2 for all the other parameters selected) were run and the program returned a list of 47 templates (see Table 8.1). A target sequence profile was then generated to help the alignment of the target sequence and the templates and 25 models for the best aligned templates were built. **3IFR** (xylulose kinase from *R. rubrum*, chain B, 2.3 Å, 498 residues[225]) was selected as "open homology model" (3IFR_HM) and **3G25** (glycerol kinase from *S. aureus* in complex with glycerol (GOL), chain B, 1.9 Å, 499 residues[226]) as "closed homology model" (3G25_HM). The open (3IFR_HM) and closed (3G25_HM) models were then aligned to see how much the binding site closes upon binding of the sugar: it is evident from Figure 2.6 that is the C-terminal domain that is moving towards the sugar (not shown in the figure) to prevent solvent from entering the catalytic cleft and to start the phosphorylation process.
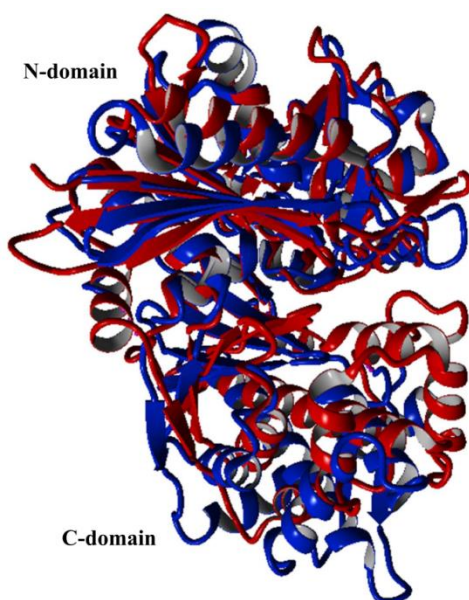
Figure 2.6: Alignment of 3IFR_HM (blue) and 3G25_HM (red). Figure created with YASARA (version 16.4.6.L.32)[219]

To prove that is the binding of the sugar (and not of ATP) that closes the binding site, a close analogue (i.e., 1GLF, glycerol kinase from *E. coli*, co-crystallized with GOL and ADP[227]) of the closed homology model was selected and aligned to it: the two 3D structures perfectly align, which means that is the sugar and not ATP (ADP in this case) responsible for the closing up of the binding site (Figure 2.7).
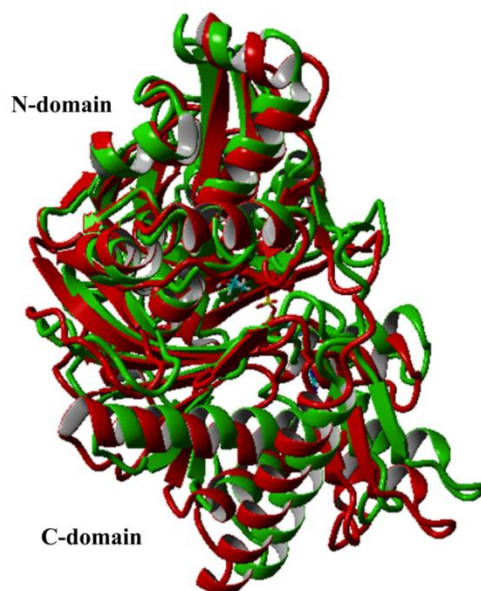
Figure 2.7: Alignment of 3G25_HM (red) and 1GLF (green). GOL and ADP from 1GLF are shown in stick in the catalytic cleft. Figure created with YASARA (version 16.4.6.L.32)[219]

A closer look to the binding site of both the open and close models was necessary to identify the conserved residues typical of kinases (e.g., DFG motif) as well as the amino acids involved in the catalytic mechanism (e.g., threonine/serine, arginine). Since the open homology model was built using as a template a crystal structure without both the ligand and ATP/ADP, GOL and ADP were taken from 1GLF and joined into the model. The same was done for the closed model. For both of the models, key residues were identified, such as threonine 21 (Thr 21), serine 91 (Ser 91), arginine 93 (Arg 93), aspartic acid 253 (Asp 253), phenylalanine 276 (Phe 276) (Figure 2.8). The same analysis of the binding site was performed also including a closed sugar inside the binding pocket selecting 2CGJ (L-rhamnulose kinase from *E. coli* in complex with L-fructose (LFR) and ADP, chain A, 2.3 Å, 489 residues[228]) as source of the ligand (LFR). The results obtained for all the four combinations (i.e., (i) open model + open sugar; (ii) open model + closed sugar; (iii) closed model + open sugar and (iv) closed model + closed sugar) were compared with each other and key-residues for the catalytic activity were identified (Figure 2.8).
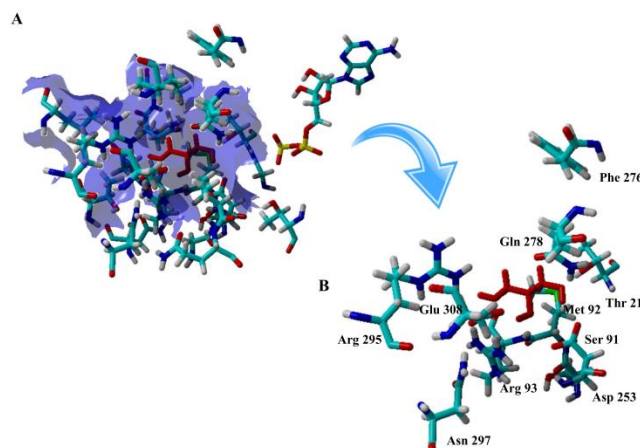
Figure 2.8: A) Analysis of the binding site of 3IFR_HM. GOL and ATP were taken from 1GLF. B) Residues conserved and involved in the catalytic mechanism

2.5   Cloning, over-expression and purification of LsrK

In collaboration with the research team of professor Martin Welch (member of the INTEGRATE[229] consortium) at the University of Cambridge (where I spent the four months March – June 2017), several attempts to solve the X-ray crystal structure of LsrK were performed.

First, LsrK cloning was attempted in *E. coli* as its maltose-binding protein (MBP)-pMAL-c2X fusion but without any success (see Chapter 8.3.3). The cloning was then repeated using pET-19m as plasmid to have LsrK as a His$_6$-tagged fusion protein (see Chapter 8.3.4).

Whole genomic DNA of *E. coli* MG1655 was extracted with Genomic DNA Purification Kit (ThermoFisher Scientific) and used as a template for LsrK gene amplification. Designated primers were employed to amplify the LsrK sequence by polymerase chain reaction (PCR). The purified gene was digested with the two restriction enzymes NdeI and XhoI and cloned into the pET-19m expression vector to generate a His$_6$-tagged construct. The sequence was confirmed by standard sequence analysis (see Chapter 8.3.4).

Four flasks (4 x 250 mL) of Luria Broth (LB) supplemented with carbenicillin disodium salt (50 mg/mL) and chloramphenicol (34 mg/mL) were inoculated with 250 μL (each) of a 10 mL overnight culture of the *E. coli* expression strain, itself grown in LB with carbenicillin disodium salt (50 mg/mL) and chloramphenicol (34 mg/mL). After testing four different conditions for the overexpression (see Chapter 8.3.4 for details and results), we found that the best ones were the ones already reported in 2013 by Zhu *et al*.[230]

The cells were grown in six flasks (6 x 1000 mL) at 37 °C with good aeration shaking at 200 rotations per minute (rpm) to an approximate optical density at 600 nanometer (OD$_{600}$) of 0.5. The temperature was then lowered to 22 °C and when the OD$_{600}$ reached 0.9, the expression was induced by adding 0.42 mM isopropyl-β-D-1-thiogalactopyranoside (IPTG). Protein expression was continued at 22 °C overnight. The cells were then harvested by centrifugation at 4 °C (14.000x *g*, 30 minutes) and the pellets were resuspended in a total volume of 100 mL of ice-cold lysis buffer (50 mM sodium phosphate, 200 mM NaCl, 10% (v/v) glycerol, pH = 8.0) supplemented with an EDTA-free protease inhibitor cocktail tablet. The bacterial suspension was lysed by sonication with continuous cooling on ice-water (8 x 30 seconds, 13 A, 1 minute

pause between pulses). The cell lysate was clarified by ultracentrifugation at 4 °C (11.000x *g*, 30 minutes) and the clarified supernatant was filtered through a 0.22 μm filter. Affinity chromatography was performed with Ni-NTA column (2 mL packed resin bed volume). The filtered lysate was loaded onto the column and purified in accordance with the manufacturer's instruction. The column was washed overnight with equilibration buffer (50 mM Tris*HCl, 200 mM NaCl, 10% (v/v) glycerol, 10 mM imidazole, pH = 7.4). The His$_6$-tagged protein was eluted with elution buffer (50 mM Tris*HCl, 200 mM NaCl, 10% (v/v) glycerol, 250 mM imidazole, pH = 7.4) and dialyzed overnight against 2 liters of dialysis buffer (50 mM Tris*HCl, 100 mM NaCl, 5% (v/v) glycerol, pH = 7.4) in the presence of His$_6$-tagged Tobacco Etch Virus nuclear-inclusion-a endopeptidase (TEV)-protease. The protein thus released was cleaned up by batch extraction in a slurry of Ni-NTA resin equilibrated in dialysis buffer and concentrated (Vivaspin, molecular weight cut-off, MWCO 30.000, Sartorium) to 12 mg/mL (estimated by A$_{280}$ using ε_{calc} ~ 93.390 M^{-1} cm^{-1}). The mixture was snap-frozen in liquid nitrogen in aliquots of 1 mL and stored at -80 °C. Sodium Dodecyl Sulphate - PolyAcrylamide Gel Electrophoresis (SDS-PAGE) confirmed the presence of a protein corresponding to the mass of the pET-19m-LsrK fusion protein (57.5 kDa) and some impurities (Figure 2.9).

Crystallization conditions were screened using sitting drop vapor diffusion with 12 mg/mL and 6.2 mg/mL purified protein. Three different crystallization plates (EB Wizard I & II, QN PEGs I, MD JCSG$^+$, Molecular Dimensions) were filled but, even after 21 days, no crystals were observed. Perhaps the lack of the natural substrate (i.e., *S*-DPD) and/or ATP in the plates as well as the protein purity (~ 80%, as estimated by SDS-PAGE) may have affected the crystallization. Therefore, as a target-based design of novel potential LsrK kinase inhibitors was mined by the lack of a 3D structure, a ligand-based approach was pursued (see Chapter 6).
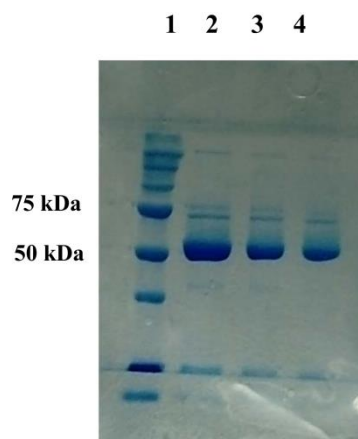
Figure 2.9: Purification of LsrK. The figure shows a Coomassie Brilliant Blue G250-stained polyacrylamide gel (12%) run in SDS buffer showing the purification of LsrK. Lane 1: protein molecular marker; lane 2: LsrK eluted from Ni-NTA column (20 μL); lane 3: LsrK eluted from Ni-NTA column (10 μL); lane 4: LsrK eluted from Ni-NTA column (5 μL)

In June 2018, three crystal structures of LsrK/HPr (a phosphocarrier protein) alone or in complex with ATP and ADP (PDB ID: 5YA0, 5YA1, 5YA2, respectively) were published.[199]

3. 4,5-DIHYDROXY-2,3-PENTANEDIONE (DPD): STATE OF THE ART

As discussed in Chapter 1, Quorum Sensing is a cell-to-cell communication process that allows bacteria to act as a population instead of as single organisms. In both Gram-negative and Gram-positive bacteria, QS is mediated by the exchange of small signaling molecules collectively termed AI-2. The precursor of AI-2 is DPD, a small chemical entity that spontaneously rearranges to generate different QS mediators. This compound has a great interest from a medicinal chemistry stand point and, over the years, numerous syntheses have been reported and a better knowledge of this molecule has been gained. In this chapter I will describe its peculiarities and summarize the procedures described in the literature for its synthesis both as a racemic mixture and as enantiopure *S*-DPD.

3.1 DPD's equilibrium and stability

DPD may look like a small, simple, linear molecule but it is actually a complex mixture of different coexisting structures (see Chapter 1, Figure 1.6). DPD is not stable unless in diluted solutions: Meijler *et al.* observed only minimal polymerization ($< 1\%$) when DPD was kept at a concentration lower than 3 mM and in such conditions it was stable for at least one month while, at higher concentrations (not specified), the stability decreased significantly.[231] Different results were published in 2005 by Semmelhack's group: the stability of a 30 mM DPD solution was monitored via ^{1}H NMR at pH = 1.5 and 20 °C and no decomposition products were observed after 5 hours. No loss of activity in the *V. harveyi* assay was also noted by the same research group for a 100 mM solution kept at 20 °C and pH = 1.3 for 16 hours.[232] Despite these results may seem contradictory, it has to be noted that Semmelhack's experiments were performed over a limited timeline. Longer experiments (e.g., one month) were done only with diluted solutions so it is still unclear whether solutions up to 100 mM can be stable for such amount of time or not.

Normal practice in DPD's reported syntheses (see later) is to remove a protecting group in the last step under acidic conditions and, in order to avoid further manipulation of such complicated mixture, to use the solution as such for biological experiments. Therefore, the equilibrium of the different DPD's species has been initially studied at pH values between 1 and 2 and it has been noted that, under these strong acidic conditions, the linear form of DPD is in equilibrium with its two cyclic isomers (i.e., *S*-DHMF and *R*-DHMF, see Chapter 1, Figure 1.6) in a ratio 1:2:2.[232] In 2012, Globish *et al.*[233] decided to explore the various forms of DPD in equilibrium at physiological pH. To do so, an aqueous solution of DPD was buffered to pH = 7 using 1M phosphate buffer (1M NaD_2PO_4/Na_2DPO_4). The changes in the intensity and number of signals detected by ^{1}H NMR in the methyl region (i.e., δ = 1.3 ppm – 2.4 ppm) and in core structure (i.e., $C_4 - C_5$, δ = 3.5 ppm – 4.4 ppm), prompted the group to investigate more deeply the pH-dependency of DPD's equilibrium. Therefore, DPD was titrated with NaOD in D_2O (0.1 M) to pH = 7 and major changes were observed in the methyl region where new signals appeared at pH values between 4 and 5.

The signals became even more dominant when DPD was titrated to pH = 10 and the three major methyl signals typical of acidic conditions completely disappeared. The changes proved to be reversible as acidification of the solution to pH = 1 resulted in the same ^{1}H NMR as before any manipulation.

These findings revealed an unexpected stability over a wide range of pH values, in complete contrast with other QS molecules like AHLs and AIPs which are known to be susceptible to hydrolytic degradation.[233–236] To gain further knowledge in this complicate equilibrium of structures, the same research group synthesized compounds **1** and **2** (Figure 3.1) as model systems for the linear and cyclic forms of DPD. Methylation of the C_5-OH (i.e., **1**, Figure 3.1) resulted in a linear DPD-analogue, incapable of any ring closure. Titration from pH = 1 to pH = 7 revealed the presence of only a major species over the entire pH range where only the ketone at C_3 was hydrated. For the cyclic model, CF_3-DPD **2** was selected as it exists only in the cyclic form. ^{1}H NMR revealed that the equilibrium of **2** is pH-dependent: signal changes in the core structure (i.e., C_4-C_5 positions) were very similar to the ones previously observed for the cyclic isomers of DPD. The authors concluded that, at physiological pH, DPD is hydrated at C_3 (*S*-THP, see Chapter 1, Figure 1.6) and in equilibrium with both the hydrated forms *S*-THMF and *R*-THMF (see Chapter 1, Figure 1.6).[233]
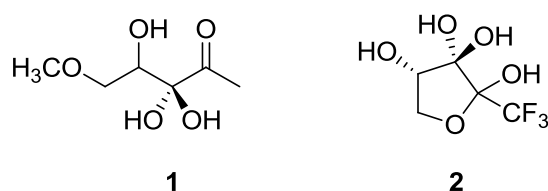
Figure 3.1: Linear (**1**) and cyclic (**2**) model compounds to study DPD's equilibrium

DPD can be purified from complex mixtures taking advantage of its affinity for boron. In 2004, Semmelhack *et al.* developed a "catch-and-release" technique from aminophenylboronic acid immobilized on polyacrylamide beads. In the protocol, the beads are washed with saturated $NaHCO_3$ and the broth containing DPD is passed through a tube containing the resin. DPD is released from the resin with 20% aqueous formic acid and the eluate is immediately buffered at pH = 7.8. Further addition of borate to form *S*-THMF-borate (see Chapter 1, Figure 1.6) can be used to stabilize the solution and directly test it in the *V. harveyi* bioluminescence assay (see further) where it has shown to increase > 600-fold the biological activity when compared to the crude enzymatic preparation.[237]

3.2   Identification and quantification of DPD

The complex equilibrium of DPD's structures has hampered its full characterization and quantification: the low ionization potential, the high polarity, the absence of chromophores and the low concentration of AI-2 in biological samples have thwarted the development of a robust, reproducible and reliable direct method for its direct identification and quantification. To date, the most common method used for AI-2 detection is the *V. harveyi* bioluminescence assay where, in response to AI-2 in cell-free supernatants, the engineered reporter strain produces bioluminescence upon binding of *S*-THMF-borate to LuxP (see Chapter 7.1 for additional details).[238] Unfortunately, this assay is not quantitative and, despite having a limit of detection (LOD) in the low nanomolar (nM) range, it is particularly sensitive to assay conditions (e.g., pH, growth conditions and borate concentration) and to culture to culture variability which affect the reproducibility. In addition, the sensitivity can be altered by the presence of other molecules in the cell-free supernatants.[239–241]

Therefore, novel LuxP-FRET-(fluorescence resonance energy transfer) based methods have been developed over the years. In 2007, Rajamani *et al.* fused two fluorescent proteins to the N- and C-termini of LuxP to measure the FRET response upon binding of *S*-THMF-borate. The assay had limited sensitivity and was susceptible to the interference from other species in the sample.[242] Similarly, in 2008 Zhu *et al.* modified LuxP and LsrB near their ligand binding sites with environmentally sensitive fluorophores to generate a fast responding, highly sensitive, novel assay. Unfortunately, this method was time consuming and expensive as the proteins had to be purified and labeled and suffered from selectivity as compounds other than AI-2 could be detected.[243]

Another common method for AI-2 detection is the reaction of *S*-DPD with *o*-phenylendiamine to form Quinoxaline-*S*-DPD that can be identified by high performance liquid chromatography (HPLC, Scheme 3.1).
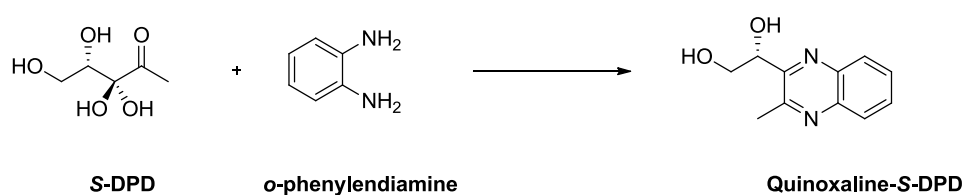
Scheme 3.1: Formation of Quinoxaline-*S*-DPD

In 2009, Thiel *et al.* developed a reliable gas chromatography-mass spectrometry (GC-MS) method for the qualitative and quantitative analysis of AI-2. The trimethylsilylated quinoxaline **3** was produced by treatment of Quinoxaline-*S*-DPD with *N*-methyl-*N*-(trimethylsilyl)trifluoroacetamide (MSTFA) in order to have a derivative accessible for GC-MS analysis. In a similar manner, the isotopically labeled derivative **6** was synthesized as an internal standard and absolute quantification was directly measured by measuring the relative ion-intensities of the labeled **6** and unlabeled **3** derivatives. This method is reproducible, linear and sensitive and allows for configuration determination by analysis of derivative **6** with chiral GC-MS (Scheme 3.2).[244]
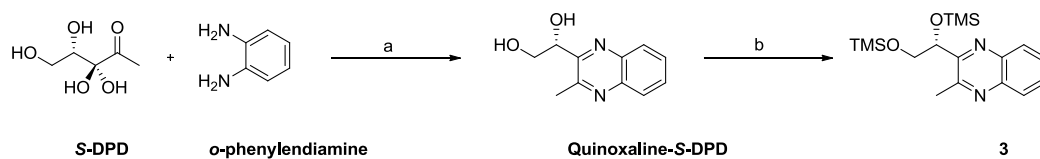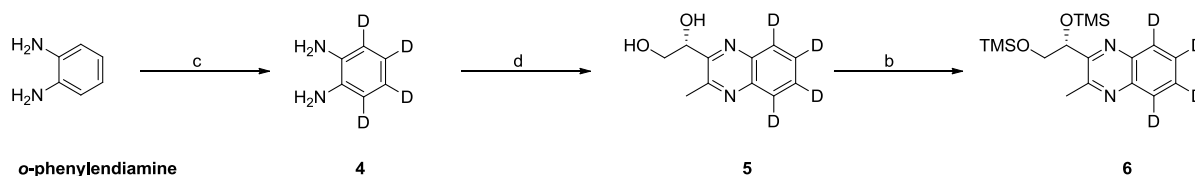
Scheme 3.2: A) Derivatization of *S*-DPD for GC-MS analysis and B) Synthesis of the internal standard **6**. Reagents and conditions: (a) DCM, rt; (b) MSTFA, DCM, 60 °C; (c) Pt/C, D$_2$O, 180 °C, 24 h (3 cycles)

A similar protocol was reported by Campagna *et al.* and applied to the detection of AI-2 in *E. coli* and *V. harveyi*. Different functionalized *o*-diaminobenzenes (i.e., **7** – **12**, Figure 3.2A) were reacted with synthetic *S*-DPD (2.35 mM, pH = 1.8) and analyzed via liquid chromatography tandem mass spectrometry (LC-MS/MS). With diamine **12**, the reaction was completed in ~ one hour and derivative **13** was isolated (Figure 3.2B). ^{13}C-DPD **14** and ^{13}C-quinoxaline-DPD-derivative **15** were both used as internal standard and the concentration of DPD was measured by multiplying the concentration of the standard added with the ratio of the integrated peak intensity for the labeled and unlabeled derivatives. When ^{13}C-DPD **14** was employed as internal standard, the concentration of *S*-DPD measured was higher than the one measured through ^{13}C-quinoxaline-DPD-derivative **15** probably because *S*-DPD was partially lost in the biological matrix during handling of the sample or (less likely) the Maillard reaction did not go to completion in such a complex media.[245]
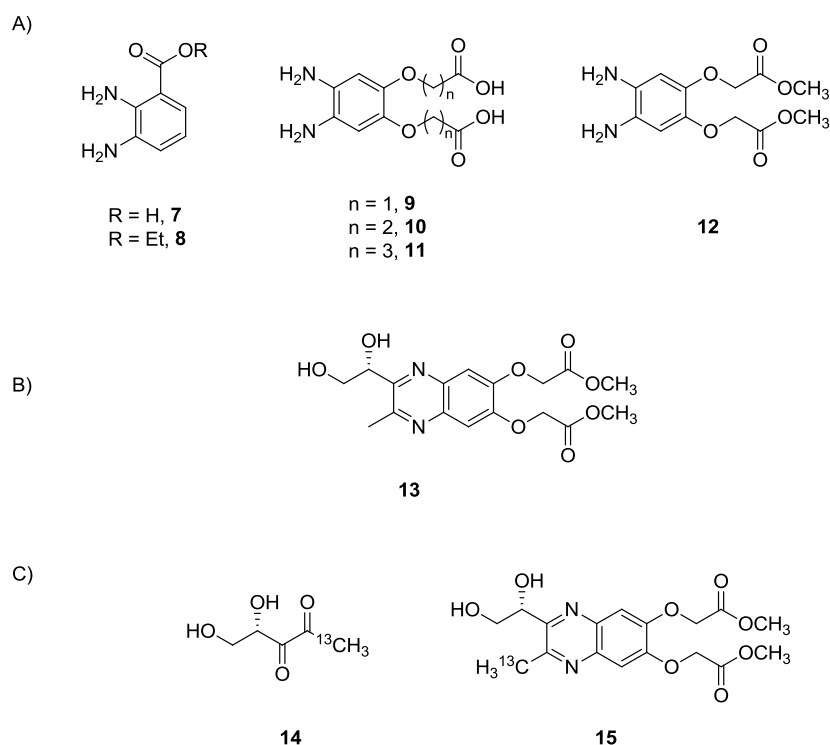
Figure 3.2: A) *o*-diaminobenzenes reacted with *S*-DPD; B) Derivative **13** and C) Isotope labeled standards used for internal calibration

3.3   Synthesis of racemic and homochiral DPD: literature-reported procedures

The first synthesis of *S*-DPD was published in 2004 by Meijler *et al*. The synthesis started from commercially available *S*-**16** which was oxidized to *S*-**17** in Swern's conditions. Corey-Fuchs homologation afforded acetal protected alkyne *S*-**19**. Deprotection and conversion to orthoformate *S*-**21** were followed by

KMnO$_4$-mediated oxidation. Final acidic deprotection under mild acidic buffer afforded *S*-DPD with an overall yield of 3.2% (Scheme 3.3).[231]
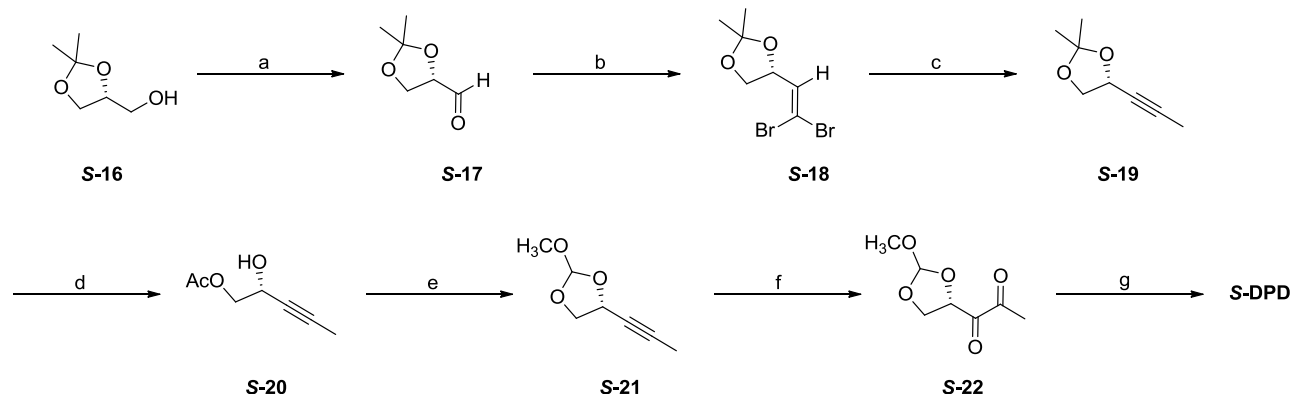
Scheme 3.3: Synthesis of *S*-DPD by Meijler *et al*. Reagents and conditions: (a) oxalyl chloride (1.1 eq), DMSO (2.5 eq), Et$_3$N (5.0 eq), DCM, - 78 °C, 30 min.; (b) CBr$_4$ (1.8 eq), PPh$_3$ (1.8 eq), Zn^0 (2.0 eq), DCM, 0 °C, 50 h; (c) *n*-BuLi (1.6 M in hexane, 3.0 eq), MeI (5.5 eq), THF, - 78 °C to rt, overnight; (d) AcOH (60%), THF, rt, 4 h (81%); (e) CH(OMe)$_3$ (neat), H$_2$SO$_4$ (cat.), rt, 1 h (73% over two steps); (f) MgSO$_4$ (4.2 eq), NaHCO$_3$ (0.6 eq), KMnO$_4$ (3.9 eq), acetone, rt, 20 min. (10%); 40 mM phosphate buffer (pH = 6.5), D$_2$O, rt, 36 h[231]

Instead of the orthoformate as protecting group, Semmelhack *et al*. introduced a cyclohexylidene group. L-gulonic acid γ-lactone **23** was prepared in 75% yield from L-ascorbic acid. Oxidative cleavage with KIO$_4$ resulted in aldehyde *S*-24. Similarly to Meijler *et al.*, Corey-Fuchs homologation led to the formation of alkyne *S*-26a with 43% yield over two steps. The critical oxidation step was performed following Zibuck *et al.*[246] and RuO$_2$*H$_2$O/NaIO$_4$ were used to generate diketone *S*-27a in 70% yield. Strong acidic deprotection (i.e., D$_2$SO$_4$) afforded *S*-DPD with an overall yield of 24% (Scheme 3.4). Notably, the byproduct of the deprotection (i.e., cyclohexanone) doesn't inhibit cell growth at concentrations < 1M.[232]
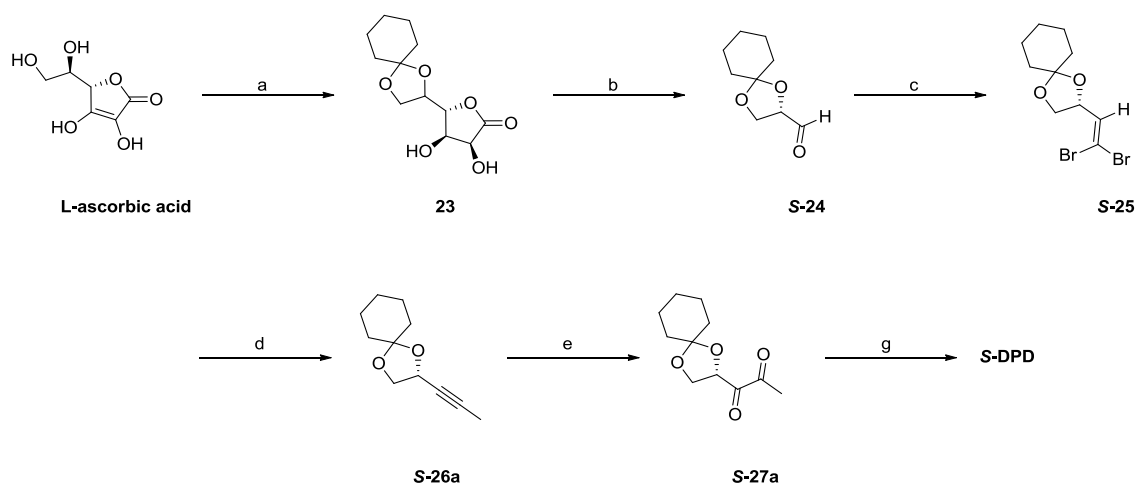
Scheme 3.4: Synthesis of *S*-DPD by Semmelhack *et al*. Reagents and conditions: (a) 1,1-dimethoxy cyclohexane (1.7 eq), *p*-TSA (cat.), DMF, rt, 36 h – 48 h; (a') Et$_3$N (cat.), PhMe, -20 °C, 24 h (75% over two steps); (b) KIO$_4$ (2.2 eq), KHCO$_3$ (4.6 eq), H$_2$O/DCM (1:1.8), rt, 18 h (76%); (c) CBr$_4$ (1.2 eq), PPh$_3$ (2.3 eq), DCM, 0 °C, 2 h (67%); (d) *n*-BuLi (2.5 M in hexane, 1.3 eq), MeI

(2.0 eq), THF, - 78 °C to rt, 4 h (98%); (e) NaIO$_4$ (2.3 eq), Ru$_2$O*H$_2$O (2.5% mol), CCl$_4$/ACN/H$_2$O (1:1:1.5), rt, 15 min. (70%); (f) D$_2$O, D$_2$SO$_4$ (cat., pD = 1.5), rt, 5 h[232]

In 2005, Frezza *et al.* published a three-step synthesis of racemic DPD (*rac*-DPD). Coupling of commercially available aldehyde **28** with 2-butenone in Baylis-Hillman's conditions and further TBAF-mediated removal of the TBDMS protecting group yielded the α-methylene-β,γ-dihydroxy ketone **30**. Reductive ozonolysis of the carbon-carbon double bond using dimethyl sulfide as reducing agent was chosen because the resulting byproducts (i.e., formaldehyde and dimethylsulfoxide) were reputed non-toxic at least at low concentrations.[247]
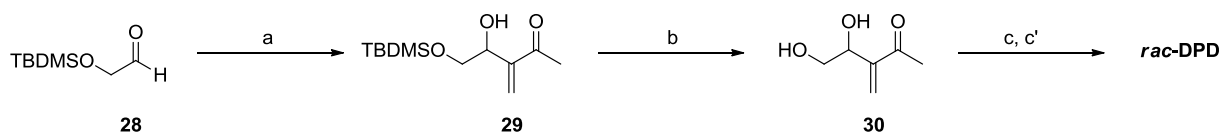
Scheme 3.5: Synthesis of *rac*-DPD by Frezza *et al.* Reagents and conditions: (a) 2-butenone (4.0 eq), DABCO (0.25 eq), THF, 0 °C, 21 h; (b) TBAF (1.0 eq), THF, rt, 21 h; (c) O$_3$, MeOH, - 78 °C, 30 min; (c') DMS, - 78 °C to rt, 16 h[247]

The same synthetic strategy was also applied to the synthesis of the elongated chain analogue ethyl-DPD **31**, the C$_5$-methyl-DPD **32**, the two 5-*O*-acylated derivatives **33** and **34** and, two years later, of the *bis*-acetylated-DPD **35** (Figure 3.3, see also Chapter 5, Scheme 5.9).[247]
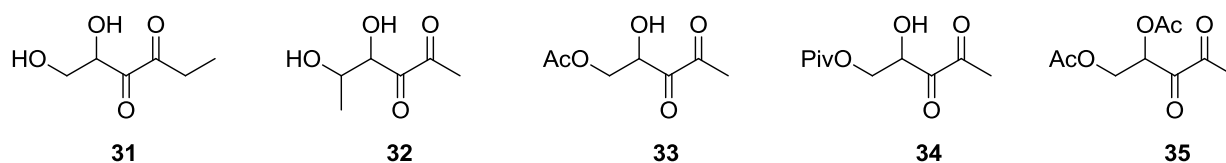
Figure 3.3: DPD analogues synthesized by Frezza *et al.*[247]

A similar approach, where reductive ozonolysis was the key step, was developed in the same year by De Keersmaecker *et al.* Commercially available methyl (*S*)-2,2-dimethyl-1,3-dioxolane-4-carboxylate **S-36** was converted into the corresponding amide **S-37**. Grignard addition with isopropenylmagnesium bromide and further acetal deprotection with an acidic Dowex resin resulted in the isolation of enone **S-39**. Ozonolysis and *in situ* reductive cleavage of the ozonide intermediate with dimethylsulfide, followed by addition of water and evaporation of the volatile byproducts, yielded a solution of *S*-DPD (Scheme 3.6).[252]
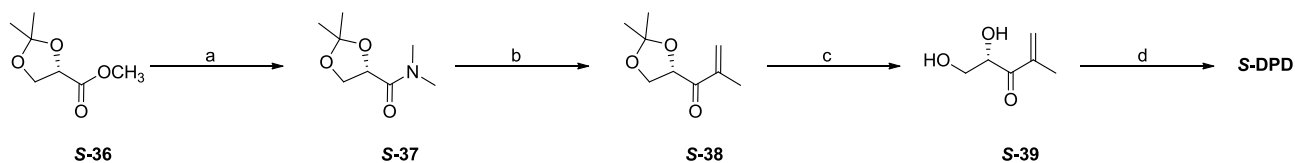
Scheme 3.6: Synthesis of *S*-DPD by De Keersmaecker *et al.* Reagents and conditions: (a) dimethylamine (6.0 eq), EtOH, rt, 2 days (86%); (b) isopropenylmagnesium bromide (0.5 M in THF, 1.4 eq), Et$_2$O, 0 °C, 10 min. (53%); (c) Dowex 50WX8, MeOH, 50 °C, 1.5 h (74%); (d) O$_3$, MeOH, - 78 °C; (d') DMS, - 78 °C to rt[248]

Following Semmelhack *et al.*'s strategy, in 2008, Lowery and coworkers synthesized *S*-DPD and a small set of six DPD-analogues starting from aldehyde *S*-24 which was converted, in one step, to the terminal alkyne *S*-40. Alkylation with *n*-BuLi and the corresponding alkyl iodide (methyl iodide in the case of *S*-DPD) was followed by RuO$_2$*H$_2$O/NaIO$_4$-mediated oxidation and final acidic removal of the protecting group (Scheme 3.7, see also Chapter 5, Scheme 5.1).[249]
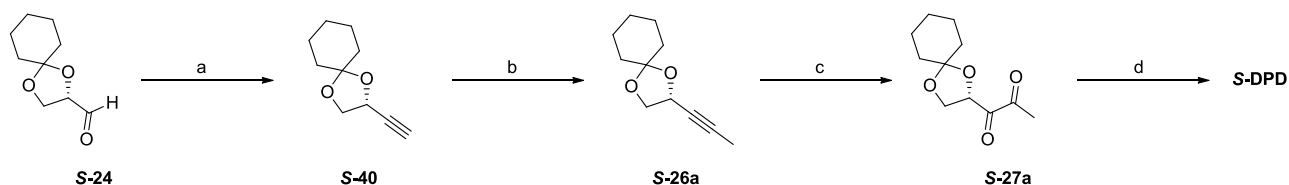
Scheme 3.7: Synthesis of *S*-DPD by Lowery *et al.* Reagents and conditions: (a) DIPA (1.5 eq), *n*-BuLi (1.4 eq), TMSCHN$_2$ (1.6 eq), THF, - 78 °C to rt, 7 h (71%); (b) *n*-BuLi (2.0 eq), MeI (2.0 eq), THF, - 78 °C to rt, 12 h (70%); (c) NaIO$_4$ (2.3 eq), Ru$_2$O*H$_2$O (2.5% mol), CCl$_4$/ACN/H$_2$O (1:1:1.5), rt, 15 min. (70%); (d) D$_2$SO$_4$ (cat.), D$_2$O/d_6-DMSO (4:1), rt, 6 h[249]

In 2009, Smith's group developed a two-pot strategy amenable for the synthesis of both *rac*-DPD and a variety of C$_1$-DPD-analogues (see also Chapter 5, Scheme 5.4). After coupling acyl chlorides (acetyl chloride in the case of *rac*-DPD) with diazomethane, the resulting diazocarbonyls were condensed with aldehyde **28**. TBAF deprotection of the diazo-diol intermediates was followed by oxidation with dimethyl dioxirane to generate *rac*-DPD (and C$_1$-DPD-analogues). The oxidizing agent was chosen to minimize manipulation of sensitive DPD: dioxirane (as well as its byproduct acetone) is volatile and can be easily evaporated (Scheme 3.8).[250]
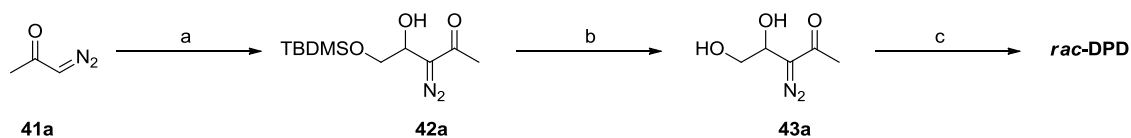
Scheme 3.8: Synthesis of *rac*-DPD by Smith *et al.* Reagents and conditions: (a) **28** (1.0 eq), DBU (20% mol), ACN, rt, 4 h; (b) TBAF (2.0 eq), THF, 0 °C to rt, 1 h (50% over two steps); (c) dimethyl dioxirane in acetone, rt, 2 h[250]

Kadirvel and coworkers developed a new synthesis for both *R*- and *S*-DPD starting from cheap and commercially available D-mannitol which was first protected as an acetal with 2,2-dimethoxypropane. Oxidative cleavage with NaIO$_4$ provided aldehyde *R*-17. Wittig olefination gave a mixture of *E* and *Z* alkenes and OsO$_4$-mediated dihydroxylation of *R*-45 and *R*-46 afforded the diastereoisomeric diols **47/48** and **49/50**, respectively. Oxidation with PCC to isolate diketone *R*-51 and acid-catalyzed deprotection of the acetonide group led to *R*-DPD in 6.3% overall yield (Scheme 3.9A).[251] The same strategy was also applied to the synthesis of *S*-DPD starting from alcohol *S*-16. PCC-mediated oxidation was followed by Wittig olefination. Dihydroxylation of the resulting olefins, oxidation and deprotection provided *S*-DPD (Scheme 3.9B).
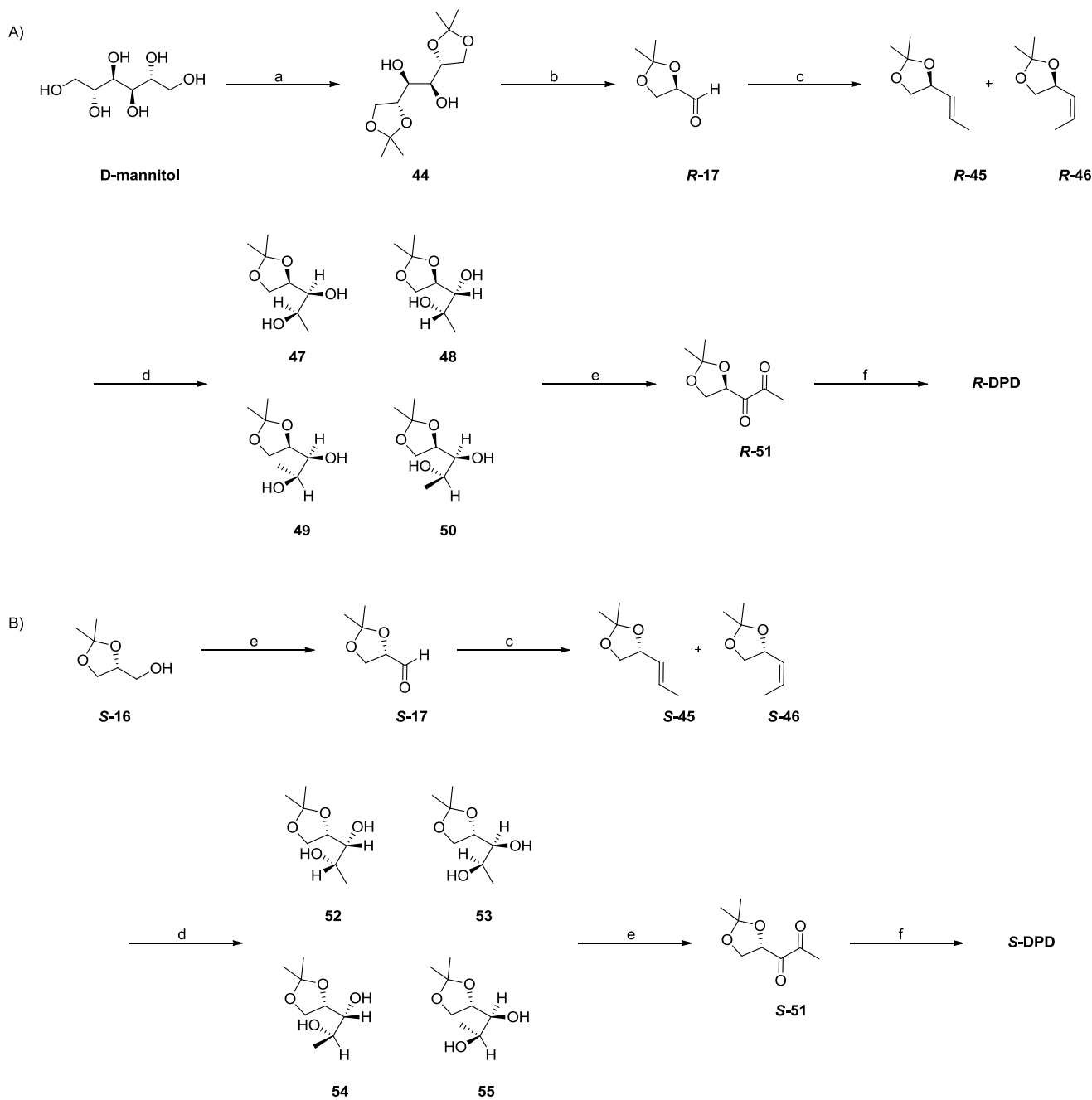
Scheme 3.9: Synthesis of A) *R*-DPD and B) *S*-DPD by Kadirvel and coworkers. Reagents and conditions: a) 2,2-dimethoxypropane (2.1 eq), *p*-TSA (10% mol), DMF, rt, overnight (57%); (b) $NaIO_4$ (2.0 eq), $NaHCO_3$ (sat. solution), DCM, rt, 3 h (75%); (c) *n*-BuLi (1.6 eq), (ethyl)triphenylphosphonium bromide (1.25 eq), THF, - 78 °C, 1 h (70%); (d) NMO (3.25 eq), 4% OsO_4 (5% mol), acetone/H_2O (1:1), rt, overnight (70%); (e) PCC (3.8 eq), DCM, rt, 1 h (30%); (f) D_2SO_4 (cat.), D_2O, rt, 4 h[251]

R-bis-acetyl- and *bis*-benzyl-protected-DPD (**57** and **58**, respectively, Figure 3.4) were also synthesized from alkenes **R-45** and **R-46** by protection, dihydroxylation and PCC-oxidation.[251]
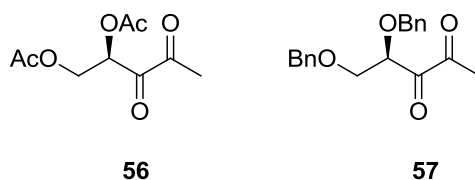
Figure 3.4: *R-bis*-acetyl-DPD **56** and *R-bis*-benzyl-DPD **57** by Kadirvel and coworkers[251]

All the enantioselective syntheses reported so far rely on the use of chiral starting materials. In 2011, Ascenso *et al*. reported a novel synthesis where the chiral center was generated from asymmetric reduction of ketone **62**. The hydroxyl group of methyl glycolate **58** was protected with *t*-butyldiphenylsilyl chloride; saponification of the ester and Weinreb amide formation were followed by incorporation of the acetylenic group using lithiated propyne to generate **62**. Asymmetric reduction with *S*-alpine borane and TBAF-removal of the TBDPS group afforded *S*-**64**. Diol *S*-**64** was protected with a cyclohexyliden group, oxidized with $RuO_2*H_2O/NaIO_4$ and final acidic removal of the protecting group led to the formation of *S*-DPD. The same procedure was also applied to the synthesis of *R*-DPD using *R*-alpine borane as a reducing agent (Scheme 3.10).[252]
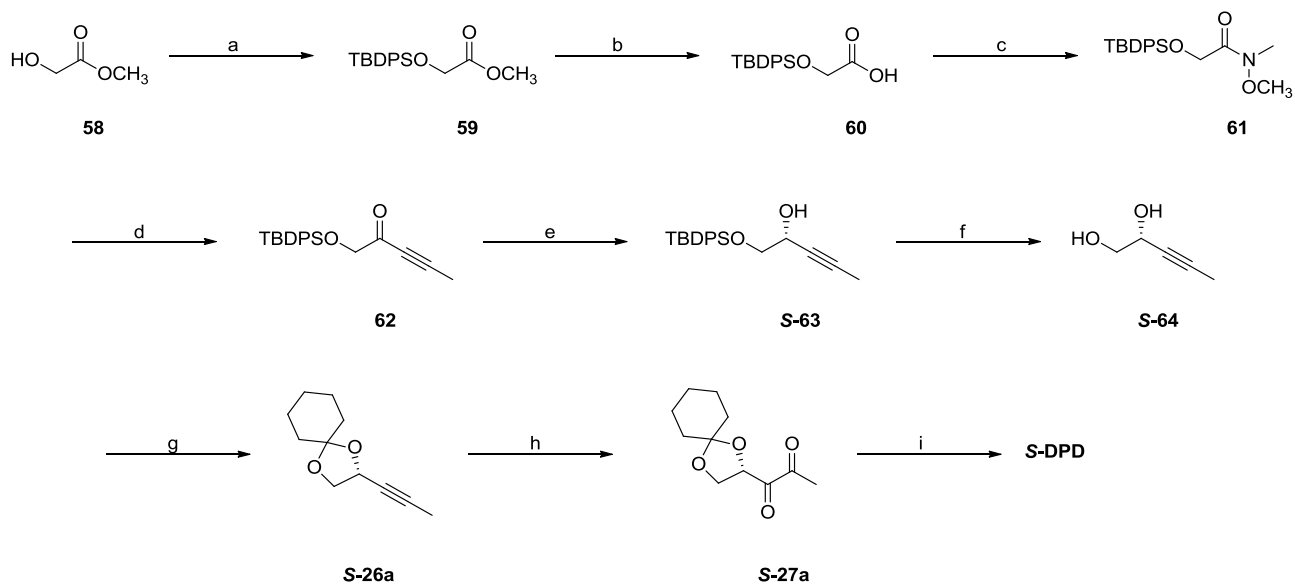
Scheme 3.10: Synthesis of *S*-DPD by Ascenso *et al*. Reagents and conditions: (a) TBDPSCl (1.1 eq), DMAP (cat.), pyridine, 0 °C to rt, overnight (97%); (b) LiOH (2.7 eq), THF/H_2O (4:1), rt (94%); (c) MeNHOMe*HCl (3.0 eq), DCC (3.0 eq), DCM, 40 °C (85%); (d) Propyne (1.45 M in THF, 1.2 eq), *n*-BuLi (1.2 eq), THF, - 78 °C to rt, 1 h; (e) (*S*)-alpine borane (1.5 eq), THF, rt, 2 days (67%); (f) TBAF (1.2 eq), THF, rt, 1 h (86%); (g) 1,1-dimethoxy cyclohexane (2.0 eq), H_2SO_4 (cat.), DMF, rt, overnight (91%); (h) $NaIO_4$ (2.3 eq), Ru_2O*H_2O (2.5% mol), $CCl_4/ACN/H_2O$ (1:1:1.5), rt, (86%); (i) Dowex 50WX8 100-200 mesh, H_2O, rt, overnight[252]

4. SET UP OF A NOVEL SYNTHETIC STRATEGY OF RACEMIC-DPD

As explained in the previous chapters, the goal of my research project was to validate, within the INTEGRATE[229] consortium, the impact of LsrK kinase inhibition on Quorum Sensing. To do so, I designed and synthesized DPD-analogues as potential LsrK kinase inhibitors. Before starting with such plan, I wanted to familiarize myself with the chemistry related to my target and synthesize DPD. The summary of DPD's syntheses described in the previous chapter (i.e., Chapter 3) underlines the difficulties that one would face when trying to synthesize such small, polar and unstable (unless in diluted solutions) molecule. Enantioselective syntheses are demanding as they require chiral and expensive starting materials (e.g., aldehyde *S*-24) as well as purification of most of the intermediates while the synthesis of racemic-DPD proceeds smoothly and it can be performed in only three steps and with a single column chromatography (see Frezza *et al.*[247] and Smith *et al.*[250]). I therefore decided to develop a new synthesis of racemic DPD that does not necessitate reductive ozonolysis (see Frezza *et al.*[247]) or the use of dangerous and explosive diazomethane (see Smith *et al.*[250]) as not all of the laboratories have such equipment or can perform such reactions. The new strategy is short, robust and it requires only one purification step.

Scheme 4. 1: Synthesis of *rac*-DPD (attempt 1). Reagents and conditions: (a) 1-propynylmagnesium bromide (0.5 M in THF, 1.3 eq), THF, 0 °C to rt, 3 h (96%); (b) TBDMSCl (1.2 eq), NaH (2.0 eq), THF, rt, 3 h (90%); (c) NaIO$_4$ (4.4 eq), Ru$_2$O*H$_2$O (2.5% mol), CHCl$_3$/ACN/H$_2$O (1:1:1), rt, 1 h (52%); (d) see Table 4.2

Grignard addition of 1-propynylmagnesium bromide to aldehyde **28** was followed by protection of the resulting secondary alcohol with TBDMSCl. To avoid the use of carcinogenic CCl$_4$, normally employed with RuO$_2$*H$_2$O/NaIO$_4$ oxidation, different oxidative conditions (Table 4.1) were screened and the mixture CHCl$_3$/ACN/H$_2$O (1:1:1) was found to be suitable to be used with the system RuO$_2$*H$_2$O/NaIO$_4$ providing the desired product in 52% yield (Table 4.1, entry 5).

Entry	Solvent	Oxidant and eq	Time	Yield (%)
1	Acetone	KMnO$_4$/NaHCO$_3$/MgSO$_4$ 3.8/0.6/2.0	Overnight	SM
2	Acetone	KMnO$_4$/NaHCO$_3$/MgSO$_4$ 3.9/0.6/4.2	Overnight	Traces
3	CCl$_4$/ACN (1:1)	NaIO$_4$/RuO$_2$*H$_2$O 2.2 eq/2.5% mol	3 h	Traces
4	CCl$_4$/ACN (1:1)	NaIO$_4$/RuO$_2$*H$_2$O 4.4 eq/2.5% mol	3 h	23
5	CHCl$_3$/ACN/H$_2$O (1:1:1)	NaIO$_4$/RuO$_2$*H$_2$O 4.4 eq/2.5% mol	1h	52

Table 4.1: Screening of oxidative conditions. All the reactions were performed at room temperature

Final acidic removal of the two TBDMS groups proved to be challenging and failed after several attempts. Decomposition was observed when H$_2$SO$_4$ (or D$_2$SO$_4$), TBAF or NH$_4$F were employed (Table 4.2, entry 1 – 6) while partial removal of the two protecting groups (up to a maximum of 30% in total) was achieved with the use of acetic acid or Dowex50WX8 (Table 4.2, entry 7 – 9).

Entry	Solvent	Deprotecting agent	Temp (° C)	Time	Result
1	D$_2$O/DMSO-$_{d6}$ (4:1) (10 mM conc.)	D$_2$SO$_4$ (final 5 mM conc.)	Rt	Overnight	Decomposition
2	D$_2$O/DMSO-$_{d6}$ (4:1) (10 mM conc.)	D$_2$SO$_4$ (final 5 mM conc.)	0	Overnight	Decomposition
3	D$_2$O/DMSO-$_{d6}$ (4:1) (10 mM conc.)	H$_2$SO$_4$ (cat.)	0→100	2 days	Decomposition
4	MeOD (10 mM conc.)	D$_2$SO$_4$ (final 5 mM conc.)	Rt	Overnight	Decomposition
5	THF	TBAF (1.1 eq)	Rt	Overnight	Decomposition
6	ACN-d_3 (10 mM conc.)	NH$_4$F (4.0 eq)	Rt	Overnight	SM
7	ACN-d_3/D$_2$O (1:1) (10 mM conc.)	AcOD-d_3 (3.0 eq)	Rt	Overnight	~10 % deprotection
8	MeOD (10 mM conc.)	Dowex 50WX8 100-200 mesh	Rt	Overnight	~30 % deprotection
9	ACN-d_3 (10 mM conc.)	Dowex 50WX8 100-200 mesh	Rt	Overnight	~30 % deprotection

Table 4.2: Screening of the conditions for the acidic removal of the two TBDMS groups of compound **67**

As the bulkiness of the TBDMS group was thought to be the reason that impeded the deprotection, TBDMS was replaced with the smaller TMS group (Scheme 4.2). Unfortunately, the results were similar and a maximum of 40% cleavage (for both the TBDMS and TMS groups) was achieved when Dowex50WX8 and ACN-d_3 were used (data not shown).
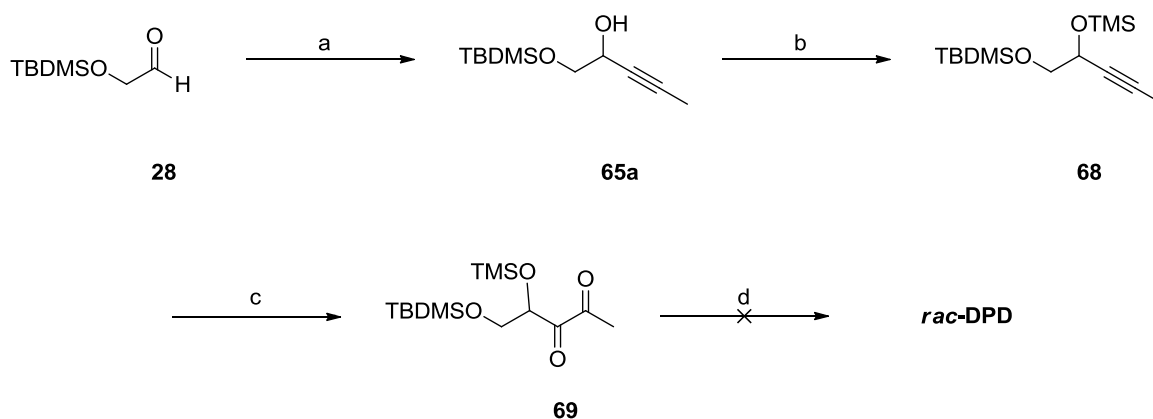
Scheme 4.2: Synthesis of *rac*-DPD (attempt 2). Reagents and conditions: (a) 1-propynylmagnesium bromide (0.5 M in THF, 1.3 eq), THF, 0 °C to rt, 3 h (96%); (b) TMSCl (1.2 eq), NaH (2.0 eq), THF, rt, 3 h (92%); (c) NaIO$_4$ (4.4 eq), Ru$_2$O*H$_2$O (2.5% mol), CHCl$_3$/ACN/H$_2$O (1:1:1), rt, 1 h (65%); (d) Dowex50WX8 100-200 mesh, ACN-d_3 (10 mM), rt, overnight

Since the main goal of my PhD project was to produce DPD-analogues, a synthetic strategy that allowed to generate racemic-DPD and was suitable also for the synthesis of small sets of analogues was planned. Intermediate **65** was deprotected in acidic conditions (Dowex50WX8) and the resulting diol **64a** was protected with a cyclohexyliden group. This two intermediates, slightly modified (see Chapter 6.1), became the two starting points for the synthesis of all the DPD-related compounds prepared during my PhD. Oxidation of **26a** with our previously established protocol (see Table 4.1, entry 5) was followed by Dowex50WX8-mediated removal of the protecting group and the success of the reaction was confirmed by addition of *o*-phenylendiamine to the mixture to produce **Quinoxaline-*rac*-DPD** (Scheme 4.3). ^{1}H NMR was consistent with previously reported data[247] and **Quinoxaline-*rac*-DPD** was also isolated and fully characterized. To prove the validity of such strategy, phenyl-DPD (Ph-DPD) was also synthesized (Scheme 4.3) using phenylethynylmagnesium bromide as Grignard reagent and confirming once again the positive results by comparison of ^{1}H NMR with literature data and by isolation of **Quinoxaline-*rac*-Ph-DPD**.

To sum up, the newly developed approach allows for the rapid production of racemic-DPD in five steps and it does not require (i) the use of dangerous or expensive reagents nor (ii) of particular equipment (i.e., ozonolysator); furthermore, (iii) only one column chromatography is necessary and (iv) it can be employed for the synthesis of Ph-DPD as well as other C$_1$-DPD analogues (as long as the corresponding Grignard reagent can be purchased or produced).
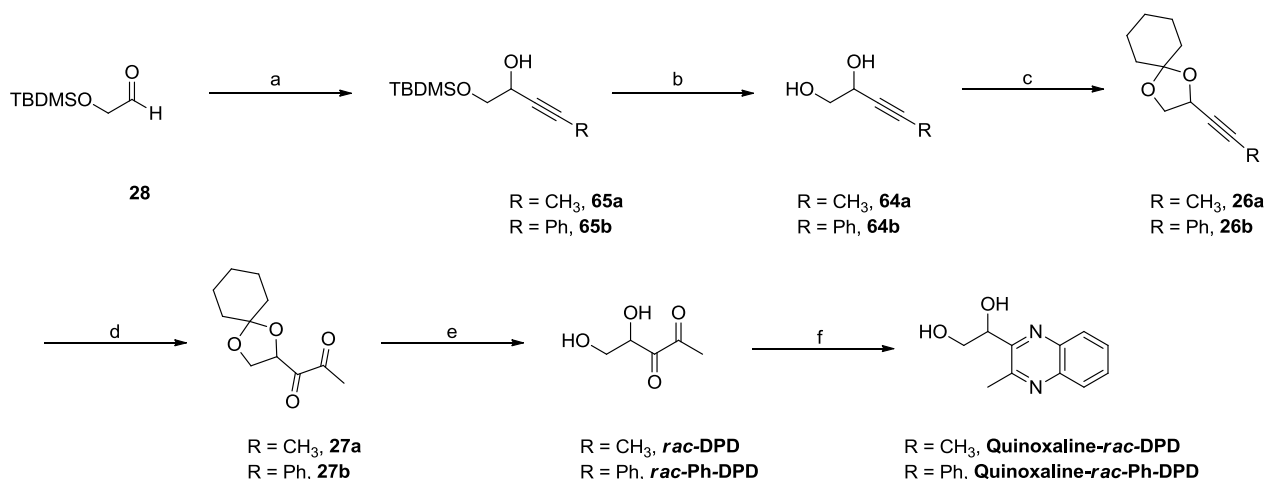
Scheme 4.3: Synthesis of *rac*-DPD (attempt 3) and Ph-DPD. Reagents and conditions: (a) 1-propynylmagnesium bromide (0.5 M in THF, 1.3 eq), THF, 0 °C to rt, 3 h (96%); (b) Dowex50WX8 100-200 mesh, MeOH, rt, overnight (98%); (c) 1,1-dimethoxy cyclohexane (3.0 eq), *p*-TSA (cat.), rt, overnight (84%); (d) NaIO$_4$ (4.4 eq), Ru$_2$O*H$_2$O (2.5% mol), CHCl$_3$/ACN/H$_2$O (1:1:1), rt, 1 h (54%); (e) Dowex50WX8 100-200 mesh, D$_2$O (10 mM), rt, overnight; (f) *o*-phenylendiamine (2.0 eq), rt, overnight

The results described in this chapter have been reported in the manuscript entitled "*A Versatile Strategy for the Synthesis of 4,5-Dihydroxy-2,3-Pentanedione (DPD) and Related Compounds as Potential Modulators of Bacterial Quorum Sensing*" published in *Molecules* on October 6th 2018 (Stotani S. *et al*., Molecules **2018**, *23(10)*, 2545)[253] (see Appendix 1).

4.1 Enzymatic synthesis of DPD

During my four months (March – June 2017) visiting period at the University of Cambridge I've also produced DPD enzymatically following the procedure described in 2002 by Winzer *et al.*[254] The two enzymes necessary (i.e., Pfs and LuxS, see Chapter 1.4.3, Figure 1.7) were cloned in *E. coli* as His$_6$-tagged fusion proteins. Designated primers were employed to amplify both genes by PCR. The purified genes were digested with restriction enzymes NdeI and XhoI and cloned into the pET-19m expression vector to generate the corresponding His$_6$-tagged constructs. The sequences were confirmed by standard sequence analysis (see Chapter 8.3.2). Two flasks (2 x 1000 mL, one for each protein) of LB supplemented with carbenicillin disodium salt (50 mg/mL) and chloramphenicol (34 mg/mL) were inoculated with 1 mL (each) of a 10 mL overnight culture of the *E. coli* expression strain, itself grown in LB with carbenicillin disodium salt (50 mg/mL) and chloramphenicol (34 mg/mL). The cells were grown at 37 °C with good aeration (shaking at 200 rpm) to an approximate OD$_{600}$ of 0.5. The temperature was then lowered to 20 °C and the expression was induced by addition of 1 mM IPTG. Protein expression was continued at 20 °C overnight. The cells were then harvested by centrifugation at 4 °C (14.000x *g*, 30 minutes) and the pellets were resuspended in a total volume of 50 mL of ice-cold lysis buffer (50 mM sodium phosphate, 200 mM NaCl, 10% (v/v) glycerol, pH = 8.0) supplemented with an EDTA-free protease inhibitor cocktail tablet. The bacterial suspensions were lysed by sonication with continuous cooling on ice-water (8 x 30 seconds, 13 A, 1 minute pause between pulses). The cell lysates were clarified by ultracentrifugation at 4 °C (11.000x *g*, 30 minutes) and the clarified supernatants were filtered through a 0.22 μm filter. Affinity chromatography was performed

with Ni-NTA columns (2 mL packed resin bed volume). The filtered lysates were loaded onto the columns and purified in accordance with the manufacturer's instruction. The columns were washed overnight with equilibration buffer (50 mM Tris*HCl, 200 mM NaCl, 10% (v/v) glycerol, 10 mM imidazole, pH = 7.4). The His$_6$-tagged proteins were eluted with elution buffer (50 mM Tris*HCl, 200 mM NaCl, 10% (v/v) glycerol, 250 mM imidazole, pH = 7.4) and dialyzed overnight against 1 liter (each) of dialysis buffer (50 mM Tris*HCl, 100 mM NaCl, 5% (v/v) glycerol, pH = 7.4). The proteins thus released were concentrated (Vivaspin MWCO 10.000, Sartorium) to 180 mg/mL (Pfs, estimated by A$_{280}$ using $\varepsilon_{calc} \sim 10.095$ M^{-1} cm^{-1}) and 59 mg/mL (LuxS, estimated by A$_{280}$ using $\varepsilon_{calc} \sim 24.353$ M^{-1} cm^{-1}). The mixtures were snap-frozen in liquid nitrogen in aliquots of 100 µL and stored at -80 °C. SDS-PAGE confirmed the presence of proteins corresponding to the mass of the pET-19m-Pfs fusion protein (24 kDa) and of the pET-19m-LuxS fusion protein (19 kDa) (Figure 4.1).
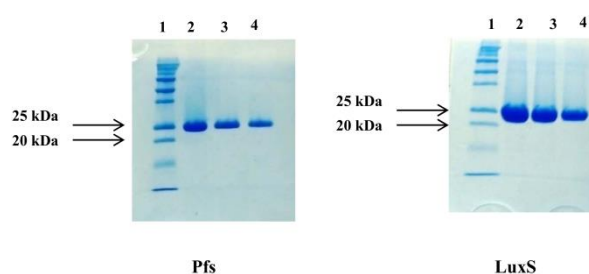
Figure 4.1: Purification of Pfs and LuxS. The figure shows two Coomassie Brilliant Blue G250-stained polyacrylamide gels (12%) run in SDS buffer showing the purification of Pfs and LuxS. Lane 1: protein molecular marker; lane 2: Pfs (or LuxS) eluted from Ni-NTA column (20 µL); lane 3: Pfs (or LuxS) eluted from Ni-NTA column (10 µL); lane 4: Pfs (or LuxS) eluted from Ni-NTA column (5 µL)

Having in my hands the two enzymes, following Winzer *et al*,.[254] 2 mM SAH in 50 mM Tris*HCl buffer pH = 7.8 was incubated at 37 °C with 100 µg/mL of Pfs under nitrogen atmosphere. The reaction was monitored by LC-MS: every 30 minutes, a 5 µL aliquot of reaction mixture was diluted with 1 mL of ACN/MeOH (1:1). The reaction was completed after 30 minutes and was irreversible (Figure 4.2).
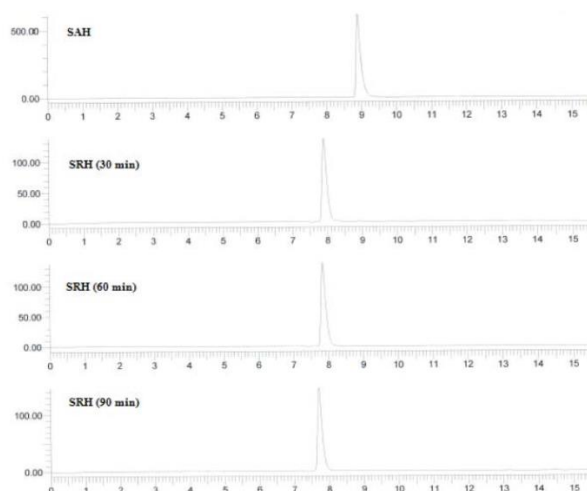
Figure 4.2: SAH conversion to SRH measured after 30, 60 and 90 minutes of incubation at 37 °C with 100 µg/mL of Pfs

Pfs was filtered off and to the resulting mixture was added 500 µg/mL of LuxS. The solution was incubated at 37 °C. Homocysteine production (as a result of DPD formation, see Chapter 1.4.3, Figure 1.7) was measured through the Ellman's reagent. 5,5'-dithiobis-(2-nitrobenzoic acid) (DTNB or Ellman's reagent) reacts with free thiols (in this case, the homocysteine released) to generate 2-nitro-5-thiobenzoate (TNB^-), which ionizes to the TNB^{2-} dianion in water at neutral and alkaline pH. The TNB^{2-} ion has a yellow color and absorbs at 412 nm (Figure 4.3).
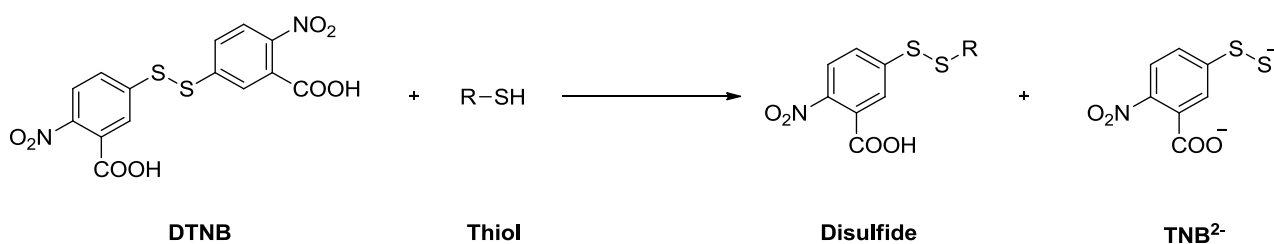
Figure 4.3: Reaction of DTNB with a thiol (R-SH)

The absorbance was measured every 15 minutes incubating at room temperature for 15 minutes 50 µL of reaction mixture with a previously prepared solution containing 500 mL of reaction buffer (0.1 M sodium phosphate, pH = 8.0, containing 1 mM EDTA) and 10 µL of Ellman's reagent solution (containing 4 mg Ellman's Reagent in 1 mL of Reaction Buffer). The reaction was completed in 30 minutes (Figure 4.4) and a decrease in the absorbance was observed over the time, probably due to oxidation of the reaction mixture or time-dependent decomposition.
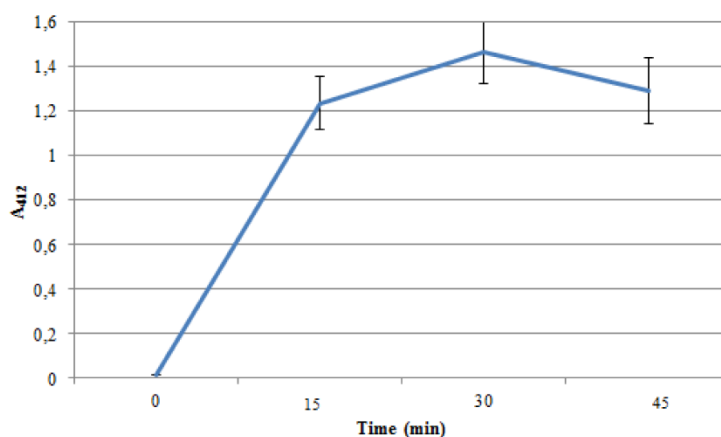
Figure 4.4: Absorbance at 412 nm of homocysteine released during DPD's enzymatic biosynthesis

5. DPD-ANALOGUES AS QS INHIBITORS: STATE OF THE ART

The goal of my PhD project was to assess the relevance of LsrK kinase inhibition in the QS machinery. Studies showed that in LsrK mutants, *lsr* transcription is reduced and, as a result, the production of the Lsr transporter decreases and AI-2 accumulates in the extracellular medium.[223] Potentially, LsrK kinase inhibition would result in lower *lsr* transcription and, therefore, in QS quenching. Since at the time I started my PhD no crystal structure of LsrK was available (and therefore a structure-based design of potential inhibitors was not possible), I decided to follow a ligand-based approach to validate my hypothesis.

Before rationalizing the design of the different sets of molecules, biological data for natural and synthetic DPD-analogues reported in the literature will be herein summarized.

5.1 Natural DPD-analogues

Semmelhack *et al.* tested the ability of six different DPD-related compounds to chelate boron and measured their biological activity in the *V. harveyi* bioluminescence assay (see Chapter 7.1 for additional details).[237] The natural product laurencione (from *Laurencia spectabilis*, Figure 5.1) had an activity 100-fold lower than that of enzymatically prepared *S*-DPD while HMF (Figure 5.1) despite having similar activity, did not show boron complexation. D-ribose and analogues **70** – **72** (Figure 5.1) were not active and only D-ribose and **70** were able to bind boron.
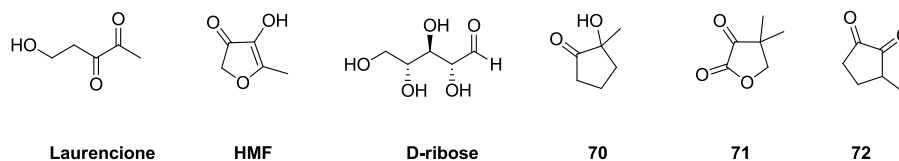
Figure 5.1: Structure of the natural DPD-analogues investigated by Semmelhack *et al.*[237]

Similarly, Lowery and coworkers tested a small panel of natural and non-natural DPD-analogues (Figure 5.2) to better understand the importance of the chelation of boron and the position of the hydroxyl group in the binding to LuxP.[255]
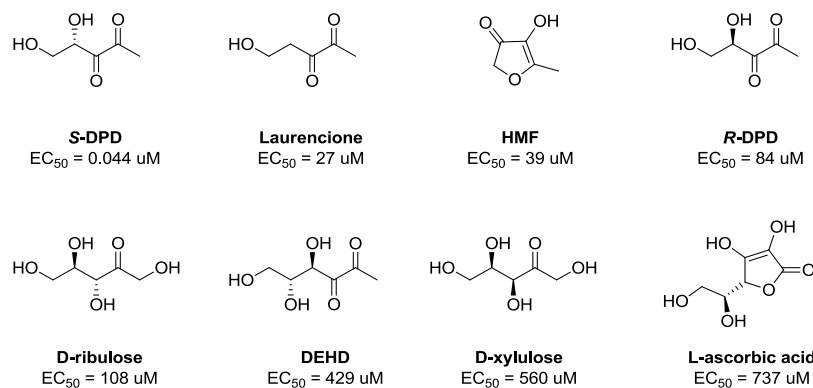
Figure 5.2: Structures and activities of natural and non-natural DPD-analogues reported by Lowery and coworkers[255]

The non-natural enantiomer of DPD (i.e., *R*-DPD, Figure 5.2) displayed only residual QS activity (EC_{50} = 84 µM, ~2000-fold reduction compared to *S*-DPD). Analysis of the LuxP crystal structure (PDB ID: 1JX6)[256] suggested the possible inaccessibility of the OH group for H-bonding due to inversion of the stereochemistry. In a similar manner, laurencione, lacking a hydroxyl group at position 4 (therefore lacking two potential H-bonds), had an activity ~1000-fold less than *S*-DPD (approximately in agreement with Semmelhack's *et al.* results[257]). Extension of the backbone by a hydroxymethyl moiety (DEHD, 1-deoxy-D-erythro-hexo-2,3-diulose, Figure 5.2), resulted also in low QS activity (EC_{50} = 429 µM). All the modifications to the DPD core structure reported by Lowery and coworkers led to lower bioluminescence activities and demonstrated the specificity of LuxP towards *S*-DPD.[255]

5.2 Synthetic DPD-analogues

5.2.1 C_1-modifications

The majority of the work related to the modulation of AI-2-based QS has focused on the synthesis of C_1-substituted DPD-analogues. In 2008, Lowery's research group synthesized six C_1-alkyl/aryl DPD-derivatives and assayed them for QS modulation in *V. harveyi* and *S. typhimurium* (Scheme 5.1 and Table 5.1).[249] The synthesis was based on previously reported routes[231,232] and began with the transformation, in one step, of the known aldehyde **S-24** into the terminal alkyne **S-40** which was then alkylated with *n*-BuLi and six different alkyl iodides. Oxidation and acidic deprotection afforded the desired products **S-73b-g** (Scheme 5.1 and Table 5.1).[249]
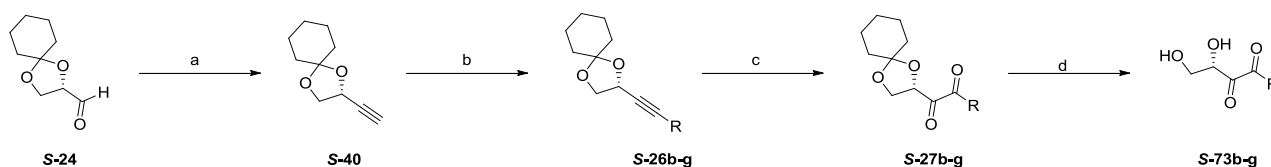
Scheme 5.1: Synthesis of C_1-alkyl/aryl DPD-derivatives **S-73b-g** from Lowery's research group. Reagents and conditions: (a) *n*-BuLi (1.4 eq), TMSCHN$_2$ (2M in hexane, 2.0 eq), DIPA (1.5 eq), THF, - 78 °C to rt, 6 h (71%); (b) *n*-BuLi (2 M in hexane, 2.0 eq), RI (2.0 eq), THF, - 78 °C to rt, 12 h (40% − 75%); (c) RuO$_2$*H$_2$O (2.5% mol), NaIO$_4$ (2.25 eq), ACN/CCl$_4$/H$_2$O (1:1:1.5), rt, 15 min. (36% − 70%); (d) 10 mM, D$_2$SO$_4$ (cat.), DMSO/D$_2$O (1:4), pD = 1.5, 6 h (99%)[249]

Compound	R	IC$_{50}$ in *S. typhimurium* (µM)	Fold-activation in *V. harveyi*
S-**73b**	Ethyl	>50	6.30±0.72
S-**73c**	Propyl	5.30±0.43	7.69±0.30
S-**73d**	Butyl	5.04±0.61	6.05±0.93
S-**73e**	Hexyl	24.9±5.4	2.74±0.24
S-**73f**	Phenyl	>50	1.81±0.12
S-**73g**	Azidobutyl	20.3±1.3	7.44±0.77

Table 5.1: Activities of the C_1-alkyl/aryl DPD-derivatives **S-73b-g** from Lowery's research group[249]

Modulation of bioluminescence was measured with *V. harveyi* MM32. Only ethyl-DPD **S-73b** exhibited weak agonistic activity (data not shown) while for all the compounds of the series a synergistic agonistic activity was observed when they were incubated with *V. harveyi* and 1 μM DPD (Table 5.1). In the presence of DPD, all the analogues enhanced the bioluminescence detected when compared to the bioluminescence of DPD alone (i.e., DPD-enhanced AI-2-induced bioluminescence). In *S. typhimurium*, agonistic (without DPD) and antagonistic (with 50 μM DPD) activity was measured via the β-galactosidase assay (see Chapter 7.1 for additional details). No agonists were detected but all the compounds were found to act as antagonists in the presence of 50 μM DPD without affecting bacterial growth. Propyl-DPD **S-73c** and butyl-DPD **S-73d** were the most potent inhibitors, with IC$_{50}$ values of 5.30 μM and 5.04 μM, respectively.[249] Similar results were obtained in 2009 by Ganin and coworkers.[258] The group measured the bioluminescence of a series of C$_1$-alkylated DPD-analogues (ranging from ethyl to heptyl, **S-73b-e**, **S-73h-i**, Scheme 5.2 and Table 5.2) and observed a synergistic activity which decreased as the length of the alkyl chain increased. The synthesis followed again previously reported strategies[231,232] but this time the terminal alkyne **S-40** was obtained in two steps by Corey-Fuchs homologation of aldehyde **S-24**. Alkylation according to Shintani *et al.*[259] and further oxidation and deprotection yielded the six analogues **S-73b-e**, **S-73h-i** (Scheme 5.2 and Table 5.2).
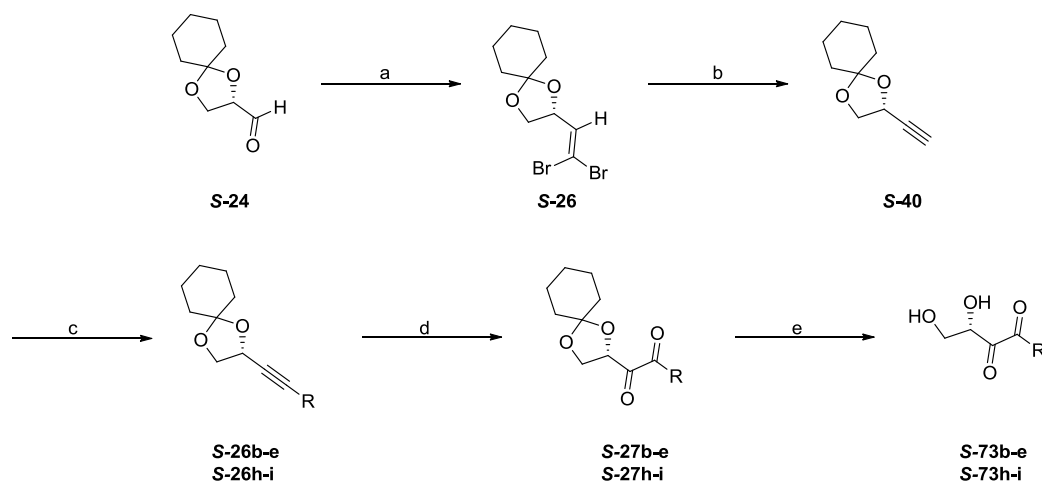
Scheme 5.2: Synthesis of the C$_1$-alkyl DPD-derivatives **S-73b-e**, **S-73h-i** from Ganin and coworkers. Reagents and conditions: (a) PPh$_3$, CBr$_4$, DCM (40%); (b) *n*-BuLi, - 78 °C to rt, 1.5 h, H$_2$O (67%); (c) *n*-BuLi, RI, - 78 °C to − 55 °C to 50 °C, 19 h (51% − 83%); (d) RuO$_2$*H$_2$O (2.5% mol), NaIO$_4$ (2.3 eq), ACN/CCl$_4$/H$_2$O (1:1:1.5), rt, 30 min. (25% − 70%); (e) 10 mM, H$_2$SO4 (cat.), H$_2$O, rt, 24 h[258]

Since the compounds displayed an agonistic effect only when DPD was present, the authors hypothesized (i) a possible binding with an allosteric site on LuxP or (ii) the interaction with another protein responsible for an increment in the synthesis of DPD or a reduction of its degradation (or both). Notably, butyl- and pentyl-DPD (**S-73d** and **S-73h**) reduced the production of pyocyanin, a virulence factor in *P. aeruginosa*, most likely by interfering with the LasR system.[258]

Compound	R	EC_{50} in *V. harveyi* BB170 (µM)
S-73b	Ethyl	0.58±0.24
S-73c	Propyl	0.75±0.23
S-73d	Butyl	1.01±0.37
S-73h	Pentyl	1.35±0.24
S-73e	Hexyl	1.52±0.30
S-73i	Heptyl	1.81±0.86

Table 5.2: Activities of the C_1-alkyl DPD-derivatives *S*-73b-e, *S*-73h-i from Ganin and coworkers[28]

A naphthalenyl group was installed at C_1 by Mandabi and coworkers.[260] The Bestmann-Ohira reagent was employed to convert aldehyde *S*-24 to alkyne *S*-40 under mild conditions. Since alkylation with *n*-BuLi and bromethylnaphthalene failed, a Sonogashira coupling using $PdCl_2(CH_3CN)_2$ and Sphos was performed, providing the desired alkylated product *S*-27j in moderate yield (44%). Further oxidation with $RuO_2/NaIO_4$ and acidic removal of the protecting group afforded naphthalenyl-DPD *S*-73j which was used to measure *V. harveyi* bioluminescence (Scheme 5.3).
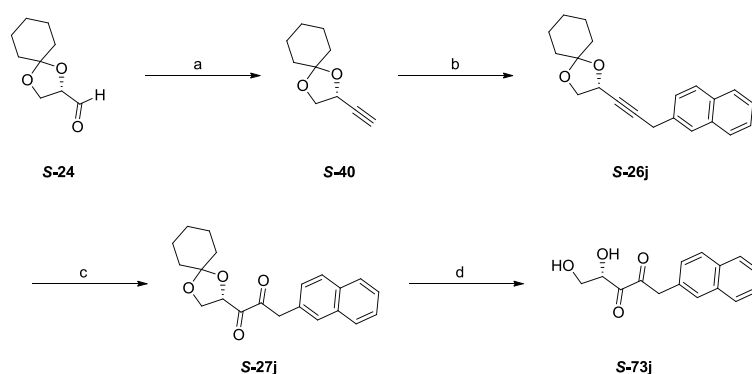
Scheme 5.3: Synthesis of naphthalenyl-DPD *S*-73j by Mandabi and coworkers. Reagents and conditions: (a) Bestmann-Ohira reagent (1.5 eq), K_2CO_3 (1.5 eq), MeOH, rt, overnight (77%); (b) $PdCl_2(CH_3CN)_2$ (5% mol), Sphos (10% mol), 2-(bromomethyl)naphthalene (0.7 eq), THF, 66 °C, 24 h (44%); (c) RuO_2*H_2O (2.5% mol), $NaIO_4$ (5.1 eq), ACN/CCl_4/H_2O (1:1:1.5), rt, 2 h (17% − 22%); (d) H_2SO_4, pH = 1.5, rt, 24 h (100%)[260]

In *V. harveyi* BB120, a dose-dependent increase in QS activity was observed. When *S*-73j was tested in *V. harveyi* MM32, no QS response was measured in the absence of DPD while, upon addition of 200 nM DPD, a synergistic (dose-dependent) activation was observed. To explain the synergism, the authors hypothesized the binding of naphthalenyl-DPD to one LuxPQ moiety and the binding of DPD to the other domain. This new hybrid structure would then be responsible for conformational changes able to speed up LuxQ dimerization and activate QS.[260]

No agonistic activity was measured by Smith *et al.* in a series of linear, branched, cyclic and deoxy C_1-DPD-analogues (*rac*-74b-z, Scheme 5.4, Table 5.3 and Figure 5.3).[261–263]
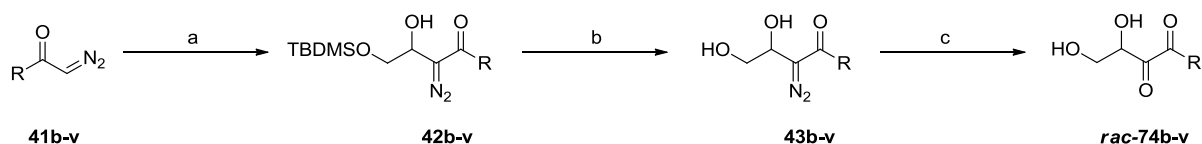
Scheme 5.4: Synthesis of C$_1$- linear, branched and cyclic DPD-analogues **rac-74b-v** reported by Smith *et al.* Reagents and conditions: (a) **28** (1.0 – 1.5 eq), DBU (0.16 – 0.20 eq), ACN, rt, 4 – 8 h; (b) TBAF (1.0 – 2.0 eq), THF, 0 °C to rt, 1 – 3 h (20% – 52%, over two steps); (c) dioxirane, acetone, rt, 1 – 2 h.[261–263]

The compounds were synthesized following a two-pot strategy where the appropriate diazocarbonyl was condensed with aldehyde **28** in the presence of DBU. The resulting products were directly deprotected using TBAF in THF to give the corresponding diols after column chromatography. Due to the difficulty in purifying DPD, oxirane was chosen as oxidating agent because it is volatile and the sole byproduct of the reaction is acetone (Scheme 5.4). Compounds **rac-74b-d,h,l,m,p** were not able to induce bioluminescence in *V. harveyi* on their own but, when tested together with DPD, all of them enhanced AI-2-mediated bioluminescence. Since no trend could be observed based on the size/shape of the analogues and their activity, the authors suggested promiscuity in the receptors that mediate the synergistic agonism.[261]

Compounds **rac-74b-k**, **rac-74w-z** were tested in *E. coli* and *S. typhimurium* to evaluate their ability to modulate QS. None of the compounds, except **rac-74b**, increased *lsr* expression (agonistic activity). All the linear analogues with at least three carbons (**rac-74c-g**, Table 5.3) acted as antagonists in *E. coli* while only **rac-74d** reduced *lsr* expression in *S. typhimurium*. Among the non-linear analogues, **rac-74h-i**, **rac-74k** knocked down *lsr* expression only in *E. coli* while **rac-74j** in both the bacterial species being the first effective cross-species QS inhibitor reported. Based on these results, the authors concluded that the QS machinery of *E. coli* is promiscuous because it can be silenced by DPD-analogues having different sizes and shapes while the *S. typhimurium* QS circuitry appears to be more specific. In the same paper, the promiscuity of LsrK was also demonstrated: all the compounds, although to a different extent, were phosphorylated, except analogues **rac-74w-z** (Figure 5.3), lacking the primary hydroxyl moiety that is phosphorylated by LsrK.[222] (Note that for the synthesis of the deoxy analogues, instead of aldehyde **28** acetaldehyde was used and no TBAF-mediated deprotection of the TBDMS moiety was necessary).[262]

Phosphorylation was proved to be essential for the analogues to act either as agonists or antagonists (**rac-74b-d** did not affect QS in an LsrK knockout strain) but not the only criterion: despite being phosphorylated, **rac-74m** did not repress *lsr* expression; on the other hand, **rac-74f**, which was less phosphorylated than **rac-74m**, repressed *lsr* expression to a higher extent.[262]

Compound	R	Ref.
rac-**74b**	Ethyl	[261,262]
rac-**74c**	Propyl	[261,262]
rac-**74d**	Butyl	[261,262]
rac-**74e**	Pentyl	[262]
rac-**74f**	Hexyl	[262]
rac-**74g**	Septyl	[262]
rac-**74h**	Isopropyl	[261,262]
rac-**74i**	Neopentyl	[262]
rac-**74j**	Isobutyl	[262]
rac-**74k**	*Sec*-butyl	[262]
rac-**74l**	*Tert*-butyl	[261]
rac-**74m**	Cyclopropyl	[261–263]
rac-**74n**	Cyclobutyl	[263]
rac-**74o**	Cyclopentyl	[263]
rac-**74p**	Cyclohexyl	[261,263]
rac-**74q**	CH_2-cyclohexyl	[263]
rac-**74r**	Cycloheptyl	[263]
rac-**74s**	Furanyl	[263]
rac-**74t**	Phenyl	[263]
rac-**74u**	*p*-Fluorophenyl	[263]
rac-**74v**	*p*-Nitrophenyl	[263]

Table 5.3: Structures of C_1-linear, branched and cyclic DPD-analogues *rac*-**74b-v** reported by Smith *et al.*[261–263]

In order to better understand the promiscuity/specificity of the QS proteins, the research group expanded the set of C_1-DPD-analogues including four new cyclic analogues (*rac*-**74n-o**, *rac*-**74q-r**, Table 5.3) and four aromatic (*rac*-**74s-v**, Table 5.3) C_1-DPD-derivatives. The compounds were assayed in *E. coli* and *S. typhimurium* to evaluate their ability to modulate QS. None of them had agonistic activity in both bacterial species. Different results were obtained when 20 μM DPD was added to the culture: in *E. coli* all the cyclic analogues (except *rac*-**74m**) reduced *lsr* expression while in *S. typhimurium* *rac*-**74o** and *rac*-**74p** acted as synergistic agonists increasing *lsr* expression (for all the other cyclic compounds no significant variation in *lsr* expression was observed when compared with DPD alone).[263]

Deoxy-methyl-DPD, *rac*-**74w**   Deoxy-isobutyl-DPD, *rac*-**74z**
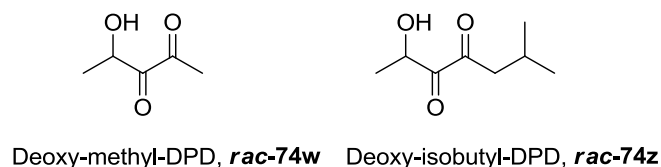
Figure 5.3: C_1-deoxy-DPD-analogues *rac*-**74w-z** reported by Smith and coworkers[262]

Minimal or no effects were measured with the aromatic compounds (*rac*-**74s-v**, Table 5.3) with the exception of *rac*-**74v** that acted as agonist in *S. typhimurium*. LsrK-mediated phosphorylation was measured for all the analogues: cyclic compounds with more than five carbons (*rac*-**74p-r**, Table 5.3) as well as the aromatic analogues were weakly or not phosphorylated displaying minimal or no attenuation of *lsr* expression.[263]

Using a Baylis-Hillman/ozonolysis approach (see Chapter 3, Scheme 3.5), Frezza *et al.* synthesized CF_3-DPD both as a racemic mixture (*rac*-**83**, Scheme 5.5 A) and as *S*-**83** (Schemes 5.5 A and 5.5 B). The Baylis-Hillmann condensation of aldehyde **28** with 1,1,1,3,3,3,-hexafluoroisopropyl acrylate **75** in the presence of DABCO afforded a mixture of **76** and **77** which was further converted into the corresponding α-methylene β-hydroxy ester **78**. Acetal protection followed by treatment with trifluoromethyltrimethylsilane (TMSCF$_3$) and acetal deprotection resulted in the hemiketal **82**. Reductive ozonolysis generated *rac*-CF$_3$-DPD *rac*-**83** (Scheme 5.5 A). The same synthetic approach was applied to produce *S*-**83** with the asymmetric Baylis-Hillmann step performed using the acrylamide *R*-**84**[264] derived from the Oppolzer sultam (Scheme 5.5 B).[265]
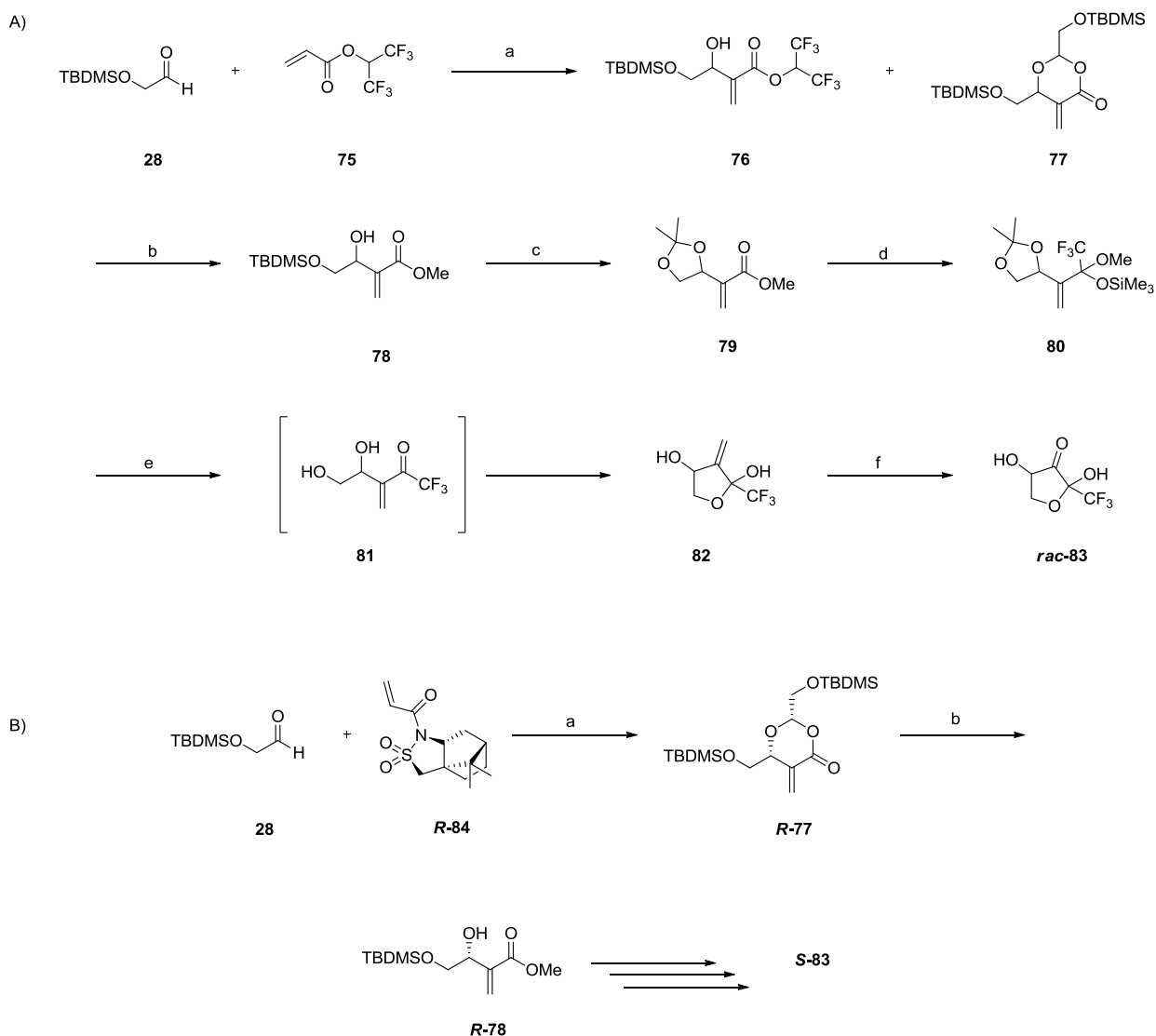
Scheme 5.5: Synthesis of A) *rac*-CF$_3$-DPD *rac*-**83** and B) *S*-CF$_3$-DPD *S*-**83** by Frezza *et al.* Reagents and conditions: (a) **28** (2.0 eq), DABCO (0.25 eq), THF, 0 °C, 2 h, (b) Et$_3$N (2.8 eq), MeOH, rt, 2 h (84%); (c) camphorsulfonic acid (cat.), MeOH, rt, 25 min then 2,2-dimethoxypropane, rt, 1 h (78%); (d) TMSCF$_3$ (1.5 eq), CsF (2.9% mol), rt, 26 h; (e) 3M HCl, THF, rt, 18 h; (f) O$_3$, MeOD, - 78 °C then DMS (10.0 eq), rt, 24 h[265]

Due to the strong electronegativity of the CF$_3$ moiety, *S*-**83** exists only in its hemiketal (hydrated at C$_3$) form *S*-**86** and, as the majority of the C$_1$-DPD-analogues, it could not be isolated because of its instability. The activity of the crude mixture was evaluated in the *V. harveyi* bioluminescence assay. *S*-**87** was found to act as a weak agonist being 10-fold less active than *rac*-DPD with an IC$_{50}$ value of ~ 30 μM (IC$_{50}$ for *rac*-DPD ~ 3 μM, Figure 5.4).[265]
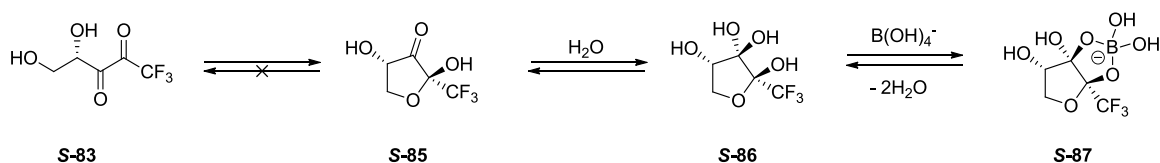
Figure 5.4: Structures of *S*-CF$_3$-DPD *S*-**83** synthesized by Frezza *et al.*[265]

5.2.2 C₃-modifications

The majority of the modifications to DPD structure have focused on the synthesis of C_1-analogues. So far, the carbonyl group at position C_2 has never been substituted while there's only a paper about the replacement of the ketone at C_3 with geminal di-halogens. In 2013, the transcriptional regulator LsrR was co-crystallized with P-DPD (see Chapter 1, Figure 1.6, PDB ID: 4L4Z[133]). Therefore, in 2015, Guo *et al.* rationalized the insertion of di-halogens at position C_3 as isosteric replacement of the 3-hydrated moiety of DPD, postulating the possible formation of halogen bonds.

Since the synthesis of the di-halogens-DPD-analogues was hampered by the volatility of the final products, the corresponding butyl esters **rac-91a-f** were isolated (Schemes 5.6 A and 5.6 B). Grignard addition to chlorodifluoroacetic acid **88** was followed by zinc-catalyzed condensation of the resulting intermediate with previously prepared **90** to afford products **rac-91a-b** (Scheme 5.6 A). The remaining four analogues **rac-91c-f** were produced in one step by condensation of **93** with the corresponding di-halogenated ketones **92c-f** (Scheme 5.7 B).
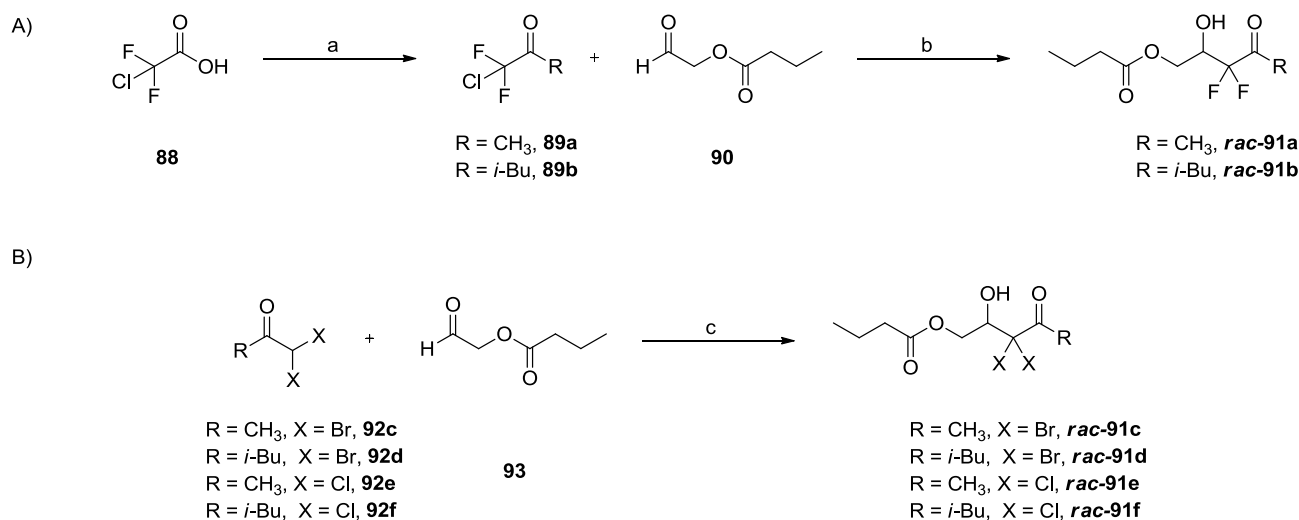
Scheme 5.6: Synthesis of A) geminal di-halogens **rac-91a-b** and B) **rac-91c-f** from Guo *et al.* Reagents and conditions: (a) RMgBr (2M in Et₂O), Et₂O, - 20 °C, 12 h; (b) **93**, Zn⁰ (3.0 eq), CuI (10% mol), THF, 60 °C to rt, 4 h (**rac-91a**, 35%; **rac-91b**, 67%); (c) **93** (1.0 eq), *t*-BuOK (10% mol), THF, - 78 °C to rt, overnight (**rac-91c**, 61%; **rac-91d**, 40%; **rac-91e**, 64%; **rac-91f**, 61%)[266]

The six compounds were evaluated in the β-galactosidase assay in *E. coli*. None of them resulted toxic at 100 µM concentration and both **rac-91c** and **rac-91e** induced transcription of β-*gal*. As previously observed by Roy *et al.*[267], compounds with at least three carbons at position C_1 act as antagonists. In accordance, the isobutyl di-bromo **rac-91d** and di-chloro **rac-91f** derivatives were found to be antagonists of LsrR. The lack of activity (both as agonists and as antagonists) of the two di-fluoro analogues **rac-91a** and **rac-91b** was explained with the smaller size of the two fluorine atoms compared to the two hydroxyl groups (steric effect) and with the higher electron-withdrawing nature of the fluorine which could result in hydration at position C_2 (electronic effect).[266]

5.2.3 C$_4$-modifications

Fluorine is often used as an isosteric and isoelectronic replacement for a hydroxyl group. In 2014, Kadirvel and coworkers measured the effect of *rac*-4-fluoro-DPD **rac-99** on *V. harveyi*'s bioluminescence and biofilm formation. The synthesis of **rac-99** started with the benzylation of glycidol followed by organolithium-mediated ring opening and alkylation of the resulting terminal alkyne. Intermediate **96** was fluorinated with Xtal-Fluor-E and the F-alkyne was oxidized using RuO$_2$*H$_2$O. Ultimately, the benzyl group was removed to afford **rac-99** (Scheme 5.7). At 12.5 μM concentration, **rac-99** completely inhibited *V. harveyi* BB170's bioluminescence and biofilm formation was reduced by over 90% at 200 μM.[268]
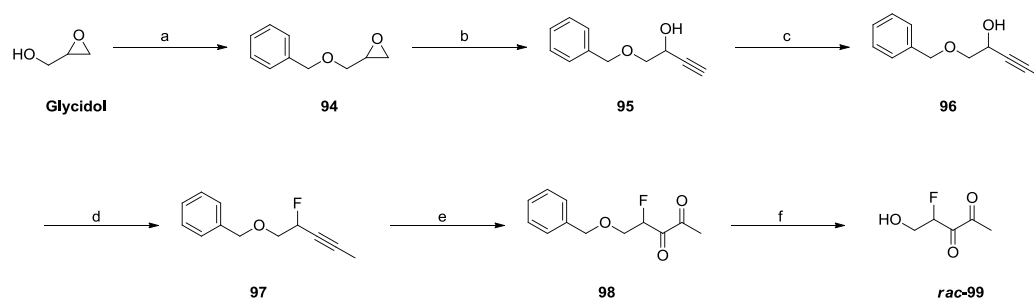
Scheme 5.7: Synthesis of *rac*-4-fluoro-DPD **rac-99** by Kadirvel and coworkers. Reagents and conditions: (a) NaH (1.5 eq), BnBr (1.3 eq), DMF, 0 °C to rt, 48 h (70%); (b) lithium acetylide ethylendiamine complex (90%) (1.5 eq), DMSO, 0 °C to rt, overnight (68%); (c) *t*-BuOK (4.0 eq), DMSO, rt, 1 h (64%); (d) Et$_3$N*3HF (2.2 eq), Xtal-Fluor-E (2.0 eq), Et$_3$N (1.0 eq), DCM, - 72 °C to rt, 3 h (73%); (e) NaIO$_4$ (2.3 eq), RuO$_2$*H$_2$O (1.4% mol), ACN/CCl$_4$/H$_2$O (1:1:1.5), rt, 15 min. (71%); (e) DDQ (2.0 eq), DCM/H$_2$O (10:1), rt, 3 h (40%)[268]

All the examples reported so far have underlined how minimal structural changes in DPD's structure can significantly impact QS-mediated processes. An interesting finding is the discovery, in 2012, of two QS agonists (out of five compounds synthesized) 10-fold more potent than DPD in *V. harveyi*.[269] The small set of molecules was generated upon protection of the hydroxyl group at position C$_4$. Starting from the readily available 1-((*t*-butyldimethylsilyl)oxy)pen-3-yn-2-ol **65**[270] (see Chapter 4, Scheme 4.1 for its synthesis), five different alkyl groups were installed at C$_4$ under standard conditions (Scheme 5.7). Further ruthenium-catalyzed oxidation and acidic deprotection afforded the desired C$_4$-alkoxy-5-hydroxy-2,3-pentanediones (C$_4$-alkoxy-HDPs, **rac-102a-e**, Scheme 5.8 and Table 5.4).[269]
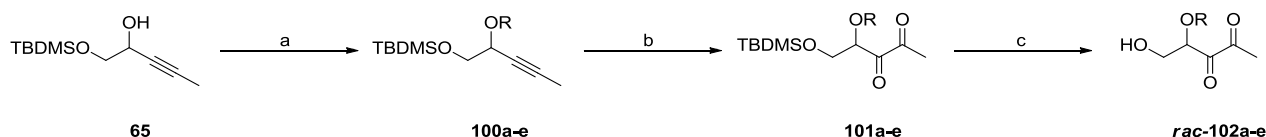
Scheme 5.8: Synthesis of C$_4$-alkoxy-HDPs **rac-102a-e** from Tsuchikama *et al*. Reagents and conditions: (a) NaH (1.2 eq), RBr (or RI) (1.5 eq), THF, 0 °C to rt, 4 h (18% − 68%); (b) NaIO$_4$ (2.25 eq), RuO$_2$*H$_2$O (2.5% mol), ACN/CCl$_4$/H$_2$O (1:1:1), rt, 20 min. (25% − 67%); (c) D$_2$SO$_4$ (5 mM), DMSO-d_6/D$_2$O (1:4), rt, overnight[269]

The analogues were tested in *V. harveyi* MM32 and *S. typhimurium* strain Met844. In *V. harveyi* the activity was dependent on the length of the alkyl chain: C_4-HexO-HDP *rac*-**102d** and C_4-BnO-HDP *rac*-**102e** showed weak or no bioluminescence induction while C_4-MeO-HDP *rac*-**102a** displayed moderate activity and C_4-EtO-HDP *rac*-**102b** and C_4-PrO-HDP *rac*-**102c** were better ligands than *S*-DPD. Remarkably, *rac*-**102c** had an EC_{50} almost 10-fold lower than the natural ligand *S*-DPD (EC_{50} *rac*-**102c** = 0.15±0.03 µM and EC_{50} *S*-DPD = 1.07±0.06 µM, Table 5.4). Since the cyclic form is the one that complexes borate to generate *S*-THMF-borate, the active specie in *V. harveyi*, a possible explanation to this phenomenon can be the higher ratio of linear/cyclic form (~ 10:90) for the five analogues when compared to *S*-DPD (ratio of linear/cyclic 10:80). Additionally, LuxP can have an allosteric site where analogue *rac*-**102c** can access while the bulkier derivatives *rac*-**102d** and *rac*-**102e** can't. In *S. typhimurium* none of the compounds was found to act as agonist neither as antagonist. In enteric bacteria, P-DPD is the active form recognized by LsrR. The lack of activity can be attributed to the absence of LsrK-mediated phosphorylation for all the analogues suggesting that the hydroxyl group at position C_4 should be free to allow phosphorylation.[269]
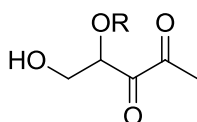
Compound	R	β-galactosidase activity in *S. typhimurium* strain Met844 (µM)	EC_{50} in *V. harveyi* MM32 (µM)
S-DPD		100±2.9	1.07±0.06
rac-**102a**	Methyl	<5	7.60±0.45
rac-**102b**	Ethyl	<5	0.79±0.05
rac-**102c**	Propyl	<5	0.15±0.03
rac-**102d**	Hexyl	<5	Not determined
rac-**102e**	Benzyl	<5	Not determined

Table 5.4: Activities of the C_4-alkoxy-HDPs *rac*-**102a-e** from Tsuchikama *et al*.[269]

As already explained, the main problem that one would face when synthesizing DPD-analogues is related to their instability. To overcome this issue, in 2007 Frezza and coworkers prepared the *bis*-acetate protected version of DPD (Ac_2-DPD) believing that, after *in situ* hydrolysis of the two esters, it would have the same activity as DPD.[271] Ac_2-DPD was synthesized both as a racemic mixture *rac*-**107** and as enantiopure *S*-**107**. *rac*-**107** was prepared following the methodology previously reported by the group (see Chapter 3, Scheme 3.5)[247]: acetylation of the Baylis-Hillmann product **105** and subsequent ozonolysis (Scheme 5.9 A). *S*-**107** was instead produced using De Keersmaecker *et al.*'s methodology starting from the dihydroxy enone *S*-**39** (see Chapter 3, Scheme 3.6) which was first acetylated and then subjected to ozonolysis (Scheme5.9 B).[248] When tested in *V. harveyi*, both *rac*-**107** and *S*-**107** induced the same activity as *rac*-**DPD** and *S*-**DPD** with IC_{50} values of 2.1 µM, 2.6 µM, 2.6 µM and 3.3 µM, respectively. Similar effects were observed in *S.*

typhimurium, where **S-107** strongly induced β-galactosidase production and in the Gram-positive bacterium *B. cereus* where it inhibited biofilm formation.[271]

A)

B)
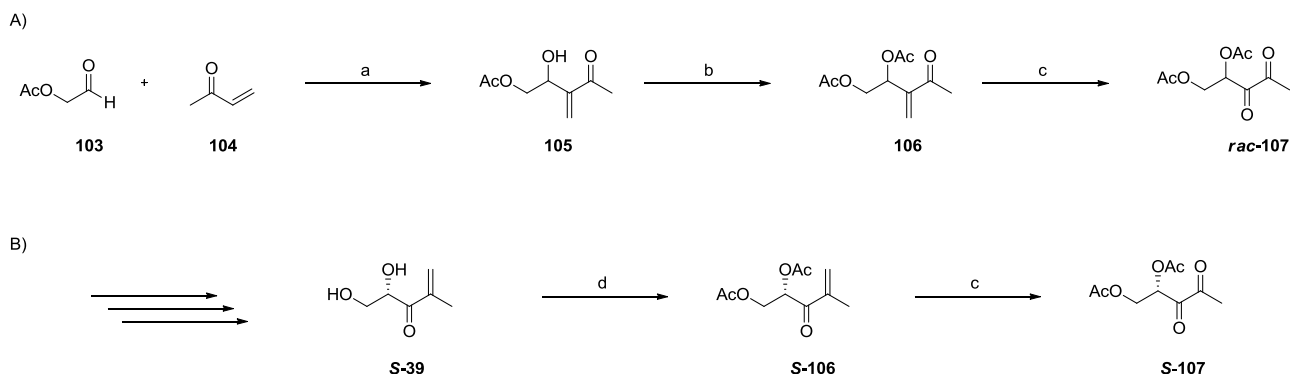
Scheme 5.9: Synthesis of A) **rac-107** and B) **S-107** by Frezza *et al.* Reagents and conditions: (a) **104** (4.0 eq), DABCO (0.25 eq), THF, 0 °C, 20 h (87%); (b) Ac$_2$O (2.5 eq), DMAP (1.0 eq), DCM, rt, 2 h, (70%); (c) O$_3$, MeOH, - 78 °C then DMS (10.0 eq), - 78 °C to rt, 24 h; (**rac-107**, 55%; **S-107**, 87%) (d) Ac$_2$O (5.0 eq), pyridine (2.2 eq), Et$_3$N (0.1 eq), DCM, 0 °C, 18 h (90%)[271]

Since ester protection of DPD proved to increase its stability while retaining its activity after *in situ* hydrolysis of the protecting groups, Guo and coworkers synthesized a series of *bis*-ester-protected analogues of DPD and measured their activity in *E. coli* and *S. typhimurium*.[272] Protection as esters (methyl, propyl, butyl, pentyl) of the corresponding methyl-, hexyl- and isobutyl-diazocarbonyls **43a,e,j** (produced as in Scheme 5.4) was followed by oxidation of the diazo *bis*-esters **108a-l** to afford the targeted compounds **rac-109a-l** (Scheme 5.10). In *E. coli* all the analogues were found to act as agonists, while in *S. thypimurium* only *bis*-butyl-DPD **rac-109c** was as good as DPD in activating *lsr* expression. When measuring antagonistic activity, in *E coli* both the *bis*-methyl and the *bis*-propyl esters of isobutyl (**rac-109e** and **rac-109f**, respectively) and hexyl DPD (**rac-109i** and **rac-109j**, respectively) were QS inhibitors but the inhibitory activity decreased/disappeared as the length of the ester chain increased (*bis*-butyl and *bis*-pentyl esters of isobutyl (**rac-109g** and **rac-109h**, respectively) and hexyl (**rac-109k** and **rac-109l**, respectively) DPD were slightly/not active).
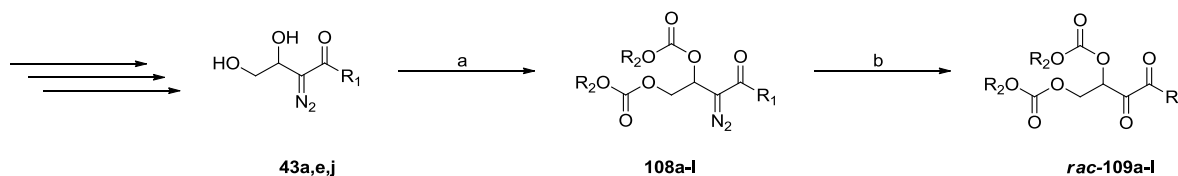
Scheme 5.10: Synthesis of *bis*-ester-protected DPD-analogues **rac-109a-l** by Guo and coworkers. Reagents and conditions: (a) (R$_1$CO)$_2$O (2 – 3 eq), DCM, rt, 2– 3 h; b) dimethyldioxirane (in acetone), acetone, rt, 1 h – 2h[272]

In *S. typhimurium* instead none the analogues acted as QS antagonists. Despite having similar QS systems and despite the fact that *rac*-isobutyl-DPD **rac-74j** reduces *lsr* expression in both *E. coli* and *S. typhimurium*,[267] the lack of activity of all the protected versions of isobutyl-DPD in the latter can allow for selective QS modulation within the two species. The reason for such selectivity remains unknown, perhaps

the analogues can permeate the bacterial cell wall in a different rate or the esterases responsible for the *in situ* hydrolysis of the protecting groups can have different sensitivity.[272]

5.2.4 C₅-modifications

As already underlined in paragraph 5.1, the stereochemistry at position C_4 of DPD seems to play an important role in determining its activity.[255] To further confirm the importance of the *S*-sterochemistry, in 2012 Rui *et al.* introduced a second stereocenter at C_5 generating four diastereoisomeric analogues of DPD (Figure 5.5).[273]

(4*S*, 5*S*)-**110**   (4*R*, 5*S*)-**110**   (4*S*, 5*R*)-**110**   (4*R*, 5*R*)-**110**
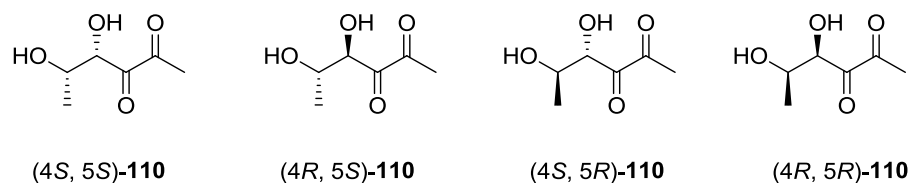
Figure 5.5: C₅-DPD-analogues (4*S*, 5*S*)-**126**, (4*R*, 5*S*)-**126**, (4*S*, 5*R*)-**126** and (4*S*, 5*S*)-**126** synthesized by Rui *et al.*[273]

The four compounds were prepared starting from *S*- and *R*-methyl lactate. For the sake of simplicity, here below is reported the synthetic procedure only from *S*-methyl lactate (Scheme 5.11). The starting material was first protected as TBDPS ether then the ester was hydrolyzed, coupled with *N,O*-dimethylhydroxylamine hydrochloride and the corresponding Weinreb amide was homologated to give the silyloxyhexynone *S*-**114**. Two different stereoselective reducing methods were employed: (i) *S*-alpine borane in THF (Scheme 5.11 A; with *R*-methyl lactate, *R*-alpine borane was used); and (ii) $CeCl_3 \cdot 7H_2O$ with $NaBH_4$ in MeOH (Luche reduction, Scheme 5.11 B). The resulting alcohols (*S*-**115** and *S*-**119**, respectively) were deprotected using TBAF and protected as cyclohyliden acetals. Oxidation to diketone and acidic hydrolysis afforded the two desired isomers ((4*S*, 5*S*)-**110** and (4*R*, 5*S*)-**110**). The same procedure was applied starting from *R*-methyl lactate, to generate (4*S*, 5*R*)-**110** and (4*R*, 5*R*)-**110**.

The activity of the four diastereoisomers was evaluated in *E. coli* and *V. harveyi*. In *E. coli* none of the compounds showed agonistic or antagonistic activity but, when tested with 20 μM DPD, the analogues with natural *S* configuration (i.e., (4*S*, 5*S*-**110**) and (4*S*, 4*R*-**110**)) increased *lsr* expression (synergistic agonists). In *V. harveyi* two different assays were performed: (i) a LuxP-FRET assay to measure binding to LuxP through measurement of the fluorescence resonance energy transfer and (ii) a bioluminescence assay with strain MM32. The FRET assay revealed binding for all the four analogues with the *S*-isomers (4*S*, 5*S*)-**110** and (4*S*, 5*R*)-**110** being the most active (Table 5.5). The C₅-configuration affects binding to LuxP with a 10-fold stronger response to (4*S*, 5*R*)-**110** than to (4*S*, 5*S*)-**110** (Table 5.5).
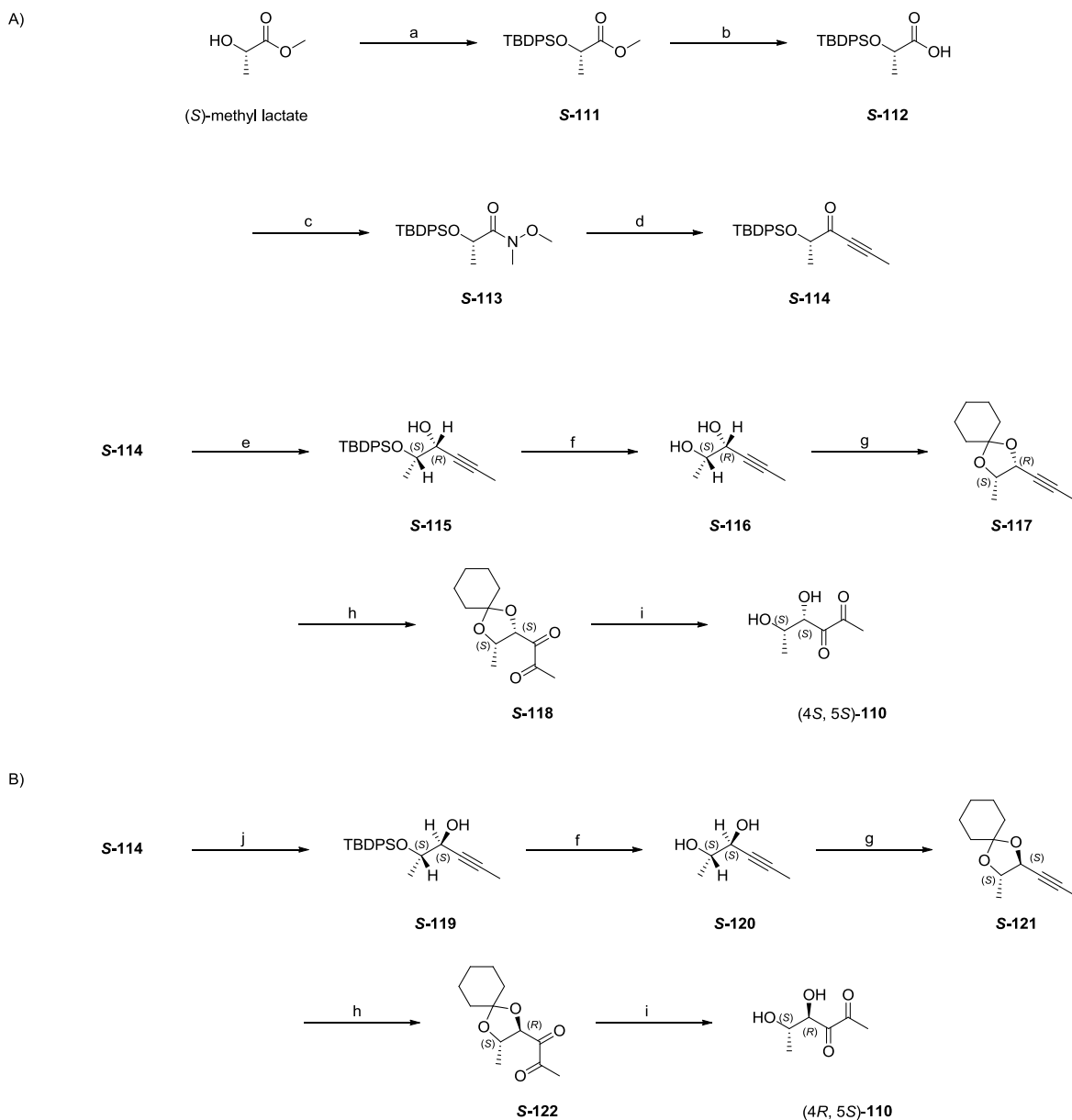
Scheme 5.11: Synthesis of C$_5$-DPD-analogues A) (4*S*, 5*S*)-**110**, (4*R*, 5*S*)-**110**; B) (4*S*, 5*R*)-**110** and (4*S*, 5*S*)-**110** by Rui *et al.* Reagents and conditions: (a) TBDPSCl (1.1 eq), Et$_3$N (1.1 eq), DMAP (0.4 eq), DCM, rt, 15 h (92%); (b) LiOH (3.0 eq), THF/H$_2$O (1:5), rt, 18 h (100%); (c) CH$_3$NHOCH$_3$*HCl (1.0 eq), CDMT (1.2 eq), NMM (3.0 eq), THF, rt, 5 h (84%); (d) propyne (1.5 eq), *n*-BuLi (1.4 eq), THF, - 78 °C to – 20 °C, 1 h (73%); (e) (*S*)-alpine borane (0.5 M in THF, 2.0 eq), THF, rt, 36 h; (f) TBAF (1.0 M in THF), THF, rt, 5 h (36% over two steps); (g) 1,1-dimethoxy cyclohexane (1.2 eq), H$_2$SO$_4$ (cat.), DMF, rt, 30 min (83%); (h) NaIO$_4$ (2.25 eq), RuO$_2$*H$_2$O (2.5% mol), ACN/CCl$_4$/H$_2$O (1:1:1.4), rt, 5 min (46%); (i) H$_2$SO$_4$ 0.01 M, D$_2$O, 4 °C, 18 h; (j) CeCl$_3$*7H$_2$O (1.2 eq), NaBH$_4$ (1.5 eq), MeOH, - 50 °C, 20 min (53%).[273]

In the bioluminescence assay, all the diastereoisomers acted as agonists but higher concentrations compared to DPD were required to reach maximum induction (partial agonists). Once more, the *R*-configuration is responsible for higher activity with (4*S*, 5*R*)-**110** being 10-fold more potent than (4*S*, 5*S*)-**110** (Table 5.5). When tested with 0.1 μM DPD, (4*S*, 5*S*)-**110** was the strongest antagonist (IC$_{50}$ = 57.54±0.29 μM) and at 0.1 mM all the compounds inhibited growth and did not show toxicity.[273]

Compound	EC$_{50}$ in LuxP-FRET assay (μM)	EC$_{50}$ in *V. harveyi* MM32 (μM)[a]	IC$_{50}$ in *V. harveyi* MM32 (μM)[b]
S-DPD	0.032±0.0015	0.076±0.002	N.D.[c]
(4*S*, 5*R*)-**110**	0.14±0.019	0.65±0.05	169±19
(4*S*, 5*S*)-**110**	1.87±0.22	6.21±0.46	57.54±0.29
(4*R*, 5*S*)-**110**	11.6±2.8	19.5±6.3	159.7±8.4
(4*R*, 5*R*)-**110**	10.0±2.4	26.5±8.4	N.D.[c]

Table 5.5: Activities of the four C$_5$-DPD-analogues (4*S*, 5*S*)-**110**, (4*R*, 5*S*)-**110**, (4*S*, 5*R*)-**110** and (4*S*, 5*S*)-**110** synthesized by Rui *et al.*[273]

Beside the stereochemistry, both hydration at C$_3$ and the ratio of open/cyclic form are important in determining DPD-analogues' activity (see geminal di-halogens-DPD-analogues[266] and C$_4$-alkoxy-HDP[269]). In 2016, Collins and coworkers synthesized *rac*-C$_5$-SH-DPD, whose closed form was proposed, by DFT (density functional theory) calculations, to exist mainly hydrated at C$_3$ and they also introduced an halide (i.e., fluoro, chloro, bromo) at C$_5$ as isosteric replacement for the hydroxyl group, to see if the resulting compounds could mimic *S*-THP, the linear and hydrated form of *S*-DPD. Lastly, they measured the activity of the previously synthesized (but not tested)[233] *rac*-C$_5$-OMe-DPD (Scheme 5.12).[274] The synthesis started with the Grignard addition to the Weinreb amides **123a** and **123b** or with the alkynilation of chloroacetyl chloride **124**. The three resulting ketones **127a-c** were reduced under Luche conditions and the chloride in **128c** was displaced to introduce a thioacetate group. TBS protection, oxidation and acidic deprotection afforded the desired compounds *rac*-**131a-d** (Scheme 5.12 A). Compound *S*-**131e** was instead prepared as enantiopure. L-gulonic acid γ lactone **23** was converted into *S*-**64a** in five steps as previously described.[232] After protection of both the primary and the secondary alcohols as tosilate and TBS-ether, respectively, ruthenium-catalyzed oxidation yielded diketone *S*-**134**. Tosyl displacement and installation of the bromine were followed by acidic deprotection to give *S*-**131e** (Scheme 5.12 B).
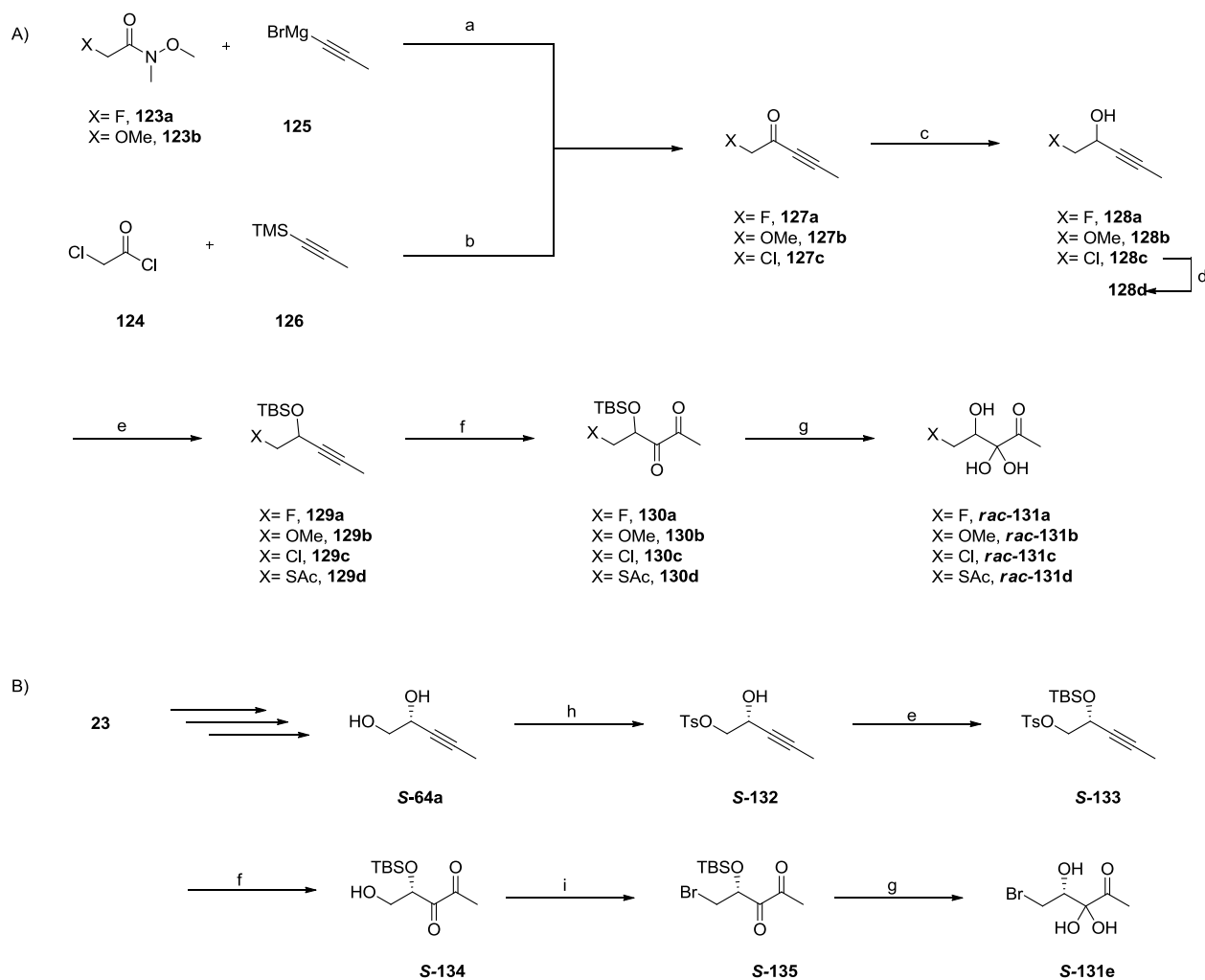
Scheme 5.12: Synthesis of C_5-DPD-analogues A) *rac*-**131a-d** and B) *S*-**131e** by Collins and coworkers. Reagents and conditions: (a) **125** (1.5 eq), THF, 0 °C, 5h (89%); (b) **126** (1.0 eq), AlCl$_3$ (1.1 eq), DCM, 0 °C, 3h (97%); (c) CeCl$_3$*7H$_2$O (1.1 eq), NaBH$_4$ (1.2 eq), MeOH, 0 °C, 1 h (**128a**, 37%; **128b**, 40%; **128c**, 66%); (d) KSAc (1.1 eq), DMF, 0 °C to rt, 72 h (60%); (e) TBDMSCl (2.5 eq), imidazole (5.0 eq), DCM, rt, 17 h (**129a**, 77%; **129b**, 62%; **129c**, 74%; **129d**, 81%; *S*-**133**, 81%); (f) NaIO$_4$ (2.3 eq), RuO$_2$*H$_2$O (2% mol), ACN/CCl$_4$/H$_2$O (1:1:3.1), rt, 20 min (**130a**, 40%; **130b**, 68%; **130c**, 56%; **130d**, 38%; **134**, 18%); (g) D$_2$SO$_4$ (cat.), DMSO-d_6/D$_2$O (1:4), rt, 24 h; (h) TosCl (1.2 eq), pyridine/DCM (9:5), 0 °C to rt, 22 h; (i) LiBr (1.0 eq), acetone, rt, 24 h (78%).[274]

The compounds were tested in *S. typhimurium* and *V. harveyi* both as agonists and as antagonists. *rac*-**131a-c** were found to be stable and existed only as their linear form while *S*-**131e** slowly hydrolyzed to DPD so its biological activity was not evaluated. In *S. typhimurium* none of the compounds was active (neither as agonist nor as antagonist). In *V harveyi* no antagonism was observed but *rac*-**131c** and *rac*-**131d** showed, respectively, moderate and weak agonism. Since the closed form of DPD (i.e., *S*-THMF) is the one able to complex borate and generate the borate ester *S*-THMF-borate that binds to LuxP, it was proposed that *rac*-**131c**, similarly to *S*-**131e**, slowly hydrolyses to form DPD. Indeed, reaction with 1,2-phenylendiamine showed the formation of the quinoxaline product *rac*-**136**, explaining the agonistic activity (Figure 5.6).[274]
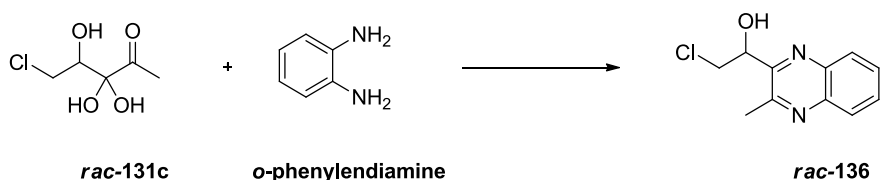
Figure 5.6: Reaction of **rac-131c** with *o*-phenylendiamine[274]

5.2.5 Carbocyclic DPD-analogues

As the synthesis of DPD-analogues is hampered by the rapid interconversion of the latter to different linear and cyclic structures and since the closed form of DPD is the one recognized by LuxP and by the enteric LsrB transporter, in 2011 Tsuchikama and coworkers decided to synthesize carbocyclic analogues of this active form and to investigate them as potential DPD-mimics.[275] The synthesis began with the TBS protection of commercially available **137**. *m*-CPBA mediated epoxidation followed by reduction with NaBH$_4$ afforded epoxide **140** as a single diastereoisomer. Acidic deprotection yielded racemic *cis*-2,5-dihydroxy-2-methylcyclopentanone (*cis*-DHMP) **141** in quantitative yield. *Trans*-DHMP **146** was instead produced after deprotection of *trans*-**145** which was synthesized from **142** through sylilation, OsO$_4$-catalyzed dihydroxylation and TEMPO oxidation. The synthesis of the four 1,2,3-trihydroxy-1-methylpentane (TriHMP) started from previously reported **147**.[276] **147** was derivatized to the four benzylated diols **148a-d** by osmium-mediated dyhdroxylation and *m*-CPBA oxidation followed by acidic ring opening. The four diols were then de-benzylated under standard Pd-catalyzed conditions to give **149a-d**. The six compounds were evaluated in *V. harveyi* BB170 and MM32 and in *S. typhimurium* Met844. Both in *S. typhimurium* and in *V. harveyi* MM32 no agonists or antagonists were discovered. In *V. harveyi* BB170 none of the analogues displayed agonistic activity but **149a-c** exhibited weak (33% inhibition) to moderate (44% and 51% inhibition, respectively) antagonistic effect.[275]
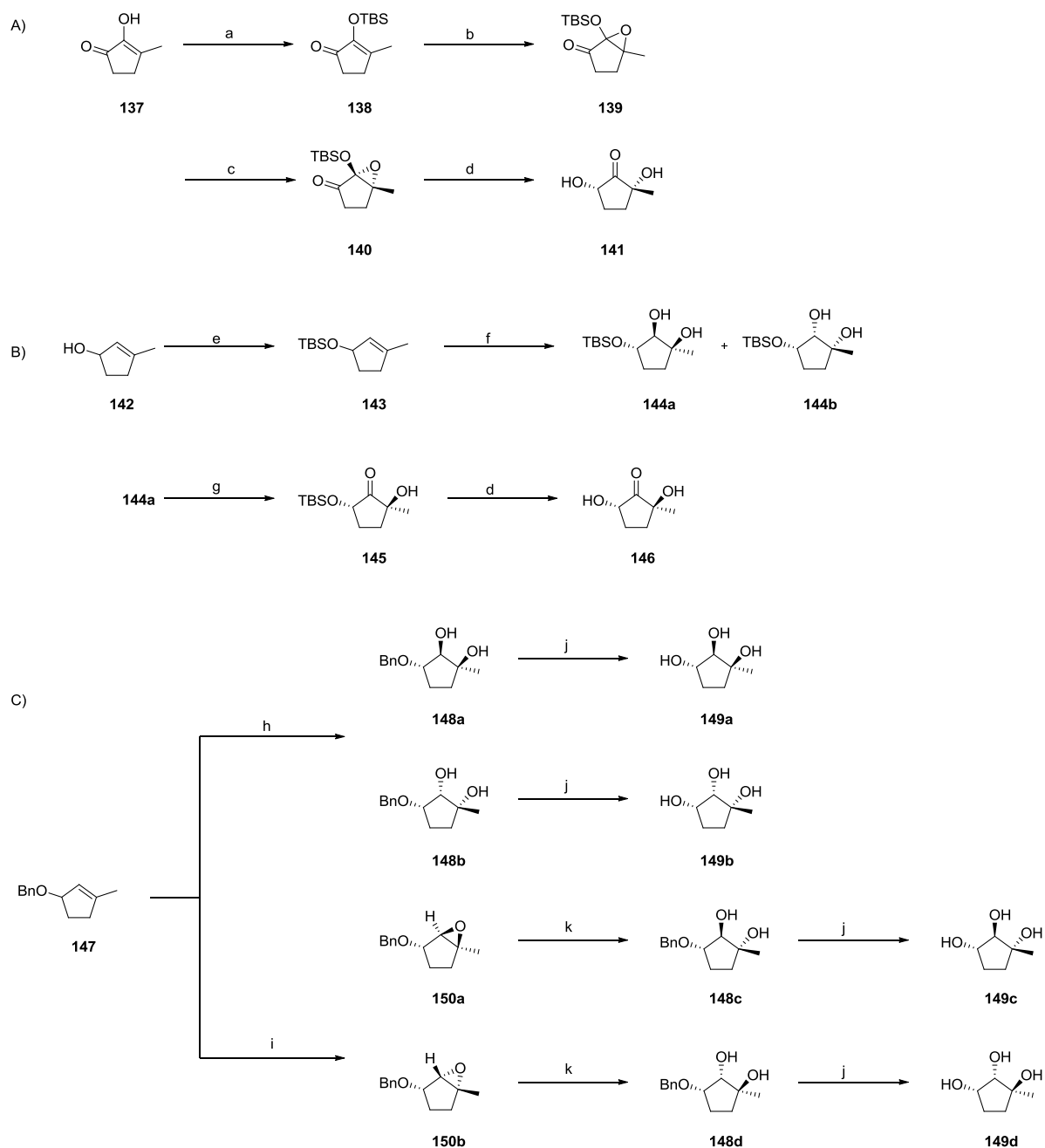
Scheme 5.13: Synthesis of carbocyclic-DPD-analogues from Tsuchikama *et al.* Reagents and conditions: (a) TBSCl (1.05 eq), Et$_3$N (2.0 eq), DMAP (10% mol), DCM, rt, 12 h (88%); (b) *m*-CPBA (2.0 eq), DCM, rt, 2 h; (c) NaBH$_4$ (2.0 eq), MeOH 0 °C, 5 min. (95% over two steps, single diastereoisomer); (d) H$_2$SO$_4$ (pH = 2), D$_2$O/DMSO-d_6 (1:1), rt, 12 h; (e) TBMSSCl (1.1 eq), imidazole (2.0 eq), DMF, rt, 12 h; (f) OsO$_4$ (5% mol), DMAP (1% mol), NMO (1.5 eq), Acetone/H$_2$O (3:1), rt, 18 h (**144a**, 43% over two steps; **144b**, 7% over two steps); (g) TEMPO (10% mol), KBr (10% mol), NaOCl (2.0 eq), DCM/10% NaHCO$_3$ (2.6:1), 0 °C, 20 min. (98%); (h) OsO$_4$ (1% mol), NMO (1.5 eq), Acetone/H$_2$O (2:1), rt, 16 h (**148a**, 54%; **148b**, 13%); (i) *m*-CPBA (2.0 eq), NaHCO$_3$ (10.0 eq), DCM, 0 °C, 2 h (**150a**, 49%; **150b**, 19%); (j) Pd(OH)$_2$/C (20% mol), THF, rt, 1 h (**149a-d**, quant.); (k) 1% H$_2$SO$_4$, H$_2$O, rt, 3 h (**148c**, 70%; **148d**, 78%).[275]
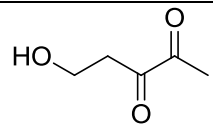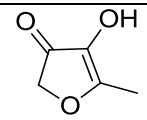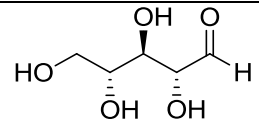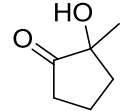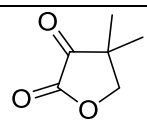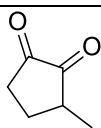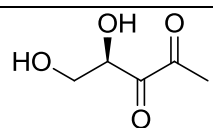
The complete lack of activity in *S. typhimurium* can be attributed to the locked cyclopentane scaffold of the compounds. In enteric bacteria, the LsrB transporter binds to the closed form of DPD (i.e., *R*-THMF) but then is the alcohol at C$_5$ of the linear hydrated form (i.e., *S*-THP) to be phosphorylated by LsrK: the absence
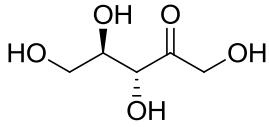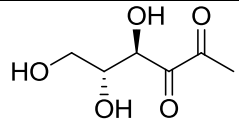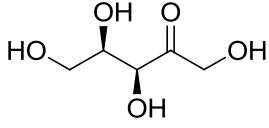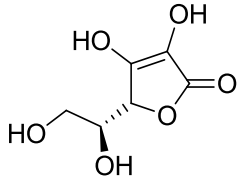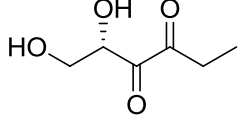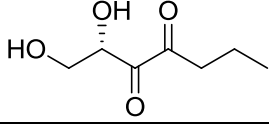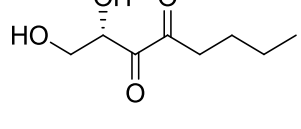
of a primary alcohol and the locked carbocyclic conformation are preventing phosphorylation and therefore activity. On the other hand, in *V. harveyi* the closed conformation is the one recognized by the LuxP receptor. The absence of activity of the two DHMPs **141** and **146** can be ascribed to the replacement of the heterocyclic oxygen of DPD with a carbon atom and to the insufficient hydration at C_3, both responsible for the loss of hydrogen bonds in the binding site. The replacement of the ketone at C_3 with an hydrogen bond donor (i.e., an hydroxyl group) and the consequent restoration of an hydrogen bond, may be responsible for the poor activity of **149a-c**, although the antagonistic (rather than agonistic) effect is probably caused by the general toxicity of the TriHMPs analogues.[275]
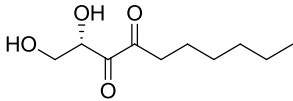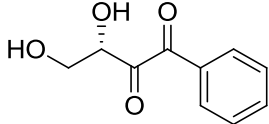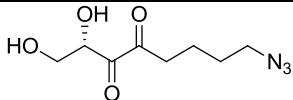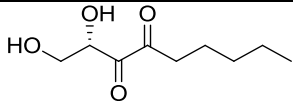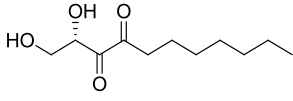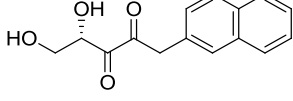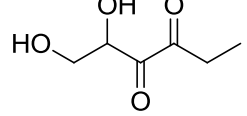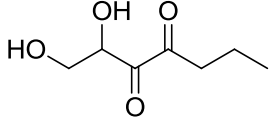
This overview of natural and synthetic DPD-analogues reported in the literature (see Table 5.6 for a schematic summary) underlines the paucity of natural derivatives tested and the lack of synthetic compounds derived from modifications at C_2 (Figure 5.7): the majority of the substitutions on DPD structure have been performed at C_1, where the methyl has been substituted with a wide range of alkyl (short, long, cyclic) groups, one heteroaromatic and four aromatic rings.[247,249,260,263,267,277,278] The ketone at C_3 has been isosterically replaced with geminal dihalogens[279] while the two hydroxyl groups at C_4 and C_5 have been protected as esters [247,251,271,272] and ethers,[233,280] exchanged with halogens[268274] or removed[267]. Lastly, a methyl has been installed at C_5, resulting in four diastereoisomers.[273]
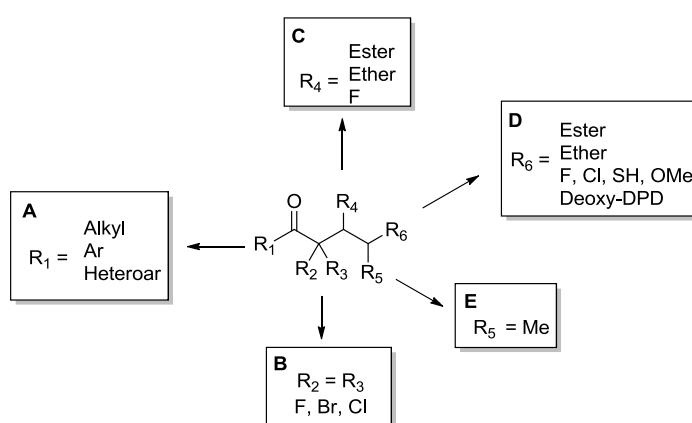
Figure 5.7: DPD-analogues reported in the literature
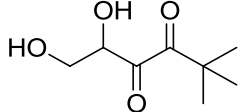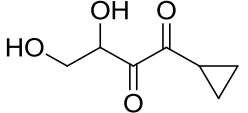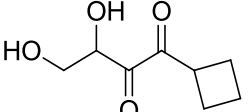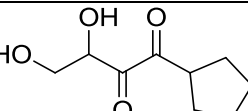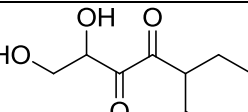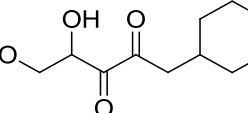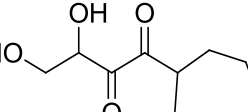
Entry	Compound Structure	Compound Name / Number	Tested in			Ref.
			V. harveyi	*S. typhimurium*	*E. coli*	
1		Laurencione	MM32			257
2		HMF	MM32			255
3		D-ribose	MM32			257
4		**70**	MM32			257
5		**71**	MM32			257
6		**72**	MM32			257
7		*R*-DPD	MM30			255
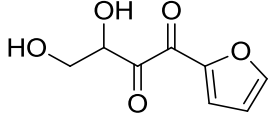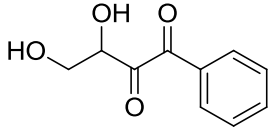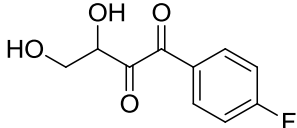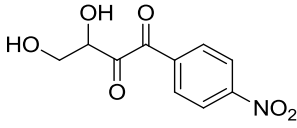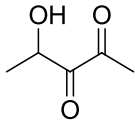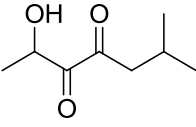
72

Entry	Compound Structure	Compound Name / Number	Tested in			Ref.
			V. harveyi	*S. typhimurium*	*E. coli*	
8		D-ribulose	MM30			255
9		DEHD	MM30			255
10		D-xylulose	MM30			255
11		L-ascorbic acid	MM30			255
12		*S*-73b	MM32, BB170, MM30	Met844		249,258
13		*S*-73c	MM32, BB170, MM30	Met844		249,258
14		*S*-73d	MM32, BB170, MM30	Met844		249,258
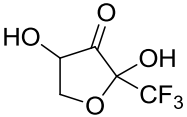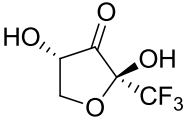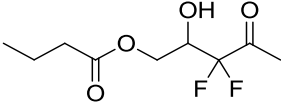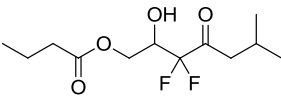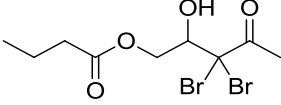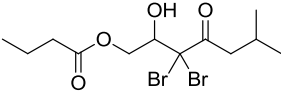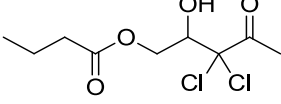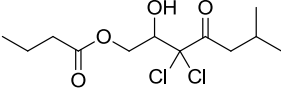
Entry	Compound Structure	Compound Name / Number	Tested in			Ref
			V. harveyi	*S. typhimurium*	*E. coli*	
15		*S*-**73e**	MM32, BB170, MM30	Met844		[249,258]
16		*S*-**73f**	MM32	Met844		[249]
17		*S*-**73g**	MM32	Met844		[249]
18		*S*-**73h**	BB170, MM30			[258]
19		*S*-**73i**	BB170, MM30			[258]
20		*S*-**73j**	BB120, MM32			[260]
21		*rac*-**74b**	MM32, BB170	Met715, Met708	LW7 pLW11, ZK126 pLW11, W3110 pCT6	[247,261,267]
22		*rac*-**74c**	MM32, BB170	Met715, Met708	LW7 pLW11, ZK126 pLW11, W3110 pCT6	[261,267]
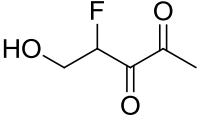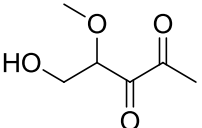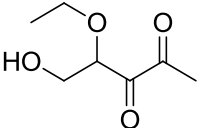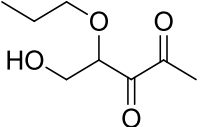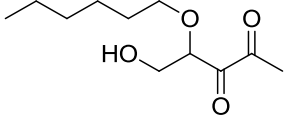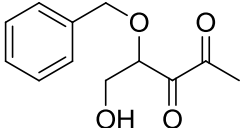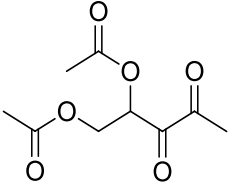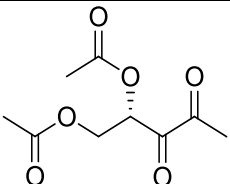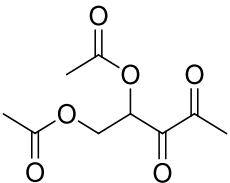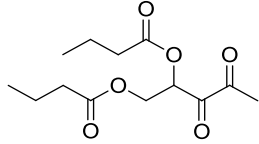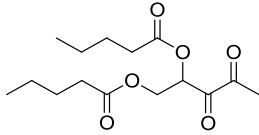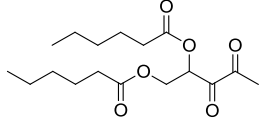
74

Entry	Compound Structure	Compound Name / Number	Tested in			Ref
			V. harveyi	*S. typhimurium*	*E. coli*	
23		*rac*-**74d**	MM32, BB170	Met715, Met708	LW7 pLW11, ZK126 pLW11, W3110 pCT6	[261,267]
24		*rac*-**74e**	BB170	Met715, Met708	LW7 pLW11, ZK126 pLW11, W3110 pCT6	[267]
25		*rac*-**74f**	BB170	Met715, Met708	LW7 pLW11, ZK126 pLW11, W3110 pCT6	[267]
26		*rac*-**74g**	BB170	Met715, Met708	LW7 pLW11, ZK126 pLW11, W3110 pCT6	[267]
27		*rac*-**74h**	MM32, BB170	Met715, Met708	LW7 pLW11, ZK126 pLW11, W3110 pCT6	[261,267]
28		*rac*-**74i**	BB170	Met715, Met708	LW7 pLW11, ZK126 pLW11, W3110 pCT6	[267]
29		*rac*-**74j**	BB170	Met715, Met708	LW7 pLW11, ZK126 pLW11, W3110 pCT6	[267]
30		*rac*-**74k**	BB170	Met715, Met708	LW7 pLW11, ZK126 pLW11, W3110 pCT6	[267]
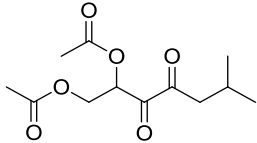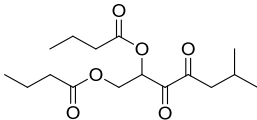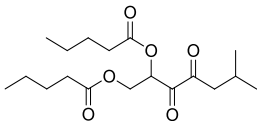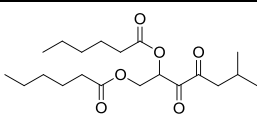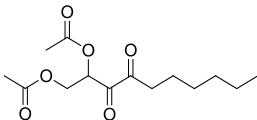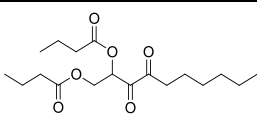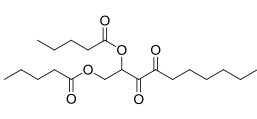
Entry	Compound Structure	Compound Name / Number	Tested in			Ref
			V. harveyi	*S. typhimurium*	*E. coli*	
31		*rac*-**74l**	MM32			[261]
32		*rac*-**74m**	MM32, BB170	Met715, Met708	LW7 pLW11, ZK126 pLW11, W3110 pCT6	[261,263,267]
33		*rac*-**74n**		Met708, Met715	ZK126 pLW11, W3110 pCT6 dsRED	[263]
34		*rac*-**74o**		Met708, Met715	ZK126 pLW11, W3110 pCT6 dsRED	[263]
35		*rac*-**74p**	MM32	Met708, Met715	ZK126 pLW11, W3110 pCT6 dsRED	[261,263]
36		*rac*-**74q**		Met708, Met715	ZK126 pLW11, W3110 pCT6 dsRED	[263]
37		*rac*-**74r**		Met708, Met715	ZK126 pLW11, W3110 pCT6 dsRED	[263]
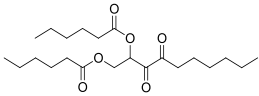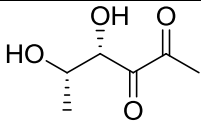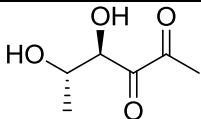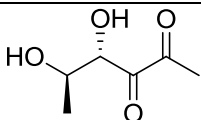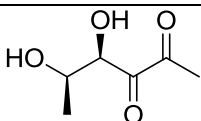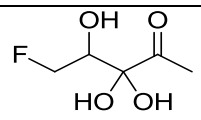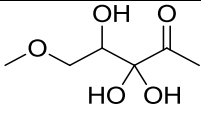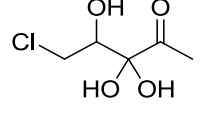
76

Entry	Compound Structure	Compound Name / Number	Tested in			Ref
			V. harveyi	*S. typhimurium*	*E. coli*	
38		*rac*-**74s**		Met708, Met715	ZK126 pLW11, W3110 pCT6 dsRED	263
39		*rac*-**74t**		Met708, Met715	ZK126 pLW11, W3110 pCT6 dsRED	263
40		*rac*-**74u**		Met708, Met715	ZK126 pLW11, W3110 pCT6 dsRED	263
41		*rac*-**74v**		Met708, Met715	ZK126 pLW11, W3110 pCT6 dsRED	263
42		*rac*-**74w**	BB170	Met715, Met708	LW7 pLW11, ZK126 pLW11, W3110 pCT6	276
43		*rac*-**74z**	BB170	Met715, Met708	LW7 pLW11, ZK126 pLW11, W3110 pCT6	267

Entry	Compound Structure	Compound Name / Number	Tested in			Ref
			V. harveyi	*S. typhimurium*	*E. coli*	
44		*rac*-83	BB170			265
45		*S*-83	BB170			265
46		*rac*-91a			LW7, W3110 pCT6	266
47		*rac*-91b			LW7, W3110 pCT6	266
48		*rac*-91c			LW7, W3110 pCT6	266
49		*rac*-91d			LW7, W3110 pCT6	266
50		*rac*-91e			LW7, W3110 pCT6	266
51		*rac*-91f			LW7, W3110 pCT6	266
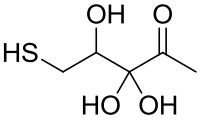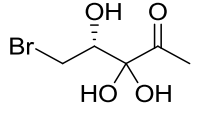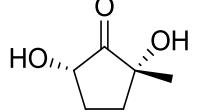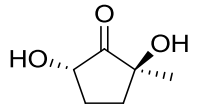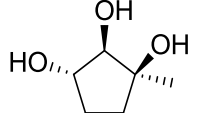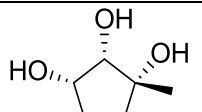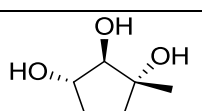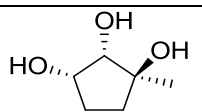
78

Entry	Compound Structure	Compound Name / Number	Tested in			Ref
			V. harveyi	*S. typhimurium*	*E. coli*	
52		*rac*-99	BB170			[268]
53		*rac*-102a	MM32	Met844		[269]
54		*rac*-102b	MM32	Met844		[269]
55		*rac*-102c	MM32	Met844		[269]
56		*rac*-102d	MM32	Met844		[269]
57		*rac*-102e	MM32	Met844		[269]

Entry	Compound Structure	Compound Name / Number	Tested in			Ref
			V. harveyi	*S. typhimurium*	*E. coli*	
58		*rac*-**107**	BB170	Met844		[271]
59		*S*-**107**	BB170	Met844		[271]
60		*rac*-**109a**		Met715	LW7	[272]
61		*rac*-**109b**		Met715	LW7	[272]
62		*rac*-**109c**		Met715	LW7	[272]
63		*rac*-**109d**		Met715	LW7	[272]

Entry	Compound Structure	Compound Name / Number	Tested in			Ref
			V. harveyi	*S. typhimurium*	*E. coli*	
64		*rac*-109e		Met715	LW7	272
65		*rac*-125f		Met715	LW7	272
66		*rac*-109g		Met715	LW7	272
67		*rac*-109h		Met715	LW7	272
68		*rac*-109i		Met715	LW7	272
69		*rac*-109j		Met715	LW7	272
70		*rac*-109k		Met715	LW7	272

Entry	Compound Structure	Compound Name / Number	Tested in			Ref
			V. harveyi	*S. typhimurium*	*E. coli*	
71		*rac*-109l		Met715	LW7	[272]
72		(4*S*, 5*S*)-110	MM32		KX1446	[273]
73		(4*R*, 5*S*)-110	MM32		KX1446	[273]
74		(4*S*, 5*R*)-110	MM32		KX1446	[273]
75		(4*R*, 5*R*)-110	MM32		KX1446	[273]
76		*rac*-131a	BB170, MM32[274]	Met844		[274]
77		*rac*-131b	BB170, MM32[274]	Met844		[233,274]
78		*rac*-131c	BB170, MM32	Met844		[274]

Entry	Compound Structure	Compound Name / Number	Tested in			Ref
			V. harveyi	*S. typhimurium*	*E. coli*	
79		*rac*-131d	BB170, MM32	Met844		[274]
80		*S*-131e	BB170, MM32	Met844		[274]
81		141	BB170, MM32	Met844		[275]
82		146	BB170, MM32	Met844		[275]
83		149a	BB170, MM32	Met844		[275]
84		149b	BB170, MM32	Met844		[275]
85		149c	BB170, MM32	Met844		[275]
86		149d	BB170, MM32	Met844		[275]

Table 5.6: Summary of the DPD-analogues reported in the literature

6. SYNTHESIS OF SMALL SETS OF DPD-RELATED COMPOUNDS

With the "state of the art" of all the DPD-analogues reported in the literature in my hands, I decided to move forward to the design and synthesis of novel DPD-related compounds. Considering that (i) no modifications at C_2 have been reported; (ii) position C_3 has poorly been explored and (iii) no heteroaromatic substituents (except for a furan) were installed on the DPD-scaffold by other research groups, I designed eight series of compounds where the diketo moiety of DPD was embedded in heteroaromatic rings (Figure 6.1). This choice was made because (i) a locked and stable conformation where the open/closed equilibrium (typical of the majority of DPD-analogues reported) is not possible would allow for column chromatography purification of the samples and (ii) the increased UV activity and MW (due to the addition of heteroaromatic groups) would make compound detection by classical analytical methods (e.g., UHPLC-MS) easier compared to non UV active and very polar analogues.
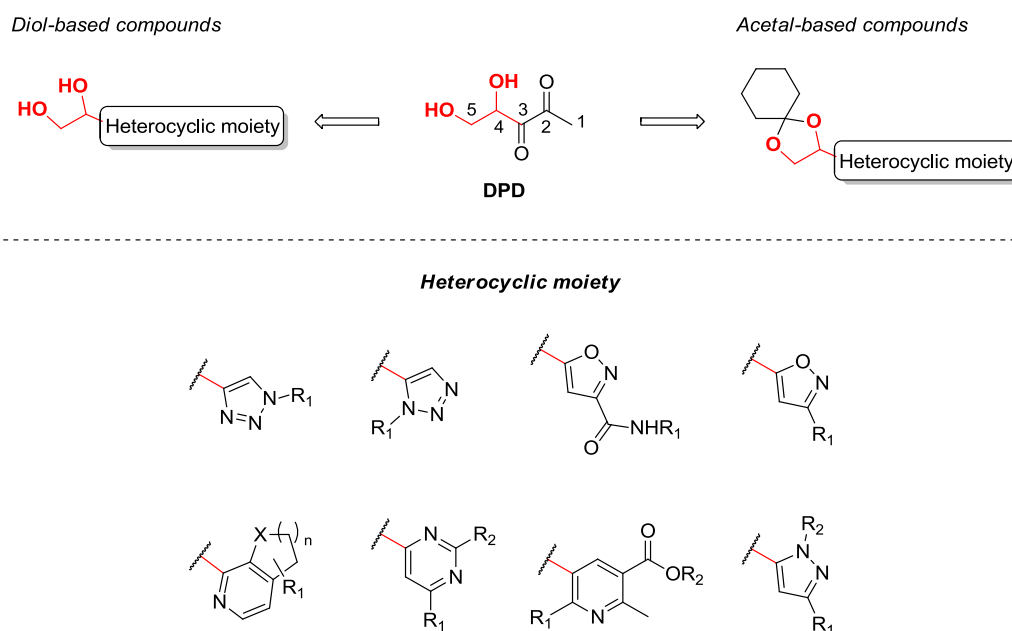
Figure 6.1: DPD-related compounds presented in this chapter

When selecting the heterocyclic moieties to install as a replacement of the dicarbonyl system of DPD, triazole, isoxazole, isoquinoline, pyrimidine, pyridine and pyrazole were selected as they can be found in many natural products as well as in marketed drugs. Such heterocycles play crucial roles in medicinal chemistry, being used as antifungal (hedaquinium chloride, fluconazole, terconazole),[281–285] anticancer (crizotinib),[286] antibacterial (sulfamethoxazole, trimethoprim, sulfamethazine),[287–289] anti-inflammatory (valdecoxib, lonazolac, celecoxib),[287,290,291] anti-reumatic (leflunomide),[287] antidepressant (fezolamine),[290,291] antiobesity (rimonabant),[290,291] anti-acid (esomeprazole),[286] antihistaminic (tripelennamine, mepyramine, thonzylamine),[286,288,289] antihypertensive (minoxidil),[287,288] anestetic (dimethisoquin),[282–285] disinfectant (N-laurylisoquinolinium bromide)[282–285] (Figure 6.2).
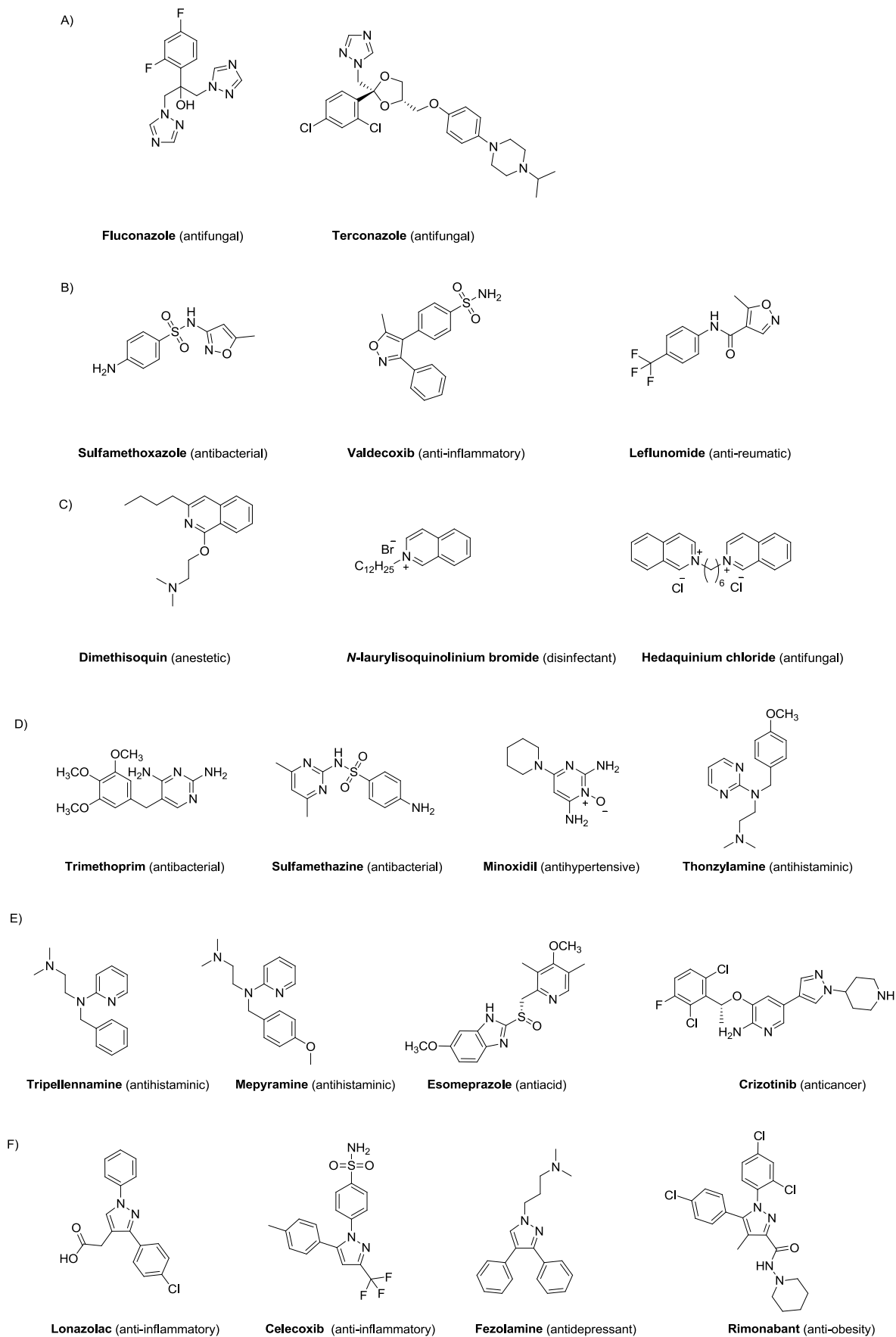
Figure 6.2: Examples of heterocyclic-containing drugs: A) triazoles; B) isoxazoles; C) isoquinolines; D) pyrimidines; E) pyridines and F) pyrazoles

All the compounds were purified before being assayed and characterized by UHPLC-MS (purity > 90%), ^{1}H NMR and ^{13}C NMR. At this stage of the research, I decided to prepare racemic compounds to speed up the synthetic protocol and the achievement of the results, having in mind that, for the most active compounds (i.e., IC_{50} in the nM range), preparation of homochiral derivatives would have been necessary. The newly established synthesis of racemic-DPD (see Chapter 4) was used as a template to design the synthetic routes towards all the DPD-analogues. Two building blocks (i.e., **150** and **40**, Scheme 6.1) were used as starting materials for all the planned synthesis and all the compounds were obtained from them in a few (maximum four) synthetic steps in such a way that, in case of positive hit(s), further derivatization and SAR studies would have not required to start from the very first step but directly from one of the two precursors.

6.1 Synthesis of the starting materials

The first of the two building blocks necessary to start the synthesis of all the analogues presented in this chapter was produced by Grignard addition of ethynylmagnesium bromide to the readily available (*t*-butyldimethylsilyloxy)acetaldehyde[292] **28** followed by acidic removal of the TBDMS protecting group. Further protection of the resulting diol **152** as acetal using 1,1-dimethoxy cyclohexane afforded the second building block compound **40** (Scheme 6.1).
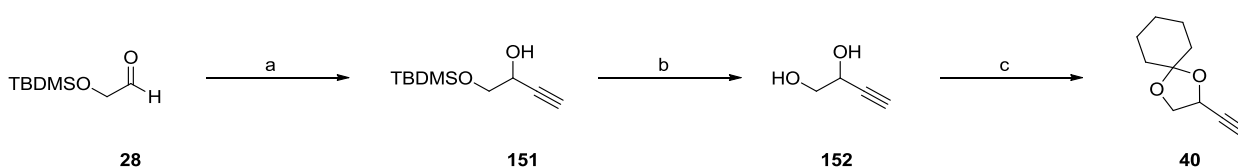
Scheme 6.1: Synthesis of the starting materials **152** and **40**. Reagents and conditions: (a) ethynylmagnesium bromide (0.5 M in THF, 1.3 eq), THF, 0 °C to rt, 3h (99%); (b) Dowex50WX8 100-200 mesh, MeOH, rt, overnight (99%); (c) 1,1-dimethoxy cyclohexane (3.0 eq), *p*-TSA (cat.), rt, overnight (57%)

As compounds **152** and **40** were necessary in high amounts (at least 30g each) to proceed towards the synthesis of all of our sets analogues, we needed to purchase aldehyde **28** in big quantity (> 50g). After checking several suppliers we found out that the price was really demanding (254 € / 5g) and the estimated delivery was 4 – 6 weeks. To avoid to waste time and money, we produced compound **28** by ourselves (following the previously reported procedure from Paterson *et a.l*[292]) in 75g scale (Scheme 6.2). TBDMS protection of cheap glycerol (50€ / 1L) and oxidation of the resulting intermediate allowed us to have, in one day, the required amount of **28** spending ~ 80€ / 5g thus saving more than 1/3 of money and plenty of time.
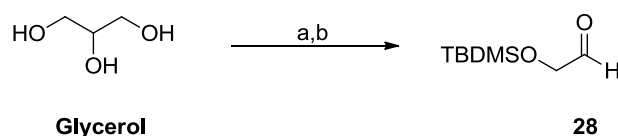
Scheme 6.2: Synthesis of aldehyde **28**. Reagents and conditions: (a) imidazole (0.15 eq), TBDMSCl (0.05 eq), DCM/DMF (3:1), rt, 2h; (b) $NaIO_4$ (3.3 eq), DCM/H_2O (1:1), rt, overnight (80% over two steps)

## 6.2 Synthesis of 1,4- and 1,5-disubstituted 1,2,3-triazoles

1,2,3-triazoles (both 1,4- and 1,5-disubstituted) can be synthesized applying azide-alkyne Huisgen cycloaddition conditions where an azide is reacted with an alkyne in a 1,3-dipolar cycloaddition reaction. The limitations of such a procedure (i.e., it requires high temperatures and produces mixtures of two regioisomers) were overcome in 2002 by Sharpless *et al.* with the introduction of a copper (I)-catalyzed variant termed the Copper (I)-catalyzed Azide-Alkyne Cycloaddition (CuAAC).[293] The addition of a catalyst (i.e., copper) increases the reaction rate of 10^7 to 10^8 when compared to the uncatalyzed cycloaddition. A broad range of functional groups are tolerated as well as an extended range of temperatures (0 °C – 160 °C). The reaction proceeds well in aqueous conditions, is insensitive to pH variations (4 – 12), is highly regioselective towards 1,4-disubstitution and pure products can be easily isolated by filtration or extraction. The *in situ* generation of Cu(I) catalyst by reduction of Cu(II) with a reducing agent (e.g., sodium ascorbate) is usually preferred over the use of Cu(I) salts (e.g., bromide or iodide) as it eliminates the need of a base. Polar aprotic solvents (e.g., THF, DMSO, ACN, DMF) are commonly used as well as mixtures such as *t*-BuOH/H_2O. The *in situ* generated Cu(I) forms a π-complex with the triple bond of the terminal alkyne (Figure 6.3, step A). The acidic proton of the alkyne is abstracted by a base forming a Cu-acetylide intermediate where one copper atom activates the azide while the other is bound to the acetylide. The azide coordinates the copper complex to generate a copper-azide-acetylide complex (Figure 6.3, step B). Cyclization (Figure 6.3, step C) and further protonation (by the hydrogen removed from the terminal alkyne by the base) results in the formation of product and the release of the catalyst which is re-used for another catalytic cycle (Figure 6.3, step D). The addition of ligands is essential to prevent Cu(I) oxidation to Cu(II) and, as they can function as proton acceptor, they make the base no longer necessary.[294–299]
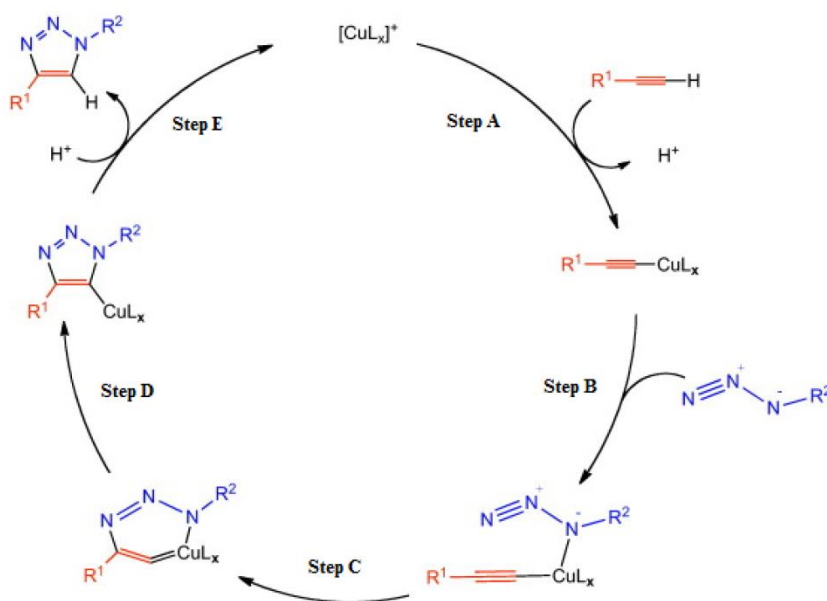
Figure 6.3: CuAAC reaction mechanism. Figure adapted with permission from *Coord. Chem. Rev.* **2011**, *255* (23), 2933–2945. Copyright © 2011 Elsevier

Before starting with the synthesis of a small library of 1,2,3-triazoles, I decided to test three different CuAAC conditions in order to establish the best ones and apply them to synthesize all the planned compounds. (2-Azidoethyl)benzene **154a** was chosen as reference azide (Table 6.1). First we used CuI (10% mol) and DIPEA (15% mol) in nonaqueous, nonprotic THF to afford the desired product with 58% isolated yield (Table 6.1, entry 1).[300] As the addition of AcOH was found to accelerate the protonation of the Cu-C bond[301–303] (thus facilitating the formation of the product), a catalytic amount of AcOH was added to the mixture (containing 2% mol CuI and 4% mol DIPEA) and this acid-base jointly promoted CuAAC resulted in a 14% increase of the isolated yield (Table 6.1, entry 2) when compared to the previous conditions (Table 6.1, entry 1).[304] As previously explained, the use of ligands is beneficial for the reaction as it prevents Cu(I) oxidation and avoids the use of base. Therefore it is not surprising that the *in situ* generation of Cu(I) by reduction of $CuSO_4*5H_2O$ from sodium ascorbate together with the use of L-ascorbic acid (both as a ligand and acidic source) raised the yield up to 89% (Table 6.1, entry 3).[305]
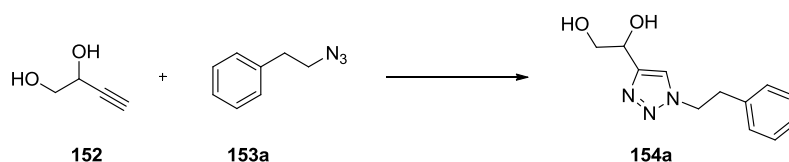
Entry	153a (Eq)	Solvent	Cu species	Yield 154a (%)[a]	Ref.
1	1.1	THF	CuI (10% mol) DIPEA (15% mol)	58	300
2	1.05	DCM	CuI (2% mol) DIPEA (4% mol) AcOH (cat)	72	304
3	1.0	*t*-BuOH/H$_2$O (1:1)	$CuSO_4*5H_2O$ (5% mol) Na ascorbate (0.5 eq)	89	305

Table 6.1: Screening of conditions for the CuAAC. All the reactions were performed overnight at room temperature
[a]Isolated yield

Once optimal conditions for the regioselective synthesis of 1,4-disubstituted 1,2,3-triazoles were established, five different azides (aromatic, heteroaromatic, aliphatic) were produced by stirring overnight at room temperature the corresponding bromo compounds with an excess (1.5 eq) of sodium azide. The five azides were reacted with alkyne **152** applying the previously found conditions and products **154b-f** were isolated in good yields (Table 6.2).

Entry	R$_1$	Product	Yield (%)
1	(CH$_2$)-Ph	**154b**	73
2	(CH$_2$)$_2$-*o*-F-Ph	**154c**	60
3	(CH$_2$)$_2$-*m*-Pyr	**154d**	72
4	(CH$_2$)$_5$-CN	**154e**	62
5	(CH$_2$)$_2$-CyH	**154f**	88

**Table 6.2**: Isolated yields for the 1,4-disubstituted triazoles **154b-f**

The 1,4-disubstitution was confirmed by HMBC (Heteronuclear Multiple Bond Correlation) of compound **154a** (see Chapter 8.1.4 and Appendix I, SI) and, as a proof of concept, the corresponding 1,5-disubstituted 1,2,3-triazole **155a** was synthesized. The regioselective synthesis of 1,5-disubstituted 1,2,3-triazoles is achieved with the use of Ruthenium-catalyzed Azide-Alkyne Cycloaddition (RuAAC) conditions. RuAAC can be used also with internal alkynes affording fully substituted 1,2,3-triazoles. The reaction starts (Figure 6.4, step A) with the displacement of the ligand (from the ruthenium-ligand complex) to generate an activated complex (not shown) which is converted, via oxidative coupling of the alkyne and the azide, to a six-membered ruthenium containing metallocycle (ruthenacycle, Figure 6.4, step B). The new C-N bond is formed between the terminal electrophilic nitrogen of the azide and the more electronegative carbon of the alkyne (Figure 6.4, step C). Reductive elimination and release of the triazole product regenerate the catalyst for further reaction cycles (Figure 6.4, step D). The most common ruthenium catalysts are Cp*RuCl(PPh$_3$)$_2$, Cp*Ru(COD) and Cp*[RuCl$_4$].[306,307]
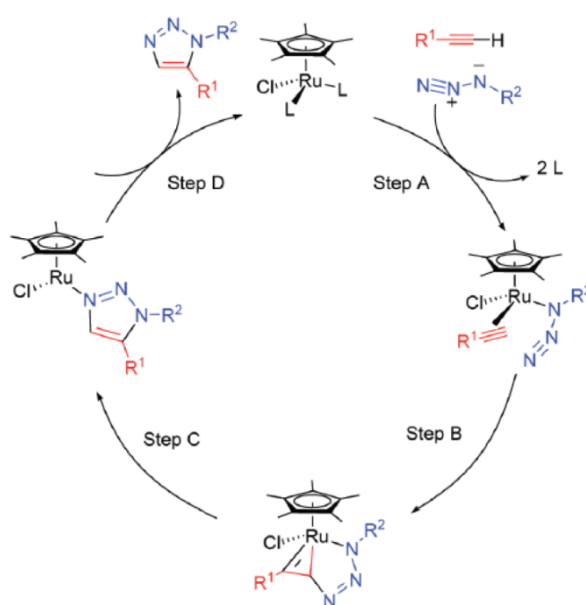
Figure 6.4: RuAAC reaction mechanism. Figure adapted with permission from *J. Am. Chem. Soc.*, **2008**, *130 (28)*, 8923–8930. Copyright © 2008 American Chemical Society

Azide **153a** was reacted with terminal alkyne **152** in the presence of 2% mol pentamethylcyclopentadienylbis (triphenylphosphine)ruthenium(II) chloride (Cp*RuCl(PPh$_3$)$_2$) regioselectively yielding, after stirring overnight the mixture in refluxing 1,4-dioxane, the corresponding 1,5-disubstituted 1,2,3-triazole **155a** (Scheme 6.3). ^{1}H NMR, ^{13}C NMR, TLC, UHPLC-MS, HMBC definitely confirm the different nature of the two compounds (see Chapter 8.1.4 and Appendix I, SI).[307]
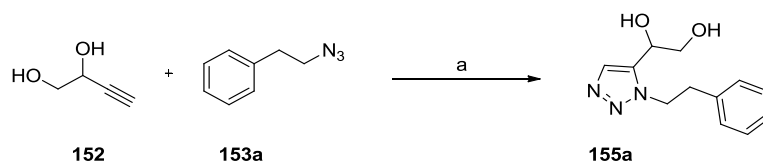
Scheme 6.3: Synthesis of 1,5-disubstituted 1,2,3-triazole **155a**. Reagents and conditions: (a) **153a** (1.0 e), Cp*RuCl(PPh$_3$)$_2$ (2% mol), 1,4-dioxane, 60 °C, overnight (87%)

As the synthesis of trialzoles substituted with short alkyl chains (e.g., methyl, butyl) was mined by safety issues related to the explosive and unstable nature of the small azides necessary, the desired substituents were installed on the triazole scaffold via alkylation. The use of a single, small and dangerous azide (i.e., $TMSN_3$) was privileged over the use of four different ones. The acetal protected terminal alkyne **40** was carefully reacted with an excess (10.0 eq) of $TMSN_3$ under previously established CuAAC conditions. The resulting unsubstituted triazole (**156**, Scheme 6.4) was both deprotected under acidic conditions (**154g**, Scheme 6.4) and, to install the desired substituents, alkylated with four different (methyl, cyclopropylmethyl, butyl, ethoxyethyl) bromides (Scheme 6.4).
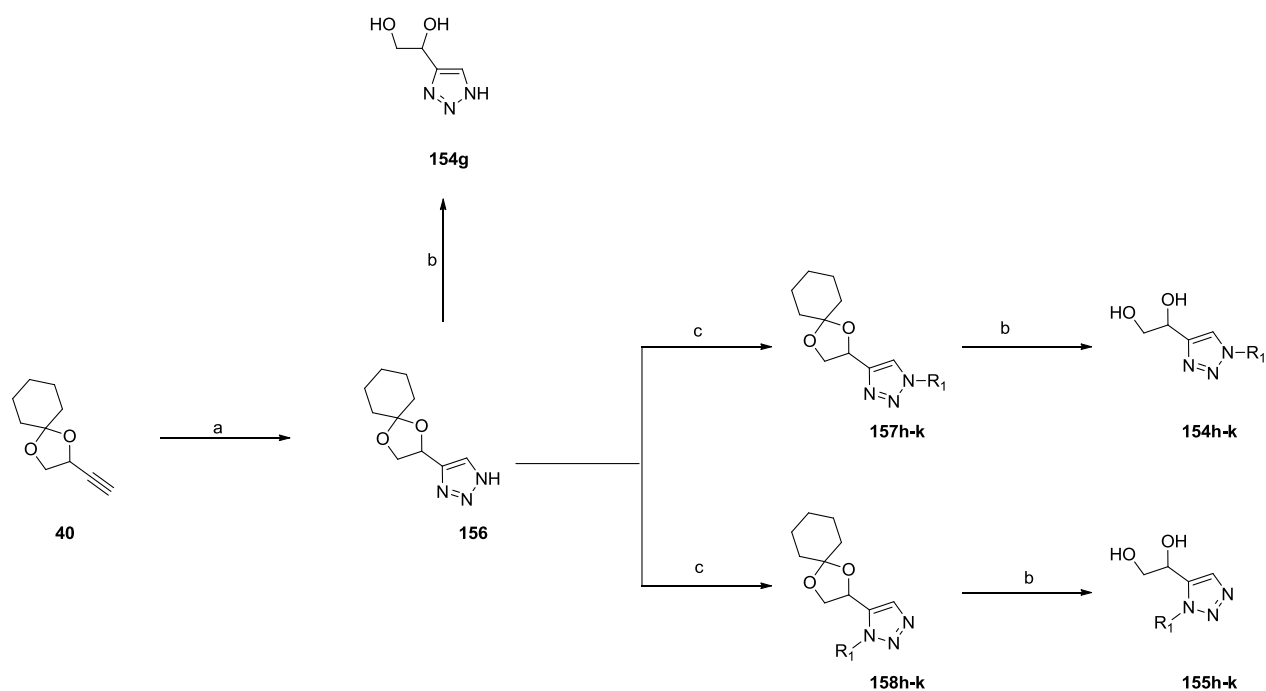
Scheme 6.4: Synthesis of 1,4-disubstituted 1,2,3-triazoles **154g-k** and 1,5-disubstituted 1,2,3-triazoles **155h-k**. Reagents and conditions: (a) $TMSN_3$ (10.0 eq), $CuSO_4*5H_2O$ (5% mol), Na ascorbate (0.5 eq), t-BuOH/H_2O (1:1), rt, overnight (36%); (b) 12M HCl (cat.), 1,4-dioxane, 0 °C to rt, 3h (98%); (c) R_1Br (1.5 eq), K_2CO_3 (2.0 eq), THF, 40 °C, overnight; (29% − 62%).

As expected, no regioselectivity was observed and both the 1,4- and the 1,5-disubstituted 1,2,3-triazoles formed. Playing with the equivalent of the base (i.e., 1.1 eq, 1.3 eq and 1.5 eq of K_2CO_3) and/or the alkylbromides (i.e., 0.8 eq and 0.9 eq of R_1Br) did not consistently changed the ratio of the two regioisomers (data not shown). For each substituent, the two corresponding regioisomers were isolated by preparative HPLC. The resulting eight products **157h-k** and **158h-k** were lastly deprotected with catalytic amount of concentrated hydrochloric acid. The ratio of the two regioisomers was determined by crude ^{1}H NMR: for all of the four couples, the 1,4-dibustituted 1,2,3-triazoles formed in excess when compared to the respective 1,5-regioisomers and, as predictable, the ratio decreases as the sterical hindrance of the R_1 substituent increases (Table 6.3). Concentrated HCl was preferred over Dowex 50WX8 100-200 mesh for the removal of the acetal protecting group for (i) the shorter reaction time (1 hour vs overnight) and (ii) the simpler workup (no filtration to remove the acidic resin required).

Entry	R_1	Product	Ratio 170:171
1	CH_3	157h / 158h	10:1
2	CH_2-Cyp	157i / 158i	6:1
3	n-Bu	157j / 158j	3:1
4	CH_2-O-CH_3CH_2	157k / 158k	2:1

Table 6.3: ^{1}H NMR ratio of the regioisomers **157h-k**:**158h-k**

6.3 Synthesis of 3,5-disubstituted isoxazoles

The first step in the synthesis of the set of 3,5-disubstituted isoxazoles was the production of the chloro-oximes necessary for the 1,3-dipolar cycloaddition with diol **152**. Seven aldehydes were converted into their corresponding oximes using an excess (3.0 eq) of hydroxylamine hydrochloride and the resulting crudes were directly chlorinated by reaction with *N*-chlorosuccinimide. The same conditions as for the synthesis of the 1,4-disubstituted 1,2,3-triazoles (i.e., 5% mol $CuSO_4*5H_2O$ and 0.5 eq of Na ascorbate in a 1:1 mixture of *t*-BuOH/H_2O, see Table 6.1) were applied, with the addition of an excess of potassium bicarbonate (4.3 eq) to form the nitrile oxide necessary for the cycloaddition. Seven 3,5-disubstituted isoxazoles **162a-g** were obtained in good to excellent yield (i.e., 63% − 89%, Table 6.4) after preparative HPLC purification (Scheme 6.5).[305]
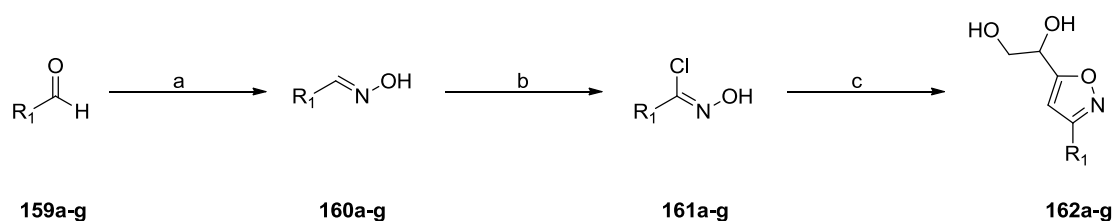
Scheme 6.5: Synthesis 3,5-disubstituted isoxazoles **162a-g**. Reagents and conditions: (a) $NH_2OH*HCl$ (3.0 eq), Et_3N (1.5 eq), H_2O/EtOH (1:1), rt, 1 − 3 h (80% − 98%); (b) NCS (1.0 eq), DMF, rt, 1 − 2 h (75% − 92%); (c) **152** (1.0 eq), $CuSO_4*5H_2O$ (5% mol), Na ascorbate (0.5 eq), $KHCO_3$ (4.3 eq), *t*-BuOH/H_2O (1:1), rt, overnight (63% − 89%)

Entry	R_1	Product	Yield (%)
1	*p*-CH_3-Ph	**162a**	82
2	*m*-Cl-Ph	**162b**	87
3	*o*,*p*-di-F-Ph	**162c**	78
4	*m*-Pyr	**162d**	71
5	Cyp	**162e**	63
6	*m*-THF	**162f**	77
7	CyH	**162g**	89

Table 6.4: Isolated yields for the 3,5-disubstituted isoxazoles **162a-g**

To produce the series of DPD-analogues where an amide moiety was installed at position 3 of the 3,5-disubstituted isoxazoles, the synthetic strategy was slightly modified and the protected precursor **40** was employed for the 1,3-dipolar cycloaddition instead of its unprotected version **152**, due to incompatibility of a free 1,3-diol with the reagents necessary in the following steps (e.g., NaOH, DIPEA, Scheme 6.8). Formation of the nitrile oxide for the cycloaddition was attempted by dehydration of ethyl nitroacetate with several bases (i.e., DABCO, DMAP, DBU, NMI, Scheme 6.6 conditions a) and also with a combination of PhNCO/Et$_3$N (Scheme 6.6 conditions b), commonly used to activate nitro groups. All of the aforementioned methods resulted in a mixture of unreacted starting materials.[308,309]
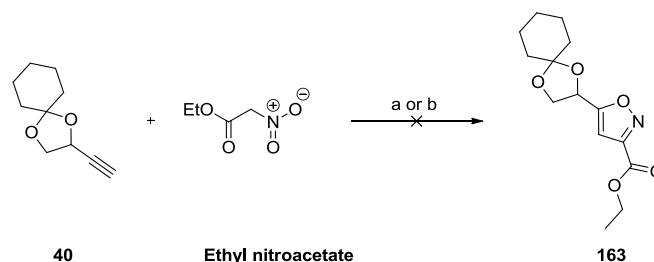
Scheme 6.6: Attempts for the synthesis of intermediate **163**. Reagents and conditions: (a) base (1.5 eq), CHCl$_3$, 60 °C, 3 days; (b) PhNCO (2.0 eq), Et$_3$N (1.5 eq), PhMe, 100 °C, 3 days

The 1,3-dipole specie was then changed to the chloro-oxime of ethyl glyoxalate (50% solution in toluene) which was synthesized as previously described (see Scheme 6.5, conditions a and b). Classical Sharpless conditions (see Scheme 6.5, conditions c) did not yield the desired product while the simple use of an equimolar amount of Et$_3$N gave only traces of **163**.[305,310]
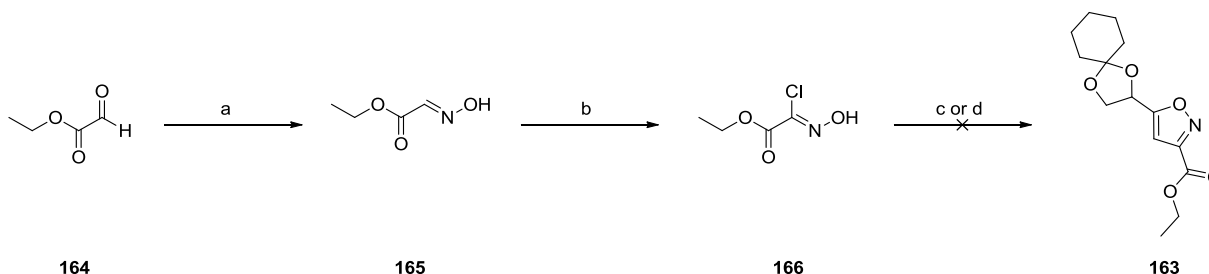
Scheme 6.7: Attempts for the synthesis of intermediate **163**. Reagents and conditions: (a) NH$_2$OH*HCl (3.0 eq), Et$_3$N (1.5 eq), H$_2$O/EtOH (1:1), rt, 3 h (80%); (b) NCS (1.0 eq), DMF, rt, 2 h (70%); (c) **40** (1.0 eq), CuSO$_4$*5H$_2$O (5% mol), Na ascorbate (0.5 eq), KHCO$_3$ (4.3 eq), *t*-BuOH/H$_2$O (1:1), rt, overnight; (d) **40** (1.0 eq), Et$_3$N (1.0 eq), THF, rt, overnight

The oxime of ethyl glyoxalate (i.e., compound **165**) was then reacted with an excess (40.0 eq) of sodium hypochlorite, both as a chlorinating agent and as base to form the corresponding nitrile oxide.[311] Different reaction times as well as ratios of dipolarophile **40** and 1,3-dipole **165** were tested (Table 6.5) in order to improve the initially poor yield (i.e., 16%, Table 6.5, entry 1). Increasing the equivalents of 1,3-dipole enhanced the formation of intermediate **163** up to a maximum of 36% isolated yield (Table 6.5, entry 4) with complete consumption of the dipolarophile **40** followed by removal of the excess of **165** by column chromatography.
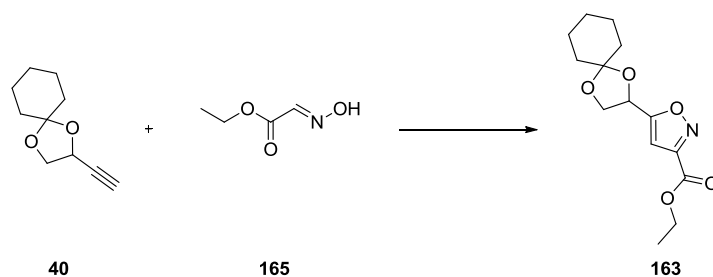
Entry	40 (Eq)	165 (Eq)	Time (h)	Yield 163 (%)[a]
1	1.2	1	96	16
2	1	1.2	72	18
3	1	1.5	24	21
4	1	2	12	36

Table 6.5: Different ratios of dipolarophile **40** and 1,3-dipole **165** tested for the synthesis of intermediate **163**
[a] Isolated yield

Once a solution for the key 1,3-dipolar cycloaddition step was found, the rest of the synthetic pathway proceeded smoothly. Saponification of the ethyl ester was followed by amidification of the resulting carboxylic acid moiety using HOBt as coupling agent and employing both primary and secondary amines (aliphatic, aromatic, heteroaromatic). Final acidic removal of the acetal protecting group afforded nine 3,5-disubstituted isoxazoles (with an amide moiety at position 3) **170h-m** in moderate to very good yields (i.e., 42% − 89%, Table 6.6). Two more products were isolated after acidic deprotection of intermediates **163** and **167** (i.e., **166** and **168**, respectively).
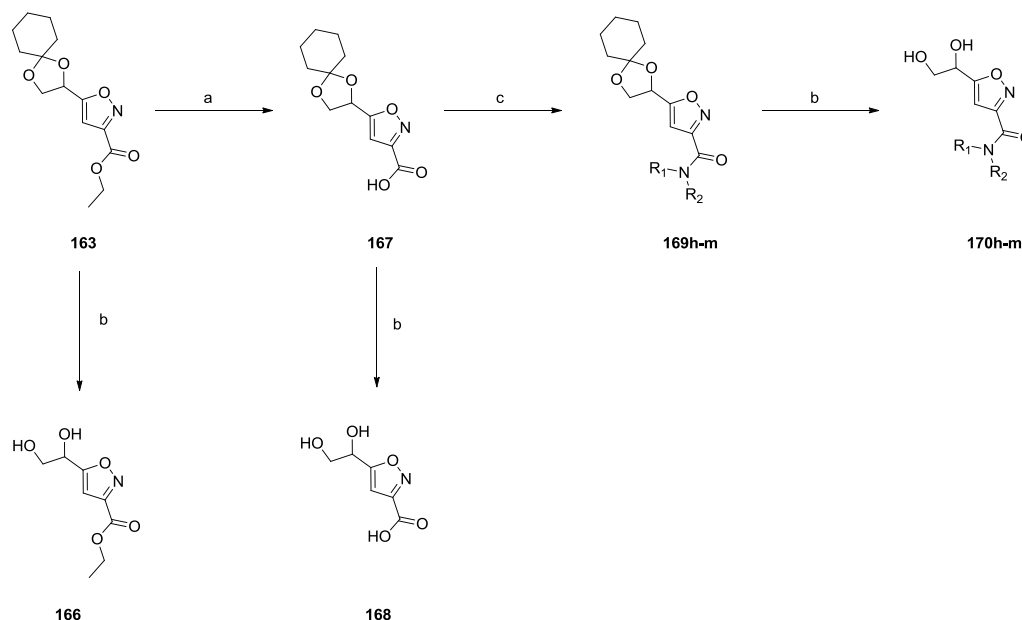
Scheme 6.8: Synthesis of 3,5-disubstituted isoxazoles with an amide moiety at position 3 **170h-m**. Reagents and conditions: (a) NaOH 1M (3.0 eq), THF, rt, overnight (99%); (b) 12 M HCl (cat.), 1,4-dioxane, 0 °C to rt, 1h − 3h (**166**, 46%; **168**, 55%, **170h-m**, 42% − 89%); (c) amine (2.0 eq), HOBt (2.0 eq), EDC*HCl (2.0 eq), Et$_3$N, DCM, rt, overnight (35% − 78%)

Entry	R₁	R₂	Product	Yield (%)
1	H	CH$_2$-Ph	**170h**	56
2	H	*p*-F-Ph	**170i**	58
3	H	CH$_2$-thiophene	**170j**	45
4	H	CH$_2$-*m*-Pyr	**170k**	42
5	H	(CH$_2$)$_2$-O-CH$_3$	**170l**	78
6	Pyrrolidine		**170m**	68

Table 6.6: Isolated yields for the 3,5-disubstituted isoxazoles with an amide moiety at position 3 **170h-m**

The results described in paragraphs 2 and 3 have been reported in the manuscript entitled "*A Versatile Strategy for the Synthesis of 4,5-Dihydroxy-2,3-Pentanedione (DPD) and Related Compounds as Potential Modulators of Bacterial Quorum Sensing*" published in *Molecules* on 6th October 2018 (Stotani S. *et al.*, Molecules **2018**, *23(10)*, 2545)[253] (see Appendix 1).

6.4   Synthesis of monosubstituted isoquinolines and derivatives

Traditional isoquinoline synthetic methods based on strong acidic catalysis (e.g., Pomeranz−Fritsch,[312] Bischler-Napieralski,[313] Pictet-Spengler[314]) have been superseded over the years with milder late transition metal catalyzed approaches. For the synthesis of the set of monosubstituted isoquinolines (and derivatives) a one pot, microwave-assisted and palladium catalyzed strategy where terminal alkyne **40** was coupled with *o*-bromoaldehydes was selected. The resulting Sonogashira products were then reacted with ammonium acetate as imination reagent and, lastly, deprotected.[315] Following Yang *et al.*, alkyne **40** was dissolved in DMF together with Pd(OAc)$_2$, PPh$_3$, KOAc and the corresponding *o*-bromoaldehyde. After microwave irradiation for 1h – 2h, disappearance of the starting material and formation of the corresponding alkynilation products were confirmed by UHPLC. Further addition of an excess (1.8 eq) of ammonium acetate resulted, after 2h – 3h, in the formation of the desired protected products **173a-g** (Scheme 6.9).
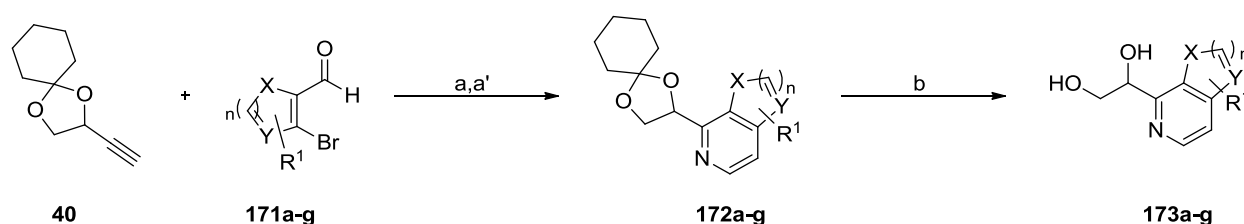
Scheme 6.9: Synthesis of monosubstituted isoquinolines and derivatives **173a-g**. Reagents and conditions: (a) **171a-g** (0.9 eq), Pd(OAc)$_2$ (1.8% mol), PPh$_3$ (3.6% mol), KOAc (1.8 eq), DMF, MW, 80 °C, 1h – 2h; (a') NH$_4$OAc (1.8 eq), MW, 150 °C, 2h – 3h; (b) 12M HCl (cat.), 1,4-dioxane, 0°C to rt, 1h – 3h

Both electron donating (i.e., CH$_3$ and OH, **171b** and **171c**, respectively) and electron withdrawing groups (i.e., F, **171d**) in different positions on the *o*-bromobenzaldehyde were well tolerated. To further increase the variability of our set of compounds, heteroaromatic *o*-bromoaldehydes (i.e., 3-bromo-2-formylfuran, 3-bromothiophene-2-carbaldehyde and 5-bromo-2-methyl-4-thiazolecarboxaldehyde) were selected to isolate the corresponding furopyridine, thienopyridine and thiazolopyridine **172e-g**. Final acidic removal of the

acetal protecting group yielded the desired seven novel monosubstituted isoquinolines (and derivatives) compounds **173a-g** (Table 6.7).

Entry	n	X	Y	R$_1$	Product	Yield (%)
1	2	H	H	H	**173a**	90
2	2	H	H	*p*-CH$_3$-Ph	**173b**	54
3	2	H	H	*m*-OH-Ph	**173c**	67
4	2	H	H	*o*-F-Ph	**173d**	42
5	1	O	H	H	**173e**	48
6	1	S	H	H	**173f**	73
7	1	S	N	CH$_3$	**173g**	70

Table 6.7: Isolated yields for monosubstituted isoquinolines and derivatives **173a-g**

6.5 Synthesis of 2,4,6-trisubstituted pyrimidines

From a synthetic point of view, pyrimidines are versatile substrates and this has facilitated, over the years, the generation of several structurally diverse derivatives bearing substitutions at C$_2$, C$_4$, C$_5$, C$_6$ or on the pyrimidinic nitrogen.[316,317] To access to the small set of 2,4,6-trisubstituted pyrimidines DPD-related compounds, was originally selected a one pot Sonogashira coupling of terminal alkyne **40** and acyl chlorides, followed by addition, to the corresponding ynone, of amidinium salts.[318] Choosing benzoyl chloride as acylating agent and acetamidine hydrochloride as amidinium salt and performing the reaction in one pot (following Karpov *et al.*[318]) resulted in a complex mixture and no formation of the corresponding ynone was observed. Ynone **174a** was therefore isolated prior to add the amidinium salt and, surprisingly, the yield was only 15%.
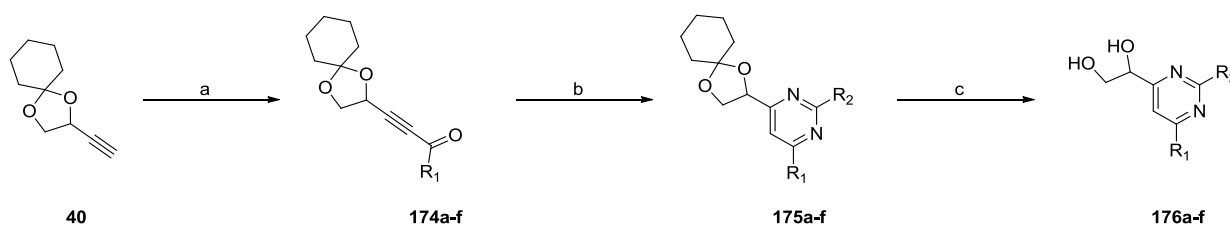
Scheme 6.10: Synthesis of 2,4,6-trisubstituted pyrimidines **190a-f**. Reagents and conditions: (a) R$_1$COCl (1.5 eq), PdCl$_2$(PPh$_3$)$_2$ (9% mol), CuI (3% mol), Et$_3$N (1.25 eq), THF, rt, overnight (52% – 71%); (b) R$_2$NHNH$_2$*HCl (1.2 eq), Na$_2$CO$_3$*10 H$_2$O (3.0 eq), 40 °C, overnight (42% – 62%); (c) 12M HCl (cat.), 1,4-dioxane, 0 °C to rt, 3h (43% – 82%).

Three different conditions were therefore tested to optimize ynone formation. (Table 6.8). Copper-, ligand- and solvent-free acylation (Table 6.8, entry 1)[319] as well as the use of a mixture of PdCl$_2$(CH$_3$CN)$_2$, Sphos and Cs$_2$CO$_3$ (Table 6.8, entry 2)[260] didn't show product formation by UHPLC. Lastly, the use of the copper- and palladium-catalyzed system proposed by Karpov *et al.*[318] resulted in **174a** with 87% yield.

Entry	PhCOCl (eq)	Solvent	Catalyst/Base	Time (h)	Temp (°C)	Yield (%)	Ref.
1	1.0	THF	Pd(OAc)$_2$ (2% mol) Et$_3$N (1.0 eq)	12	rt	–	[319]
2	1.5	THF	PdCl$_2$(CD$_3$CN)$_2$ (5% mol) Sphos (10% mol) Cs$_2$CO$_3$ (1.2 eq)	24	60	–	[260]
3	1.5	THF	PdCl$_2$(PPh$_3$)$_2$ (9% mol) CuI (3% mol) Et$_3$N (1.25 eq)	12	rt	87	[320]

Table 6.8: Screening of the conditions for the synthesis of ynone **174a**

Three different acyl chlorides (i.e., benzoyl chloride, cyclopropane carbonyl chloride and 2-thiophenecarbonyl chloride) were selected to be coupled with terminal alkyne **40**. To further speed up the synthetic protocol, the corresponding ynones were not isolated but the reaction mixtures were worked up to remove salts and metal catalysts before addition of six different amidinium salts. Final acidic deprotection under acidic conditions afforded the desired 2,4,6-trisubstituted pyrimidines **176a-f** with moderate to excellent yields (i.e., 43% – 82%, Table 6.9).

Entry	R$_1$	R$_2$	Product	Yield (%)
1	Ph	CH$_3$	**176a**	54
2	Ph	Cyp	**176b**	53
3	Cyp	Ph	**176c**	46
4	Cyp	*p*-Pyr	**176d**	67
5	2-thiophene	*n*-Propyl	**176e**	71
6	2-thiophene	*m*-F-Ph	**176f**	82

Table 6.9: Isolated yields for the 2,4,6-trisubstituted pyrimidines **176a-f**

6.6 Synthesis of 2,3,4,6-tetrasubstituted pyridines

Since the development of the Bohlmann-Rahtz pyridine synthesis in 1957,[321] many variations of this Michael addition between an enamine with an electron-withdrawing (EWG) group and an ynone have been reported. Having established optimal conditions to produce the Michael acceptors (i.e., ynones), β-aminocrotonate was selected as nucleophile. Following Bagley *et al.*, to a mixture of the latter and **174a** was added acetic acid as Brønsted acid to promote the conjugate addition (Table 6.10, entry 1).[322] Neither the pyridine product nor the intermediate (i.e., the Michael adduct) could be observed by ^{1}H NMR and UHPLC. Following a microwave-assisted protocol developed by the same research group to prepare tri- or tetrasubstituted pyridines, the desired 2,3,4,6-tetrasubstituted pyridine **177a** could be isolated after 20 minutes of microwave irradiation at 170 °C of a DMSO solution of the two starting materials (Table 6.10, entry 2).[323] The absence of the Brønsted acid (i.e., acetic acid) proved to be beneficial for the success of the reaction and prompted me to test a new, one-pot, three-component and acid-free methodology developed by Bagley's group. This heteroannulation combines an alkynone (i.e., the Michael acceptor) with a 1,3-dicarbonyl compound (i.e., the nucleophile) in the presence of an excess (10.0 eq) of ammonium acetate (to generate, *in situ*, the

enamine).[324] Ethyl acetoacetate was selected as nucleophile to have, as for the case of β-aminocrotonate, an additional diversification point (i.e., the carboxylic ester moiety) and reaction with **174a** in refluxing ethanol provided intermediate **177a** with 92% yield (Table 6.10, entry 3).
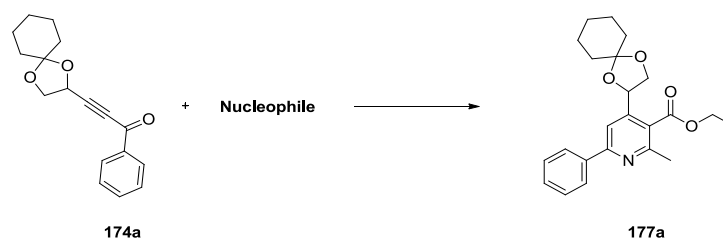
Entry	Nucleophile, eq	Solvent	Time (h)	Temp (°C)	Yield 191a(%)	Ref.
1	β-aminocrotonate, 0.8	PhMe: AcOH (5:1)	12	50	–	322
2	β-aminocrotonate, 2.0	DMSO	0.3	170 (MW)	6	323
3	Ethyl acetoacetate, 10.0	EtOH	12	50	92	324

Table 6.10: Screening of the conditions for the synthesis of **177a**

Having in my hands tetrasubstituted pyridines **177a-b**, my plan was to follow two different strategies: (i) remove the acetal to have the corresponding free diols **178a-b** still maintaining the carboxylic ester moiety and (ii) hydrolize the ester and deprotect the acetal to isolate the free diols **180a-b** with a carboxylic acid moiety at position 3 (Scheme 6.11).
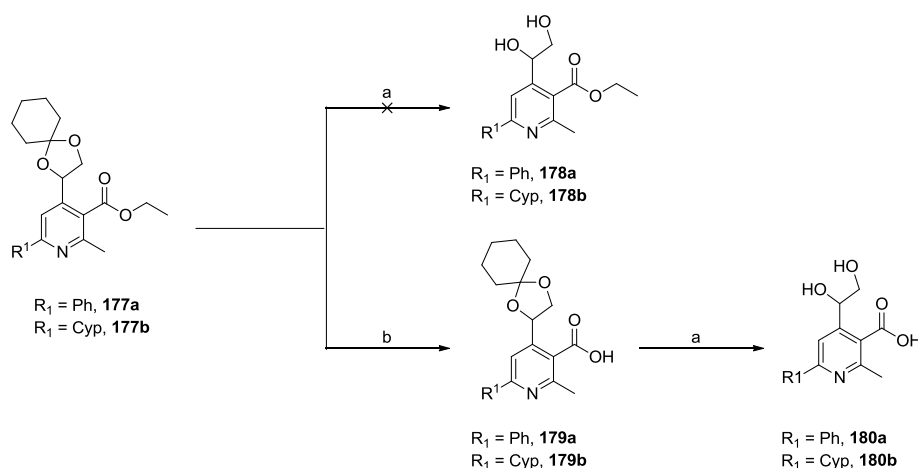
Scheme 6.11: Different strategies for the manipulation of **177a-b**. Reagents and conditions: (a) 12M HCl (cat.), 1,4-dioxane, 0°C to rt, 1h – 3h (80% for **180a** and 72% for **180b**); (b) 1M NaOH (3.0 eq), EtOH, 0 °C to rt, overnight.

This second approach proceeded smoothly: basic hydrolysis of the ester was followed by acidic removal of the acetal protecting group to isolate the desired compounds **180a-b** with excellent yields (i.e., 80% and 72%, respectively). Deprotect the acetal while keeping the carboxylic ester moiety at position 3 proved to be challenging: five different conditions were screened and none of them was successful. The use of our

standard deprotection protocol (i.e., 12M HCl (cat.), 1,4-dioxane, 0 °C to rt) on intermediate **177b** resulted in acetal removal as well as hydrolysis of the ester to obtain compound **180b** instead of **178b** (Table 6.11, entry 1). The same outcome was achieved with EtOH as a solvent and diluted HCl. (Table 6.11, entry 2). Milder conditions (i.e., AcOH, Dowex50WX8, TFA Table 6.11, entry 3 – 5) were not able to remove the protecting group even when the mixtures were stirred for longer time (i.e., 12 hours instead of one hour) and at 40 °C.

Entry	Acid	Solvent	Temp (°C)	Time (h)	Result
1	12M HCl (cat.)	1,4-dioxane	0 to rt	1	**180b**
2	1M HCl (cat.)	EtOH	0 to rt	1	**180b**
3	AcOH	–	0 to 40	12	**177b**
4	Dowex50WX8 100-200 mesh	MeOH	Rt	12	**177b**
5	TFA	–	0 to 40	12	**177b**

Table 6.11: Acidic conditions tested for the deprotection of **177b**

6.7 Synthesis of 3,5-disubtituted and 1,3,5-trisubstituted pyrazoles

Classical synthetic approaches towards substituted pyrazoles are based on the condensation between hydrazines and 1,3-dicarbonyls (or α,β-unsaturated carbonyls) such as the Paal-Knorr synthesis or on [3+2] intermolecular cycloadditions of dipolarophiles (e.g., alkenes and alkynes) with diazo compounds (e.g., Pechmann-pyrazole synthesis).[325–333] Novel methodologies have been developed during the years like the regioselective condensation of ynones and (un)substituted hydrazines. The regioselectivity is the result of an initial 1,4-conjugate addition of the more nucleophilic hydrazinic nitrogen to the ynone's triple bond followed by cyclization of the second hydrazinic nitrogen with the carbonyl group in a favored 5-*exo*-trig process and final dehydration (Figure 6.5).[329]
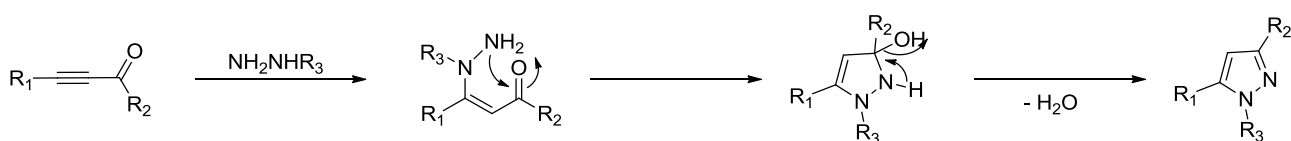
Figure 6.5: Mechanism of the regioselective condensation of ynones and (un)substituted hydrazines

Three additional aliphatic (i.e., isopropyl, cyclopentyl and adamantane) and one aromatic (i.e., furanyl) ynones were synthesized and each of the seven ynones in my hands was reacted with two different hydrazines (i.e., hydrazine and methylhydrazine) to generate, respectively, 3,5-disubstituted and 1,3,5-trisubstituted protected pyrazoles. Final acidic deprotection afforded the targeted products **183a-g** and **184a-g** with excellent yields (i.e., 67% – 92%, Scheme 6.12 and Table 6.12).
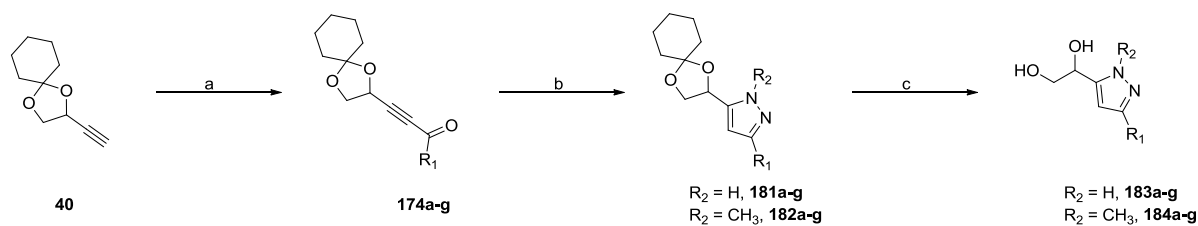
Scheme 6.12: Synthesis of 3,5-disubstituted and 1,3,5-trisubstitted pyrazoles **183a-g** and **184a-g**. Reagents and conditions: (a) R_1COCl (1.5 eq), $PdCl_2(PPh_3)_2$ (9% mol), CuI (3% mol), Et_3N (1.25 eq), THF, rt, overnight (49% − 80%); (b) R_2NHNH_2 (1.3 eq), EtOH, rt, overnight (52% − 89%); (c) 12 M HCl (cat.), 1,4-dioxane, 0 °C to rt, 1h − 3h (67% − 92%)

Entry	R_1	R_2	Product	Yield (%)
1	Ph	H	**183a**	88
2	Ph	CH_3	**184a**	79
3	2-furanyl	H	**183b**	82
4	2-furanyl	CH_3	**184b**	85
5	2-thiophene	H	**183c**	83
6	2-thiophene	CH_3	**174c**	76
7	*i*-Pr	H	**183d**	87
8	*i*-Pr	CH_3	**184d**	77
9	Cyp	H	**183e**	89
10	Cyp	CH_3	**184e**	92
11	Cypentyl	H	**183f**	82
12	Cyclopentyl	CH_3	**184f**	78
13	Adamantane	H	**183g**	75
14	Adamantane	CH_3	**184g**	67

Table 6.12: Isolated yields for the 3,5-disubstituted and 1,3,5-trisubstituted pyrazoles **183a-g** and **184a-g**.

An additional set of six 1,3,5-trisubstituted pyrazoles was prepared strating from ynone **174a**. The N_1-nitrogen was derivatized with aliphatic (linear, branched and cyclic) and aromatic substituents by addition of an excess (1.3 eq) of the corresponding hydrazine. No final acidic deprotection was required in order to keep constant the six member ring protection of the acetal (Scheme 6.13 and Table 6.13).
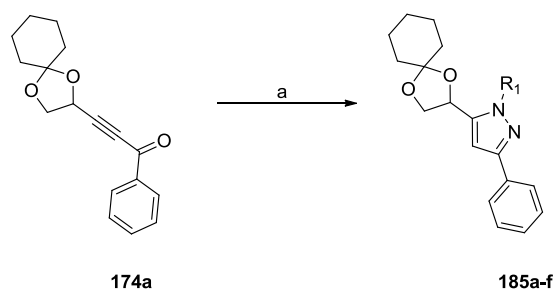
Scheme 6.13: Synthesis of the first new set of 1,3,5-trisubstituted pyrazoles **185a-f**. Reagents and conditions: (a) R_1NHNH_2 (1.3 eq), EtOH, rt, overnight (41% − 70%).

Entry	R_1	Product	Yield (%)
1	CH_2-CH_3	**185a**	44
2	*i*-Pr	**185b**	60
3	Cyp	**185c**	54
4	$(CH_2)_2$-CN	**185d**	41
5	Cyclopentyl	**185e**	70
6	Ph	**185f**	55

Table 6.13: Isolated yields for the first new set of 1,3,5-trisubstituted pyrazoles **185a-f**

To generate the second new set of pyrazoles where the phenyl at position three was replaced with other aliphatic, aromatic and heteroaromatic rings, the same conditions as Scheme 6.12 were reproduced and seven ynones were synthesized and afterward condensed with methylhydrazine (Scheme 6.14 and Table 6.14).
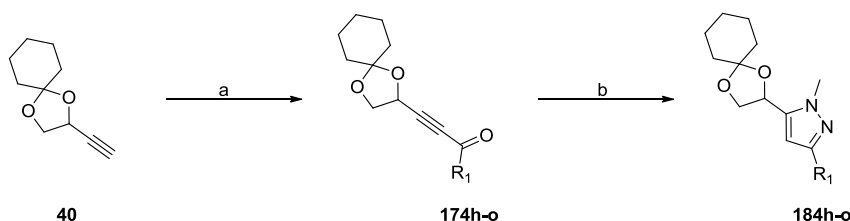
Scheme 6.14: Synthesis of the second new set of 1,3,5-trisubstituted pyrazoles **184h-o**. Reagents and conditions: (a) R_1COCl (1.5 eq), $PdCl_2(PPh_3)_2$ (9% mol), CuI (3% mol), Et_3N (1.25 eq), THF, rt, overnight (52% − 81%); (b) $MeNHNH_2$ (1.3 eq), EtOH, rt, overnight (41% − 65%)

Entry	R_1	Product	Yield (%)
1	*m*-CH_3-Ph	**184h**	54
2	*m*-CN-Ph	**184i**	65
3	*m*-F, *m*-Cl-Ph	**184j**	61
4	*p*-NH_2-Ph	**184k**	41
5	3-isoxazole	**184l**	55
6	2-indole	**184m**	46
7	*m*-Pyr	**184n**	47
8	CyHex	**184o**	55

Table 3.14: Isolated yields for the second new set of 1,3,5-trisubstituted pyrazoles **184h-o**

More efforts were required for the third and last set of diversifications concerning the acetal protection. To completely remove the latter (and therefore the diol moiety), benzoyl chloride was reacted with 1-propyne and the resulting ynone with methylhydrazine (Scheme 6.15 A). To change the size of the protecting group, free diol **152** was protected with an excess (3.0 eq) of the corresponding ketone and a catalytic amount of *p*-TSA in neat conditions. Further acylation with benzoyl chloride and condensation with methylhydrazine afforded the desired five new pyrazoles **189a-d** (Scheme 6.15 B and Table 6.15). 4-piperidone was found not to be suitable for our purpose as the free basic nitrogen impeded the Sonogashira coupling with benzoyl chloride while *N*-acetylpiperidone did not show any reactivity issue and compound **189d** could be isolated with good yield (i.e., 44%, Table 6.15, entry 3).
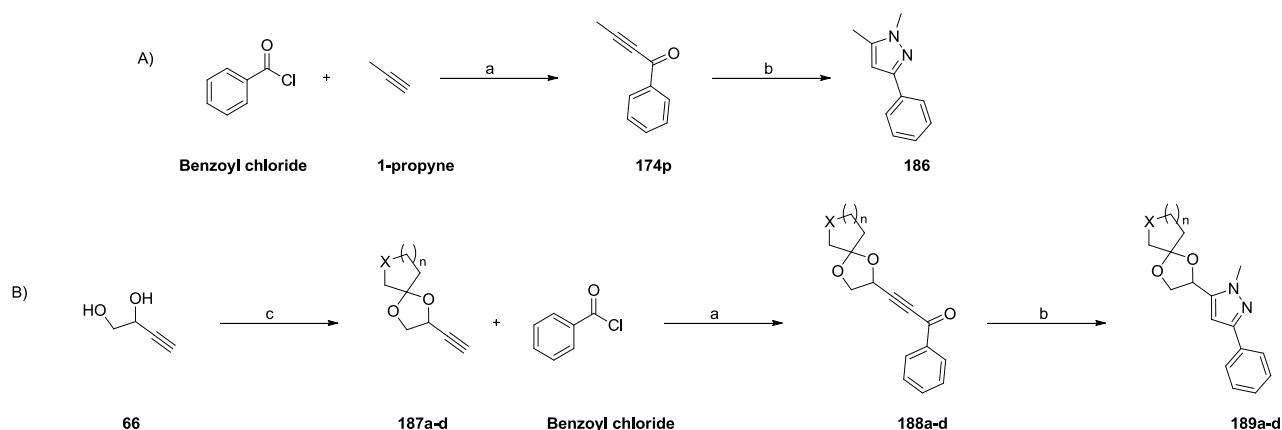
Scheme 6.15: Synthesis of the third new set of 1,3,5-trisubstituted pyrazoles. A) Synthesis of compound **186** and B) Synthesis of compounds **189a-d**. Reagents and conditions: (a) 1-propyne (1.5 eq), PdCl$_2$(PPh$_3$)$_2$ (9% mol), CuI (3% mol), Et$_3$N (1.25 eq), THF, rt, overnight (42% − 79%); (b) MeNHNH$_2$ (1.3 eq), EtOH, rt, overnight (44% − 85%); (c) Ketone (3.0 eq), *p*-TSA (cat.), rt, overnight (35% − 72%)

Entry	X	n	Product	Yield (%)
1	H	0	**189a**	69
2	H	2	**189b**	57
3	O	1	**189c**	85
4	*N*-Ac	1	**189d**	44

Table 6.15: Isolated yields for the third new set of 1,3,5-trisubstituted pyrazoles **189a-d**

The results described in paragraphs 4 − 7 have and 3 have been submitted to *Journal of Medicinal Chemistry* on January 5th in a manuscript entitled *"DPD-inspired discovery of novel LsrK kinase inhibitors: an opportunity to fight antimicrobial resistance"*.

6.8   Synthesis of disubstituted indoles and derivatives

In this paragraph I will describe the attempts to synthesize an additional series of DPD-derivatives with an indole core. Indole is a popular pharmacophore in several research areas (e.g., agrochemicals, fragrances, pharmaceuticals) and many efforts have been devoted in the last decades to the development of more and efficient synthetic protocols towards its preparation and functionalization.

Four different one pot synthetic strategies, all based on consecutive metal-catalyzed Sonogashira coupling followed by intramolecular cyclization, were screened in parallel (Table 6.16).

The coupling of *o*-chloroiodobenzene **190a** with **40** in a multicatalytic system (HIPrCl, Pd(OAc)$_2$ and CuI) and subsequent addition of *p*-fluoroaniline in basic conditions (Table 6.16, entry 1) did not show any sign of product formation by UHPLC.[334] Same unsuccessful outcome derived from a one pot three component Sonogashira-Cacchi domino reaction where *o*-iodo-*N*-trifluoroacetylanilide **190b** was mixed with **40**, catalytic amounts of Pd(OAc)$_2$ and PPh$_3$ and an excess of K$_2$CO$_3$ and PhBr in DMF and stirred at 60 °C overnight: a complicate mixture was observed by UHPLC and the major peaks could not be identified (Table 6.16, entry 2).[335] Inconclusive chromatogram was the result of a one pot consecutive palladium-catalyzed Sonogashira reaction followed by amidopalladation and reductive elimination (Table 6.16, entry 3).[336]

Lastly, a palladium-free domino coupling/cyclization of **40** with *o*-bromo-*N*-trifluoroacetylanilide **190c** afforded the desired indole **191b** (Table 6.16, entry 4). The CuI/L-proline system and the ortho-substituent effect of the trifluoroacetamido group allowed coupling and the subsequent CuI-mediated cyclization process.[337]
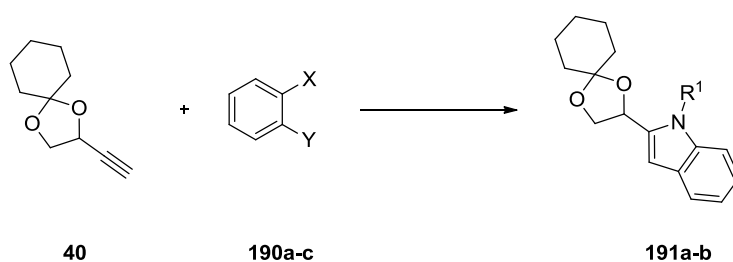
Entry	190a-c, eq	X	Y	R$_1$	Solvent	Catalyst/Base	Product	Time(h)	Temp (°C)	Ref
1	**190a**, 0.7	I	Cl	*p*-F-Ph (1.2 eq)	PhMe	CuI (10% mol) Pd(OAc)$_2$ (10% mol) HIPrCl (10% mol) Cs$_2$CO$_3$ (1.5 eq) *t*-BuOK (1.5 eq)	**191a**	20	105	334
2	**190b**, 0.8	I	NHCOCF$_3$	H	DMF	Pd(OAc)$_2$ (5% mol) PPh$_3$ (0.2 eq) K$_2$CO$_3$ (4.0 eq) PhBr (1.2 eq)	**191b**	12	60	335
3	**190c**, 1.0	Br	NHCOCF$_3$	H	DMF	PdCl$_2$(PhCN)$_2$ (3% mol) X-Phos (12% mol) Cs$_2$CO$_3$ (3.0 eq) PhBr (1.2 eq)	**191b**	12	80	336
4	**190c**, 1.0	Br	NHCOCF$_3$	H	DMF	CuI (2% mol) L-proline (6% mol) K$_2$CO$_3$ (2.0 eq)	**191b**	24	80	337

Table 6.16: Screening of the conditions for the synthesis of indoles **191a-b**

Prompted by the success of the last conditions screened (intermediate **191b** was isolated in 50% yield), I proceeded further with the production of a small indole-based library of DPD-related compounds. The starting materials for the coupling (i.e., the *o*-bromotrifluroacetanylides) were synthesized in excellent yields (i.e., 80% − 97%, see Chapter 8.1.10) by acylation of the corresponding *o*-bromoanilines.
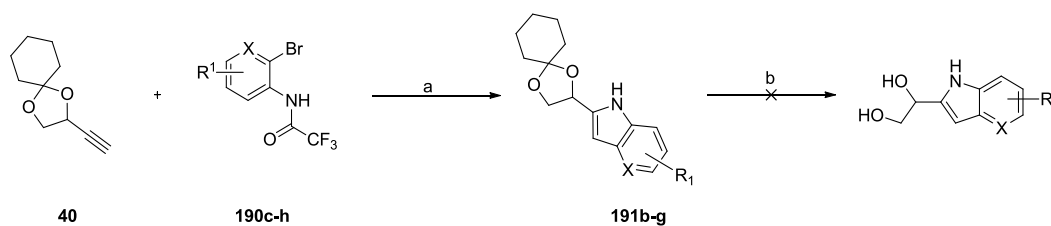
Scheme 6.16: Synthesis of substituted indoles **191b-g**. Reagents and conditions: (a) **190c-h** (1.0 eq), CuI (2% mol), L-proline (6% mol) K$_2$CO$_3$ (2.0 eq), DMF, 80 °C, 2d – 7d (3% – 14%); (b) see Table 6.18

Entry	X	R$_1$	Product	Yield (%)
1	H	H	**191b**	50
2	H	p-OMe	**191c**	7
3	H	m-CF$_3$	**191d**	14
4	H	p-COOMe	**191e**	3
5	H	m-Cl	**191f**	5
6	N	H	**191g**	9

Table 6.17: Isolated yields for the substituted indoles and derivatives **191b-g**

Independently from the electron withdrawing or electron donating nature of the substituents on the starting materials, all of the products were isolated with insignificant yields (i.e., <15%, Table 6.17) and the reactions proceeded very slow (2 days – 7 days). Additional problems were encountered in the removal of the acetal protecting group as none of the conditions tested was effective. Decomposition was observed when using a catalytic amount of concentrated or diluted HCl in both 1,4-dioxane and THF (Table 6.18, entry 1 – 3 and 5 – 6). Milder acidic conditions (i.e., TFA or AcOH, Table 6.18, entry 4 and 8, respectively) resulted in unreacted starting materials. Transacetalization with acetone and p-TSA (Table 6.18, entry 9), deprotection with Dowex 50WX8 (Table 6.18, entry 7) or the use of p-toluenesulfonyl hydrazide polymer as ketone scavenger (Table 6.18, entry 10) caused, respectively, decomposition or no reaction. Unfortunately, the desired DPD-analogues with an indole core could not be synthesized and we were able to isolate, with very poor yields, only their corresponding acetal protected precursors **191b-g**. As the removal of the acetal failed, I decided not to focus on increasing the yields for the indole formation.

Entry	Starting material	Acid	Solvent	Temp (°C)	Result
1	**191b**	12M HCl (cat.)	1,4-dioxane	0 to rt	Decomposition
2	**191b**	1M HCl (cat.)	1,4-dioxane	0 to rt	Decomposition
3	**191b**	1M HCl (cat.)	THF	0 to rt	Decomposition
4	**191b**	TFA	–	Rt	**190c**
5	**191c**	1M HCl (cat.)	1,4-dioxane	0 to rt	Decomposition
6	**191c**	1M HCl (cat.)	THF	0 to rt	Decomposition
7	**191c**	Dowex 50WX8 100-200 mesh	MeOH	Rt	Decomposition
8	**191c**	AcOH (cat.)	Water	Rt	**190d**
9	**191c**	*p*-TSA (cat.)	Acetone	Rt	Decomposition
10	**191c**	In(Otf)$_3$ (cat.) *p*-toluenesulfonyl hydrazide polymer	THF	rt to 40	**190d**

Table 6.18: Conditions tested to deprotect indoles **191b-c**

7. BIOLOGICAL RESULTS

In Chapter 5 I described the state of the art of all the DPD-analogues reported in the literature. The compounds were often evaluated as QSI in *E. coli*, *S. thyphimurium* and *V. harveyi* using mostly two types of assays: QS-induced bioluminescence (for *V. harveyi* strains BB120, BB170, MM30, MM32) and QS-mediated induction of β-galactosidase (for *E. coli* and *S. thyphimurium*). In this chapter I will briefly describe this two assays and the D-luciferin-based assay developed by my collaborators at the University of Helsinki (Finland) to evaluate LsrK kinase inhibition. The chapter also includes the results of the biological evaluation of the sets of compounds described in Chapter 6.

7.1 *V. harveyi* and β-galactosidase bioluminescence assays

Three different QS signals have been identified in *V. harveyi:*

1) AHL, produced by LuxM it binds to the membrane bound protein LuxN;
2) AI-2, produced by LuxS it binds (in the form of the furanosyl borate ester ‚*S*-THMF-borate) to LuxP (PDB ID: 1JX6[129]) and the *S*-THMF-borate-LuxP-complex interacts with LuxQ in the membrane;
3) CAI-1, produced by CqsA, it interacts with CqsS.

The three cognate receptors (i.e., LuxN, LuxQ and CsqQ) are histidine sensor kinases bound to the cell membrane. At low cell density, the three receptors phosphorylate LuxO (via LuxU) to form phospho-LuxO (P-LuxO). Together with σ54, P-LuxO synthesizes silent RNAs (sRNAs) that, upon interaction with the RNA chaperon hfq, degrade *luxR* mRNA. At high cell density, the receptors bind their respective autoinducers and switch from kinases to phosphatases. Phosphate is removed from LuxO allowing translation of *luxR* mRNA and LuxR-mediated bioluminescence (Figure 7.1).[95,129,338]
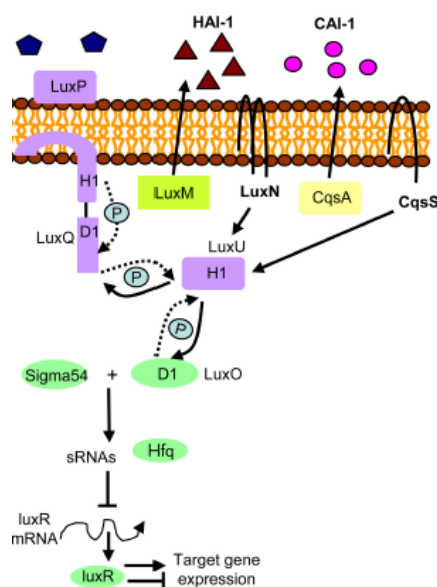
Figure 7.1: Quorum Sensing pathways in *V. harveyi*. Figure adapted with permission from *Enzyme Microb. Technol.* **2011**, *49* (2), 113–123. Copyright 2011 Elsevier

In chapter 5, the synthesis and biological evaluation of different DPD-analogues is reported. The strains used to measure bioluminescence are BB120, BB170, MM30 and MM32.

BB120 is the *wild type*;

BB170 is a LuxN (-) mutant;

MM30 is a LuxS (-) mutant;

MM32 is a LuxN (-)/ LuxS (-) double mutant

The strains are chosen based on the scope of the authors: a LuxN (-) mutant can produce bioluminescence through the AI-2-mediated pathway but not through the AHL system. The use of *V. harveyi* BB170 therefore excludes the possibility of the tested compounds to be recognized by the AHL receptor and, if they affect bioluminescence, they do it through the AI-2 system.

β-galactosidase is an enzyme that breaks glycosidic bonds to hydrolyze β-galactosides into monosaccharides. In *E. coli* and *S. thyphimurium*, the structural gene for β-galactosidase is the *lacZ* gene. The strains used in the assays reported in Chapter 5 to measure AI-2 mediated-QS (Met708, Met715 and Met844) are LuxS(-), *lsr-lacZ* fusion and they are incapable of producing their own DPD. The *lsr-lacZ* fusion encodes for β-galactosidase under the control of the *lsr* promoter and AI-2-dependent lsr expression can be measured based on the residual β-galactosidase activity: the higher is the residual activity, the lower is the activity of the inhibitors.[339]

7.2 The D-luciferin-based LsrK kinase assay

The assay developed by Zhu *et al.*[230] to measure LsrK kinase activity is a coupled assay where ATP consumption (and the corresponding production of ADP) is coupled with pyruvate kinase- and lactate dehydrogenase-mediated oxidation of NADH (see Chapter 2, Figure 2.5).

My collaborators at the University of Helsinki (Finland) developed a D-luciferin-based bioluminescence assay that could be automatized to screen up to 1536 well plates.

The previously reported assay requires the overexpression of two additional enzymes (i.e., pyruvate kinase and lactate dehydrogenase) and also suffers from signal instability. The new assay uses the Glo Luminescence kit from Promega (USA) where the luminescent signal is inversely proportional to the amount of kinase activity and supports up to 500 μM ATP. To reduce interference between wells on the 384 well plate, 100 μM ATP was used. Reagents stability and concentration, DMSO tolerance (up to 5%) and signal stability (up to 5 hours upon addition of Glo Luminescence kit components) were carefully evaluated. Optimal reaction time was estimated to be 15 minutes. All the assay components were found to be stable at room temperature and functional after 5 freeze/thaw cycles with the only exception of *S*-DPD for which fresh aliquots should be used each time.

To evaluate enzymatic activity, LsrK was overexpressed and purified as described in Chapter 8.3.5. The activity was detected in the presence of 200 nM LsrK, 200 μM *S*-DPD (from OMM Scientific) and 20 μM ATP in a 96 well plate format (Figure 7.2).
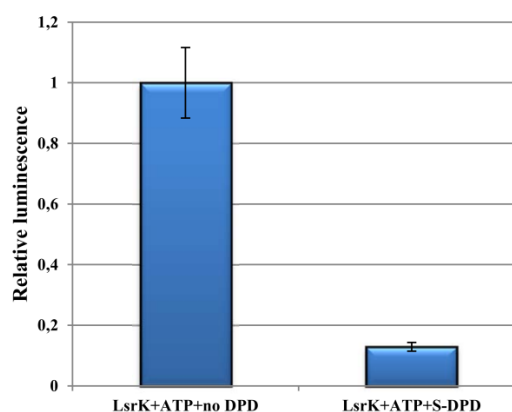
Figure 7.2: Activity of LsrK. 200 nM LsrK, 20 μM ATP, 200 μM *S*-DPD. Glycerokinase activity: 0.5 μg/mL glycerokinase, 200 μM glycerol, 20 μM ATP

LsrK is a member of the FGGY kinase family, a family of kinases that phosphorylate different sugars. To test LsrK specificity, a small set of sugars (i.e., glycerol, meso erythritol, 6-phosphogluconic acid, D-ribulose, L-ribulose) with similar structure to DPD was evaluated using the same ATP depletion assay previously reported. All the compounds were tested at 200 μM and 400 μM (Figure 7.3).
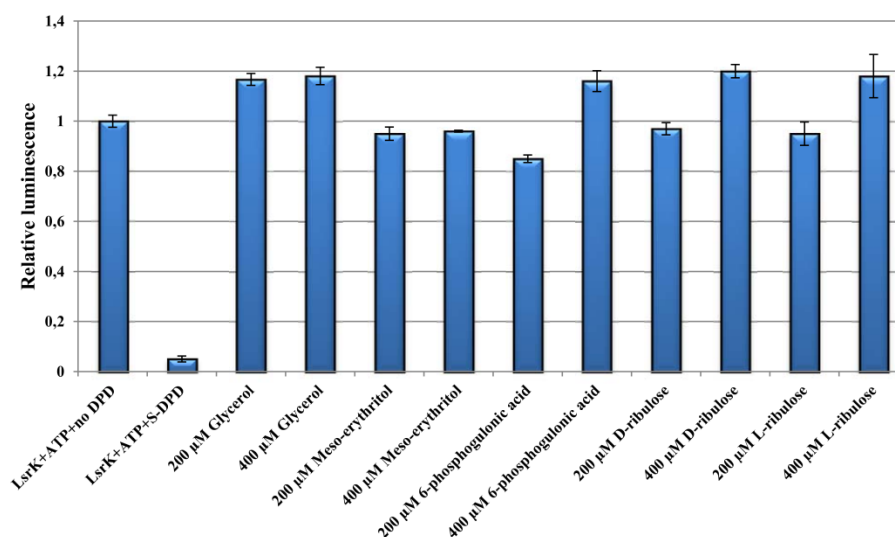
Figure 7.3: LsrK activity in the presence of different sugars

7.3 Activity of synthesized DPD and DPD-related compounds

The activity of the synthetized racemic-DPD (see Chapter 4) and DPD-related compounds (see Chapter 6) was evaluated with the newly developed bioluminescence-based assay against LsrK (see Chapter 8.3.6 and 8.3.7, respectively). Racemic-DPD prepared as described in Chapter 4 is efficiently phosphorylated by LsrK. In fact, the level of ATP is significantly reduced by the addition of racemic DPD, resulting in a light emission lower than the sample including only LsrK and ATP. Although phosphorylation of *S*-DPD, the enantiomer recognized by the protein, is higher, the results confirmed the validity of the newly developed racemic synthesis of DPD (described in Chapter 4). The aforementioned results have been reported in the
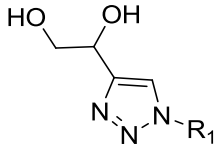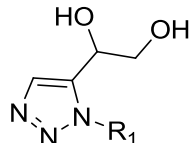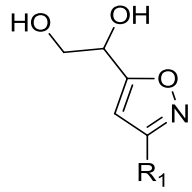
manuscript entitled "*A Versatile Strategy for the Synthesis of 4,5-Dihydroxy-2,3-Pentanedione (DPD) and Related Compounds as Potential Modulators of Bacterial Quorum Sensing*" published in *Molecules* on October 6th 2018 (Stotani S. *et al.*, Molecules **2018**, *23(10)*, 2545)[253] (see Appendix 1, SI).

The same assay was used to measure LsrK kinase inhibition of the eight small libraries of compounds described in Chapter 6 in order to assess their ability to compete with DPD in binding LsrK and therefore their potential as LsrK kinase inhibitors. Table 7.1 shows the percentage of inhibition for each of the synthesized compounds which was measured at 200 µM in the presence of 300 µM DPD.

Four compounds (i.e., **181a**, **182a**, **181b**, **182b**) displayed a percentage of inhibition higher than 40% (Table 7.1) and, for those molecules, dose-response curves were determined at seven different compound concentrations (i.e., 25 µM, 50 µM, 100 µM, 200 µM, 300 µM, 400 µM, 500 µM) and the corresponding IC_{50} values were extrapolated (Figure 7.4). These resulst were submitted to *Journal of Medicinal Chemistry* on January 5th in a manuscript entitled "*DPD-inspired discovery of novel LsrK kinase inhibitors: an opportunity to fight antimicrobial resistance*".
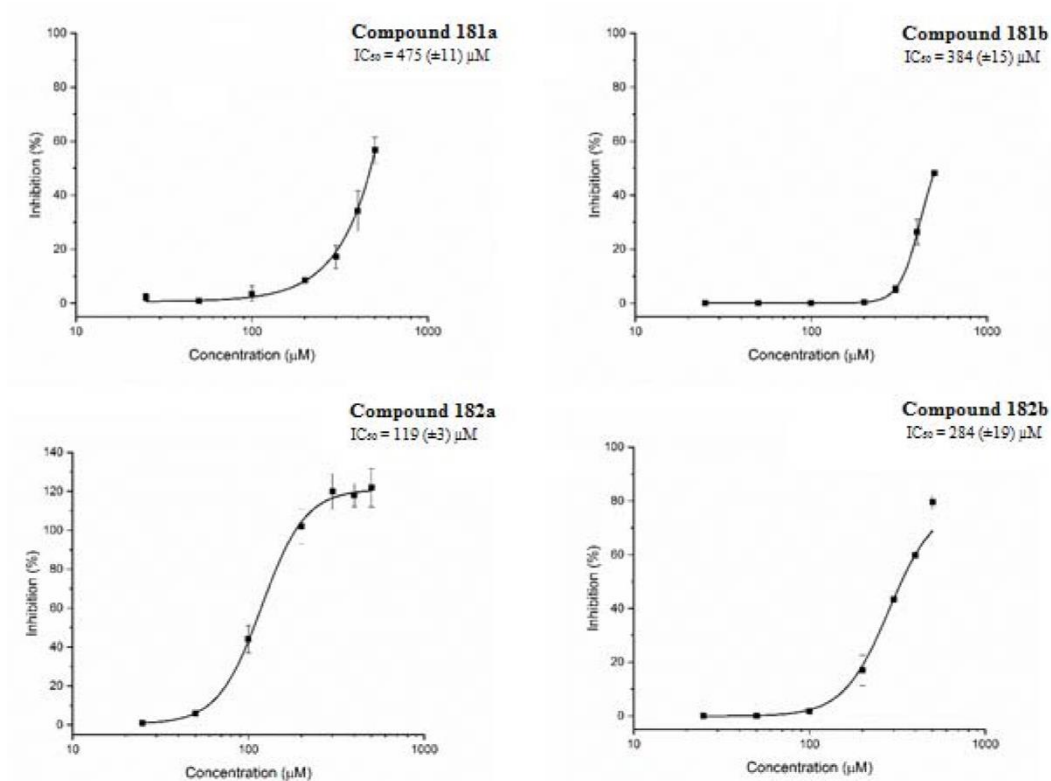
Figure 7.4: IC_{50} values for LsrK kinase inhibition of compounds **181a**, **182**a, **181b**, **182b**

Series	Structure	Compound	R^1	R^2	X	Y	N	Inhibition (%)	SD
1,4-disubstituted 1,2,3-triazoles		154a	$(CH_2)_2$-Ph	—	—	—	—	0	0.14
		154b	(CH_2)-Ph					1.9	1.87
		154c	$(CH_2)_2$-o-F-Ph					3.3	0.54
		154d	$(CH_2)_2$-m-Pyr					0.1	0.37
		154e	$(CH_2)_5$-CN					2.2	2.66
		154f	$(CH_2)_2$-CyH					2.7	0.93
		154g	H					2.3	0.44
		154h	CH_3					2.0	0.12
		154i	CH_2-Cyp					2.5	0.06
		154j	n-Bu					5.5	0.03
		154k	$(CH_2)_2$-O-CH_3CH_2					2.2	0.20
1,5-disubstituted 1,2,3-triazoles		155a	$(CH_2)_2$-Ph	—	—	—	—	2.0	0.31
		155h	CH_3					2.5	0.04
		155i	CH_2-Cyp					1.6	1.16
		155j	n-Bu					2.4	8.64
		155k	$(CH_2)_2$-O-CH_3CH_2					2.0	0.32
3,5-disubstituted isoxazoles		162a	p-CH_3-Ph	—	—	—	—	1.9	0.66
		162b	m-Cl-Ph					0.1	0.40
		162c	o, p-di-F-Ph					0.2	0.27
		162d	m-Pyr					4.8	1.90
		162e	Cyp					8.4	1.13
		162f	m-THF					0.8	1.18
		162g	CyH					5.5	0.27

Series	Structure	Compound	R^1	R^2	X	Y	N	Inhibition (%)	SD
3,5-disubstituted isoxazoles		169h	CH$_2$-Ph	H				2.9	0.46
		169i	p-F-Ph	H				16.9	23.83
		169j	CH$_2$-thiophene	H				31.3	14.31
		169k	CH$_2$-m-Pyr	H	—	—	—	0	0.52
		169l	(CH$_2$)$_2$-O-CH$_3$	H				0	0.08
		169m	Pyrrolidine					0	0.26
3,5-disubstituted isoxazoles		175h	CH$_2$-Ph	H				2.5	0.25
		170i	p-F-Ph	H				2.5	0.11
		170j	CH$_2$-thiophene	H				2.5	0.15
		170k	CH$_2$-m-Pyr	H				1.2	1.15
		170l	(CH$_2$)$_2$-O-CH$_3$	H	—	—	—	1.0	0.90
		170m	Pyrrolidine					2.5	0.35
Isoquinoline and detrivatives		172a	H	—	H	H	H	14.91	1.53
		172b	p-CH$_3$		H	H	2	1.66	1.22
		172c	m-OH		H	H	2	28.55	3.83
		172d	o-F		H	H	2	1.76	0.94
		172e	H		O	H	1	5.75	1.41
		172f	H		S	H	1	11.06	4.02
		172g	CH$_3$		S	N	1	6.32	2.35

110

Series	Structure	Compound	R^1	R^2	X	Y	N	Inhibition (%)	SD
Isoquinoline and detrivatives		173a	H		H	H	2	0.48	0.63
		173b	p-CH$_3$		H	H	2	0.40	0.39
		173c	m-OH		H	H	2	1.67	1.55
		173d	o-F	—	H	H	2	0.65	0.41
		173e	H		O	H	1	2.07	1.00
		173f	H		S	H	1	0.17	0.42
		173g	CH$_3$		S	N	1	0.10	0.42
2,4,6-trisubstituted pyrimidines		175a	Ph	CH$_3$				9.41	1.41
		175b	Ph	Cyp				15.18	4.39
		175c	Cyp	Ph	—	—	—	0.76	0.74
		175d	Cyp	p-Pyr				21.22	3.23
		175e	2-thiophene	n-propyl				0.96	0.85
		175f	2-thiophene	m-F-Ph				0.20	0.33
2,4,6-trisubstituted pyrimidines		176a	Ph	CH$_3$				0.22	0.69
		176b	Ph	Cyp				24.48	3.32
		176c	Cyp	Ph	—	—	—	21.65	2.37
		176d	Cyp	p-Pyr				2.94	1.11
		176e	2-thiophene	n-propyl				47.76	2.94
		176f	2-thiophene	m-F-Ph				19.79	1.42
2,3,4,6-tetrasubstituted pyridines		177a	Ph	CH$_3$CH$_2$				0.10	0.07
		177b	Cyp	CH$_3$CH$_2$				0.36	0.66
		179a	Ph	H	—	—	—	0	1.69
		179b	Cyp	H				6.26	0.65

Series	Structure	Compound	R^1	R^2	X	Y	N	Inhibition (%)	SD
2,3,4,6-tetrasubstituted pyridines	HO, HO, O, OH, R^1, N (structure)	180a	Ph	—	—	—	—	0.81	0.59
		180b	Cyp	—	—	—	—	1.33	0.49
3,5-disubstituted and 1,3,5-trisubstitted pyrazoles	O, O, R^2, N, N, R^1 (structure)	181a	Ph	H				53.60	5.67
		181b	2-furanyl	H				43.48	26.98
		181c	2-thiophene	H				26.50	5.52
		181d	i-Pr	H	—	—	—	7.14	1.78
		181e	Cyp	H				1.47	0.26
		181f	Cyclopentyl	H				0	0.21
		181g	Adamantane	H				0	0.81
		182a	Ph	CH_3				78.05	3.44
		182b	2-furanyl	CH_3				51.63	11.91
		182c	2-thiophene	CH_3				0	0.22
		182d	i-Pr	CH_3				0	0.67
		182e	Cyp	CH_3				0	0.57
		182f	Cyclopentyl	CH_3				0	0.82
		182g	Adamantane	CH_3				0	0.11
		182h	m-CH_3-Ph	CH_3	—	—	—	1.07	0.91
		182i	m-CN-Ph	CH_3				0	0.51
		182j	m-Cl-,m-F-Ph	CH_3				4.42	2.14
		182k	p-N(CH_3)$_2$-Ph	CH_3				0.19	1.11
		182l	3-isoxazole	CH_3				9.83	1.74
		182m	2-indole	CH_3				4.38	2.39
		182n	m-Pyr	CH_3				4.92	5.13
		182o	CyHex	CH_3				1.51	1.50

112

Series	Structure	Compound	R^1	R^2	X	Y	N	Inhibition (%)	SD
3,5-disubstituted and 1,3,5-trisubstitted pyrazoles		183a	Ph	H				0	0.02
		183b	Cyp	H				0	0.05
		183c	2-thiophene	H				0	1.16
		183d	i-Pr	H	—	—	—	0	0.06
		183e	Cyclopentyl	H				0	0.08
		183f	Adamantane	H				0	0.96
		183g	2-furanyl	H				0	0.44
		184a	Ph	CH_3				0	0.46
		184b	Cyp	CH_3				0	0.66
		184c	2-thiophene	CH_3				0	0.05
		184d	i-Pr	CH_3	—	—	—	0	0.24
		184e	Cyclopentyl	CH_3				0	0.47
		184f	Adamantane	CH_3				0	0.32
		184g	2-furanyl	CH_3				0	0.72
3,5-disubstituted pyrazoles		185a	CH_3CH_2					0	0.62
		185b	i-Pr					0	0.96
		185c	Cyp		—	—	—	—	0	0.70
		185d	$(CH_2)_2$-CN					0	0.83
		185e	Cyclopentyl					0	0.59
		185f	Ph					0	0.53

Series	Structure	Compound	R^1	R^2	X	Y	N	Inhibition (%)	SD
3,5-disubstituted pyrazoles		184h	CyHex	—	—	—	—	1.07	0.91
		184i	m-CH$_3$-Ph					0	0.51
		184j	m-CN-Ph					4.42	2.14
		184k	m-Cl-,m-F-Ph					0.19	1.11
		184l	p-NH$_2$-Ph					9.83	1.74
		184m	3-isoxazole					4.38	2.39
		184n	2-indole					4.92	5.13
		184o	m-Pyr					1.51	1.50
3,5-disubstituted pyrazoles		186	—	—	—	—	—	2.01	0.78
3,5-disubstituted pyrazoles		489a	—	—	H	—	0	5.56	2.34
		189b			H		2	0	0.64
		189c			O		1	31.13	1.83
		189d			N-Ac		1	2.07	1.65

Table 7.1: Activities of the synthesized DPD-related compounds (reported in Chapter 6)

8. EXPERIMENTAL

8.1 Chemistry

8.1.1 General

Chemicals and solvents were obtained from commercial suppliers and were used without further purification. All dry reactions were performed under nitrogen atmosphere using commercial dry solvents. Flash column chromatography was performed on a silica column using 230400 mesh silica gel or Grace Reveleris X2 flash chromatography system using silica gel packed Macherey Nagel Chromabond Flash BT cartridges (60 Å, 45 µm) and Grace Reveleris flash Cartridges (60 Å, 40 µm). Thin layer chromatography was performed on Macherey Nagel precoated TLC aluminum sheets with silica gel 60 UV254 (5µm – 17µm). TLC visualization was accomplished by irradiation with a UV lamp (254 nm) and/or staining with $KMnO_4$ solutions. ^{1}H NMR spectra were recorded at room temperature on a Bruker Avance spectrometer operating at 300 MHz. Chemical shifts are given in parts per million (δ, ppm) from tetramethylsilane as an internal standard or residual solvent peak. Significant ^{1}H NMR data are tabulated in the following order: multiplicity (s, singlet; d, doublet; t, triplet; q, quartet; m, multiplet; dd, doublet of doublets; dt, doublet of triplets; td, triplet of doublets; br, broad), coupling constant(s) in hertz, number of protons. Proton decoupled ^{13}C NMR data were acquired at 100 MHz. ^{13}C chemical shifts are reported in parts per million (δ, ppm). All NMR data were collected at room temperature (25 °C). Analytical, preparative HPLC and Electron Spray Ionization (ESI) mass spectra were performed on an Agilent UHPLC (1290 Infinity) and an Agilent Prep-HPLC (1260 Infinity) both equipped with a Diode Array Detector and a Quadrupole MS using mixture gradients of formic acid/water/acetonitrile as solvents. High-resolution electrospray ionization mass spectra (ESI-FTMS) were recorded on a Thermo LTQ Orbitrap (high-resolution mass spectrometer from Thermo Electron) coupled to an 'Accela' HPLC system supplied with a 'Hypersil GOLD' column (Termo Electron).

8.1.2 Failed attempts for the synthesis of DPD

Synthesis of 66 and 68: the procedure for the synthesis of compounds **66** and **68** is described in *Molecules* **2018**, *23(10)*, 2545 (see Appendix 1, SI).[253]

2,2,3,3,8,8,9,9-octamethyl-5-(prop-1-yn-1-yl)-4,7-dioxa-3,8-disiladecane (66): the compound is described in *Molecules* **2018**, *23(10)*, 2545 (see Appendix 1, SI).[253]

2,2,7,7,8,8-hexamethyl-4-(prop-1-yn-1-yl)-3,6-dioxa-2,7-disilanonane (68): the compound is described in *Molecules* **2018**, *23(10)*, 2545 (see Appendix 1, SI).[253]

Synthesis of 67 and 69: the procedure for the synthesis of compounds **67** and **69** is described in *Molecules* **2018**, *23(10)*, 2545 (see Appendix 1, SI).[253]

4,5-bis[(*t*-butyldimethylsilyl)oxy]pentane-2,3-dione (67): the compound is described in *Molecules* **2018**, *23(10)*, 2545 (see Appendix 1, SI).[253]

5-[(*t*-butyldimethylsilyl)oxy]-4-[(trimethylsilyl)oxy]pentane-2,3-dione (69): the compound is described in *Molecules* **2018**, *23(10)*, 2545 (see Appendix 1, SI).[253]

8.1.3 Successful synthesis of *rac*-DPD and *rac*-Ph-DPD

Synthesis of 65a and 65b: the procedure for the synthesis of compounds **65a** and **65b** is described in *Molecules* **2018**, *23(10)*, 2545 (see Appendix 1).[253]

1-[(*t*-butyldimethylsilyl)oxy]pent-3-yn-2-ol (65a): the compound is described in *Molecules* **2018**, *23(10)*, 2545 (see Appendix 1).[253]

1-[(*t*-butyldimethylsilyl)oxy]-4-phenylbut-3-yn-2-ol (65b): the compound is described in *Molecules* **2018**, *23(10)*, 2545 (see Appendix 1).[253]

Synthesis of 64a and 64b: the procedure for the synthesis of compounds **66** and **73** is described in *Molecules* **2018**, *23(10)*, 2545 (see Appendix 1).[253]

Pent-3-yne-1,2-diol (64a): the compound is described in *Molecules* **2018**, *23(10)*, 2545 (see Appendix 1).[253]

4-phenylbut-3-yne-1,2-diol (64b): the compound is described in *Molecules* **2018**, *23(10)*, 2545 (see Appendix 1).[253]

Synthesis of 26a and 26b: the procedure for the synthesis of compounds **26a** and **26b** is described in *Molecules* **2018**, *23(10)*, 2545 (see Appendix 1, SI).[253]

2-(prop-1-yn-1-yl)-1,4-dioxaspiro[4.5]decane (26a): the compound is described in *Molecules* **2018**, *23(10)*, 2545 (see Appendix 1).[253]

2-(2-phenylethynyl)-1,4-dioxaspiro[4.5]decane (26b): the compound is described in *Molecules* **2018**, *23(10)*, 2545 (see Appendix 1).[253]

Synthesis of 27a and 27b: the procedure for the synthesis of compounds **27a** and **27b** is described in *Molecules* **2018**, *23(10)*, 2545 (see Appendix 1).[253]

1-{1,4-dioxaspiro[4.5]decan-2-yl}propane-1,2-dione (27a): the compound is described in *Molecules* **2018**, *23(10)*, 2545 (see Appendix 1).[253]

1-{1,4-dioxaspiro[4.5]decan-2-yl}-2-phenylethane-1,2-dione (27b): the compound is described in *Molecules* **2018**, *23(10)*, 2545 (see Appendix 1).[253]

Synthesis of *rac*-DPD and *rac*-Ph-DPD: the procedure for the synthesis of compounds *rac*-DPD and *rac*-Ph-DPD is described in *Molecules* **2018**, *23(10)*, 2545 (see Appendix 1).[253]

4,5-dihydroxy-2,3-pentanedione (*rac*-DPD): the compound is described in *Molecules* **2018**, *23(10)*, 2545 (see Appendix 1).[253]

3,4-dihydroxy-1-phenylbutane-1,2-dione (*rac*-Ph-DPD): the compound is described in *Molecules* **2018**, *23(10)*, 2545 (see Appendix 1).[253]

8.1.4 Synthesis, ^{1}H and ^{13}C NMR of 1,4- and 1,5-disubstituted triazoles

Synthesis of 153a-f: the procedure for the synthesis of compounds **153a-f** is described in *Molecules* **2018**, *23(10)*, 2545 (see Appendix 1).[253]

(2-azidoethyl)benzene (153a): the compound is described in *Molecules* **2018**, *23(10)*, 2545 (see Appendix 1, SI).[253]

(azidomethyl)benzene (153b): the compound is described in *Molecules* **2018**, *23(10)*, 2545 (see Appendix 1, SI).[253]

1-(2-azidoethyl)-2-fluorobenzene (153c): the compound is described in *Molecules* **2018**, *23(10)*, 2545 (see Appendix 1, SI).[253]

2-(2-azidoethyl)pyridine (153d): the compound is described in *Molecules* **2018**, *23(10)*, 2545 (see Appendix 1, SI).[253]

6-azidohexanenitrile (153e): the compound is described in *Molecules* **2018**, *23(10)*, 2545 (see Appendix 1, SI).[253]

(2-azidoethyl)cyclohexane (153f): the compound is described in *Molecules* **2018**, *23(10)*, 2545 (see Appendix 1, SI).[253]

Different conditions tested for the synthesis of 154a: three different conditions for the synthesis of **154a** are described in *Molecules* **2018**, *23(10)*, 2545 (see Appendix 1, SI).[253]

Synthesis of 154a-f: the procedure for the synthesis of compounds **167a-f** is described in *Molecules* **2018**, *23(10)*, 2545 (see Appendix 1).[253]

1-[1-(2-phenylethyl)-1*H*-1,2,3-triazol-4-yl]ethane-1,2-diol (154a): the compound is described in *Molecules* **2018**, *23(10)*, 2545 (see Appendix 1).[253]

1-(1-benzyl-1*H*-1,2,3-triazol-4-yl)ethane-1,2-diol (154b): the compound is described in *Molecules* **2018**, *23(10)*, 2545 (see Appendix 1).[253]

1-{1-[2-(2-fluorophenyl)ethyl]-1*H*-1,2,3-triazol-4-yl}ethane-1,2-diol (154c): the compound is described in *Molecules* **2018**, *23(10)*, 2545 (see Appendix 1).[253]

1-{1-[2-(pyridin-2-yl)ethyl]-1*H*-1,2,3-triazol-4-yl}ethane-1,2-diol (154d): the compound is described in *Molecules* **2018**, *23(10)*, 2545 (see Appendix 1).[253]

6-[4-(1,2-dihydroxyethyl)-1*H*-1,2,3-triazol-1-yl]hexanenitrile (154e): the compound is described in *Molecules* **2018**, *23(10)*, 2545 (see Appendix 1).[253]

1-[1-(2-cyclohexylethyl)-1*H*-1,2,3-triazol-4-yl]ethane-1,2-diol (154f): the compound is described in *Molecules* **2018**, *23(10)*, 2545 (see Appendix 1).[253]

Synthesis of 155a: the procedure for the synthesis of compound **155a** is described in *Molecules* **2018**, *23(10)*, 2545 (see Appendix 1).[253]
1,5-disubstitution was confirmed by HMBC and by comparison of the HMBC spectrum with the one's of 1,4-disubstituted triazole 154a. Additional data are available in *Molecules* **2018**, *23(10)*, 2545 (see Appendix 1, SI).[253]

1-[1-(2-phenylethyl)-1*H*-1,2,3-triazol-5-yl]ethane-1,2-diol (155a): the compound is described in *Molecules* **2018**, *23(10)*, 2545 (see Appendix 1).[253]

Synthesis of 156: the procedure for the synthesis of compound **156** is described in *Molecules* **2018**, *23(10)*, 2545 (see Appendix 1).[253]

4-{1,4-dioxaspiro[4.5]decan-2-yl}-1*H*-1,2,3-triazole (156): the compound is described in *Molecules* **2018**, *23(10)*, 2545 (see Appendix 1).[253]

Synthesis of 157h-k and 158h-k: the procedure for the synthesis of compounds **157h-k and 158h-k** is described in *Molecules* **2018**, *23(10)*, 2545 (see Appendix 1).[253]
1,4- and 1,5-disubstitution was determined by HMBC of one representative sample (157h, see Appendix 1, SI).[253]

4-{1,4-dioxaspiro[4.5]decan-2-yl}-1-methyl-1*H*-1,2,3-triazole (157h): the compound is described in *Molecules* **2018**, *23(10)*, 2545 (see Appendix 1, SI).[253]

5-{1,4-dioxaspiro[4.5]decan-2-yl}-1-methyl-1*H*-1,2,3-triazole (158h): the compound is described in *Molecules* **2018**, *23(10)*, 2545 (see Appendix 1, SI).[253]

1-(cyclopropylmethyl)-4-{1,4-dioxaspiro[4.5]decan-2-yl}-1*H*-1,2,3-triazole (157i): the compound is described in *Molecules* **2018**, *23(10)*, 2545 (see Appendix 1, SI).[253]

1-(cyclopropylmethyl)-5-{1,4-dioxaspiro[4.5]decan-2-yl}-1*H*-1,2,3-triazole (158i): the compound is described in *Molecules* **2018**, *23(10)*, 2545 (see Appendix 1, SI).[253]

1-butyl-4-{1,4-dioxaspiro[4.5]decan-2-yl}-1*H*-1,2,3-triazole (157j): the compound is described in *Molecules* **2018**, *23(10)*, 2545 (see Appendix 1, SI).[253]

1-butyl-4-{1,4-dioxaspiro[4.5]decan-2-yl}-1*H*-1,2,3-triazole (158j): the compound is described in *Molecules* **2018**, *23(10)*, 2545 (see Appendix 1, SI).[253]

4-{1,4-dioxaspiro[4.5]decan-2-yl}-1-(2-ethoxyethyl)-1*H*-1,2,3-triazole (157k): the compound is described in *Molecules* **2018**, *23(10)*, 2545 (see Appendix 1, SI).[253]

4-{1,4-dioxaspiro[4.5]decan-2-yl}-1-(2-ethoxyethyl)-1*H*-1,2,3-triazole (158k): the compound is described in *Molecules* **2018**, *23(10)*, 2545 (see Appendix 1, SI).[253]

Synthesis of 154g-k and 155h-k: the procedure for the synthesis of compounds **154g-k and 155h-k** is described in *Molecules* **2018**, *23(10)*, 2545 (see Appendix 1).[253]

1-(1*H*-1,2,3-triazol-4-yl)ethane-1,2-diol (154g): the compound is described in *Molecules* **2018**, *23(10)*, 2545 (see Appendix 1).[253]

1-(1-methyl-1*H*-1,2,3-triazol-4-yl)ethane-1,2-diol (154h): the compound is described in *Molecules* **2018**, *23(10)*, 2545 (see Appendix 1).[253]

1-(1-methyl-1*H*-1,2,3-triazol-5-yl)ethane-1,2-diol (155h): the compound is described in *Molecules* **2018**, *23(10)*, 2545 (see Appendix 1).[253]

1-[1-(cyclopropylmethyl)-1*H*-1,2,3-triazol-4-yl]ethane-1,2-diol (154i): the compound is described in *Molecules* **2018**, *23(10)*, 2545 (see Appendix 1).[253]

1-[1-(cyclopropylmethyl)-1*H*-1,2,3-triazol-5-yl]ethane-1,2-diol (155i): the compound is described in *Molecules* **2018**, *23(10)*, 2545 (see Appendix 1).[253]

1-(1-butyl-1*H*-1,2,3-triazol-4-yl)ethane-1,2-diol (154j): the compound is described in *Molecules* **2018**, *23(10)*, 2545 (see Appendix 1).[253]

1-(1-butyl-1*H*-1,2,3-triazol-5-yl)ethane-1,2-diol (155j): the compound is described in *Molecules* **2018**, *23(10)*, 2545 (see Appendix 1).[253]

1-[1-(2-ethoxyethyl)-1*H*-1,2,3-triazol-4-yl]ethane-1,2-diol (154k): the compound is described in *Molecules* **2018**, *23(10)*, 2545 (see Appendix 1).[253]

1-[1-(2-ethoxyethyl)-1*H*-1,2,3-triazol-4-yl]ethane-1,2-diol (155k): the compound is described in *Molecules* **2018**, *23(10)*, 2545 (see Appendix 1).[253]

^{1}H NMR (300 MHz, CD$_3$CN) 1-[1-(2-phenylethyl)-1H-1,2,3-triazol-4-yl]ethane-1,2-diol (154a)

7.56, 7.31, 7.28, 7.26, 7.25, 7.23, 7.22, 7.21, 7.20, 7.17, 7.16, 7.14, 4.77, 4.76, 4.75, 4.73, 4.59, 4.57, 4.54, 3.75, 3.73, 3.71, 3.69, 3.63, 3.61, 3.59, 3.57, 3.20, 3.17, 3.15, 2.23

1.00 3.09 3.16 1.95 0.97 1.91 1.91 2.61 1.12

5.0

0.0

ppm (t1)

^{13}C NMR (100 MHz, CD$_3$CN) 1-[1-(2-phenylethyl)-1H-1,2,3-triazol-4-yl]ethane-1,2-diol (154a)

149.4, 138.8, 129.7, 129.4, 127.6, 122.8, 68.5, 66.8, 51.9, 36.9

200   150   100   50   0

ppm (t1)

120
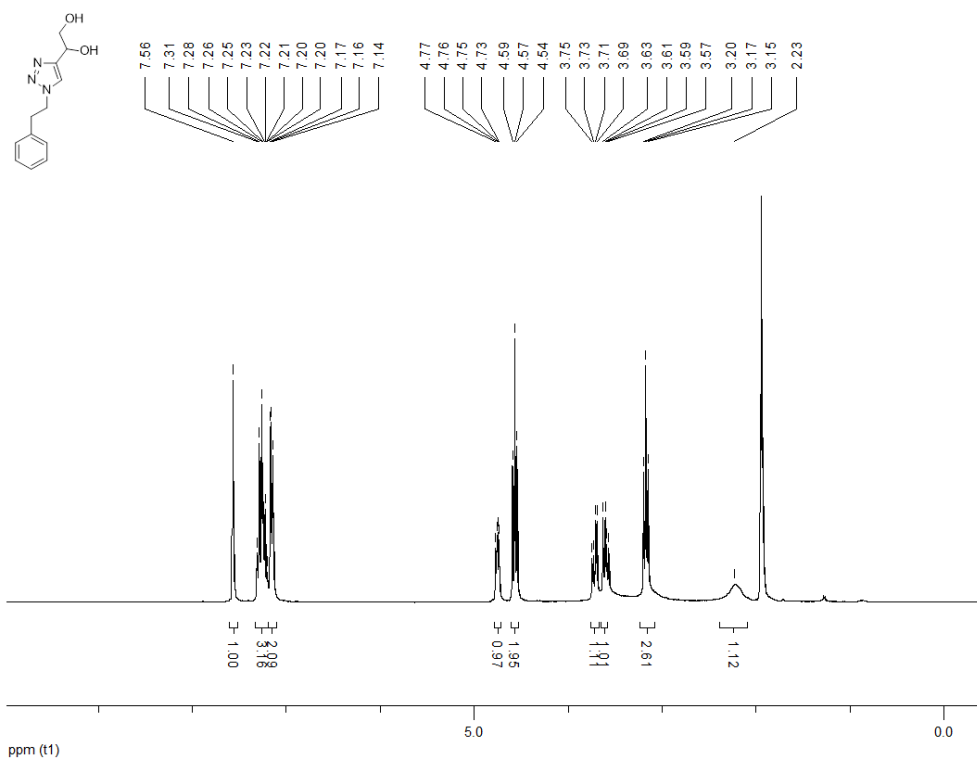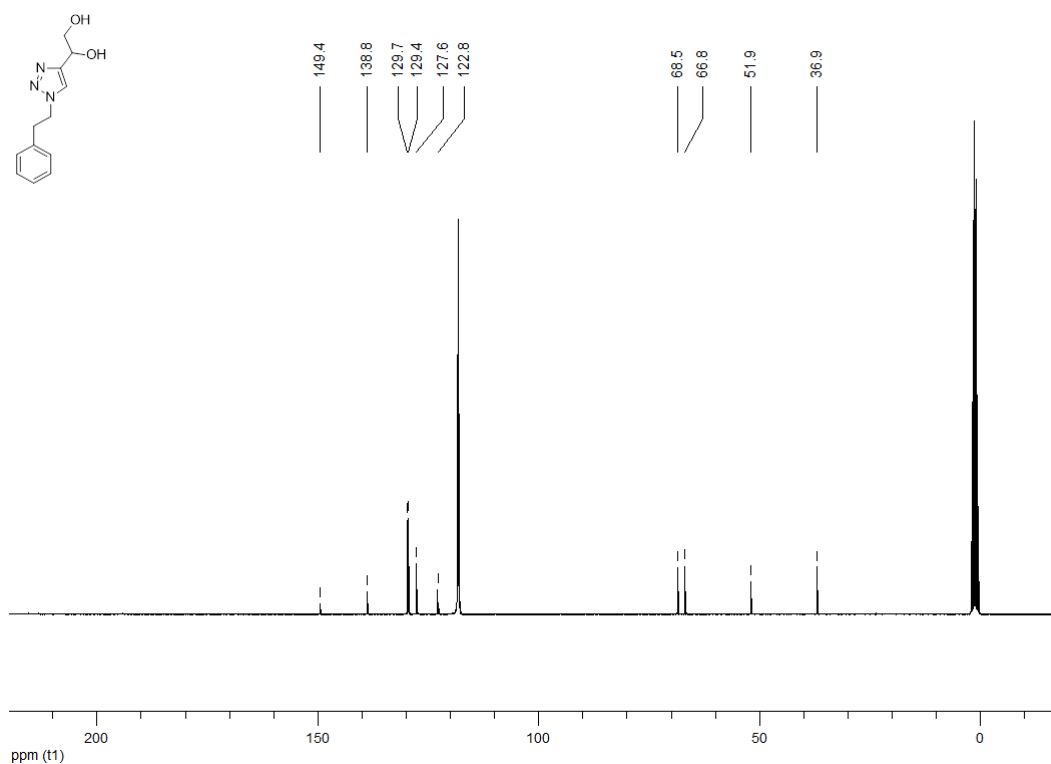
^{1}H NMR (300 MHz, CD$_3$CN) 1-(1-benzyl-1H-1,2,3-triazol-4-yl)ethane-1,2-diol (154b)
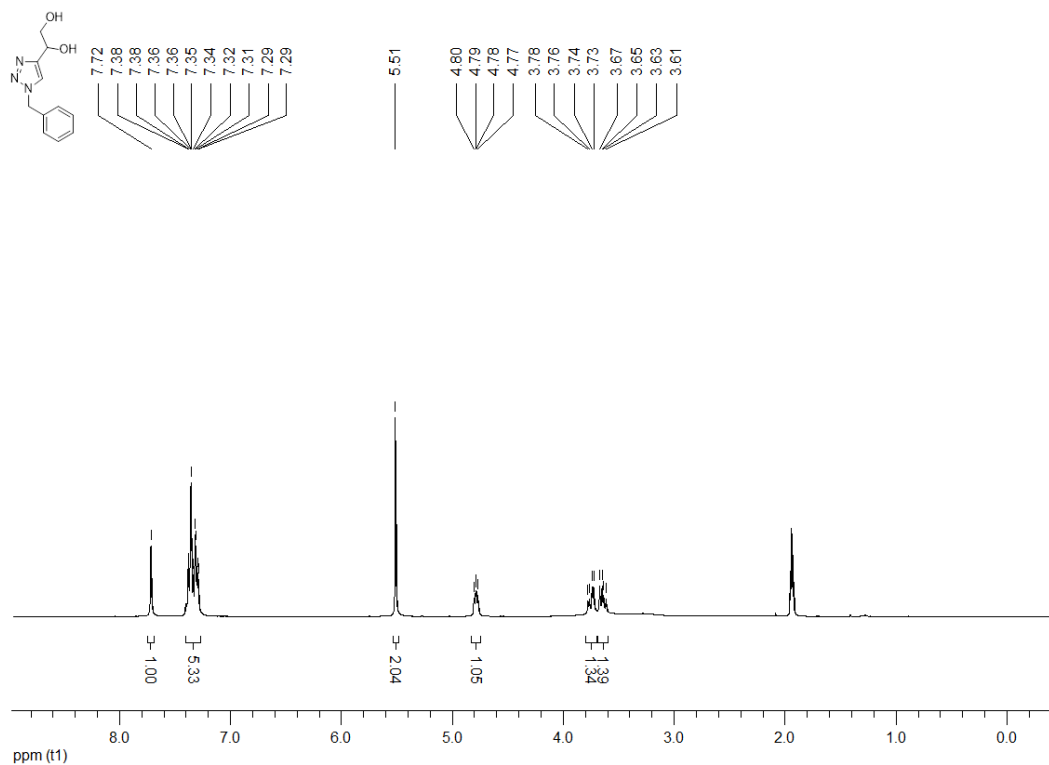
^{13}C NMR (100 MHz, CD$_3$CN) 1-(1-benzyl-1H-1,2,3-triazol-4-yl)ethane-1,2-diol (154b)
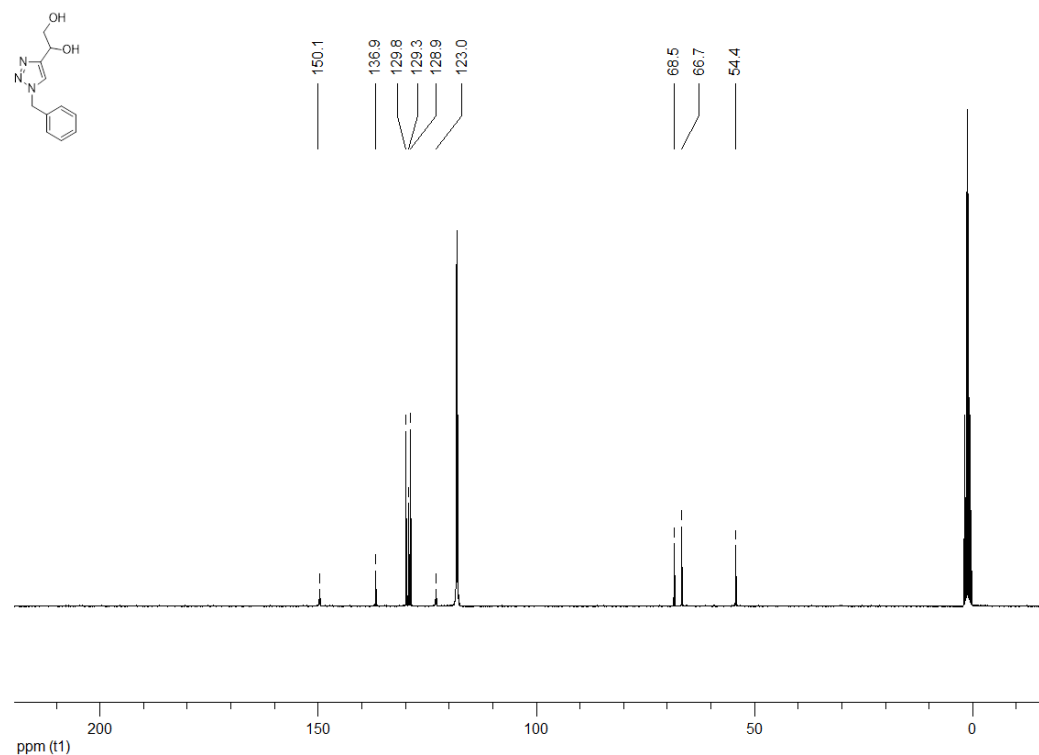
^{1}H NMR (300 MHz, CD$_3$CN) 1-{1-[2-(2-fluorophenyl)ethyl]-1H-1,2,3-triazol-4-yl}ethane-1,2-diol (154c)
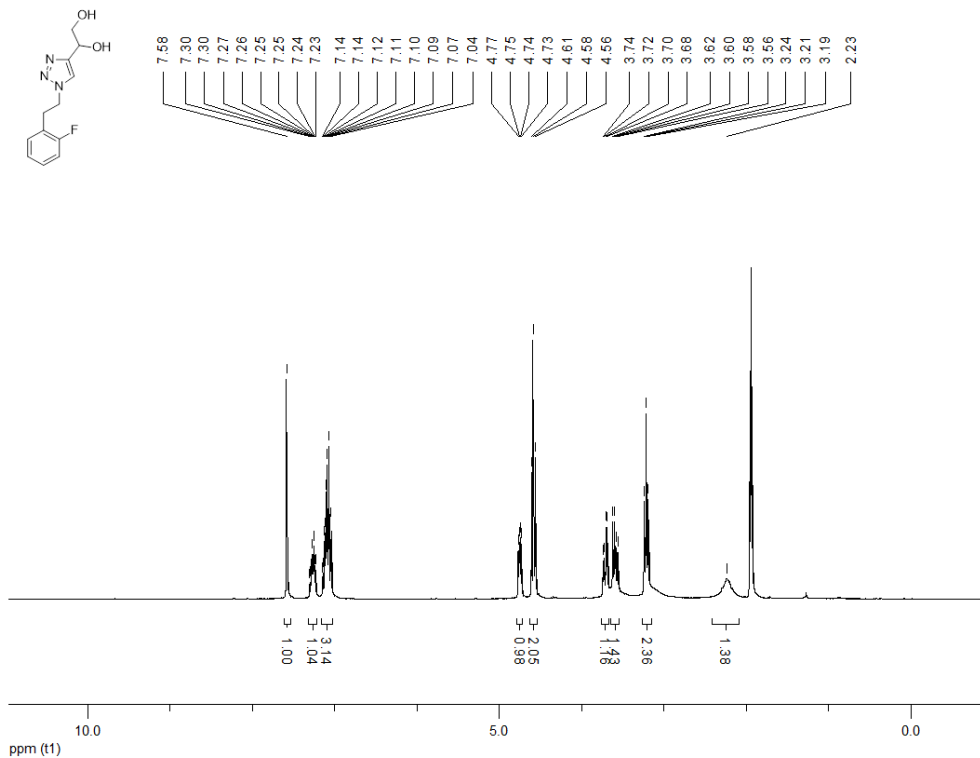
^{13}C NMR (100 MHz, CD$_3$CN) 1-{1-[2-(2-fluorophenyl)ethyl]-1H-1,2,3-triazol-4-yl}ethane-1,2-diol (154c)
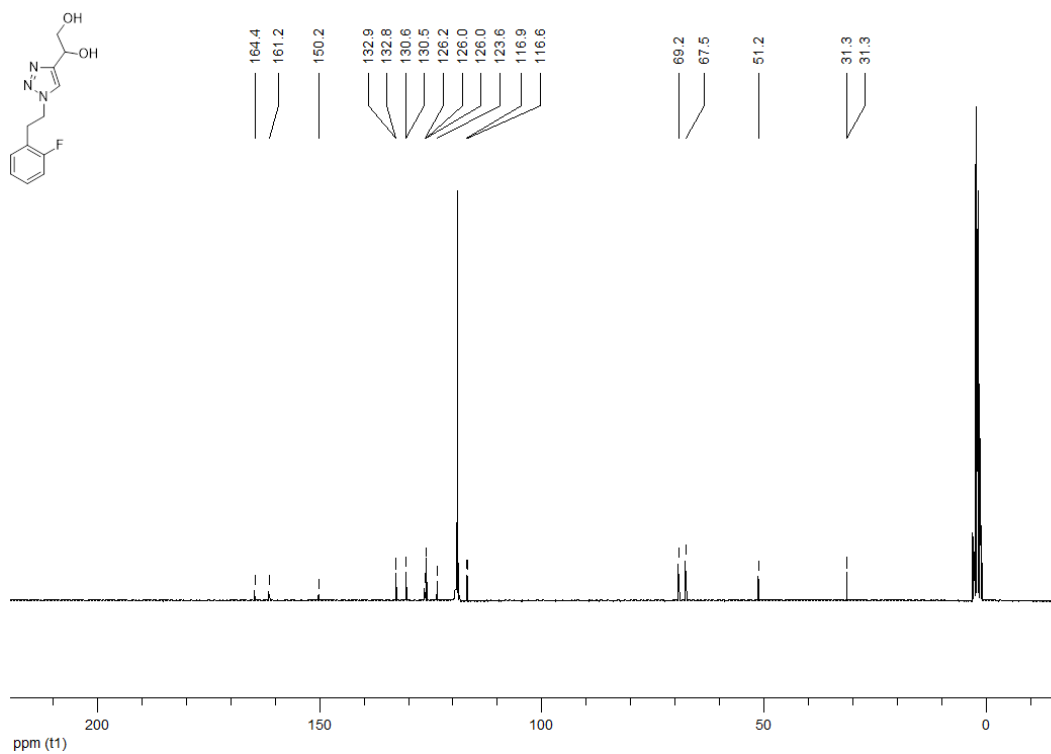
^{1}H NMR (300 MHz, CD3CN) 1-{1-[2-(pyridin-2-yl)ethyl]-1H-1,2,3-triazol-4-yl}ethane-1,2-diol (154d)
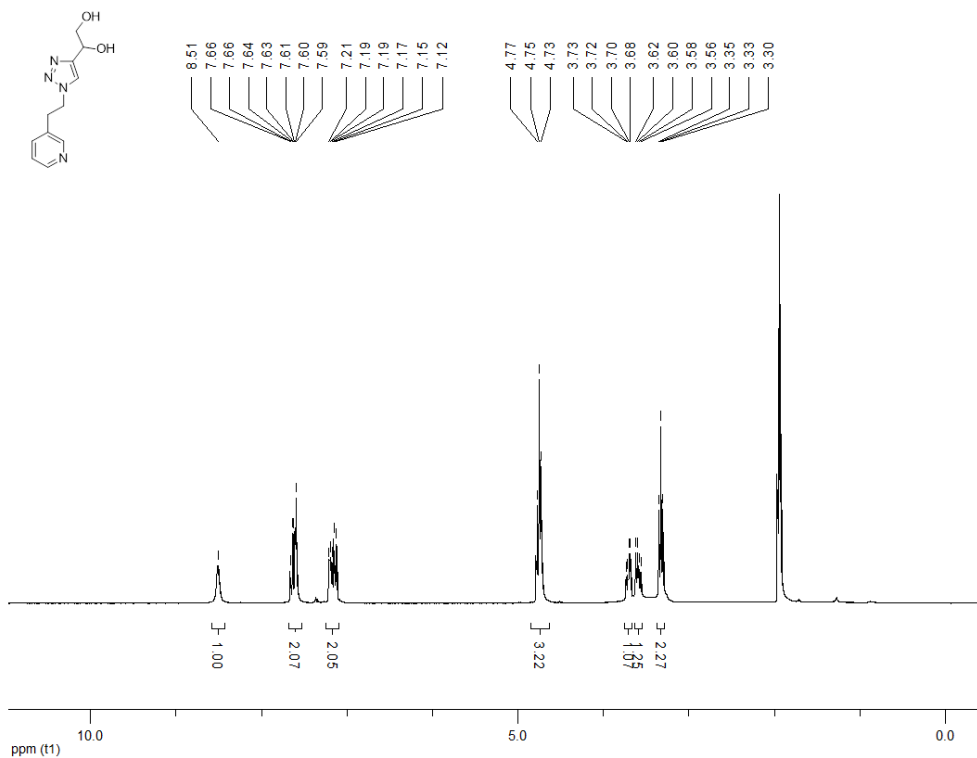
^{13}C NMR (100 MHz, CD3CN) 1-{1-[2-(pyridin-2-yl)ethyl]-1H-1,2,3-triazol-4-yl}ethane-1,2-diol (154d)
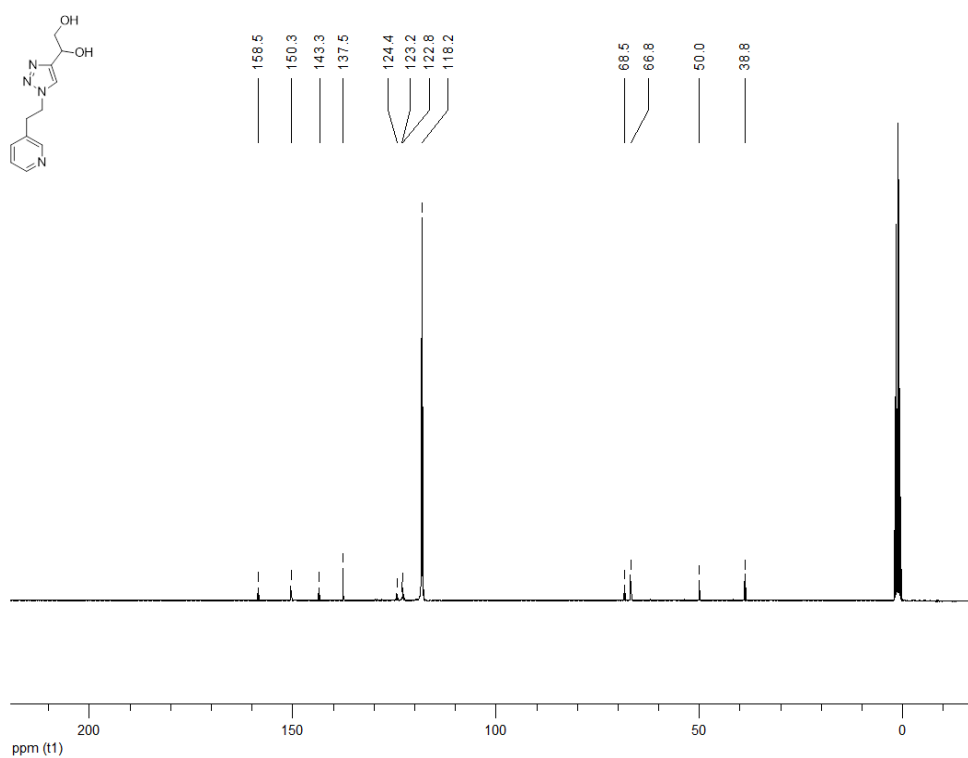
^{1}H NMR (300 MHz, CD$_3$CN) 6-[4-(1,2-dihydroxyethyl)-1*H*-1,2,3-triazol-1-yl]hexanenitrile (154e)
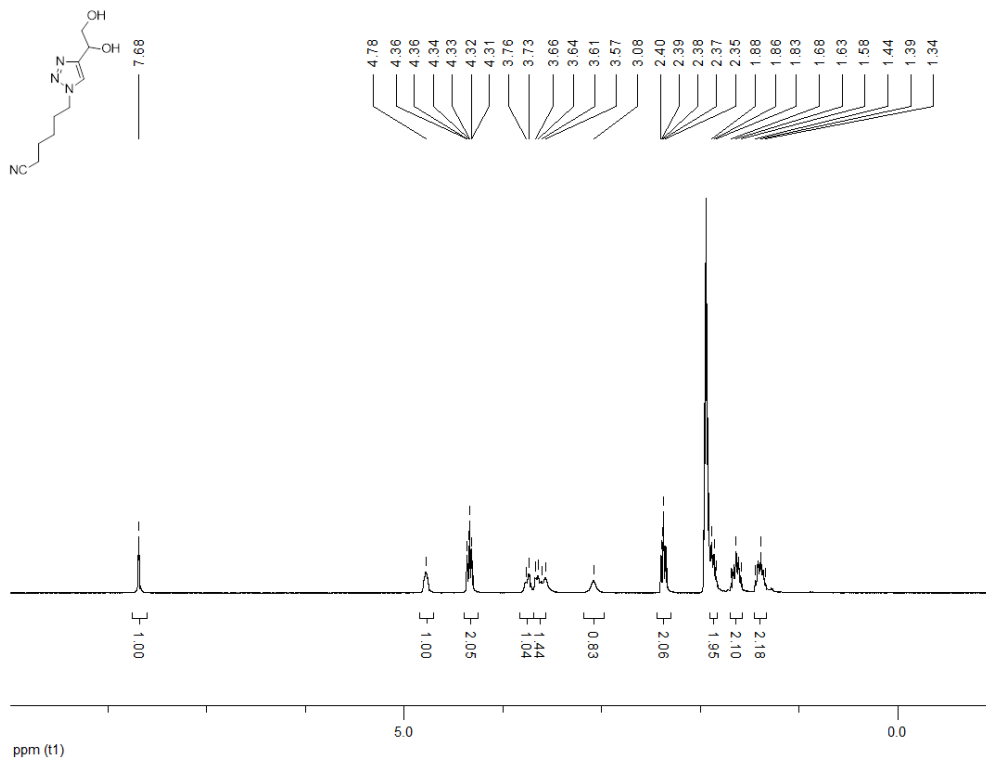
^{13}C NMR (100 MHz, CD$_3$CN) 6-[4-(1,2-dihydroxyethyl)-1*H*-1,2,3-triazol-1-yl]hexanenitrile (154e)
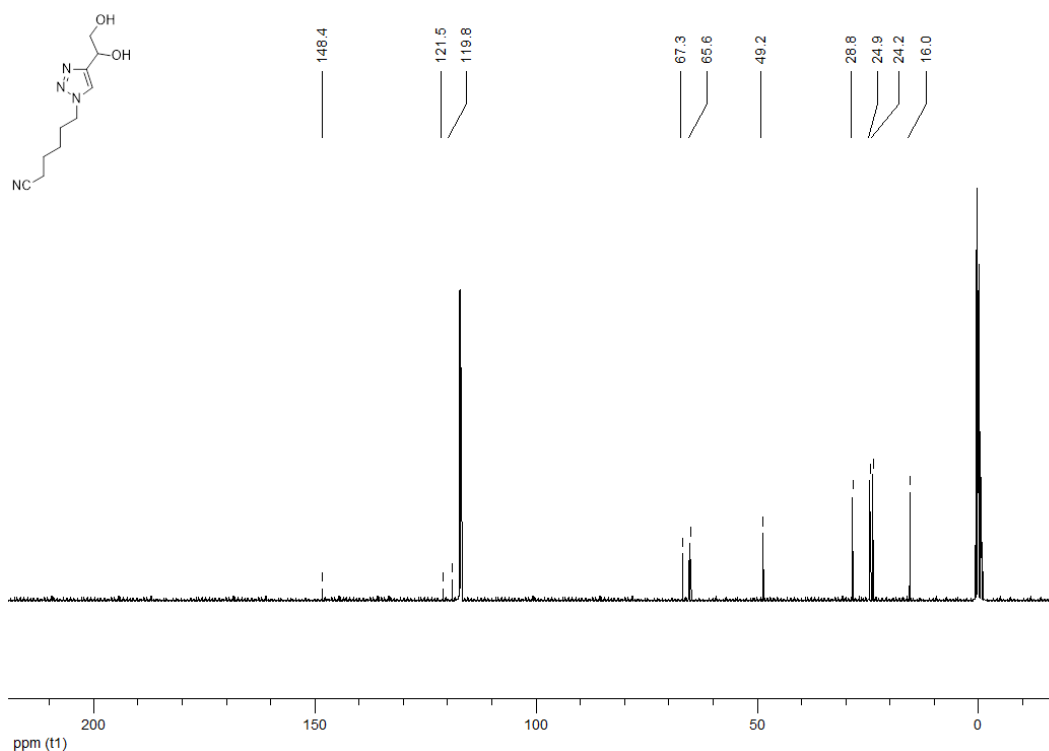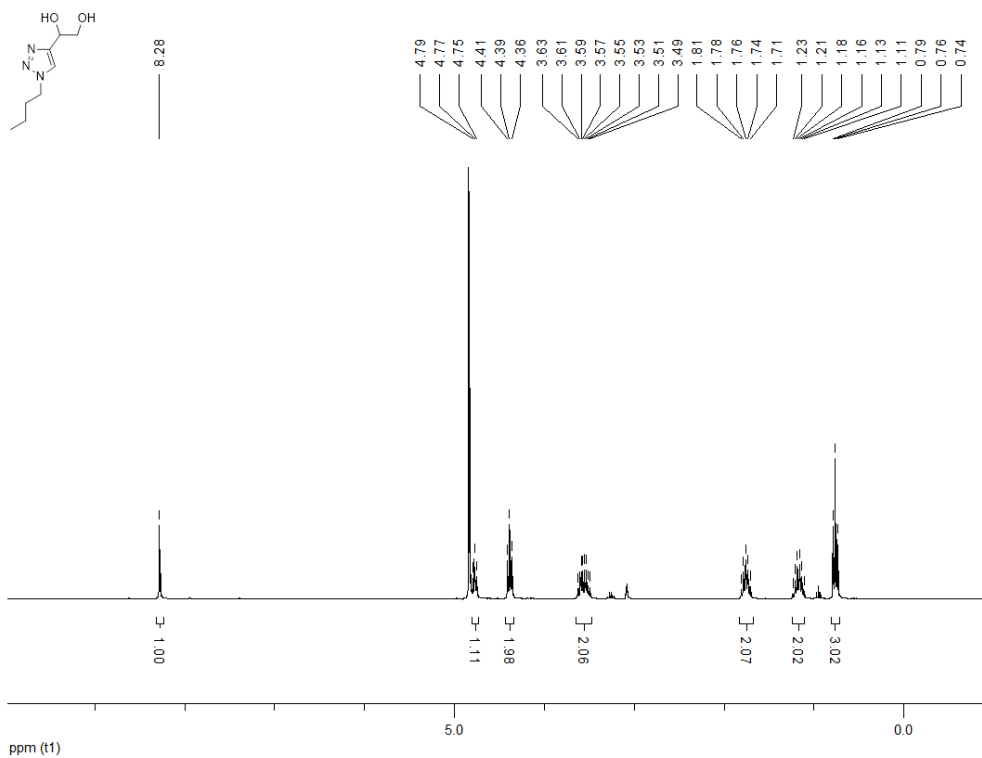
¹H NMR (300 MHz, CD₃CN) 1-[1-(2-cyclohexylethyl)-1*H*-1,2,3-triazol-4-yl]ethane-1,2-diol (154f)
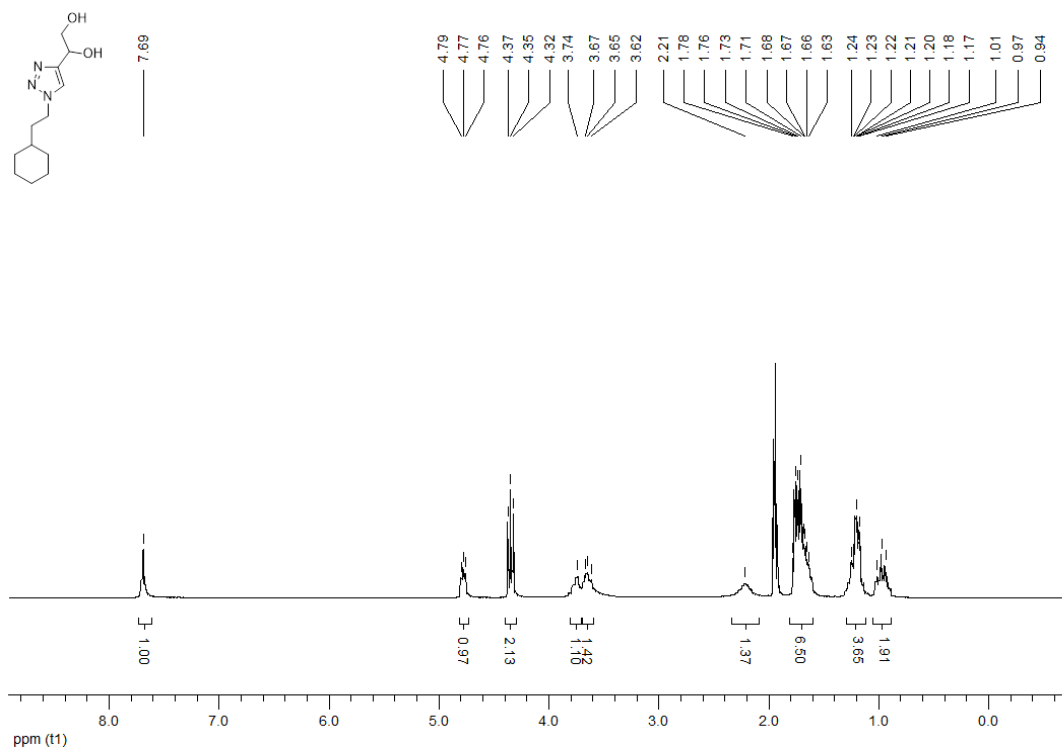
¹³C NMR (100 MHz, CD₃CN) 1-[1-(2-cyclohexylethyl)-1*H*-1,2,3-triazol-4-yl]ethane-1,2-diol (154f)
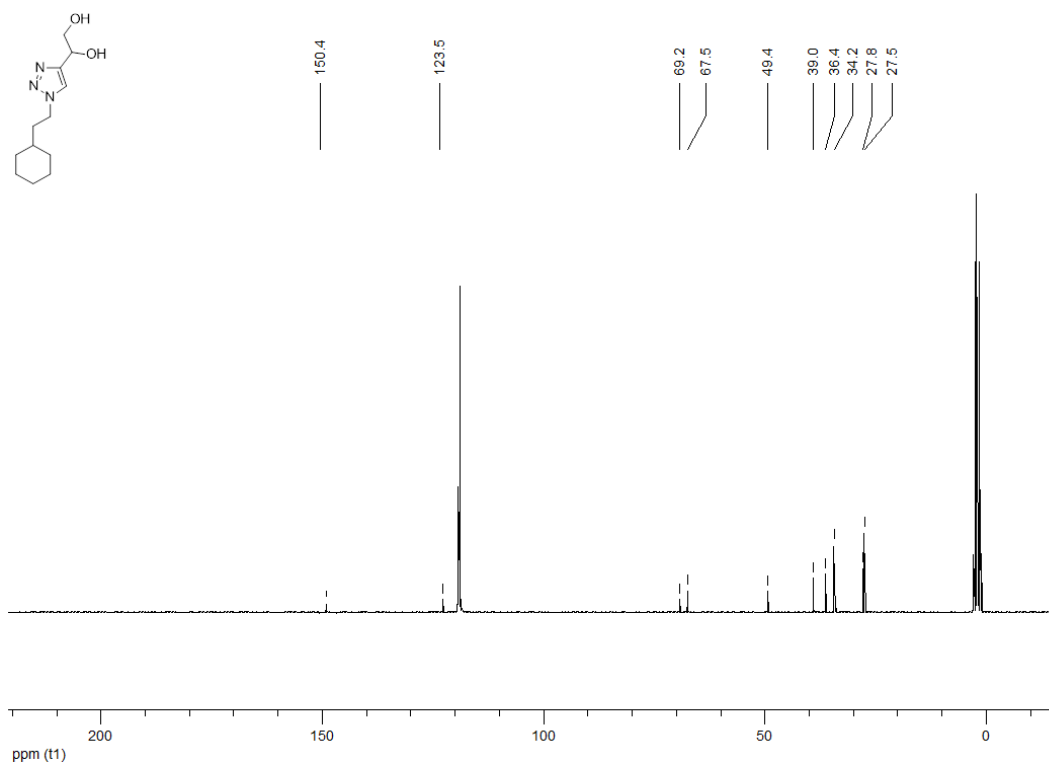
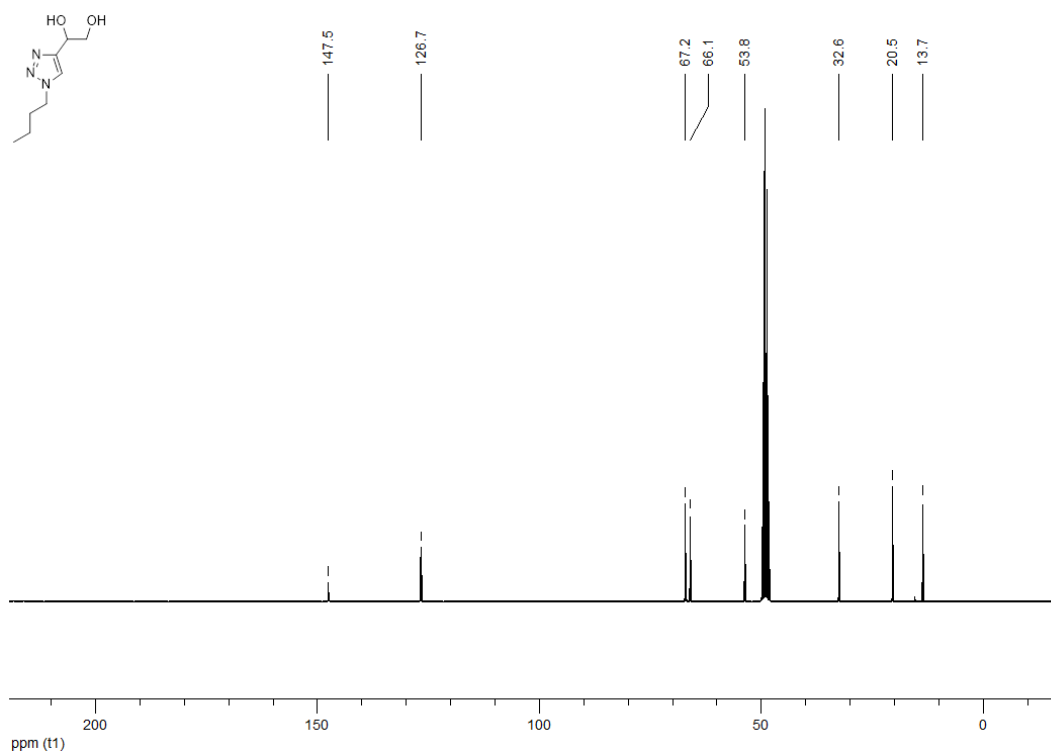**¹H NMR (300 MHz, CD₃CN) 1-[1-(2-phenylethyl)-1*H*-1,2,3-triazol-5-yl]ethane-1,2-diol (155a)**
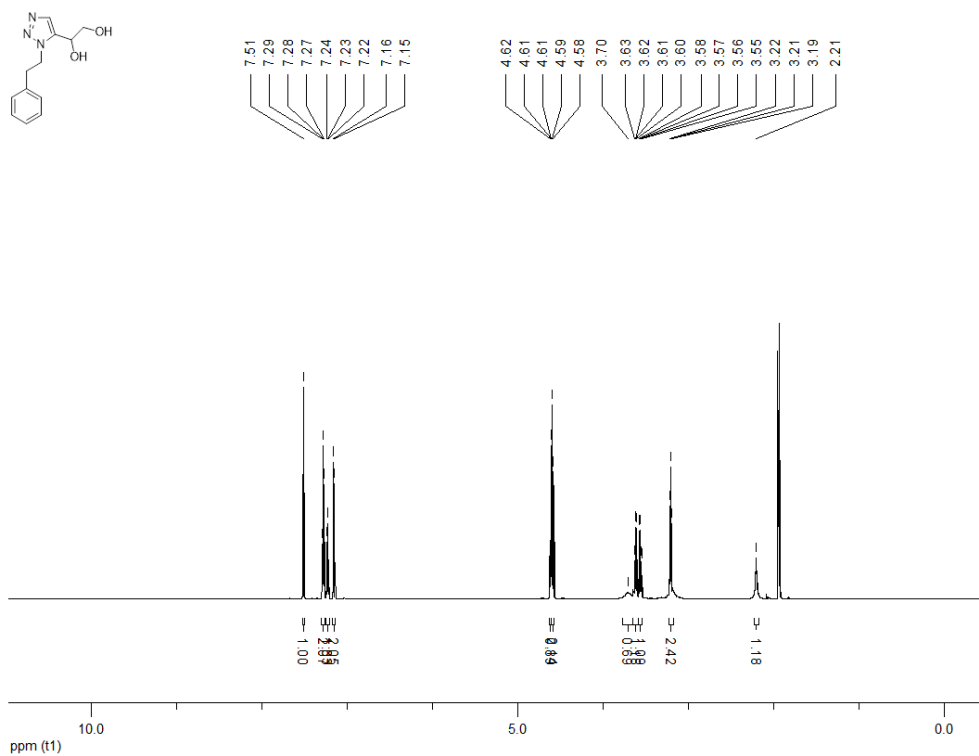
¹³C NMR (100 MHz, CD₃CN) 1-[1-(2-phenylethyl)-1*H*-1,2,3-triazol-5-yl]ethane-1,2-diol (155a)
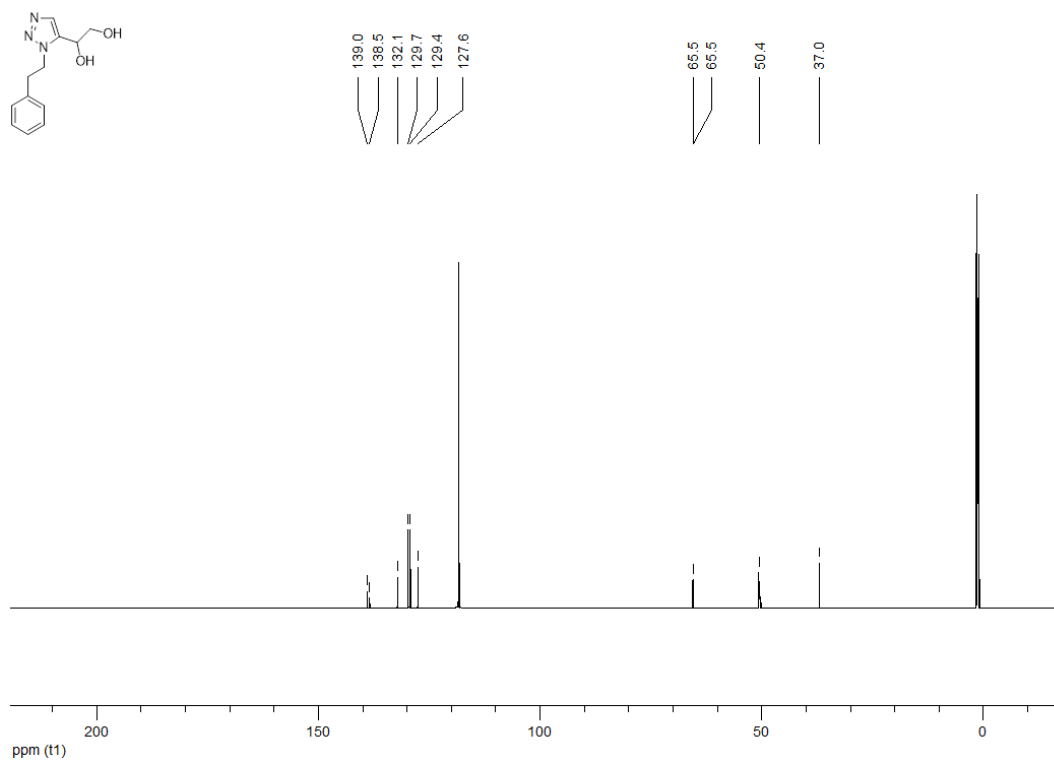
^{1}H NMR (300 MHz, CD$_3$CN) 4-{1,4-dioxaspiro[4.5]decan-2-yl}-1H-1,2,3-triazole (156)
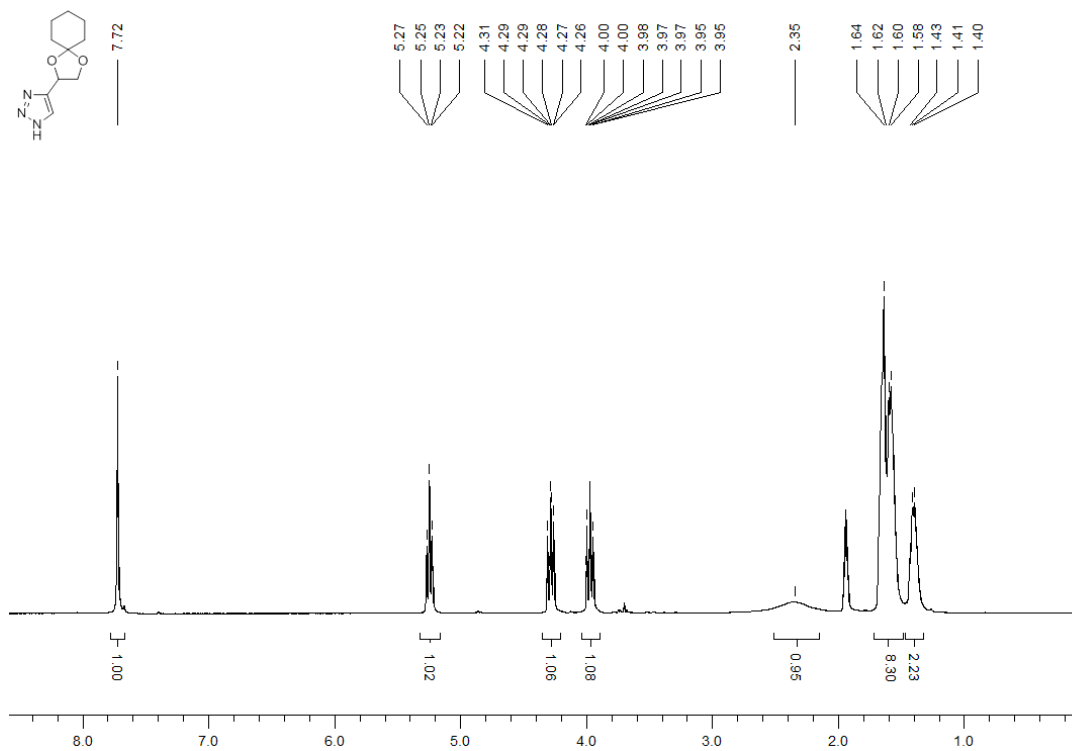
^{13}C NMR (100 MHz, CD$_3$CN) 4-{1,4-dioxaspiro[4.5]decan-2-yl}-1H-1,2,3-triazole (156)

¹H NMR (300 MHz, CDCl₃) 4-{1,4-dioxaspiro[4.5]decan-2-yl}-1-methyl-1*H*-1,2,3-triazole (157h)

7.59

5.22
5.20
5.18

4.38
4.36
4.35
4.33

4.11
4.08
4.06
4.05
4.03

1.69
1.68
1.66
1.64
1.63
1.61
1.60
1.58
1.56
1.42
1.41

1.00

1.07

1.11

3.23

8.22

2.36

8.0   7.0   6.0   5.0   4.0   3.0   2.0   1.0   0.0
ppm (t1)

¹³C NMR (100 MHz, CDCl₃) 4-{1,4-dioxaspiro[4.5]decan-2-yl}-1-methyl-1*H*-1,2,3-triazole (157h)

135.3
131.9

111.5

67.9
67.5

35.9
35.4
34.6

24.9
23.8
23.8

200   150   100   50   0
ppm (t1)

128
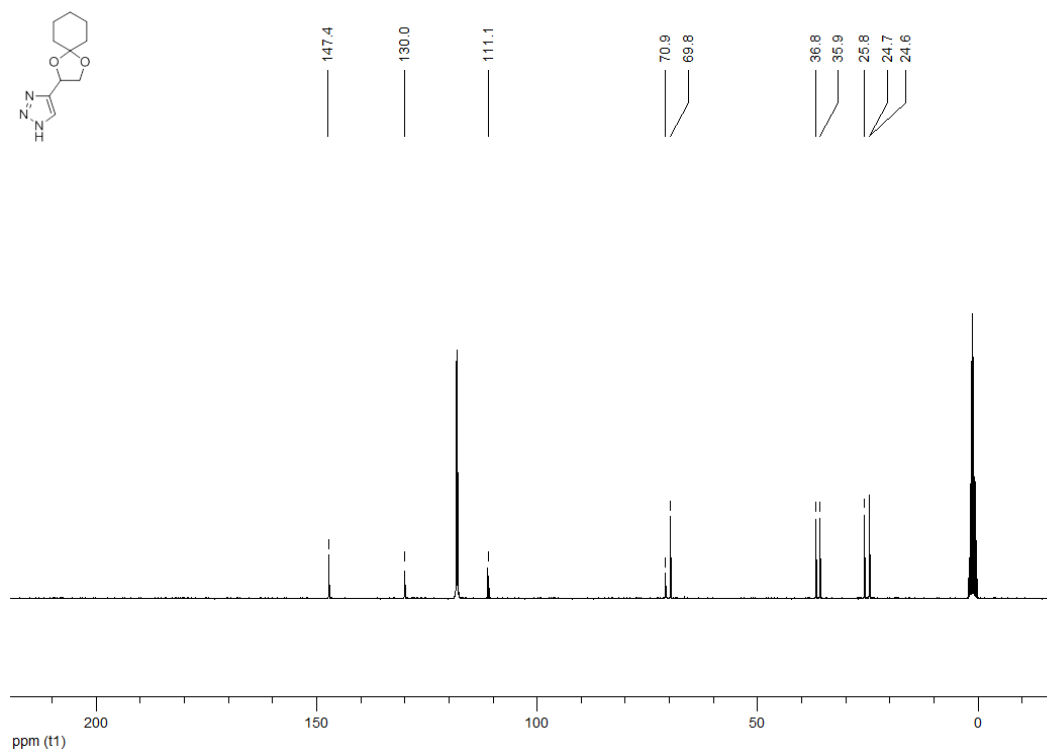
1H NMR (300 MHz, CDCl3) 5-{1,4-dioxaspiro[4.5]decan-2-yl}-1-methyl-1H-1,2,3-triazole (157h)
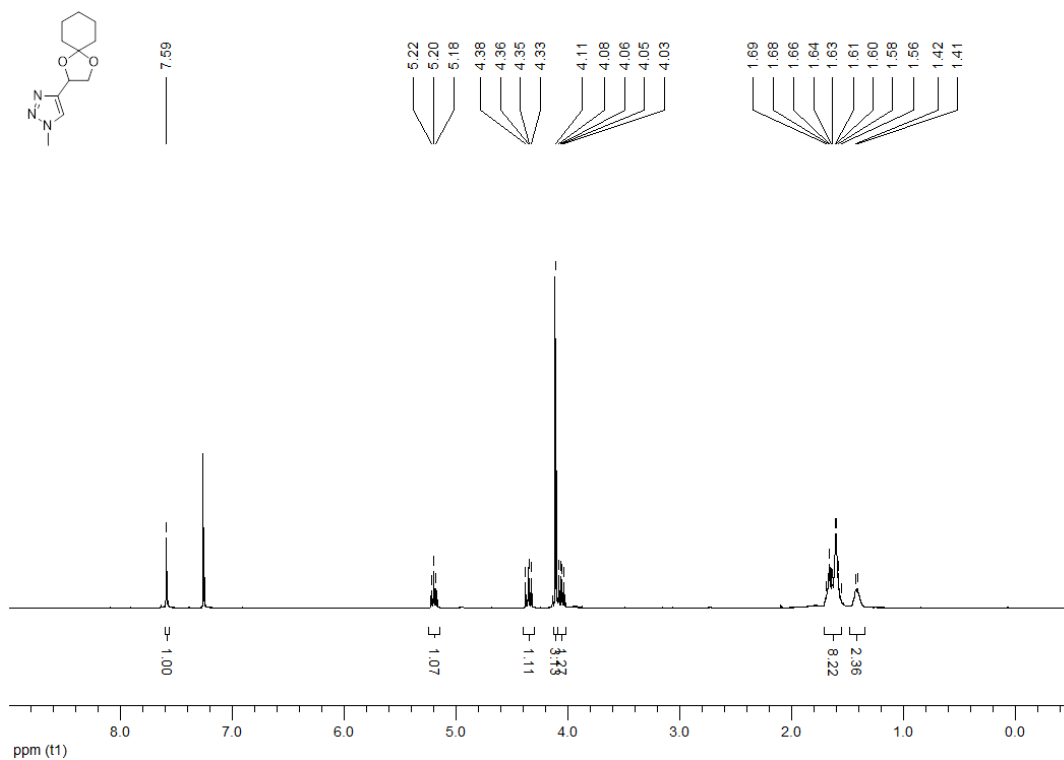
13C NMR (100 MHz, CDCl3) 5-{1,4-dioxaspiro[4.5]decan-2-yl}-1-methyl-1H-1,2,3-triazole (157h)
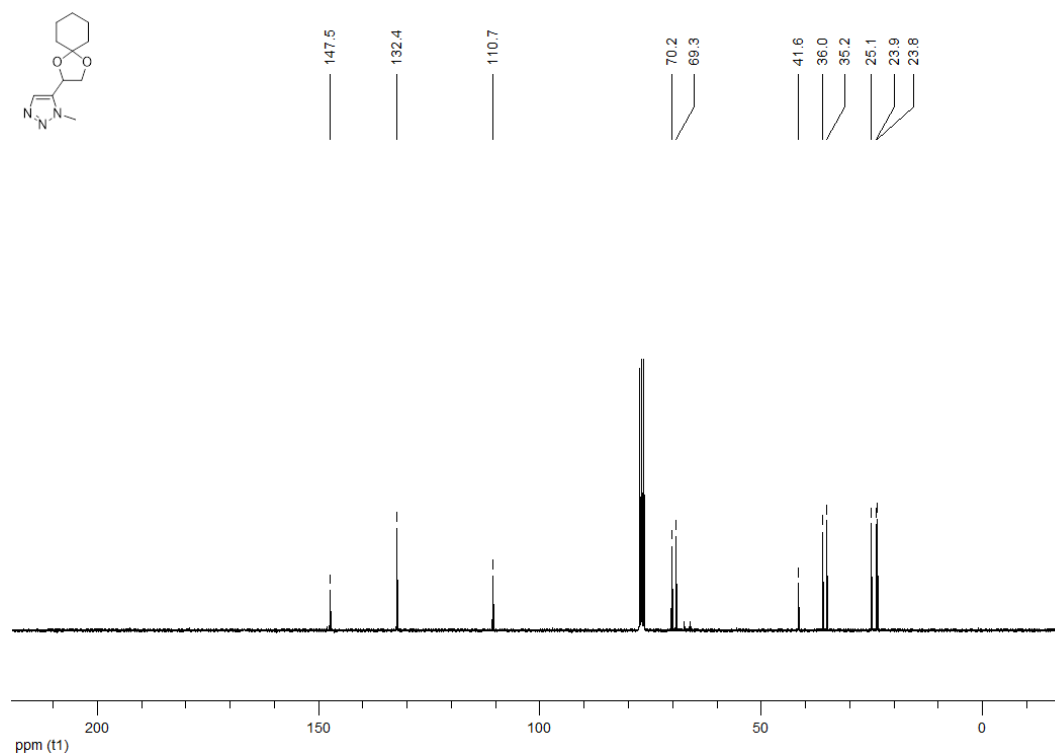
^{1}H NMR (300 MHz, CDCl$_3$) 1-(cyclopropylmethyl)-4-{1,4-dioxaspiro[4.5]decan-2-yl}-1H-1,2,3-triazole (157i)
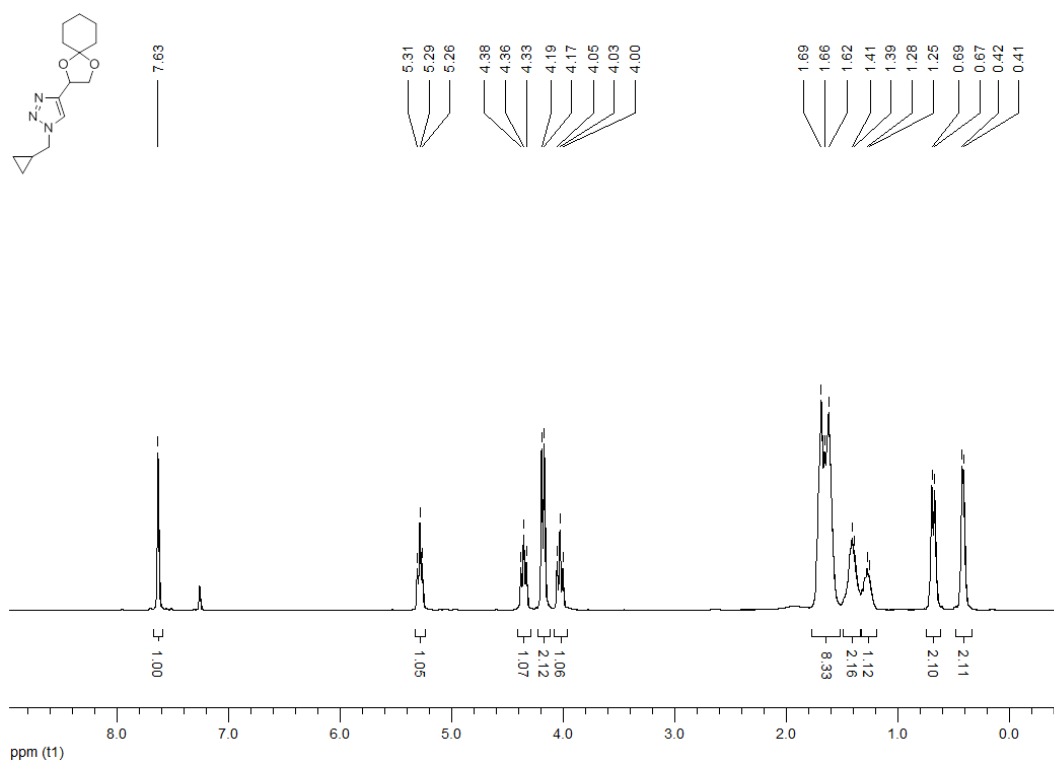
^{13}C NMR (100 MHz, CDCl$_3$) 1-(cyclopropylmethyl)-4-{1,4-dioxaspiro[4.5]decan-2-yl}-1H-1,2,3-triazole (157i)
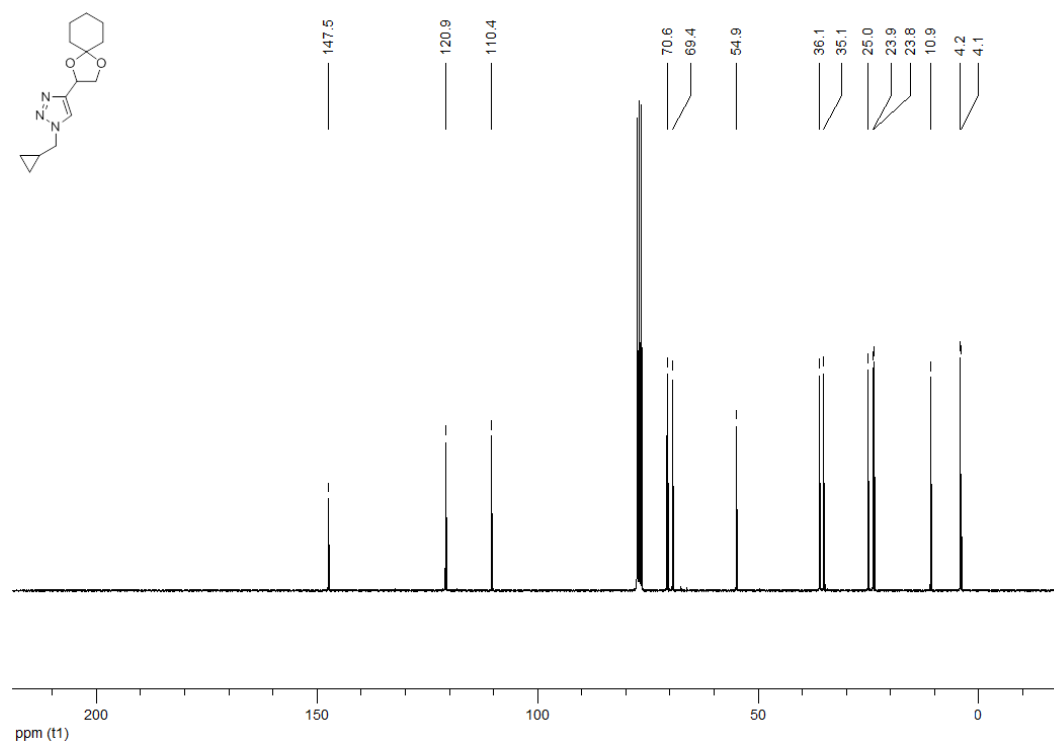
¹H NMR (300 MHz, CDCl₃) 1-(cyclopropylmethyl)-5-{1,4-dioxaspiro[4.5]decan-2-yl}-1*H*-1,2,3-triazole (157i)
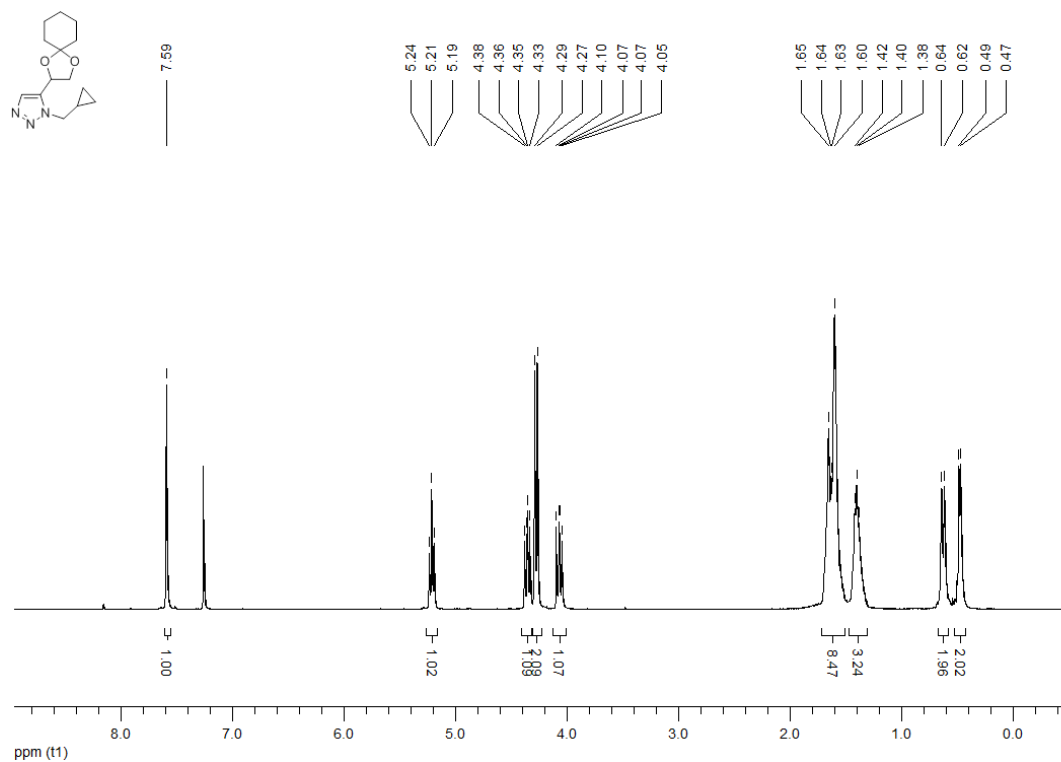
¹³C NMR (100 MHz, CDCl₃) 1-(cyclopropylmethyl)-5-{1,4-dioxaspiro[4.5]decan-2-yl}-1*H*-1,2,3-triazole (157i)
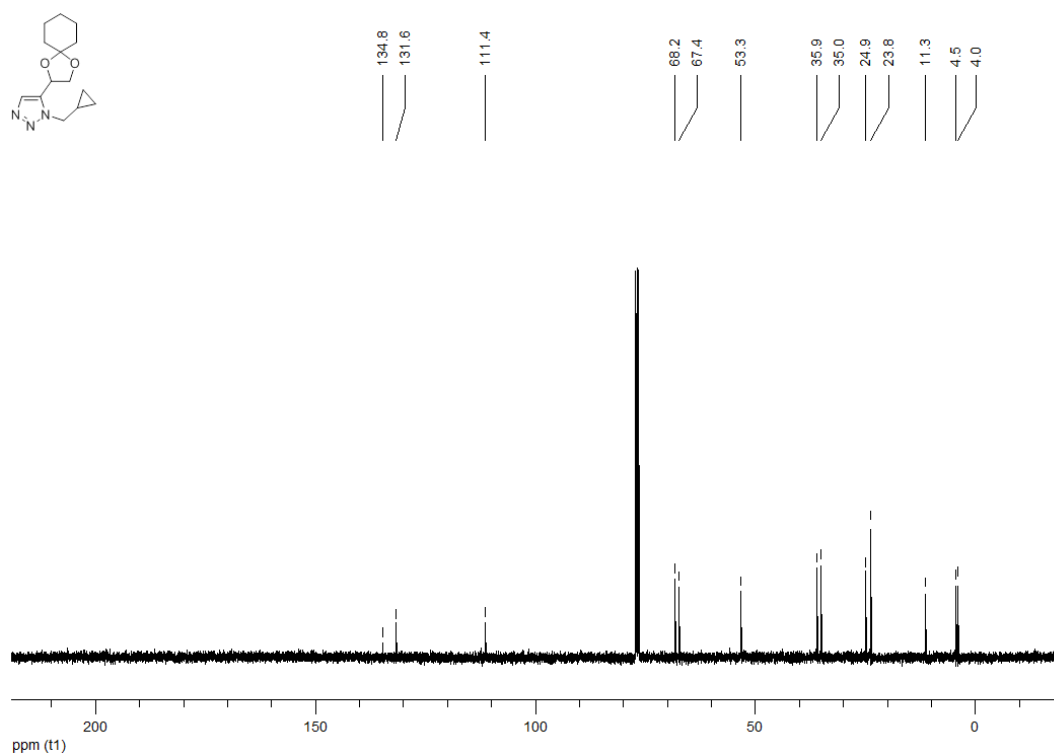
¹H NMR (300 MHz, CDCl₃) 1-butyl-4-{1,4-dioxaspiro[4.5]decan-2-yl}-1H-1,2,3-triazole (157j)
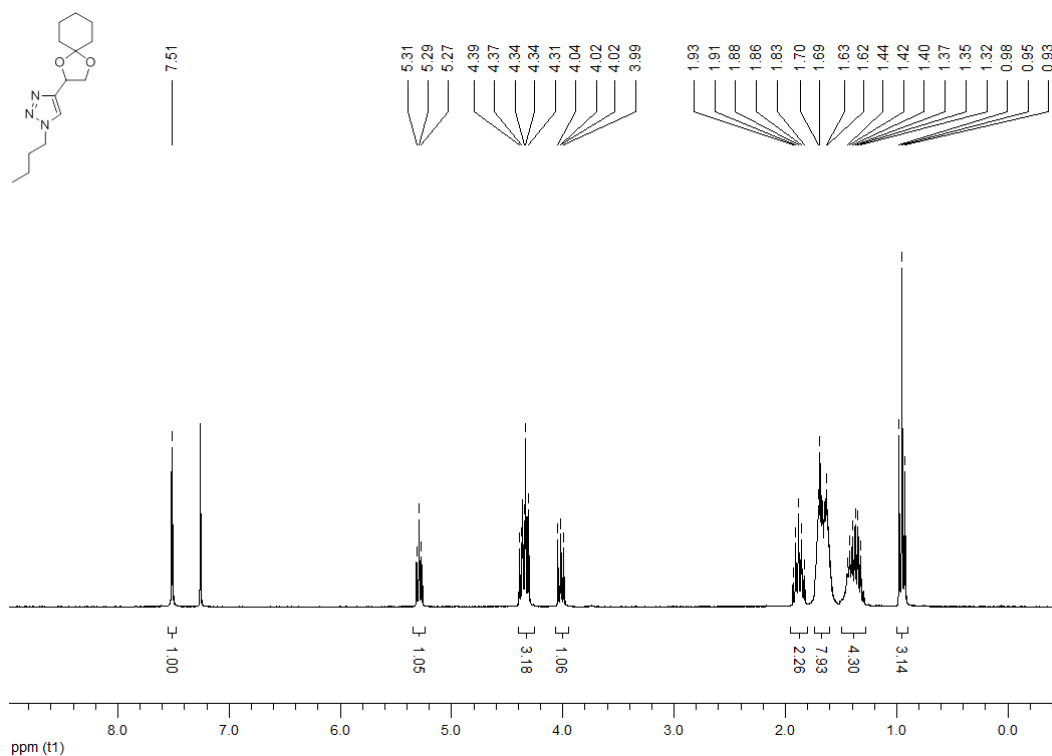
¹³C NMR (100 MHz, CDCl₃) 1-butyl-4-{1,4-dioxaspiro[4.5]decan-2-yl}-1H-1,2,3-triazole (157j)
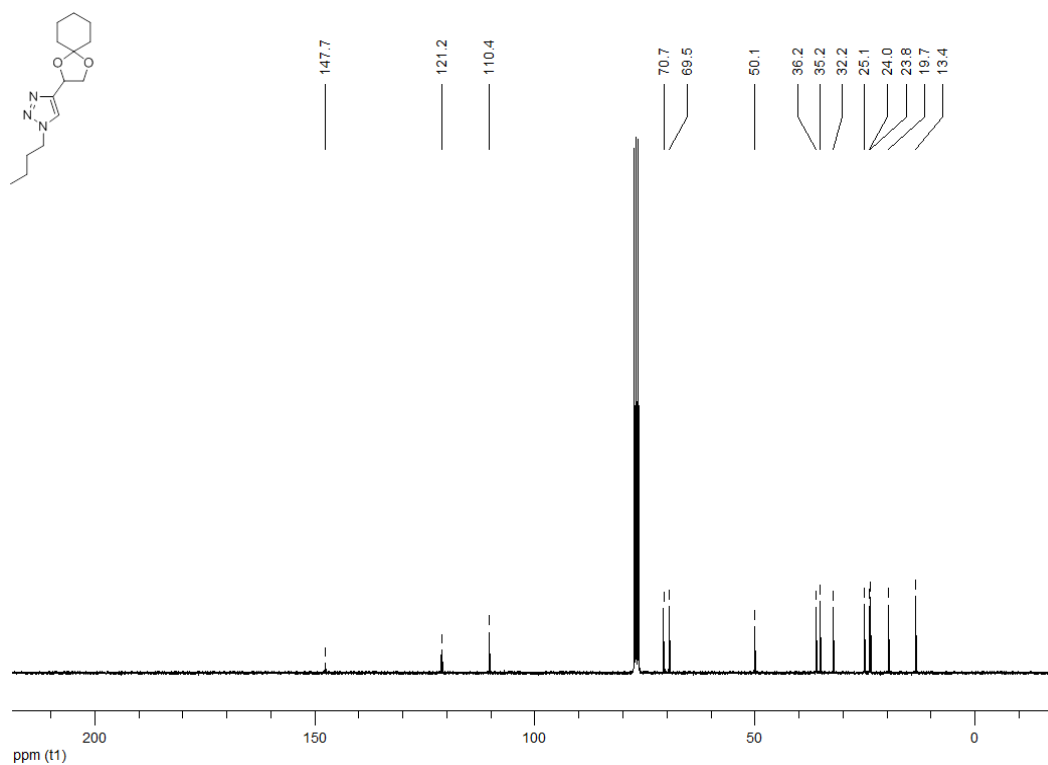
¹H NMR (300 MHz, CDCl₃) 1-butyl-4-{1,4-dioxaspiro[4.5]decan-2-yl}-1*H*-1,2,3-triazole (158j)

¹³C NMR (100 MHz, CDCl₃) 1-butyl-4-{1,4-dioxaspiro[4.5]decan-2-yl}-1*H*-1,2,3-triazole (158j)
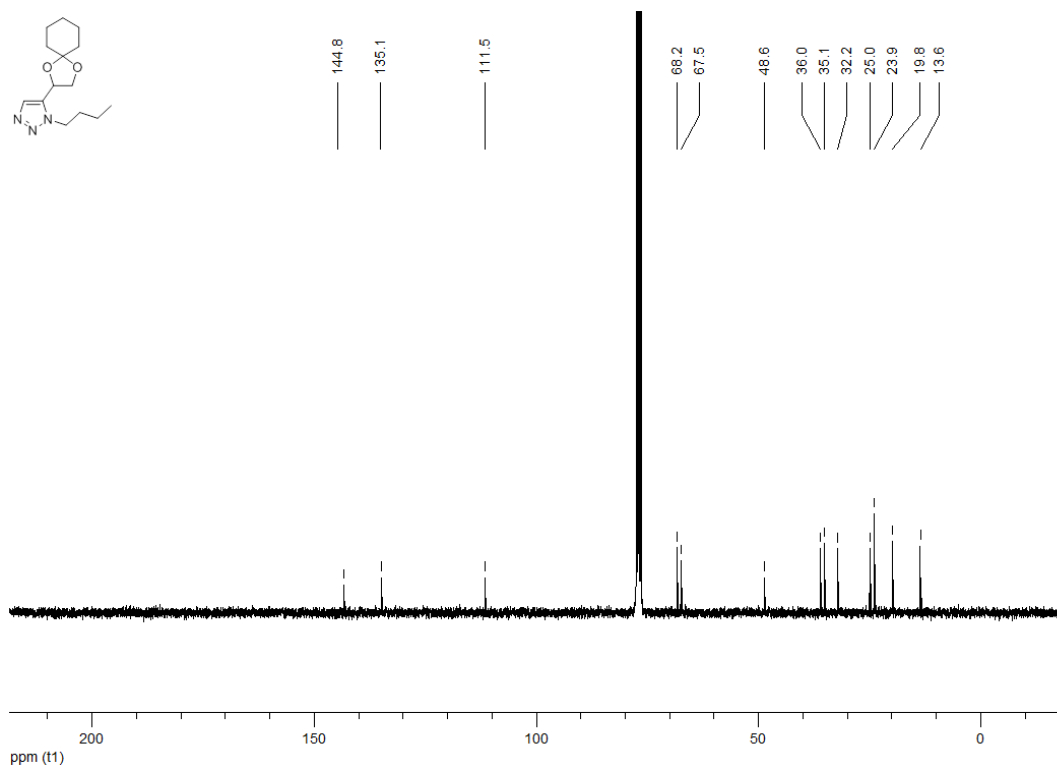
H NMR (300 MHz, CDCl₃) 4-{1,4-dioxaspiro[4.5]decan-2-yl}-1-(2-ethoxyethyl)-1*H*-1,2,3-triazole (158k)

¹H NMR (300 MHz, CDCl₃) 4-{1,4-dioxaspiro[4.5]decan-2-yl}-1-(2-ethoxyethyl)-1*H*-1,2,3-triazole (158k)
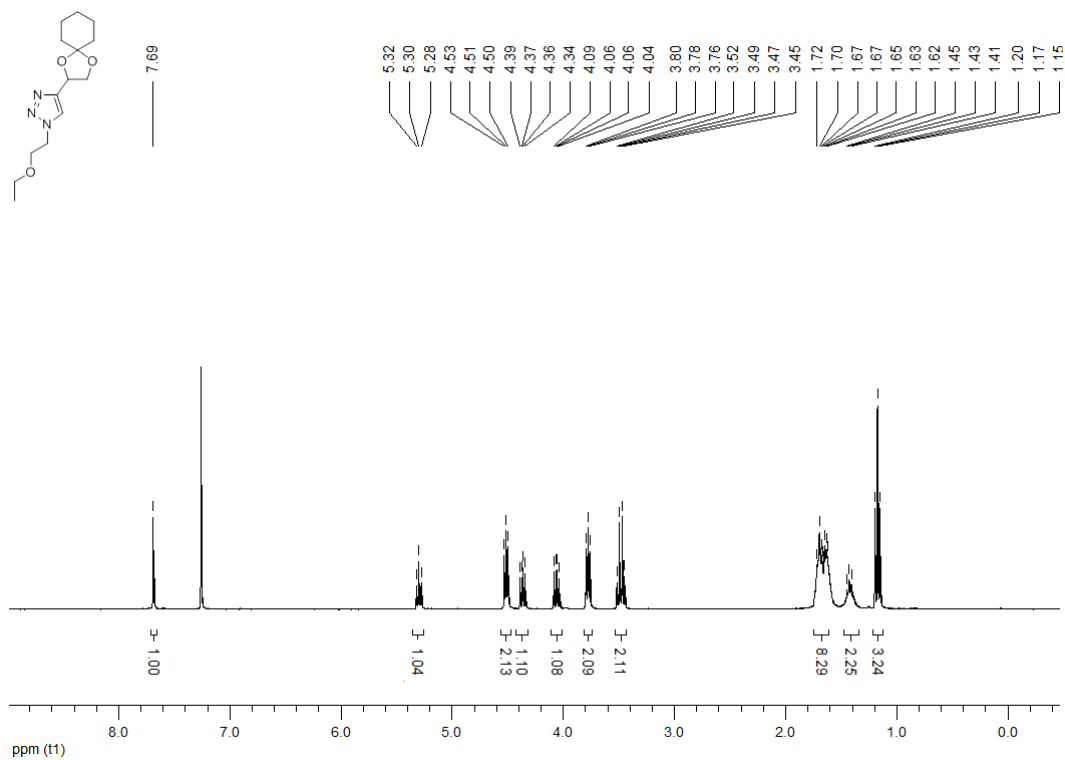
¹³C NMR (100 MHz, CDCl₃) 4-{1,4-dioxaspiro[4.5]decan-2-yl}-1-(2-ethoxyethyl)-1*H*-1,2,3-triazole (158k)
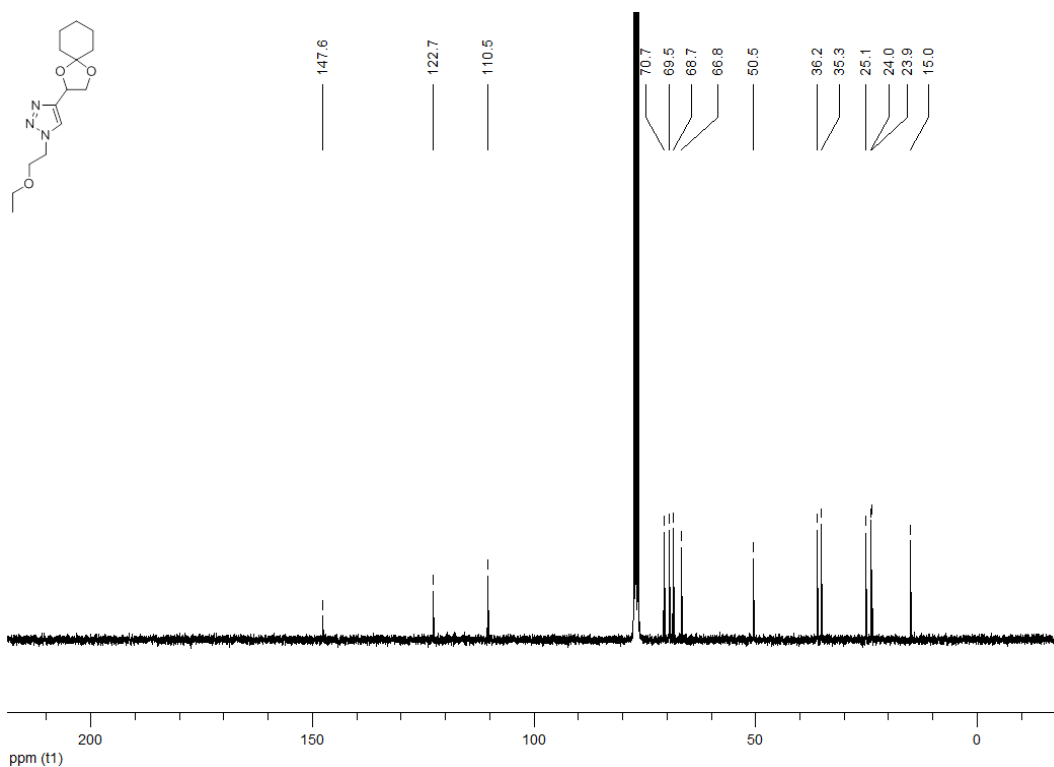
¹H NMR (300 MHz, CDCl₃) 4-{1,4-dioxaspiro[4.5]decan-2-yl}-1-(2-ethoxyethyl)-1*H*-1,2,3-triazole (158k)
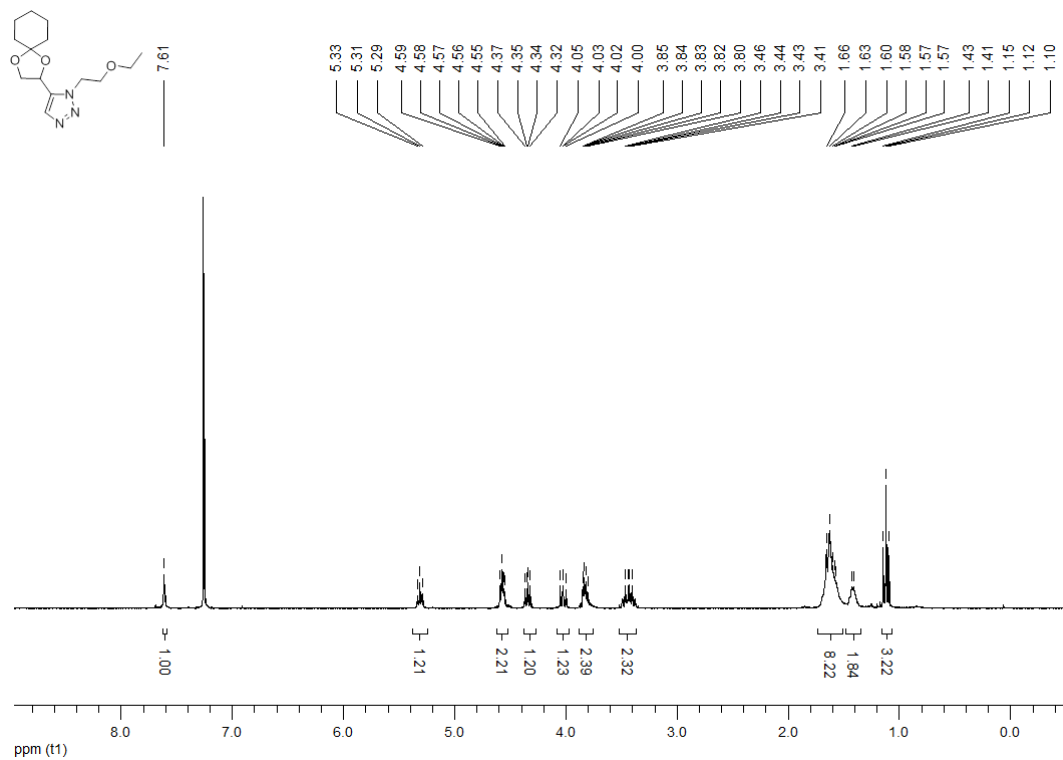
¹³C NMR (100 MHz, CDCl₃) 4-{1,4-dioxaspiro[4.5]decan-2-yl}-1-(2-ethoxyethyl)-1*H*-1,2,3-triazole (158k)
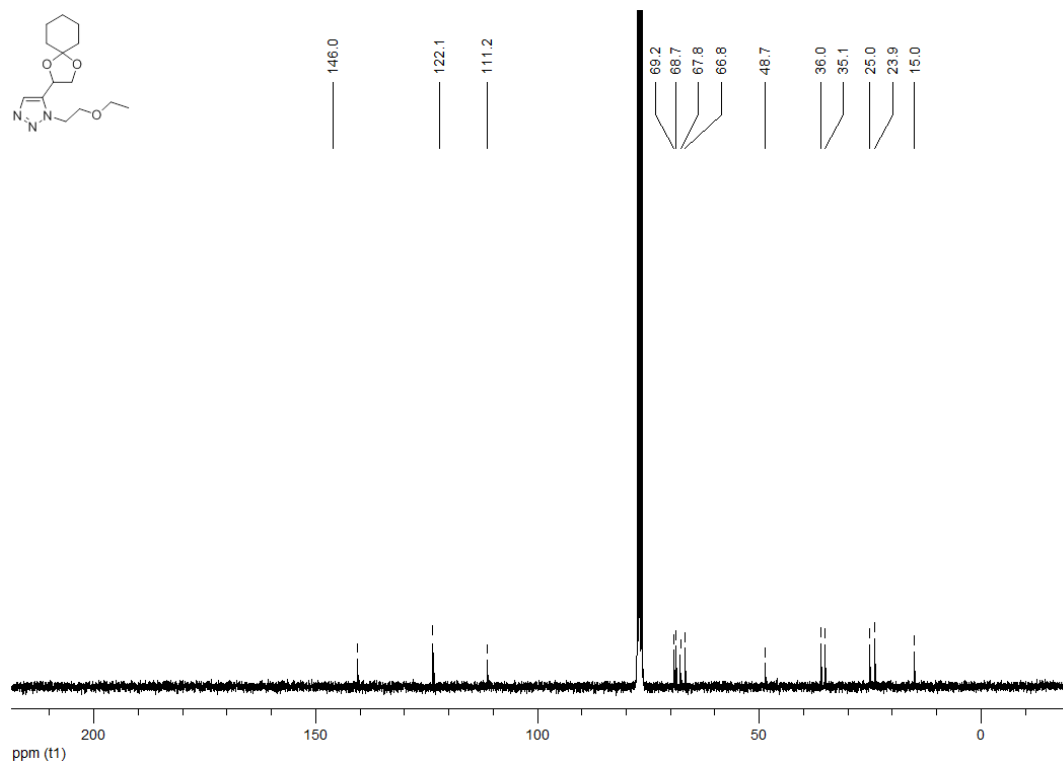
¹H NMR (300 MHz, MeOD) 1-(1*H*-1,2,3-triazol-4-yl)ethane-1,2-diol (154g)
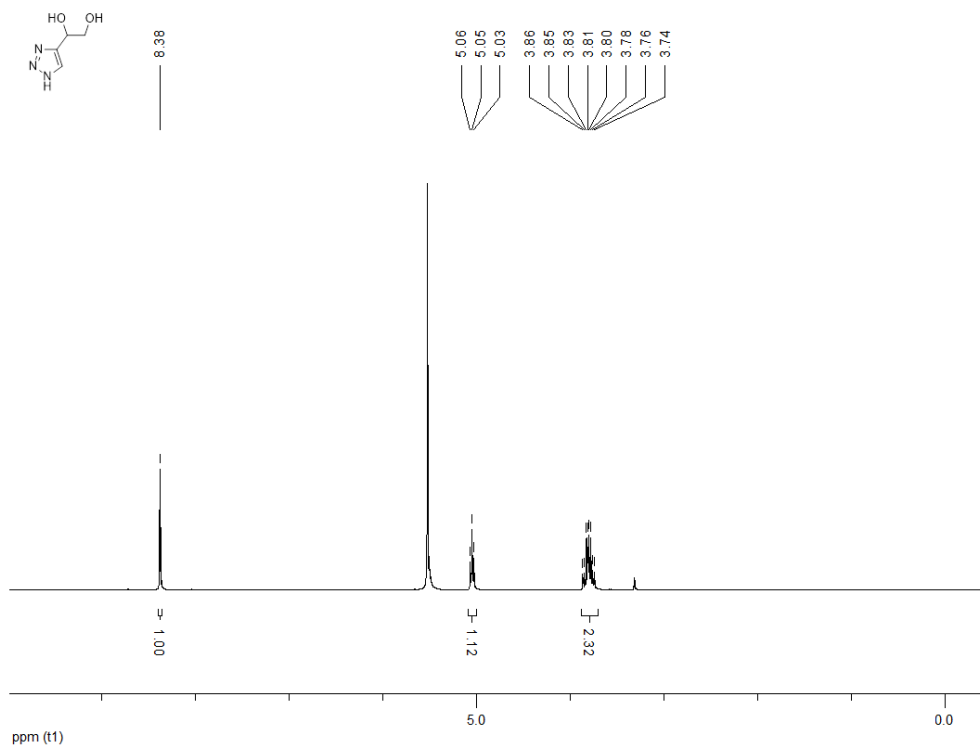
¹³C NMR (100 MHz, MeOD) 1-(1*H*-1,2,3-triazol-4-yl)ethane-1,2-diol (154g)
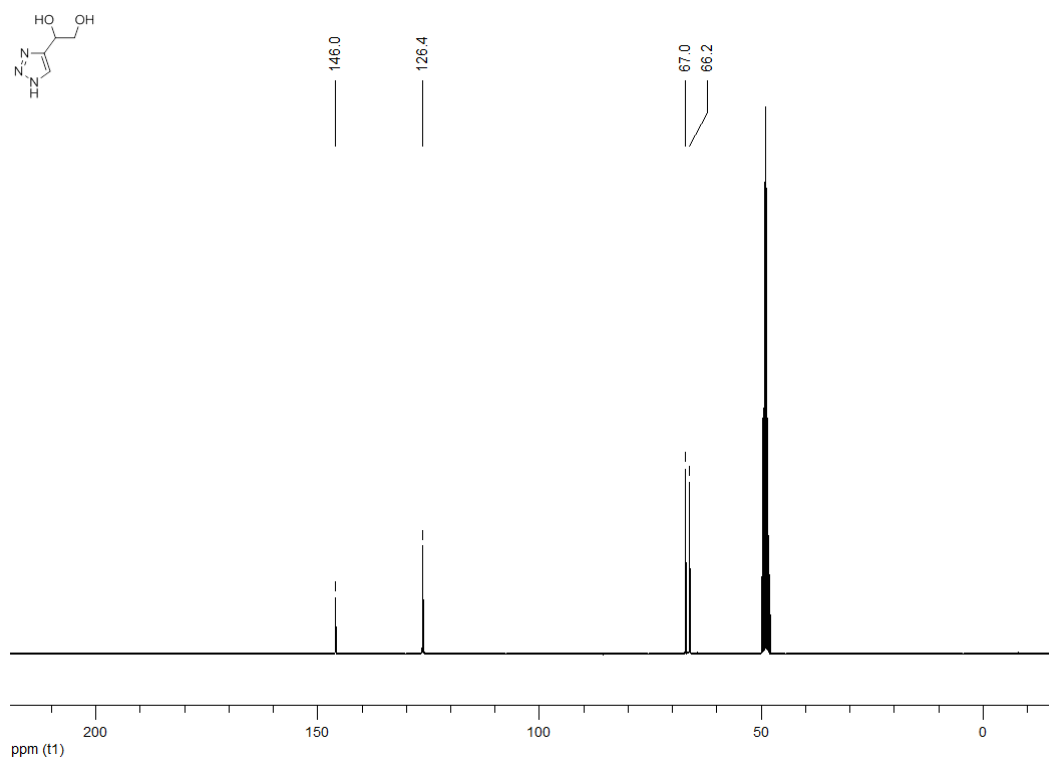
¹H NMR (300 MHz, MeOD) 1-(1-methyl-1*H*-1,2,3-triazol-4-yl)ethane-1,2-diol (154h)
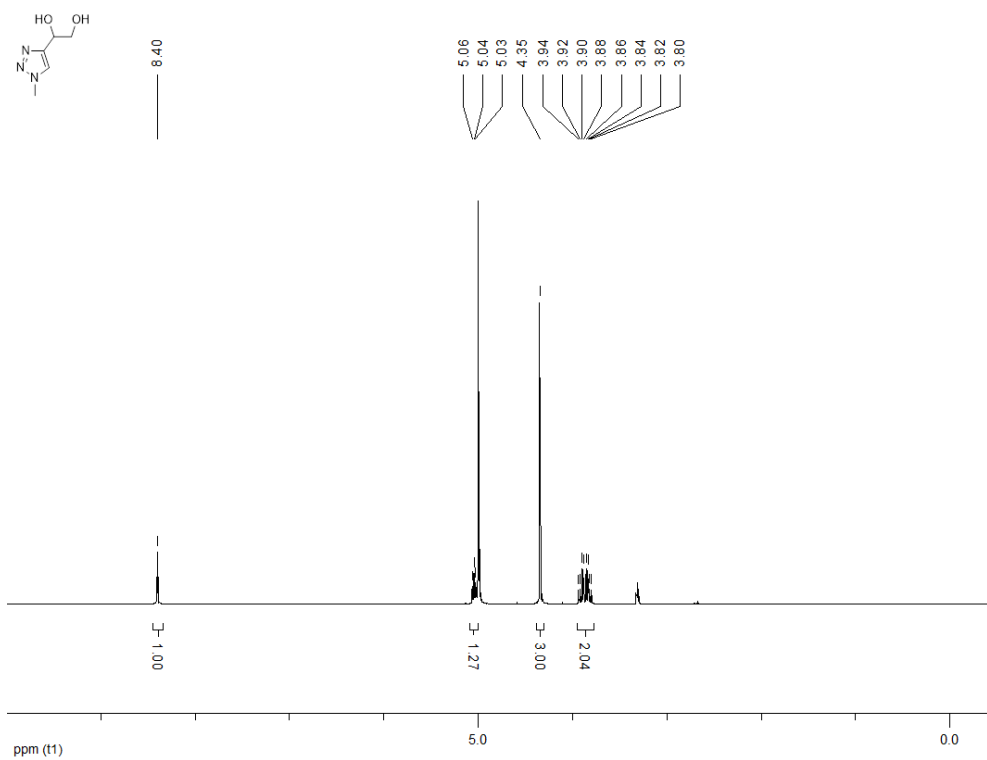
¹³C NMR (100 MHz, MeOD) 1-(1-methyl-1*H*-1,2,3-triazol-4-yl)ethane-1,2-diol (154h)
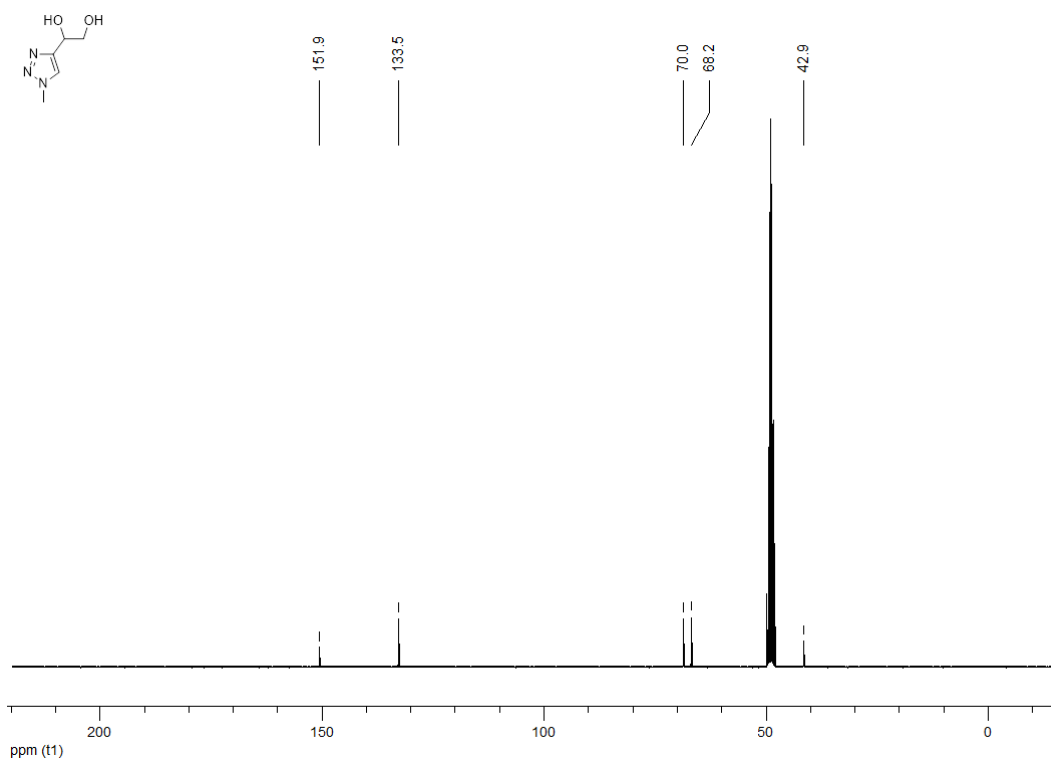
^{1}H NMR (300 MHz, MeOD) 1-(1-methyl-1*H*-1,2,3-triazol-5-yl)ethane-1,2-diol (155h)
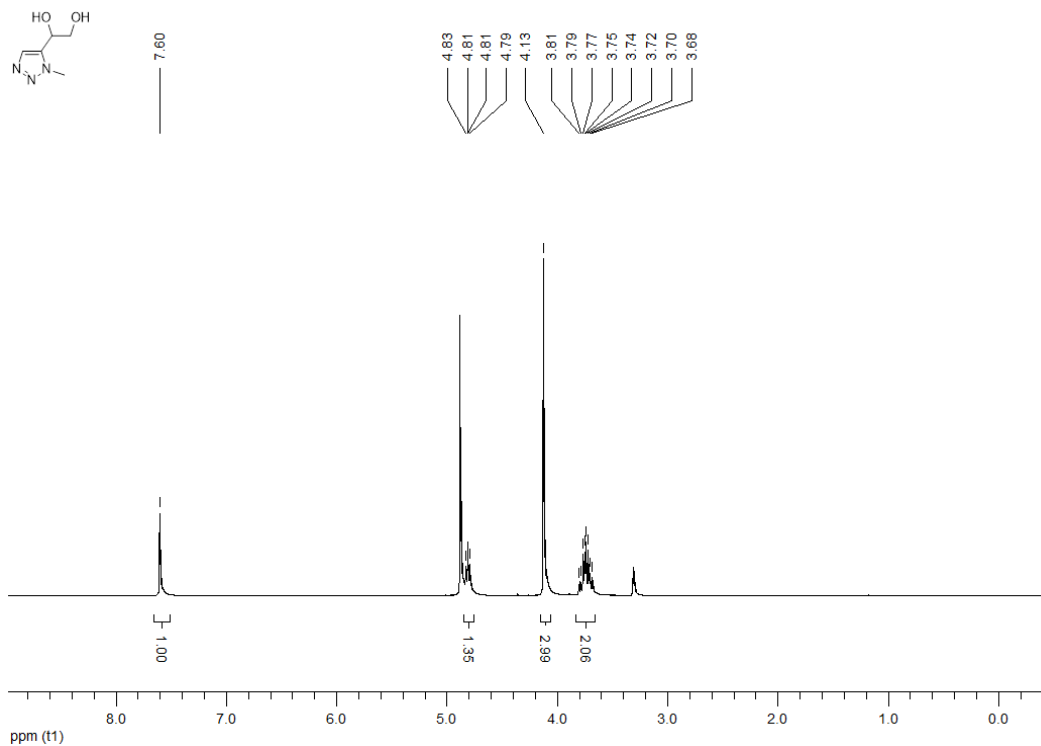
^{13}C NMR (100 MHz, MeOD) 1-(1-methyl-1*H*-1,2,3-triazol-5-yl)ethane-1,2-diol (155h)
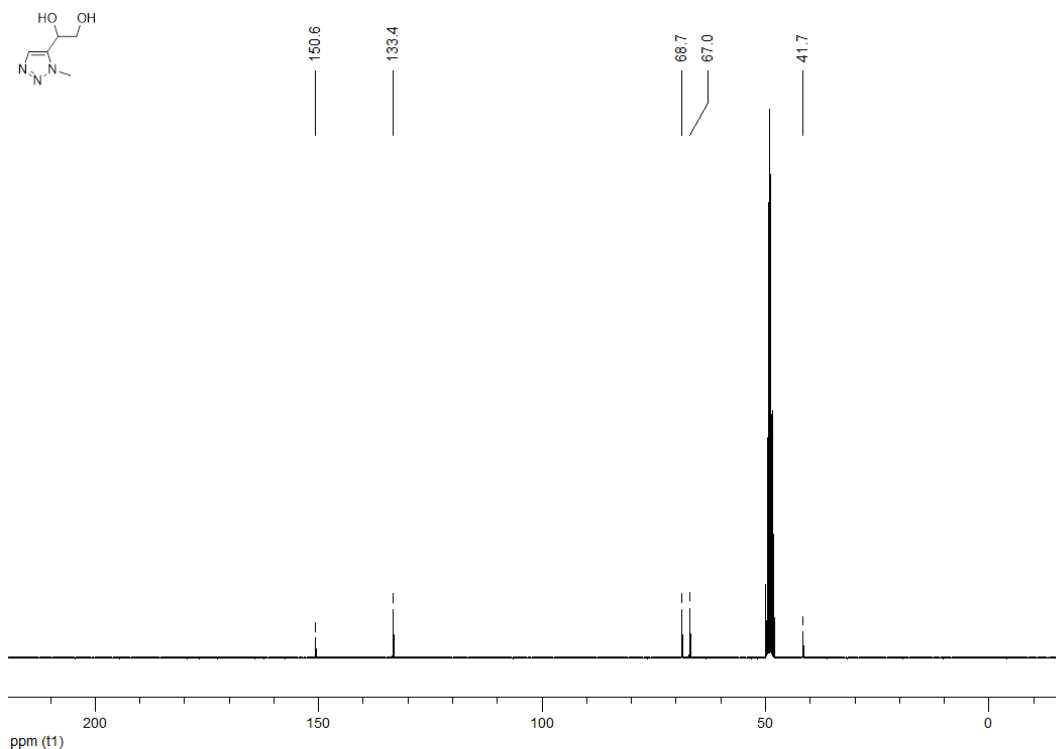
¹H NMR (300 MHz, CD₃CN) 1-[1-(cyclopropylmethyl)-1*H*-1,2,3-triazol-4-yl]ethane-1,2-diol (154i)
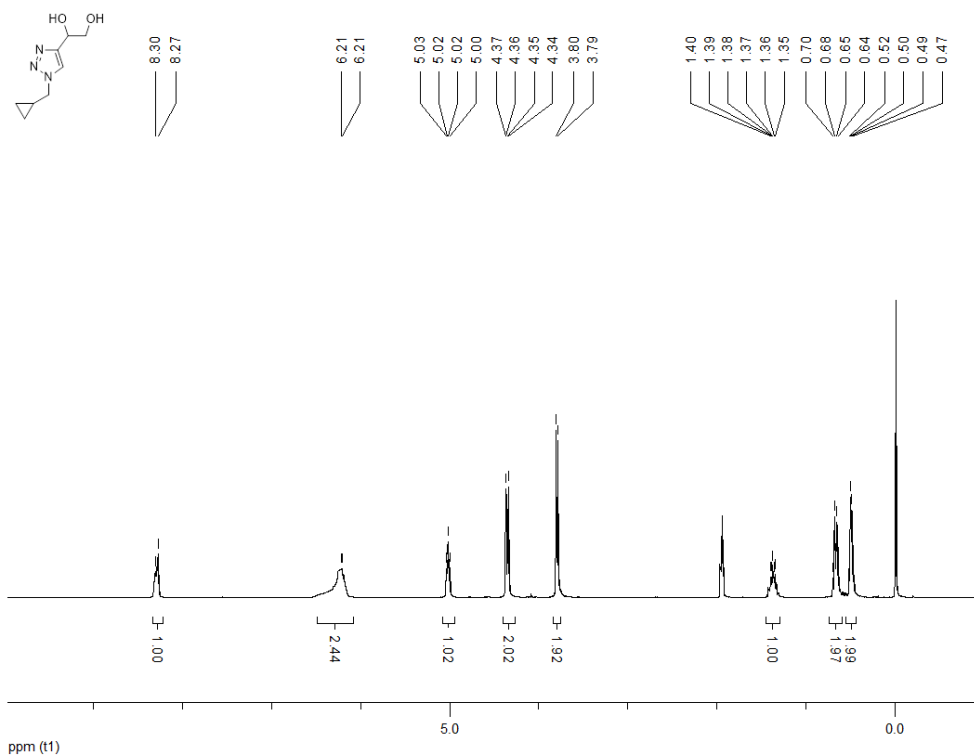
¹C NMR (100 MHz, CD₃CN) 1-[1-(cyclopropylmethyl)-1*H*-1,2,3-triazol-4-yl]ethane-1,2-diol (154i)
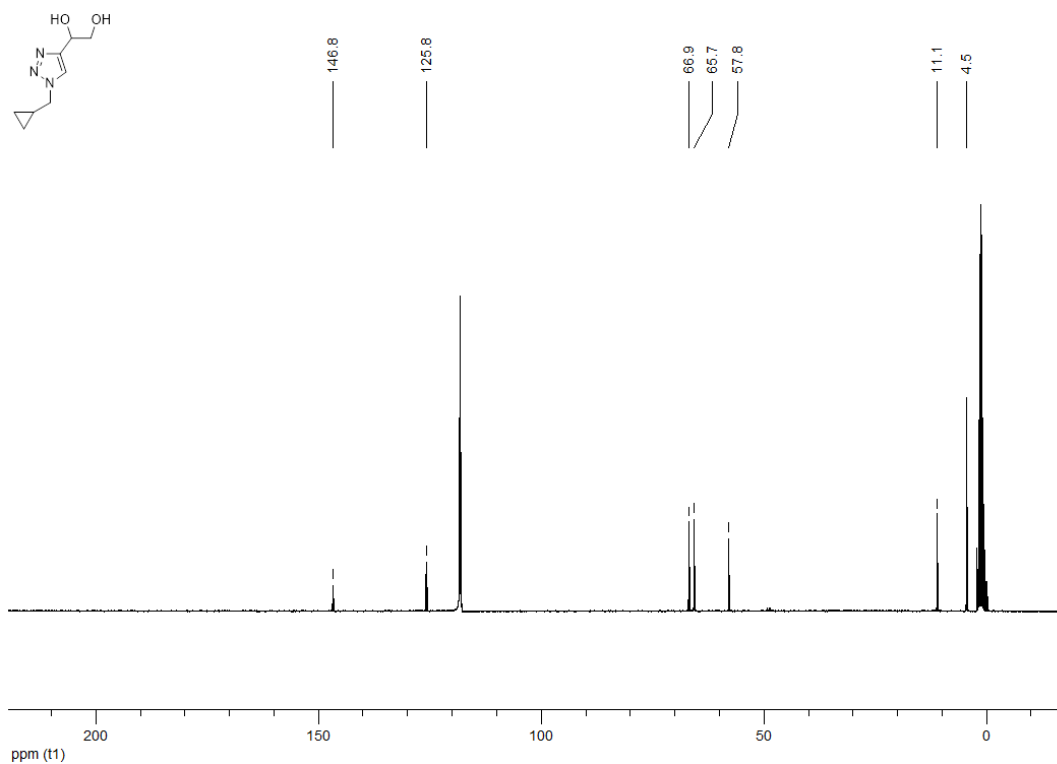
¹H NMR (300 MHz, CD₃CN) 1-[1-(cyclopropylmethyl)-1<i>H</i>-1,2,3-triazol-5-yl]ethane-1,2-diol (155i)
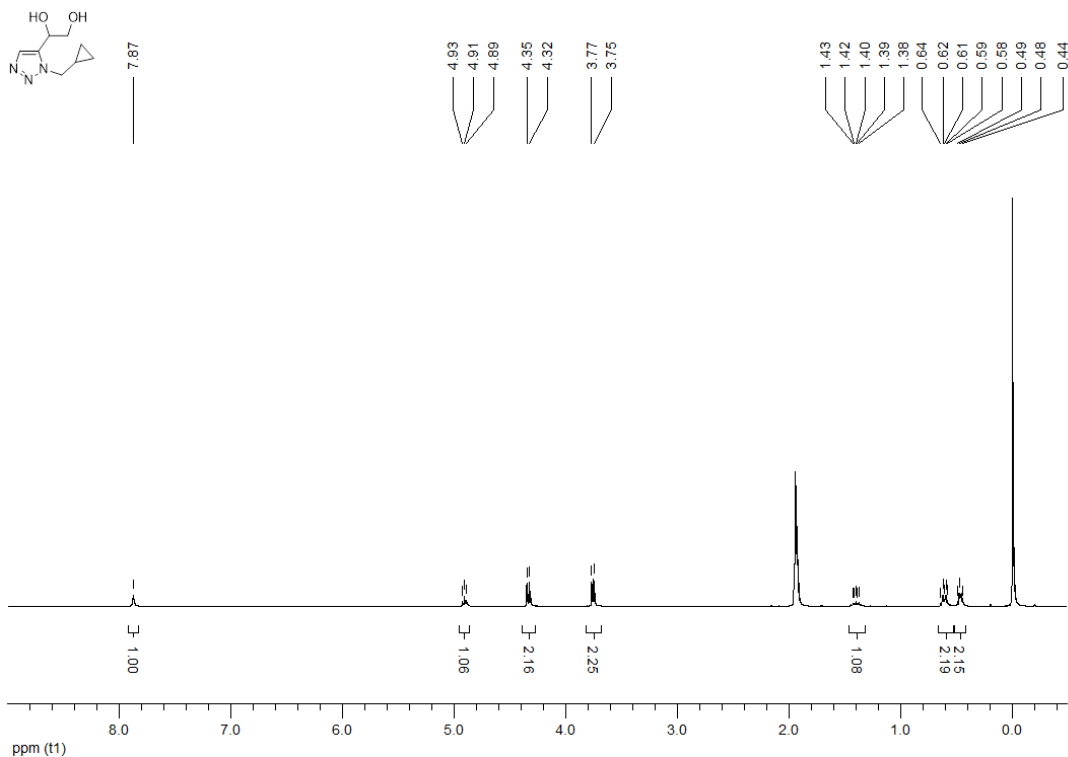
¹C NMR (100 MHz, CD₃CN) 1-[1-(cyclopropylmethyl)-1<i>H</i>-1,2,3-triazol-5-yl]ethane-1,2-diol (155i)
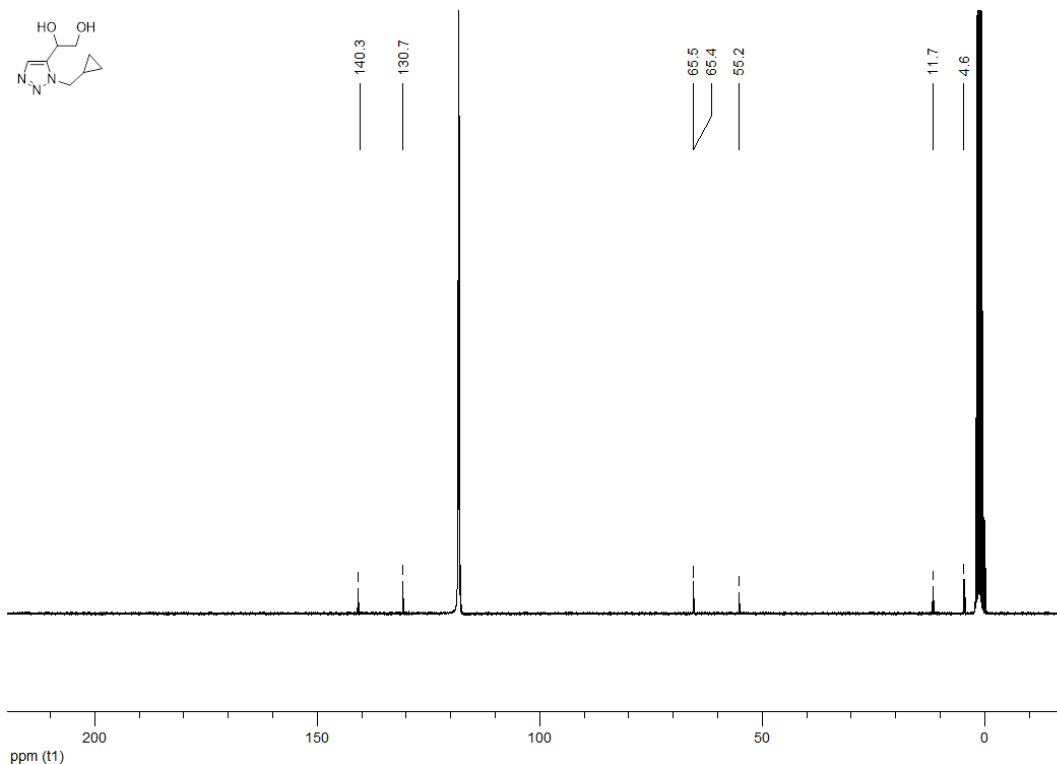
¹H NMR (300 MHz, MeOD) 1-(1-butyl-1*H*-1,2,3-triazol-4-yl)ethane-1,2-diol (154j)

¹³C NMR (100 MHz, MeOD) 1-(1-butyl-1*H*-1,2,3-triazol-4-yl)ethane-1,2-diol (154j)

¹H NMR (300 MHz, MeOD) 1-(1-butyl-1*H*-1,2,3-triazol-5-yl)ethane-1,2-diol (155j)
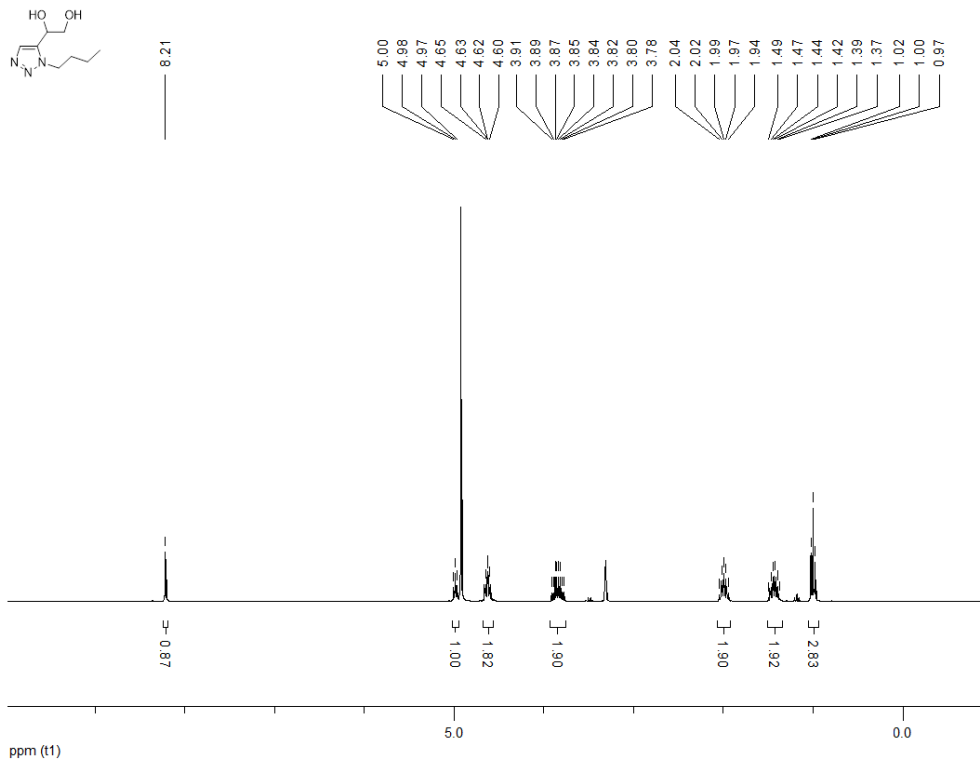
¹³C NMR (100 MHz, MeOD) 1-(1-butyl-1*H*-1,2,3-triazol-5-yl)ethane-1,2-diol (155j)
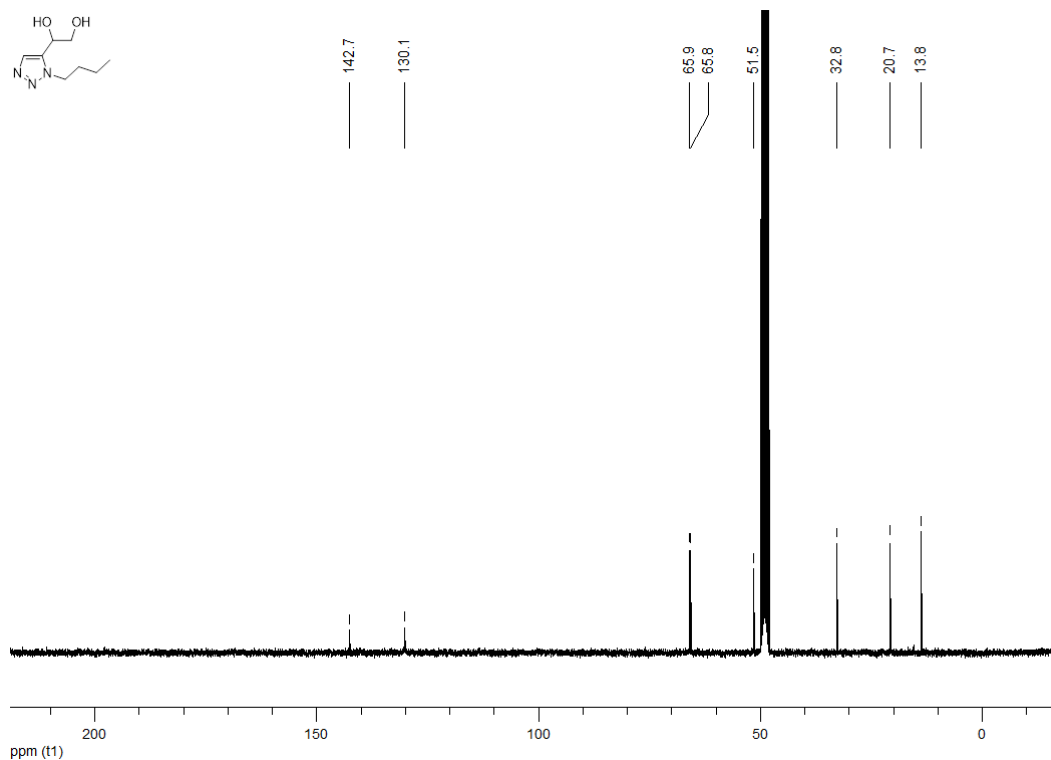
^{1}H NMR (300 MHz, CD$_3$CN) 1-[1-(2-ethoxyethyl)-1H-1,2,3-triazol-4-yl]ethane-1,2-diol (154k)
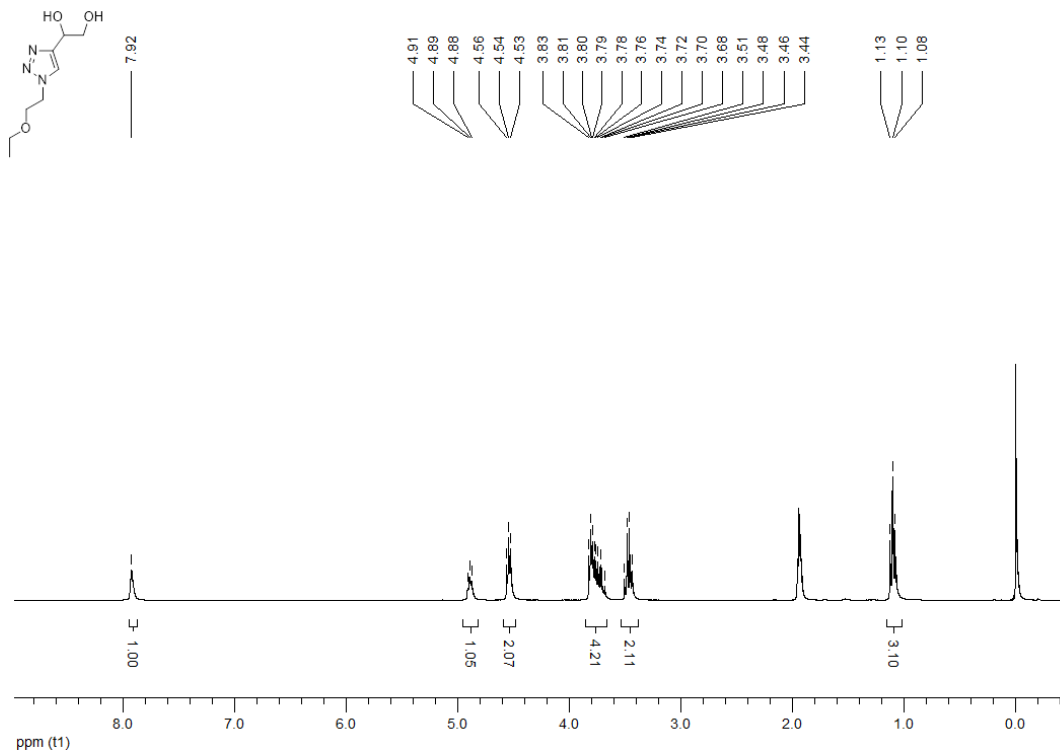
^{13}C NMR (100 MHz, CD$_3$CN) 1-[1-(2-ethoxyethyl)-1H-1,2,3-triazol-4-yl]ethane-1,2-diol (154k)
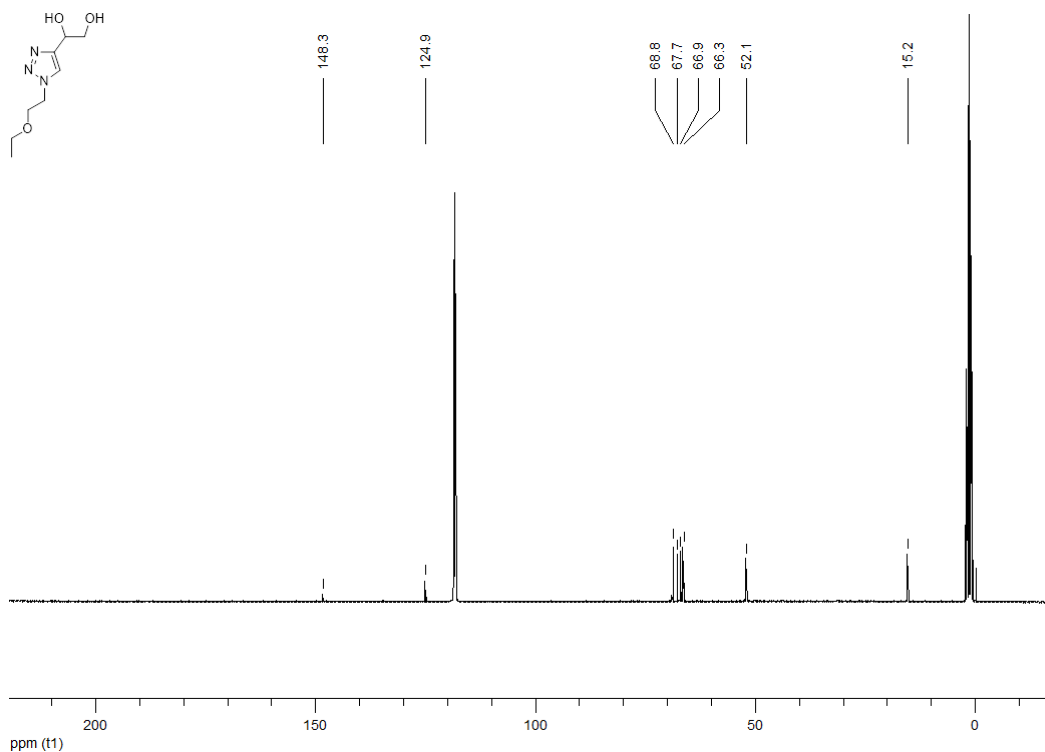
¹H NMR (300 MHz, MeOD) 1-[1-(2-ethoxyethyl)-1*H*-1,2,3-triazol-4-yl]ethane-1,2-diol (155k)
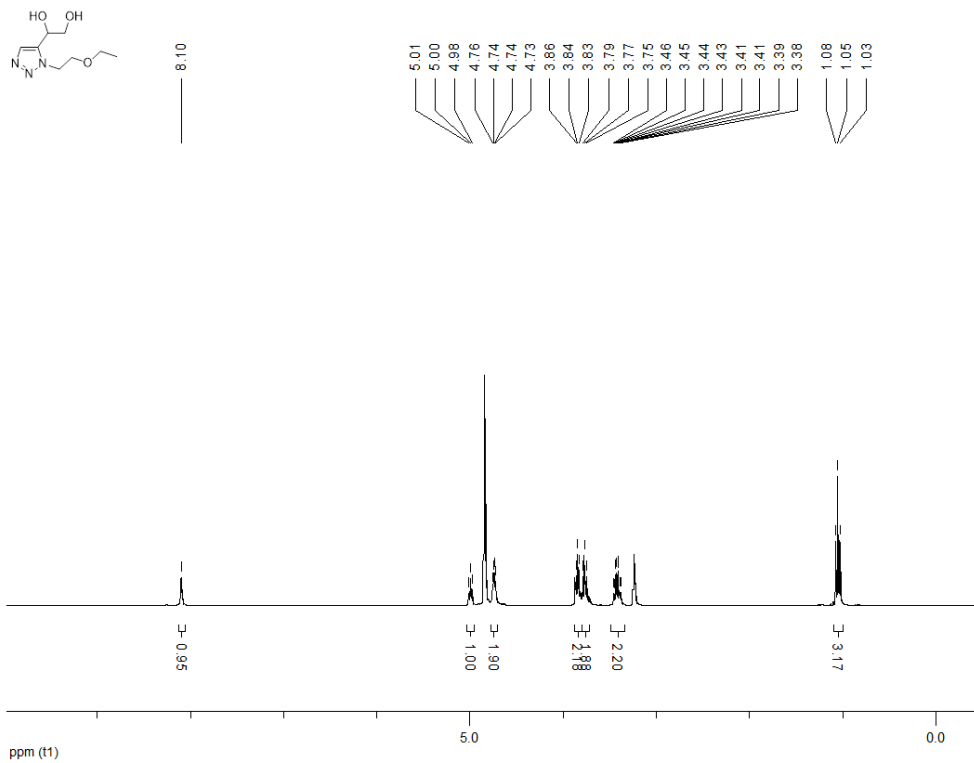
¹³C NMR (100 MHz, MeOD) 1-[1-(2-ethoxyethyl)-1*H*-1,2,3-triazol-4-yl]ethane-1,2-diol (155k)
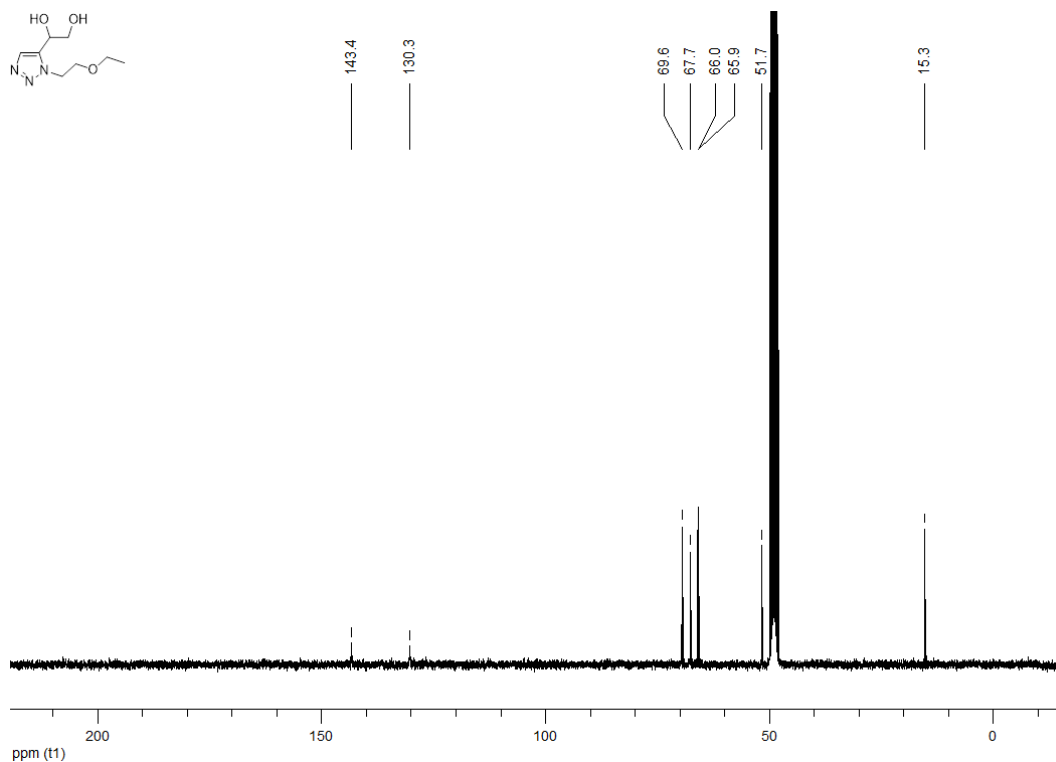
8.1.5 Synthesis, ^{1}H and ^{13}C NMR of 3,5-disubstituted isoxazoles

Synthesis of 160a-g: the procedure for the synthesis of compounds **160a-g** is described in *Molecules* **2018**, *23(10)*, 2545 (see Appendix 1).[253]

(*E*)-*N*-[(4-methylphenyl)methylidene]hydroxylamine (160a): the compound is described in *Molecules* **2018**, *23(10)*, 2545 (see Appendix 1, SI).[253]

(*E*)-*N*-[(3-chlorophenyl)methylidene]hydroxylamine (160b): the compound is described in *Molecules* **2018**, *23(10)*, 2545 (see Appendix 1, SI).[253]

(*E*)-*N*-[(2,4-difluorophenyl)methylidene]hydroxylamine (160c): the compound is described in *Molecules* **2018**, *23(10)*, 2545 (see Appendix 1, SI).[253]

(*E*)-*N*-[(pyridin-3-yl)methylidene]hydroxylamine (160d): the compound is described in *Molecules* **2018**, *23(10)*, 2545 (see Appendix 1, SI).[253]

(*E*)-*N*-(cyclopropylmethylidene)hydroxylamine (160e): the compound is described in *Molecules* **2018**, *23(10)*, 2545 (see Appendix 1, SI).[253]

(*E*)-*N*-[(oxolan-3-yl)methylidene]hydroxylamine (160f): the compound is described in *Molecules* **2018**, *23(10)*, 2545 (see Appendix 1, SI).[253]

(*E*)-*N*-(cyclohexylmethylidene)hydroxylamine (160g): the compound is described in *Molecules* **2018**, *23(10)*, 2545 (see Appendix 1, SI).[253]

Synthesis of 161a-g: the procedure for the synthesis of compounds **161a-g** is described in *Molecules* **2018**, *23(10)*, 2545 (see Appendix 1).[253]

(*Z*)-*N*-hydroxy-4-methylbenzene-1-carbonimidoyl chloride (161a): the compound is described in *Molecules* **2018**, *23(10)*, 2545 (see Appendix 1, SI).[253]

(*Z*)-3-chloro-*N*-hydroxybenzene-1-carbonimidoyl chloride (161b): the compound is described in *Molecules* **2018**, *23(10)*, 2545 (see Appendix 1, SI).[253]

(*Z*)-2,4-difluoro-*N*-hydroxybenzene-1-carbonimidoyl chloride (161c): the compound is described in *Molecules* **2018**, *23(10)*, 2545 (see Appendix 1, SI).[253]

(*Z*)-*N*-hydroxypyridine-3-carbonimidoyl chloride (161d): the compound is described in *Molecules* **2018**, *23(10)*, 2545 (see Appendix 1, SI).[253]

(*Z*)-*N*-hydroxycyclopropanecarbonimidoyl chloride (161e): the compound is described in *Molecules* **2018**, *23(10)*, 2545 (see Appendix 1, SI).[253]

(Z)-N-hydroxyoxolane-3-carbonimidoyl chloride (161f): the compound is described in *Molecules* **2018**, *23(10)*, 2545 (see Appendix 1, SI).[253]

(Z)-N-hydroxycyclohexanecarbonimidoyl chloride (161g): the compound is described in *Molecules* **2018**, *23(10)*, 2545 (see Appendix 1, SI).[253]

Synthesis of 162a-g: the procedure for the synthesis of compounds **162a-g** is described in *Molecules* **2018**, *23(10)*, 2545 (see Appendix 1).[253]

1-[3-(4-methylphenyl)-1,2-oxazol-5-yl]ethane-1,2-diol (162a): the compound is described in *Molecules* **2018**, *23(10)*, 2545 (see Appendix 1).[253]

1-[3-(3-chlorophenyl)-1,2-oxazol-5-yl]ethane-1,2-diol (162b): the compound is described in *Molecules* **2018**, *23(10)*, 2545 (see Appendix 1).[253]

1-[3-(2,4-difluorophenyl)-1,2-oxazol-5-yl]ethane-1,2-diol (162c): the compound is described in *Molecules* **2018**, *23(10)*, 2545 (see Appendix 1).[253]

1-[3-(pyridin-3-yl)-1,2-oxazol-5-yl]ethane-1,2-diol (126d): the compound is described in *Molecules* **2018**, *23(10)*, 2545 (see Appendix 1).[253]

1-(3-cyclopropyl-1,2-oxazol-5-yl)ethane-1,2-diol (162e): the compound is described in *Molecules* **2018**, *23(10)*, 2545 (see Appendix 1).[253]

1-[3-(oxolan-3-yl)-1,2-oxazol-5-yl]ethane-1,2-diol (162f): the compound is described in *Molecules* **2018**, *23(10)*, 2545 (see Appendix 1).[253]

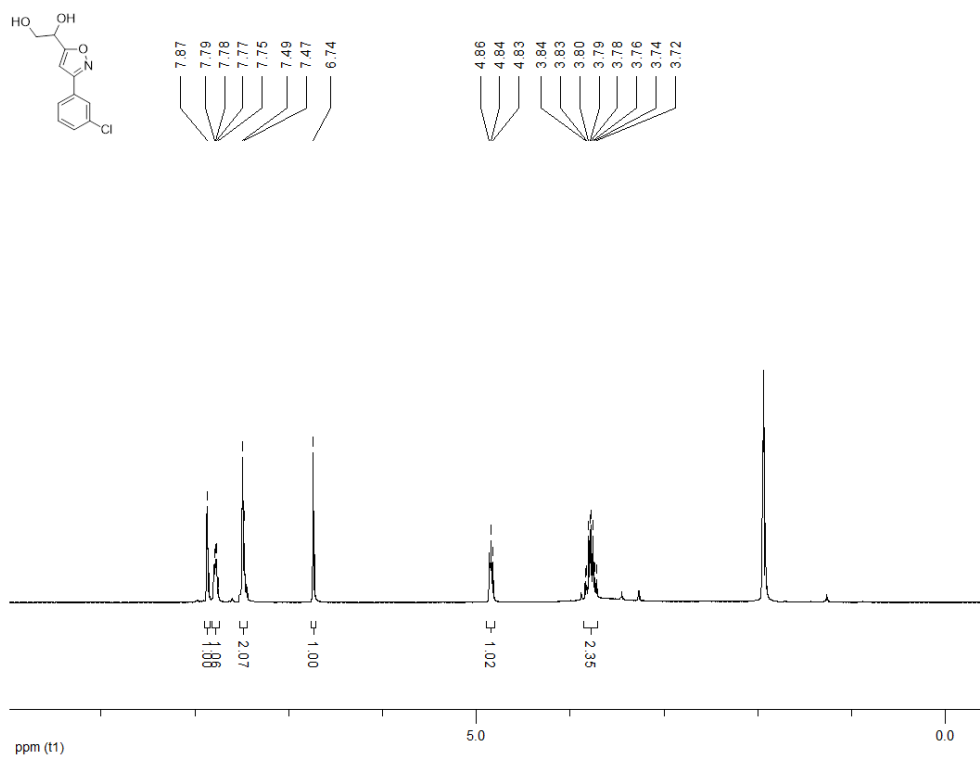**1-(3-cyclohexyl-1,2-oxazol-5-yl)ethane-1,2-diol (162g):** the compound is described in *Molecules* **2018**, *23(10)*, 2545 (see Appendix 1).[253]

Synthesis of 164: the procedure for the synthesis of compound **4** is described in *Molecules* **2018**, *23(10)*, 2545 (see Appendix 1).[253]

Ethyl (2E)-2-(hydroxyimino)acetate (164): the compound is described in *Molecules* **2018**, *23(10)*, 2545 (see Appendix 1).[253]

Synthesis of 163: the procedure for the synthesis of compound **163** is described in *Molecules* **2018**, *23(10)*, 2545 (see Appendix 1).[253]

Ethyl 5-{1,4-dioxaspiro[4.5]decan-2-yl}-1,2-oxazole-3-carboxylate (163): the compound is described in *Molecules* **2018**, *23(10)*, 2545 (see Appendix 1).[253]

Synthesis of 167: the procedure for the synthesis of compound **167** is described in *Molecules* **2018**, *23(10)*, 2545 (see Appendix 1).[253]

5-{1,4-dioxaspiro[4.5]decan-2-yl}-1,2-oxazole-3-carboxylic acid (167): the compound is described in *Molecules* **2018**, *23(10)*, 2545 (see Appendix 1).[253]

Synthesis of 169h-m: the procedure for the synthesis of compounds **169h-m** is described in *Molecules* **2018**, *23(10)*, 2545 (see Appendix 1).[253]

***N*-benzyl-5-{1,4-dioxaspiro[4.5]decan-2-yl}-1,2-oxazole-3-carboxamide (169h):** the compound is described in *Molecules* **2018**, *23(10)*, 2545 (see Appendix 1, SI).[253]

5-{1,4-dioxaspiro[4.5]decan-2-yl}-*N*-(4-fluorophenyl)- 1,2-oxazole-3-carboxamide (169i): the compound is described in *Molecules* **2018**, *23(10)*, 2545 (see Appendix 1, SI).[253]

5-{1,4-dioxaspiro[4.5]decan-2-yl}-*N*-[(thiophen-2-yl)methyl]-1,2-oxazole-3-carboxamide (169j): the compound is described in *Molecules* **2018**, *23(10)*, 2545 (see Appendix 1, SI).[253]

5-{1,4-dioxaspiro[4.5]decan-2-yl}-*N*-[(pyridin-3-yl)methyl]-1,2-oxazole-3-carboxamide (169k): the compound is described in *Molecules* **2018**, *23(10)*, 2545 (see Appendix 1, SI).[253]

5-{1,4-dioxaspiro[4.5]decan-2-yl}-*N*-(2-methoxyethyl)-1,2-oxazole-3-carboxamide (169l): the compound is described in *Molecules* **2018**, *23(10)*, 2545 (see Appendix 1, SI).[253]

5-{1,4-dioxaspiro[4.5]decan-2-yl}-3-(pyrrolidine-1-carbonyl)-1,2-oxazole (169m): the compound is described in *Molecules* **2018**, *23(10)*, 2545 (see Appendix 1, SI).[253]

Synthesis of 166, 168, 170h-m: the procedure for the synthesis of compounds **166, 168, 1704h-m** is described in *Molecules* **2018**, *23(10)*, 2545 (see Appendix 1).[253]

Ethyl 5-(1,2-dihydroxyethyl)-1,2-oxazole-3-carboxylate (166): the compound is described in *Molecules* **2018**, *23(10)*, 2545 (see Appendix 1).[253]

5-(1,2-dihydroxyethyl)-1,2-oxazole-3-carboxylic acid (168): the compound is described in *Molecules* **2018**, *23(10)*, 2545 (see Appendix 1).[253]

***N*-benzyl-5-(1,2-dihydroxyethyl)-1,2-oxazole-3-carboxamide (170h):** the compound is described in *Molecules* **2018**, *23(10)*, 2545 (see Appendix 1).[253]

5-(1,2-dihydroxyethyl)-*N*-(4-fluorophenyl)-1,2-oxazole-3-carboxamide (170i): the compound is described in *Molecules* **2018**, *23(10)*, 2545 (see Appendix 1).[253]

5-(1,2-dihydroxyethyl)-*N*-[(thiophen-2-yl)methyl]-1,2-oxazole-3-carboxamide (170j): the compound is described in *Molecules* **2018**, *23(10)*, 2545 (see Appendix 1).[253]

5-(1,2-dihydroxyethyl)-*N*-[(pyridin-3-yl)methyl]-1,2-oxazole-3-carboxamide (170k): the compound is described in *Molecules* **2018**, *23(10)*, 2545 (see Appendix 1).[253]

5-(1,2-dihydroxyethyl)-*N*-(2-methoxyethyl)-1,2-oxazole-3-carboxamide (170l): the compound is described in *Molecules* **2018**, *23(10)*, 2545 (see Appendix 1).[253]

1-[3-(pyrrolidine-1-carbonyl)-1,2-oxazol-5-yl]ethane-1,2-diol (170m): the compound is described in *Molecules* **2018**, *23(10)*, 2545 (see Appendix 1).[253]

¹H NMR (300 MHz, CD₃CN) 1-[3-(4-methylphenyl)-1,2-oxazol-5-yl]ethane-1,2-diol (162a)
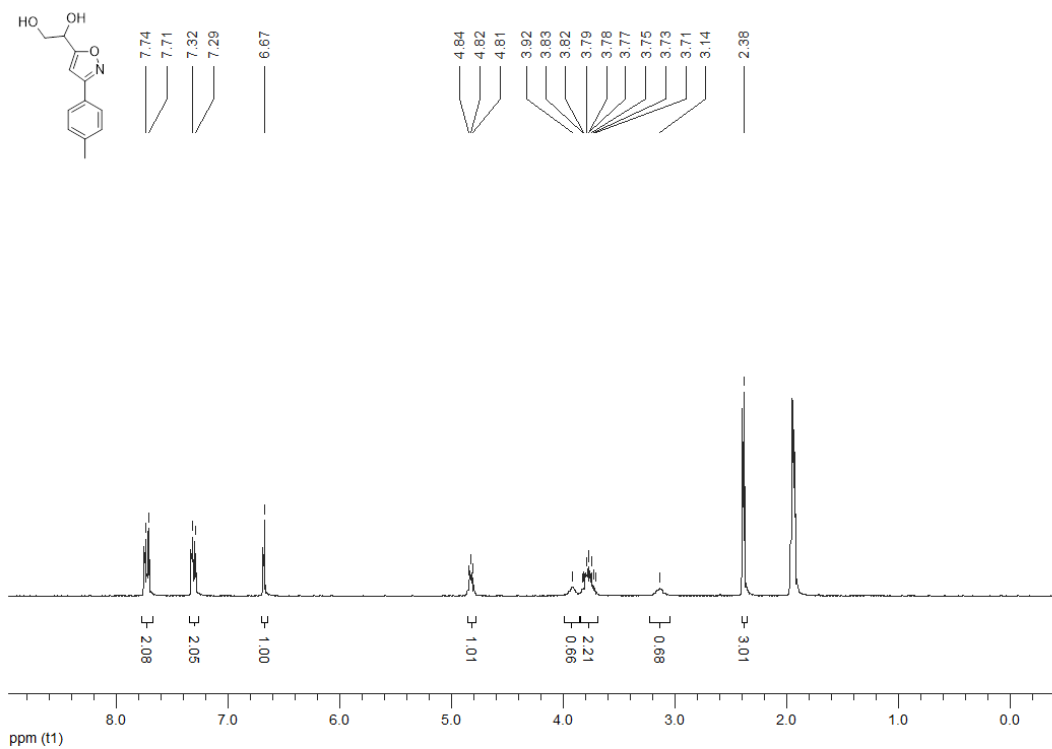
¹³C NMR (100 MHz, CD₃CN) 1-[3-(4-methylphenyl)-1,2-oxazol-5-yl]ethane-1,2-diol (162a)
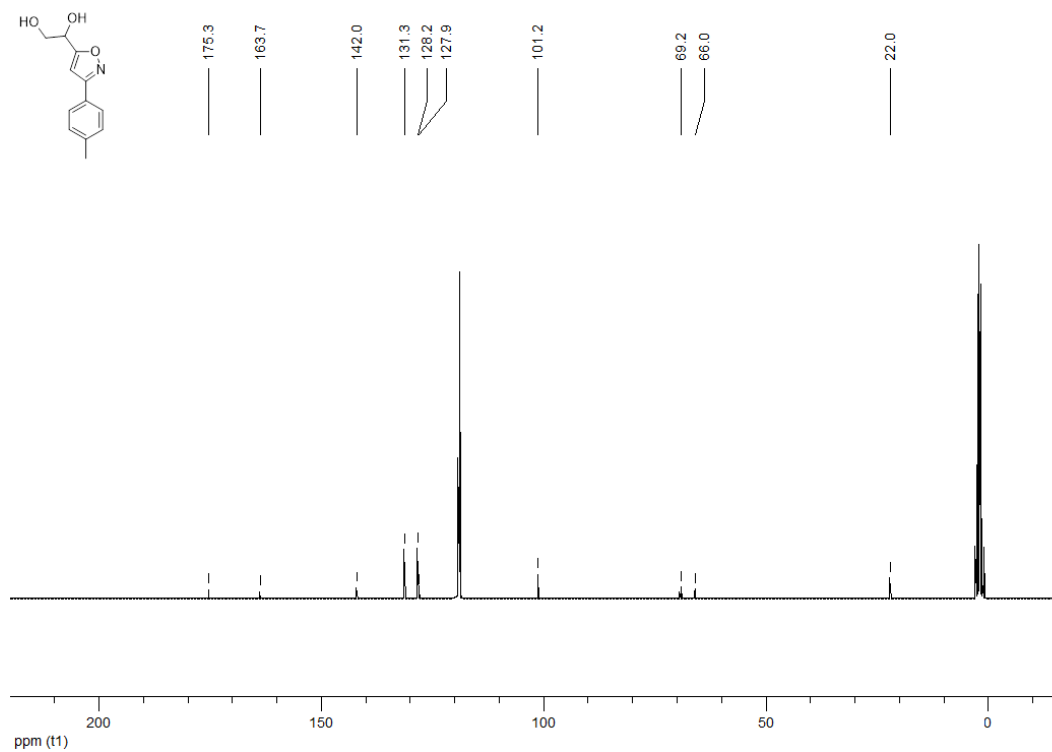
**¹H NMR (300 MHz, CD₃CN) 1-[3-(3-chlorophenyl)-1,2-oxazol-5-yl]ethane-1,2-diol (162b)**

¹³C NMR (100 MHz, CD₃CN) 1-[3-(3-chlorophenyl)-1,2-oxazol-5-yl]ethane-1,2-diol (162b)
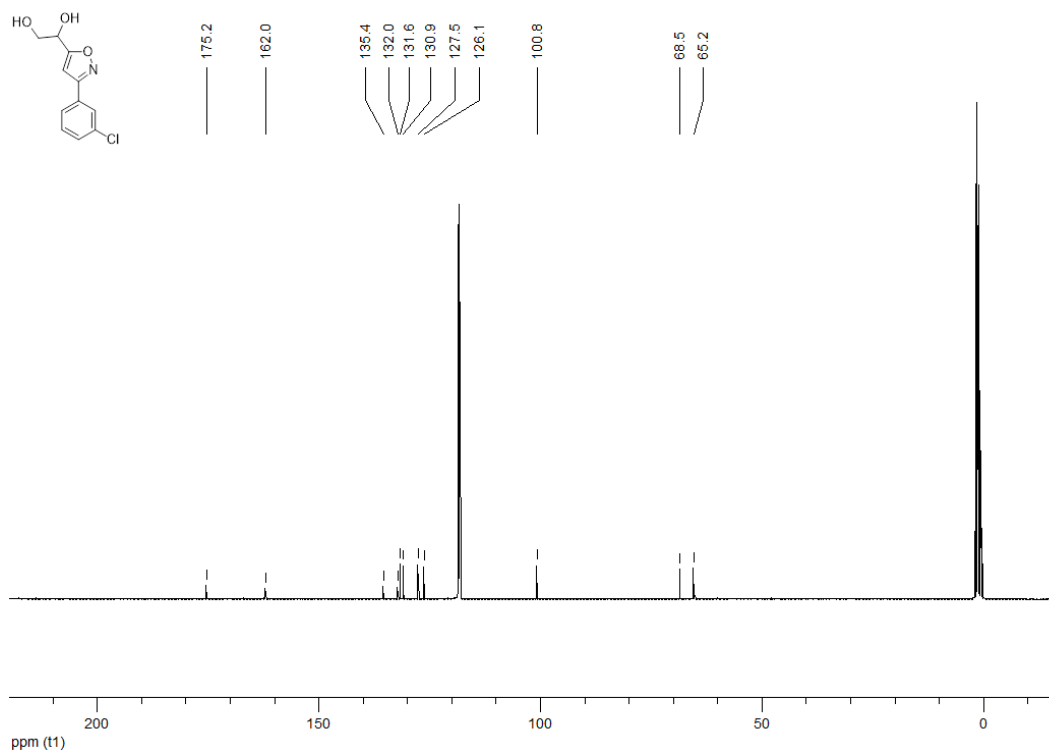
¹H NMR (300 MHz, CD₃CN) 1-[3-(2,4-difluorophenyl)-1,2-oxazol-5-yl]ethane-1,2-diol (162c)
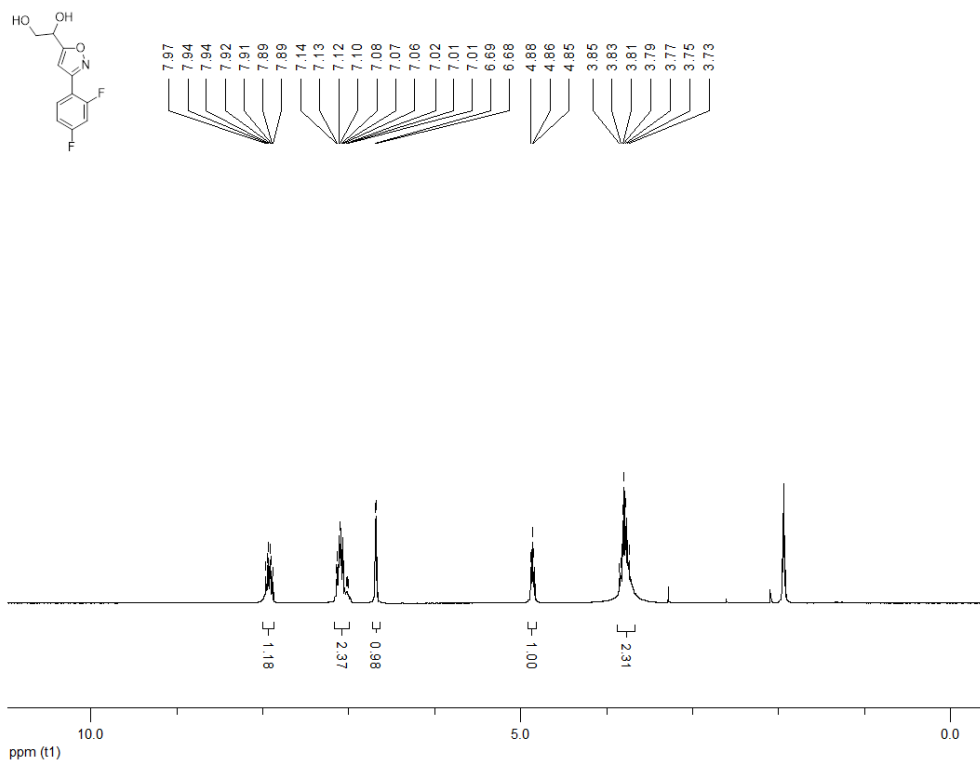
¹³C NMR (100 MHz, CD₃CN) 1-[3-(2,4-difluorophenyl)-1,2-oxazol-5-yl]ethane-1,2-diol (162c)

¹H NMR (300 MHz, CD₃CN) 1-[3-(pyridin-3-yl)-1,2-oxazol-5-yl]ethane-1,2-diol (162d)
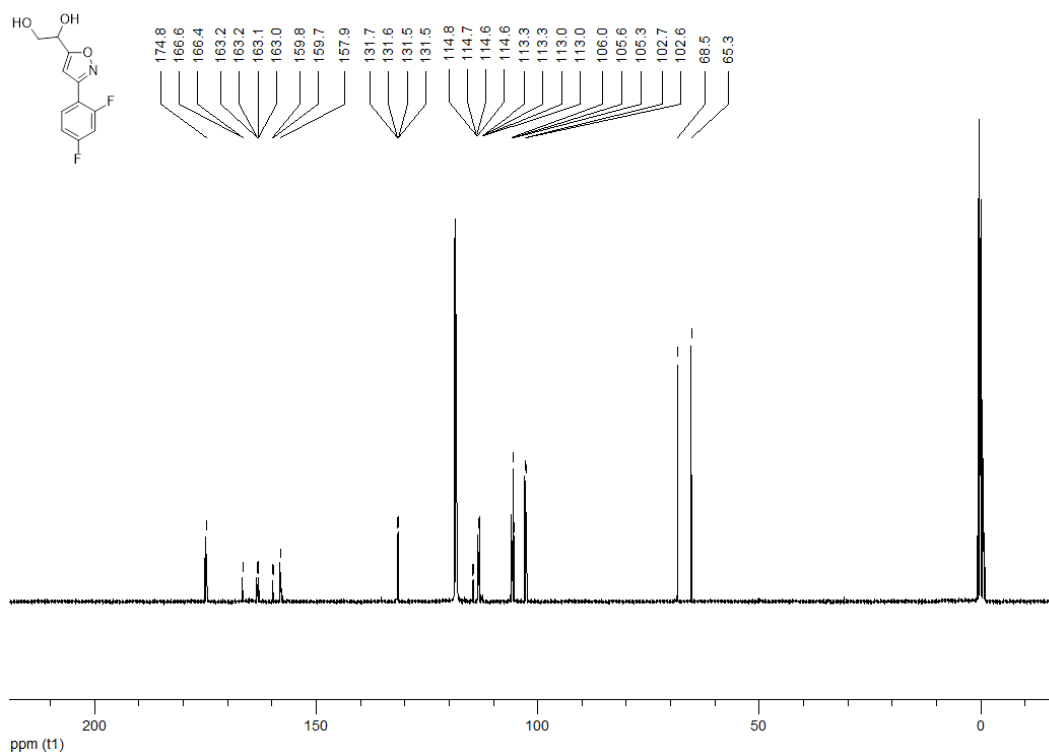
¹H NMR (300 MHz, CD₃CN) 1-[3-(pyridin-3-yl)-1,2-oxazol-5-yl]ethane-1,2-diol (162d)
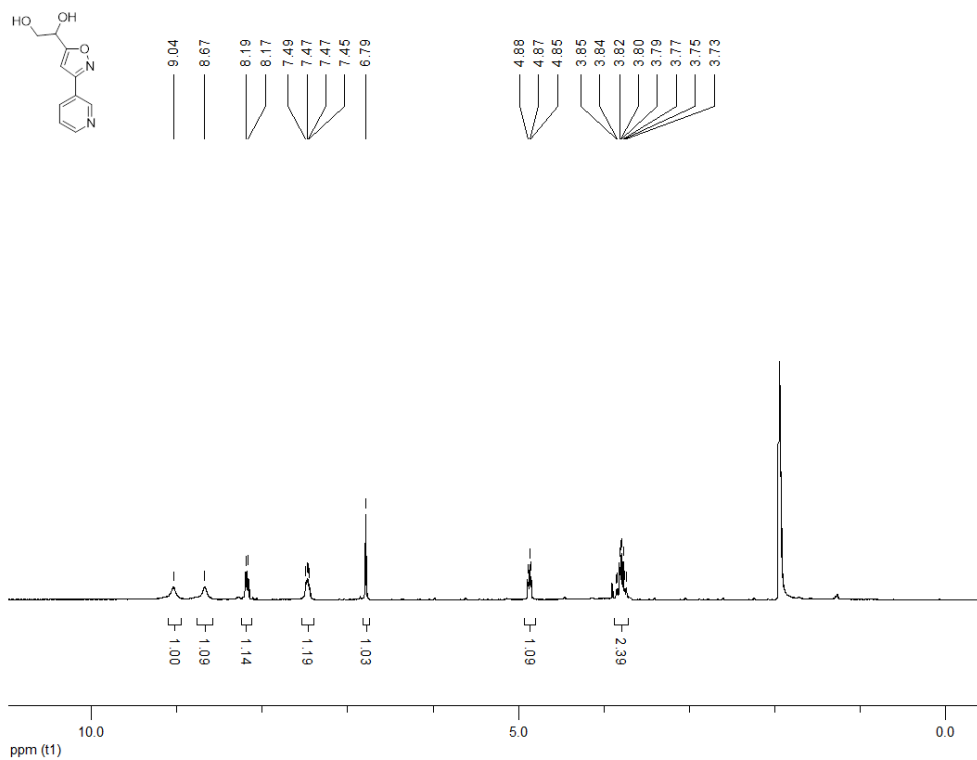
¹³C NMR (100 MHz, CD₃CN) 1-[3-(pyridin-3-yl)-1,2-oxazol-5-yl]ethane-1,2-diol (162d)
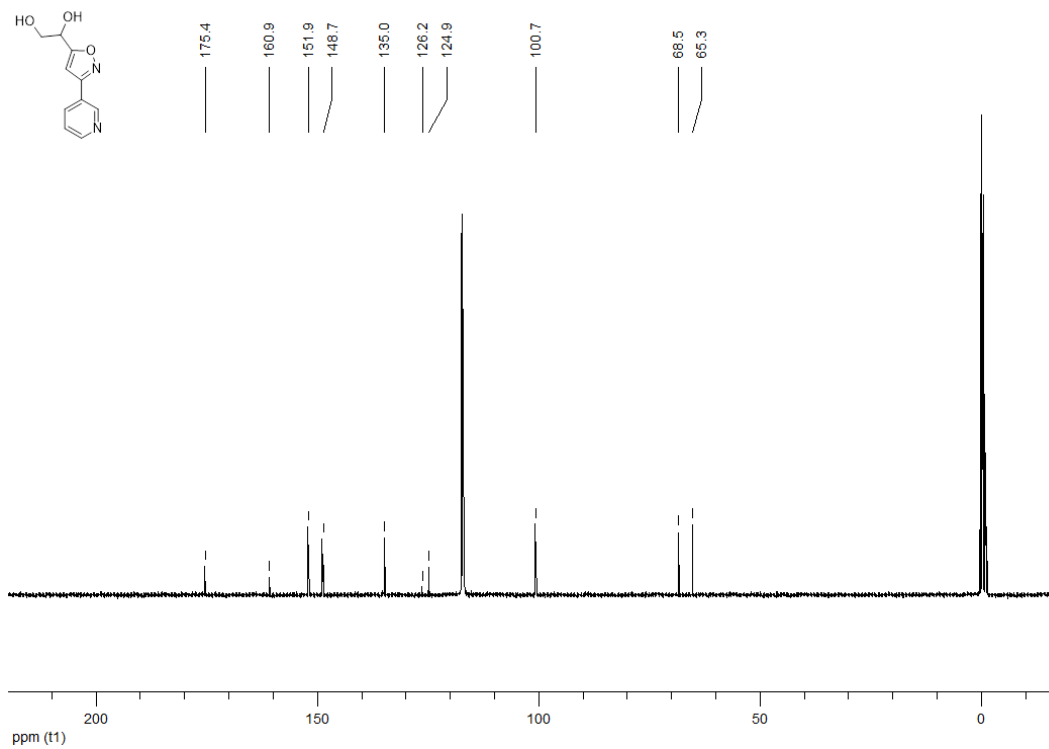
¹H NMR (300 MHz, CD₃CN) 1-(3-cyclopropyl-1,2-oxazol-5-yl)ethane-1,2-diol (162e)
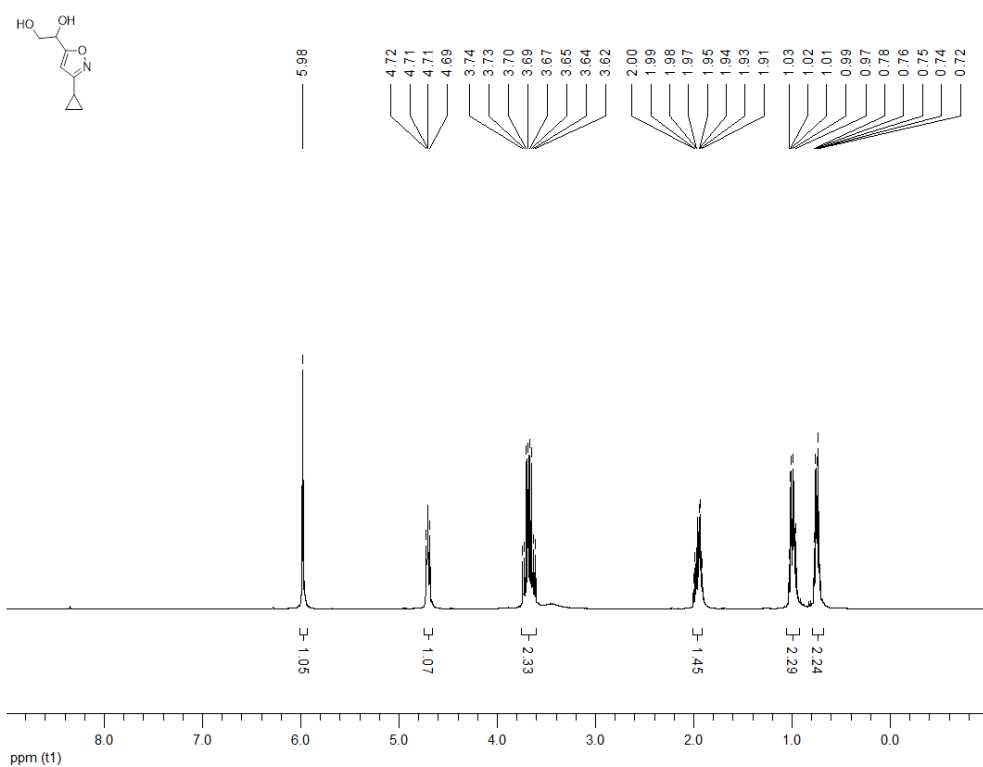
¹³C NMR (100 MHz, CD₃CN) 1-(3-cyclopropyl-1,2-oxazol-5-yl)ethane-1,2-diol (162e)
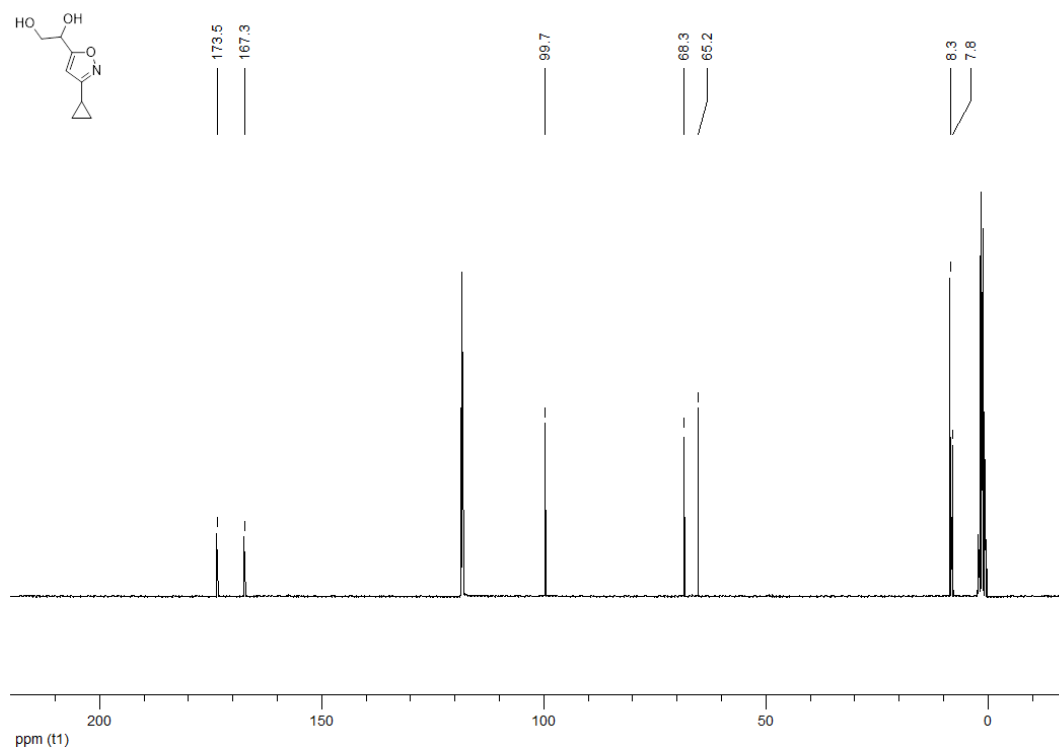
¹H NMR (300 MHz, CD₃CN) 1-[3-(oxolan-3-yl)-1,2-oxazol-5-yl]ethane-1,2-diol (162f)
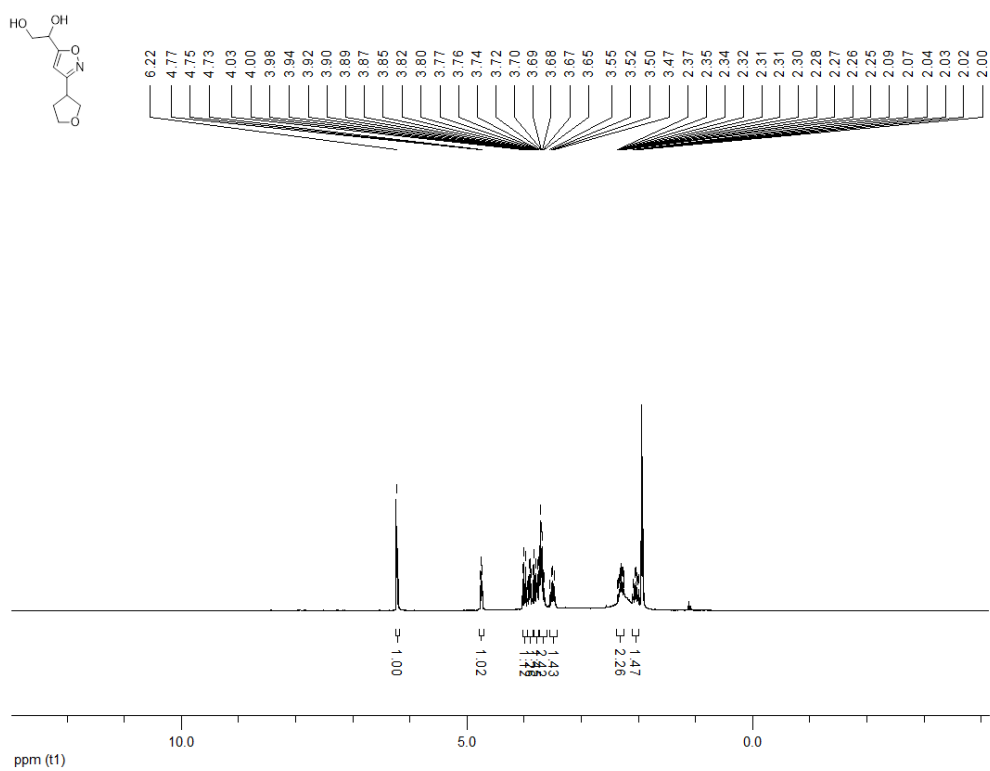
¹³C NMR (100 MHz, CD₃CN) 1-[3-(oxolan-3-yl)-1,2-oxazol-5-yl]ethane-1,2-diol (162f)
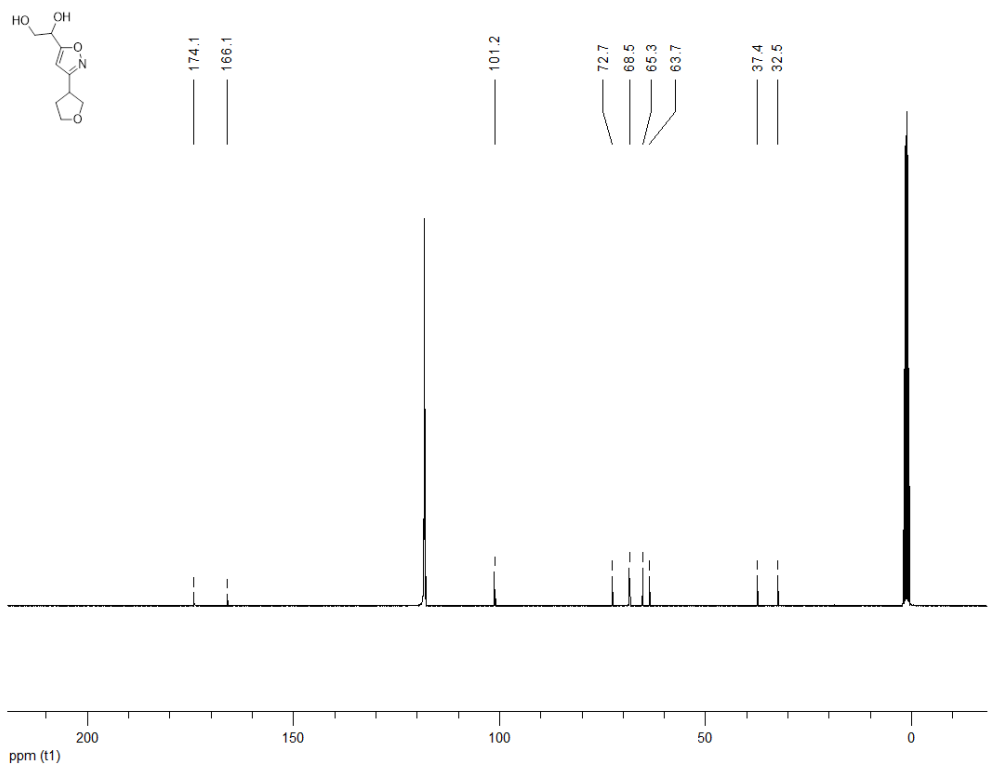
1H NMR (300 MHz, CD3CN) 1-(3-cyclohexyl-1,2-oxazol-5-yl)ethane-1,2-diol (162g)
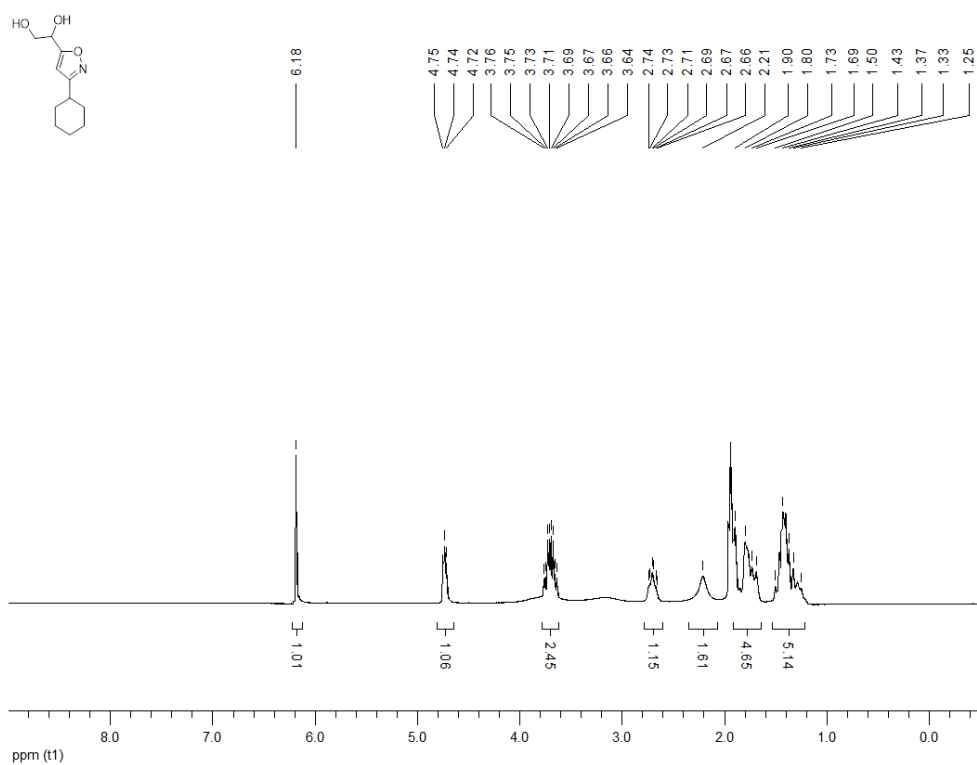
13C NMR (100 MHz, CD3CN) 1-(3-cyclohexyl-1,2-oxazol-5-yl)ethane-1,2-diol (162g)
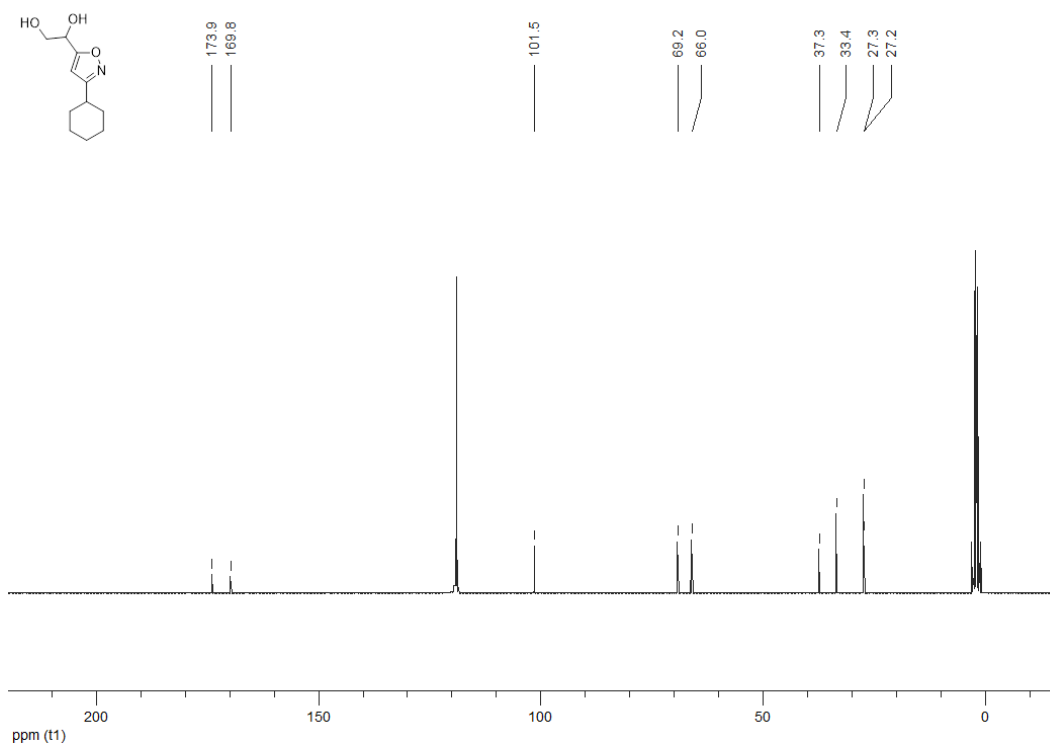
^{1}H NMR (300 MHz, CDCl$_3$) ethyl 5-{1,4-dioxaspiro[4.5]decan-2-yl}-1,2-oxazole-3-carboxylate (163)
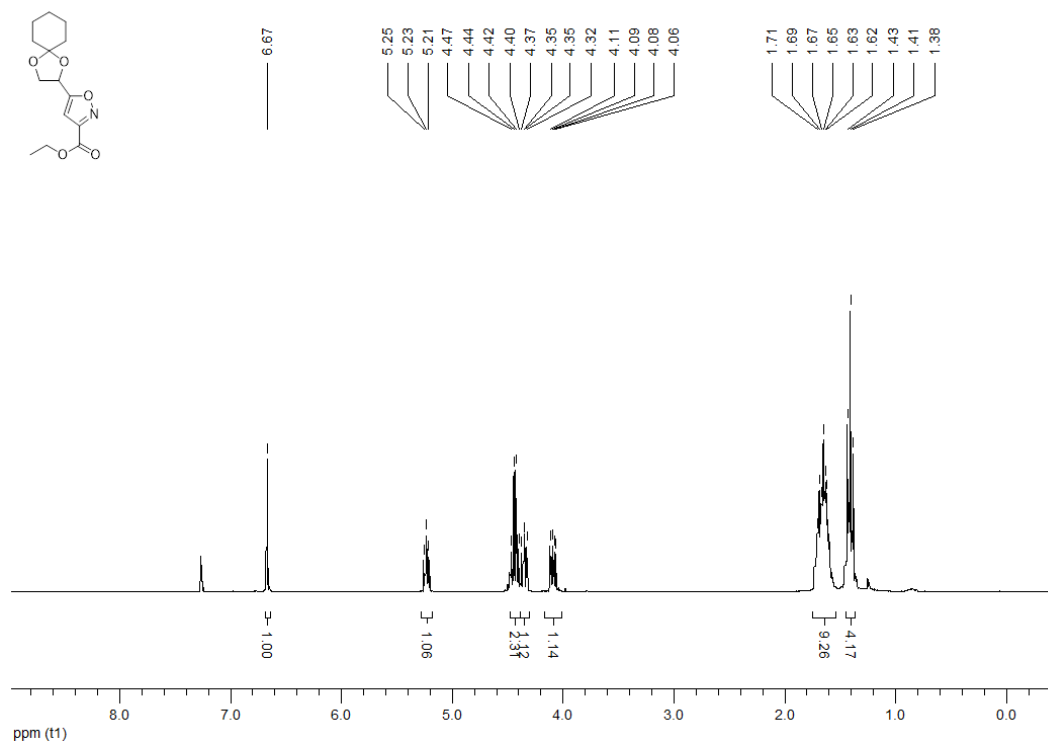
^{13}C NMR (100 MHz, CDCl$_3$) ethyl 5-{1,4-dioxaspiro[4.5]decan-2-yl}-1,2-oxazole-3-carboxylate (163)
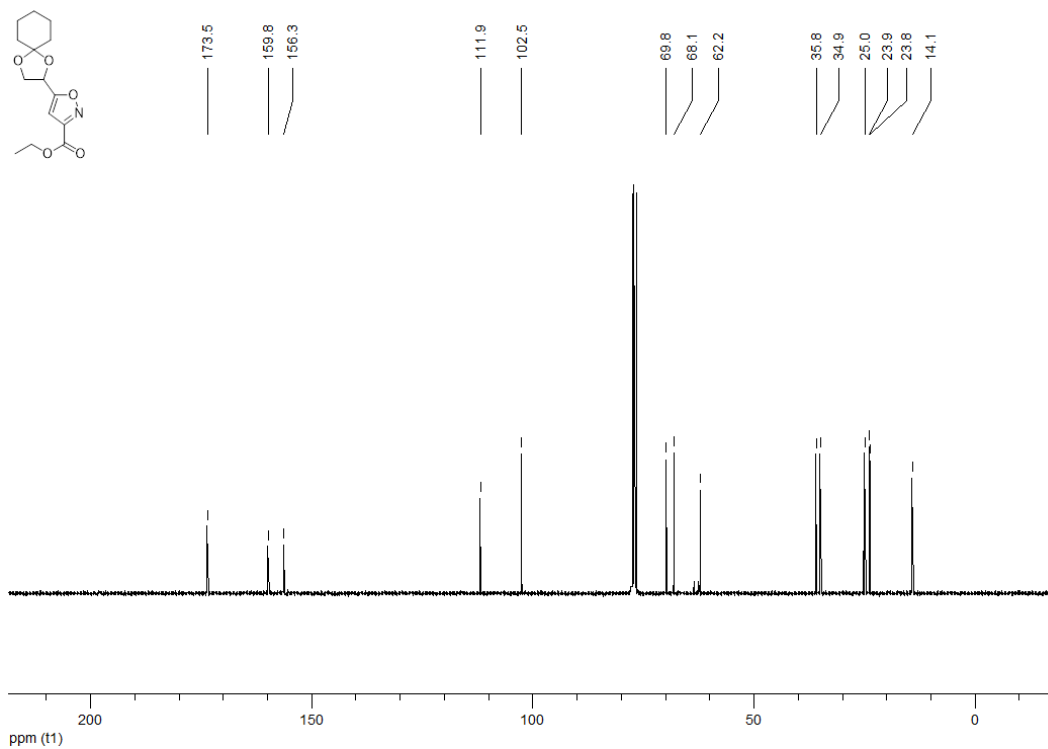
¹H NMR (300 MHz, CDCl₃) 5-{1,4-dioxaspiro[4.5]decan-2-yl}-1,2-oxazole-3-carboxylic acid (167)
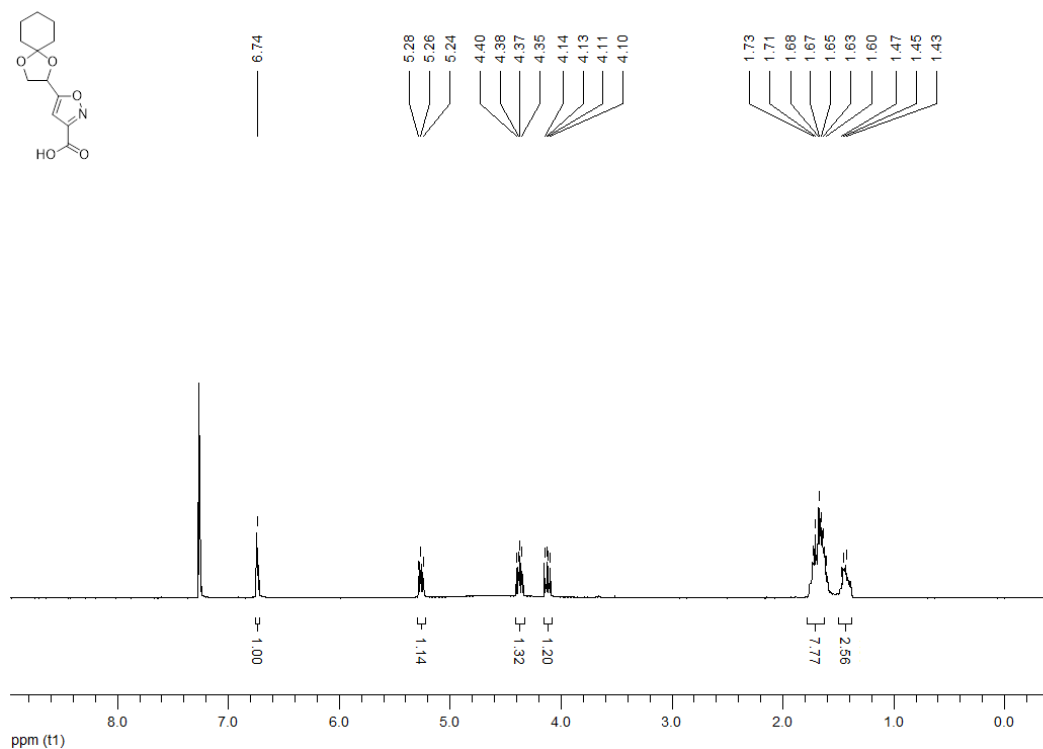
¹³C NMR (100 MHz, CDCl₃) 5-{1,4-dioxaspiro[4.5]decan-2-yl}-1,2-oxazole-3-carboxylic acid (167)

157
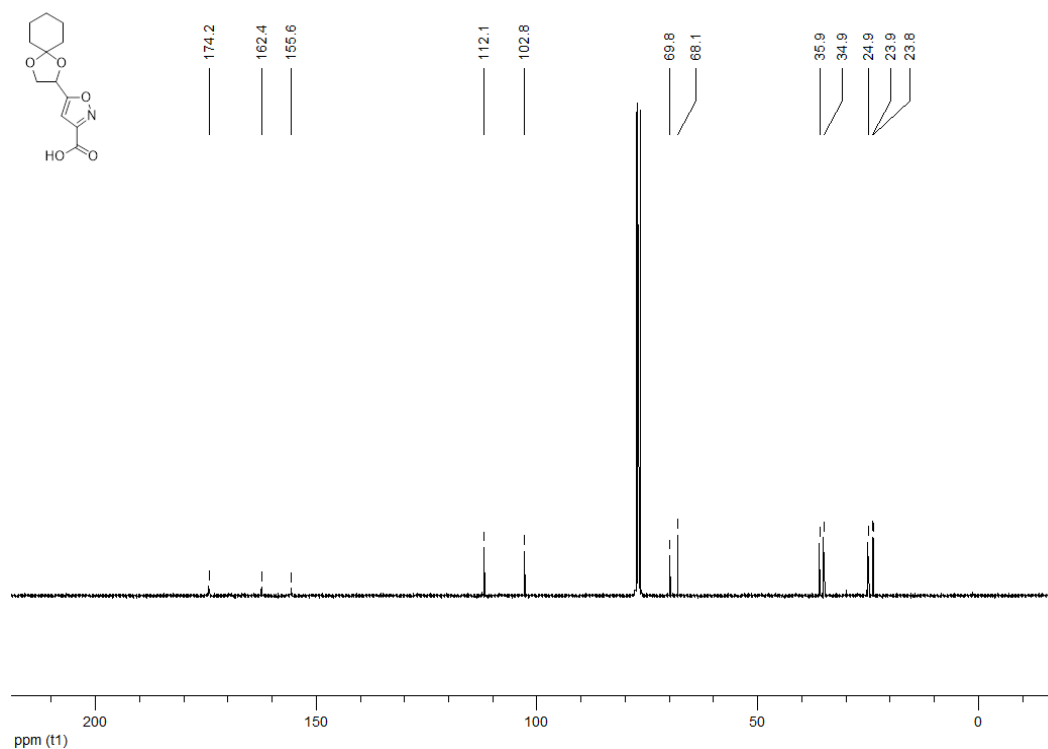
^{1}H NMR (300 MHz, CDCl$_3$) *N*-benzyl-5-{1,4-dioxaspiro[4.5]decan-2-yl}-1,2-oxazole-3-carboxamide (169h)
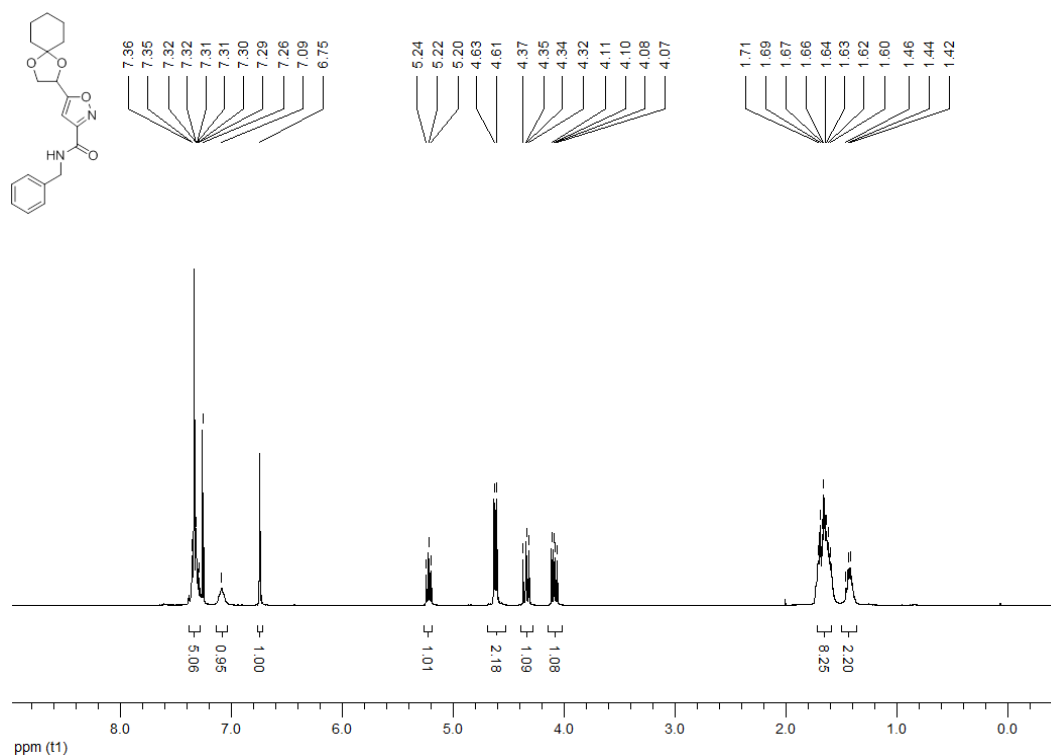
^{13}C NMR (100 MHz, CDCl$_3$) *N*-benzyl-5-{1,4-dioxaspiro[4.5]decan-2-yl}-1,2-oxazole-3-carboxamide (169h)
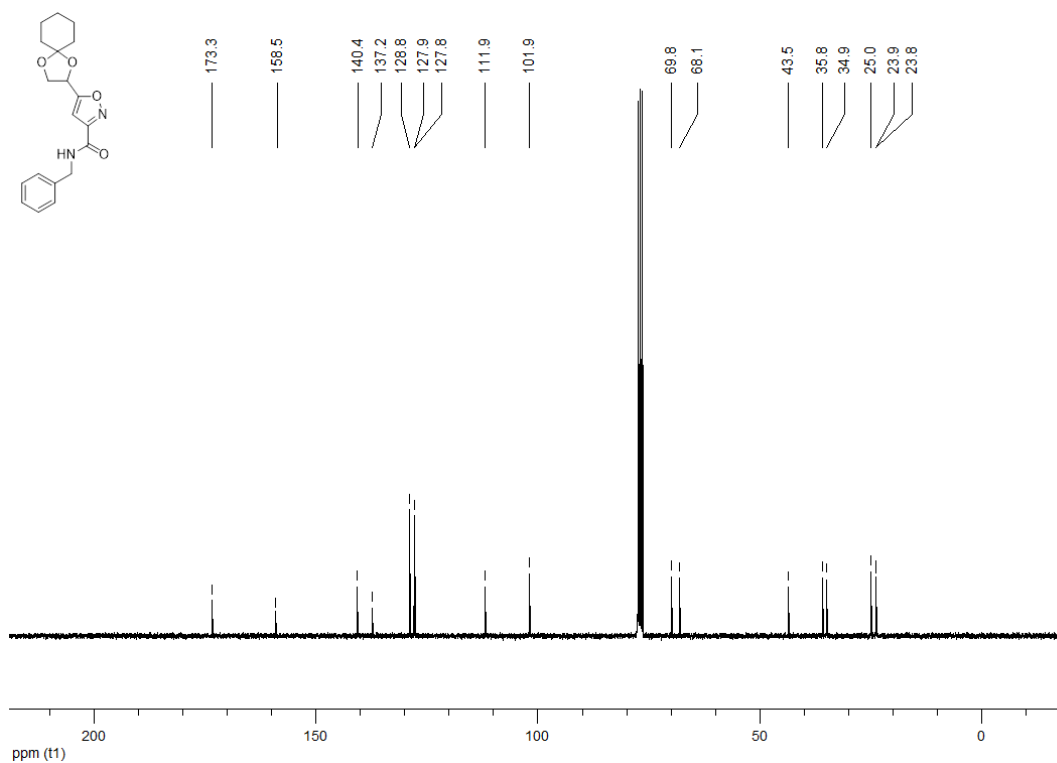
1H NMR (300 MHz, CDCl₃) 5-{1,4-dioxaspiro[4.5]decan-2-yl}-*N*-(4-fluorophenyl)- 1,2-oxazole-3-carboxamide (169i)
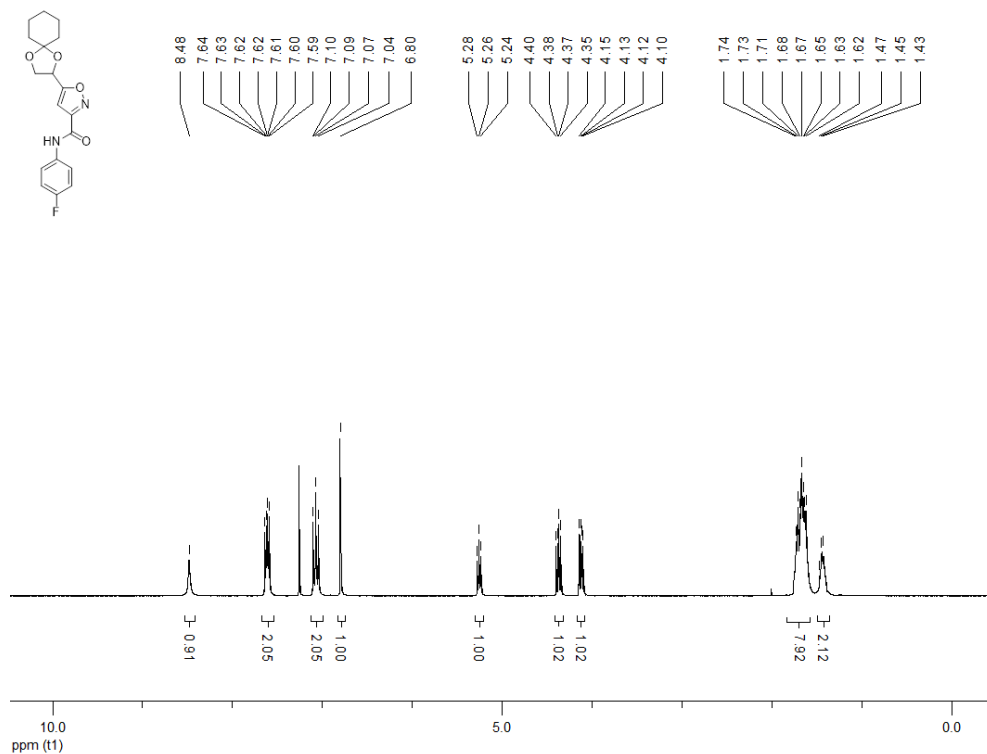
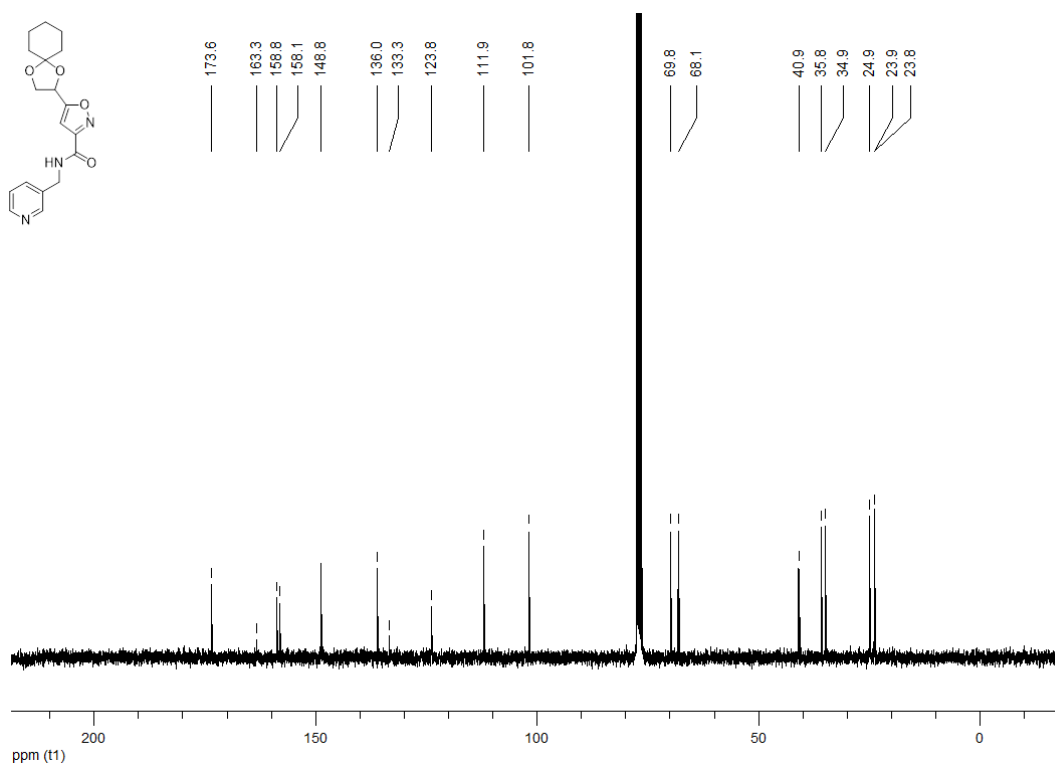**¹³C NMR (100 MHz, CDCl₃) 5-{1,4-dioxaspiro[4.5]decan-2-yl}-*N*-(4-fluorophenyl)- 1,2-oxazole-3-carboxamide (169i)**
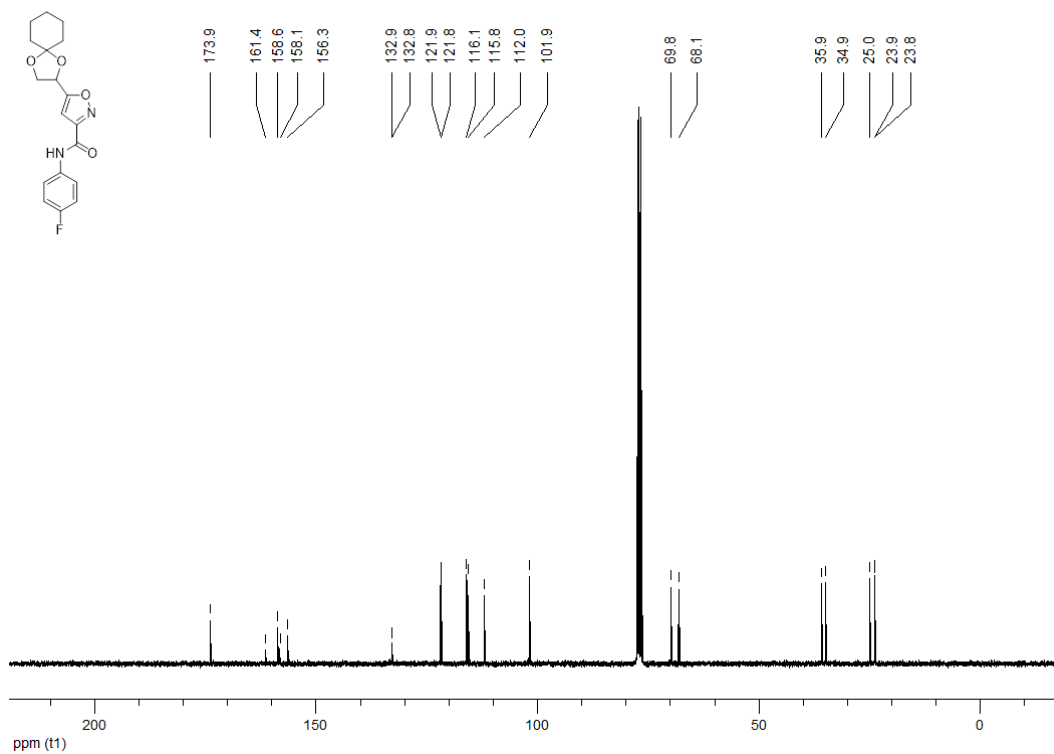
¹H NMR (300 MHz, CDCl₃) 5-{1,4-dioxaspiro[4.5]decan-2-yl}-*N*-[(thiophen-2-yl)methyl]-1,2-oxazole-3-carboxamide (169j)
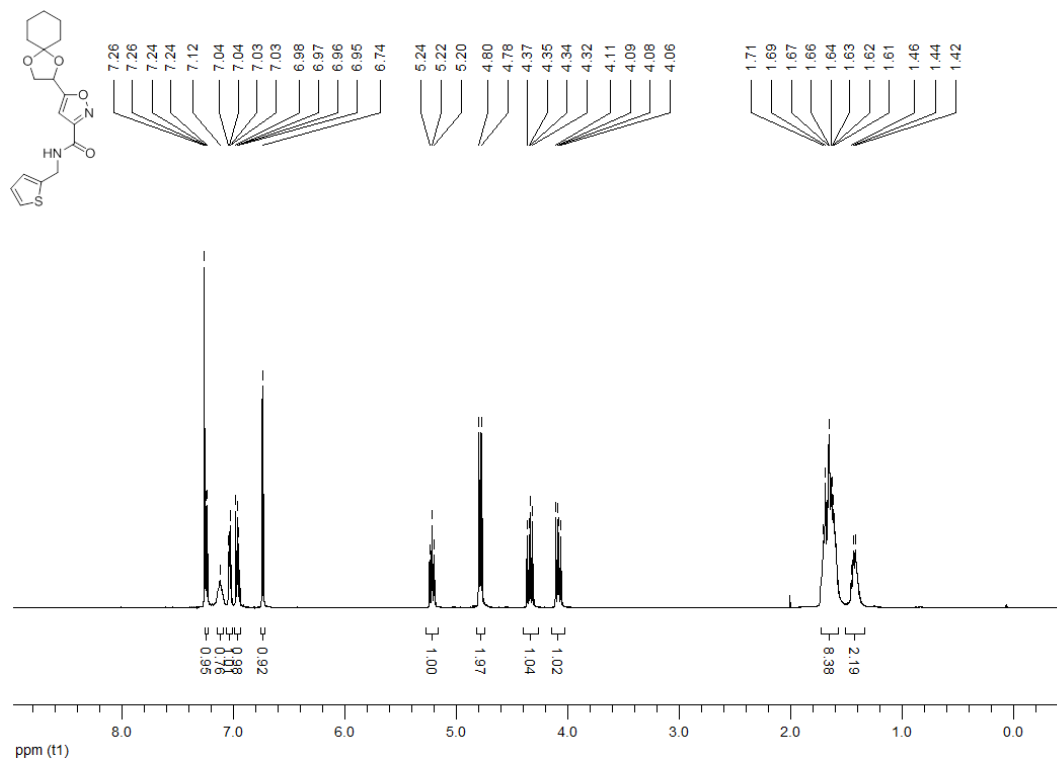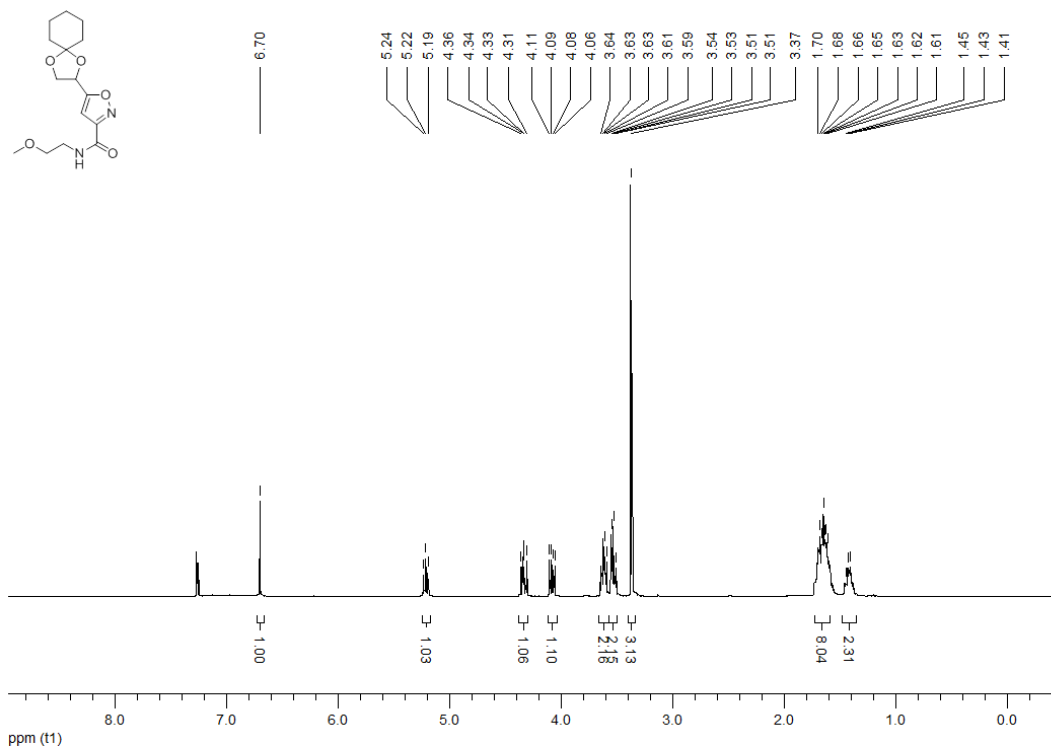

¹³C NMR (100 MHz, CDCl₃) 5-{1,4-dioxaspiro[4.5]decan-2-yl}-*N*-[(thiophen-2-yl)methyl]-1,2-oxazole-3-carboxamide (169j)
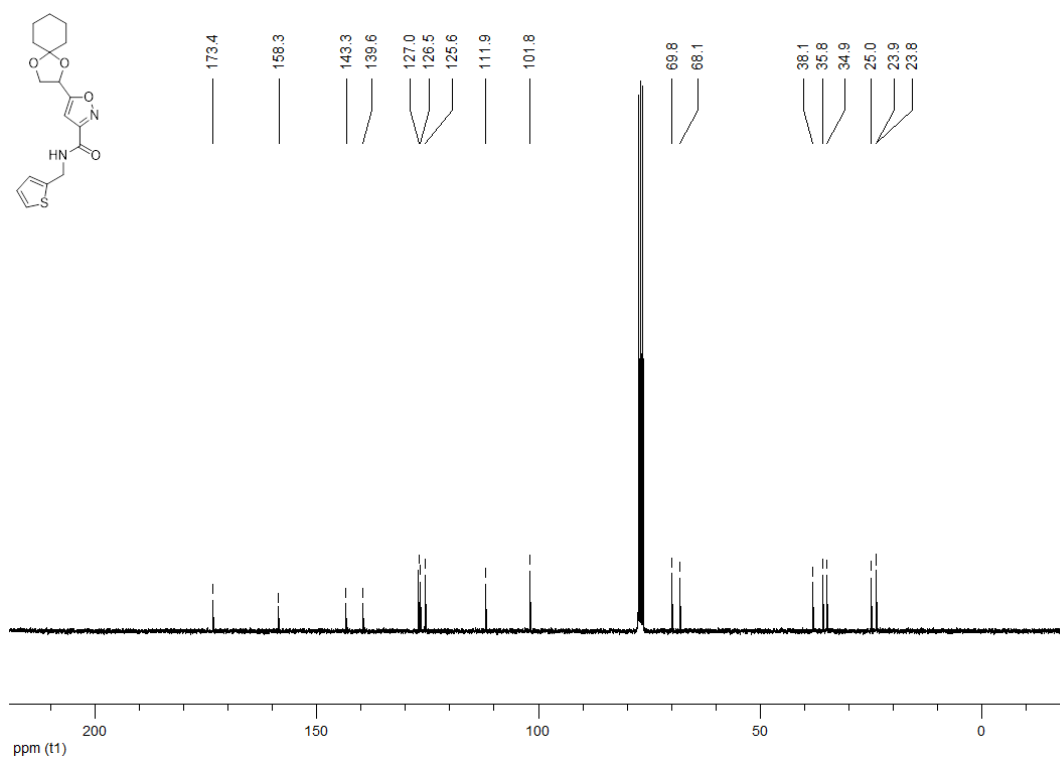
¹H NMR (300 MHz, CDCl₃) 5-{1,4-dioxaspiro[4.5]decan-2-yl}-*N*-[(pyridin-3-yl)methyl]-1,2-oxazole-3-carboxamide (169k)
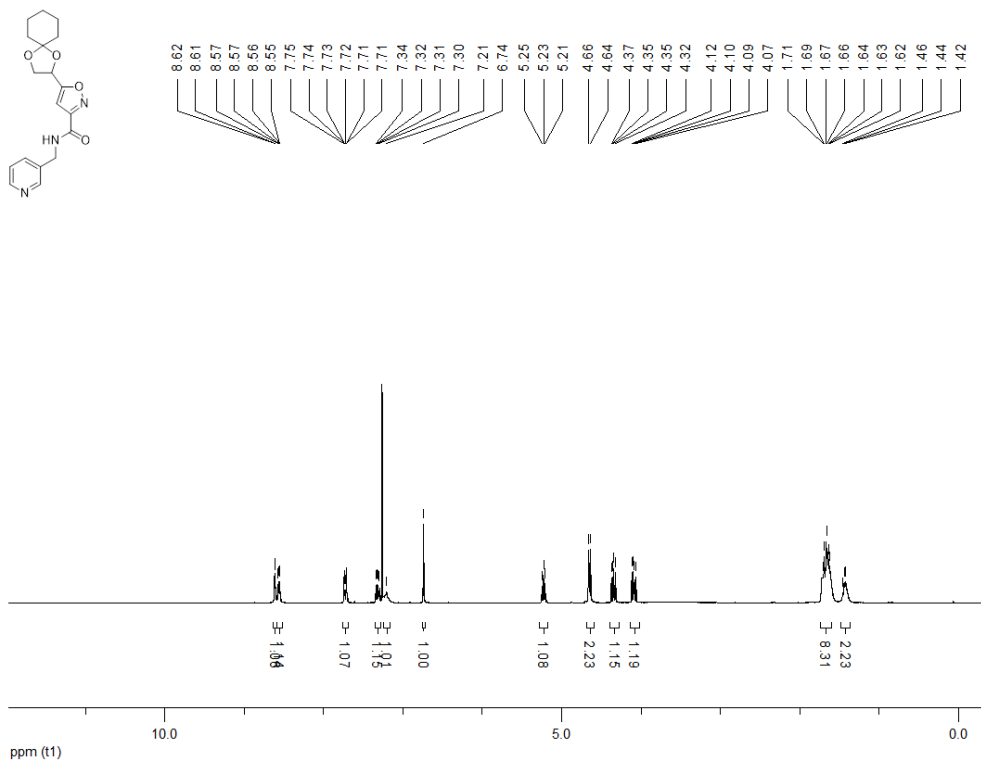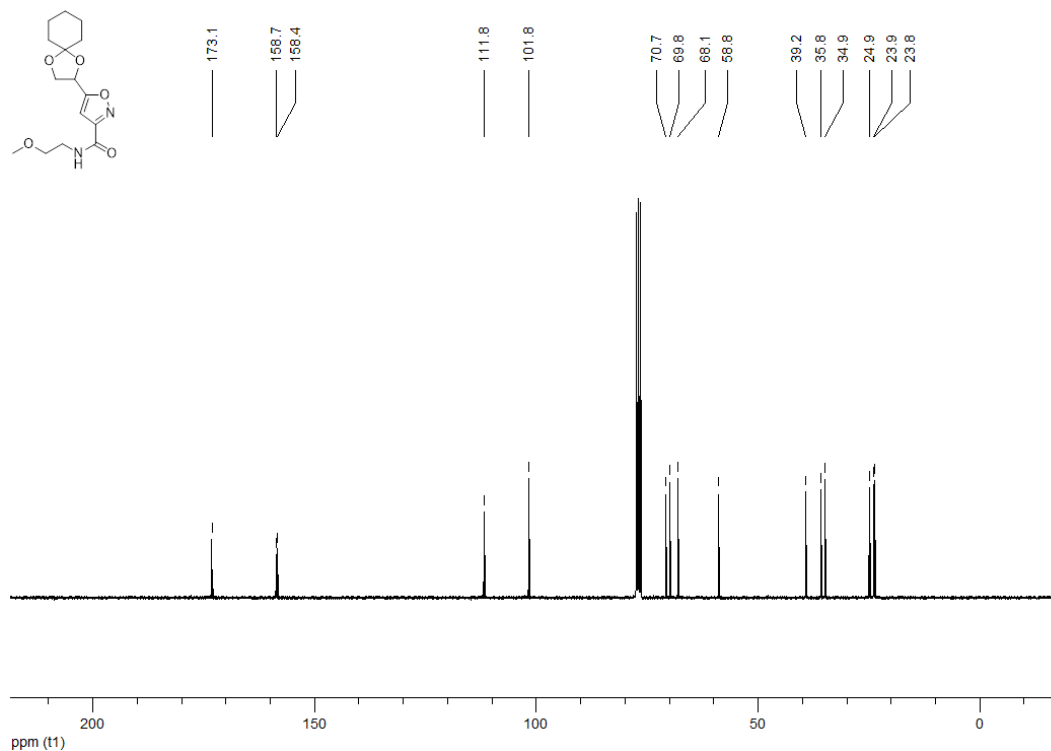

¹³C NMR (100 MHz, CDCl₃) 5-{1,4-dioxaspiro[4.5]decan-2-yl}-*N*-[(pyridin-3-yl)methyl]-1,2-oxazole-3-carboxamide (169k)

¹H NMR (300 MHz, CDCl₃) 5-{1,4-dioxaspiro[4.5]decan-2-yl}-*N*-(2-methoxyethyl)-1,2-oxazole-3-carboxamide (169l)
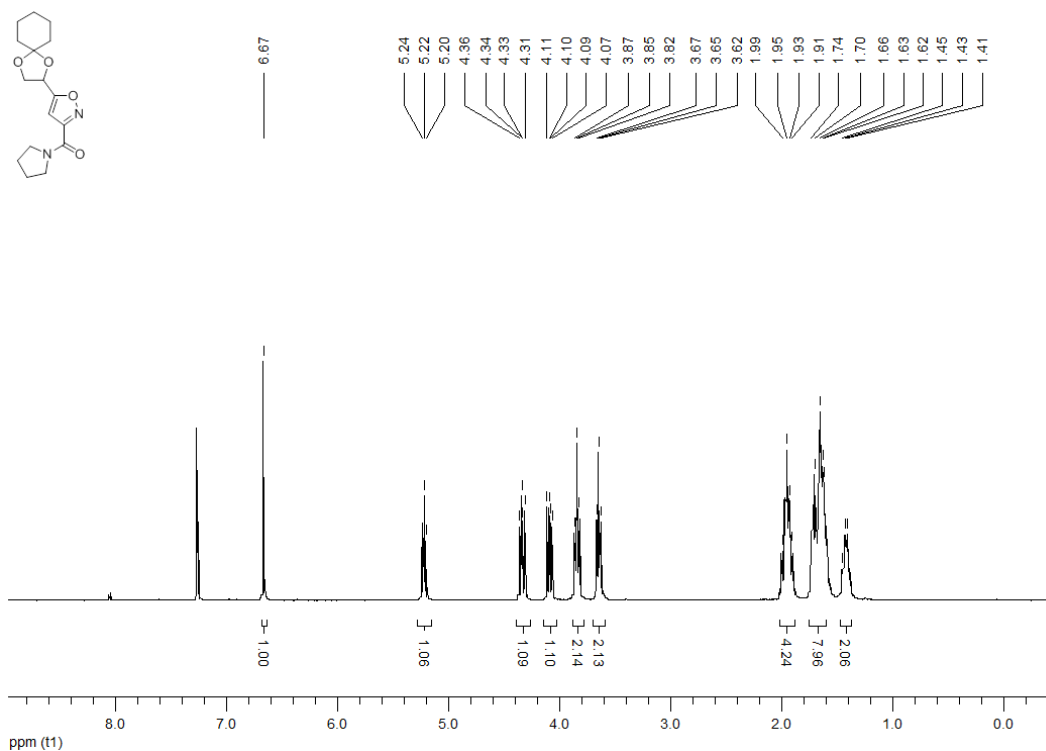

¹³C NMR (100 MHz, CDCl₃) 5-{1,4-dioxaspiro[4.5]decan-2-yl}-*N*-(2-methoxyethyl)-1,2-oxazole-3-carboxamide (169l)
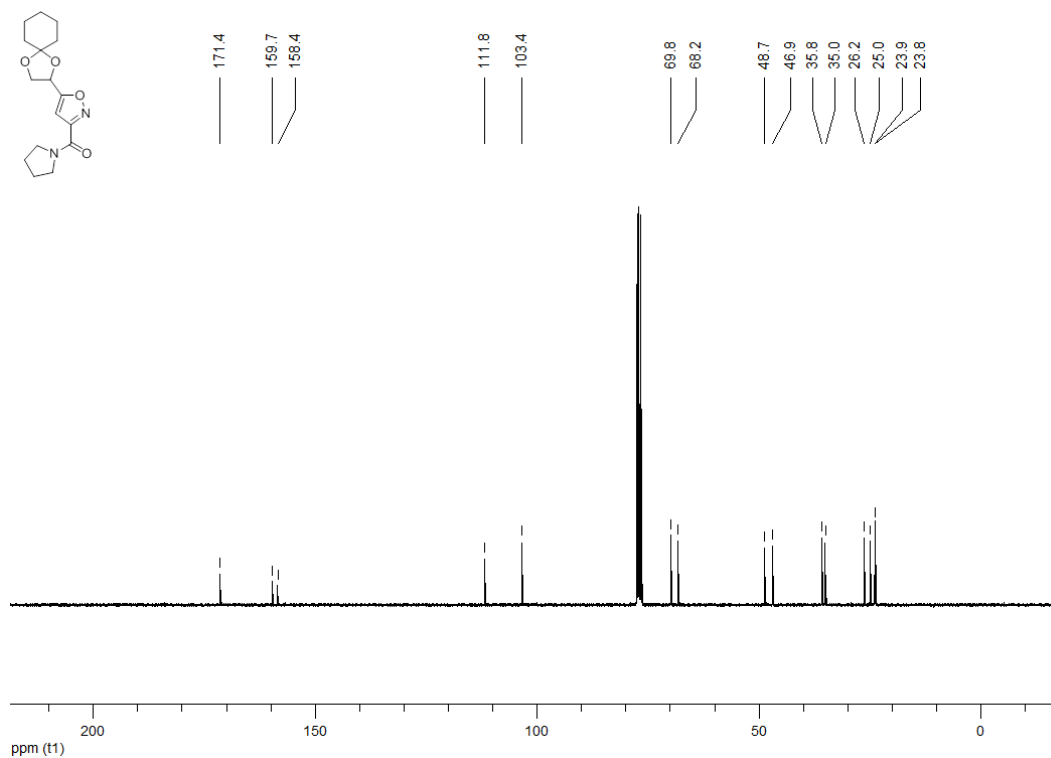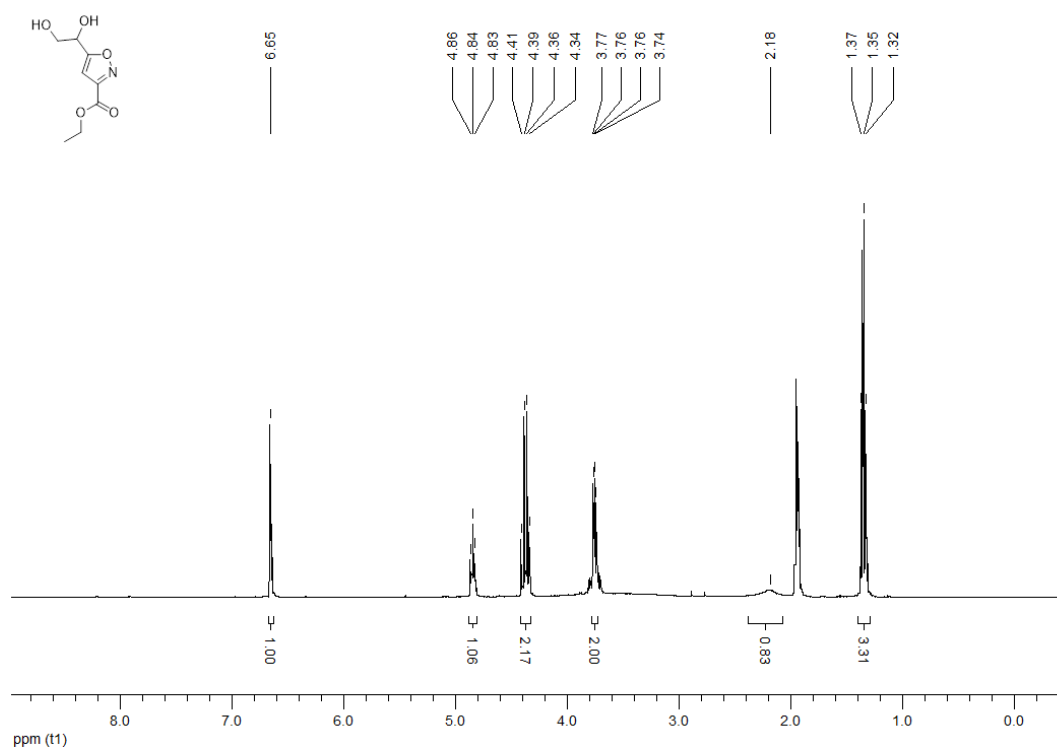
¹H NMR (300 MHz, CDCl₃) **¹H NMR (300 MHz, CDCl₃) 5-{1,4-dioxaspiro[4.5]decan-2-yl}-3-(pyrrolidine-1-carbonyl)-1,2-oxazole (169m)**

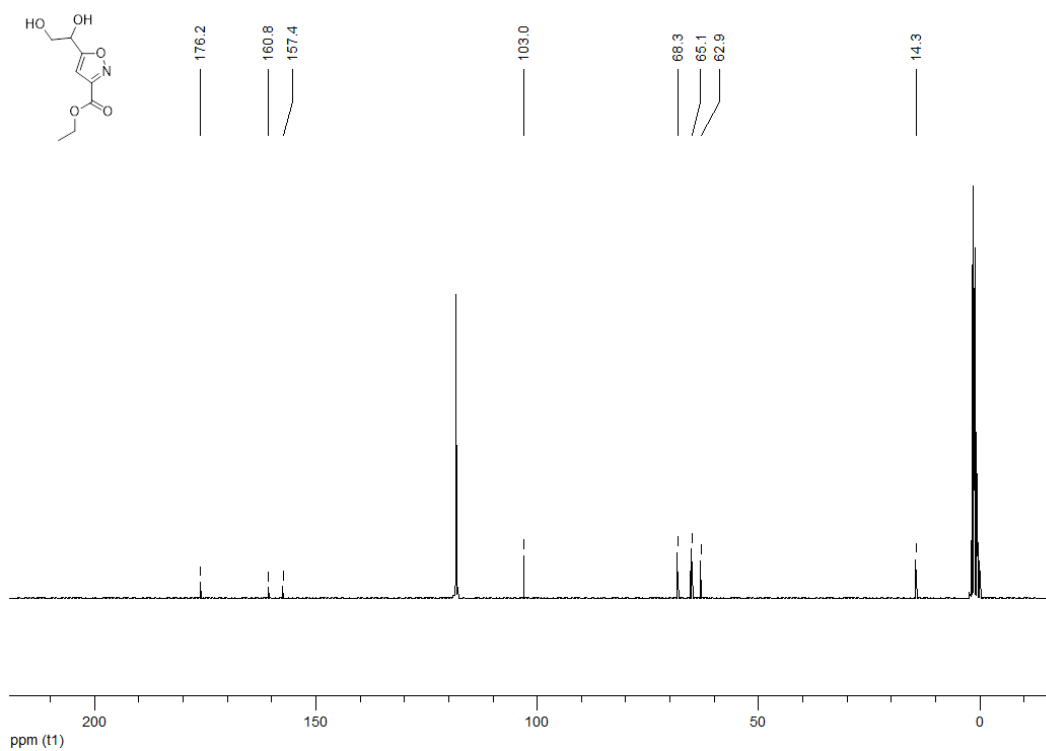

¹³C NMR (100 MHz, CDCl₃) 5-{1,4-dioxaspiro[4.5]decan-2-yl}-3-(pyrrolidine-1-carbonyl)-1,2-oxazole (169m)
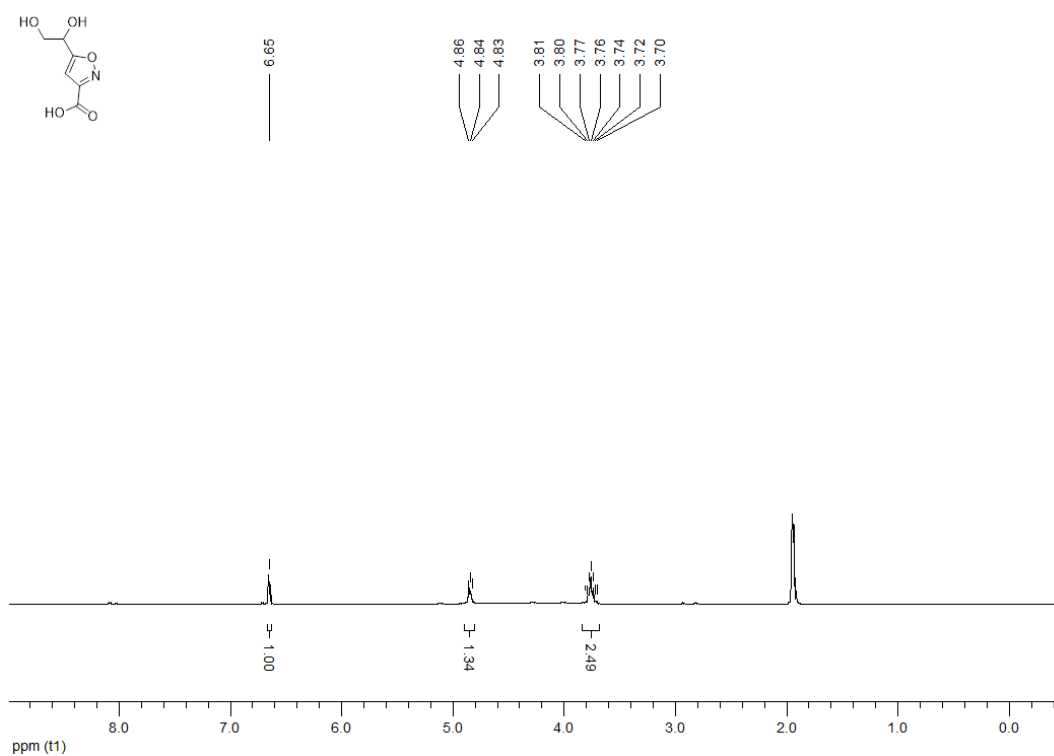
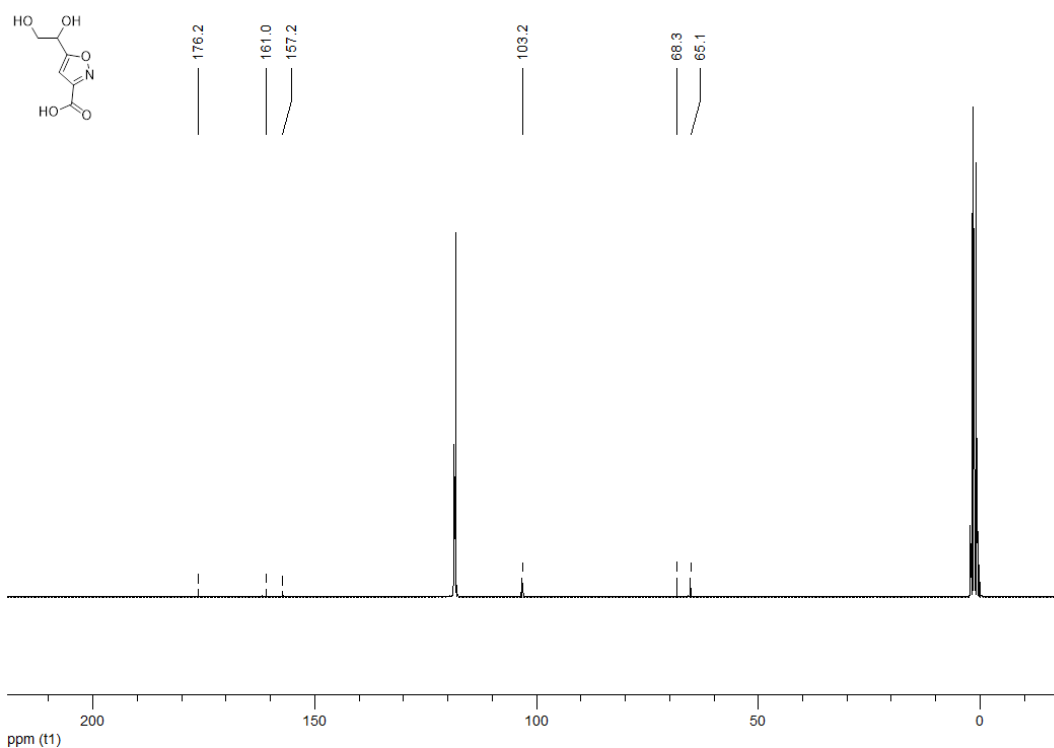**¹H NMR (300 MHz, CD₃CN) ethyl 5-(1,2-dihydroxyethyl)-1,2-oxazole-3-carboxylate (166)**

¹³C NMR (100 MHz, CD₃CN) ethyl 5-(1,2-dihydroxyethyl)-1,2-oxazole-3-carboxylate (166)
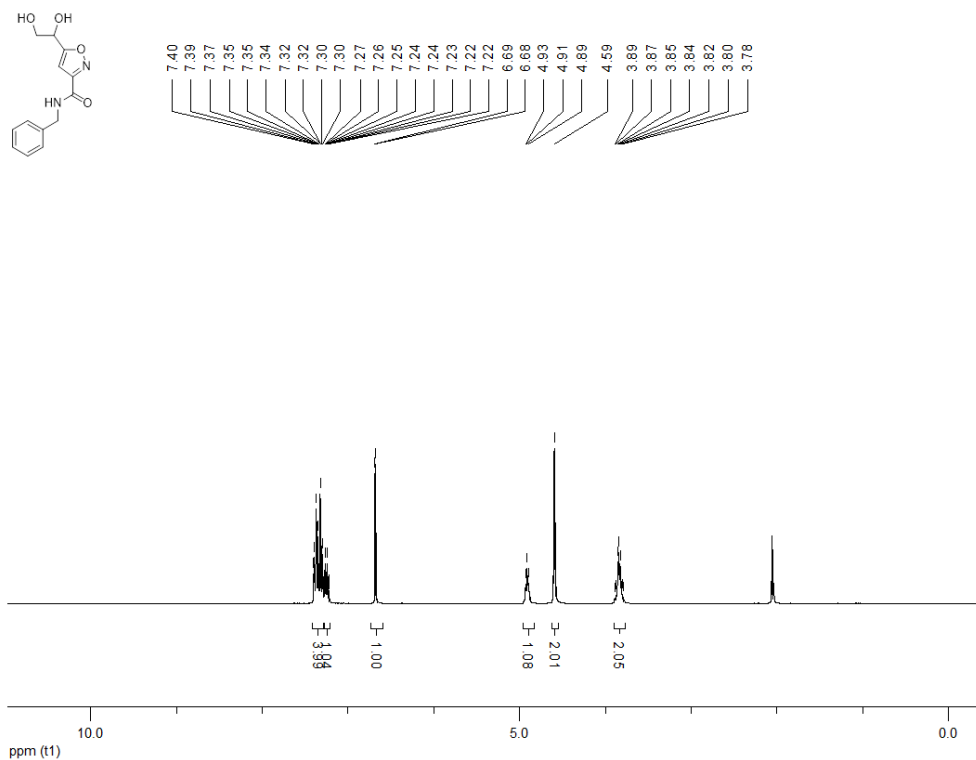
¹H NMR (300 MHz, CD₃CN) 5-(1,2-dihydroxyethyl)-1,2-oxazole-3-carboxylic acid (168)

¹³C NMR (100 MHz, CD₃CN) 5-(1,2-dihydroxyethyl)-1,2-oxazole-3-carboxylic acid (168)

¹H NMR (300 MHz, Acetone-*d₆*) ***N*-benzyl-5-(1,2-dihydroxyethyl)-1,2-oxazole-3-carboxamide (170h)**

¹³C NMR (100 MHz, Acetone-*d₆*) ***N*-benzyl-5-(1,2-dihydroxyethyl)-1,2-oxazole-3-carboxamide (170h)**
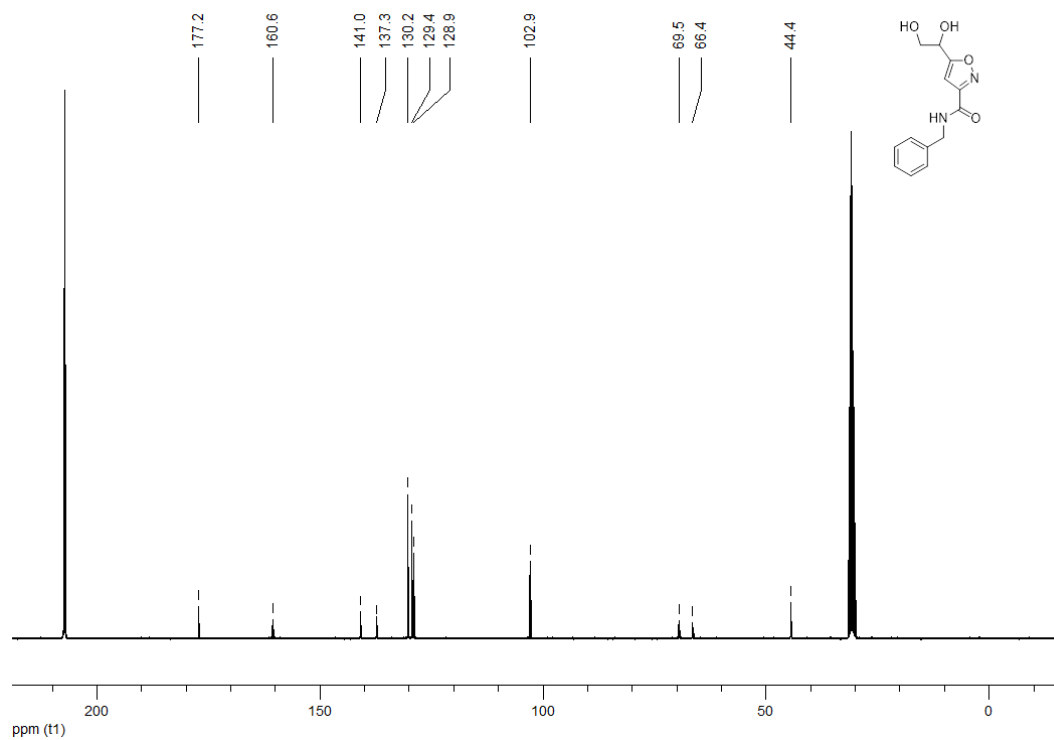
¹H NMR (300 MHz, Acetone-*d₆*) 5-(1,2-dihydroxyethyl)-*N*-(4-fluorophenyl)-1,2-oxazole-3-carboxamide (170i)
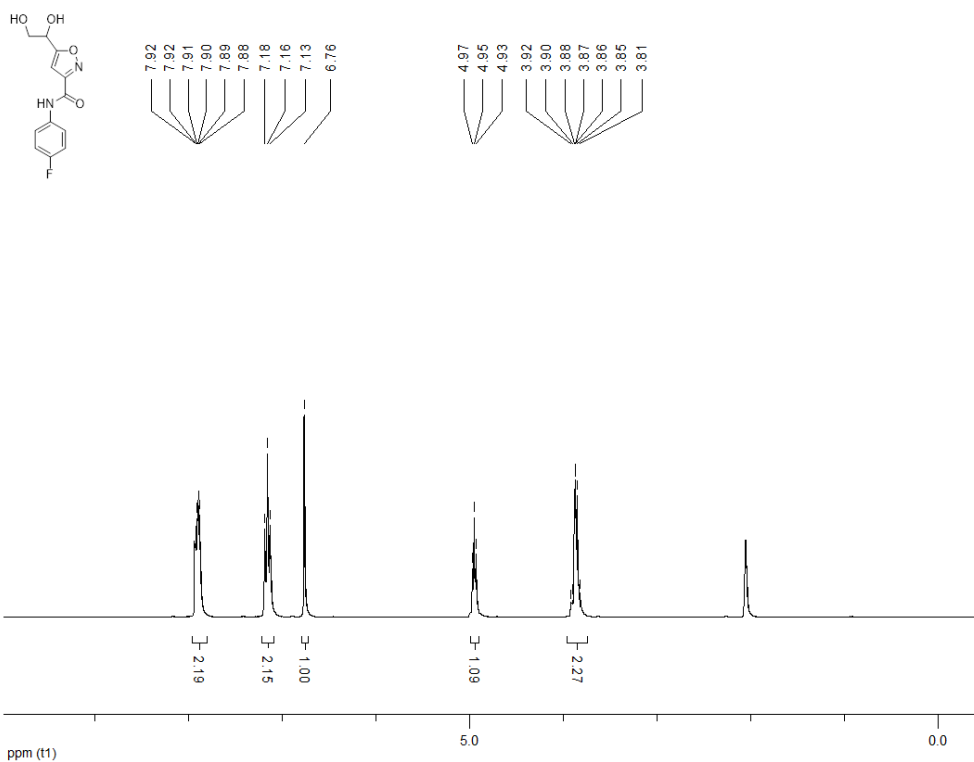
¹³C NMR (100 MHz, Acetone-*d₆*) 5-(1,2-dihydroxyethyl)-*N*-(4-fluorophenyl)-1,2-oxazole-3-carboxamide (170i)
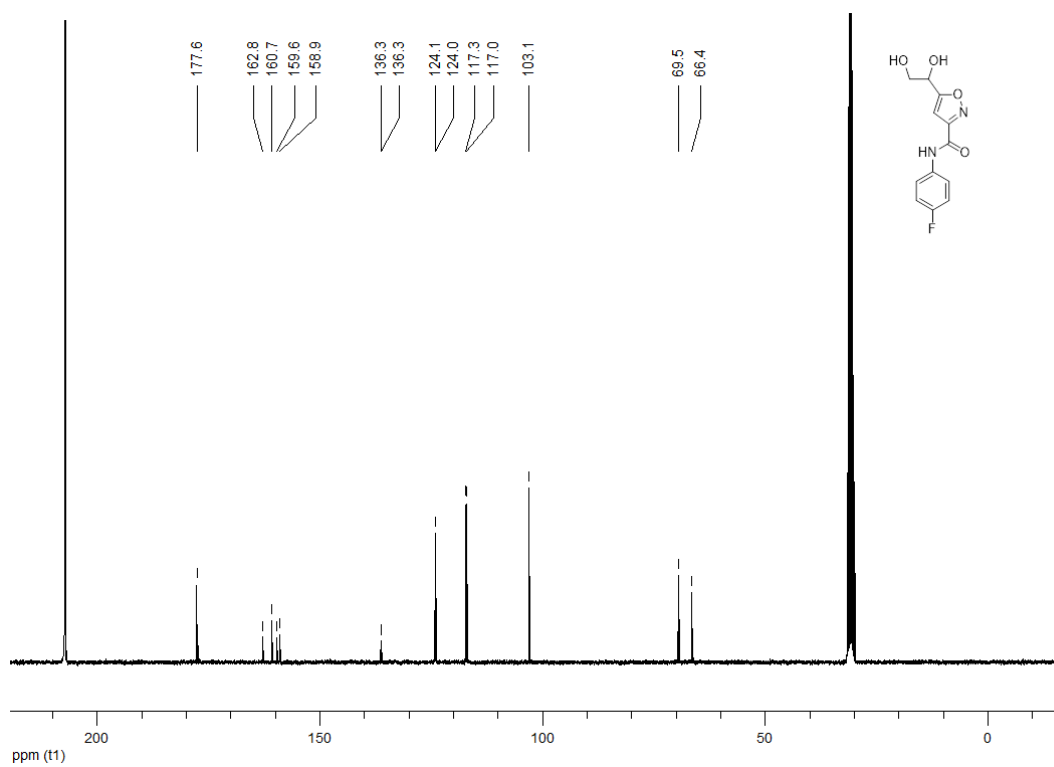
^{1}H NMR (300 MHz, Acetone-d_6) 5-(1,2-dihydroxyethyl)-N-[(thiophen-2-yl)methyl]-1,2-oxazole-3-carboxamide (170j)
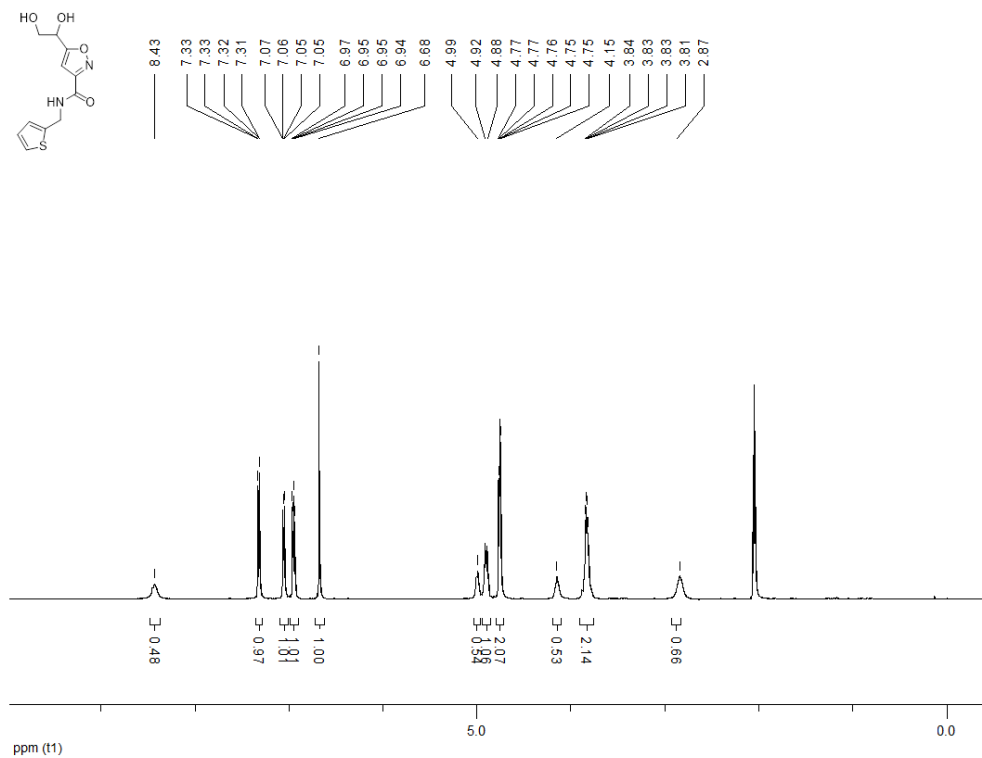
^{13}C NMR (100 MHz, Acetone-d_6) 5-(1,2-dihydroxyethyl)-N-[(thiophen-2-yl)methyl]-1,2-oxazole-3-carboxamide (170j)

1H NMR (300 MHz, MeOD) 5-(1,2-dihydroxyethyl)-*N*-[(pyridin-3-yl)methyl]-1,2-oxazole-3-carboxamide (170k)

13C NMR (100 MHz, MeOD) 5-(1,2-dihydroxyethyl)-*N*-[(pyridin-3-yl)methyl]-1,2-oxazole-3-carboxamide (170k)
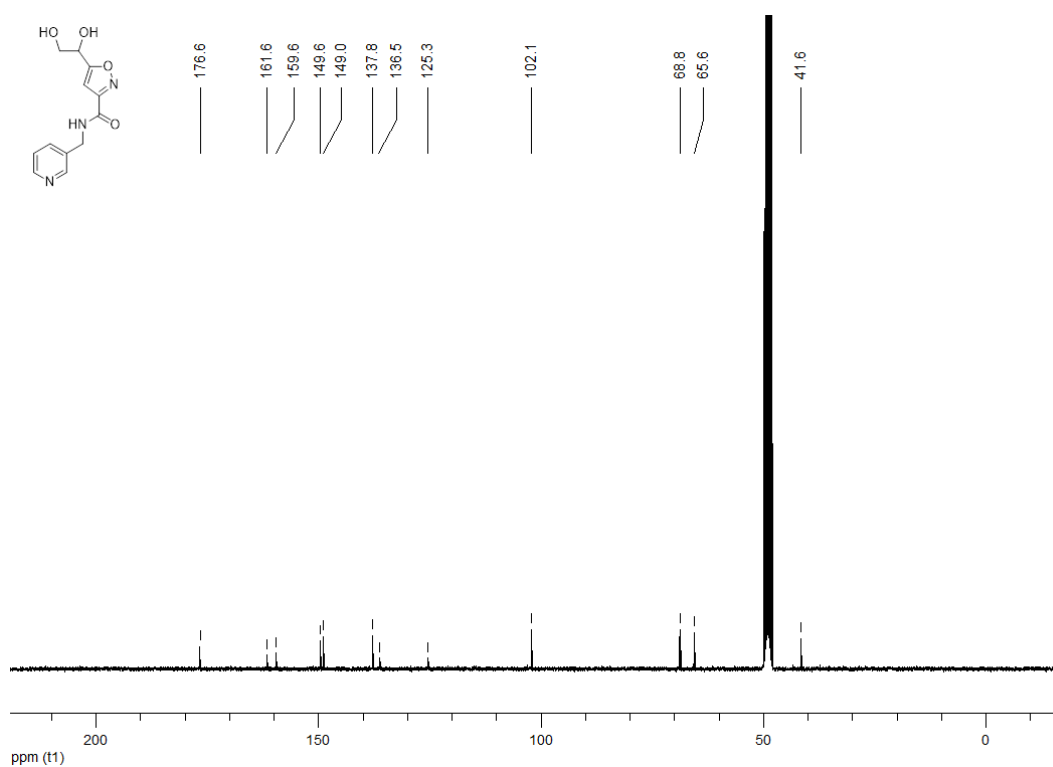
^{1}H NMR (300 MHz, Acetone-d_6) 5-(1,2-dihydroxyethyl)-N-(2-methoxyethyl)-1,2-oxazole-3-carboxamide (170l)
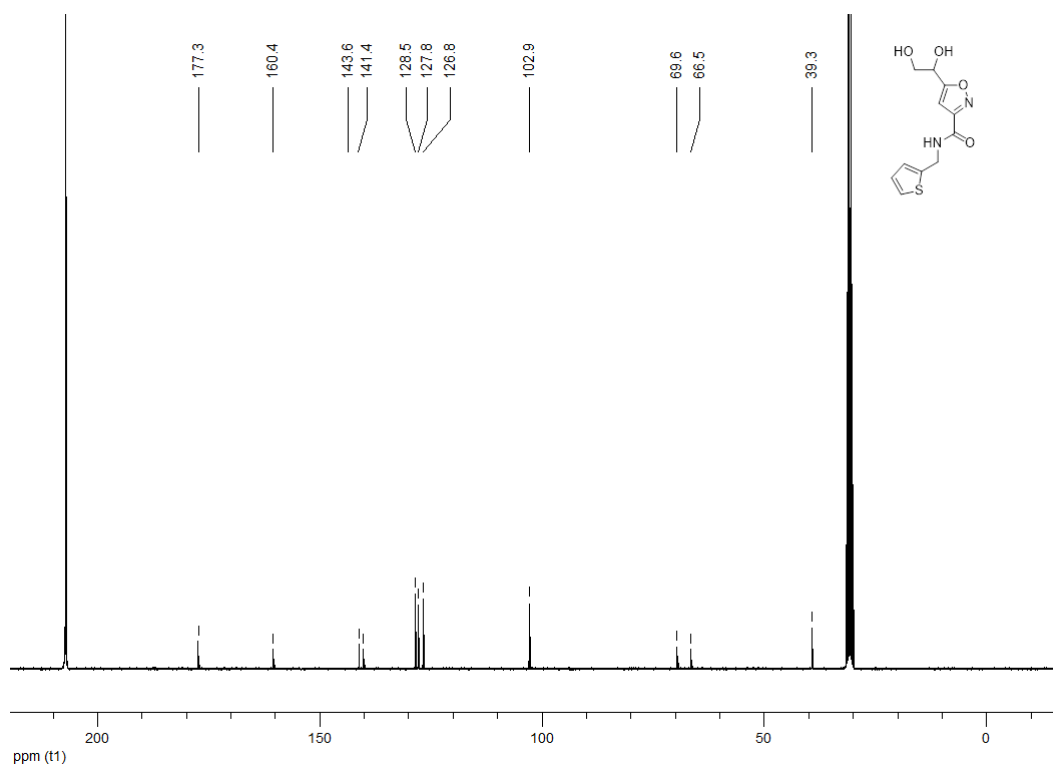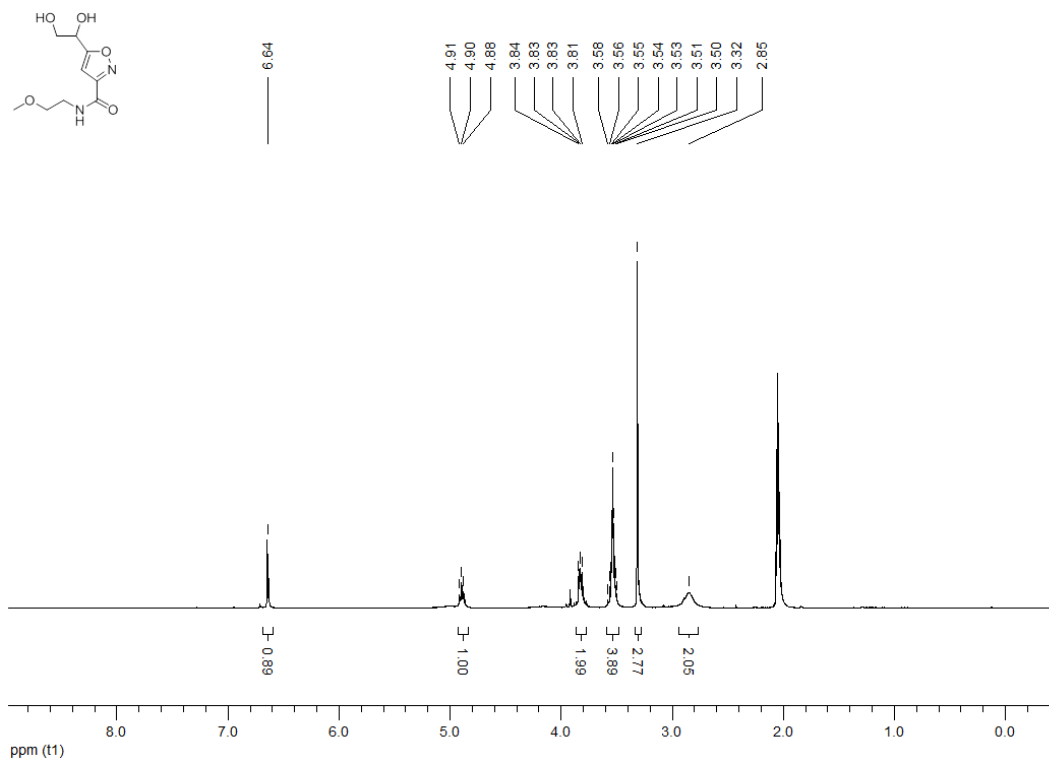

^{13}C NMR (100 MHz, Acetone-d_6) 5-(1,2-dihydroxyethyl)-N-(2-methoxyethyl)-1,2-oxazole-3-carboxamide (170l)
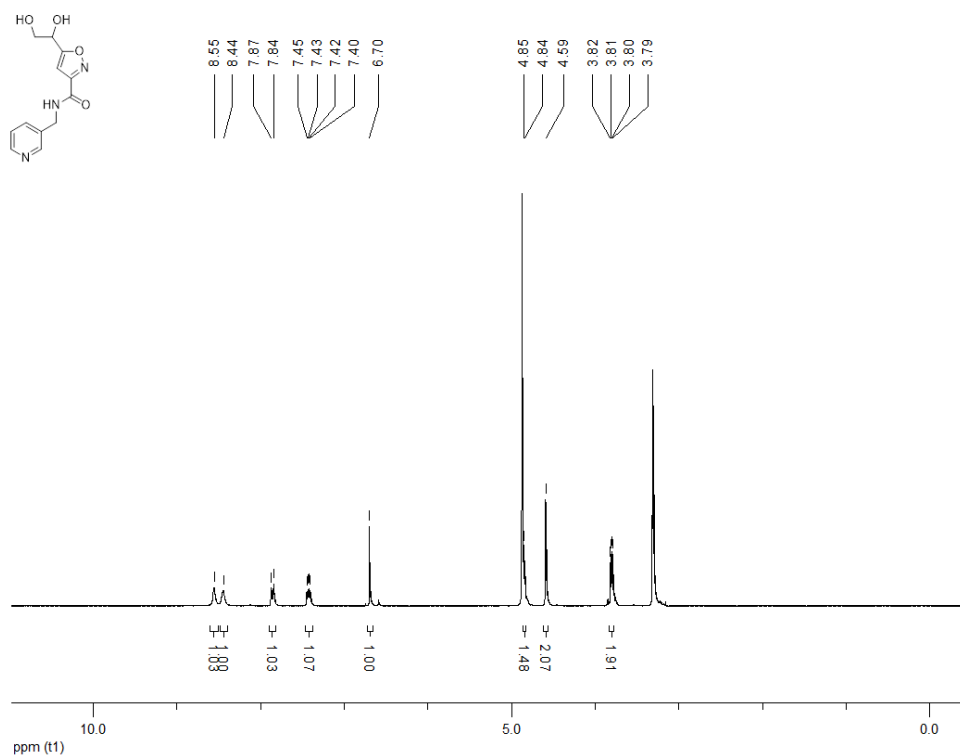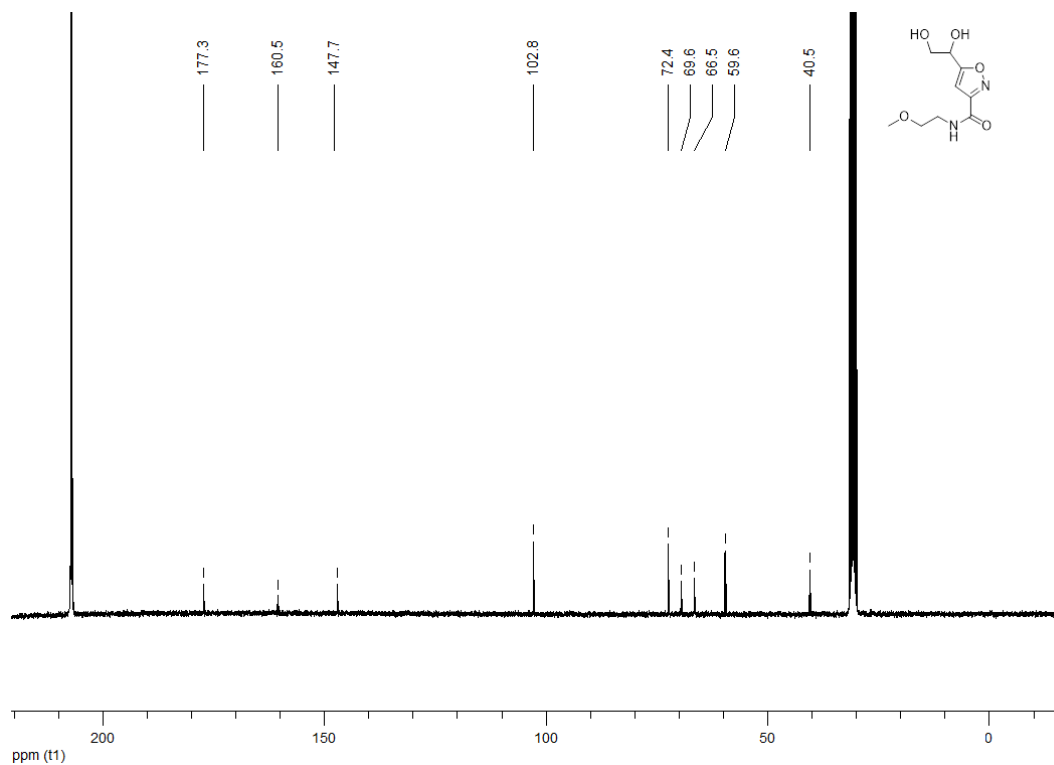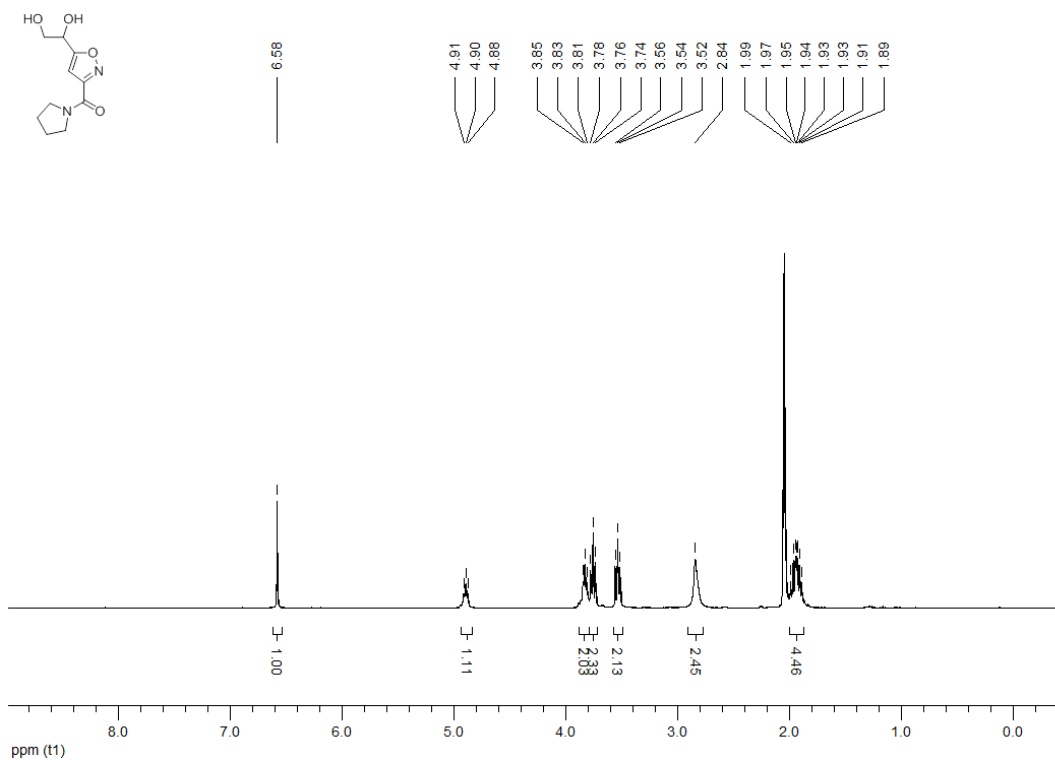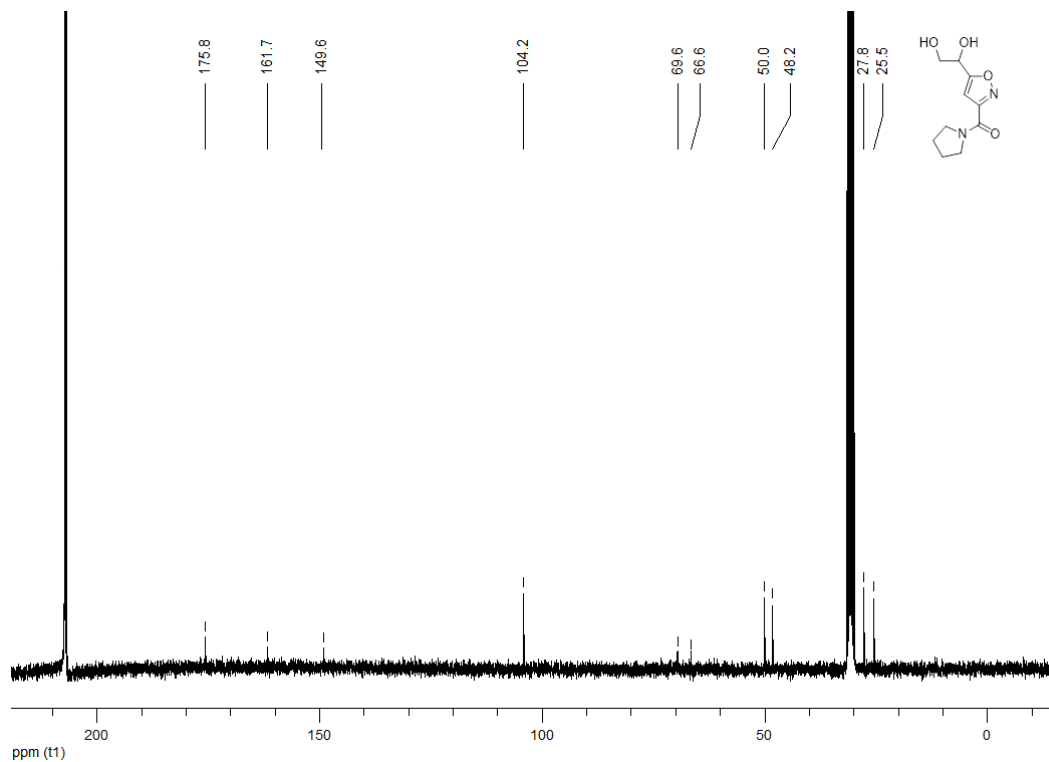
**¹H NMR (300 MHz, Acetone-*d₆*) 1-[3-(pyrrolidine-1-carbonyl)-1,2-oxazol-5-yl]ethane-1,2-diol (170m)**

¹³C NMR (100 MHz, Acetone-*d₆*) 1-[3-(pyrrolidine-1-carbonyl)-1,2-oxazol-5-yl]ethane-1,2-diol (170m)

8.1.6 Synthesis, ^{1}H and ^{13}C NMR of monosubstituted isoquinolines and derivatives

Synthesis of 172a-g: 41 (1.1 eq), Pd(OAc)$_2$ (2%mol), PPh$_3$ (4% mol), KOAc (2.0 eq) and the corresponding 2-bromoaryl(heteroaryl)aldehyde (1.0 eq) in dry DMF were mixed in a 5 mL microwave vial under N$_2$ atmosphere. The mixture was stirred at 80 °C under microwave irradiation until starting material disappearance (usually 1 – 2 hours). After cooling to room temperature, NH$_4$OAc (2.0 eq) was added and the mixture was stirred at 150 °C under microwave irradiation until disappearance of the corresponding Sonogashira product (usually 2 – 3 hours). The mixture was diluted with EtOAc and washed five times with water. The organic layer was dried over MgSO$_4$, filtered and concentrated *in vacuo.* The crude was redissolved in ACN (1 mL), filtered and purified by preparative HPLC.[340]
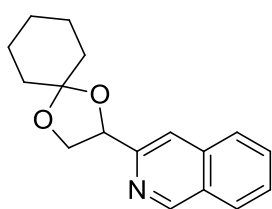
3-{1,4-dioxaspiro[4.5]decan-2-yl}isoquinoline (172a): brown oil, 55%, R_f = 0.15 (CyH/EtOAc 9:1), UHPLC-ESI-MS: R_t = 2.96, m/z = 270.2 [M + H] $^+$. ^{1}H NMR (300 MHz, CDCl$_3$) δ 9.18 (s, 1H), 7.95 (d, J = 8.1 Hz, 1H), 7.87 – 7.82 (m, 2H), 7.68 (t, J = 7.5 Hz, 1H), 7.57 (t, J = 7.5 Hz, 1H), 5.39 (t, J = 6.7 Hz, 1H), 4.55 (t, J = 7.5 Hz, 1H), 4.01 (t, J = 7.5 Hz, 1H), 1.86 – 1.63 (m, 8H), 1.49 – 1.46 (m, 2H) ppm; ^{13}C NMR (100 MHz, CDCl$_3$) δ 153.7, 152.1, 136.3, 130.5, 127.9, 127.5, 127.0, 126.7, 116.1, 110.8, 77.8, 70.1, 36.1, 35.2, 25.2, 24.0, 23.9 ppm.
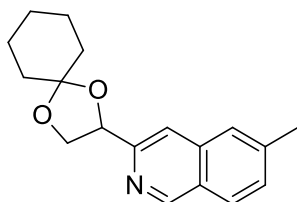
3-{1,4-dioxaspiro[4.5]decan-2-yl}-7-methylisoquinoline (172b): orange oil, 43%, R_f = 0.45 (CyH/EtOAc 3:1), UHPLC-ESI-MS: R_t = 2.94, m/z = 284.2 [M + H] $^+$. ^{1}H NMR (300 MHz, CDCl$_3$) δ 9.11 (s, 1H), 7.85 (d, J = 4.8 Hz, 1H), 7.79 (s, 1H), 7.61 (s, 1H), 7.41 (dd, J = 1.5 Hz, J = 8.4 Hz, 1H), 5.37 (t, J = 7.0 Hz, 1H), 4.54 (dd, J = 6.8 Hz, J = 8.2 Hz, 1H), 4.00 (dd, J = 6.8 Hz, J = 8.2 Hz, 1H), 2.54 (s, 3H), 1.86 – 1.77 (m, 4H), 1.74 – 1.63 (m, 4H), 1.49 – 1.47 (m, 2H) ppm; ^{13}C NMR (100 MHz, CDCl$_3$) δ 153.7, 151.6, 140.9, 136.6, 129.3, 127.3, 126.4, 125.7, 115.6, 110.8, 77.8, 70.2, 36.1, 35.3, 25.2, 24.1, 23.9, 22.1 ppm.
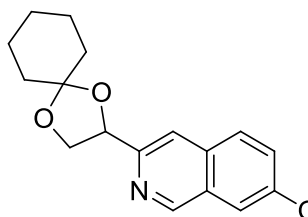
3-{1,4-dioxaspiro[4.5]decan-2-yl}isoquinolin-7-ol (172c): brown oil, 45%, R_f = 0.25 (CyH/EtOAc 3:1), UHPLC-ESI-MS: R_t = 2.29, m/z = 286.2 [M + H]$^+$. ^{1}H NMR (300 MHz, MeOD) δ 8.99 (s, 1H), 8.21 (s, 1H), 7.85 (s, 1H), 7.38 (dd, J = 2.4 Hz, J = 8.9 Hz, 1H), 7.30 (d, J = 2.4 Hz, 1H), 5.29 (t, J = 6.7 Hz, 1H), 4.47 (dd, J = 6.6 Hz, J = 8.1 Hz, 1H), 3.92 (dd, J = 7.1 Hz, J = 8.1 Hz, 1H), 1.87 − 1.67 (m, 8H), 1.52 − 1.48 (m, 2H), ppm; ^{13}C NMR (100 MHz, MeOD) δ 158.2, 151.2, 149.7, 131.2, 129.6, 125.2, 122.1, 118.1, 112.0, 109.2, 78.9, 71.2, 37.3, 36.3, 26.4, 25.2, 25.0 ppm.
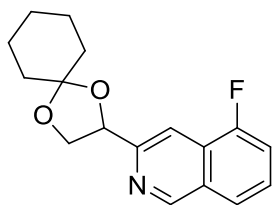

3-{1,4-dioxaspiro[4.5]decan-2-yl}-5-fluoroisoquinoline (172d): brown oil, 73%, R_f = 0.22 (CyH/EtOAc 9:1), UHPLC-ESI-MS: R_t = 3.27, m/z = 288.2 [M + H]$^+$. ^{1}H NMR (300 MHz, CDCl$_3$) δ 9.18 (s, 1H), 8.08 (s, 1H), 7.72 (d, J = 8.2 Hz, 1H), 7.48 (dt, J = 5.1 Hz, J = 7.9 Hz, 1H), 7.36 − 7.30 (m, 1H), 5.37 (t, J = 6.6 Hz, 1H), 4.53 (dd, J = 6.8 Hz, J = 8.2 Hz, 1H), 4.01 (dd, J = 6.6 Hz, J = 8.2 Hz, 1H), 1.85 − 1.73 (m, 4H), 1.68 − 1.61 (m, 4H), 1.48 − 1.45 (m, 2H) ppm; ^{13}C NMR (100 MHz, CDCl$_3$) δ 157.6 (d, J = 254.1 Hz), 154.4, 151.5 (d, J = 3.0 Hz), 128.8 (d, J = 4.9 Hz), 126.9 (d, J = 7.5 Hz), 126.6, 123.2 (d, J = 4.4 Hz), 114.0 (d, J = 19.1 Hz), 111.0, 109.1 (d, J = 3.7 Hz), 77.0, 70.0, 36.1, 35.2, 25.1, 24.0 (d, J = 8.3 Hz) ppm.
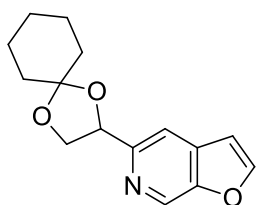
5-{1,4-dioxaspiro[4.5]decan-2-yl}furo[2,3-c]pyridine (172e): brown oil, 53%, R_f = 0.22 (CyH/EtOAc 9:1), UHPLC-ESI-MS: R_t = 2.54, m/z = 260.2 [M + H]$^+$. ^{1}H NMR (300 MHz, CDCl$_3$) δ 8.79 (s, 1H), 7.81 (s, 1H), 7.76 (d, J = 2.0 Hz, 1H), 6.82 (d, J = 1.2 Hz, 1H), 5.32 (t, J = 6.7 Hz, 1H), 4.49 (t, J = 8.1 Hz, 1H), 3.95 (t, J = 7.5 Hz, 1H), 1.81 − 1.75 (m, 5H), 1.71 − 1.64 (m, 3H), 1.50 − 1.46 (m, 2H) ppm; ^{13}C NMR (100 MHz, CDCl$_3$) δ 153.2, 151.5, 148.5, 134.8, 132.8, 112.4, 110.8, 106.3, 77.9, 70.4, 36.2, 35.2, 25.2, 24.1, 23.9 ppm.
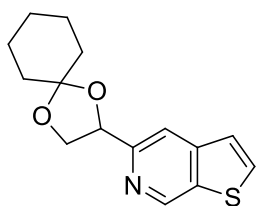
5-{1,4-dioxaspiro[4.5]decan-2-yl}thieno[2,3-c]pyridine (172f): brown oil, 66%, R_f = 0.24 (CyH/EtOAc 9:1), UHPLC-ESI-MS: R_t = 2.67, m/z = 276.2 [M + H]$^+$. ^{1}H NMR (300 MHz, CDCl$_3$) δ 9.05 (s, 1H), 7.95 (s, 1H), 7.72 (d, J = 5.3 Hz, 1H), 7.37 (d, J = 5.3 Hz, 1H), 5.35 (t, J = 6.7 Hz, 1H), 4.52 (t, J = 7.5 Hz, 1H), 3.96 (t, J = 7.5 Hz, 1H), 1.81 − 1.75 (m, 4H), 1.71 − 1.64 (m, 4H), 1.49 − 1.45 (m, 2H) ppm; ^{13}C NMR (100 MHz, CDCl$_3$) δ 154.1, 145.6, 143.8, 135.2, 132.5, 123.2, 114.0, 110.8, 77.7, 70.3, 36.1, 35.2, 25.2, 24.0 (d, J = 12.1 Hz) ppm.
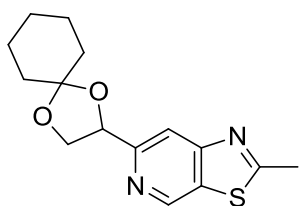
6-{1,4-dioxaspiro[4.5]decan-2-yl}-2-methyl-[1,3]thiazolo[5,4-c]pyridine (172g): brown oil, 59%, R_f = 0.23 (CyH/EtOAc 3:1), UHPLC-ESI-MS: R_t = 2.80, m/z = 291.2 [M + H]$^+$. ^{1}H NMR (300 MHz, CDCl$_3$) δ 9.13 (s, 1H), 8.03 (s, 1H), 5.33 (t, J = 6.6 Hz, 1H), 4.52 (t, J = 7.5 Hz, 1H), 3.97 (t, J = 7.5 Hz, 1H), 2.87 (s, 3H), 1.82 − 1.62 (m, 8H), 1.50 − 1.46 (m, 2H) ppm; ^{13}C NMR (100 MHz, CDCl$_3$) δ 168.2, 154.9, 149.2, 144.8, 143.3, 112.5, 111.0, 77.7, 70.2, 36.2, 35.1, 25.2, 24.1, 23.9, 20.2 ppm.

Synthesis of 173a-g: a stirred solution of the protected isoquinoline **172a-g** in 1,4-dioxane was cooled to 0 °C using an ice bath. A catalytic amount of concentrated HCl was added. The reaction was stirred at room temperature overnight. Solvent was evaporated under reduced pressure, the crude was redissolved in ACN (1 mL), filtered and purified by preparative HPLC.
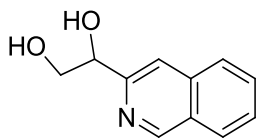
1-(isoquinolin-3-yl)ethane-1,2-diol (173a): white solid, 90%, R_f = 0.41 (CHCl$_3$/MeOH 9:1), UHPLC-ESI-MS: R_t = 1.12, m/z = 190.2 [M + H]$^+$. ^{1}H NMR (300 MHz, MeOD) δ 9.20 (s, 1H), 8.08 (d, J = 8.2 Hz, 1H), 7.94 (d, J = 7.6 Hz, 2H), 7.78 (t, J = 7.3 Hz, 1H), 7.66 (t, J = 7.4 Hz, 1H), 4.95 − 4.92 (m, 1H), 3.98 − 3.88 (m, 1H), 3.79 − 3.70 (m, 1H) ppm; ^{13}C NMR (100 MHz, MeOD) δ 155.5, 152.7, 135.1, 132.3, 128.9, 128.6, 127.8, 124.4, 118.9, 76.2, 67.7 ppm
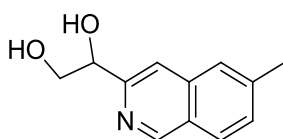
1-(6-methylisoquinolin-3-yl)ethane-1,2-diol (173b): yellowish solid, 54%, R_f = 0.23 (DCM/MeOH 19:1), UHPLC-ESI-MS: R_t = 1.31, m/z = 204.2 [M + H]$^+$. ^{1}H NMR (300

MHz, MeOD) δ 9.11 (s, 1H), 7.97 (d, J = 8.4 Hz, 1H), 7.86 (s, 1H), 7.71 (s, 1H), 7.51 (dd, J = 1.4 Hz, J = 8.4 Hz, 1H), 4.95 – 4.91 (m, 1H), 3.93 (dd, J = 4.0 Hz, J = 11.3 Hz, 1H), 3.74 (dd, J = 6.8 Hz, J = 11.3 Hz, 1H), 2.56 (s, 3H) ppm; ^{13}C NMR (100 MHz, MeOD) δ 155.4, 152.2, 143.3, 138.4, 130.9, 128.7, 127.9, 126.7, 118.5, 76.1, 67.7, 22.1 ppm.
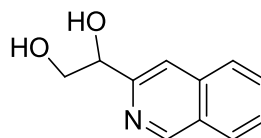
1-(7-hydroxyisoquinolin-3-yl)ethane-1,2-diol (173c): yellow oil, 67%, R_f = 0.50 (CHCl$_3$/MeOH 9:1), UHPLC-ESI-MS: R_t = 0.41, m/z = 206.0 [M + H]$^+$. ^{1}H NMR (300 MHz, MeOD) δ 9.14 (s, 1H), 7.97 (dd, J = 9.4 Hz, J = 16.6 Hz, 2H), 7.51 (dd, J = 1.5 Hz, J = 8.7 Hz, 1H), 7.41 (s, 1H), 4.98 – 4.95 (m, 1H), 3.89 (dd, J = 4.5 Hz, J = 11.3 Hz, 1H), 3.79 (dd, J = 6.2 Hz, J = 11.2 Hz, 1H) ppm; ^{13}C NMR (100 MHz, MeOD) δ 164.9, 159.2, 148.5, 133.8, 130.8, 129.9, 127.5, 120.7, 109.8, 74.4, 67.4 ppm.
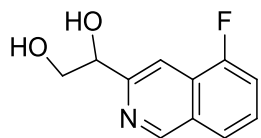
1-(5-fluoroisoquinolin-3-yl)ethane-1,2-diol (173d): white solid, 42%, R_f = 0.47 (CHCl$_3$/MeOH 9:1), UHPLC-ESI-MS: R_t = 1.44, m/z = 208.2 [M + H]$^+$. ^{1}H NMR (300 MHz, MeOD) δ 9.25 (s, 1H), 8.11 (s, 1H), 7.91 (d, J = 7.8 Hz, 1H), 7.65 – 7.58 (m, 1H), 7.52 – 7.46 (m, 1H), 4.97 – 4.94 (m, 1H), 3.97 (dd, J = 3.9 Hz, J = 11.3 Hz, 1H), 3.77 (dd, J = 6.4 Hz, J = 11.3 Hz, 1H) ppm; $^{13}$C NMR (100 MHz, MeOD) δ 158.6 (d, J = 252.4 Hz), 156.3 (d, J = 1.5 Hz), 152.3 (d, J = 2.9 Hz), 130.1 (d, J = 4.6 Hz), 128.4 (d, J = 7.7 Hz), 127.8 (d, J = 17.9 Hz), 124.6 (d, J = 4.4 Hz), 115.3 (d, J = 19.3 Hz), 111.0 (d, J = 3.9 Hz), 75.9, 67.3 ppm.
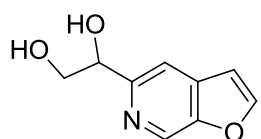
1-{furo[3,2-c]pyridin-6-yl}ethane-1,2-diol (173e): yellow oil, 48%, R_f = 0.33 (CHCl$_3$/MeOH 9:1), UHPLC-ESI-MS: R_t = 0.48, m/z = 180.1 [M + H]$^+$. ^{1}H NMR (300 MHz, MeOD) δ 8.84 (s, 1H), 8.12 (s, 1H), 7.93 (s, 1H), 7.05 (s, 1H), 4.96 – 4.91 (m, 1H), 3.86 (dd, J = 4.2 Hz, J = 11.2 Hz, 1H), 3.73 (dd, J = 6.6 Hz, J = 11.2 Hz, 1H) ppm; ^{13}C NMR (100 MHz, MeOD) δ 154.7, 152.5, 143.5, 139.9, 132.1, 115.4, 107.7, 75.4, 67.8 ppm.
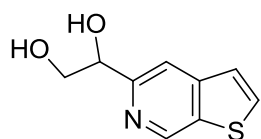
1-{thieno[3,2-c]pyridin-6-yl}ethane-1,2-diol (173f): white solid, 73%, R_f = 0.35 (CHCl$_3$/MeOH 9:1), UHPLC-ESI-MS: R_t = 0.64, m/z = 196.0 [M + H]$^+$. ^{1}H NMR (300 MHz, MeOD) δ 8.97 (s, 1H), 7.91 – 7.87 (m, 2H), 7.39 (d, J = 5.3 Hz, 1H), 4.82 (s, 1H), 3.80 (dd, J = 3.9

Hz, J = 11.2 Hz, 1H), 3.63 (dd, J = 6.8 Hz, J = 11.2 Hz, 1H) ppm; ^{13}C NMR (100 MHz, MeOD) δ 156.1, 147.7, 144.5, 136.8, 134.9, 124.3, 116.5, 76.1, 67.9 ppm.
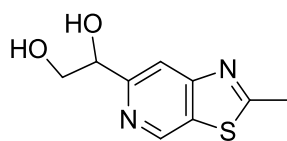
1-{2-methyl-[1,3]thiazolo[4,5-c]pyridin-6-yl}ethane-1,2-diol **(173g):** yellow oil, 70%, R_f = 0.39 (CHCl$_3$/MeOH 9:1), UHPLC-ESI-MS: R_t = 1.12, m/z = 211.2 [M + H]$^+$. ^{1}H NMR (300 MHz, MeOD) δ 9.03 (s, 1H), 8.16 (s, 1H), 4.91 (s, 1H), 3.90 (dd, J = 3.9 Hz, J = 11.3 Hz, 1H), 3.73 (dd, J = 6.4 Hz, J = 11.1 Hz, 1H), 3.70 (s, 3H) ppm; ^{13}C NMR (100 MHz, MeOD) δ 171.6, 157.2, 150.4, 146.7, 143.2, 115.4, 76.0, 67.7, 19.9 ppm.

1H NMR (300 MHz, CDCl₃) 3-{1,4-dioxaspiro[4.5]decan-2-yl}isoquinoline (172a)
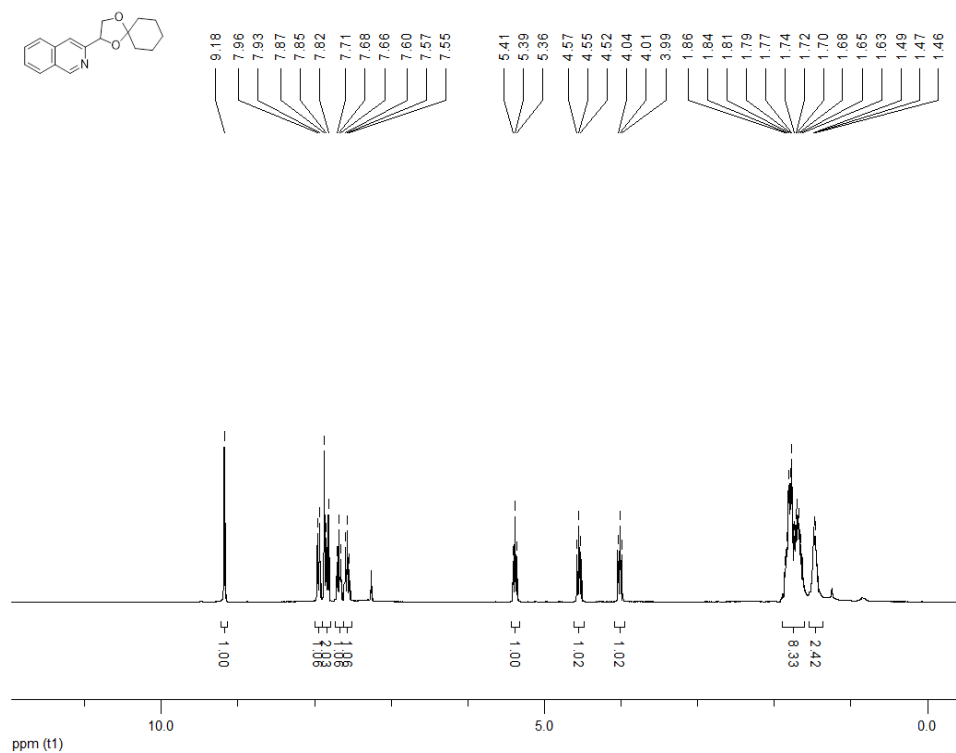
13C NMR (100 MHz, CDCl₃) 3-{1,4-dioxaspiro[4.5]decan-2-yl}isoquinoline (172a)
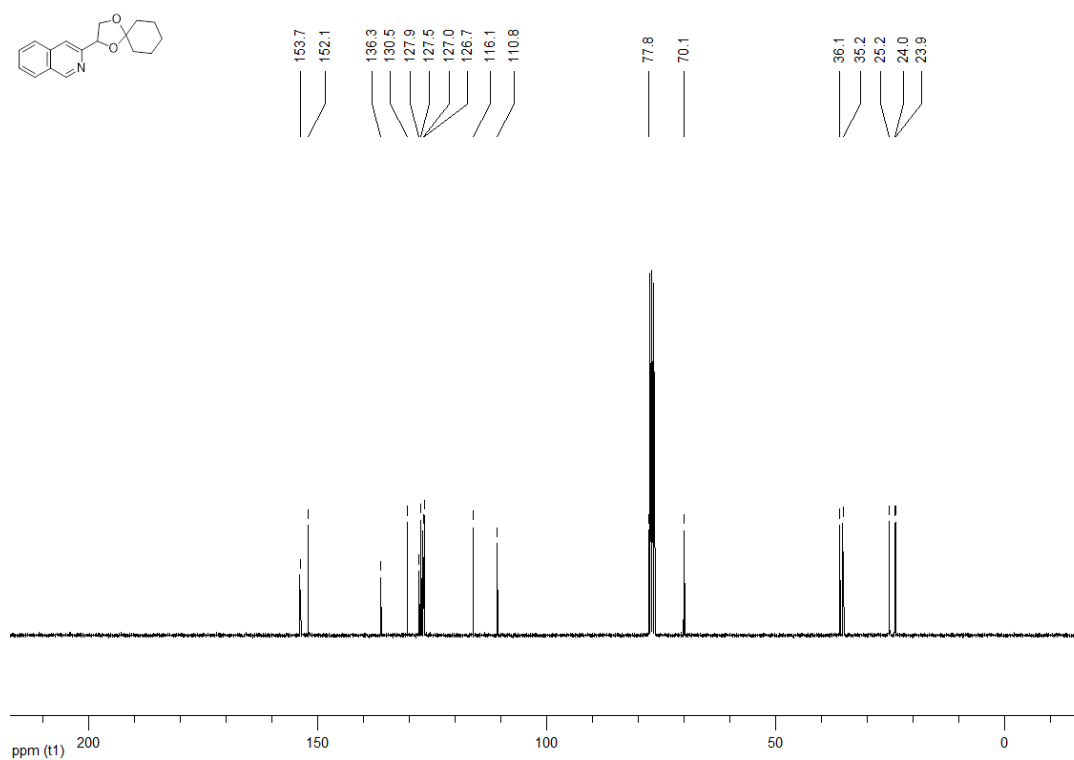
^{1}H NMR (300 MHz, CDCl$_3$) 3-{1,4-dioxaspiro[4.5]decan-2-yl}-7-methylisoquinoline (172b)
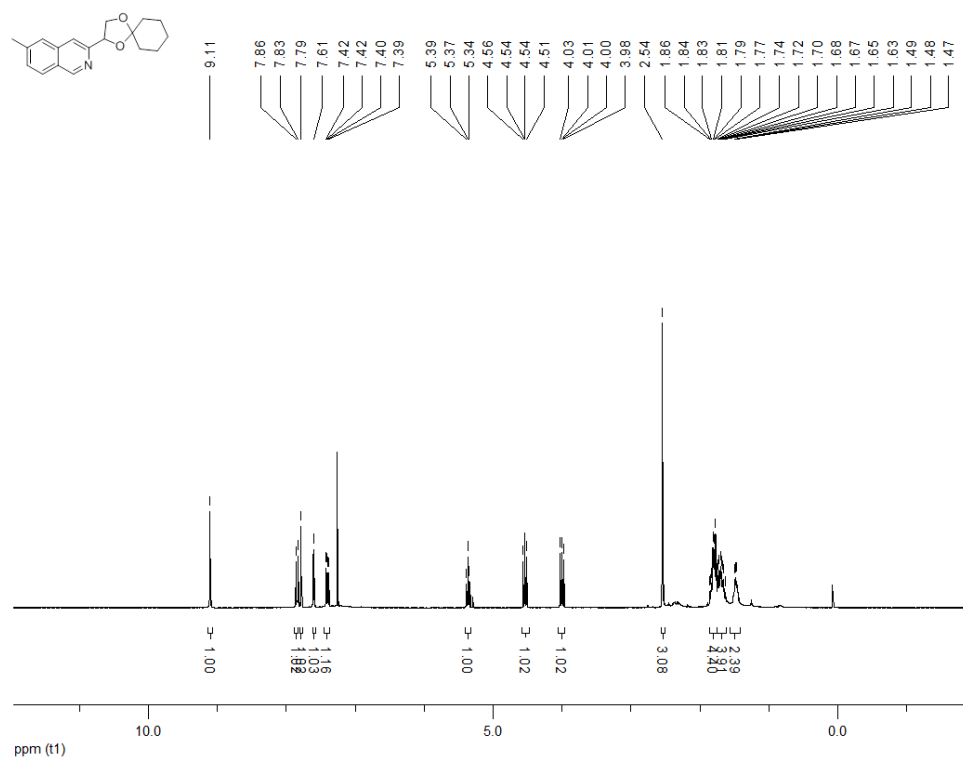
^{13}C NMR (100 MHz, CDCl$_3$) 3-{1,4-dioxaspiro[4.5]decan-2-yl}-7-methylisoquinoline (172b)
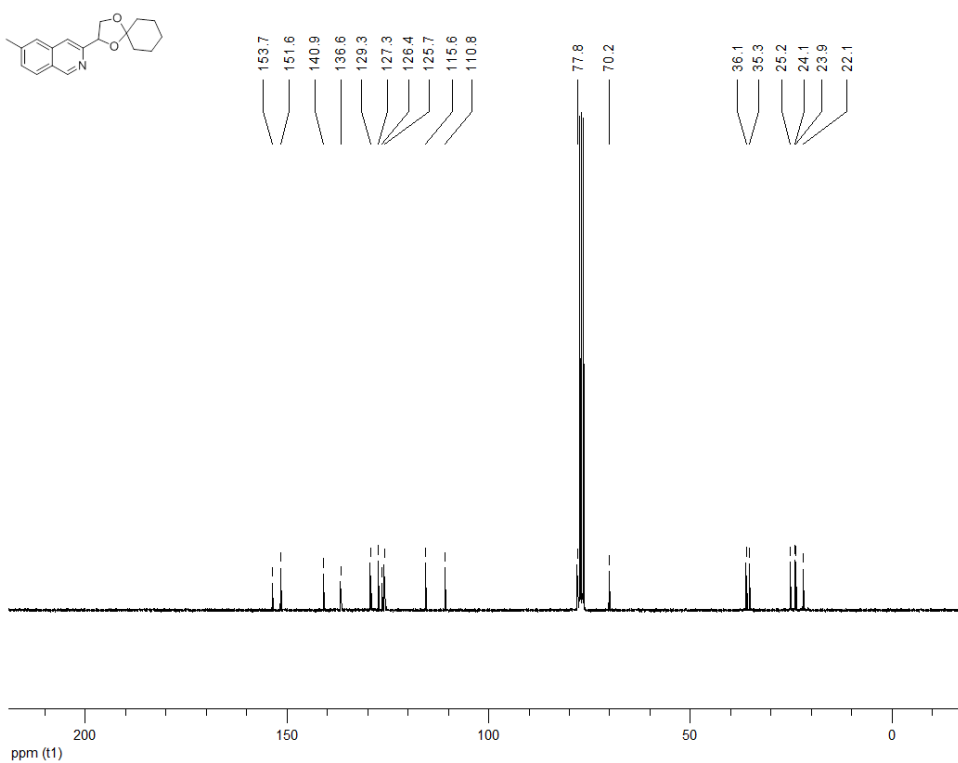
¹H NMR (300 MHz, MeOD) 3-{1,4-dioxaspiro[4.5]decan-2-yl}isoquinolin-7-ol (172c)

8.99
8.21
7.85
7.40
7.39
7.37
7.36
7.30
7.29
5.31
5.29
5.27
4.50
4.48
4.47
4.45
3.94
3.92
3.91
3.89
1.87
1.84
1.84
1.82
1.81
1.78
1.77
1.74
1.74
1.72
1.70
1.69
1.67
1.52
1.50
1.48

0.98
0.95
1.49
1.94
1.91
1.00
0.93
1.07
2.49
8.49

10.0   5.0   0.0
ppm (t1)
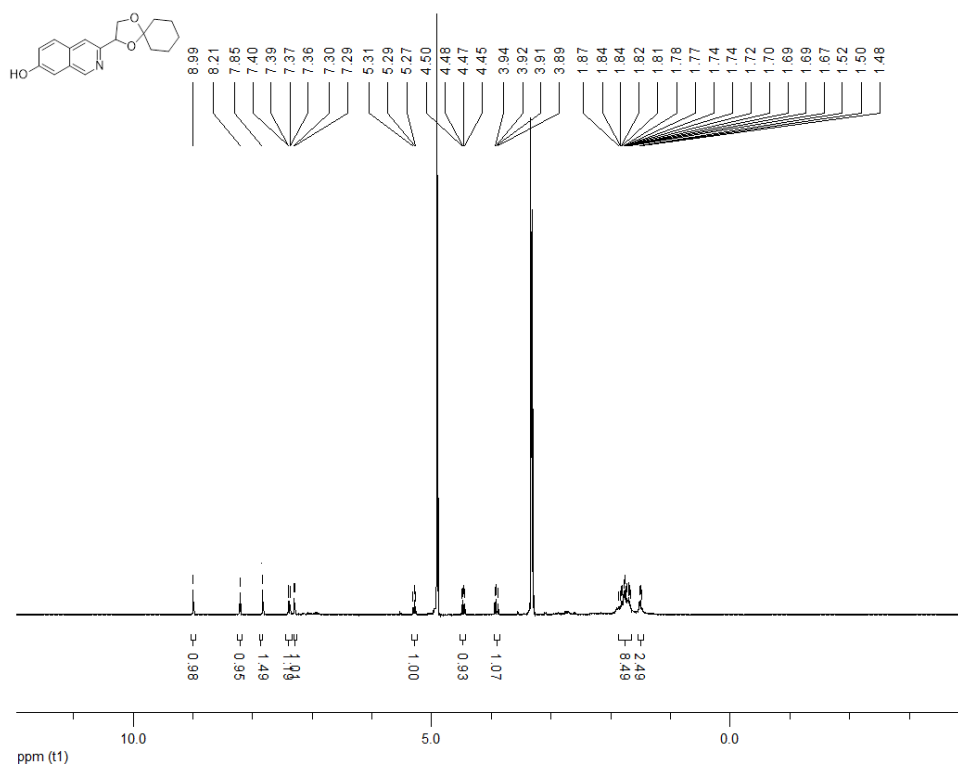
¹³C NMR (100 MHz, MeOD) 3-{1,4-dioxaspiro[4.5]decan-2-yl}isoquinolin-7-ol (172c)

158.2
151.2
149.7
131.2
129.6
125.2
122.1
118.1
112.0
109.2
78.9
71.2
37.3
36.3
26.4
25.2
25.0

200   150   100   50   0
ppm (t1)

179

^{1}H NMR (300 MHz, CDCl$_3$) 3-{1,4-dioxaspiro[4.5]decan-2-yl}-5-fluoroisoquinoline (172d)

9.18
8.08
7.73
7.71
7.51
7.50
7.49
7.47
7.46
7.44
7.36
7.32
7.30
5.40
5.37
5.35
4.56
4.54
4.53
4.51
4.03
4.01
3.98
1.85
1.84
1.80
1.79
1.76
1.73
1.68
1.65
1.63
1.61
1.48
1.47
1.45

0.97
1.00
1.00
1.04
1.02
1.00
1.02
1.05
4.74
3.58
2.42
2.04

ppm (t1)   10.0   5.0   0.0

^{13}C NMR (100 MHz, CDCl$_3$) 3-{1,4-dioxaspiro[4.5]decan-2-yl}-5-fluoroisoquinoline (172d)

159.3
155.9
154.4
151.5
151.5
128.8
128.8
126.9
126.8
126.6
123.2
123.1
114.1
113.8
111.0
109.1
109.1
77.7
70.0

36.1
35.2
25.1
24.0
23.9

ppm (t1)   200   150   100   50   0

¹H NMR (300 MHz, CDCl₃) 5-{1,4-dioxaspiro[4.5]decan-2-yl}furo[2,3-c]pyridine (172e)

8.79
7.81
7.76
7.76
6.82
6.82
5.34
5.32
5.30
4.52
4.49
4.47
3.97
3.95
3.92
1.81
1.78
1.77
1.75
1.71
1.70
1.68
1.66
1.64
1.50
1.48
1.46

1.00
1.93
1.02
1.04
1.07
1.07
3.49
3.66
2.01

10.0   5.0   0.0

ppm (t1)

¹³C NMR (100 MHz, CDCl₃) 5-{1,4-dioxaspiro[4.5]decan-2-yl}furo[2,3-c]pyridine (172e)

153.2
151.5
148.5
134.8
132.8
112.4
110.8
106.3
77.9
70.4
36.2
35.2
25.2
24.1
23.9

200   150   100   50   0

ppm (t1)
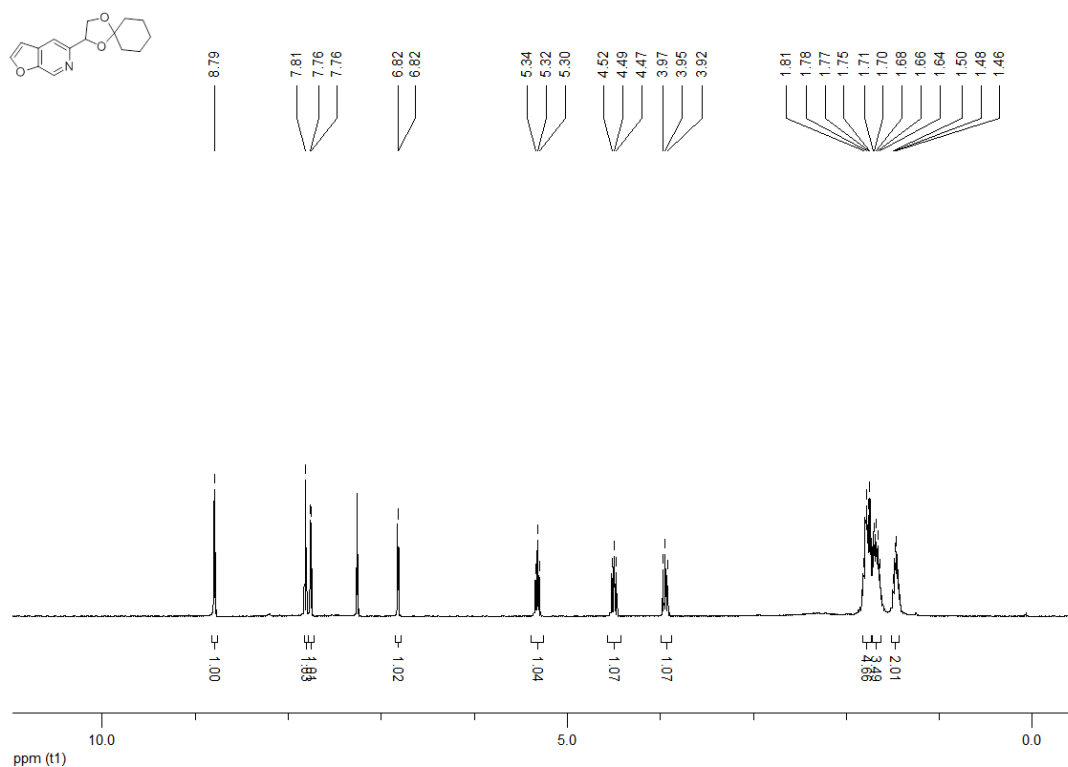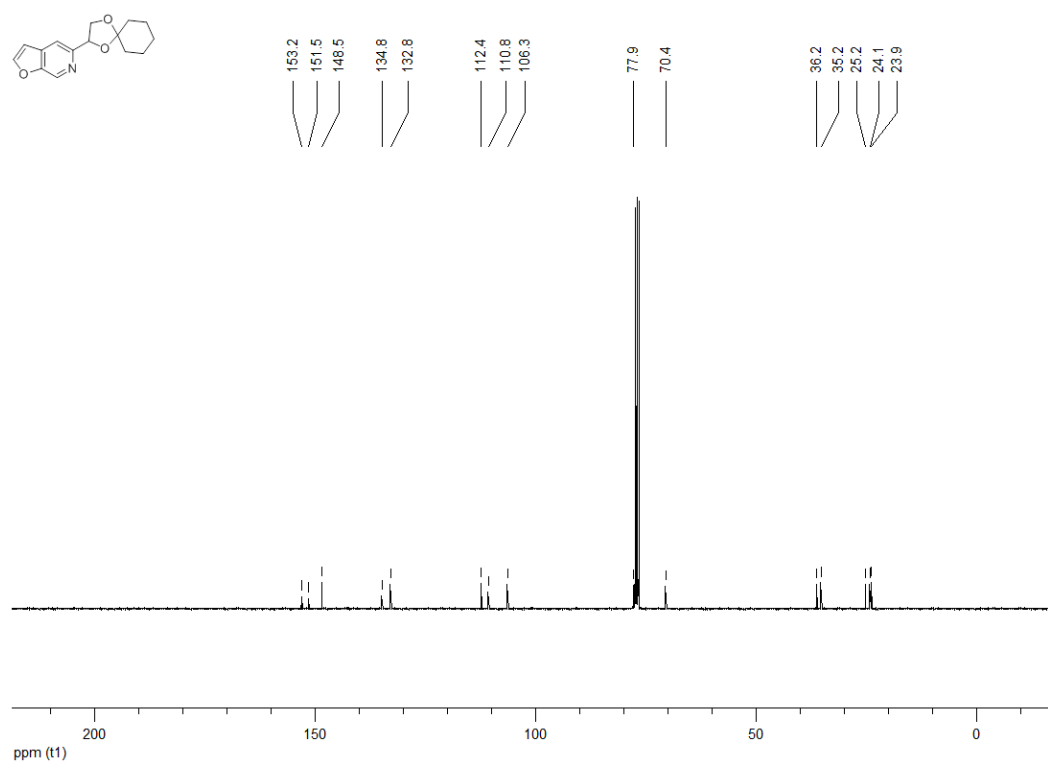
¹H NMR (300 MHz, CDCl₃) 5-{1,4-dioxaspiro[4.5]decan-2-yl}thieno[2,3-c]pyridine (172f)
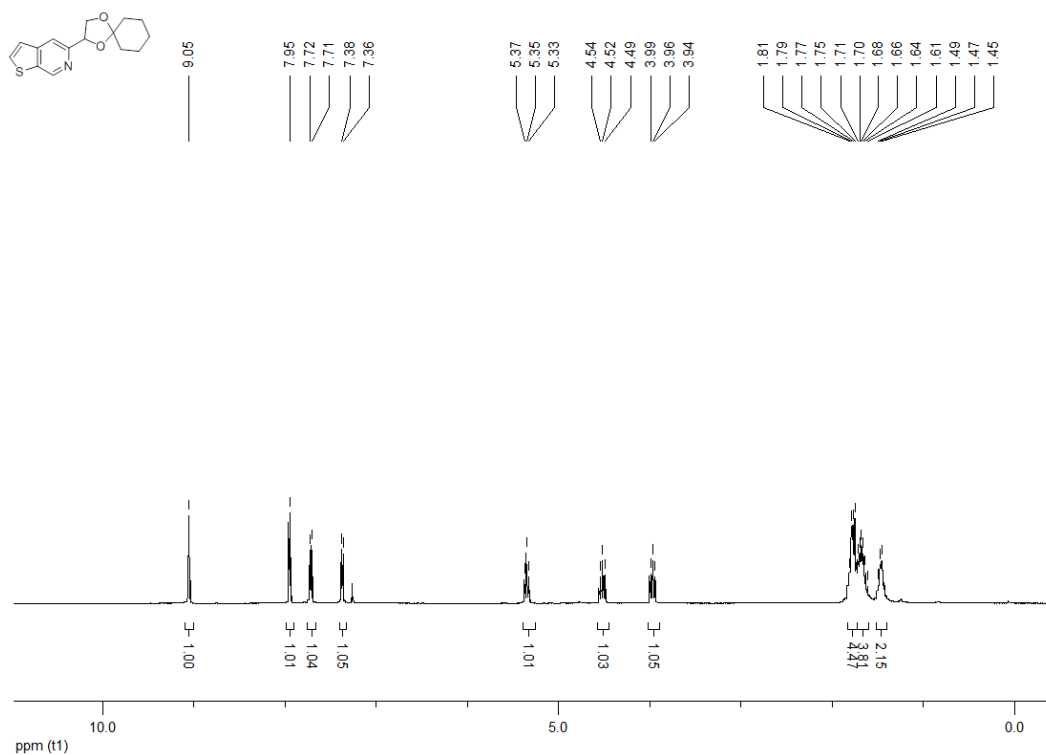
¹³C NMR (100 MHz, CDCl₃) 5-{1,4-dioxaspiro[4.5]decan-2-yl}thieno[2,3-c]pyridine (172f)
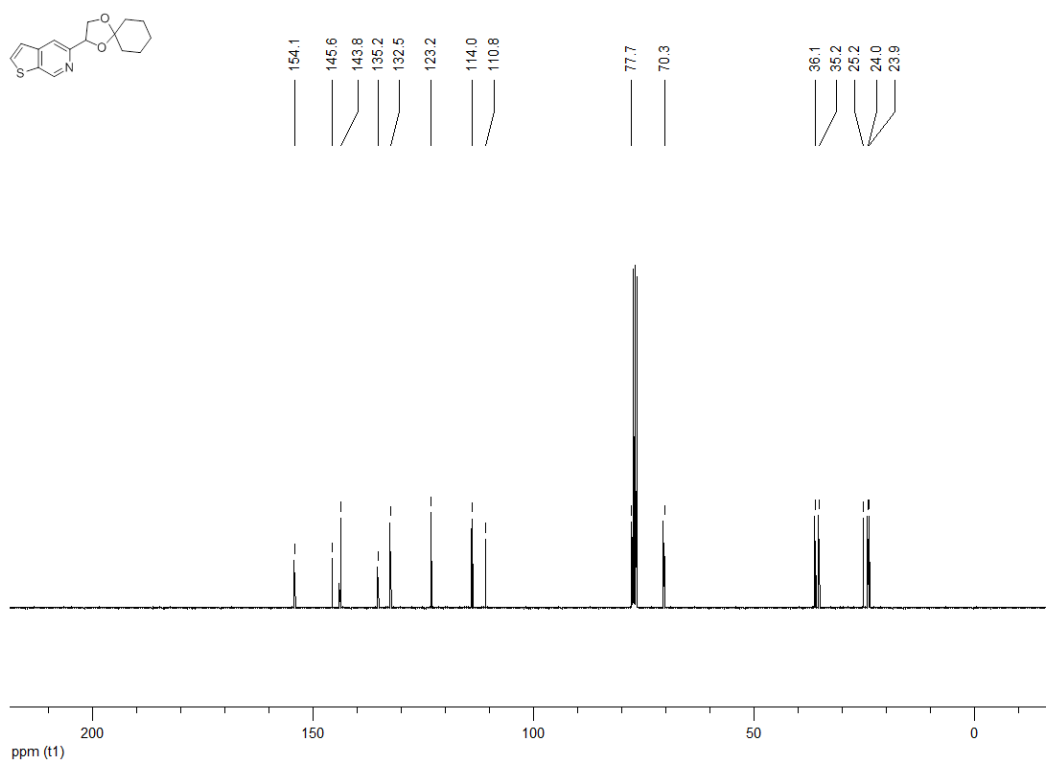
¹H NMR (300 MHz, CDCl₃) 6-{1,4-dioxaspiro[4.5]decan-2-yl}-2-methyl-[1,3]thiazolo[5,4-c]pyridine (172g)
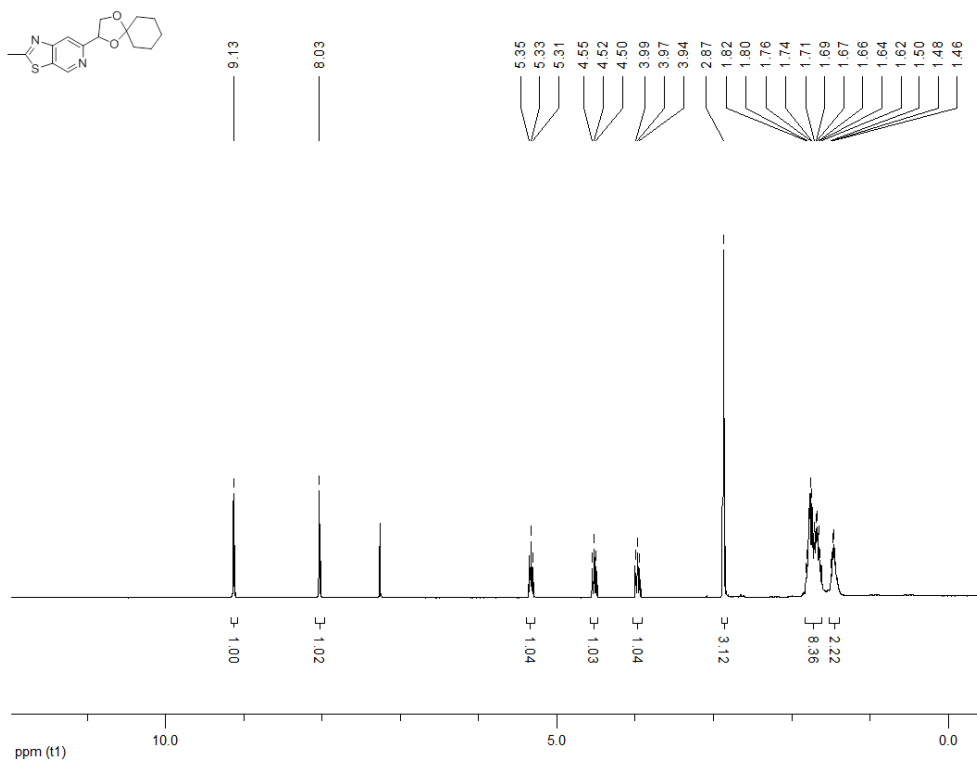
¹³C NMR (100 MHz, CDCl₃) 6-{1,4-dioxaspiro[4.5]decan-2-yl}-2-methyl-[1,3]thiazolo[5,4-c]pyridine (172g)
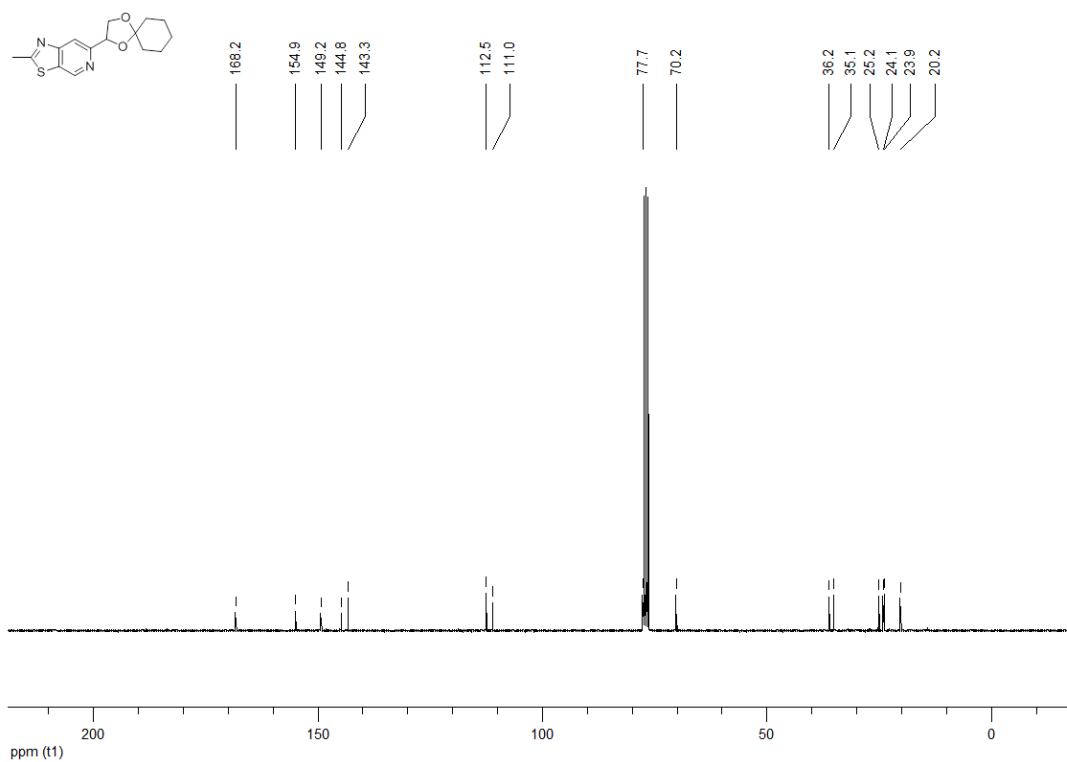
^{1}H NMR (300 MHz, MeOD) 1-(isoquinolin-3-yl)ethane-1,2-diol (173a)
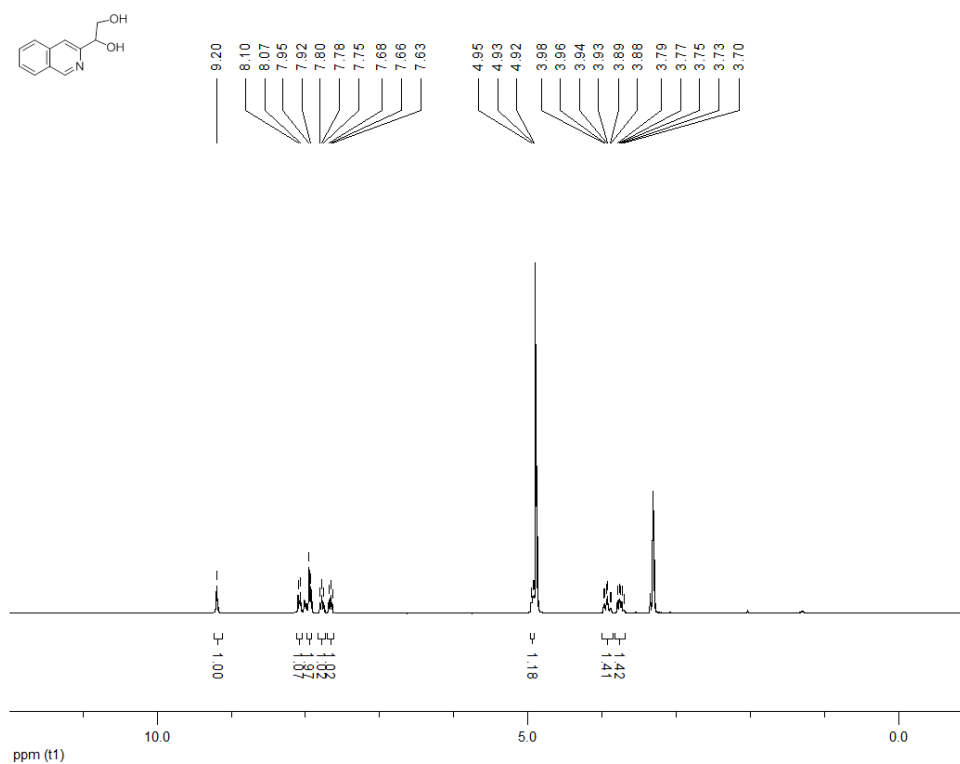
^{13}C NMR (100 MHz, MeOD) 1-(isoquinolin-3-yl)ethane-1,2-diol (173a)
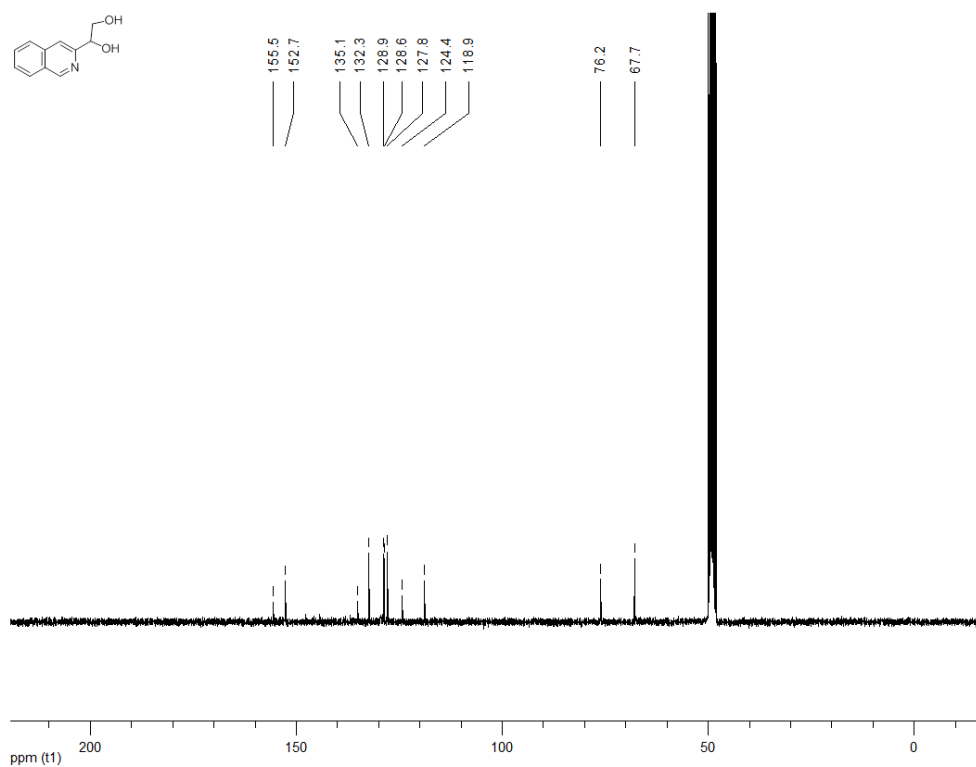
¹H NMR (300 MHz, MeOD) 1-(7-methylisoquinolin-3-yl)ethane-1,2-diol (173b)
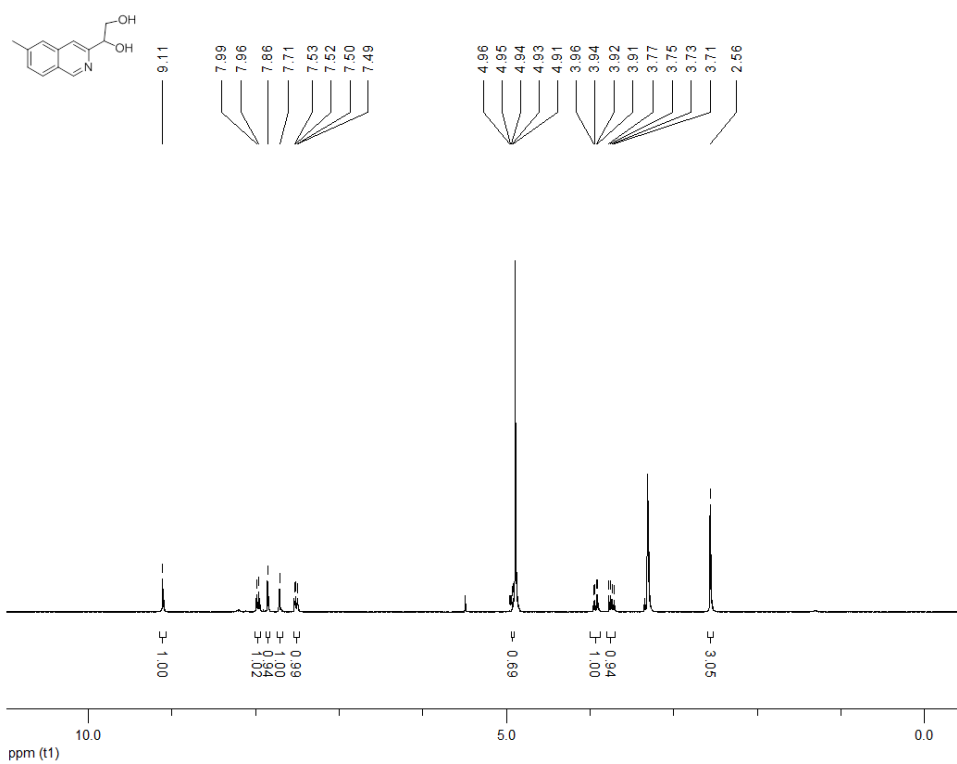
¹³C NMR (100 MHz, MeOD) 1-(7-methylisoquinolin-3-yl)ethane-1,2-diol (173b)

¹H NMR (300 MHz, MeOD) 1-(7-hydroxyisoquinolin-3-yl)ethane-1,2-diol (173c)

9.14
8.01
7.98
7.96
7.93
7.53
7.53
7.50
7.50
7.41
4.98
4.96
4.95
3.92
3.90
3.88
3.87
3.82
3.80
3.78
3.76

0.95
2.33
0.99
0.99
0.99
1.21
1.04
1.04

10.0   5.0   0.0

ppm (t1)
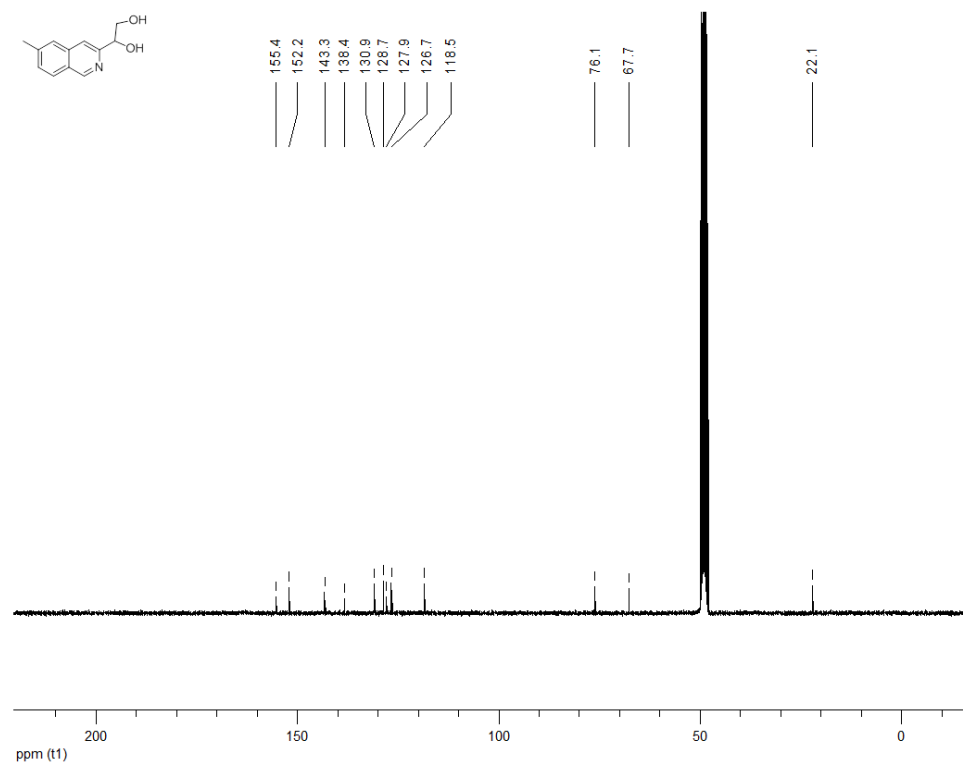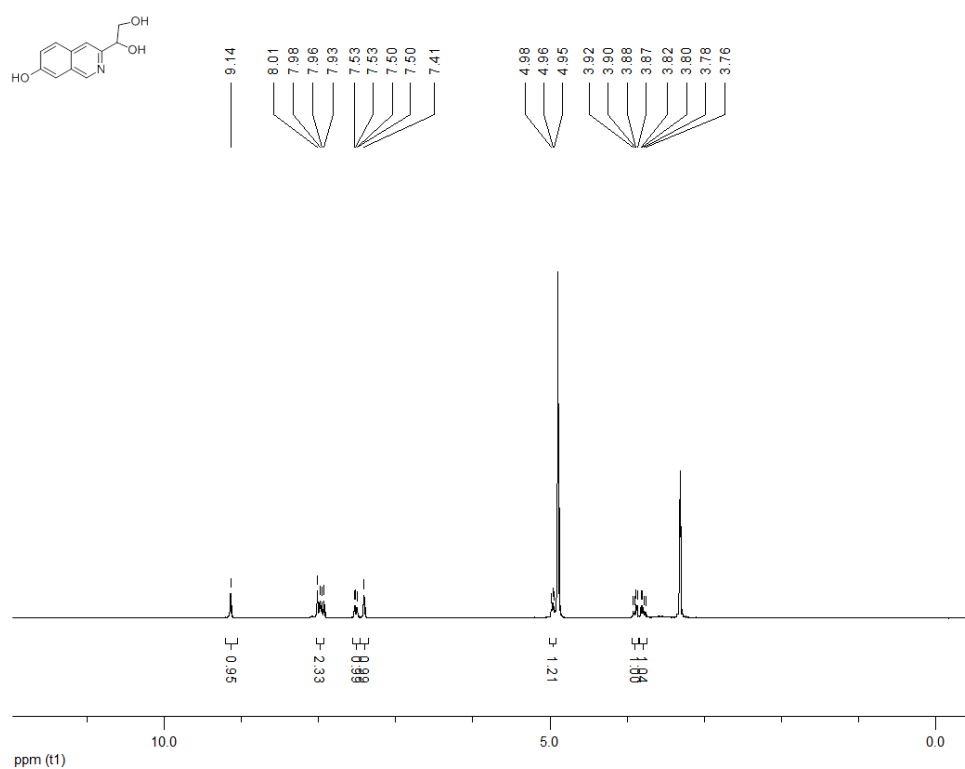
¹³C NMR (100 MHz, MeOD) 1-(7-hydroxyisoquinolin-3-yl)ethane-1,2-diol (173c)

164.9
159.2
148.5
133.8
130.8
129.9
127.5
120.7
109.8
74.4
67.4

200   150   100   50   0

ppm (t1)
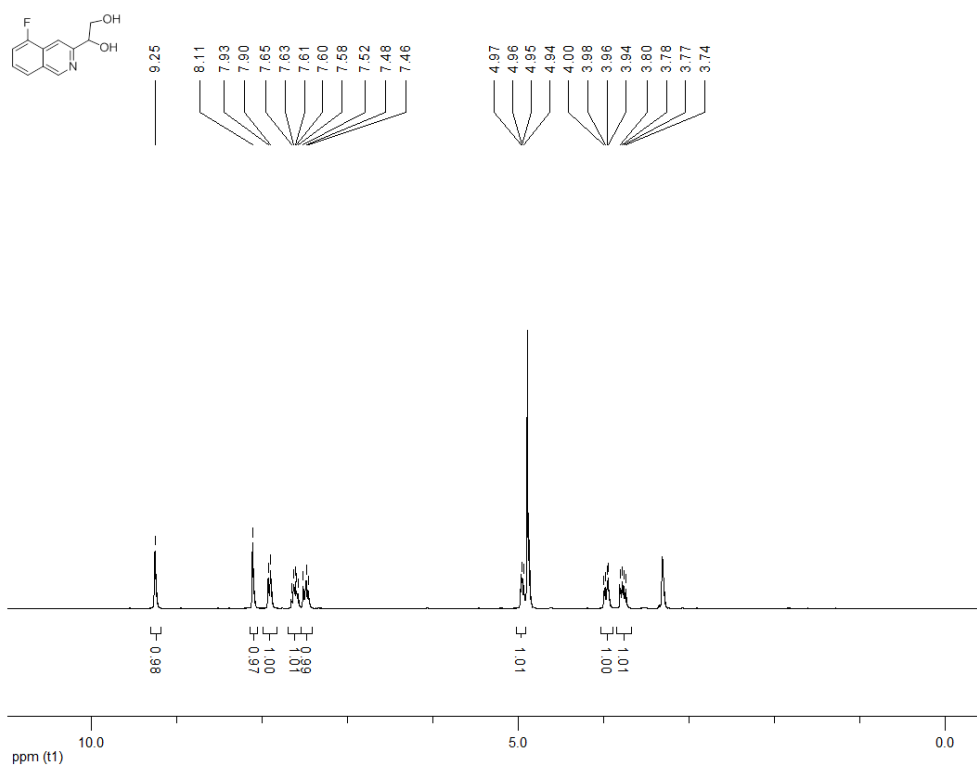
¹H NMR (300 MHz, MeOD) 1-(5-fluoroisoquinolin-3-yl)ethane-1,2-diol (173d)

¹H NMR (300 MHz, MeOD) 1-(5-fluoroisoquinolin-3-yl)ethane-1,2-diol (173d)

9.25

8.11
7.93
7.90
7.65
7.63
7.61
7.60
7.58
7.52
7.48
7.46

4.97
4.96
4.95
4.94
4.00
3.98
3.96
3.94
3.80
3.78
3.77
3.74

0.98

0.67
1.00
1.01
1.01
0.99

1.01

1.01
1.00
1.01

10.0   5.0   0.0

ppm (t1)

¹³C NMR (100 MHz, MeOD) 1-(5-fluoroisoquinolin-3-yl)ethane-1,2-diol (173d)

¹³C NMR (100 MHz, MeOD) 1-(5-fluoroisoquinolin-3-yl)ethane-1,2-diol (173d)

160.3
157.0
156.3
156.3
152.3
152.3
130.1
130.1
128.4
128.3
127.9
127.7
124.6
124.6
115.4
115.1
111.0
110.9

75.9

67.3

200   150   100   50   0

ppm (t1)
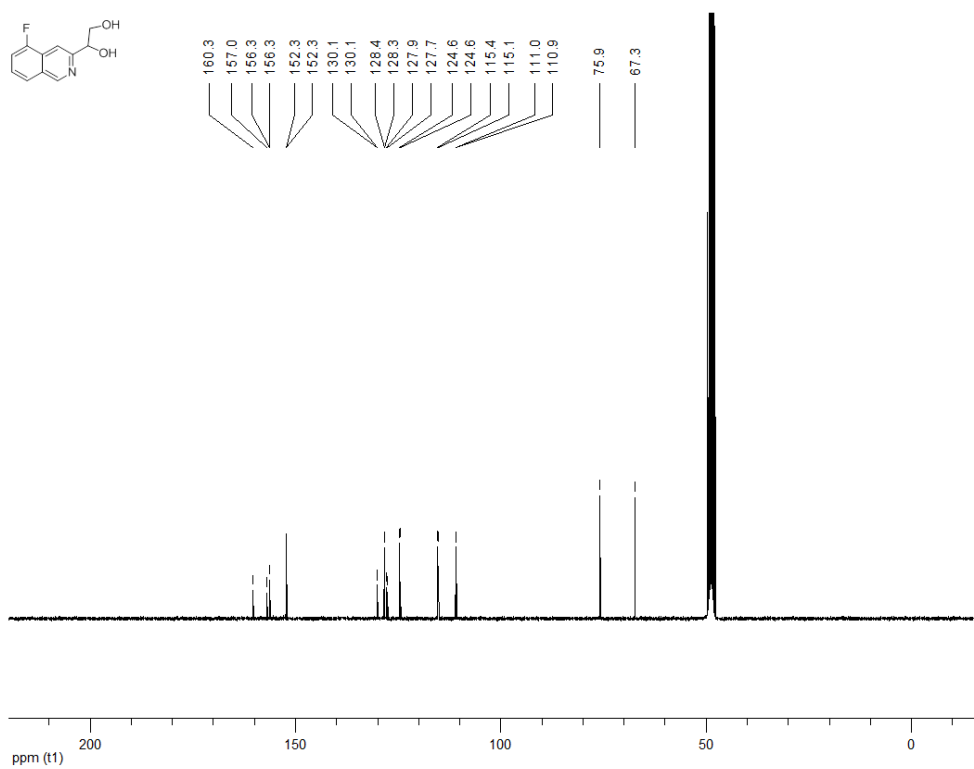
¹H NMR (300 MHz, MeOD) 1-{furo[3,2-c]pyridin-6-yl}ethane-1,2-diol (173e)

¹³C NMR (100 MHz, MeOD) 1-{furo[3,2-c]pyridin-6-yl}ethane-1,2-diol (173e)
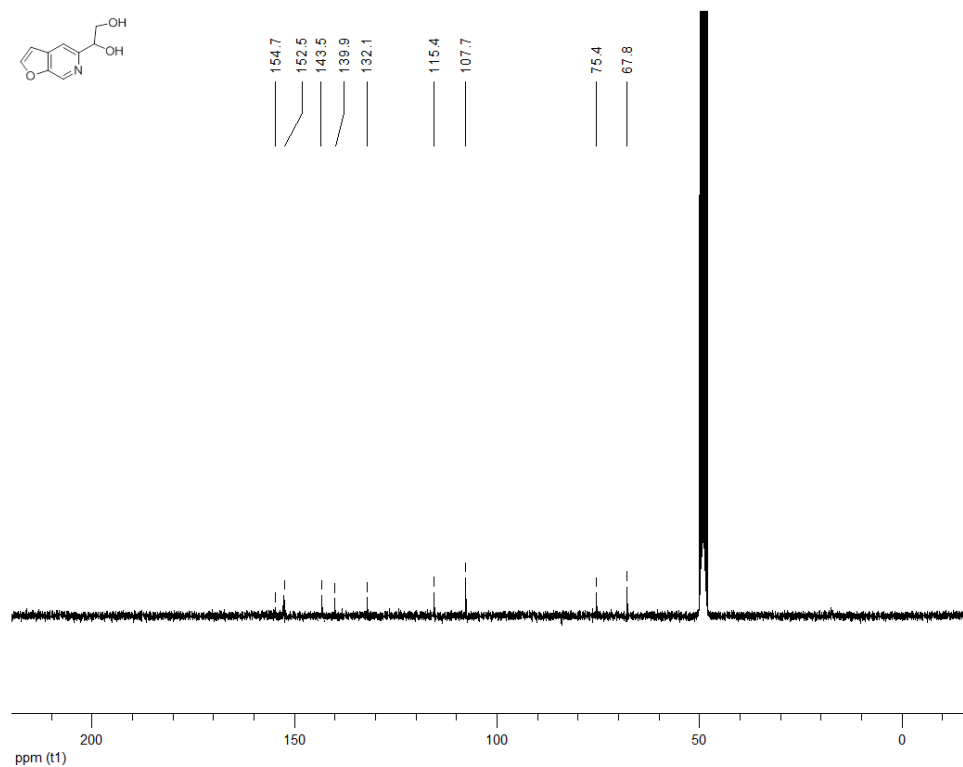
¹**H NMR (300 MHz, MeOD) 1-{thieno[3,2-c]pyridin-6-yl}ethane-1,2-diol (173f)**
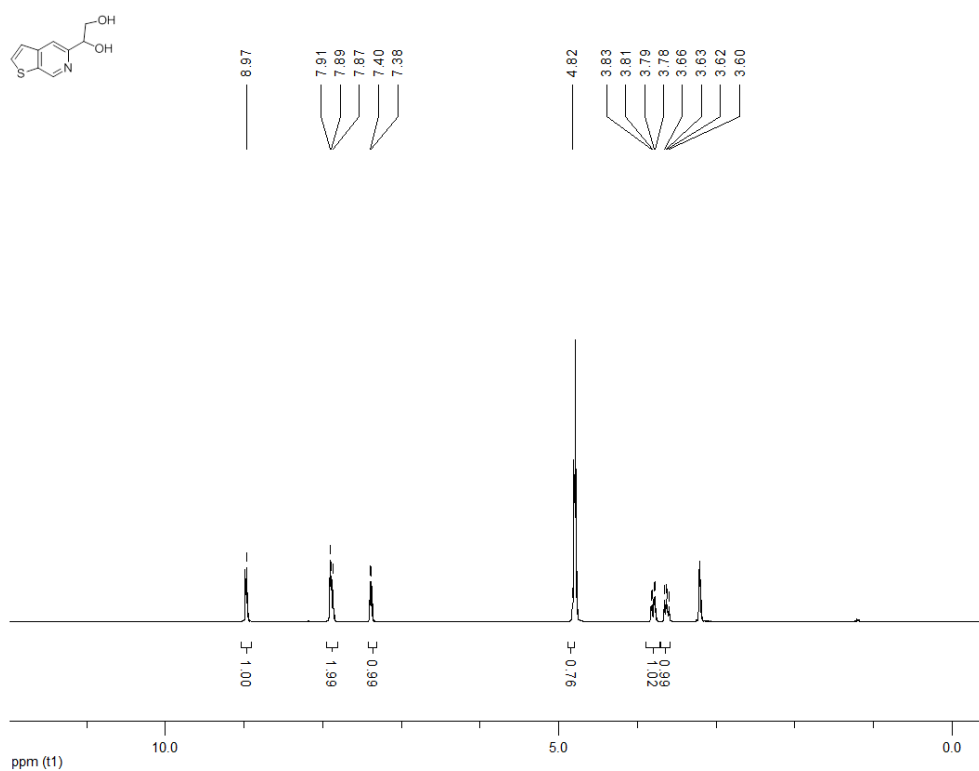
¹³**C NMR (100 MHz, MeOD) 1-{thieno[3,2-c]pyridin-6-yl}ethane-1,2-diol (173f)**
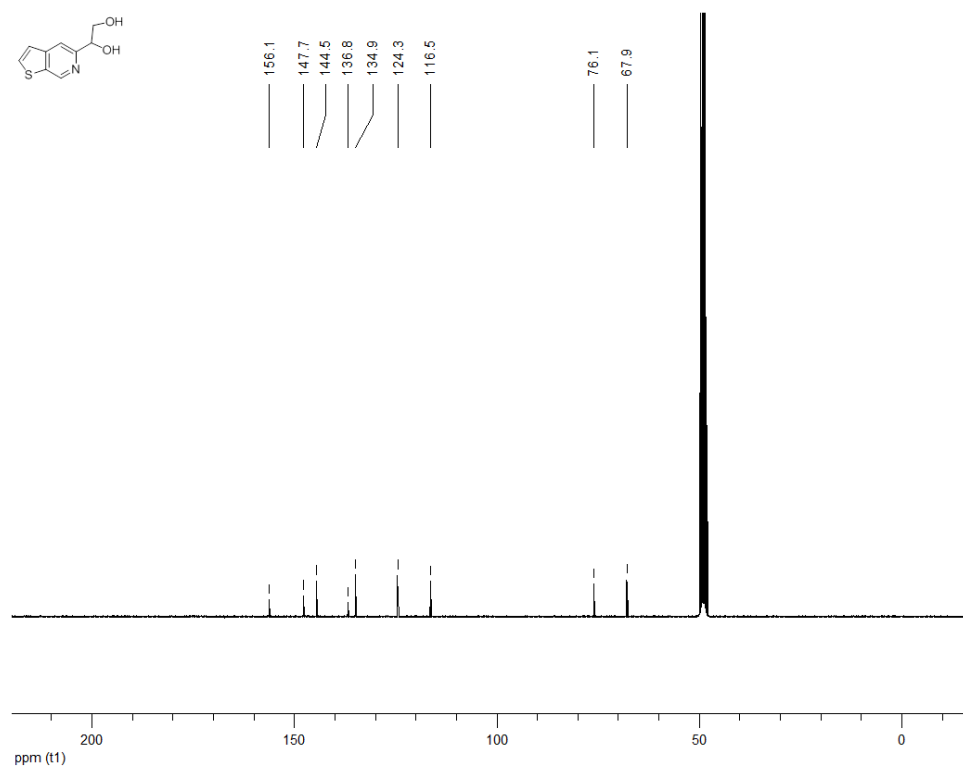
¹H NMR (300 MHz, MeOD) 1-{2-methyl-[1,3]thiazolo[4,5-c]pyridin-6-yl}ethane-1,2-diol (173g)
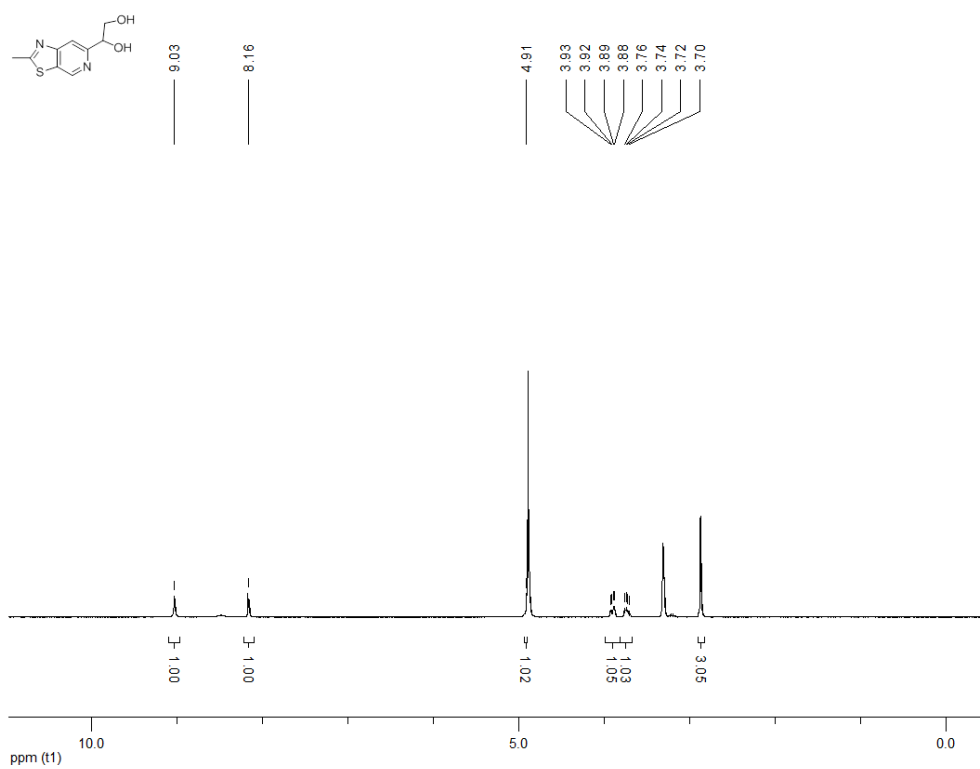
¹³C NMR (100 MHz, MeOD) 1-{2-methyl-[1,3]thiazolo[4,5-c]pyridin-6-yl}ethane-1,2-diol (173g)
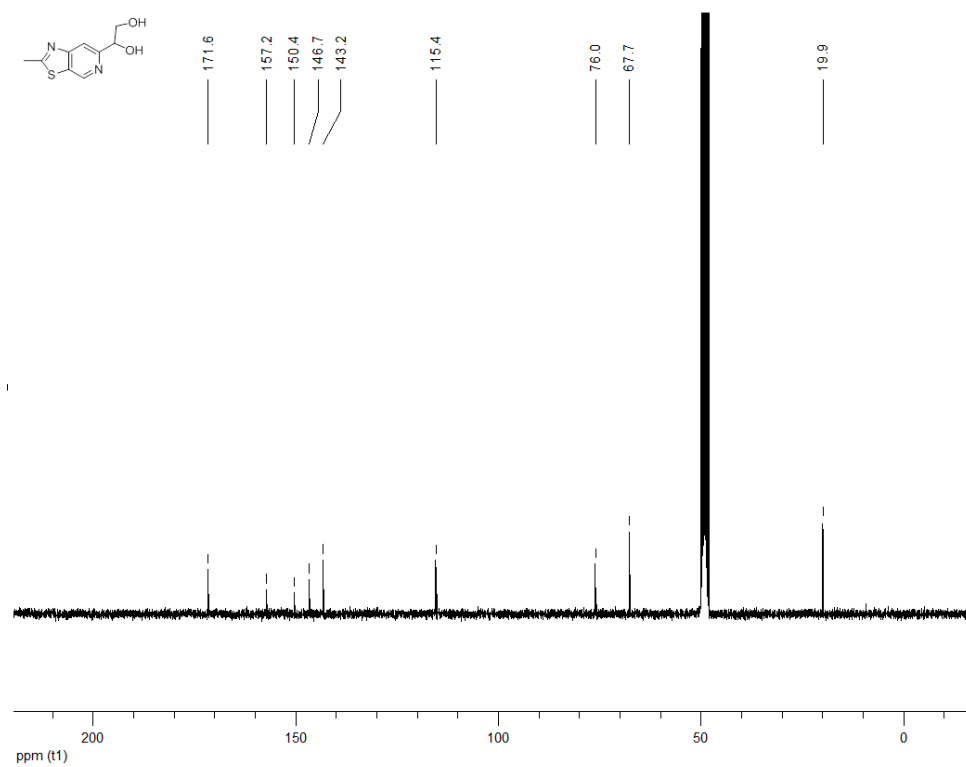
8.1.7 Synthesis, ^{1}H and ^{13}C NMR of 2,4,6-trisubstituted pyrimidines

Synthesis of 174a-p: to a stirred solution of **40** (1.0 eq) in dry THF were added PdCl$_2$(PPh$_3$)$_2$ (9%mol), CuI (3% mol) and the corresponding acyl chloride (1.5 eq). The reaction was stirred at room temperature for 2 minutes under N$_2$ atmosphere. Et$_3$N (1.25 eq) was added and the mixture was stirred at room temperature overnight. Solvent was removed under reduced pressure, the crude redissolved in EtOAc and extracted three times with water. The organic layer was dried over MgSO$_4$, filtered and concentrated *in vacuo* to yield the corresponding ynone. The products were used without being purified.

Synthesis of 175a-f: to a stirred solution of the corresponding ynone (1.0 eq) in THF was added Na$_2$CO$_3$ (2.4 eq) and the corresponding amidine hydrochloride (1.2 eq). The mixture was stirred at reflux overnight. Solvent was evaporated under reduced pressure, the crude was redissolved in EtOAc and washed three times with water. The organic layer was dried over MgSO$_4$, filtered and concentrated *in vacuo*. The crude was redissolved in ACN (1 mL), filtered and purified by preparative HPLC.[341]
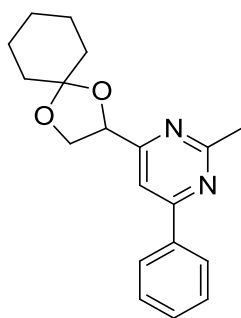
4-{1,4-dioxaspiro[4.5]decan-2-yl}-2-methyl-6-phenylpyrimidine   (175a): orange oil, 42%, R_f = 0.44 (CyH/EtOAc 9:1), UHPLC-ESI-MS: R_t = 3.48, m/z = 311.2 [M + H]$^+$. ^{1}H NMR (300 MHz, CDCl$_3$) δ 8.09 − 8.07 (m, 2H), 7.78 (s, 1H), 7.51 − 7.50 (m, 3H), 5.15 (t, J = 6.6 Hz, 1H), 4.52 (t, J = 7.8 Hz, 1H), 4.01 (dd, J = 6.2 Hz, J = 8.3 Hz, 1H), 2.76 (s, 3H), 1.76 − 1.66 (m, 8H), 1.48 − 1.46 (m, 2H) ppm; ^{13}C NMR (100 MHz, CDCl$_3$) δ 170.1, 167.7, 164.8, 137.2, 130.8, 128.9, 127.3, 111.4, 109.7, 77.3, 69.5, 36.0, 35.0, 26.1, 25.1, 24.0, 23.9 ppm.
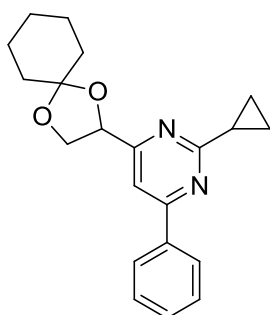
2-cyclopropyl-4-{1,4-dioxaspiro[4.5]decan-2-yl}-6-phenylpyrimidine
(175b): orange oil, 51%, R_f = 0.51 (CHCl$_3$/MeOH 9:1), UHPLC-ESI-MS: R_t = 3.85, m/z = 337.2 [M + H]$^+$. ^{1}H NMR (300 MHz, CDCl$_3$) δ 8.09 − 8.07 (m, 2H), 7.71 (s, 1H), 7.50 − 7.48 (m, 3H), 5.13 (t, J = 6.6 Hz, 1H), 4.49 (t, J = 7.8 Hz, 1H), 4.01 (dd, J = 6.7 Hz, J = 7.8 Hz, 1H), 2.29 − 2.26 (m, 1H), 1.80 − 1.63 (m, 8H), 1.47 (s, 2H), 1.21 (d, J = 4.7 Hz, 2H), 1.09 − 1.05 (m, 2H) ppm; ^{13}C NMR (100 MHz,

CDCl$_3$) δ 171.5, 169.6, 164.3, 137.3, 130.7, 128.8, 127.2, 111.3, 109.3, 77.2, 69.5, 36.0, 35.0, 25.1, 24.0, 23.9, 18.0, 10.8 (d, J = 5.2 Hz) ppm.
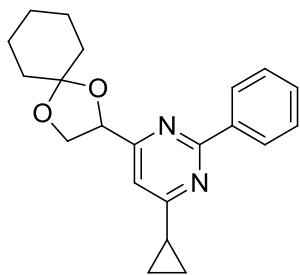
4-cyclopropyl-6-{1,4-dioxaspiro[4.5]decan-2-yl}-2-phenylpyrimidine

(175c): brown oil, 54%, R_f = 0.48 (CyH/EtOAc 9:1), UHPLC-ESI-MS: R_t = 3.94, m/z = 337.2 [M + H]$^+$. ^{1}H NMR (300 MHz, CDCl$_3$) δ 8.44 – 8.41 (m, 2H), 7.47 – 7.44 (m, 3H), 7.31 (s, 1H), 5.17 (t, J = 6.9 Hz, 1H), 4.53 (dd, J = 7.1 Hz, J = 8.4 Hz, 1H), 4.07 (dd, J = 6.3 Hz, J = 8.4 Hz, 1H), 2.09 – 2.02 (m, 1H), 1.82 – 1.64 (m, 8H), 1.51– 1.46 (m, 2H), 1.32 – 1.27 (m, 2H), 1.13 – 1.07 (m, 2H) ppm; ^{13}C NMR (100 MHz, CDCl$_3$) δ 172.4, 168.2, 163.4, 137.8, 130.3, 128.3, 128.1, 112.5, 111.2, 77.0, 69.5, 36.0, 35.1, 25.1, 24.0, 23.8, 17.2, 11.1 (d, J = 7.3 Hz) ppm.
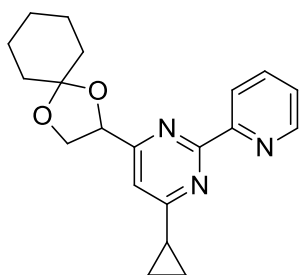
4-cyclopropyl-6-{1,4-dioxaspiro[4.5]decan-2-yl}-2-(pyridin-2-

yl)pyrimidine (175d): brown oil, 62%, R_f = 0.52 (CHCl$_3$/MeOH 5:1), UHPLC-ESI-MS: R_t = 2.62, m/z = 338.2 [M + H]$^+$. ^{1}H NMR (300 MHz, CDCl$_3$) δ 8.82 (ddd, J = 0.9 Hz, J = 1.8 Hz, J = 4.8 Hz, 1H), 8.44 (td, J = 1.0 Hz, J = 8.0 Hz, 1H), 7.82 (dt, J = 1.8 Hz, J = 7.8 Hz, 1H), 7.38 – 7.36 (m, 2H), 5.29 (t, J = 6.6 Hz, 1H), 4.55 (dd, J = 7.1 Hz, J = 8.5 Hz, 1H), 3.99 (dd, J = 6.0 Hz, J = 8.5 Hz, 1H), 2.18 – 2.12 (m, 1H), 1.79 – 1.62 (m, 8H), 1.47– 1.44 (m, 2H), 1.26 – 1.22 (m, 2H), 1.18 – 1.11 (m, 2H) ppm; ^{13}C NMR (100 MHz, CDCl$_3$) δ 173.1, 169.4, 162.6, 155.1, 149.9, 136.8, 124.6, 123.9, 113.0, 111.3, 77.1, 69.8, 36.0, 34.8, 25.1, 24.0, 23.8, 17.5, 11.4 (d, J = 2.8 Hz) ppm.
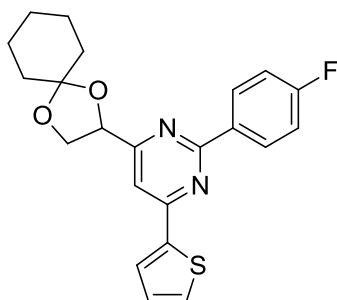
4-{1,4-dioxaspiro[4.5]decan-2-yl}-2-(3-fluorophenyl)-6-(thiophen-2-

yl)pyrimidine (175e): orange oil, 57%, R_f = 0.66 (CyH/EtOAc 9:1), UHPLC-ESI-MS: R_t = 4.03, m/z = 397.2 [M + H]$^+$. ^{1}H NMR (300 MHz, CDCl$_3$) δ 8.33 – 8.30 (m, 1H), 8.24 – 8.19 (m, 1H), 7.85 (dd, J

= 1.1 Hz, J = 3.7 Hz, 1H), 7.72 (s, 1H) 7.54 (dd, J = 1.0 Hz, J = 5.0 Hz, 1H), 7.49 – 7.42 (m, 1H), 7.21 – 7.15 (m, 2H), 5.21 (t, J = 6.6 Hz, 1H), 4.56 (dd, J = 7.1 Hz, J = 8.5 Hz, 1H), 4.13 (dd, J = 6.0 Hz, J = 8.5 Hz, 1H), 1.81 – 1.67 (m, 8H), 1.51 – 1.49 (m, 2H) ppm; ^{13}C NMR (100 MHz, CDCl$_3$) δ 170.3, 164.7, 162.7 (d, J = 3.2 Hz), 161.5, 159.6, 142.8, 139.7 (d, J = 7.8 Hz), 130.2, 129.9 (d, J = 8.0 Hz), 128.3, 127.6, 123.9 (d, J = 2.7 Hz), 117.6 (d, J = 21.4 Hz), 115.1 (d, J = 23.2 Hz), 111.4, 109.0, 77.2, 69.4, 36.0, 35.1, 25.1, 24.0, 23.9 ppm.
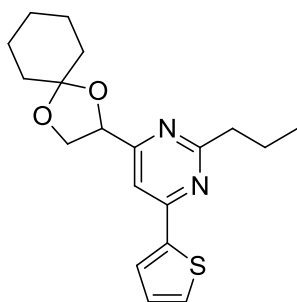
4-{1,4-dioxaspiro[4.5]decan-2-yl}-2-propyl-6-(thiophen-2-yl)pyrimidine

(175f): orange oil, 57%, R_f = 0.57 (CyH/EtOAc 9:1), UHPLC-ESI-MS: R_t = 3.77, m/z = 345.2 [M + H]$^+$. ^{1}H NMR (300 MHz, CDCl$_3$) δ 7.77 (dd, J = 1.0 Hz, J = 3.7 Hz, 1H), 7.61 (s, 1H), 7.48 (dd, J = 1.0 Hz, J = 5.0 Hz, 1H), 7.12 (dd, J = 3.8 Hz, J = 5.0 Hz, 1H), 5.10 (t, J = 6.5 Hz, 1H), 4.48 (dd, J = 7.2 Hz, J = 8.4 Hz, 1H), 3.99 (dd, J = 6.0 Hz, J = 8.4 Hz, 1H), 2.88 (t, J = 7.5 Hz, 2H), 1.89 – 1.80 (m, 2H), 1.74 – 1.62 (m, 8H), 1.45 (s, 2H), 1.00 (t, J = 7.4 Hz, 3H) ppm; ^{13}C NMR (100 MHz, CDCl$_3$) δ 170.9, 169.7, 159.3, 143.0, 129.7, 128.2, 127.2, 111.3, 107.8, 76.9, 69.4, 41.1, 35.9, 34.9, 25.1, 24.0, 23.8, 21.8, 13.8 ppm.

Synthesis of 176a-f: a stirred solution of the protected pyrimidine**189a-f** in 1,4-dioxane was cooled to 0 °C using an ice bath. A catalytic amount of concentrated HCl was added. The reaction was stirred at room temperature overnight. Solvent was evaporated under reduced pressure, the crude was redissolved in ACN (1 mL), filtered and purified by preparative HPLC.
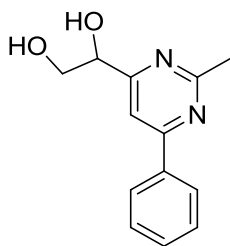
1-(2-methyl-6-phenylpyrimidin-4-yl)ethane-1,2-diol **(176a):** yellowish solid, 54%, R_f = 0.58 (CHCl$_3$/MeOH 9:1), UHPLC-ESI-MS: R_t = 1.92, m/z = 231.2 [M + H]$^+$. ^{1}H NMR (300 MHz, MeOD) δ 8.13 – 8.11 (m, 2H), 7.90 (s, 1H), 7.54 – 7.52 (m, 3H), 4.75 – 4.72 (m, 1H), 3.92 (dd, J = 3.8 Hz, J = 11.3 Hz, 1H), 3.78 (dd, J = 5.8 Hz, J = 11.3 Hz, 1H), 2.73 (s, 3H) ppm; ^{13}C NMR (100 MHz, MeOD) δ 172.7, 168.7, 166.2, 138.4, 132.1, 130.1, 128.5, 112.4, 75.7, 67.2, 25.8 ppm.
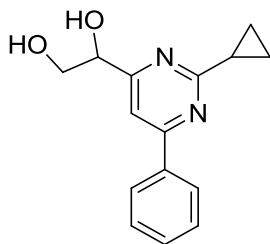
1-(2-cyclopropyl-6-phenylpyrimidin-4-yl)ethane-1,2-diol (176b): brown oil, 53%, R_f = 0.58 (CHCl$_3$/MeOH 9:1), UHPLC-ESI-MS: R_t = 2.38, m/z = 257.2 [M + H] $^+$. ^{1}H NMR (300 MHz, MeOD) δ 8.12 – 8.10 (m, 2H), 7.82 (s, 1H), 7.51 – 7.49 (m, 3H), 4.72 – 4.69 (m, 1H), 3.92 (dd, J = 3.8 Hz, J = 11.3 Hz, 1H), 3.76 (dd, J = 6.0 Hz, J = 11.2 Hz, 1H), 2.31 – 2.24 (m, 1H), 1.19 – 1.18 (m, 2H), 1.09 – 1.06 (m, 2H) ppm; ^{13}C NMR (100 MHz, MeOD) δ 172.6, 172.1, 165.7, 138.5, 132.0, 130.0, 128.3, 111.7, 75.7, 67.2, 18.7, 11.0 ppm.
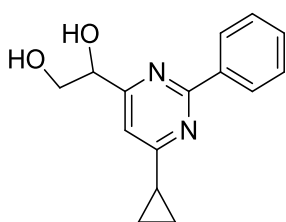
1-(6-cyclopropyl-2-phenylpyrimidin-4-yl)ethane-1,2-diol (176c): brown oil, 46%, R_f = 0.62 (CHCl$_3$/MeOH 9:1), UHPLC-ESI-MS: R_t = 2.55, m/z = 257.2 [M + H] $^+$. ^{1}H NMR (300 MHz, MeOD) δ 8.30 – 8.26 (m, 1H), 7.58 – 7.51 (m, 1H), 7.49 – 7.45 (m, 1H), 7.36 – 7.34 (m, 2H), 7.28 (s, 1H), 4.63 (dd, J = 3.9 Hz, J = 6.1 Hz, 1H), 3.87 (dd, J = 3.9 Hz, J = 11.3 Hz, 1H), 3.69 (dd, J = 6.2 Hz, J = 11.3 Hz, 1H), 2.07 – 2.00 (m, 1H), 1.15 – 1.11 (m, 2H), 1.04 – 1.00 (m, 2H) ppm; ^{13}C NMR (100 MHz, MeOD) δ 174.0, 170.7, 164.6, 139.3, 131.5, 130.1, 129.4, 114.8, 75.7, 67.3, 17.9, 11.6 (d, J = 7.0 Hz) ppm.
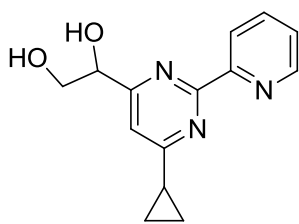
1-[6-cyclopropyl-2-(pyridin-2-yl)pyrimidin-4-yl]ethane-1,2-diol (176d): yellowish solid, 67%, R_f = 0.62 (CHCl$_3$/MeOH 9:1), UHPLC-ESI-MS: R_t = 1.50, m/z = 258.2 [M + H] $^+$. ^{1}H NMR (300 MHz, MeOD) δ 8.71 (d, J = 4.2 Hz, 1H), 8.50 (d, J = 7.9 Hz, 1H), 7.99 (t, J = 7.0 Hz, 1H), 7.55 – 7.51 (m, 1H), 7.49 – 7.47 (m, 1H), 4.80 – 4.77 (m, 1H), 3.94 (dd, J = 4.2 Hz, J = 11.3 Hz, 1H), 3.83 (dd, J = 5.8 Hz, J = 11.3 Hz, 1H), 2.23 – 2.17 (m, 1H), 1.27 (d, J = 4.1 Hz, 2H), 1.18 – 1.14 (m, 2H) ppm; ^{13}C NMR (100 MHz, MeOD) δ 174.7, 171.2, 163.2, 156.1, 150.2, 139.0, 126.5, 125.1, 116.3, 75.6, 67.2, 18.0, 11.9 (d, J = 5.3 Hz) ppm.
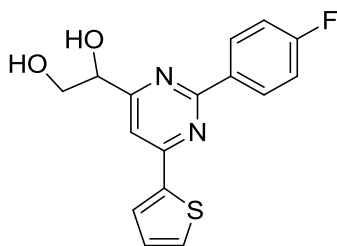
1-[2-(3-fluorophenyl)-6-(thiophen-2-yl)pyrimidin-4-yl]ethane-1,2-diol

(176e): orange solid, 71%, R_f = 0.75 (CHCl$_3$/MeOH 5:1), UHPLC-ESI-MS: R_t = 2.80, m/z = 317.0 [M + H]$^+$. ^{1}H NMR (300 MHz, MeOD) δ 8.29 (d, J = 7.8 Hz, 1H), 8.17 − 8.13 (m, 1H), 7.93 (dd, J = 0.9 Hz, J = 3.7 Hz, 1H), 7.84 (s, 1H), 7.64 (dd, J = 0.9 Hz, J = 5.0 Hz, 1H), 7.51 − 7.43 (m, 1H), 7.23 − 7.16 (m, 2H), 4.80 (dd, J = 3.8 Hz, J = 5.8 Hz, 1H), 4.03 (dd, J = 3.8 Hz, J = 11.3 Hz, 1H), 3.87 (dd, J = 6.0 Hz, J = 11.3 Hz, 1H) ppm; ^{13}C NMR (100 MHz, MeOD) δ 172.6, 166.1, 163.7 (d, J = 3.2 Hz), 162.9, 161.0, 144.0, 141.4 (d, J = 7.8 Hz), 131.5, 131.2 (d, J = 8.1 Hz), 129.4 (d, J = 36.2 Hz), 125.1 (d, J = 2.7 Hz), 118.5 (d, J = 21.6 Hz), 115.8 (d, J = 23.5 Hz), 111.3, 75.8, 67.1 ppm.
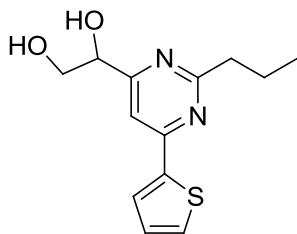
1-[2-propyl-6-(thiophen-2-yl)pyrimidin-4-yl]ethane-1,2-diol **(176f):** yellow solid, 82%, R_f = 0.78 (CHCl$_3$/MeOH 5:1), UHPLC-ESI-MS: R_t = 2.33, m/z = 265.2 [M + H]$^+$. ^{1}H NMR (300 MHz, MeOD) δ 7.90 (d, J = 3.6 Hz, 1H), 7.78 (s, 1H), 7.63 (d, J = 4.9 Hz, 1H), 7.17 (t, J = 4.5 Hz, 1H), 4.72 − 4.69 (m, 1H), 3.91 (dd, J = 3.8 Hz, J = 11.3 Hz, 1H), 3.75 (dd, J = 6.0 Hz, J = 11.3 Hz, 1H), 2.87 (t, J = 7.5 Hz, 2H), 1.90 − 1.82 (m, 2H), 1.01 (t, J = 7.4 Hz, 3H) ppm; ^{13}C NMR (100 MHz, MeOD) δ 172.1, 171.7, 161.0, 143.9, 131.4, 129.5, 129.1, 110.4, 75.6, 67.2, 41.8, 22.9, 14.2 ppm.

¹H NMR (300 MHz, CDCl₃) 4-{1,4-dioxaspiro[4.5]decan-2-yl}-2-methyl-6-phenylpyrimidine (175a)
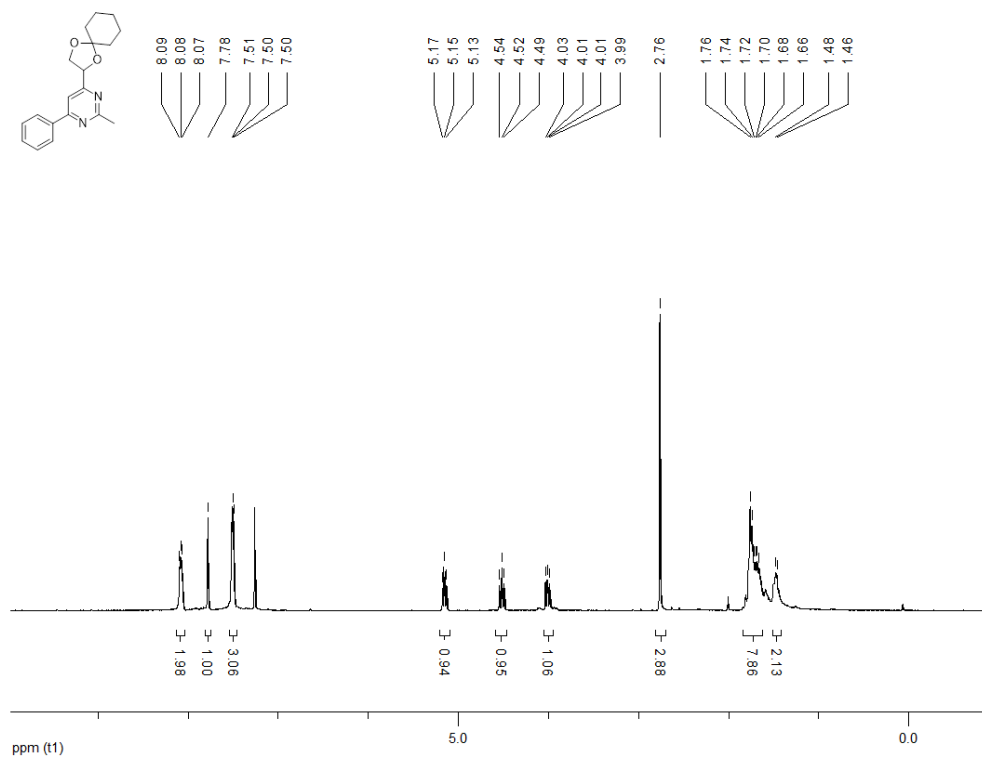
8.09, 8.08, 8.07, 7.78, 7.51, 7.50, 7.50

5.17, 5.15, 5.13, 4.54, 4.52, 4.49, 4.03, 4.01, 4.01, 3.99, 2.76, 1.76, 1.74, 1.72, 1.70, 1.68, 1.66, 1.48, 1.46

1.98, 1.00, 3.06, 0.94, 0.95, 1.06, 2.88, 7.86, 2.13

ppm (t1)   5.0   0.0

¹³C NMR (100 MHz, CDCl₃) 4-{1,4-dioxaspiro[4.5]decan-2-yl}-2-methyl-6-phenylpyrimidine (175a)

170.1, 167.7, 164.8, 137.2, 130.8, 128.9, 127.3, 111.4, 109.7, 77.3, 69.5, 36.0, 35.0, 26.1, 25.1, 24.0, 23.9

ppm (t1)   200   150   100   50   0
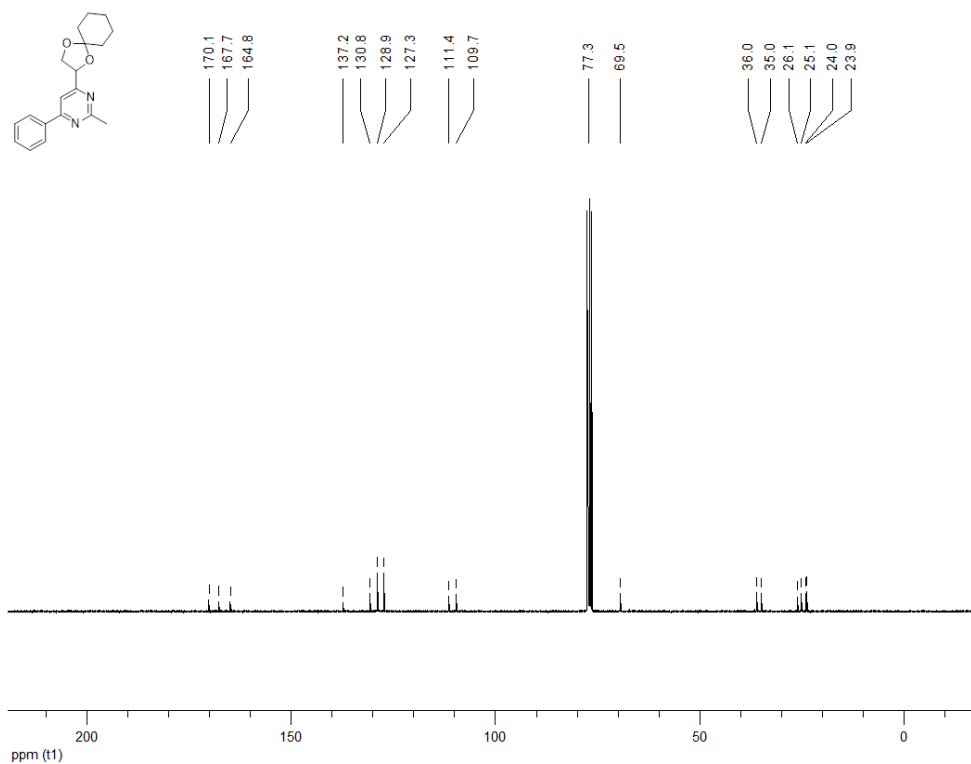
¹H NMR (300 MHz, CDCl₃) 2-cyclopropyl-4-{1,4-dioxaspiro[4.5]decan-2-yl}-6-phenylpyrimidine (175b)
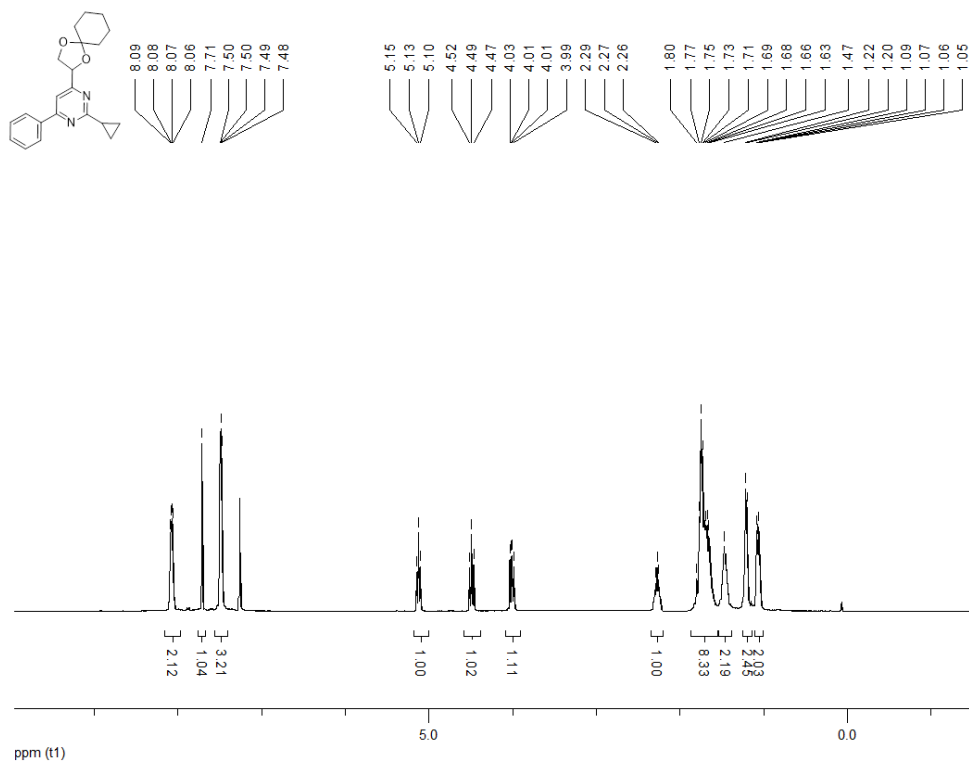
¹³C NMR (100 MHz, CDCl₃) 2-cyclopropyl-4-{1,4-dioxaspiro[4.5]decan-2-yl}-6-phenylpyrimidine (175b)
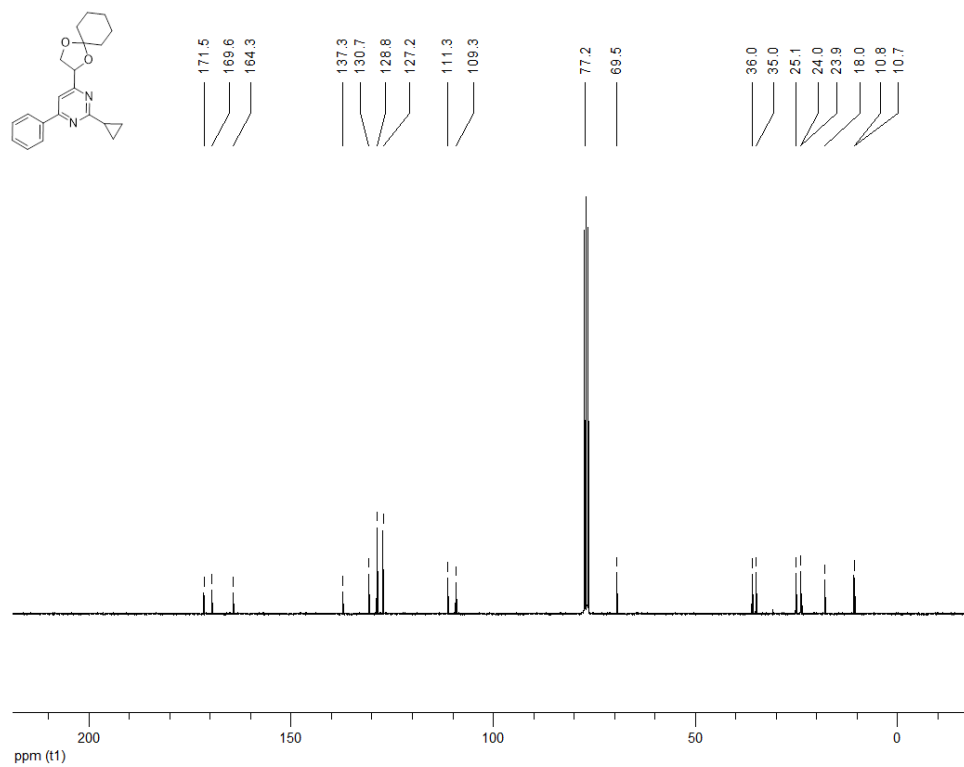
1H NMR (300 MHz, CDCl₃) 4-cyclopropyl-6-{1,4-dioxaspiro[4.5]decan-2-yl}-2-phenylpyrimidine (175c)

13C NMR (100 MHz, CDCl₃) 4-cyclopropyl-6-{1,4-dioxaspiro[4.5]decan-2-yl}-2-phenylpyrimidine (175c)
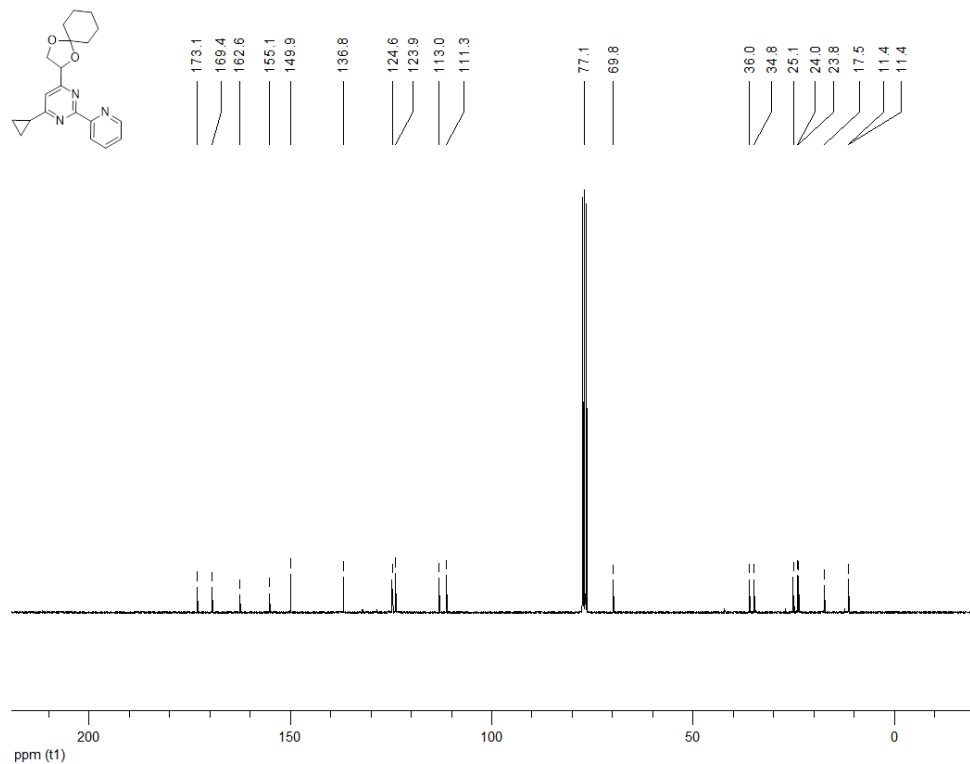
199

¹H NMR (300 MHz, CDCl₃) 4-{1,4-dioxaspiro[4.5]decan-2-yl}-2-(3-fluorophenyl)-6-(thiophen-2-yl)pyrimidine (175e)

8.33, 8.32, 8.31, 8.30, 8.24, 8.23, 8.21, 8.19, 7.86, 7.85, 7.84, 7.72, 7.55, 7.53, 7.49, 7.47, 7.44, 7.42, 7.21, 7.19, 7.18, 7.16, 7.15, 5.23, 5.21, 5.19, 4.59, 4.56, 4.53, 4.15, 4.13, 4.12, 4.10, 1.81, 1.77, 1.73, 1.70, 1.67, 1.51, 1.49

¹³C NMR (100 MHz, CDCl₃) 4-{1,4-dioxaspiro[4.5]decan-2-yl}-2-(3-fluorophenyl)-6-(thiophen-2-yl)pyrimidine (175e)

170.3, 164.7, 162.7, 162.7, 161.5, 159.6, 142.8, 139.7, 139.6, 130.2, 129.9, 129.8, 128.3, 127.6, 123.9, 123.9, 117.7, 117.4, 115.3, 114.9, 111.4, 109.0, 77.2, 69.4, 36.0, 35.1, 25.1, 24.0, 23.9

<superscript>1</superscript>H NMR (300 MHz, CDCl<subscript>3</subscript>) 4-{1,4-dioxaspiro[4.5]decan-2-yl}-2-propyl-6-(thiophen-2-yl)pyrimidine (175f)

<superscript>13</superscript>C NMR (100 MHz, CDCl<subscript>3</subscript>) 4-{1,4-dioxaspiro[4.5]decan-2-yl}-2-propyl-6-(thiophen-2-yl)pyrimidine (175f)

¹H NMR (300 MHz, MeOD) 1-(2-methyl-6-phenylpyrimidin-4-yl)ethane-1,2-diol (176a)

8.13
8.12
8.11
7.90
7.54
7.53
7.52

4.75
4.73
4.72
3.94
3.93
3.91
3.89
3.81
3.79
3.77
3.75
2.73

1.99
1.00
3.04

0.96
0.96
0.96
2.96

5.0

0.0

ppm (t1)
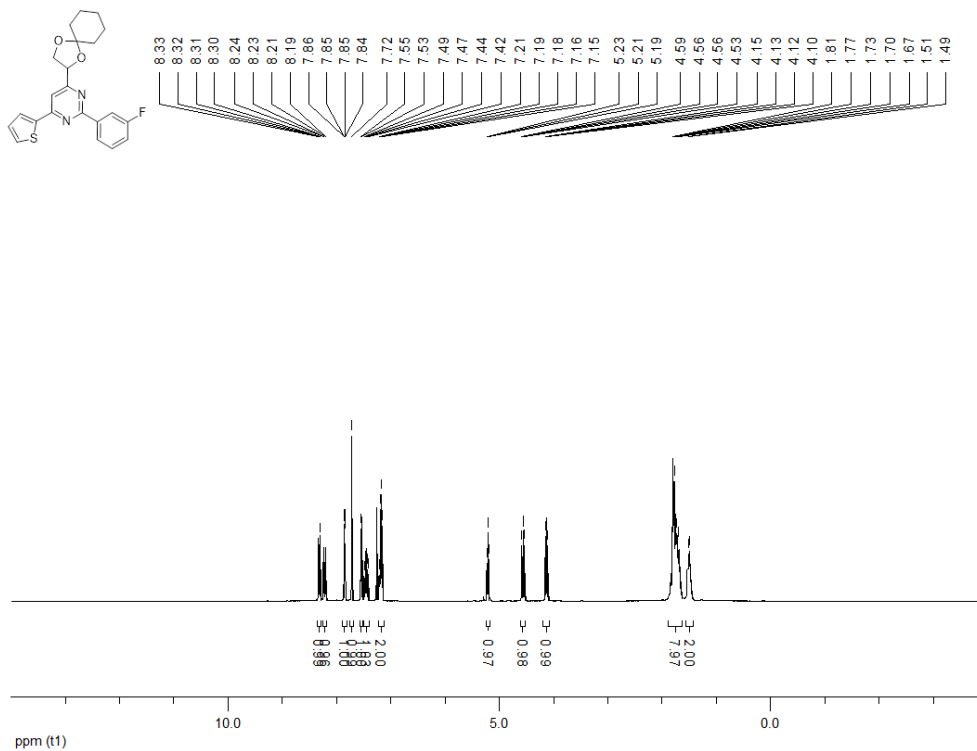
¹³C NMR (100 MHz, MeOD) 1-(2-methyl-6-phenylpyrimidin-4-yl)ethane-1,2-diol (176a)

172.7
168.7
166.2

138.4
132.1
130.1
128.5

112.4

75.7
67.2

25.8

200

150

100

50

0

ppm (t1)

¹H NMR (300 MHz, MeOD) 1-(2-cyclopropyl-6-phenylpyrimidin-4-yl)ethane-1,2-diol (176b)

ppm (t1)

¹³C NMR (100 MHz, MeOD) 1-(2-cyclopropyl-6-phenylpyrimidin-4-yl)ethane-1,2-diol (176b)

ppm (t1)
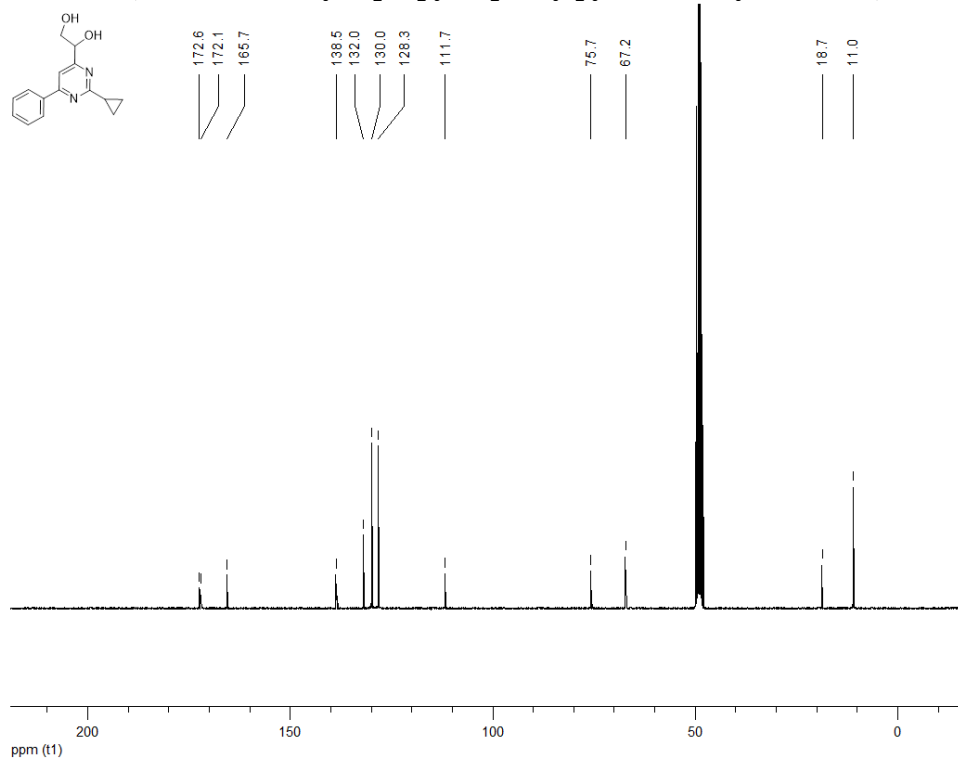
¹H NMR (300 MHz, MeOD) 1-(6-cyclopropyl-2-phenylpyrimidin-4-yl)ethane-1,2-diol (176c)
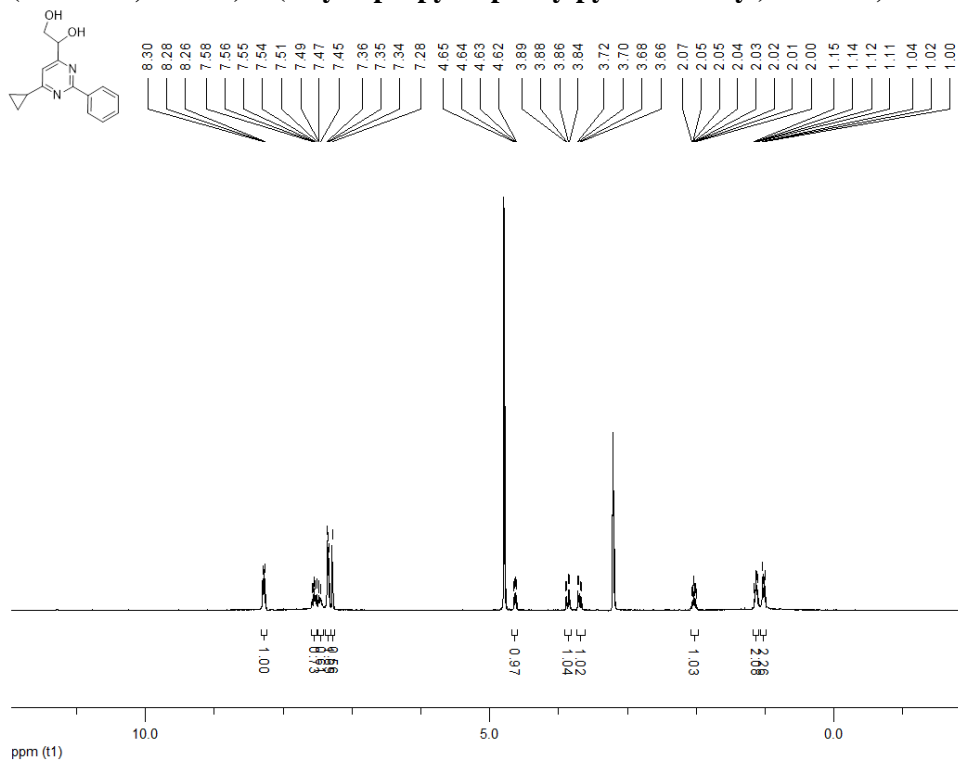
¹³C NMR (100 MHz, MeOD) 1-(6-cyclopropyl-2-phenylpyrimidin-4-yl)ethane-1,2-diol (176c)
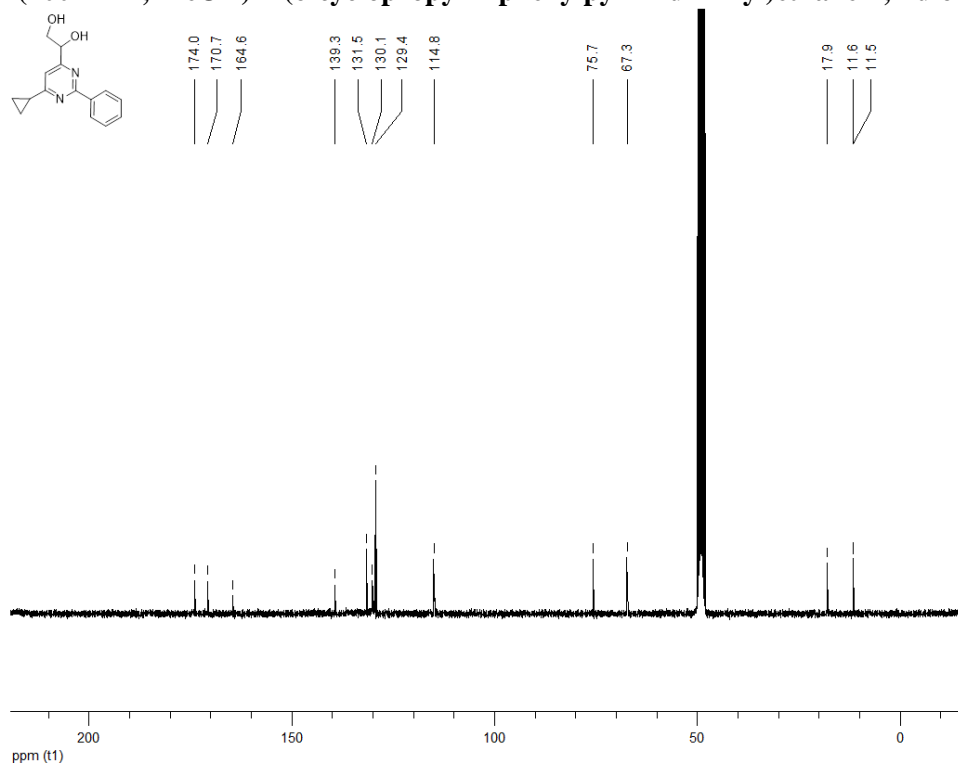
¹H NMR (300 MHz, MeOD) 1-[6-cyclopropyl-2-(pyridin-2-yl)pyrimidin-4-yl]ethane-1,2-diol (176d)
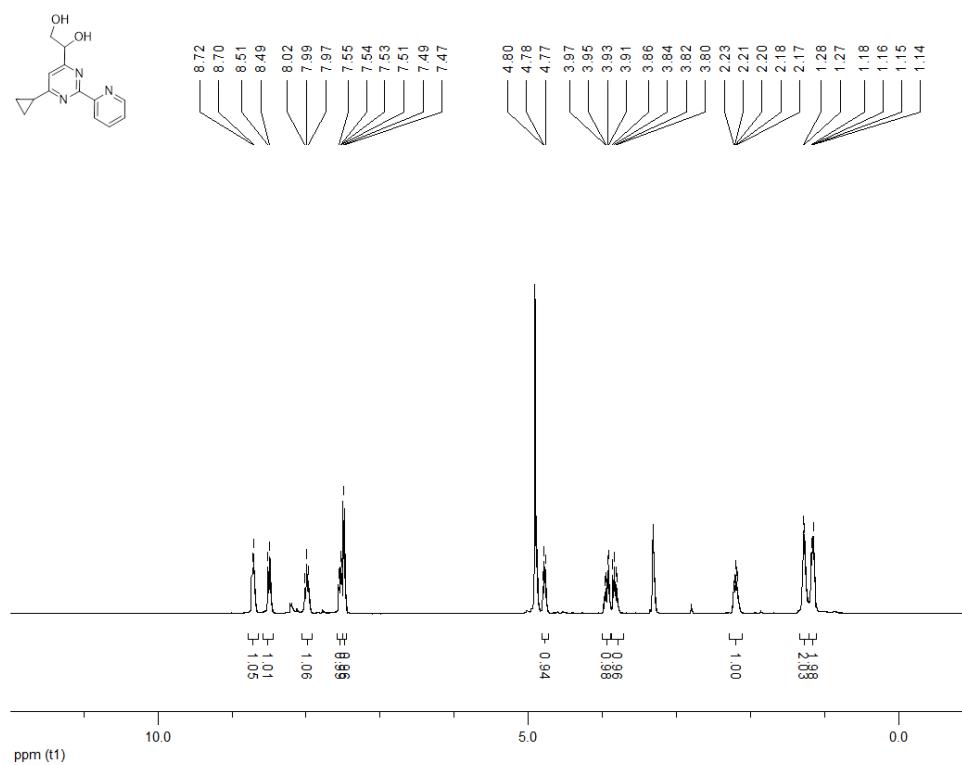
¹³C NMR (100 MHz, MeOD) 1-[6-cyclopropyl-2-(pyridin-2-yl)pyrimidin-4-yl]ethane-1,2-diol (176d)
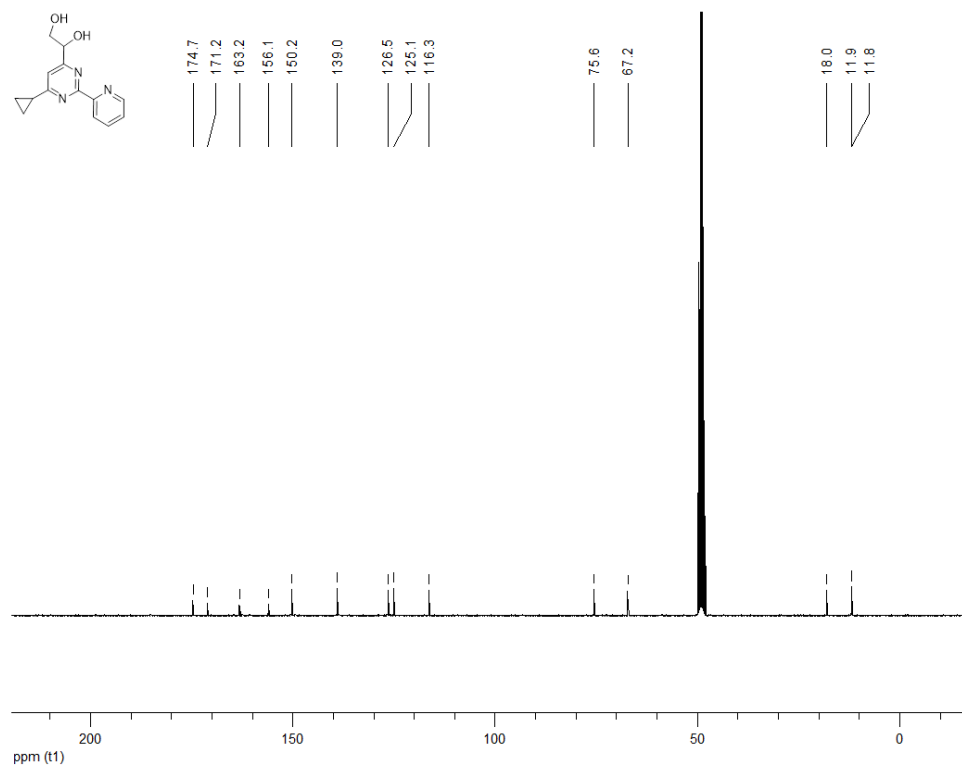
¹H NMR (300 MHz, MeOD) 1-[2-(3-fluorophenyl)-6-(thiophen-2-yl)pyrimidin-4-yl]ethane-1,2-diol (176e)
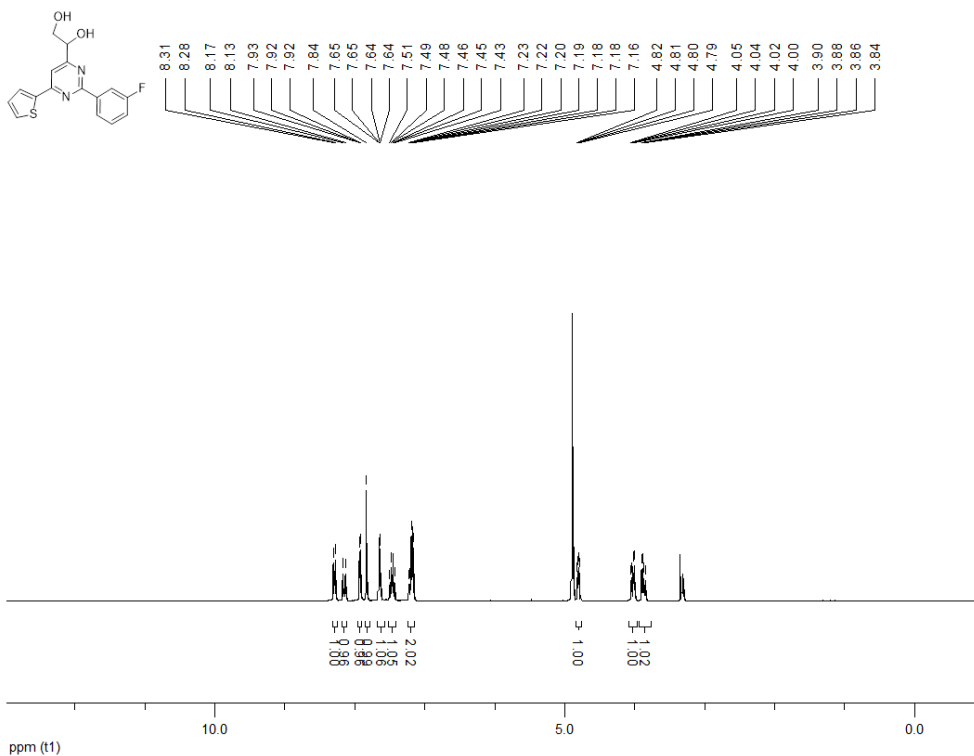
¹³C NMR (100 MHz, MeOD) 1-[2-(3-fluorophenyl)-6-(thiophen-2-yl)pyrimidin-4-yl]ethane-1,2-diol (176e)
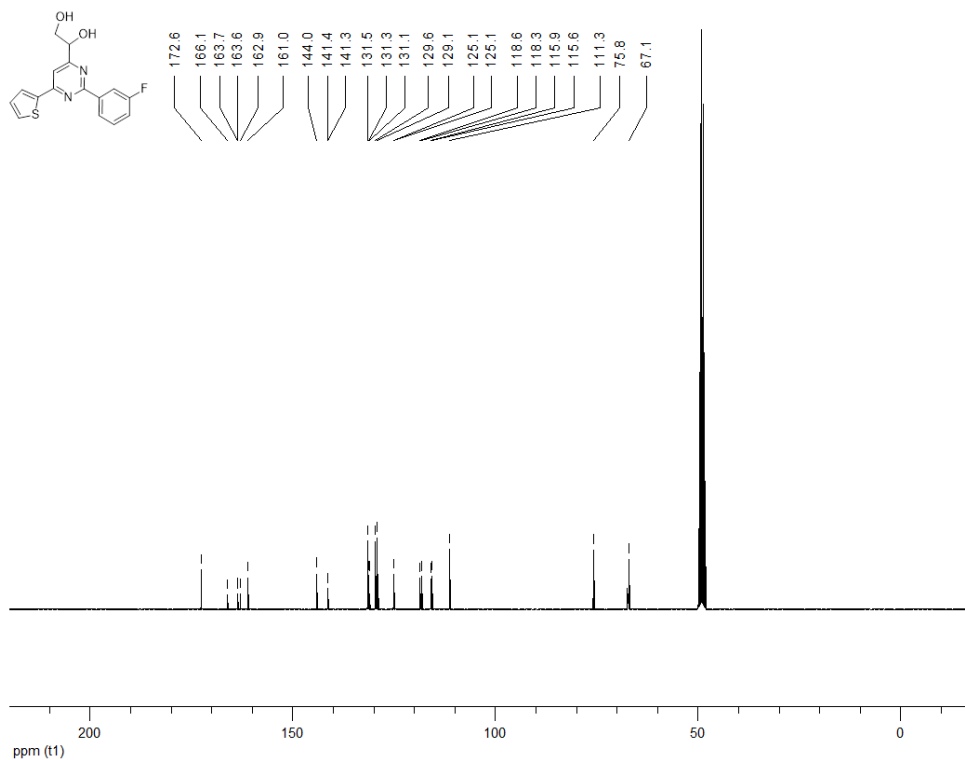
¹H NMR (300 MHz, MeOD) 1-[2-propyl-6-(thiophen-2-yl)pyrimidin-4-yl]ethane-1,2-diol (176f)
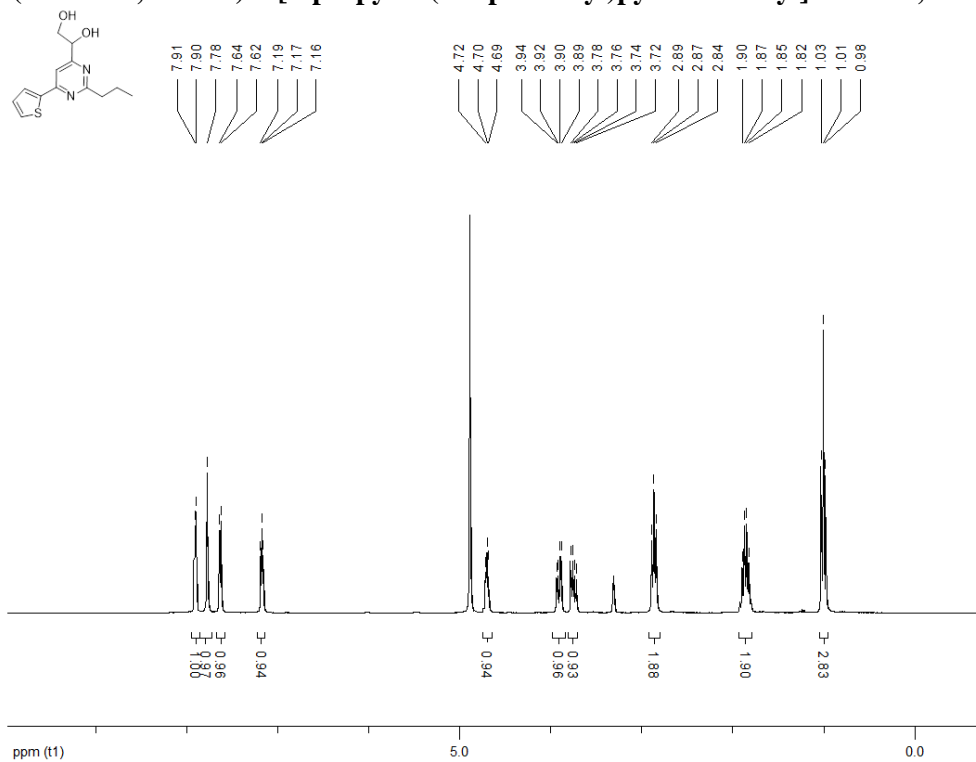
¹³C NMR (100 MHz, MeOD) 1-[2-propyl-6-(thiophen-2-yl)pyrimidin-4-yl]ethane-1,2-diol (176f)
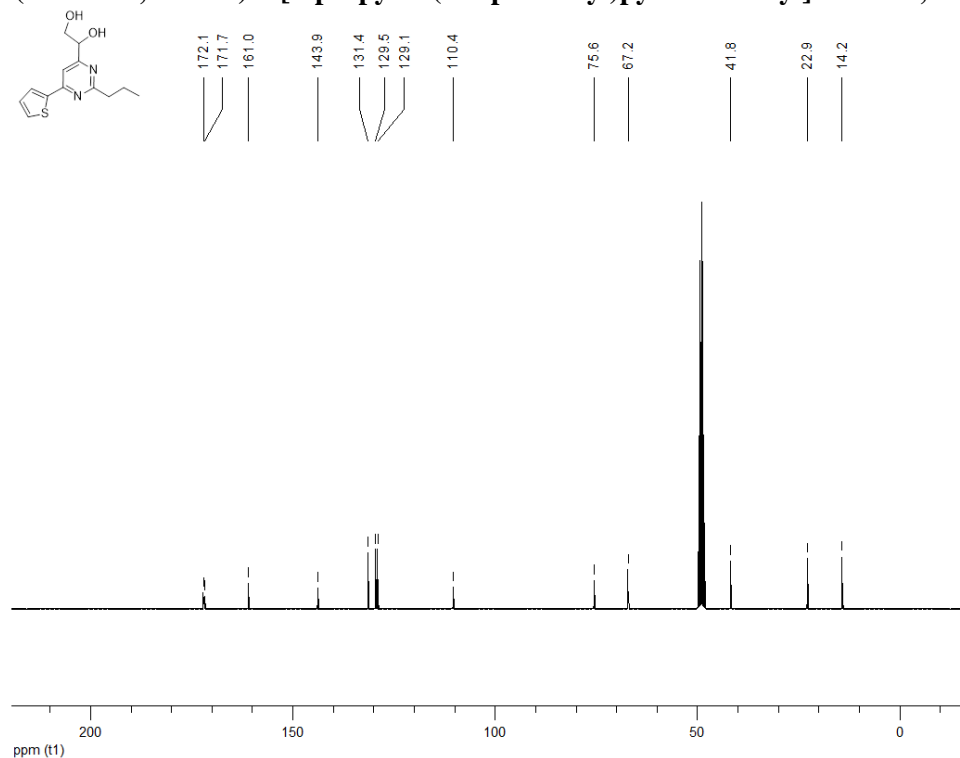
8.1.8 Synthesis, ¹H and ¹³C NMR of 2,3,4,6-tetrasubstituted pyridines

Synthesis of 177a-b: to a stirred solution of the corresponding ynone (0.6 eq) and ethyl acetoacetate (1.0 eq) in EtOH was added NH₄OAc (10.0 eq). The mixture was stirred at reflux overnight. Solvent was removed under reduced pressure, the crude was redissolved in EtOAc and washed three times with NaHCO₃ (saturated solution). The organic layer was dried over MgSO₄, filtered and concentrated *in vacuo.* The crude was redissolved in ACN (1 mL), filtered and purified by preparative HPLC.[324]
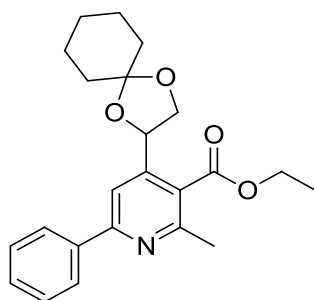
ethyl 4-{1,4-dioxaspiro[4.5]decan-2-yl}-2-methyl-6-phenylpyridine-3-carboxylate (177a): brown oil, 92%, R_f = 0.53 (CyH/EtOAc 9:1), UHPLC-ESI-MS: R_t = 3.80, m/z = 382.2 [M + H] ⁺. ¹H NMR (300 MHz, CDCl₃) δ 8.01 (dd, J = 1.5 Hz, J = 8.0 Hz, 2H), 7.87 (s, 1H), 7.51 − 7.43 (m, 3H), 5.22 (t, J = 6.9 Hz, 1H), 4.47 − 4.39 (m, 3H), 3.72 (dd, J = 7.2 Hz, J = 8.4 Hz, 1H), 2.68 (s, 3H), 1.88 − 1.81 (m, 2H), 1.76 − 1.60 (m, 6H), 1.51 − 1.47 (m, 2H), 1.42 (t, J = 7.1 Hz, 3H) ppm; ¹³C NMR (100 MHz, CDCl₃) δ 168.2, 158.0, 156.0, 149.2, 138.9, 129.4, 128.8, 127.2, 124.7, 114.4, 110.9, 74.7, 70.9, 61.7, 35.8, 35.0, 25.2, 24.0, 23.8, 23.7, 14.2 ppm.
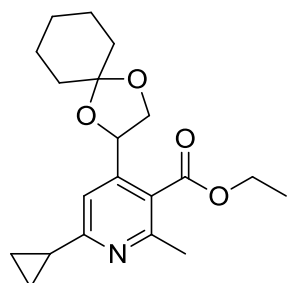
ethyl 6-cyclopropyl-4-{1,4-dioxaspiro[4.5]decan-2-yl}-2-methylpyridine-3-carboxylate (177b): brown oil, 87%, R_f = 0.50 (CyH/EtOAc 9:1), UHPLC-ESI-MS: R_t = 3.42, m/z = 346.2 [M + H] ⁺. ¹H NMR (300 MHz, CDCl₃) δ 7.21 (s, 1H), 5.13 (t, J = 6.9 Hz, 1H), 4.40 − 4.33 (m, 3H), 3.64 (d, J = 7.8 Hz, 1H), 2.50 (s, 3H), 2.08 − 1.99 (m, 1H), 1.82 − 1.73 (m, 2H), 1.70 − 1.59 (m, 6H), 1.48 − 1.44 (m, 2H), 1.37 (t, J = 7.1 Hz, 3H), 1.01 − 0.97 (m, 4H) ppm; ¹³C NMR (100 MHz, CDCl₃) δ 168.4, 164.2, 155.5, 148.1, 123.0, 114.4, 110.6, 74.5, 70.9, 61.4, 35.8, 34.8, 25.1, 23.9, 23.8, 23.6, 17.5, 14.2, 10.1 ppm.

Synthesis of 179a-b: a stirred solution of **177a** (or **177b**) in EtOH was cooled to 0 °C using an ice bath. 10 M NaOH (5.0 eq) was added dropwise. The mixture was stirred at reflux overnight. Solvent was evaporated under reduced pressure, the crude was redissolved in DCM and extracted with water. The aqueous layer was acidified with 1M HCl until pH = 1 and extracted three times with CHCl₃/*i*-

PrOH (7:3). The organic layer was dried over MgSO₄, filtered and concentrated *in vacuo*. The crude was redissolved in ACN (1 mL), filtered and purified by preparative HPLC.
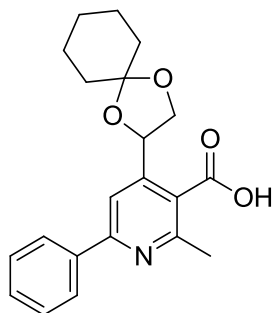
4-{1,4-dioxaspiro[4.5]decan-2-yl}-2-methyl-6-phenylpyridine-3-carboxylic acid (179a): yellow oil, 80%, R_f = 0.23 (CHCl₃/MeOH 9:1), UHPLC-ESI-MS: R_t = 2.76, m/z = 354.2 [M + H]⁺. ¹H NMR (300 MHz, CDCl₃) δ 8.01 (d, *J* = 7.3 Hz, 2H), 7.92 (s, 1H), 7.53 – 7.43 (m, 3H), 5.34 (t, *J* = 6.9 Hz, 1H), 4.46 (t, *J* = 7.7 Hz, 1H), 3.73 (t, *J* = 7.6 Hz, 1H), 2.80 (s, 3H), 1.89 – 1.82 (m, 2H), 1.79 – 1.66 (m, 6H), 1.51 – 1.47 (m, 2H) ppm; ¹³C NMR (100 MHz, CDCl₃) δ 171.2, 158.2, 156.5, 150.7, 138.2, 129.7, 128.8, 127.4, 115.2, 111.0, 74.7, 71.0, 35.8, 34.8, 25.2, 24.0, 23.8, 23.7 ppm.
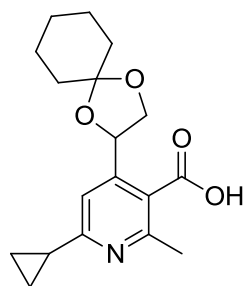
6-cyclopropyl-4-{1,4-dioxaspiro[4.5]decan-2-yl}-2-methylpyridine-3-carboxylic acid (179b): yellow oil, 83%, R_f = 0.18 (CHCl₃/MeOH 9:1), UHPLC-ESI-MS: R_t = 1.98, m/z = 318.2 [M + H]⁺. ¹H NMR (300 MHz, CDCl₃) δ 7.20 (s, 1H), 5.40 (t, *J* = 6.7 Hz, 1H), 4.46 (t, *J* = 7.9 Hz, 1H), 3.68 (t, *J* = 7.5 Hz, 1H), 2.77 (s, 3H), 2.54 – 2.49 (m, 1H), 1.71 – 1.59 (m, 8H), 1.42 (s, 2H), 1.22 (d, *J* = 8.1 Hz, 2H), 1.03 – 1.01 (m, 2H) ppm; ¹³C NMR (100 MHz, CDCl₃) δ 169.4, 159.5, 154.1, 151.1, 131.5, 113.9, 110.8, 74.6, 70.6, 35.8, 34.5, 25.0, 23.9, 23.6, 19.4, 14.4, 11.4, 11.3 ppm.

Synthesis of 180a-b: a stirred solution of the protected pyridine **177a-b** in 1,4-dioxane was cooled to 0 °C using an ice bath. A catalytic amount of concentrated HCl was added. The reaction was stirred at room temperature overnight. Solvent was evaporated under reduced pressure, the crude was redissolved in ACN (1 mL), filtered and purified by preparative HPLC.
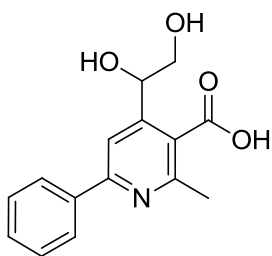
4-(1,2-dihydroxyethyl)-2-methyl-6-phenylpyridine-3-carboxylic acid (180a): white solid, 80%, R_f = 0.78 (CHCl$_3$/MeOH 5:1), UHPLC-ESI-MS: R_t = 2.34, m/z = 274.1 [M + H]$^+$. ^{1}H NMR (300 MHz, CDCl$_3$) δ 8.07 – 8.03 (m, 2H), 7.67 (s, 1H), 7.50 – 7.48 (m, 3H), 5.51 (t, J = 4.3 Hz, 1H), 4.15 (dd, J = 3.8 Hz, J = 12.3 Hz, 1H), 3.98 (dd, J = 4.9 Hz, J = 12.3 Hz, 1H), 2.92 (s, 3H) ppm; ^{13}C NMR (100 MHz, CDCl$_3$) δ 169.3, 161.0, 159.8, 156.8, 138.1, 130.3, 128.9, 127.7, 118.6, 111.3, 80.3, 63.2, 21.0 ppm.
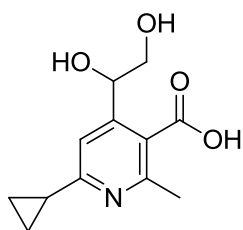
6-cyclopropyl-4-(1,2-dihydroxyethyl)-2-methylpyridine-3-carboxylic acid (180b): yellow oil, 72%, R_f = 0.46 (CHCl$_3$/MeOH 9:1), UHPLC-ESI-MS: R_t = 1.74, m/z = 238.2 [M + H]$^+$. ^{1}H NMR (300 MHz, MeOD) δ 7.17 (s, 1H), 5.38 (s, 1H), 3.94 (dd, J = 3.2 Hz, J = 12.3 Hz, 1H), 3.80 (dd, J = 3.8 Hz, J = 12.3 Hz, 1H), 2.61 (s, 3H), 2.13 – 2.04 (m, 1H), 0.99 (d, J = 6.9 Hz, 4H) ppm; ^{13}C NMR (100 MHz, MeOD) δ 171.5, 169.4, 159.8, 158.5, 118.9, 113.4, 82.3, 63.0, 20.6, 18.7, 11.7 (d, J = 7.9 Hz) ppm.

¹H NMR (300 MHz, CDCl₃) ethyl 4-{1,4-dioxaspiro[4.5]decan-2-yl}-2-methyl-6-phenylpyridine-3-carboxylate (177a)
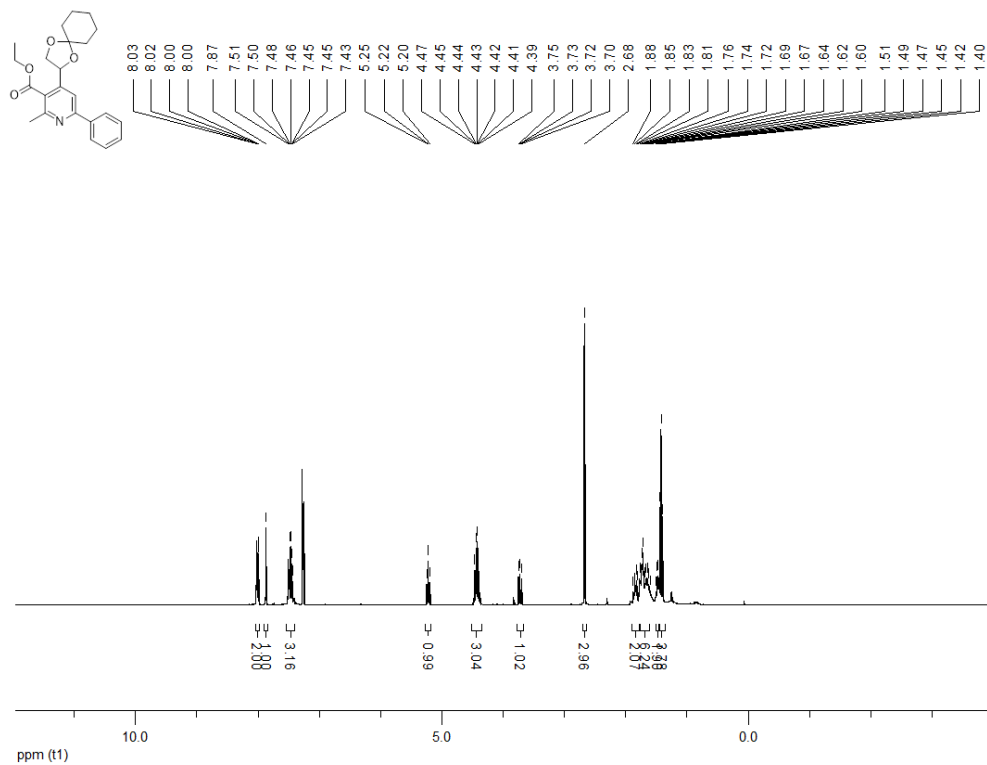
¹³C NMR (100 MHz, CDCl₃) ethyl 4-{1,4-dioxaspiro[4.5]decan-2-yl}-2-methyl-6-phenylpyridine-3-carboxylate (177a)

¹H NMR (300 MHz, CDCl₃) ethyl 6-cyclopropyl-4-{1,4-dioxaspiro[4.5]decan-2-yl}-2-methylpyridine-3-carboxylate (177b)

¹³C NMR (100 MHz, CDCl₃) ethyl 6-cyclopropyl-4-{1,4-dioxaspiro[4.5]decan-2-yl}-2-methylpyridine-3-carboxylate (177b)
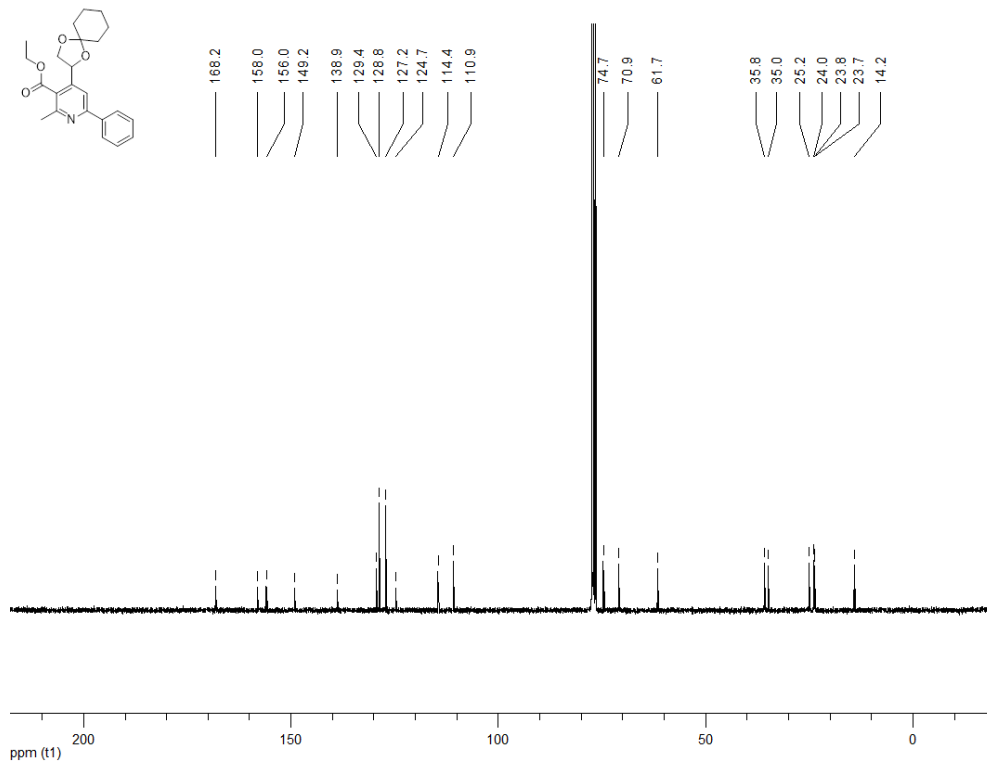
¹H NMR (300 MHz, CDCl₃) 4-{1,4-dioxaspiro[4.5]decan-2-yl}-2-methyl-6-phenylpyridine-3-carboxylic acid (179a)
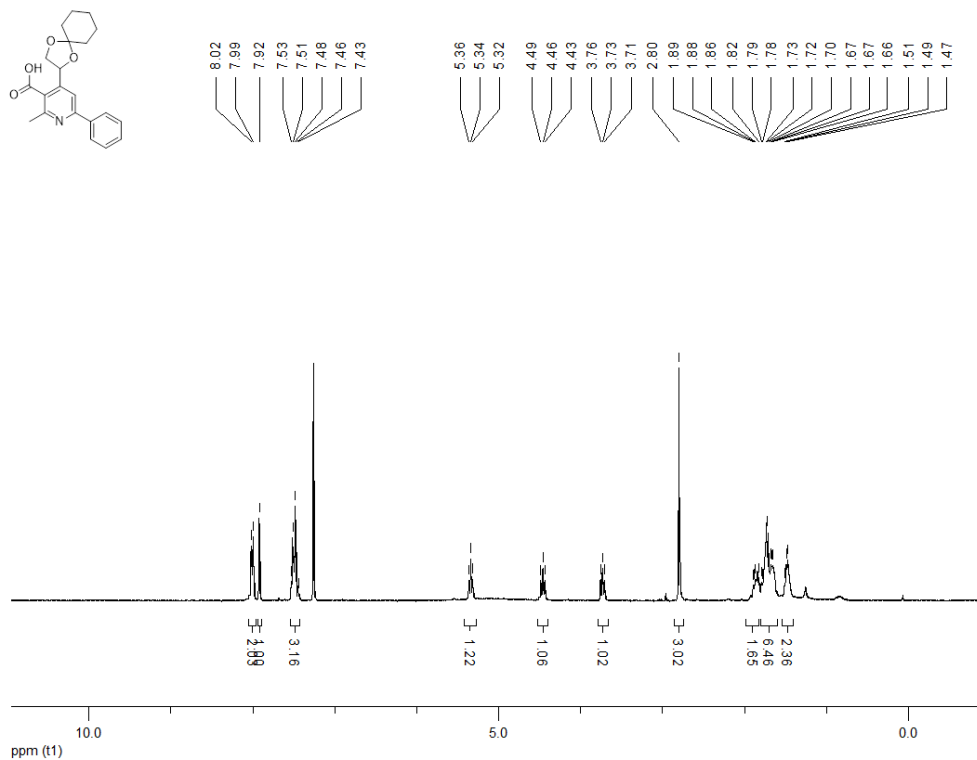
¹³C NMR (100 MHz, CDCl₃) 4-{1,4-dioxaspiro[4.5]decan-2-yl}-2-methyl-6-phenylpyridine-3-carboxylic acid (179a)
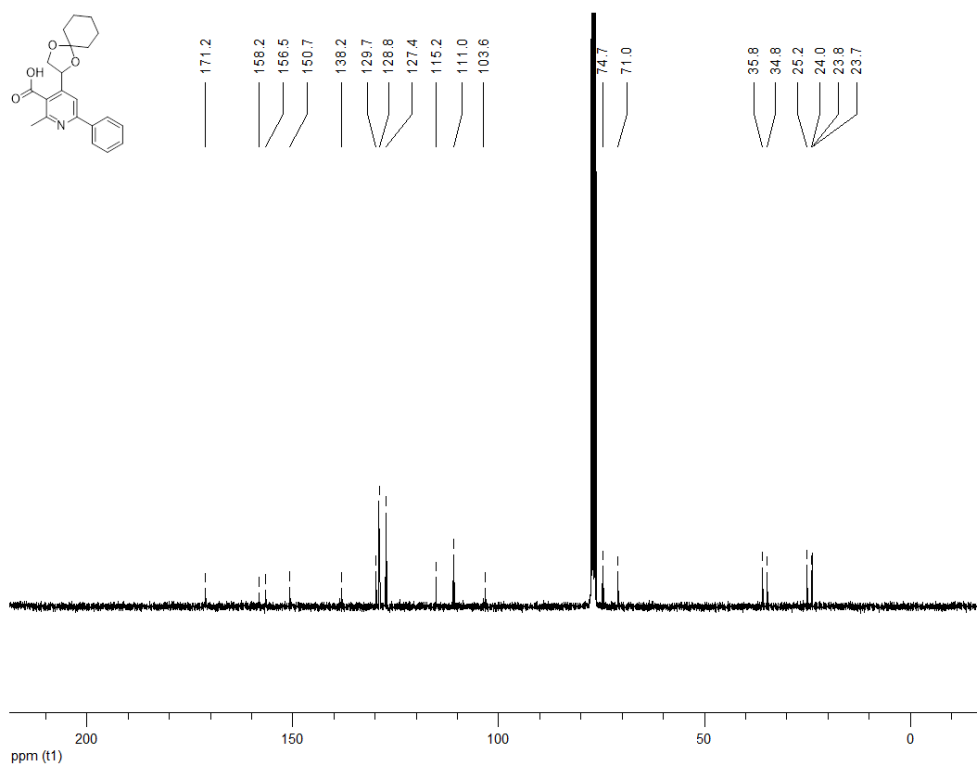
¹H NMR (300 MHz, CDCl₃) 6-cyclopropyl-4-{1,4-dioxaspiro[4.5]decan-2-yl}-2-methylpyridine-3-carboxylic acid (179b)
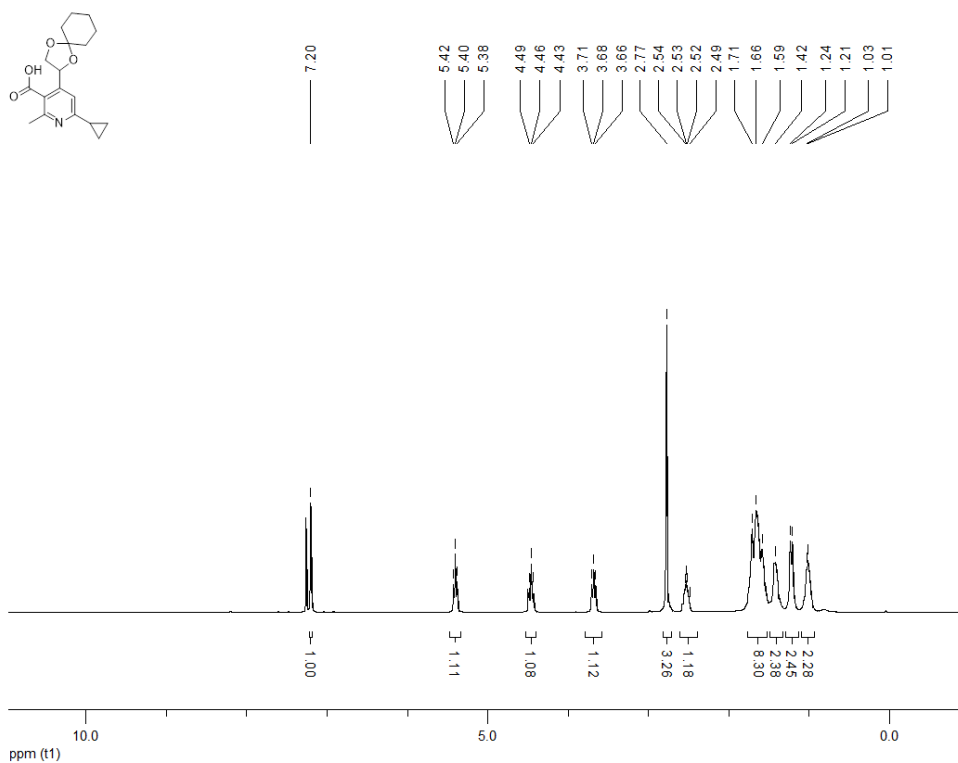
¹³C NMR (100 MHz, CDCl₃) 6-cyclopropyl-4-{1,4-dioxaspiro[4.5]decan-2-yl}-2-methylpyridine-3-carboxylic acid (179b)

¹H NMR (300 MHz, CDCl₃) 4-(1,2-dihydroxyethyl)-2-methyl-6-phenylpyridine-3-carboxylic acid (180a)

¹³C NMR (100 MHz, CDCl₃) 4-(1,2-dihydroxyethyl)-2-methyl-6-phenylpyridine-3-carboxylic acid (180a)
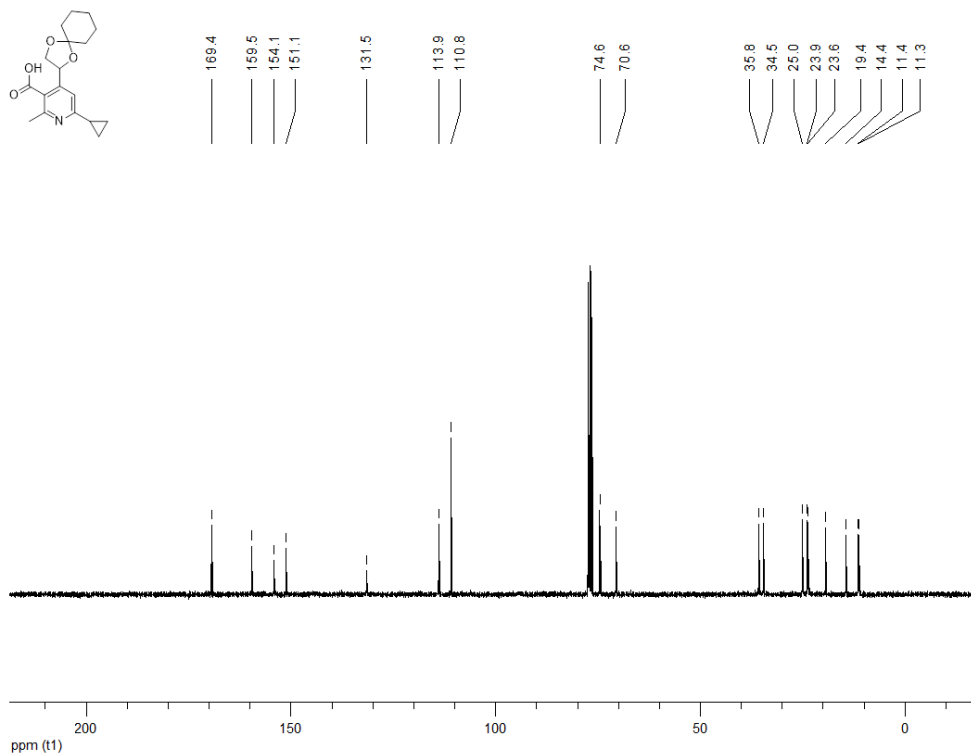
¹H NMR (300 MHz, MeOD) 6-cyclopropyl-4-(1,2-dihydroxyethyl)-2-methylpyridine-3-carboxylic acid (180b)
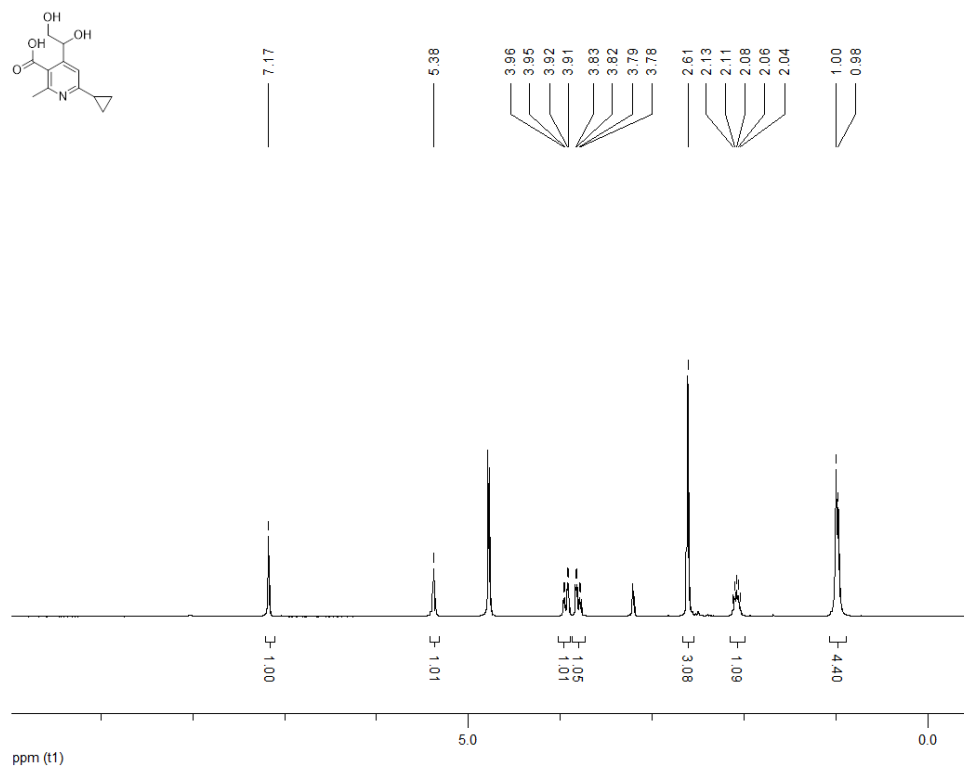
¹³C NMR (100 MHz, MeOD) 6-cyclopropyl-4-(1,2-dihydroxyethyl)-2-methylpyridine-3-carboxylic acid (180b)
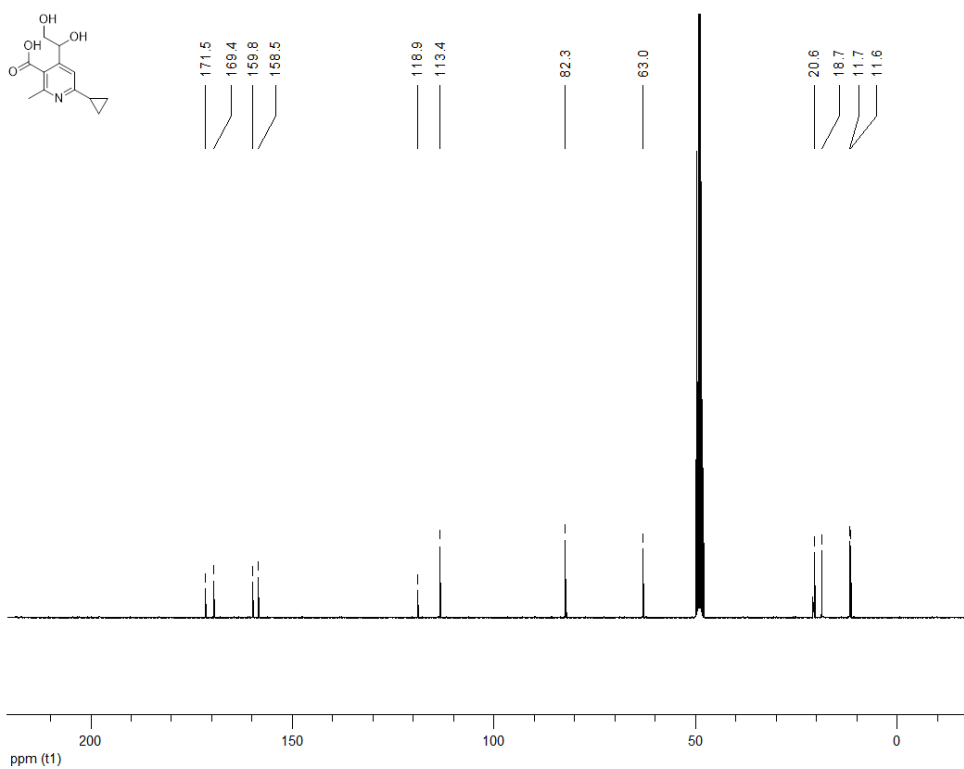
8.1.9 Synthesis, ^{1}H and ^{13}C NMR of 3,5 -disubtituted and 1,3,5-trisubstituted pyrazoles

Synthesis of 181a-g and 182h-o: to a stirred solution of the corresponding ynone (1.0 eq) in EtOH (2 mL) was added the corresponding hydrazine (hydrazine monohydrated or methyl hydrazine) (1.3 eq). The mixture was stirred at room temperature until starting material consumption (monitored by TLC) (normally 2 − 3 hours). Solvent was removed under reduced pressure, the crude was redissolved in ACN (1 mL), filtered and purified by preparative HPLC.[342]
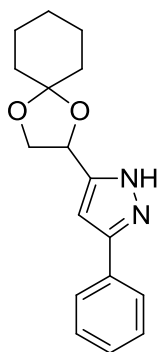
5-{1,4-dioxaspiro[4.5]decan-2-yl}-3-phenyl-1H-pyrazole (181a): yellowish oil, 57%, R_f = 0.19 (CyH/EtOAC 3:1), UHPLC-ESI-MS: R_t = 2.94, m/z = 285.2 [M + H] $^+$. ^{1}H NMR (300 MHz, CDCl$_3$) δ 7.65 (d, J = 7.1 Hz, 2H), 7.42 − 7.30 (m, 3H), 6.55 (s, 1H), 5.21 (t, J = 6.6 Hz, 1H), 4.31 (dd, J = 6.4 Hz, J = 8.1 Hz, 1H), 3.98 (t, J = 8.1 Hz, 1H), 1.76 − 1.61 (m, 8H), 1.43 − 1.40 (m, 2H) ppm; ^{13}C NMR (100 MHz, CDCl$_3$) δ 148.6, 147.9, 130.9, 128.9, 128.3, 125.6, 110.7, 100.5, 71.3, 69.5, 36.1, 35.2, 25.1, 24.0, 23.8 ppm.
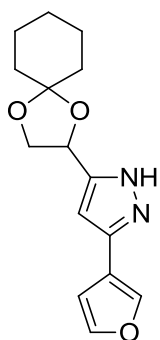
5-{1,4-dioxaspiro[4.5]decan-2-yl}-3-(furan-2-yl)-1H-pyrazole (181b): brown oil, 49%, R_f = 0.21 (CyH/EtOAc 3:1), UHPLC-ESI-MS: R_t = 2.75, m/z = 275.2 [M + H] $^+$. ^{1}H NMR (300 MHz, CDCl$_3$) δ 7.42 (d, J = 1.3 Hz, 1H), 6.62 (d, J = 3.3 Hz, 1H), 6.47 (s, 1H) 6.44 (dd, J = 1.8 Hz, J = 3.3 Hz, 1H), 5.21 (t, J = 6.6 Hz, 1H), 4.31 (dd, J = 6.3 Hz, J = 8.3 Hz, 1H), 3.96 (dd, J = 6.9 Hz, J = 8.2 Hz, 1H), 1.73 − 1.57 (m, 8H), 1.45 − 1.38 (m, 2H) ppm; ^{13}C NMR (100 MHz, CDCl$_3$) δ 148.4, 146.5, 142.1, 139.7, 111.4, 110.7, 106.4, 99.7, 71.1, 69.4, 36.1, 35.2, 25.1, 23.9, 23.8 ppm.
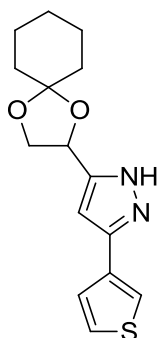
5-{1,4-dioxaspiro[4.5]decan-2-yl}-3-(thiophen-2-yl)-1*H*-pyrazole (181c): yellow oil, 63%, R_f = 0.32 (CyH/EtOAc 3:1), UHPLC-ESI-MS: R_t = 2.88, *m/z* = 291.2 [M + H]⁺. ¹H NMR (300 MHz, CDCl₃) δ 7.28 – 7.24 (m, 2H), 7.03 (dd, *J* = 3.6 Hz, *J* = 5.1 Hz, 1H), 6.42 (s, 1H), 5.19 (t, *J* = 6.5 Hz, 1H), 4.30 (dd, *J* = 6.3 Hz, *J* = 8.3 Hz, 1H), 3.95 (dd, *J* = 6.7 Hz, *J* = 8.3 Hz, 1H), 1.73 – 1.59 (m, 8H), 1.44 – 1.38 (m, 2H) ppm; ¹³C NMR (100 MHz, CDCl₃) δ 146.9, 144.4, 134.5, 127.6, 125.0, 124.1, 110.8, 100.4, 70.8, 69.4, 36.1, 35.1, 25.0, 24.0, 23.8 ppm.
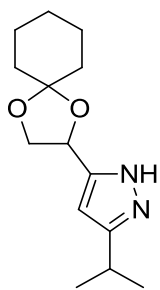
5-{1,4-dioxaspiro[4.5]decan-2-yl}-3-(propan-2-yl)-1*H*-pyrazole (181d): yellow oil, 68%, R_f = 0.25 (CyH/EtOAc 3:1), UHPLC-ESI-MS: R_t = 2.76, *m/z* = 251.6 [M + H]⁺. ¹H NMR (300 MHz, CDCl₃) δ 6.09 (s, 1H), 5.15 (t, *J* = 7.2 Hz, 1H), 4.27 (dd, *J* = 6.3 Hz, *J* = 8.2 Hz, 1H), 3.92 (t, *J* = 8.1 Hz, 1H), 2.98 (td, *J* = 6.9 Hz, *J* = 13.9 Hz, 1H), 1.74 – 1.59 (m, 8H), 1.43 – 1.40 (m, 2H), 1.27 (d, *J* = 6.9 Hz, 6H) ppm; ¹³C NMR (100 MHz, CDCl₃) δ 153.1, 149.4, 110.4, 99.7, 71.8, 69.5, 36.2, 35.3, 26.3, 25.1, 24.0, 23.8, 22.3 ppm.
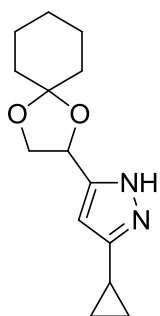
3-cyclopropyl-5-{1,4-dioxaspiro[4.5]decan-2-yl}-1*H*-pyrazole (181e): yellow oil, 49%, R_f = 0.12 (CyH/EtOAC 3:1), UHPLC-ESI-MS: R_t = 2.66, *m/z* = 249.2 [M + H]⁺. ¹H NMR (300 MHz, CDCl₃) δ 5.92 (s, 1H), 5.12 (t, *J* = 6.8 Hz, 1H), 4.25 (dd, *J* = 6.3 Hz, *J* = 8.0 Hz, 1H), 3.89 (t, *J* = 7.7 Hz, 1H), 1.90 – 1.81 (m, 1H), 1.68 – 1.60 (m, 8H), 1.43 – 1.39 (m, 2H), 0.96 – 0.89 (m, 2H), 0.72 – 0.67 (m, 2H) ppm; ¹³C NMR (100 MHz, CDCl₃) δ 149.8, 149.1, 110.3, 99.2, 71.8, 69.5, 36.1, 35.2, 25.1, 23.9, 23.8, 7.6 (d, *J* = 3.5 Hz), 7.3 ppm.
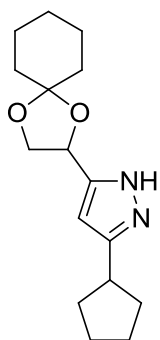
3-cyclopentyl-5-{1,4-dioxaspiro[4.5]decan-2-yl}-1H-pyrazole (181f): yellow oil, 75%, R_f = 0.14 (CyH/EtOAc 3:1), UHPLC-ESI-MS: R_t = 3.01, m/z = 277.4 [M + H]$^+$. ^{1}H NMR (300 MHz, CDCl$_3$) δ 6.08 (s, 1H), 5.14 (t, J = 7.2 Hz, 1H), 4.27 (dd, J = 6.3 Hz, J = 8.1 Hz, 1H), 3.93 (t, J = 7.8 Hz, 1H), 3.07 –3.02 (m, 1H), 2.09 – 2.03 (m, 2H), 1.78 – 1.59 (m 14H), 1.44 – 1.40 (m, 2H) ppm; ^{13}C NMR (100 MHz, CDCl$_3$) δ 151.2, 149.8, 110.3, 100.1, 72.0, 69.5, 37.2, 36.2, 35.3, 33.0, 25.1, 24.0, 23.8 ppm.
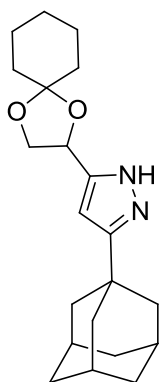
3-(adamantan-1-yl)-5-{1,4-dioxaspiro[4.5]decan-2-yl}-1H-pyrazole (181g): brown oil, 80%, R_f = 0.28 (CyH/EtOAc 3:1), UHPLC-ESI-MS: R_t = 3.51, m/z = 343.2 [M + H]$^+$. ^{1}H NMR (300 MHz, CDCl$_3$) δ 6.08 (s, 1H), 5.14 (dd, J = 6.4 Hz, J = 7.5 Hz, 1H), 4.27 (dd, J = 6.3 Hz, J = 8.1 Hz, 1H), 3.93 (t, J = 7.9 Hz, 1H), 2.06 (s, 3H), 1.91 (d, J = 2.6 Hz, 6H), 1.75 – 1.62 (m 14H), 1.44 – 1.40 (m, 2H) ppm; ^{13}C NMR (100 MHz, CDCl$_3$) δ 155.8, 149.5, 110.3, 98.7, 72.1, 69.5, 42.4, 36.5, 36.2, 35.3, 28.3, 25.1, 24.0, 23.8 ppm.
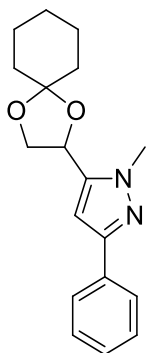
5-{1,4-dioxaspiro[4.5]decan-2-yl}-1-methyl-3-phenyl-1H-pyrazole (182a): yellowish oil, 50%, R_f = 0.39 (CyH/EtOAC 3:1), UHPLC-ESI-MS: R_t = 3.22, m/z = 299.2 [M + H]$^+$. ^{1}H NMR (300 MHz, CDCl$_3$) δ 7.74 (d, J = 7.2 Hz, 2H), 7.36 (t, J = 7.4 Hz, 2H), 7.26 (t, J = 7.2 Hz, 1H), 6.48 (s, 1H), 5.14 (t, J = 6.7 Hz, 1H), 4.31 (dd, J = 6.4 Hz, 1H, J = 8.2 Hz, 1H), 3.94 (s, 3H), 1.66 – 1.60

(m, 8H), 1.44 – 1.40 (m, 2H) ppm; ^{13}C NMR (100 MHz, CDCl$_3$) δ 150.2, 141.5, 133.3, 128.5, 127.6, 125.4, 110.0, 101.6, 69.2, 68.3, 37.2, 36.1, 35.2, 25.0, 23.9 (d, J = 2.4 Hz) ppm.
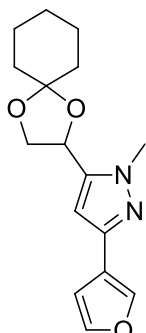
5-{1,4-dioxaspiro[4.5]decan-2-yl}-3-(furan-2-yl)-1-methyl-1*H*-pyrazole (182b): brown oil, 51%, R_f = 0.28 (CyH/EtOAc 3:1), UHPLC-ESI-MS: R_t = 2.95, m/z = 289.2 [M + H]$^+$. ^{1}H NMR (300 MHz, CDCl$_3$) δ 7.41 (d, J = 1.1 Hz, 1H), 6.60 (d, J = 3.0 Hz, 1H), 6.43 (t, J = 1.8 Hz, 1H), 6.42 (s, 1H) 5.13 (t, J = 6.6 Hz, 1H), 4.31 (dd, J = 6.3 Hz, J = 8.3 Hz, 1H), 4.05 (dd, J = 6.9 Hz, J = 8.3 Hz, 1H), 3.93 (s, 3H), 1.69 – 1.58 (m, 8H), 1.42 – 1.38 (m, 2H) ppm; ^{13}C NMR (100 MHz, CDCl$_3$) δ 148.7, 142.7, 141.6, 141.4, 111.2, 110.0, 105.3, 101.3, 69.0, 68.2, 37.2, 36.0, 35.2, 25.0, 23.9, 23.8 ppm.

5-{1,4-dioxaspiro[4.5]decan-2-yl}-1-methyl-3-(thiophen-2-yl)-1*H*-pyrazole **(182c):** yellow oil, 58%, R_f = 0.42 (CyH/EtOAc 3:1), UHPLC-ESI-MS: R_t = 3.13, m/z = 305.2 [M + H]$^+$. ^{1}H NMR (300 MHz, CDCl$_3$) δ 7.33 (dd, J = 1.0 Hz, J = 3.5 Hz, 1H), 7.27 (dd, J = 1.0 Hz, J = 5.1 Hz, 1H), 7.08 (dd, J = 3.6 Hz, J = 5.1 Hz, 1H), 6.46 (s, 1H), 5.19 (t, J = 6.6 Hz, 1H), 4.38 (dd, J = 6.3 Hz, J = 8.3 Hz, 1H), 4.11 (dd, J = 6.9 Hz, J = 8.3 Hz, 1H), 1.73 – 1.67 (m, 8H), 1.51 – 1.45 (m, 2H) ppm; ^{13}C NMR (100 MHz, CDCl$_3$) δ 145.5, 141.7, 136.5, 127.3, 124.2, 123.4, 111.0, 101.5, 69.1, 68.2, 37.2, 36.1, 35.2, 25.0, 23. 9 (d, J = 2.4 Hz) ppm.
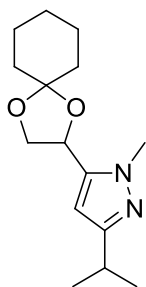
5-{1,4-dioxaspiro[4.5]decan-2-yl}-1-methyl-3-(propan-2-yl)-1*H*-pyrazole **(182d):** yellow oil, 71%, R_f = 0.55 (CyH/EtOAc 3:1), UHPLC-ESI-MS: R_t = 3.01, m/z = 265.2 [M + H]$^+$. ^{1}H

NMR (300 MHz, CDCl$_3$) δ 6.00 (s, 1H), 5.09 (t, J = 7.2 Hz, 1H), 4.27 (dd, J = 6.3 Hz, J = 8.2 Hz, 1H), 3.98 (t, J = 7.8 Hz, 1H), 3.85 (s, 3H), 2.92 (td, J = 6.9 Hz, J = 13.9 Hz, 1H), 1.66 – 1.62 (m, 8H), 1.41 – 1.39 (m, 2H), 1.23 (d, J = 6.9 Hz, 6H) ppm; ^{13}C NMR (100 MHz, CDCl$_3$) δ 158.0, 140.1, 110.7, 101.0, 69.3, 68.3, 36.7, 36.1, 35.2, 27.8, 25.1, 23.9 (d, J = 4.0 Hz), 22.9 ppm.
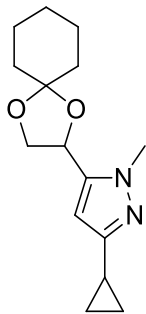
3-cyclopropyl-5-{1,4-dioxaspiro[4.5]decan-2-yl}-1-methyl-1*H*-pyrazole (182e): yellow oil, 69%, R_f = 0.28 (CyH/EtOAC 3:1), UHPLC-ESI-MS: R_t = 2.88, m/z = 263.2 [M + H]$^+$. ^{1}H NMR (300 MHz, CDCl$_3$) δ 5.84 (s, 1H), 5.07 (t, J = 6.8 Hz, 1H), 4.26 (dd, J = 6.3 Hz, J = 8.2 Hz, 1H), 3.95 (dd, J = 7.4 Hz, J = 8.0 Hz, 1H), 3.82 (s, 3H), 1.91 – 1.82 (m, 1H), 1.64 – 1.60 (m, 8H), 1.41 (d, J = 4.8 Hz, 2H), 0.90 – 0.84 (m, 2H), 0.69 – 0.64 (m, 2H) ppm; ^{13}C NMR (100 MHz, CDCl$_3$) δ 153.8, 140.5, 110.8, 100.6, 69.2, 68.3, 36.7, 36.1, 35.2, 25.0, 23.9 (d, J = 2.8 Hz), 9.0, 7.7 ppm.
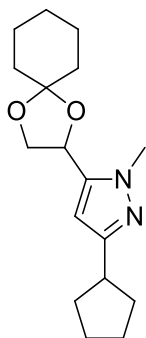
3-cyclopentyl-5-{1,4-dioxaspiro[4.5]decan-2-yl}-1-methyl-1*H*-pyrazole (182f): brown oil, 66%, R_f = 0.36 (CyH/EtOAc 3:1), UHPLC-ESI-MS: R_t = 3.25, m/z = 291.2 [M + H]$^+$. ^{1}H NMR (300 MHz, CDCl$_3$) δ 5.99 (s, 1H), 5.08 (t, J = 6.6 Hz, 1H), 4.26 (dd, J = 6.3 Hz, J = 8.2 Hz, 1H), 3.96 (t, J = 7.8 Hz, 1H), 3.84 (s, 3H), 3.06 –2.95 (m, 1H), 2.03 – 1.96 (m, 2H), 1.73 – 1.61 (m 14H), 1.43 – 1.38 (m, 2H) ppm; ^{13}C NMR (100 MHz, CDCl$_3$) δ 156.1, 140.1, 110.7, 101.5, 69.3, 68.3, 39.0, 36.7, 36.1, 35.1, 33.4, 25.3, 25.0, 23.9 (d, J = 3.9 Hz) ppm.
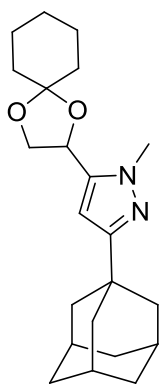
3-(adamantan-1-yl)-5-{1,4-dioxaspiro[4.5]decan-2-yl}-1-methyl-1*H*-pyrazole (182g):
brown oil, 61%, R_f = 0.55 (CyH/EtOAc 3:1), UHPLC-ESI-MS: R_t = 3.78, m/z = 357.4 [M + H] [+]. [1]H
NMR (300 MHz, CDCl$_3$) δ 6.02 (s, 1H), 5.09 (t, J = 7.2 Hz, 1H), 4.27 (dd, J = 6.3 Hz, J = 8.2 Hz, 1H),
3.97 (t, J = 8.1 Hz, 1H), 3.86 (s, 3H), 2.03 − 1.98 (m, 3H), 1.90 (d, J = 2.9 Hz, 6H), 1.75 − 1.73 (m,
6H), 1.65 − 1.61 (m, 8H), 1.44 − 1.39 (m, 2H) ppm; ^{13}C NMR (100 MHz, CDCl$_3$) δ 161.1, 139.7,
110.7, 100.2, 69.3, 68.3, 42.7, 36.8, 36.1, 35.1, 33.8, 28.6, 25.0, 23.9 (d, J = 4.5 Hz) ppm.
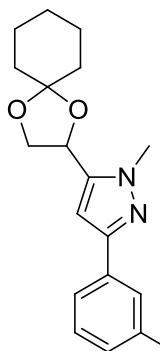
5-{1,4-dioxaspiro[4.5]decan-2-yl}-1-methyl-3-(3-methylphenyl)-1H-pyrazole
(182h): brown oil, 54%, R_f = 0.59 (CyH/EtOAC 9:1), UHPLC-ESI-MS: R_t = 3.34, m/z = 313.2 [M +
H] [+] .^{1}H NMR (300 MHz, CDCl$_3$) δ 7.61 (s, 1H), 7.54 (d, J = 7.7 Hz, 1H), 7.29 − 7.24 (m, 1H), 7.10
(d, J = 7.5 Hz, 1H), 6.49 (s, 1H), 5.17 (t, J = 6.7 Hz, 1H), 4.34 (dd, J = 6.3 Hz, 8.3 Hz, 1H), 4.08 (dd, J
= 7.1 Hz, 8.2 Hz, 1H), 3.97 (s, 3H), 1.72 − 1.60 (m, 8H), 1.44 − 1.41 (m, 2H) ppm; ^{13}C NMR (100
MHz, CDCl$_3$) δ 150.1, 141.4, 138.0, 133.1, 128.3, 128.2, 125.9, 122.5, 110.8, 101.4, 69.1, 68.1, 37.0,
36.0, 35.1, 24.9, 23.8 (d, J = 3.9 Hz), 21.3 ppm.
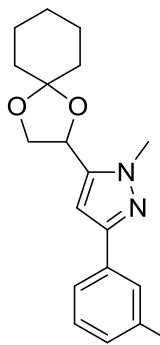
3-(5-{1,4-dioxaspiro[4.5]decan-2-yl}-1-methyl-1H-pyrazol-3-yl)benzonitrile
(182i): orange oil, 65%, R_f = 0.30 (CyH/EtOAc 3:1), UHPLC-ESI-MS: R_t = 3.14, m/z = 324.2 [M +
H] [+] .^{1}H NMR (300 MHz, CDCl$_3$) δ 8.04 (s, 1H), 7.97 (dt, J = 1.5 Hz, J = 8.1 Hz, 1H), 7.54 (dt, J = 1.4
Hz, J = 7.7 Hz, 1H), 7.45 (t, J = 7.7 Hz, 1H), 6.52 (s, 1H), 5.16 (t, J = 6.6 Hz, 1H), 4.34 (dd, J = 6.3

Hz, J = 8.3 Hz, 1H), 4.06 (dd, J = 6.9 Hz, J = 8.3 Hz, 1H), 3.96 (s, 3H), 1.70 – 1.59 (m, 8H), 1.45 – 1.39 (m, 2H) ppm; ^{13}C NMR (100 MHz, CDCl$_3$) δ 147.8, 142.2, 134.6, 130.8, 129.4, 129.3, 128.8, 118.8, 112.7, 111.1, 101.7, 69.0, 68.2, 37.4, 36.1, 35.0, 25.0, 23.8 (d, J = 4.6 Hz) ppm.
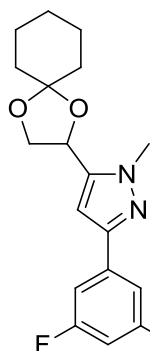

3-(3-chloro-5-fluorophenyl)-5-{1,4-dioxaspiro[4.5]decan-2-yl}-1-methyl-1H-pyrazole (182j): yellow oil, 61%, R_f = 0.49 (CyH/EtOAc 3:1), UHPLC-ESI-MS: R_t = 3.60, m/z = 351.0 [M + H]$^+$.^{1}H NMR (300 MHz, CDCl$_3$) δ 7.54 (s, 1H), 7.36 (d, J = 8.9 Hz, 1H), 6.98 (d, J = 8.3 Hz, 1H), 6.47 (s, 1H), 5.14 (t, J = 6.6 Hz, 1H), 4.33 (t, J = 7.5 Hz, 1H), 4.05 (t, J = 7.6 Hz, 1H), 3.94 (s, 3H), 1.67 – 1.65 (m, 8H), 1.42 (d, J = 4.5 Hz, 2H) ppm; ^{13}C NMR (100 MHz, CDCl$_3$) δ 162.9 (d, J = 248.2 Hz), 147.7 (d, J = 2.9 Hz), 142.1, 136.5 (d, J = 9.3 Hz), 135.1 (d, J = 11.0 Hz), 121.3 (d, J = 3.1 Hz), 114.9 (d, J = 25.0 Hz), 111.1, 110.6 (d, J = 22.8 Hz), 101.8, 69.0, 68.2, 37.3, 36.1, 35.1, 25.0, 23.8 (d, J = 4.0 Hz) ppm.

4-(5-{1,4-dioxaspiro[4.5]decan-2-yl}-1-methyl-1H-pyrazol-3-yl)benzamide **(182k)**: brown oil, 41%, R_f = 0.29 (CyH/EtOAc 3:1), UHPLC-ESI-MS: R_t = 2.79, m/z = 342.2 [M + H]$^+$. ^{1}H NMR (300 MHz, CDCl$_3$) δ 7.63 (d, J = 8.9 Hz, 2H), 6.74 (d, J = 8.9 Hz, 2H), 6.40 (s, 1H), 5.13 (t, J = 6.7 Hz, 1H), 4.31 (dd, J = 6.3 Hz, J = 8.2 Hz, 1H), 4.06 (dd, J = 7.2 Hz, J = 8.2 Hz, 1H), 3.92 (s, 3H), 2.96 (s, 6H), 1.67 – 1.59 (m, 8H), 1.45 – 1.40 (m, 2H) ppm; ^{13}C NMR (100 MHz, CDCl$_3$) δ 150.5, 150.0, 141.2, 126.3, 121.8, 112.5, 110.8, 100.6, 69.1, 68.2, 40.5, 36.9, 36.0, 35.1, 25.0, 23.8 ppm.
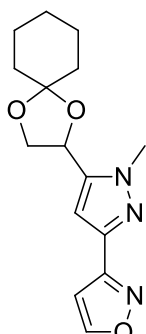
5-(5-{1,4-dioxaspiro[4.5]decan-2-yl}-1-methyl-1H-pyrazol-3-yl)-1,2-oxazole **(182l)**:
brown oil, 55%, R_f = 0.17 (CyH/EtOAc 3:1), UHPLC-ESI-MS: R_t = 2.74, m/z = 290.2 [M + H][+]. [1]H
NMR (300 MHz, CDCl$_3$) δ 8.27 (s, 1H), 6.64 (s, 1H), 6.54 (s, 1H), 5.17 (t, J = 6.5 Hz, 1H), 4.35 (dd, J
= 6.9 Hz, J = 7.8 Hz, 1H), 4.09 (d, J = 4.6 Hz, 1H), 3.99 (s, 3H), 1.73 – 1.61 (m, 8H), 1.42 (d, J = 4.4
Hz, 2H) ppm; ^{13}C NMR (100 MHz, CDCl$_3$) δ 164.1, 150.5, 142.2, 139.4, 111.3, 103.5, 98.6, 68.9,
68.1, 37.7, 36.0, 35.1, 25.0, 23.9 (d, J = 2.2 Hz) ppm.
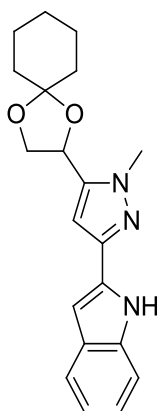
2-(5-{1,4-dioxaspiro[4.5]decan-2-yl}-1-methyl-1H-pyrazol-3-yl)-1H-indole **(182m)**:
brown oil, 46%, R_f = 0.77 (CHCl$_3$/MeOH 9:1), UHPLC-ESI-MS: R_t = 3.19, m/z = 338.2 [M + H][+]. [1]H
NMR (300 MHz, CDCl$_3$) δ 9.43 (s br, 1H), 7.62 (d, J = 7.7 Hz, 1H), 7.30 (d, J = 8.4 Hz, 1H), 7.17 (td,
J = 6.9 Hz, J = 15.0 Hz, 1H), 7.10 (td, J = 7.2 Hz, J = 14.7 Hz, 1H), 6.74 (d, J = 1.4 Hz, 1H), 6.56 (s,
1H), 5.16 (t, J = 6.6 Hz, 1H), 4.35 (dd, J = 6.4 Hz, J = 8.3 Hz, 1H), 4.10 (dd, J = 6.9 Hz, J = 8.3 Hz,
1H), 3.93 (s, 3H), 1.71 – 1.65 (m, 8H), 1.49 – 1.45 (m, 2H) ppm; ^{13}C NMR (100 MHz, CDCl$_3$) δ
143.8, 141.9, 136.2, 131.6, 128.8, 122.0, 120.4, 119.7, 111.1, 110.8, 101.9, 99.4, 69.0, 68.1, 37.1,
36.1, 35.1, 25.0, 23.9 (d, J = 3.4 Hz) ppm.
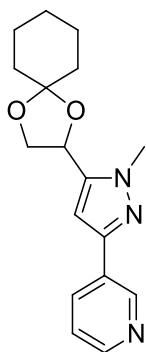
3-(5-{1,4-dioxaspiro[4.5]decan-2-yl}-1-methyl-1H-pyrazol-3-yl)pyridine **(182n)**:
brown oil, 47%, R_f = 0.76 (CHCl$_3$/MeOH 9:1), UHPLC-ESI-MS: R_t = 2.11, m/z = 300.2 [M + H][+]. [1]H

NMR (300 MHz, CDCl$_3$) δ 8.97 (s, 1H), 8.52 (d, J = 3.8 Hz, 1H), 8.09 (dt, J = 1.9 Hz, 7.9 Hz, 1H), 7.33 (dd, J = 4.9 Hz, 7.8 Hz, 1H), 6.55 (s, 1H), 5.18 (t, J = 6.6 Hz, 1H), 4.36 (dd, J = 6.4 Hz, 8.3 Hz, 1H), 4.08 (dd, J = 7.0 Hz, 8.3 Hz, 1H), 3.98 (s, 3H), 1.72 − 1.60 (m, 8H), 1.46 − 1.41 (m, 2H) ppm; ^{13}C NMR (100 MHz, CDCl$_3$) δ 148.4, 147.0, 146.8, 142.0, 132.7, 129.3, 123.5, 111.1, 101.7, 69.1, 68.2, 37.3, 36.1, 35.1, 25.0, 23.9 (d, J = 4.1 Hz) ppm.
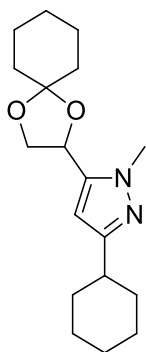
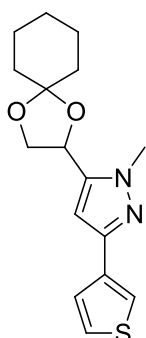**3-cyclohexyl-5-{1,4-dioxaspiro[4.5]decan-2-yl}-1-methyl-1H-pyrazole (182o)**: brown oil, 55%, R_f = 0.29 (CyH/EtOAC 9:1), UHPLC-ESI-MS: R_t = 3.40, m/z = 305.2 [M + H]$^+$. ^{1}H NMR (300 MHz, CDCl$_3$) δ 5.99 (s, 1H), 5.10 (t, J = 6.9 Hz, 1H), 4.27 (t, J = 8.1 Hz, 1H), 3.98 (t, J = 7.8 Hz, 1H), 3.85 (s, 3H), 2.61 − 2.54 (m, 1H), 1.94 (d, J = 7.8 Hz, 2H), 1.78 (d, J = 4.5 Hz, 2H), 1.66 − 1.62 (m, 8H), 1.43 − 1.33 (m, 6H), 1.29 − 1.20 (m, 2H) ppm; ^{13}C NMR (100 MHz, CDCl$_3$) δ 157.1, 139.9, 110.7, 101.2, 69.2, 68.2, 37.5, 36.7, 36.0, 35.1, 33.3, 26.4, 26.1, 25.0, 23.8 (d, J = 3.8 Hz) ppm.

Synthesis of 183a-g and 184a-g: a stirred solution of the protected pyrazole **183a-g and 184a-g** in 1,4-dioxane was cooled to 0 °C using an ice bath. A catalytic amount of concentrated HCl was added. The reaction was stirred at room temperature overnight. Solvent was evaporated under reduced pressure, the crude was redissolved in ACN (1 mL), filtered and purified by preparative HPLC.
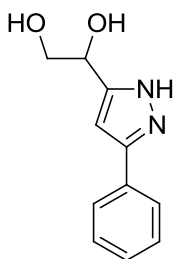
1-(3-phenyl-1H-pyrazol-5-yl)ethane-1,2-diol (183a): yellowish solid, 88%, R_f = 0.27 (CHCl$_3$/MeOH 9:1), UHPLC-ESI-MS: R_t = 1.76, m/z = 205.4 [M + H]$^+$. ^{1}H NMR (300 MHz, MeOD) δ 7.74 − 7.71 (m, 2H), 7.43 − 7.38 (m, 2H), 7.34 − 7.29 (m, 1H), 6.62 (s, 1H), 4.81 (dd, J = 5.2 Hz, J = 6.6 Hz, 1H), 3.82 − 3.72 (m, 2H) ppm; ^{13}C NMR (100 MHz, MeOD) δ 151.6, 149.2, 133.0, 129.8, 129.1, 126.6, 101.2, 69.7, 67.3 ppm.
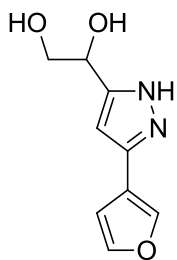
1-[3-(furan-2-yl)-1*H*-pyrazol-5-yl]ethane-1,2-diol (183b): brown oil, 82%, R_f = 0.29 (CHCl$_3$/MeOH 9:1), UHPLC-ESI-MS: R_t = 1.50, m/z = 195.2 [M + H]$^+$. ^{1}H NMR (300 MHz, MeOD) δ 7.53 (s, 1H), 6.69 (d, J = 3.3 Hz, 1H), 6.50 (d, J = 3.6 Hz, 2H), 4.79 (t, J = 6.3 Hz, 1H), 3.75 (dd, J = 2.5 Hz, J = 5.6 Hz, 2H) ppm; ^{13}C NMR (100 MHz, MeOD) δ 150.3, 148.8, 143.4, 141.9, 112.4, 107.1, 100.7, 69.4, 67.2 ppm.
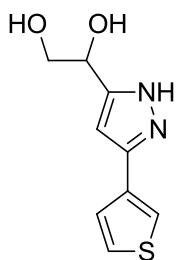
1-[3-(thiophen-2-yl)-1*H*-pyrazol-5-yl]ethane-1,2-diol (183c): yellow oil, 83%, R_f = 0.27 (CHCl$_3$/MeOH 9:1), UHPLC-ESI-MS: R_t = 1.68, m/z = 211.0 [M + H]$^+$. ^{1}H NMR (300 MHz, MeOD) δ 7.35 (dd, J = 1.2 Hz, J = 4.3 Hz, 2H), 7.06 (dt, J = 1.3 Hz, J = 4.4 Hz, 1H), 6.49 (s, 1H), 4.80 (t, J = 5.9 Hz, 1H), 3.76 – 3.74 (m, 2H) ppm; ^{13}C NMR (100 MHz, MeOD) δ 145.7, 145.5, 136.4, 128.6, 125.8, 125.1, 101.3, 69.2, 67.2 ppm.
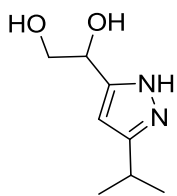
1-[3-(propan-2-yl)-1*H*-pyrazol-5-yl]ethane-1,2-diol (183d): brown oil, 87%, R_f = 0.25 (CHCl$_3$/MeOH 9:1), UHPLC-ESI-MS: R_t = 1.37, m/z = 171.2 [M + H]$^+$. ^{1}H NMR (300 MHz, MeOD) δ 6.12 (s, 1H), 4.72 (t, J = 5.9 Hz, 1H), 3.69 (dd, J = 2.8 Hz, J = 4.1 Hz, 2H), 2.98 (td, J = 6.9 Hz, J = 13.8 Hz, 1H), 1.27 (dd, J = 1.3 Hz, J = 6.9 Hz, 6H) ppm; ^{13}C NMR (100 MHz, MeOD) δ 155.1, 151.9, 100.3, 70.0, 67.3, 27.6, 22.9 ppm.
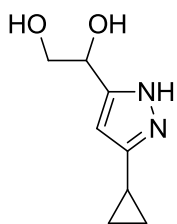
1-(3-cyclopropyl-1*H*-pyrazol-5-yl)ethane-1,2-diol (183e): yellow oil, 89%, R_f = 0.16 (CHCl$_3$/MeOH 9:1), UHPLC-ESI-MS: R_t = 1.22, m/z = 169.2 [M + H]$^+$. ^{1}H NMR (300 MHz, MeOD) δ 6.25 (s, 1H), 4.73 (t, J = 5.3 Hz, 1H), 3.62 (d, J = 5.3 Hz, 2H), 2.00 – 1.91 (m, 1H), 1.14 – 1.07 (m,

2H), 0.87– 0.80 (m, 2H) ppm; ^{13}C NMR (100 MHz, MeOD) δ 152.0, 151.7, 99.9, 69.8, 67.3, 8.4, 8.3 ppm.
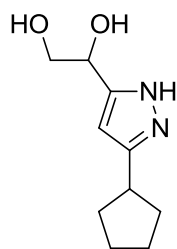
1-(3-cyclopentyl-1H-pyrazol-5-yl)ethane-1,2-diol (183f): brownish solid, 82%, R_f = 0.23 (CHCl$_3$/MeOH 9:1), UHPLC-ESI-MS: R_t = 1.68, m/z = 197.2 [M + H] $^+$. ^{1}H NMR (300 MHz, CD$_3$CN) δ 6.01 (s, 1H), 4.63 (t, J = 6.9 Hz, 1H), 3.67 – 3.56 (m, 2H), 3.07 – 3.01 (m, 1H), 2.05 – 1.99 (m, 2H), 1.77 – 1.71 (m, 2H), 1.66 – 1.54 (m, 4H) ppm; ^{13}C NMR (100 MHz, CD$_3$CN) δ 162.4, 152.0, 100.4, 69.06, 67.0, 38.1, 33.8, 25.8 ppm.
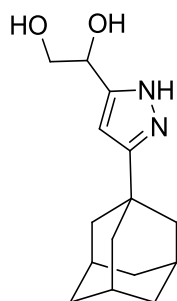
1-[3-(adamantan-1-yl)-1H-pyrazol-5-yl]ethane-1,2-diol (183g): brownish solid, 75%, R_f = 0.25 (CHCl$_3$/MeOH 9:1), UHPLC-ESI-MS: R_t = 2.24, m/z = 263.2 [M + H] $^+$. ^{1}H NMR (300 MHz, MeOD) δ 6.08 (s, 1H), 4.71 (dd, J = 5.0 Hz, J = 7.0 Hz, 1H), 3.70 (dd, J = 2.7 Hz, J = 6.0 Hz, 2H), 2.04 (s, 3H), 1.95 (d, J = 2.7 Hz, 6H), 1.81 (s, 6H) ppm; ^{13}C NMR (100 MHz, MeOD) δ 157.5. 152.0, 99.2, 70.3, 67.4, 43.5, 37.7, 34.3, 30.0 ppm.
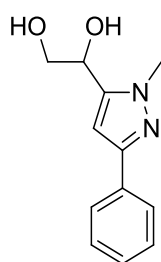
1-(1-methyl-3-phenyl-1H-pyrazol-5-yl)ethane-1,2-diol (184a): yellowish solid, 79%, R_f = 0.41 (CHCl$_3$/MeOH 9:1), UHPLC-ESI-MS: R_t = 1.88, m/z = 219.1 [M + H] $^+$. ^{1}H NMR (300 MHz, MeOD) δ 7.74 (d, J = 7.3 Hz, 2H), 7.37 (t, J = 7.2 Hz, 2H), 7.29 (d, J = 7.4 Hz, 1H), 6.62 (s, 1H), 4.82 (t, J = 5.8 Hz, 1H), 3.94 (s, 3H), 3.82 (s, 2H) ppm; ^{13}C NMR (100 MHz, MeOD) δ 151.6, 146.4, 134.6, 129.7, 128.8, 126.6, 102.5, 67.6, 66.4, 37.2 ppm.
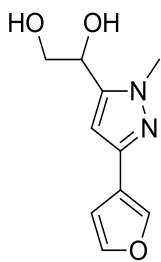
1-[3-(furan-2-yl)-1-methyl-1*H*-pyrazol-5-yl]ethane-1,2-diol (184b): brown oil, 85%, R_f = 0.42 (CHCl$_3$/MeOH 9:1), UHPLC-ESI-MS: R_t = 1.57, m/z = 209.2 [M + H]$^+$. ^{1}H NMR (300 MHz, MeOD) δ 7.50 (d, J = 1.7 Hz, 1H), 6.65 (d, J = 3.3 Hz, 1H), 6.51 (s, 1H), 6.48 (dd, J = 1.8 Hz, J = 3.3 Hz, 1H), 4.80 (t, J = 6.1 Hz, 1H), 3.92 (s, 3H), 3.80 (dd, J = 4.1 Hz, J = 6.1 Hz, 2H) ppm; ^{13}C NMR (100 MHz, MeOD) δ 150.0, 146.2, 143.9, 143.1, 112.3, 106.6, 102.2, 67.5, 66.3, 37.2 ppm.
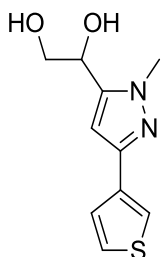
1-[1-methyl-3-(thiophen-2-yl)-1*H*-pyrazol-5-yl]ethane-1,2-diol (184c): yellow oil, 76%, R_f = 0.44 (CHCl$_3$/MeOH 9:1), UHPLC-ESI-MS: R_t = 1.76, m/z = 225.2 [M + H]$^+$. ^{1}H NMR (300 MHz, MeOD) δ 7.33 – 7.30 (m, 2H), 7.04 (dd, J = 3.6 Hz, J = 5.1 Hz, 1H), 6.51 (s, 1H), 4.80 (t, J = 6.1 Hz, 1H), 3.90 (s, 3H), 3.81 (dd, J = 3.8 Hz, J = 6.1 Hz, 2H) ppm; ^{13}C NMR (100 MHz, MeOD) δ 146.7, 146.4, 137.4, 128.5, 125.4, 124.8, 102.4, 67.5, 66.3, 37.1 ppm.
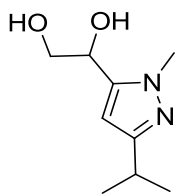
1-[1-methyl-3-(propan-2-yl)-1*H*-pyrazol-5-yl]ethane-1,2-diol (184d): brown oil, 77%, R_f = 0.47 (CHCl$_3$/MeOH 9:1), UHPLC-ESI-MS: R_t = 1.50, m/z = 185.2 [M + H]$^+$. ^{1}H NMR (300 MHz, MeOD) δ 6.09 (s, 1H), 4.74 (t, J = 6.0 Hz, 1H), 3.83 (s, 3H), 3.75 (dd, J = 4.4 Hz, J = 6.2 Hz, 2H), 2.98 (td, J = 6.9 Hz, J = 13.9 Hz, 1H), 1.22 (d, J = 7.0 Hz, 6H) ppm; ^{13}C NMR (100 MHz, MeOD) δ 159.1, 145.3, 101.6, 67.5, 66.3, 36.6, 28.9, 23.3 ppm.
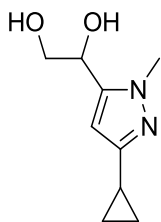
1-(3-cyclopropyl-1-methyl-1*H*-pyrazol-5-yl)ethane-1,2-diol (184e): yellow oil, 92%, R_f = 0.36 (CHCl$_3$/MeOH 9:1), UHPLC-ESI-MS: R_t = 1.37, m/z = 183.2 [M + H]$^+$. ^{1}H NMR (300 MHz, MeOD) δ 6.40 (s, 1H), 4.87 (t, J = 5.8 Hz, 1H), 4.05 (s, 3H), 3.83 (dd, J = 5.4 Hz, J = 11.3 Hz, 1H), 3.74 (dd, J = 6.1 Hz, J = 11.2 Hz, 1H), 2.10 – 2.01 (m, 1H), 1.25 – 1.18 (m, 2H), 0.97– 0.91 (m, 2H) ppm; ^{13}C NMR (100 MHz, MeOD) δ 155.0, 146.4, 101.4, 67.5, 66.3, 36.7, 9.5, 8.4 ppm
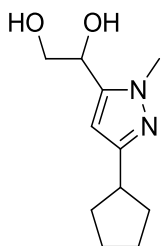
1-(3-cyclopentyl-1-methyl-1*H*-pyrazol-5-yl)ethane-1,2-diol **(184f):** brownish solid, 78%, R_f = 0.28 (CHCl$_3$/MeOH 9:1), UHPLC-ESI-MS: R_t = 1.79, m/z = 211.2 [M + H]$^+$. ^{1}H NMR (300 MHz, MeOD) δ 6.08 (s, 1H), 4.74 (t, J = 6.2 Hz, 1H), 3.82 (s, 3H), 3.75 (dd, J = 4.4 Hz, J = 6.2 Hz, 2H), 3.06 – 2.97 (m, 1H), 2.03 – 1.96 (m, 2H), 1.79 – 1.75 (m, 2H), 1.72 – 1.60 (m, 4H) ppm; ^{13}C NMR (100 MHz, MeOD) δ 157.3, 145.3, 102.1, 67.5, 66.3, 40.2, 36.6, 34.5, 26.2 ppm.
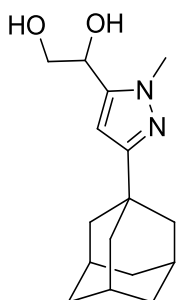
1-[3-(adamantan-1-yl)-1-methyl-1*H*-pyrazol-5-yl]ethane-1,2-diol **(184g):** brownish solid, 67%, R_f = 0.50 (CHCl$_3$/MeOH 9:1), UHPLC-ESI-MS: R_t = 2.37, m/z = 277.2 [M + H]$^+$. ^{1}H NMR (300 MHz, MeOD) δ 6.10 (s, 1H), 4.74 (t, J = 6.2 Hz, 1H), 3.83 (s, 3H) 3.75 (dd, J = 4.3 Hz, J = 6.1 Hz, 2H), 2.03 (s, 3H), 1.93 (d, J = 2.7 Hz, 6H), 1.80 (s, 6H) ppm; ^{13}C NMR (100 MHz, MeOD) δ 162.2, 144.8, 100.9, 67.6, 66.4, 43.9, 38.0, 36.5, 35.0, 30.2 ppm.

Synthesis of 185a-f: to a stirred solution of **174a** (1.0 eq) in EtOH (2 mL) was added the corresponding hydrazine (1.3 eq). The mixture was stirred at room temperature until starting material consumption (monitored by TLC) (normally 2 – 3 hours). Solvent was removed under reduced pressure, the crude was redissolved in ACN (1 mL), filtered and purified by preparative HPLC.[342]
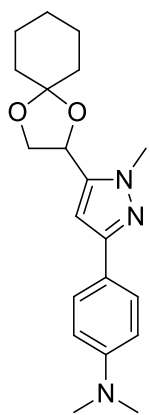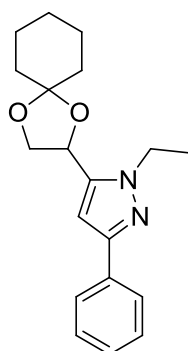
5-{1,4-dioxaspiro[4.5]decan-2-yl}-1-ethyl-3-phenyl-1H-pyrazole **(185a)**: orange oil, 44%, R_f = 0.32 (CyH/EtOAc 3:1), UHPLC-ESI-MS: R_t = 3.36, m/z = 313.2 [M + H]$^+$. ^{1}H NMR (300 MHz, CDCl$_3$) δ 7.79 – 7.76 (m, 2H), 7.40 – 7.35 (m, 2H), 7.31 – 7.28 (m, 1H), 6.49 (s, 1H), 5.17 (t, J = 6.7 Hz, 1H), 4.34 (dd, J = 6.3 Hz, J = 8.2 Hz, 1H), 4.27 (dd, J = 3.6 Hz, J = 7.2 Hz, 2H), 4.09 (dd, J = 7.2 Hz, J = 8.1 Hz, 1H), 1.70 – 1.62 (m, 8H), 1.51 (t, J = 7.2 Hz, 3H), 1.46 – 1.38 (m, 2H)

ppm; ¹³C NMR (100 MHz, CDCl₃) δ 150.3, 140.8, 133.5, 128.5, 127.5, 125.5, 110.9, 101.3, 69.0, 68.5, 45.0, 36.1, 35.2, 25.1, 23.9, 16.0 ppm.
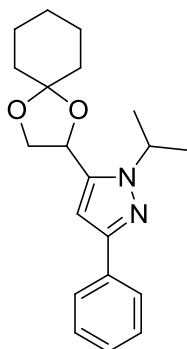
5-{1,4-dioxaspiro[4.5]decan-2-yl}-3-phenyl-1-(propan-2-yl)-1H-pyrazole (**185b**): brown oil, 60%, R_f = 0.78 (CyH/EtOAc 3:1), UHPLC-ESI-MS: R_t = 3.60, m/z = 327.2 [M + H]⁺. ¹H NMR (300 MHz, CDCl₃) δ 7.80 (d, J = 7.2 Hz, 2H), 7.38 (t, J = 7.5 Hz, 2H), 7.29 – 7.26 (m, 1H), 6.47 (s, 1H), 5.20 (t, J = 7.5 Hz, 1H), 4.69 – 4.61 (m, 1H), 4.34 (dd, J = 6.4 Hz, J = 8.1 Hz, 1H), 4.10 (t, J = 7.5 Hz, 1H), 1.69 – 1.63 (m, 8H), 1.56 (dd, J = 6.7 Hz, J = 8.7 Hz, 6H), 1.46 – 1.42 (m, 2H) ppm; ¹³C NMR (100 MHz, CDCl₃) δ 149.9, 140.2, 133.8, 128.5, 127.3, 125.5, 110.8, 100.8, 69.0, 68.4, 50.9, 36.2, 35.3, 25.1, 23.9, 22.8 (d, J = 1.8 Hz) ppm.
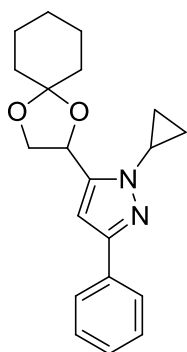
1-cyclopropyl-5-{1,4-dioxaspiro[4.5]decan-2-yl}-3-phenyl-1H-pyrazole (**185c**): yellow oil, 54%, R_f = 0.74 (CyH/EtOAc 3:1), UHPLC-ESI-MS: R_t = 3.82, m/z = 325.2 [M + H]⁺. ¹H NMR (300 MHz, CDCl₃) δ 7.89 (dd, J = 1.6 Hz, J = 8.0 Hz, 2H), 7.47 – 7.39 (m, 3H), 6.89 (s, 1H), 5.66 (t, J = 5.7 Hz, 1H), 4.51 (dd, J = 7.0 Hz, J = 8.6 Hz, 1H), 3.82 (dd, J = 5.5 Hz, J = 8.6 Hz, 1H), 3.35 – 3.30 (m, 1H), 1.84 – 1.79 (m, 2H), 1.74 – 1.63 (m, 6H), 1.50 – 1.45 (m, 2H), 1.27 – 1.24 (m, 2H), 1.18 – 1.14 (m, 2H) ppm; ¹³C NMR (100 MHz, CDCl₃) δ 154.0, 149.0, 131.9, 129.1, 128.7, 126.3, 110.7, 106.4, 72.5, 69.7, 36.1, 34.5, 25.2, 24.1, 23.8, 11.5 (d, J = 3.1 Hz) ppm.
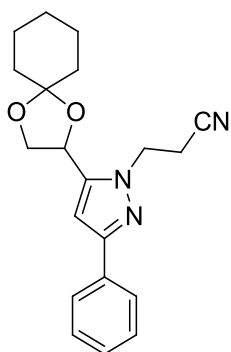
3-(5-{1,4-dioxaspiro[4.5]decan-2-yl}-3-phenyl-1H-pyrazol-1-yl)propanenitrile

(185d): orange oil, 41%, R_f = 0.28 (CyH/EtOAc 3:1), UHPLC-ESI-MS: R_t = 3.15, m/z = 338.2 [M +

H] [+]. ^{1}H NMR (300 MHz, CDCl$_3$) δ 7.76 (d, J = 7.4 Hz, 2H), 7.40 (t, J = 7.3 Hz, 2H), 7.33 (d, J = 7.2

Hz, 1H), 6.48 (s, 1H), 5.22 (t, J = 6.6 Hz, 1H), 4.65 − 4.48 (m, 2H), 4.39 (t, J = 7.5 Hz, 1H), 4.16 (t, J

= 7.6 Hz, 1H), 3.04 (dd, J = 7.2 Hz, J = 14.3 Hz, 2H), 1.69 − 1.55 (m, 8H), 1.44 (d, J = 4.8 Hz, 2H)

ppm; ^{13}C NMR (100 MHz, CDCl$_3$) δ 151.5, 141.8, 132.7, 128.7, 128.0, 125.6, 117.1, 111.4, 102.0,

68.8, 68.2, 45.5, 36.1, 35.0, 25.0, 24.0, 23.9, 19.1 ppm.
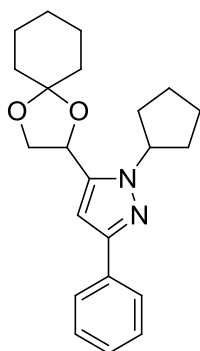
1-cyclopentyl-5-{1,4-dioxaspiro[4.5]decan-2-yl}-3-phenyl-1H-pyrazole **(185e):**

yellow oil, 70%, R_f = 0.59 (CyH/EtOAc 3:1), UHPLC-ESI-MS: R_t = 3.84, m/z = 353.2 [M + H] [+]. [1]H

NMR (300 MHz, CDCl$_3$) δ 7.81 − 7.78 (m, 2H), 7.37 (t, J = 7.5 Hz, 2H), 7.29 − 7.24 (m, 1H), 6.48 (s,

1H), 5.22 (t, J = 6.7 Hz, 1H), 4.82 − 4.72 (m, 1H), 4.34 (dd, J = 6.3 Hz, J = 8.2 Hz, 1H), 4.09 (dd, J =

7.3 Hz, J = 8.0 Hz, 1H), 2.24 − 2.11 (m, 3H), 2.09 − 1.98 (m, 3H), 1.72 − 1.61 (m, 10H), 1.46 − 1.43

(m, 2H) ppm; ^{13}C NMR (100 MHz, CDCl$_3$) δ 149.7, 141.0, 133.8, 128.4, 127.3, 125.5, 110.8, 100.9,

69.2, 68.5, 60.0, 36.2, 35.3, 33.1 (d, J = 5.8 Hz), 25.1, 24.7 (d, J = 6.2 Hz), 23.9 (d, J = 0.9 Hz) 8 ppm.
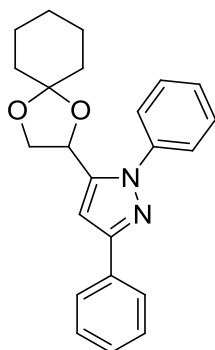
5-{1,4-dioxaspiro[4.5]decan-2-yl}-1,3-diphenyl-1H-pyrazole (185f): brown oil,

55%, R_f = 0.81 (CyH/EtOAC 9:1), UHPLC-ESI-MS: R_t = 3.56, m/z = 361.2 [M + H] [+]. ^{1}H NMR (300

MHz, CDCl$_3$) δ 7.33 − 7.20 (m, 10H), 6.58 (s, 1H), 5.27 (dd, J = 6.4 Hz, 7.4 Hz, 1H), 4.38 (dd, J = 6.3

Hz, 8.2 Hz, 1H), 4.07 (t, J = 7.8 Hz, 1H), 1.79 – 1.59 (m, 8H), 1.48 – 1.41 (m, 2H) ppm; ^{13}C NMR (100 MHz, CDCl$_3$) δ 152.1, 144.1, 139.9, 130.4, 128.8, 128.7, 128.4, 128.2, 127.4, 125.2, 110.4, 105.6, 72.4, 69.6, 36.2, 35.3, 25.1, 24.0, 23.8 ppm.

Synthesis of 187a-d: to **40** (1.0 eq) was added the corresponding ketone (3.0 eq) and a catalytic amount of p-TSA was added. The reaction was stirred at room temperature overnight. The solvent was removed under reduced pressure and the crude was re-dissolved in Et2O and washed three times with NaHCO3. The organic layer was dried over Mg
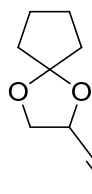
2-ethynyl-1,4-dioxaspiro[4.4]nonane (187a): yellowish oil, 76%, R_f = 0.55 (CyH/EtOAC 9:1). ^{1}H NMR (300 MHz, CDCl$_3$) δ 4.65 (dt, J = 2.1 Hz, J = 6.5 Hz, 1H), 4.13 (dd, J = 6.6 Hz, J = 8.0 Hz, 1H), 3.86 (dd, J = 6.4 Hz, J = 8.0 Hz, 1H), 2.48 (d, J = 2.1 Hz, 1H), 1.98 – 1.89 (m, 1H), 1.86 – 1.84 (m, 1H), 1.81 – 1.75 (m, 2H), 1.73 – 1.64 (m, 4H) ppm; ^{13}C NMR (100 MHz, CDCl$_3$) δ 120.2, 81.4, 73.9, 69.8, 64.8, 36.3, 36.1, 23.6, 23.3 ppm.
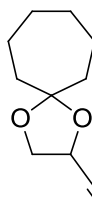
2-ethynyl-1,4-dioxaspiro[4.6]undecane (187b): yellowish oil, 82%, R_f = 0.48 (CyH/EtOAC 9:1). ^{1}H NMR (300 MHz, CDCl$_3$) δ 4.64 (d, J = 6.0 Hz, 1H), 4.11 (t, J = 7.5 Hz, 1H), 3.87 (t, J = 7.2 Hz, 1H), 2.47 (s, 1H), 1.94 (d, J = 4.5 Hz, 2H), 1.78 (d, J = 7.4 Hz, 2H), 1.55 (s, 8H) ppm; ^{13}C NMR (100 MHz, CDCl$_3$) δ 115.2, 81.4, 73.8, 69.3, 64.8, 38.9, 38.7, 29.3, 29.2, 22.4, 22.3 ppm.
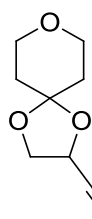
2-ethynyl-1,4,8-trioxaspiro[4.5]decane (187c): yellowish oil, 68 %, R_f = 0.33 (CyH/EtOAc 9:1). ^{1}H NMR (300 MHz, CDCl$_3$) δ 4.75 (t, J = 6.1 Hz, 1H), 4.18 (t, J = 6.9 Hz, 1H), 3.98 (t, J = 7.8 Hz, 1H), 3.83 – 3.72 (m, 4H), 2.50 (s, 1H), 1.95 – 1.83 (m, 2H), 1.73 (d, J = 3.5 Hz, 2H) ppm; ^{13}C NMR (100 MHz, CDCl$_3$) δ 108.2, 81.3, 74.1, 69.6, 65.9 (d, J = 3.7 Hz), 65.1, 36.5, 36.2 ppm.
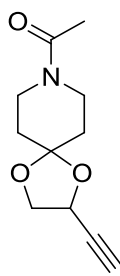
1-{2-ethynyl-1,4-dioxa-8-azaspiro[4.5]decan-8-yl}ethan-1-one (**187d**): yellowish oil, 72%, R_f = 0.46 (CyH/EtOAC 1:3). ^{1}H NMR (300 MHz, CDCl$_3$) δ 4.75 − 4.73 (m, 1H), 4.17 (dd, J = 6.3 Hz, J = 8.1 Hz, 1H), 3.96 (dd, J = 5.9 Hz, J = 8.1 Hz, 1H), 3.70 − 3.63 (m, 2H), 3.54 − 3.48 (m, 2H), 2.50 (d, J = 1.9 Hz, 1H), 2.07 (s, 3H), 1.87 − 1.77 (m, 2H), 1.69 − 1.62 (m, 2H) ppm; ^{13}C NMR (100 MHz, CDCl$_3$) δ 168.7, 108.8, 81.0 (d, J = 13.2 Hz), 74.3 (d, J = 9.1 Hz), 69.7, 65.2, 44.1, 39.3, 35.8 (d, J = 22.0 Hz), 34.9 (d, J = 24.3 Hz), 21.3 ppm.

Synthesis of 186: The compound was synthesized following the general procedure for the synthesis of ynones (using benzoylchloride and the corresponding terminal alkyne) and pyrazoles (using methylhydrazine)
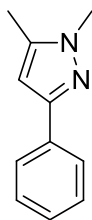
1,5-dimethyl-3-phenyl-1H-pyrazole (**186**): brownish oil, 90%, R_f = 0.38 (CyH/EtOAc 3:1), UHPLC-ESI-MS: R_t = 2.50, m/z = 173.2 [M + H] $^+$. ^{1}H NMR (300 MHz, CDCl$_3$) δ 7.78 (d, J = 7.8 Hz, 2H), 7.39 (d, J = 7.6 Hz, 2H), 7.30 (d, J = 7.3 Hz, 1H), 6.33 (s, 1H), 3.81 (s, 3H), 2.29 (s, 3H) ppm; ^{13}C NMR (100 MHz, CDCl$_3$) δ 149.8, 139.6, 133.6, 128.4. 127.2, 125.3, 102.4, 36.0, 11.1 ppm.

Synthesis of 189a-d: to a stirred solution of the corresponding ynone (1.0 eq) in EtOH (2 mL) was added methyl hydrazine (1.3 eq). The mixture was stirred at room temperature until starting material consumption (monitored by TLC) (normally 2 − 3 hours). Solvent was removed under reduced pressure, the crude was redissolved in ACN (1 mL), filtered and purified by preparative HPLC.[342]
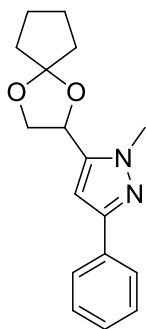
5-{1,4-dioxaspiro[4.4]nonan-2-yl}-1-methyl-3-phenyl-1H-pyrazole **(189a)**:
orange oil, 69%, R_f = 0.38 (CyH/EtOAc 3:1), UHPLC-ESI-MS: R_t = 3.02, m/z = 285.2 [M + H]$^+$.
^{1}H NMR (300 MHz, CDCl$_3$) δ 7.77 (d, J = 7.2, 2H), 7.37 (d, J = 7.7 Hz, 2H), 7.30 – 7.25 (m,
1H), 6.51 (s, 1H), 5.09 (t, J = 6.7 Hz, 1H), 4.26 (dd, J = 6.8 Hz, J = 8.1 Hz, 1H), 4.01 (dd, J =
7.0 Hz, J = 8.0 Hz, 1H), 3.92 (s, 3H), 1.90 – 1.84 (m, 4H), 1.73 – 1.68 (m, 4H) ppm; ^{13}C
NMR (100 MHz, CDCl$_3$) δ 150.0, 141.3, 133.2, 128.4, 127.4, 125.3, 120.0, 101.6, 69.1, 68.4,
37.0, 36.4, 36.1, 23.4, 23.3 ppm.
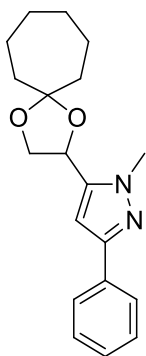
5-{1,4-dioxaspiro[4.6]undecan-2-yl}-1-methyl-3-phenyl-1H-pyrazole **(189b)**:
orange oil, 57%, R_f = 0.48 (CyH/EtOAc 3:1), UHPLC-ESI-MS: R_t = 3.36, m/z = 313.2 [M + H]$^+$.
^{1}H NMR (300 MHz, CDCl$_3$) δ 7.76 (d, J = 7.6 Hz, 2H), 7.38 (t, J = 7.5 Hz, 2H), 7.29 (d, J =
7.4 Hz, 1H), 6.50 (s, 1H), 5.11 (t, J = 6.7 Hz, 1H), 4.29 (t, J = 7.8 Hz, 1H), 4.01 (t, J = 7.7 Hz,
1H), 3.95 (s, 3H), 1.97 – 1.83 (m, 4H), 1.65 – 1.58 (m, 8H) ppm; ^{13}C NMR (100 MHz,
CDCl$_3$) δ 150.1, 141.2, 133.2, 128.5, 127.5, 125.4, 114.9, 101.6, 69.1, 68.1, 34.9, 38.3, 37.2,
29.2 (d, J = 5.7 Hz), 22.4 (d, J = 7.2 Hz) ppm.
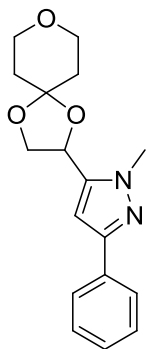
1-methyl-3-phenyl-5-{1,4,8-trioxaspiro[4.5]decan-2-yl}-1H-pyrazole **(189c)**:
brown oil, 85%, R_f = 0.27 (CyH/EtOAc 3:1), UHPLC-ESI-MS: R_t = 2.58, m/z = 301.2 [M + H]$^+$.

^{1}H NMR (300 MHz, CDCl$_3$) δ 7.77 – 7.75 (m, 2H), 7.38 (t, J = 7.4 Hz, 2H), 7.30 (d, J = 7.3 Hz, 1H), 6.50 (s, 1H), 5.20 (t, J = 6.6 Hz, 1H), 4.37 (dd, J = 6.3 Hz, J = 8.4 Hz, 1H), 4.14 (dd, J = 6.8 Hz, J = 8.4 Hz, 1H), 3.96 (s, 3H), 3.82 – 3.75 (m, 4H), 1.85 – 1.78 (m, 4H) ppm; ^{13}C NMR (100 MHz, CDCl$_3$) δ 150.2, 141.1, 133.1, 128.5, 127.6, 125.4, 108.0, 101.4, 69.3, 68.2, 65.9 (d, J = 3.7 Hz), 37.2, 36.9, 36.1 ppm.
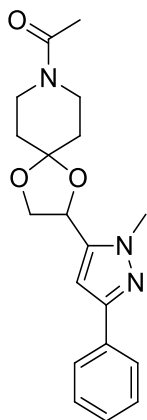
1-[2-(1-methyl-3-phenyl-1H-pyrazol-5-yl)-1,4-dioxa-8-azaspiro[4.5]decan-8-yl]ethan-1-one (189d): yellow oil, 44%, R_f = 0.66 (CHCl$_3$/MeOH 9:1), UHPLC-ESI-MS: R_t = 2.40, m/z = 342.2 [M + H] $^+$. ^{1}H NMR (300 MHz, CDCl$_3$) δ 7.76 (d, J = 7.6 Hz, 2H), 7.39 (t, J = 7.5 Hz, 2H), 7.31 (d, J = 7.2 Hz, 1H), 6.51 (s, 1H), 5.23 (dd, J = 6.1 Hz, J = 10.9 Hz, 1H), 4.40 (t, J = 6.8 Hz, 1H), 4.17 (dd, J = 7.1 Hz, J = 14.6 Hz, 1H), 3.97 (s, 3H), 3.74 – 3.68 (m, 2H), 3.59 – 3.51 (m, 2H), 2.12 (d, J = 5.6 Hz, 3H), 1.83 – 1.74 (m, 4H) ppm; ^{13}C NMR (100 MHz, CDCl$_3$) δ 169.0, 150.3, 141.1, 132.9, 128.6, 127.8, 125.5, 108.7, 101.4, 69.5 (d, J = 11.7 Hz), 68.4 (d, J = 5.7 Hz), 44.2 (d, J = 4.1 Hz), 39.5, 35.6 (d, J = 3.6 Hz), 21.3 ppm.

1H NMR (300 MHz, CDCl₃) 5-{1,4-dioxaspiro[4.5]decan-2-yl}-3-phenyl-1*H*-pyrazole (181a)
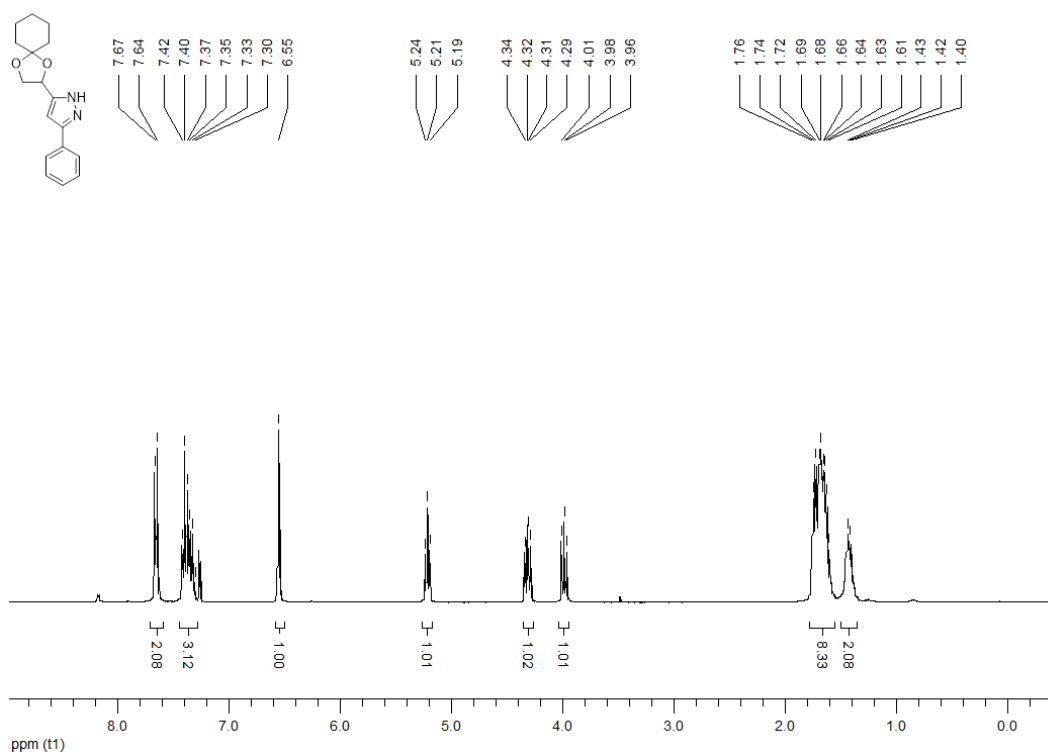
13C NMR (100 MHz, CDCl₃) 5-{1,4-dioxaspiro[4.5]decan-2-yl}-3-phenyl-1*H*-pyrazole (181a)
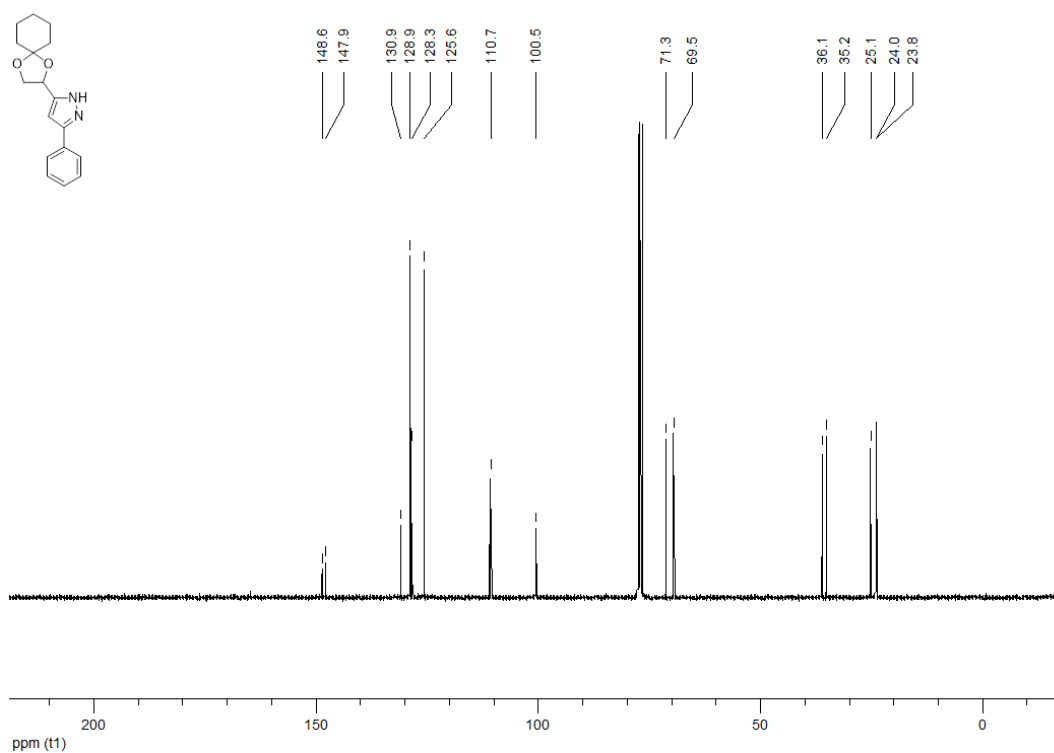
1H NMR (300 MHz, CDCl3) 5-{1,4-dioxaspiro[4.5]decan-2-yl}-3-(furan-2-yl)-1*H*-pyrazole (181b)

13C NMR (100 MHz, CDCl3) 5-{1,4-dioxaspiro[4.5]decan-2-yl}-3-(furan-2-yl)-1*H*-pyrazole (181b)

1H NMR (300 MHz, CDCl3) 5-{1,4-dioxaspiro[4.5]decan-2-yl}-3-(thiophen-2-yl)-1H-pyrazole (181c)

13C NMR (100 MHz, CDCl3) 5-{1,4-dioxaspiro[4.5]decan-2-yl}-3-(thiophen-2-yl)-1H-pyrazole (181c)
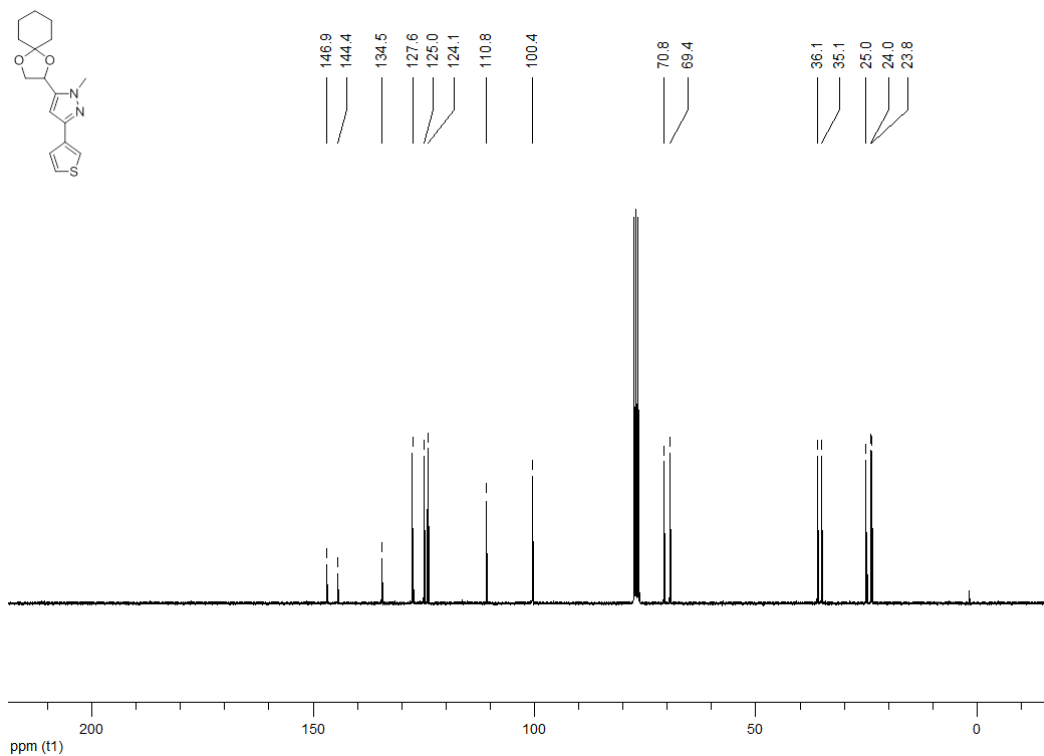
¹H NMR (300 MHz, CDCl₃) 5-{1,4-dioxaspiro[4.5]decan-2-yl}-3-(propan-2-yl)-1*H*-pyrazole (181d)

¹³C NMR (100 MHz, CDCl₃) 5-{1,4-dioxaspiro[4.5]decan-2-yl}-3-(propan-2-yl)-1*H*-pyrazole (181d)
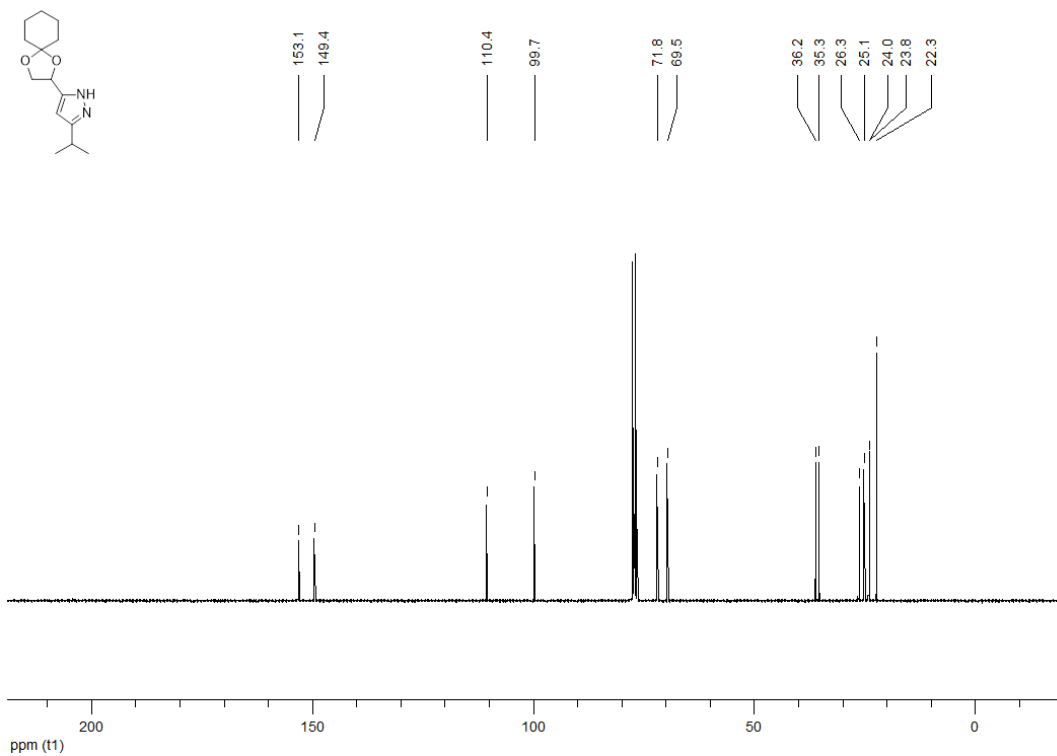
¹H NMR (300 MHz, CDCl₃) 3-cyclopropyl-5-{1,4-dioxaspiro[4.5]decan-2-yl}-1*H*-pyrazole (181e)
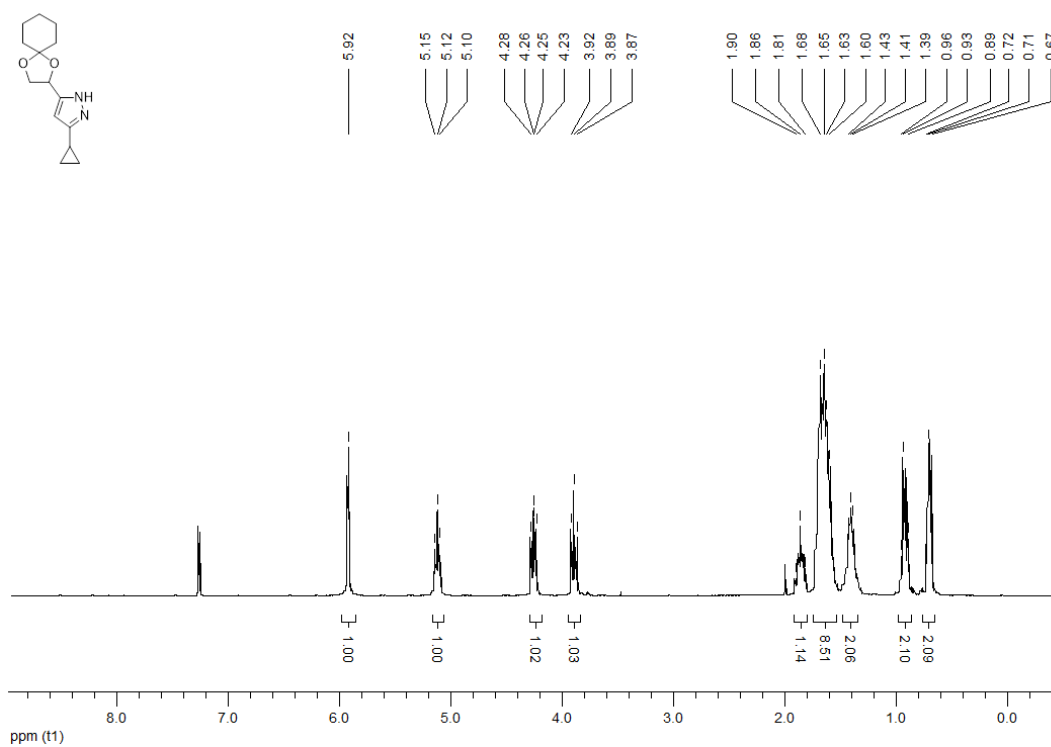
¹³C NMR (100 MHz, CDCl₃) 3-cyclopropyl-5-{1,4-dioxaspiro[4.5]decan-2-yl}-1*H*-pyrazole (181e)
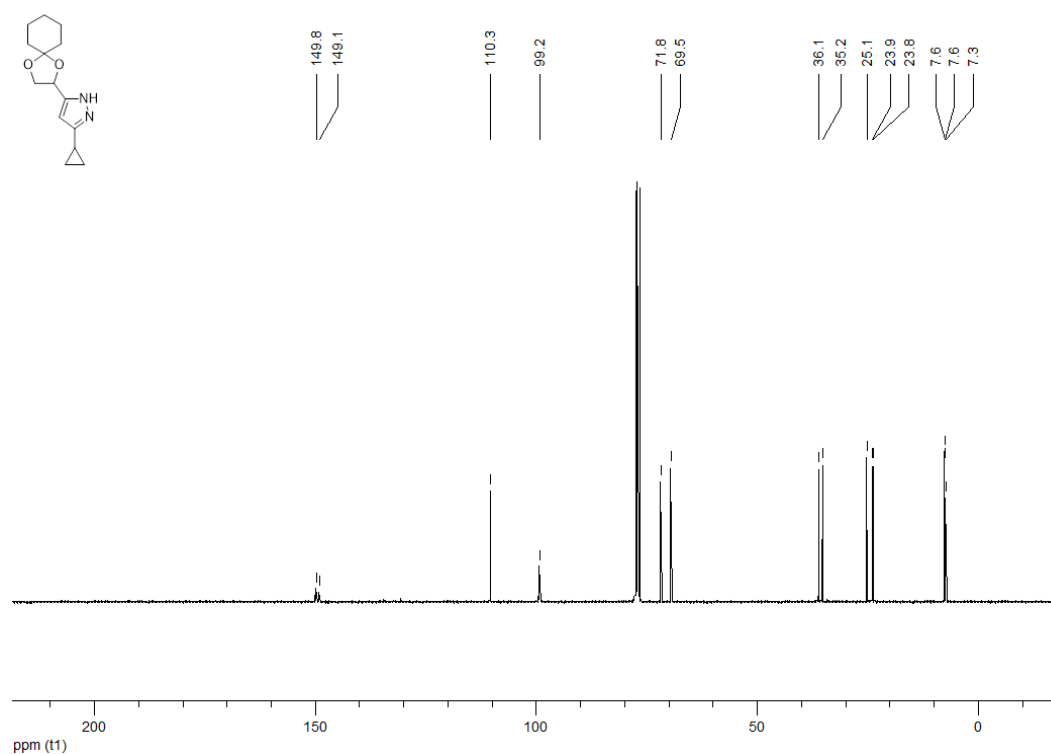
1H NMR (300 MHz, CDCl₃) 3-cyclopentyl-5-{1,4-dioxaspiro[4.5]decan-2-yl}-1H-pyrazole (181f)
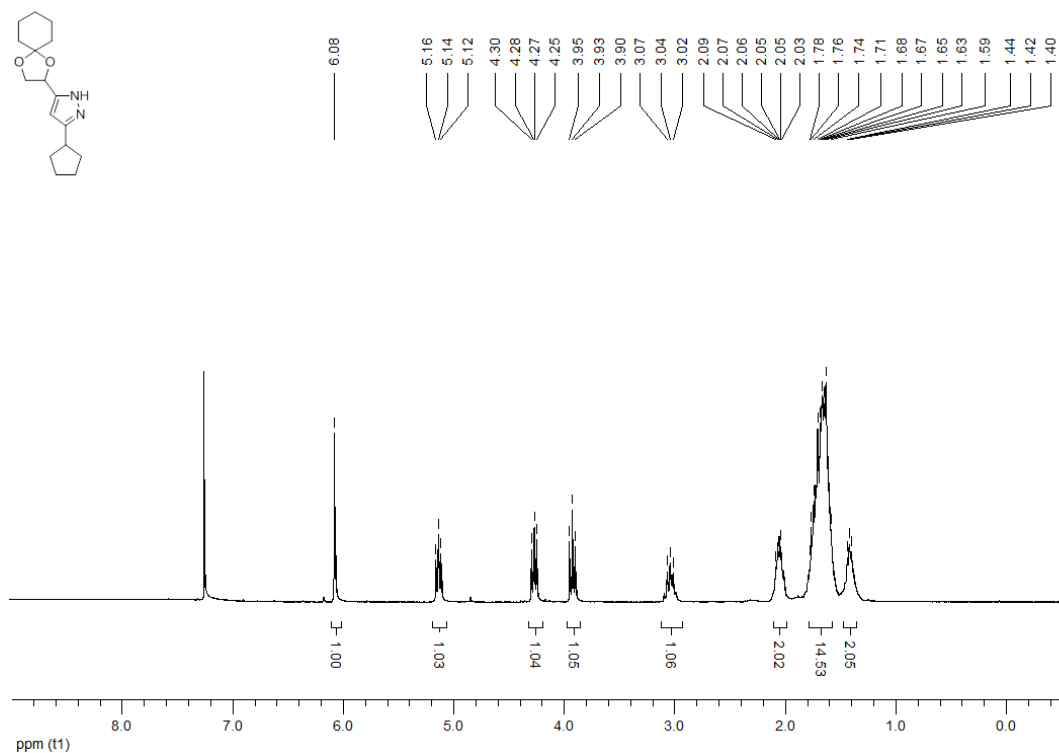
13C NMR (100 MHz, CDCl₃) 3-cyclopentyl-5-{1,4-dioxaspiro[4.5]decan-2-yl}-1H-pyrazole (181f)
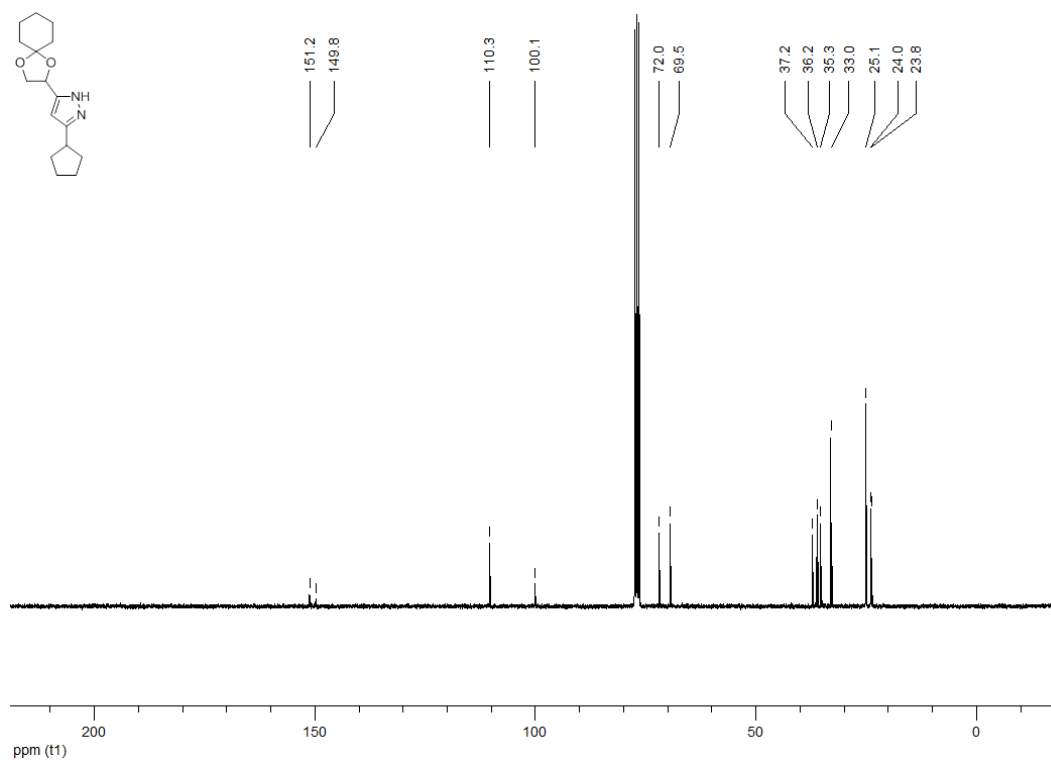
1H NMR (300 MHz, CDCl₃) 3-(adamantan-1-yl)-5-{1,4-dioxaspiro[4.5]decan-2-yl}-1H-pyrazole (181g)
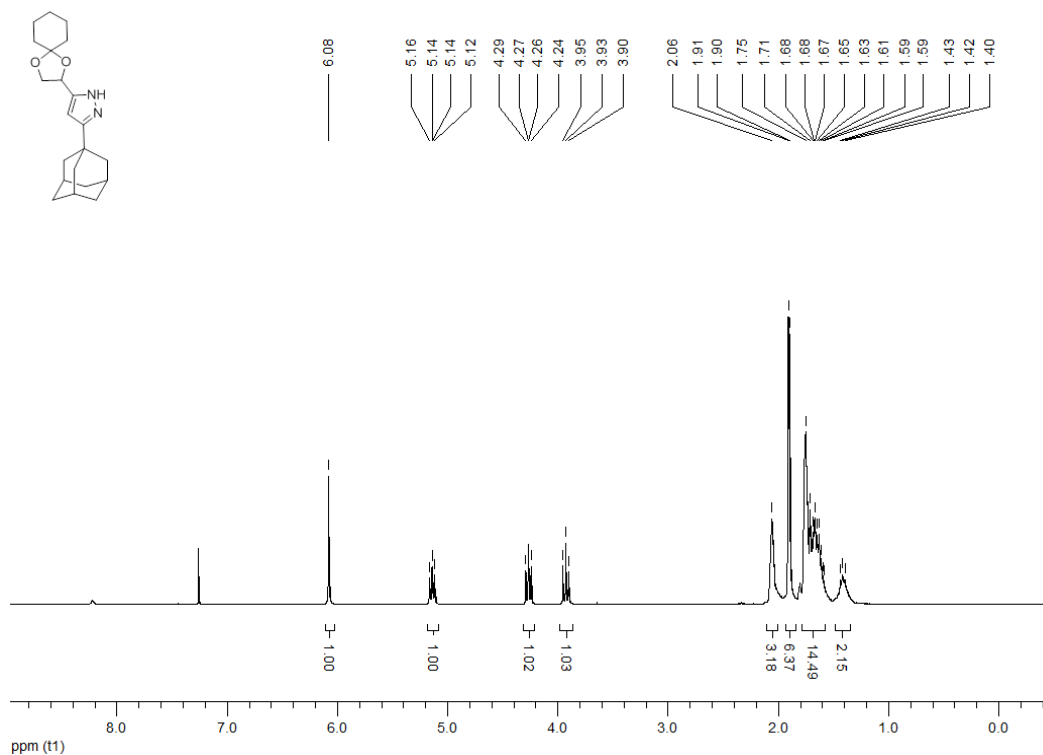
13C NMR (100 MHz, CDCl₃) 3-(adamantan-1-yl)-5-{1,4-dioxaspiro[4.5]decan-2-yl}-1H-pyrazole (181g)
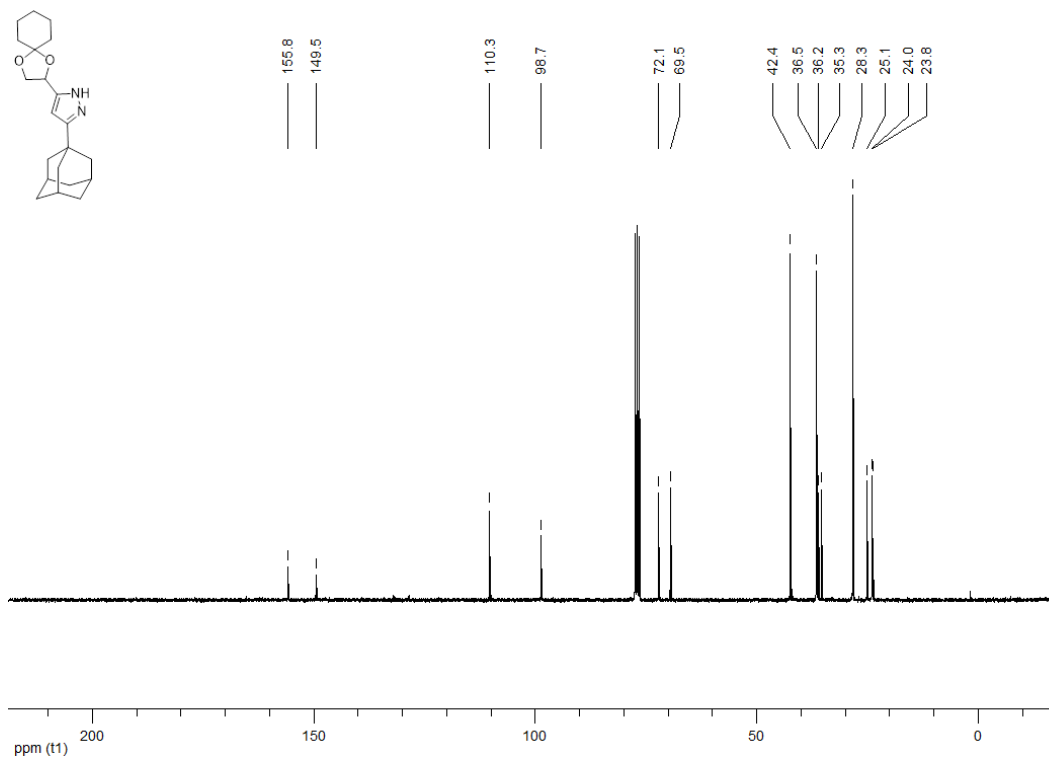
^{1}H NMR (300 MHz, CDCl$_3$) 5-{1,4-dioxaspiro[4.5]decan-2-yl}-1-methyl-3-phenyl-1*H*-pyrazole (182a)
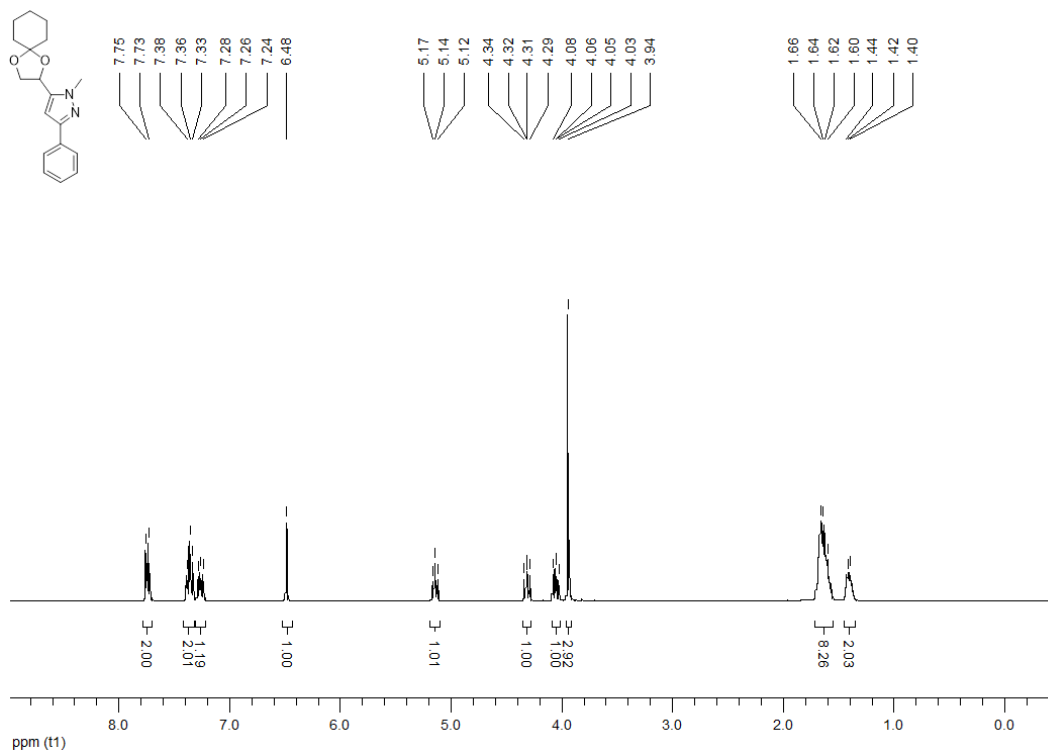
^{13}C NMR (100 MHz, CDCl$_3$) 5-{1,4-dioxaspiro[4.5]decan-2-yl}-1-methyl-3-phenyl-1*H*-pyrazole (182a)
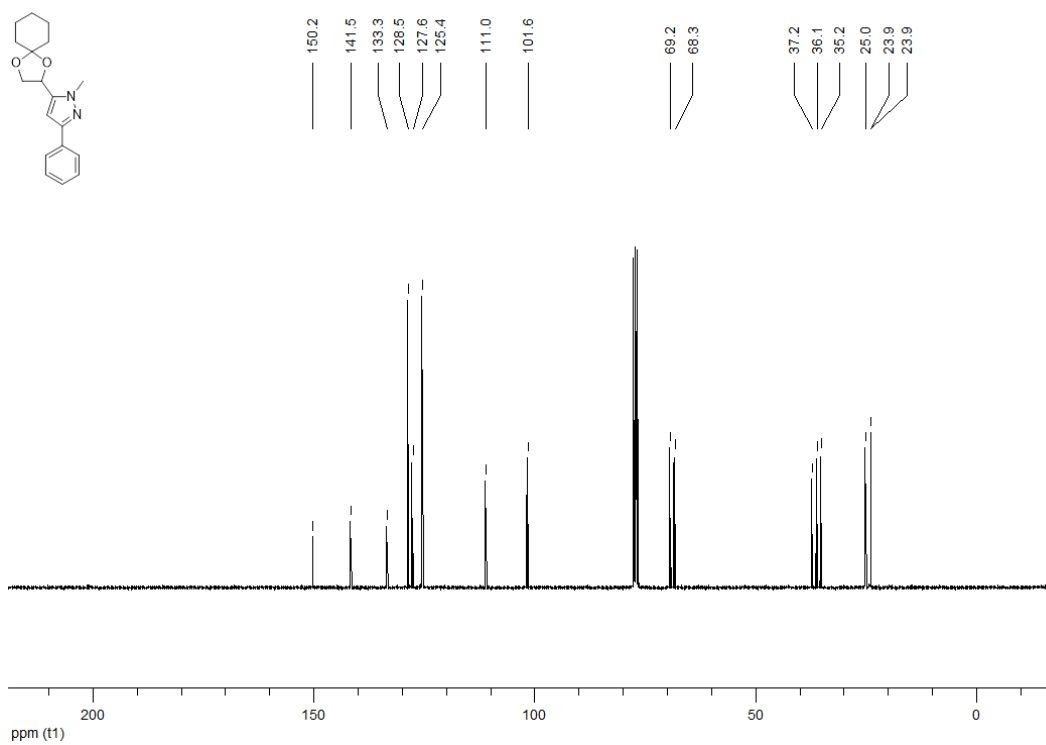
¹H NMR (300 MHz, CDCl₃) 5-{1,4-dioxaspiro[4.5]decan-2-yl}-3-(furan-2-yl)-1-methyl-1*H*-pyrazole (182b)
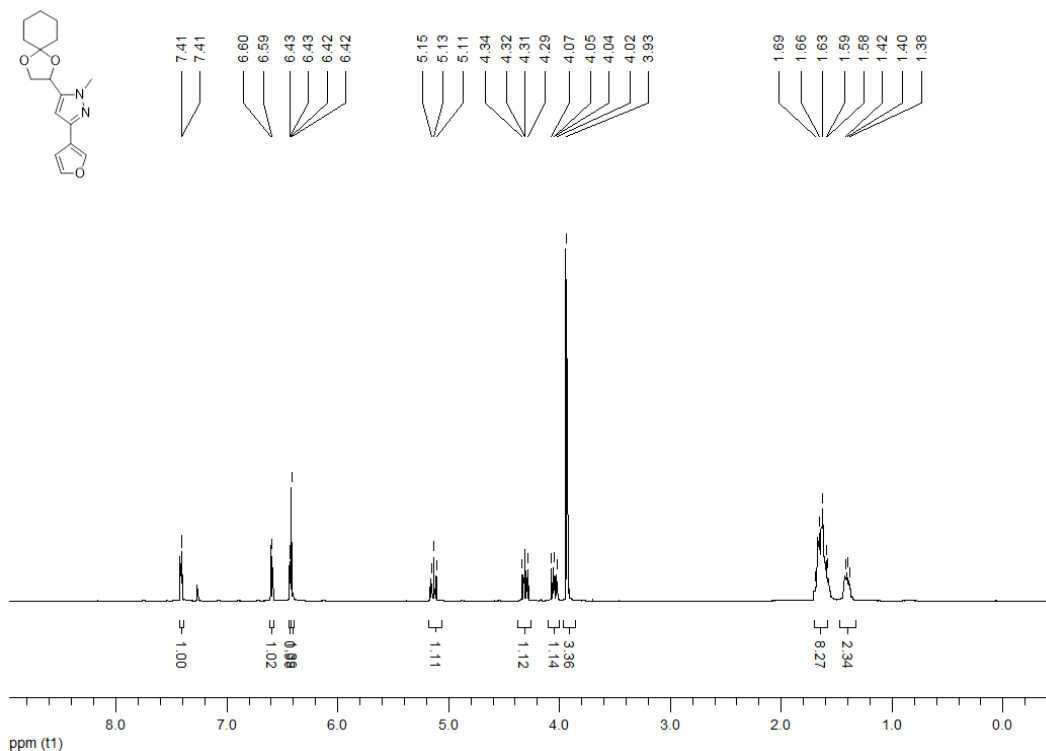
¹³C NMR (100 MHz, CDCl₃) 5-{1,4-dioxaspiro[4.5]decan-2-yl}-3-(furan-2-yl)-1-methyl-1*H*-pyrazole (182b)
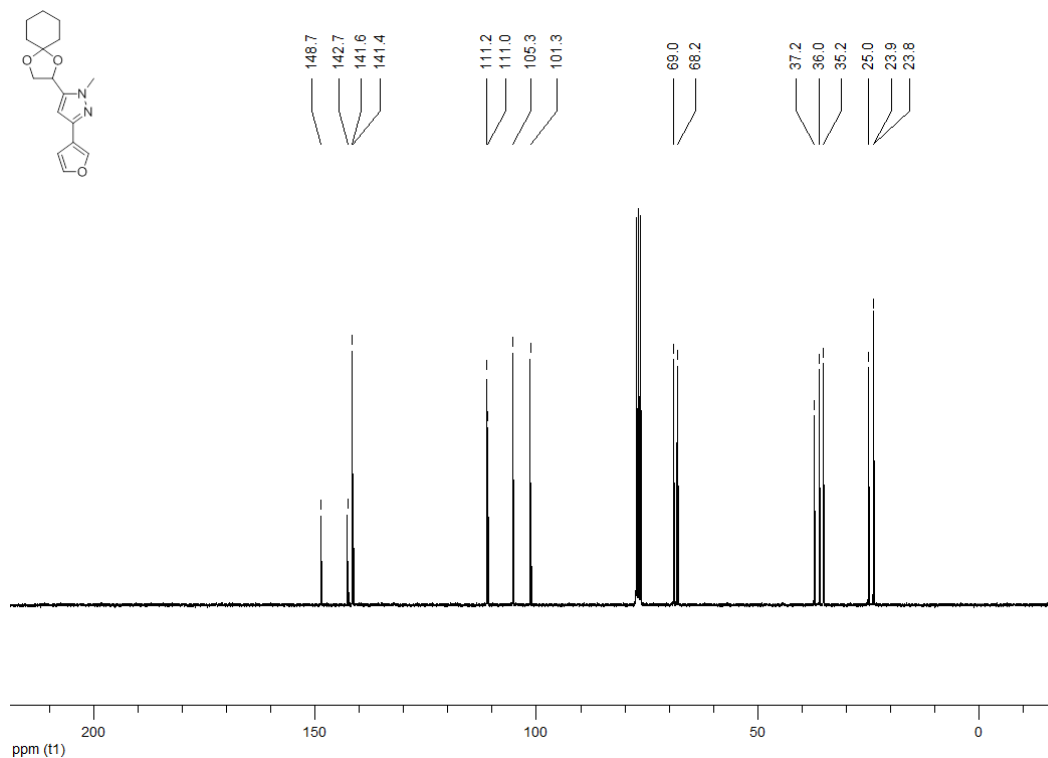
^{1}H NMR (300 MHz, CDCl$_3$) 5-{1,4-dioxaspiro[4.5]decan-2-yl}-1-methyl-3-(thiophen-2-yl)-1*H*-pyrazole (182c)
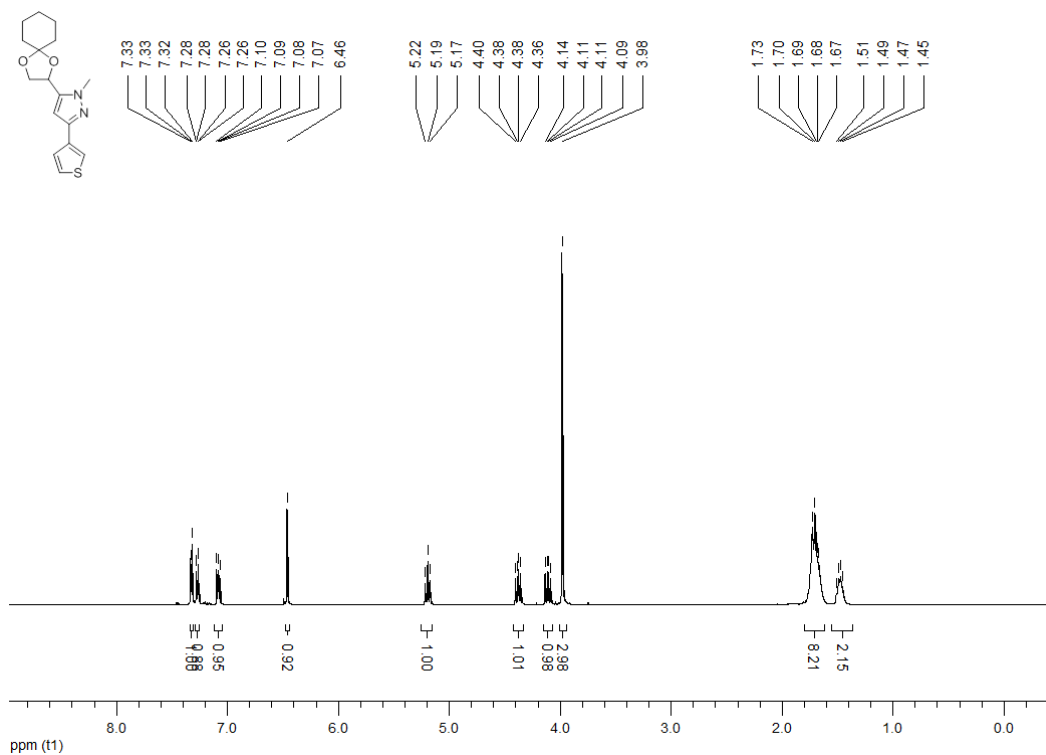
^{13}C NMR (100 MHz, CDCl$_3$) 5-{1,4-dioxaspiro[4.5]decan-2-yl}-1-methyl-3-(thiophen-2-yl)-1*H*-pyrazole (182c)
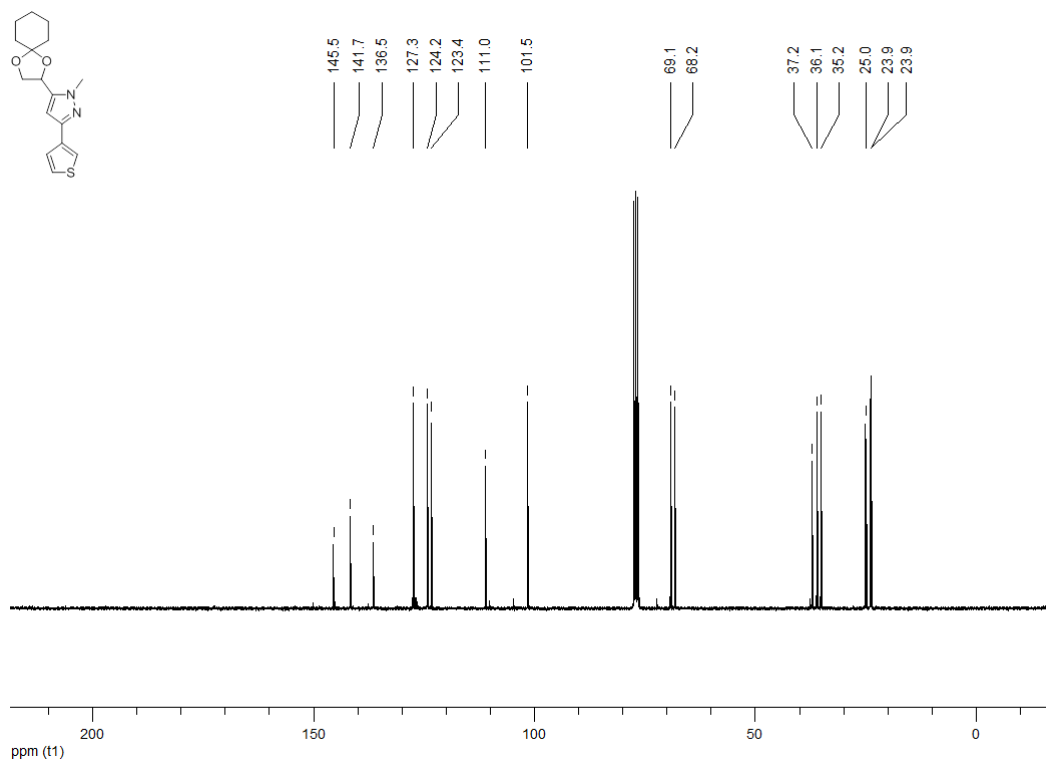
246
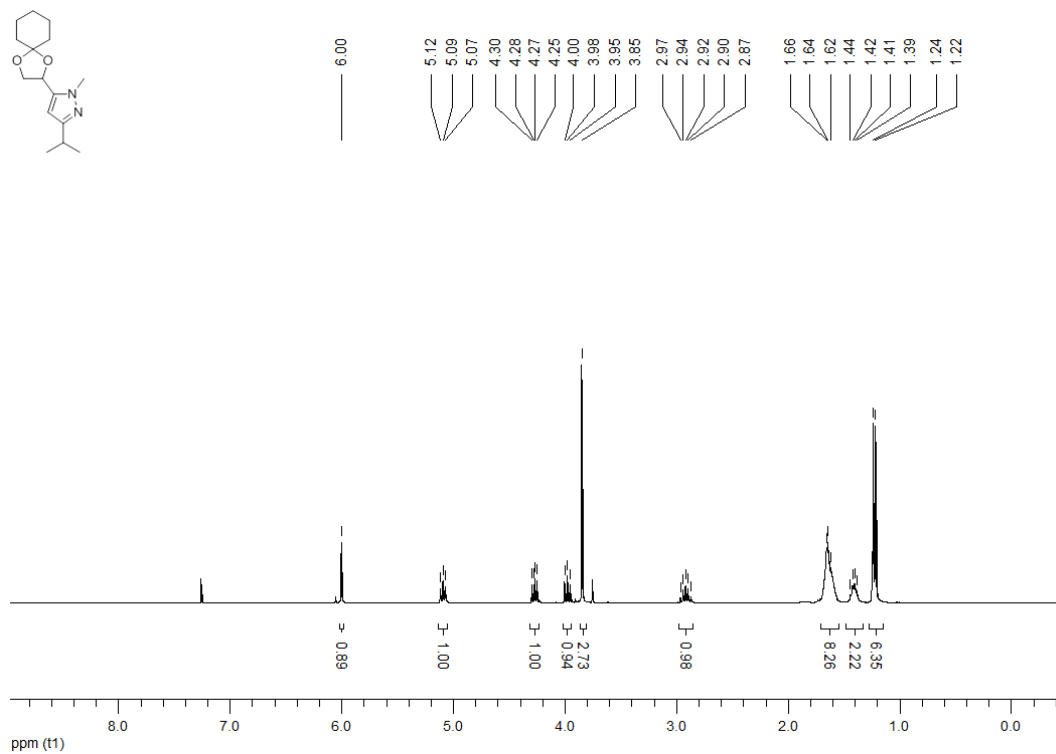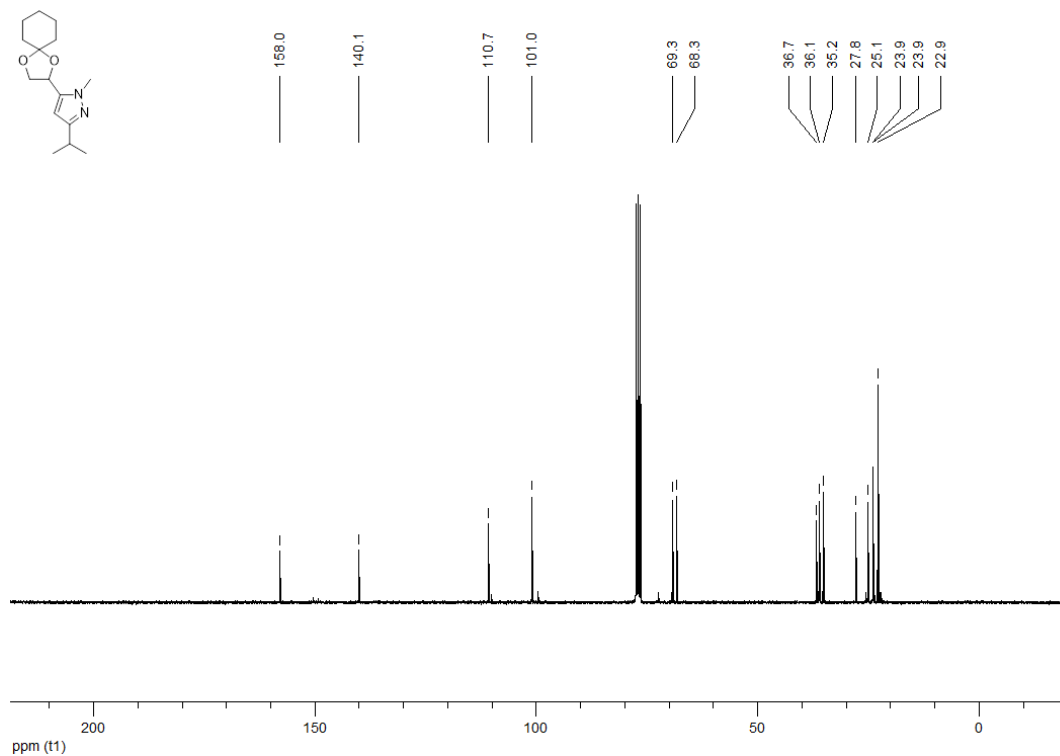
¹H NMR (300 MHz, CDCl₃) 3-cyclopropyl-5-{1,4-dioxaspiro[4.5]decan-2-yl}-1-methyl-1*H*-pyrazole (182e)
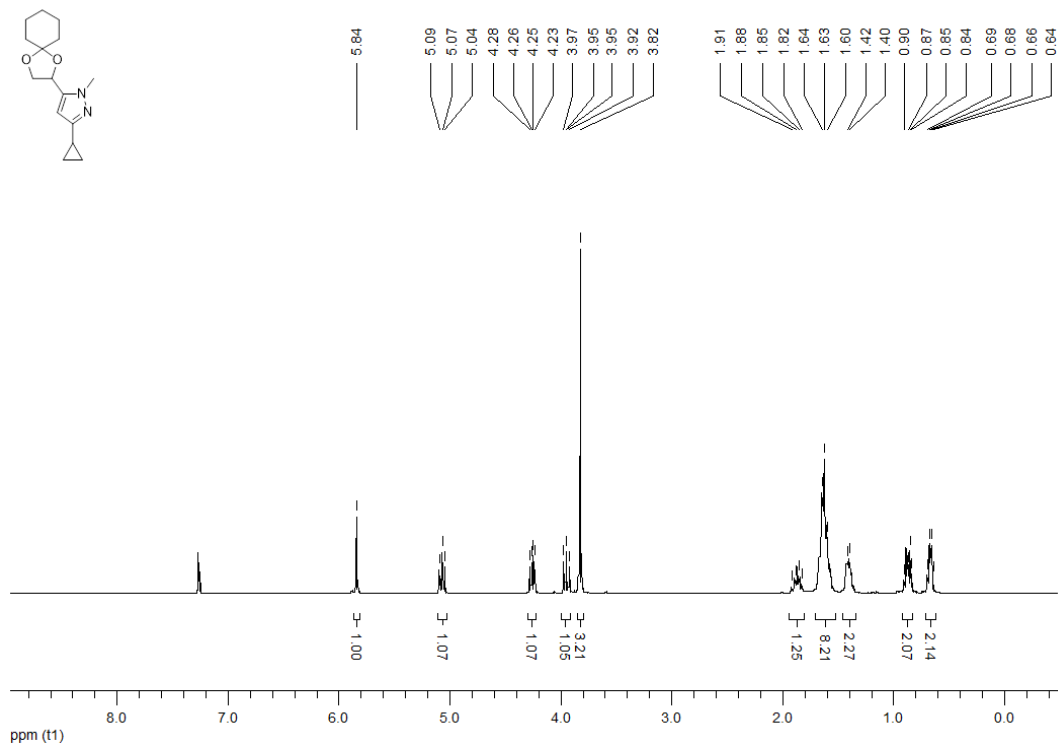
¹³C NMR (100 MHz, CDCl₃) 3-cyclopropyl-5-{1,4-dioxaspiro[4.5]decan-2-yl}-1-methyl-1*H*-pyrazole (182e)
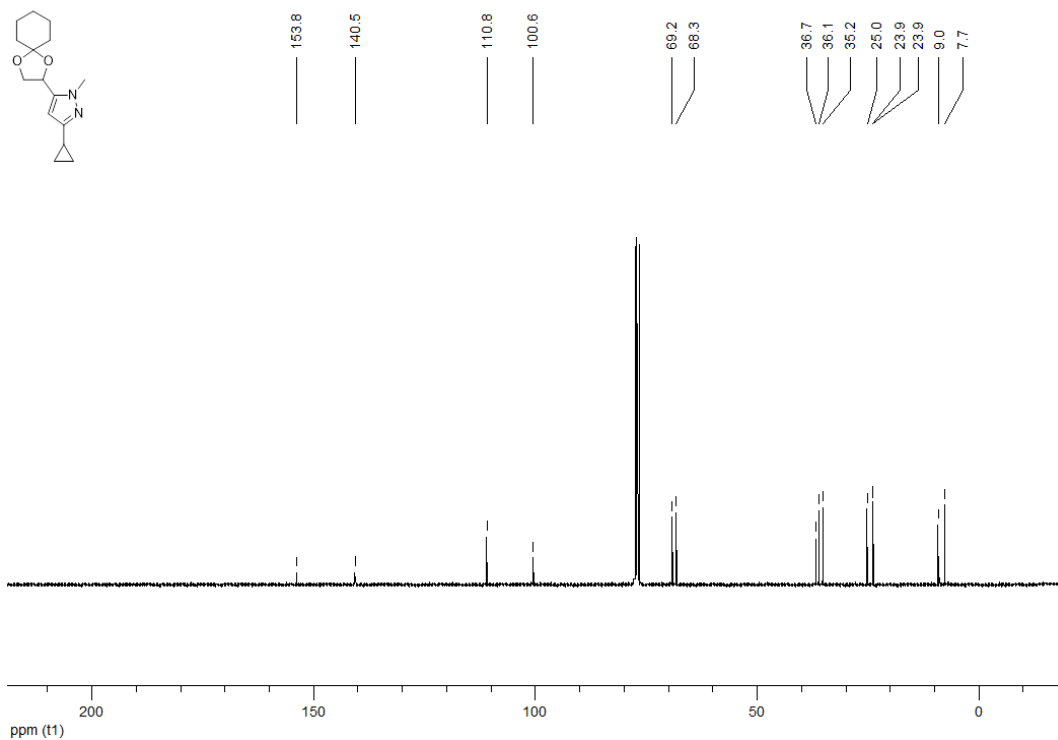
¹H NMR (300 MHz, CDCl₃) 3-cyclopentyl-5-{1,4-dioxaspiro[4.5]decan-2-yl}-1-methyl-1*H*-pyrazole (182f)
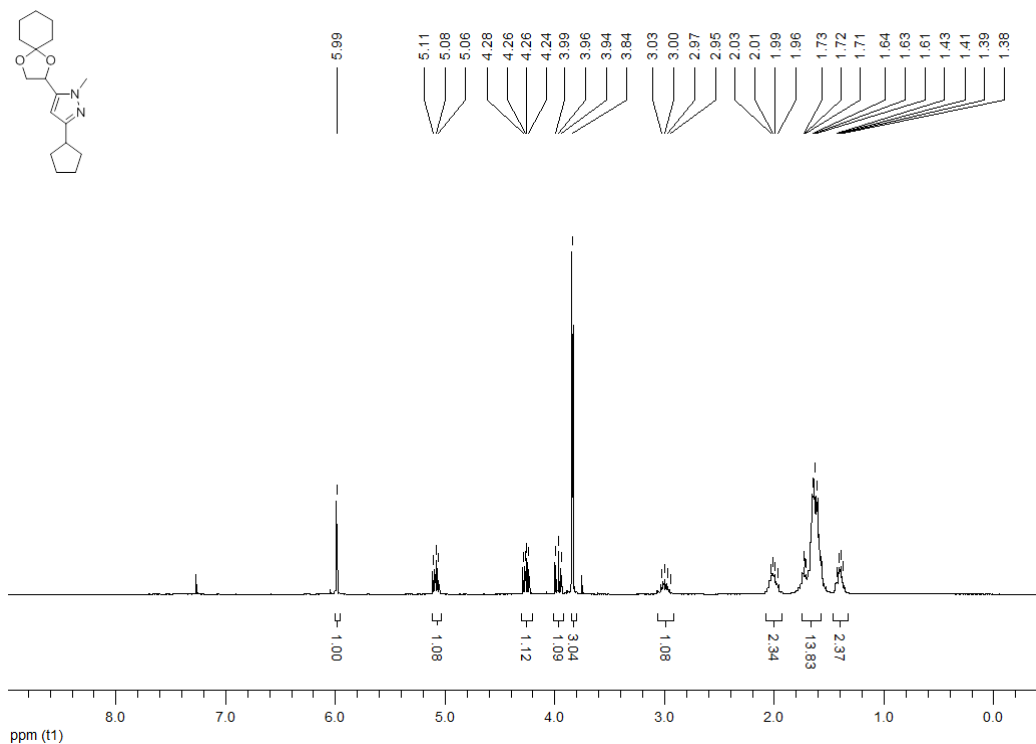
¹³C NMR (100 MHz, CDCl₃) 3-cyclopentyl-5-{1,4-dioxaspiro[4.5]decan-2-yl}-1-methyl-1*H*-pyrazole (182f)
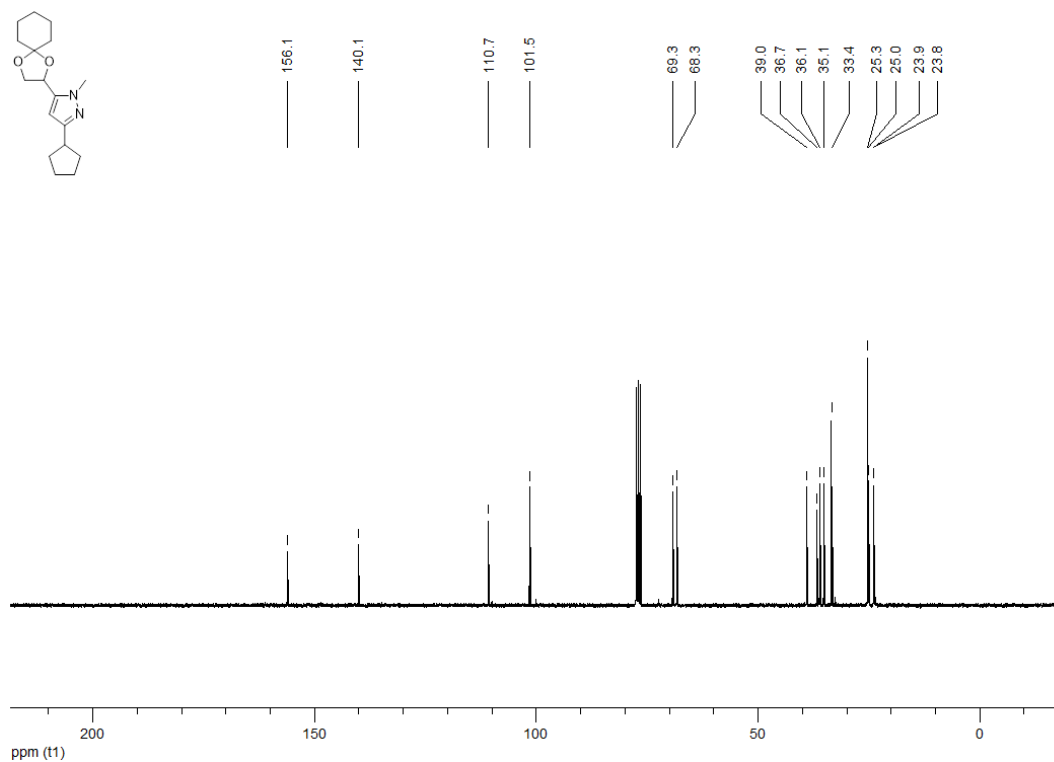
¹H NMR (300 MHz, CDCl₃) 3-(adamantan-1-yl)-5-{1,4-dioxaspiro[4.5]decan-2-yl}-1-methyl-1*H*-pyrazole (182g)
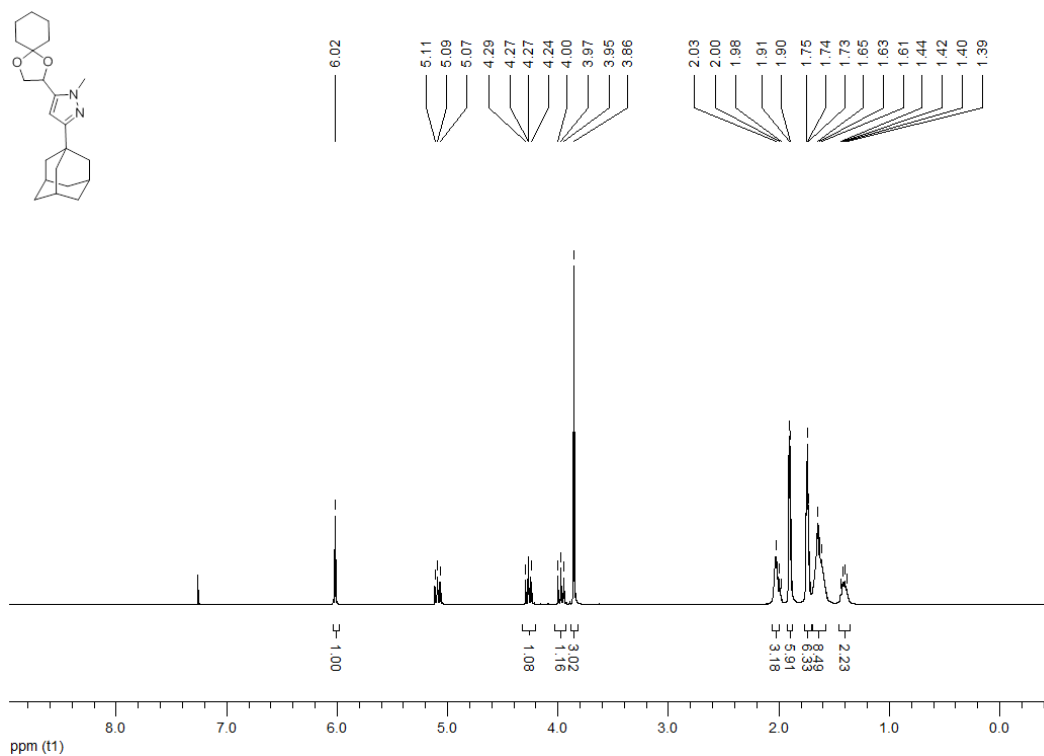
¹³C NMR (100 MHz, CDCl₃) 3-(adamantan-1-yl)-5-{1,4-dioxaspiro[4.5]decan-2-yl}-1-methyl-1*H*-pyrazole (182g)
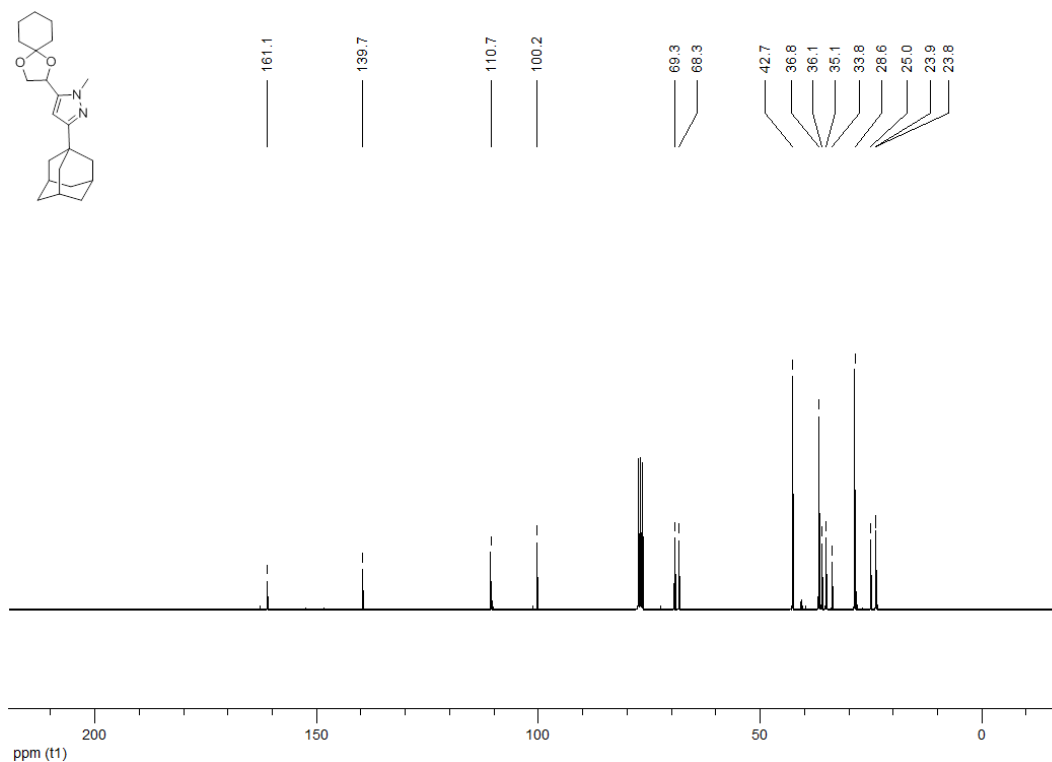
¹H NMR (300 MHz, CDCl₃) 5-{1,4-dioxaspiro[4.5]decan-2-yl}-1-methyl-3-(3-methylphenyl)-1H-pyrazole (182h)
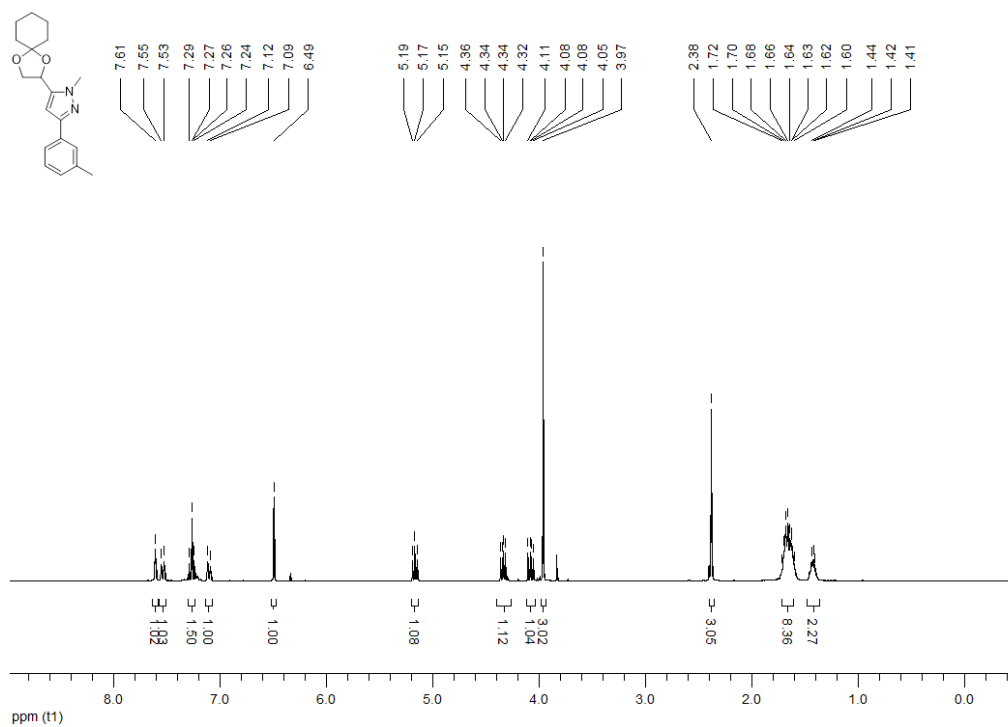
¹³C NMR (100 MHz, CDCl₃) 5-{1,4-dioxaspiro[4.5]decan-2-yl}-1-methyl-3-(3-methylphenyl)-1H-pyrazole (182h)
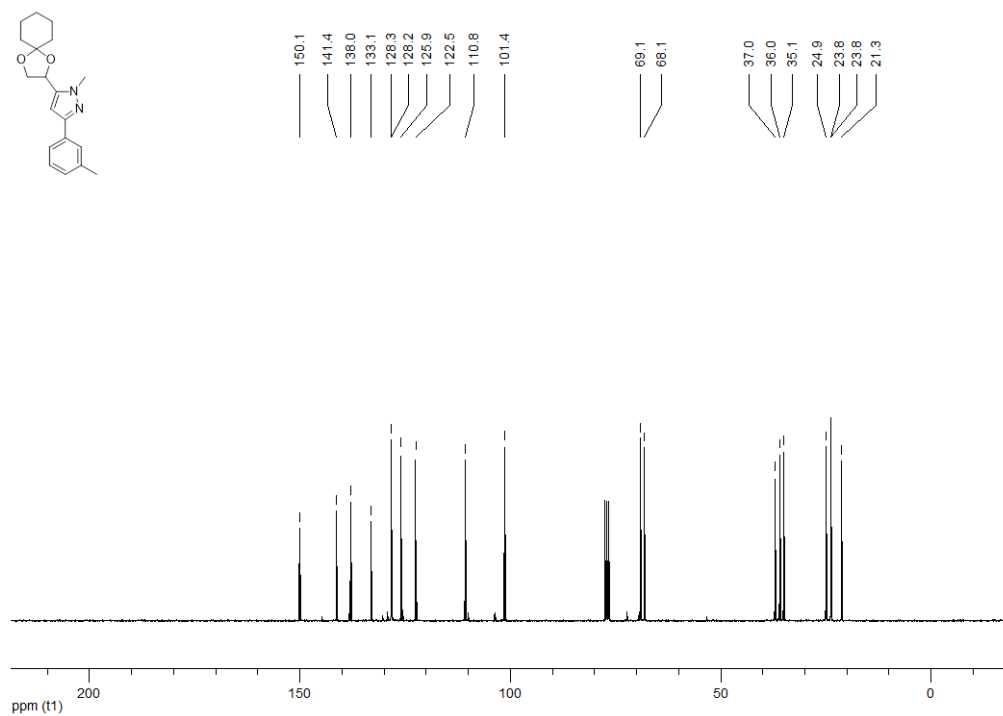
¹H NMR (300 MHz, CDCl₃) 3-(5-{1,4-dioxaspiro[4.5]decan-2-yl}-1-methyl-1H-pyrazol-3-yl)benzonitrile (182i)
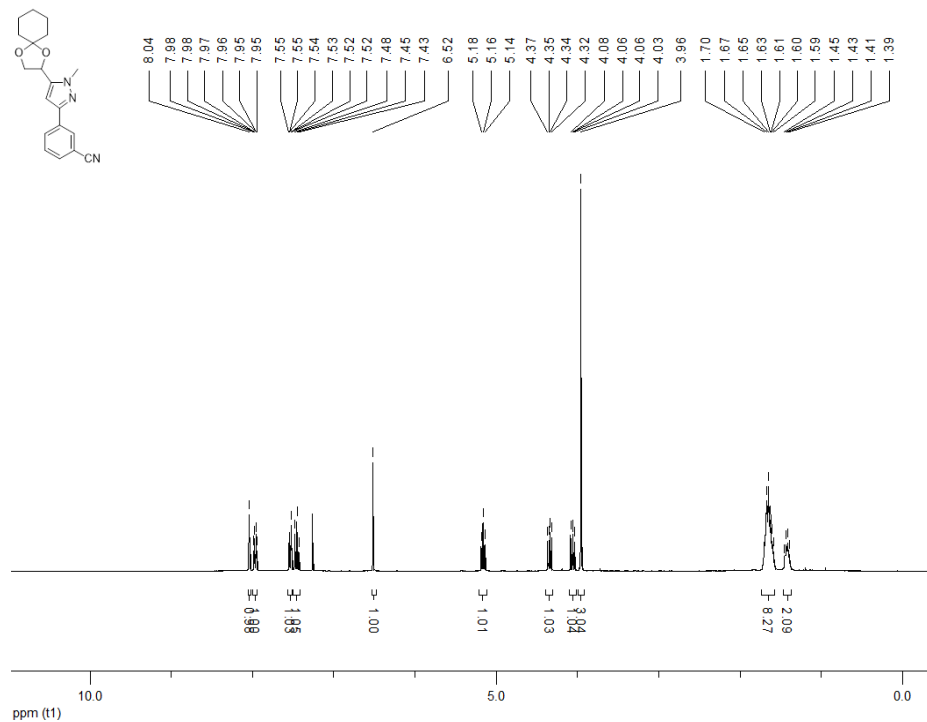
¹³C NMR (100 MHz, CDCl₃) 3-(5-{1,4-dioxaspiro[4.5]decan-2-yl}-1-methyl-1H-pyrazol-3-yl)benzonitrile (182i)

¹H NMR (300 MHz, CDCl₃) 3-(3-chloro-5-fluorophenyl)-5-{1,4-dioxaspiro[4.5]decan-2-yl}-1-methyl-1H-pyrazole (182j)

¹³C NMR (100 MHz, CDCl₃) 3-(3-chloro-5-fluorophenyl)-5-{1,4-dioxaspiro[4.5]decan-2-yl}-1-methyl-1H-pyrazole (182j)
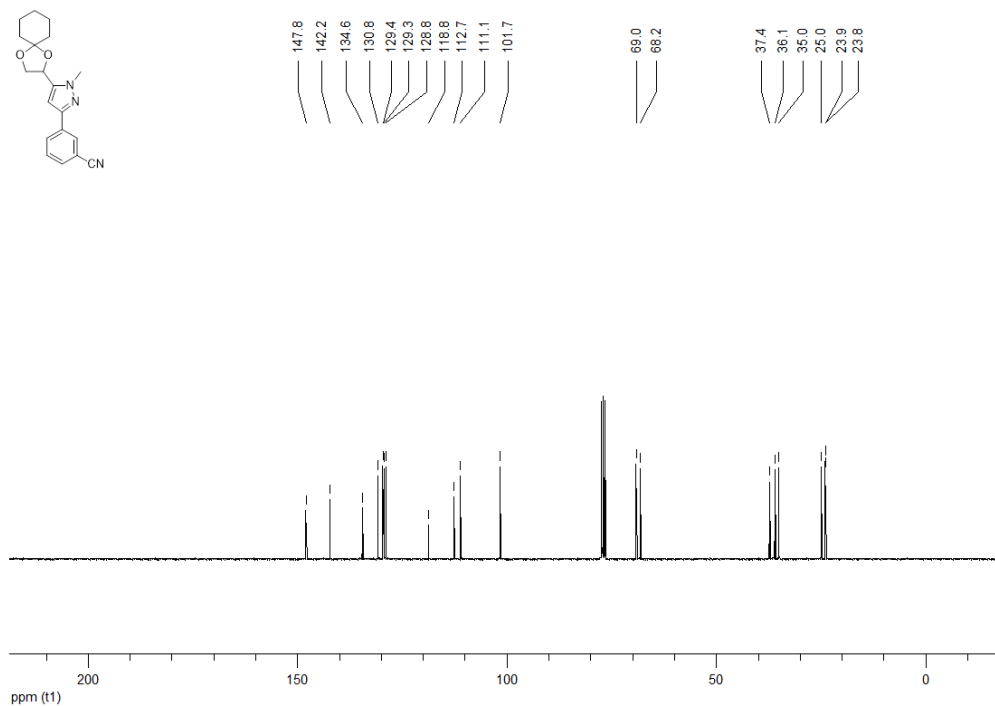
^{1}H NMR (300 MHz, CDCl$_3$) 4-(5-{1,4-dioxaspiro[4.5]decan-2-yl}-1-methyl-1H-pyrazol-3-yl)benzamide (182k)
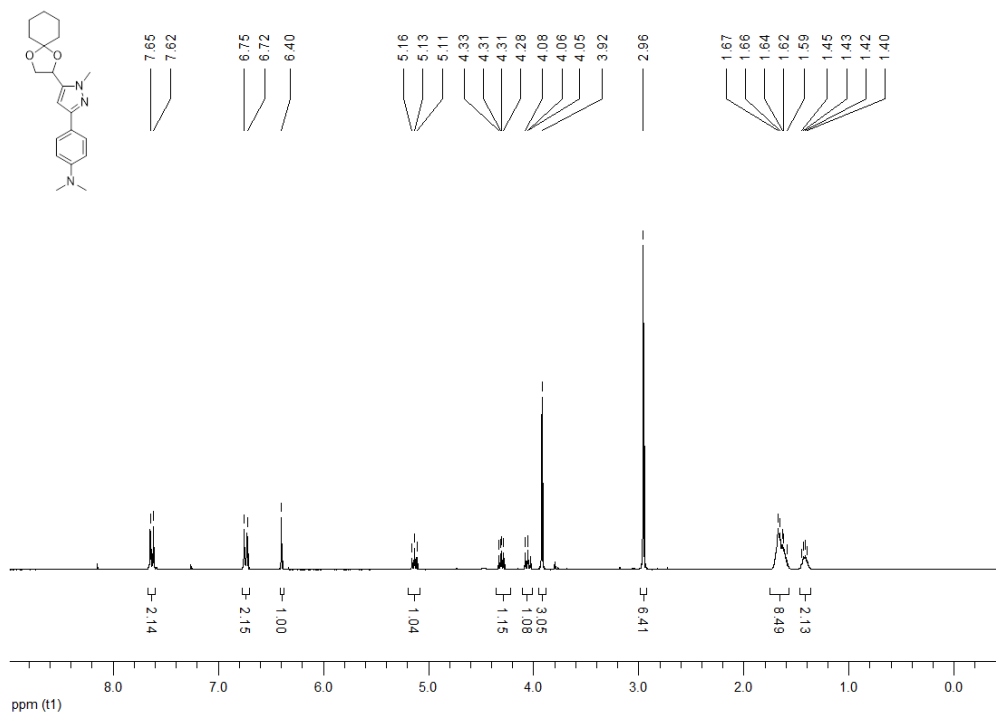
^{13}C NMR (100 MHz, CDCl$_3$) 4-(5-{1,4-dioxaspiro[4.5]decan-2-yl}-1-methyl-1H-pyrazol-3-yl)benzamide (182k)
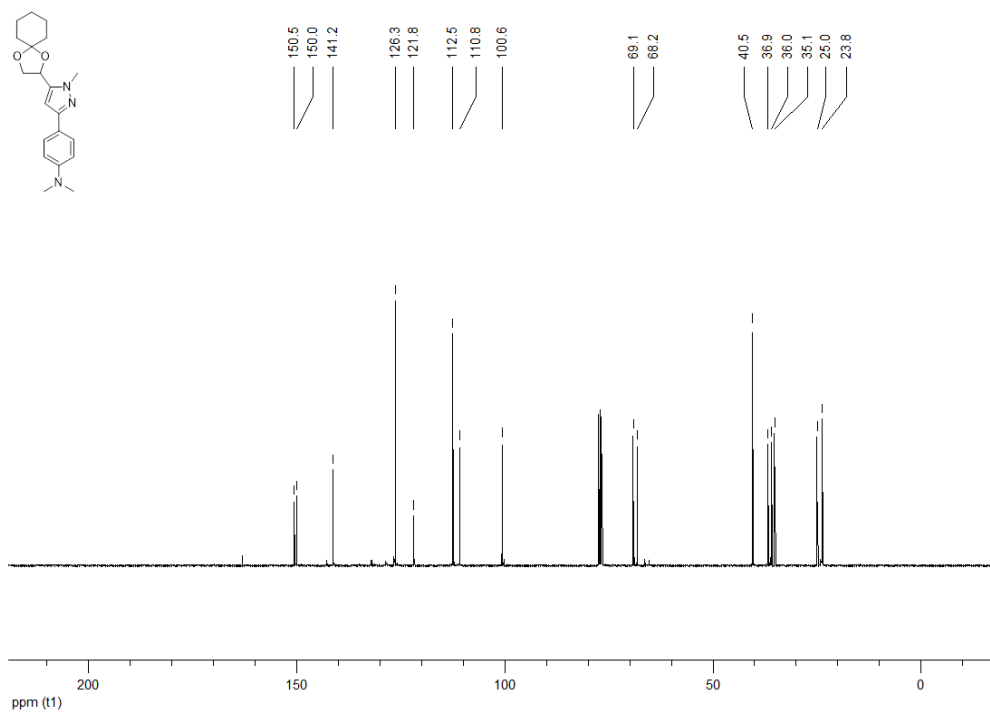
¹H NMR (300 MHz, CDCl₃) 5-(5-{1,4-dioxaspiro[4.5]decan-2-yl}-1-methyl-1H-pyrazol-3-yl)-1,2-oxazole (182l)
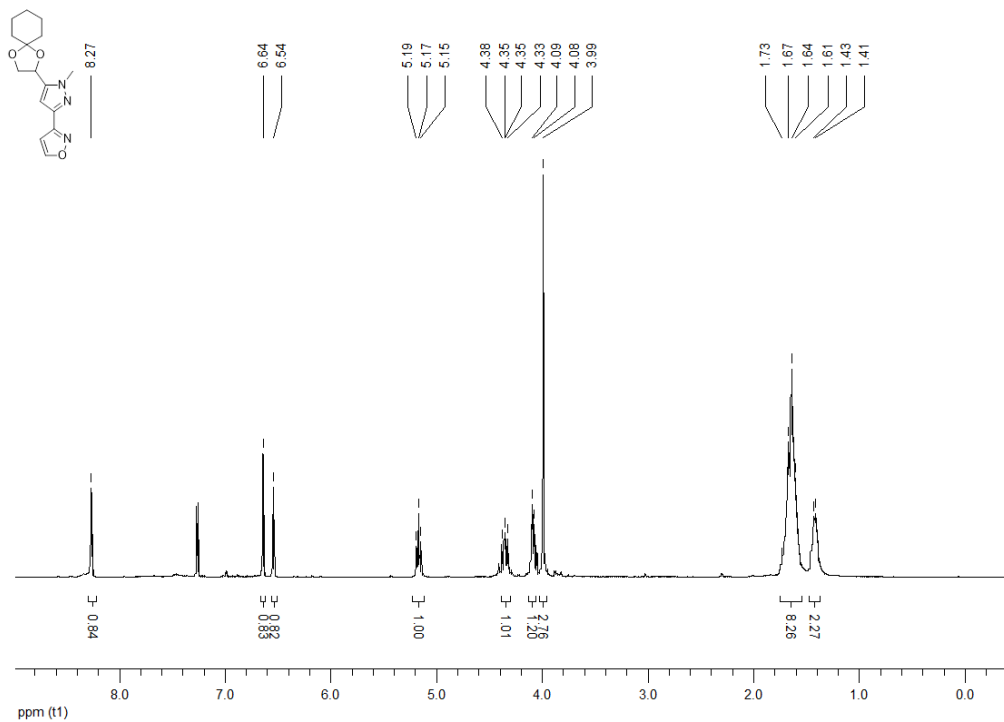
¹³C NMR (100 MHz, CDCl₃) 5-(5-{1,4-dioxaspiro[4.5]decan-2-yl}-1-methyl-1H-pyrazol-3-yl)-1,2-oxazole (182l)
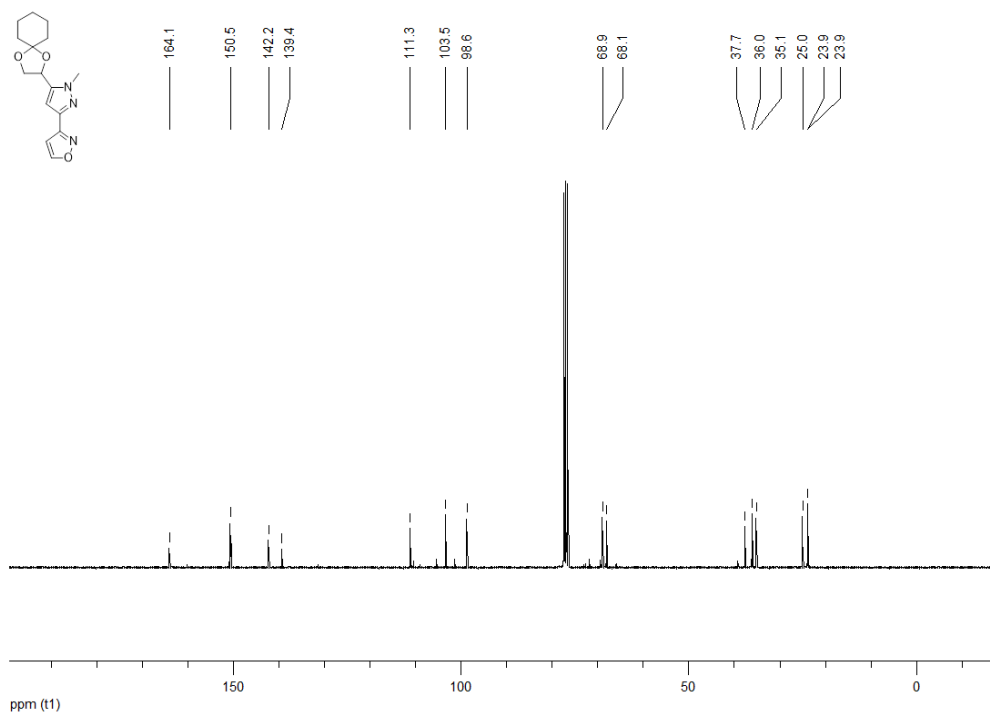
¹H NMR (300 MHz, CDCl₃) 2-(5-{1,4-dioxaspiro[4.5]decan-2-yl}-1-methyl-1H-pyrazol-3-yl)-1H-indole (182m)
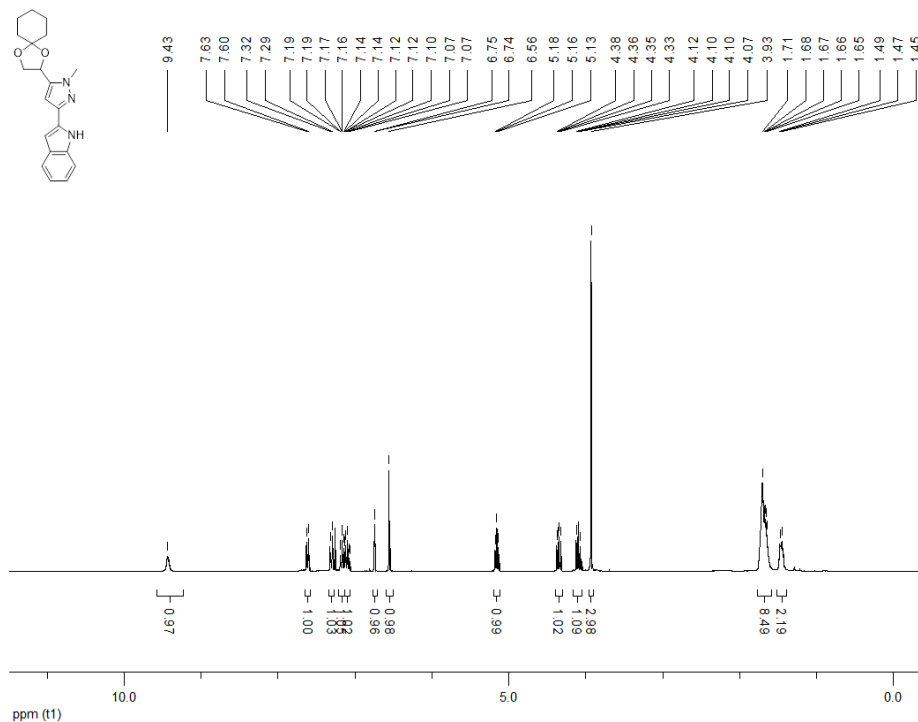
¹³C NMR (100 MHz, CDCl₃) 2-(5-{1,4-dioxaspiro[4.5]decan-2-yl}-1-methyl-1H-pyrazol-3-yl)-1H-indole (182m)
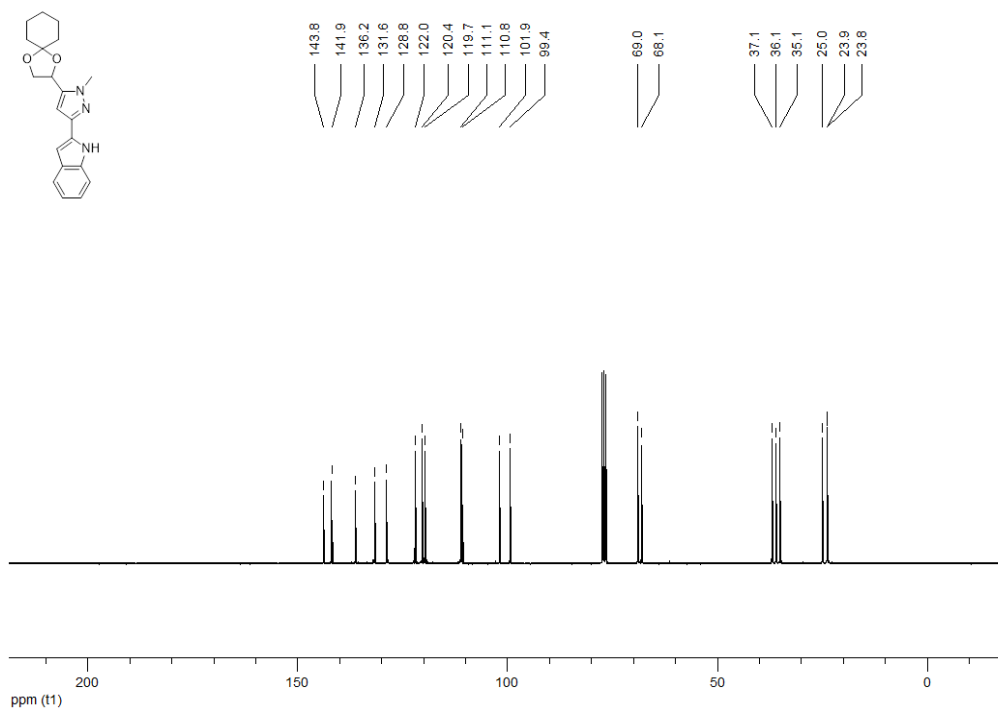
^{1}H NMR (300 MHz, CDCl$_3$) 3-(5-{1,4-dioxaspiro[4.5]decan-2-yl}-1-methyl-1H-pyrazol-3-yl)pyridine (182n)
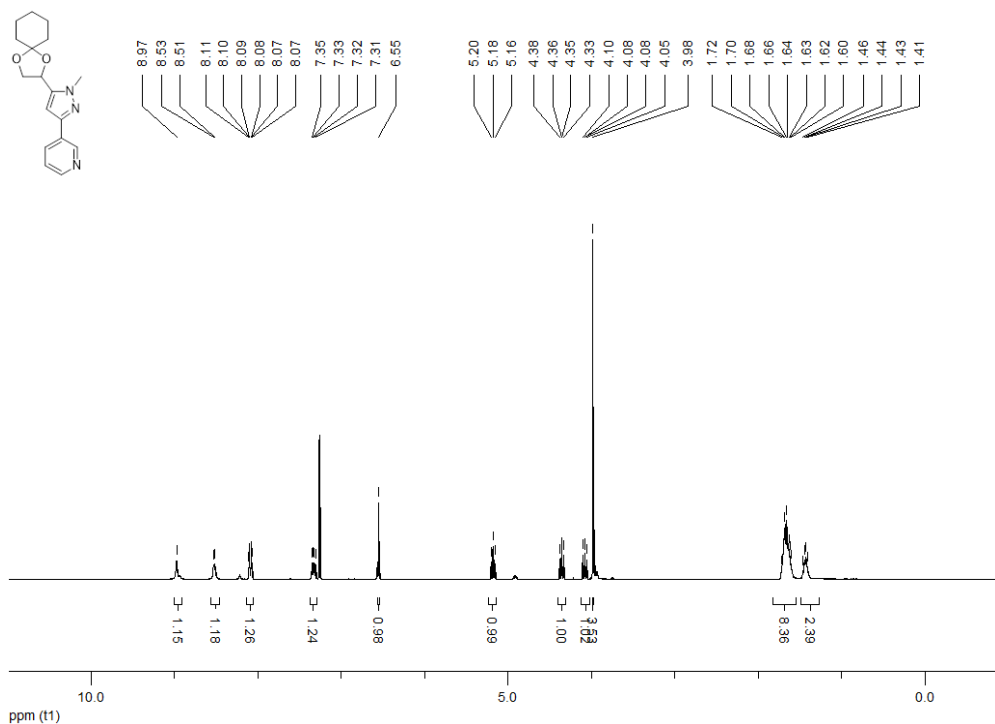
^{13}C NMR (100 MHz, CDCl$_3$) 3-(5-{1,4-dioxaspiro[4.5]decan-2-yl}-1-methyl-1H-pyrazol-3-yl)pyridine (182n)
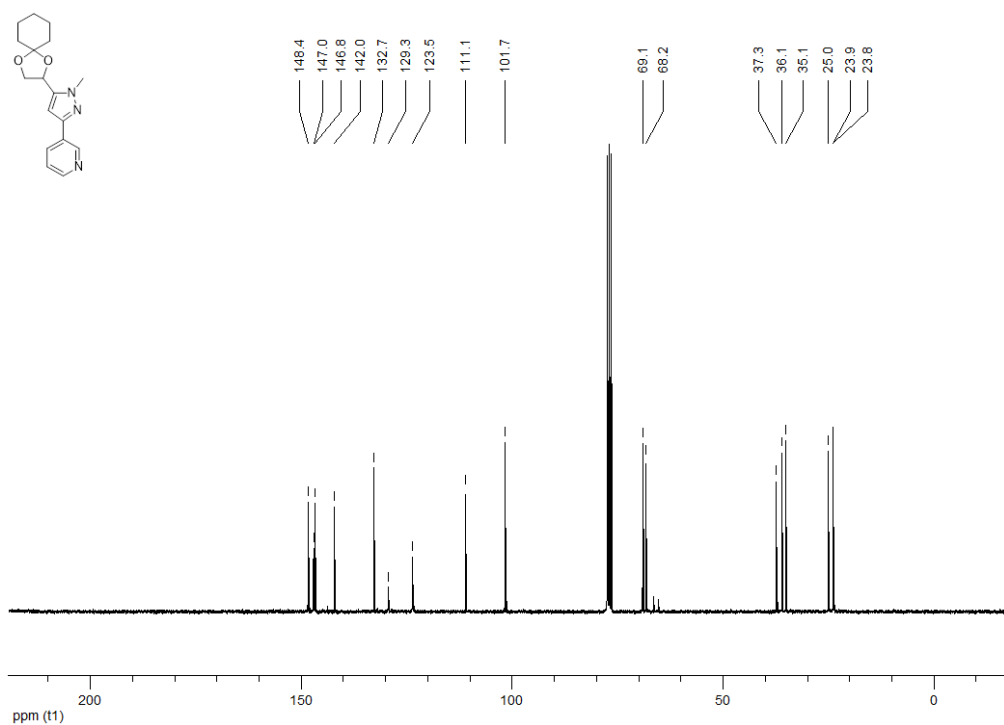
¹H NMR (300 MHz, CDCl₃) 3-cyclohexyl-5-{1,4-dioxaspiro[4.5]decan-2-yl}-1-methyl-1H-pyrazole (182o)
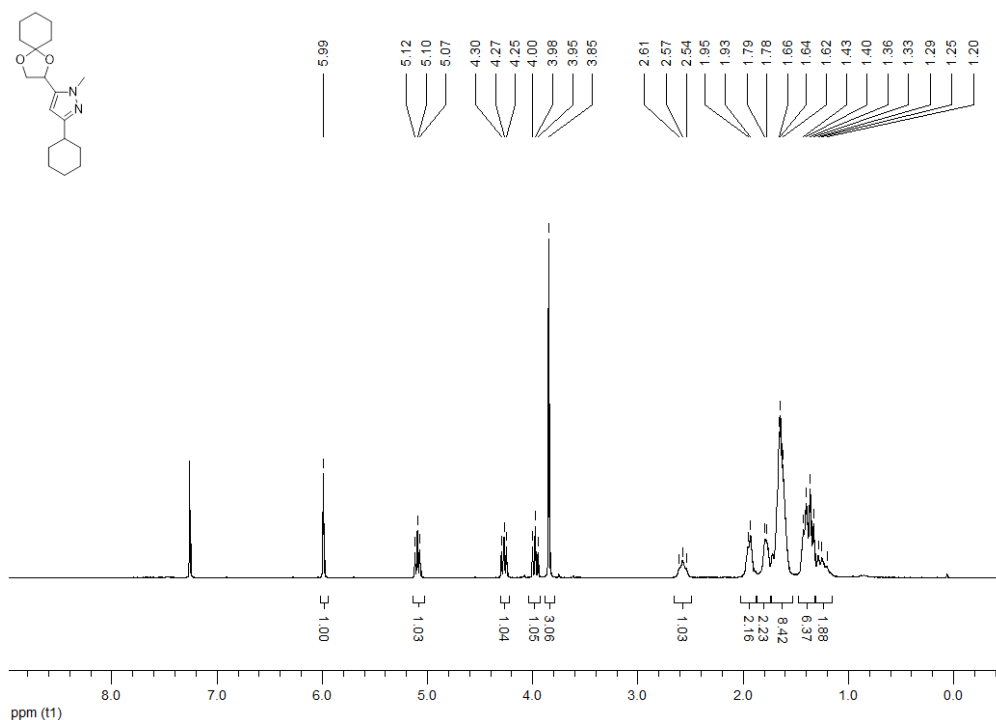
¹³C NMR (100 MHz, CDCl₃) 3-cyclohexyl-5-{1,4-dioxaspiro[4.5]decan-2-yl}-1-methyl-1H-pyrazole (182o)
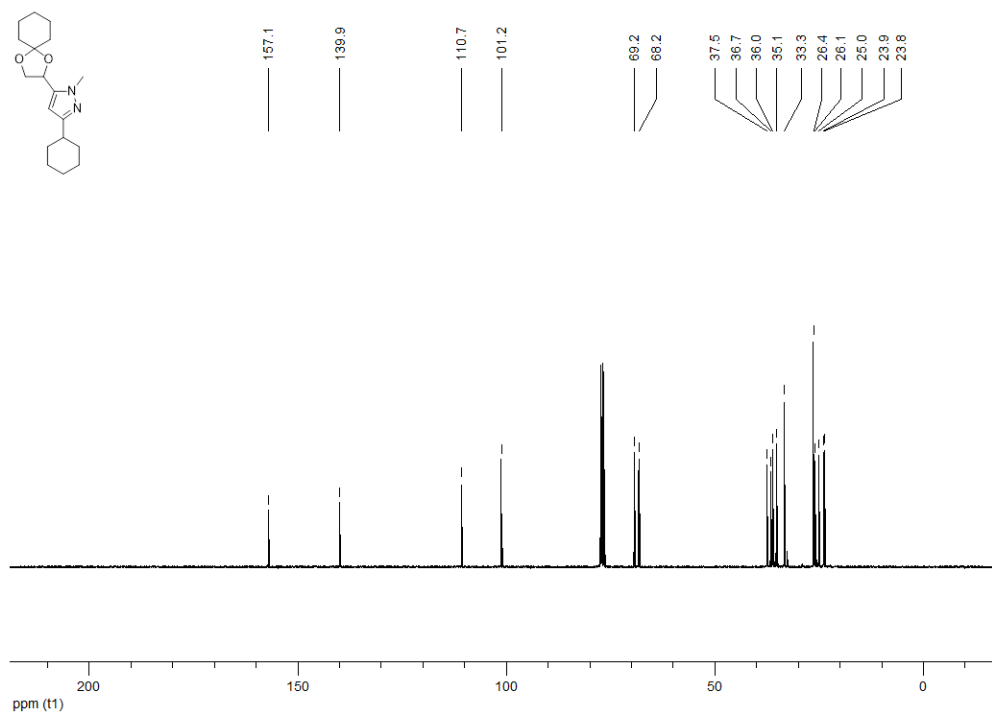
^{1}H NMR (300 MHz, MeOD) 1-(3-phenyl-1H-pyrazol-5-yl)ethane-1,2-diol (183a)
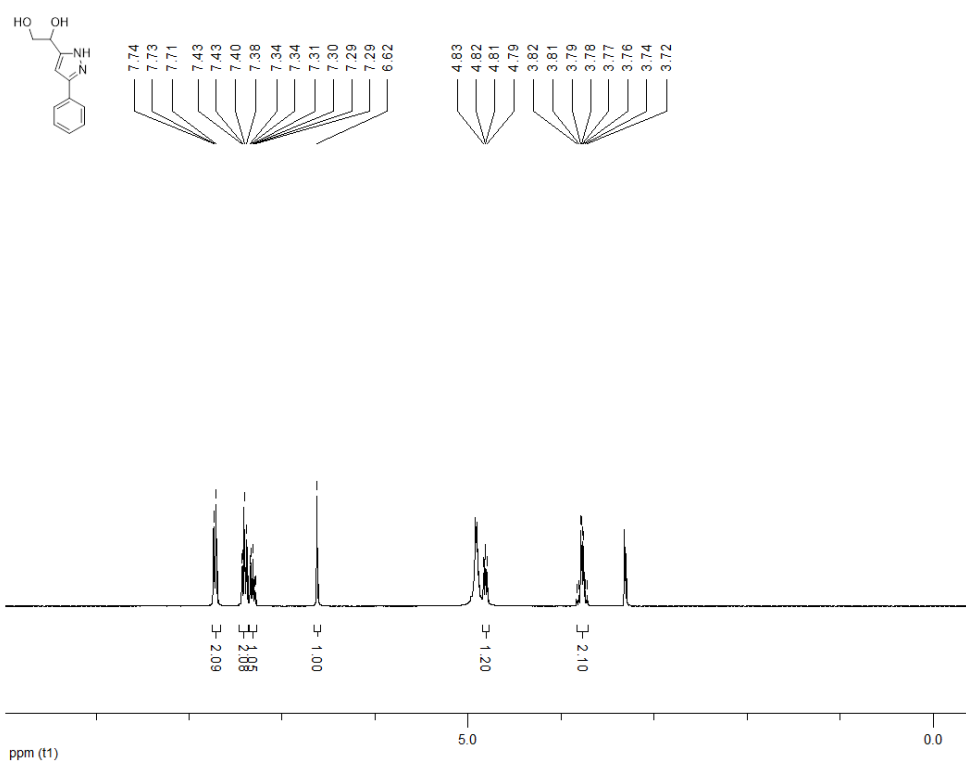
^{13}C NMR (100 MHz, MeOD) 1-(3-phenyl-1H-pyrazol-5-yl)ethane-1,2-diol (183a)
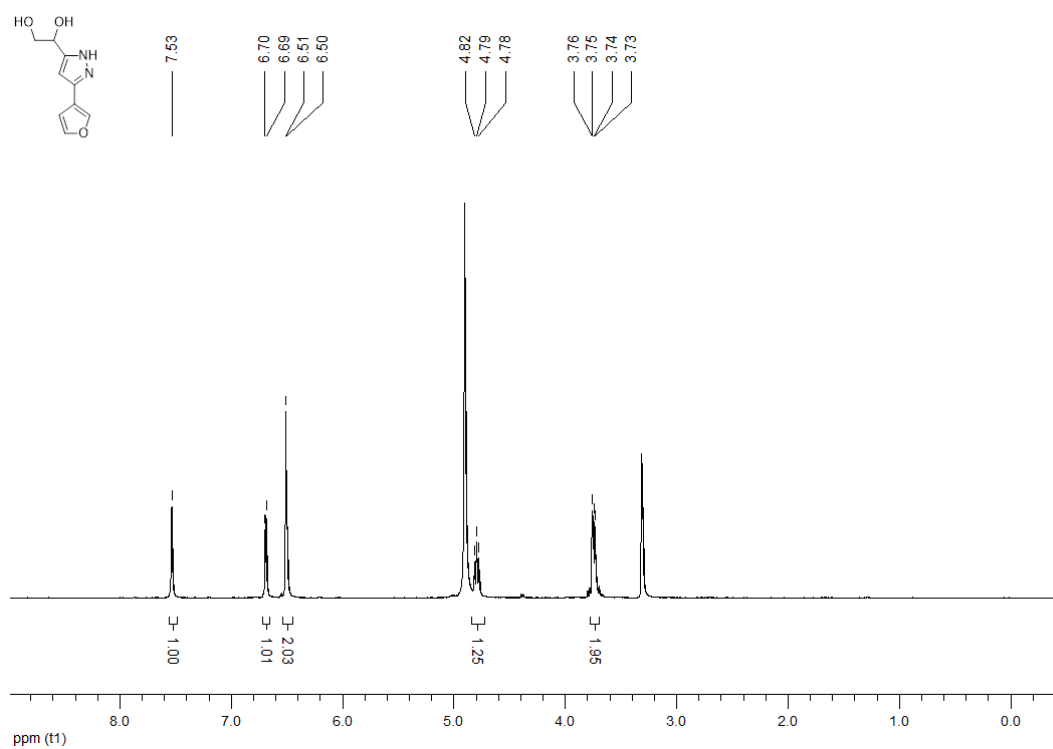
1H NMR (300 MHz, MeOD) 1-[3-(thiophen-2-yl)-1*H*-pyrazol-5-yl]ethane-1,2-diol (183c)

13C NMR (100 MHz, MeOD) 1-[3-(thiophen-2-yl)-1*H*-pyrazol-5-yl]ethane-1,2-diol (183c)
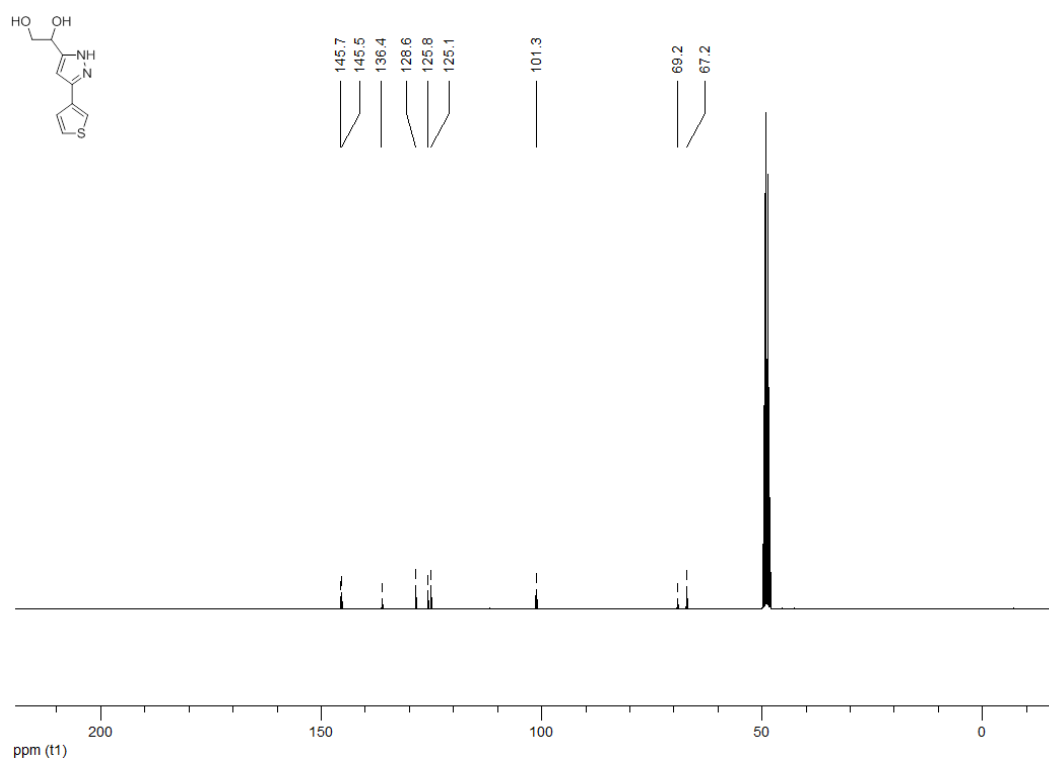
¹H NMR (300 MHz, MeOD) 1-[3-(propan-2-yl)-1*H*-pyrazol-5-yl]ethane-1,2-diol (183d)
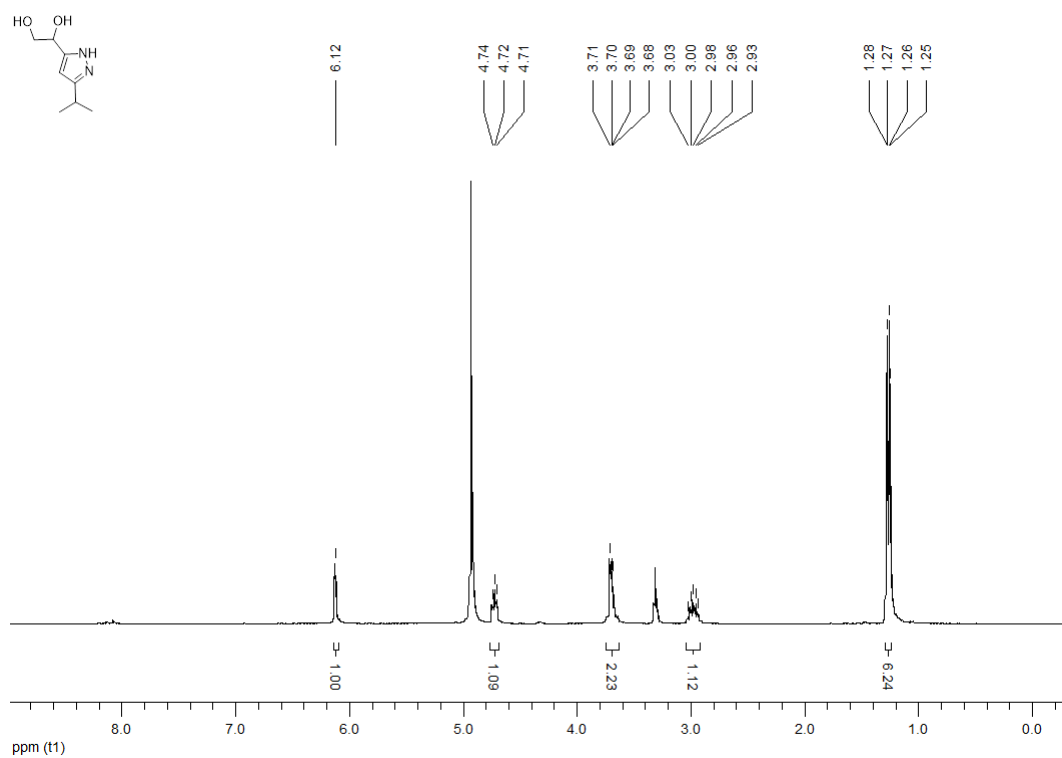
¹³C NMR (100 MHz, MeOD) 1-[3-(propan-2-yl)-1*H*-pyrazol-5-yl]ethane-1,2-diol (183d)
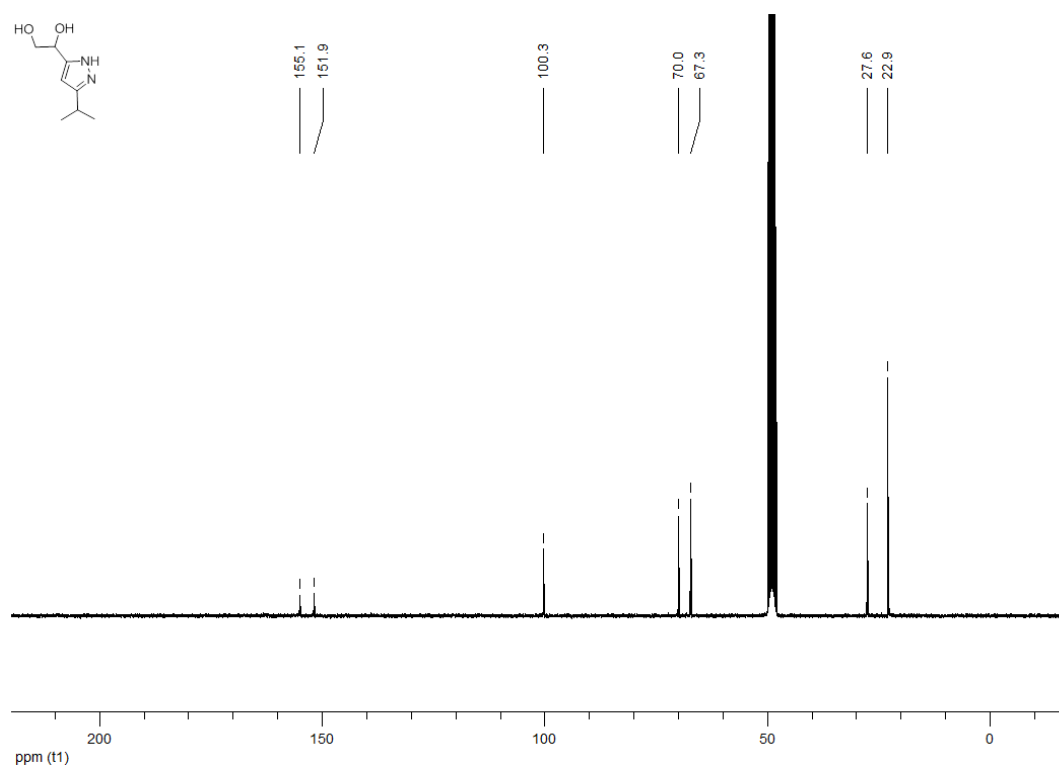
¹H NMR (300 MHz, MeOD) 1-(3-cyclopropyl-1*H*-pyrazol-5-yl)ethane-1,2-diol (183e)
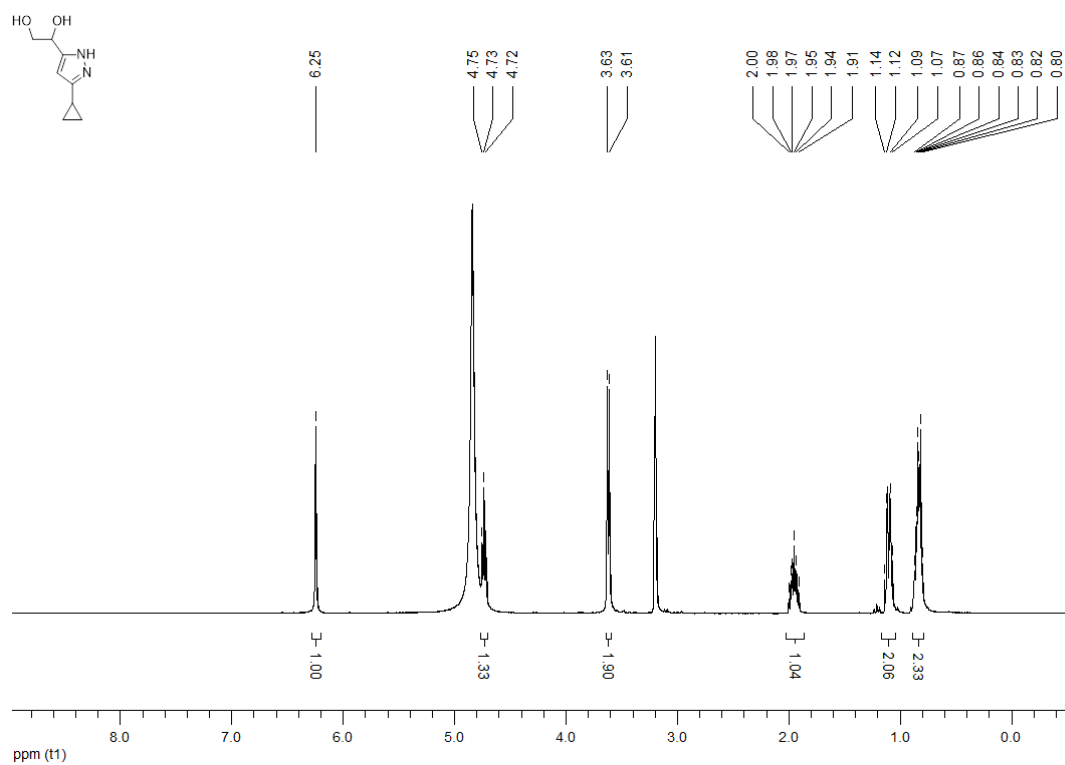
¹³C NMR (100 MHz, MeOD) 1-(3-cyclopropyl-1*H*-pyrazol-5-yl)ethane-1,2-diol (183e)
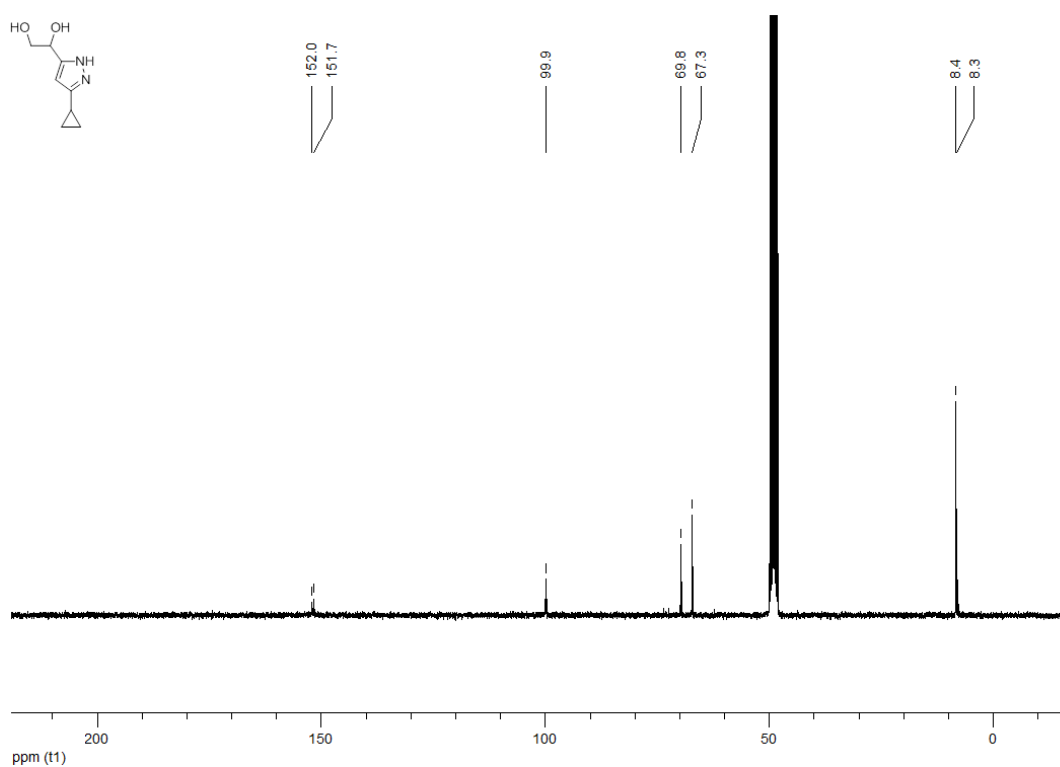
¹H NMR (300 MHz, CD₃CN) 1-(3-cyclopentyl-1*H*-pyrazol-5-yl)ethane-1,2-diol (183f)
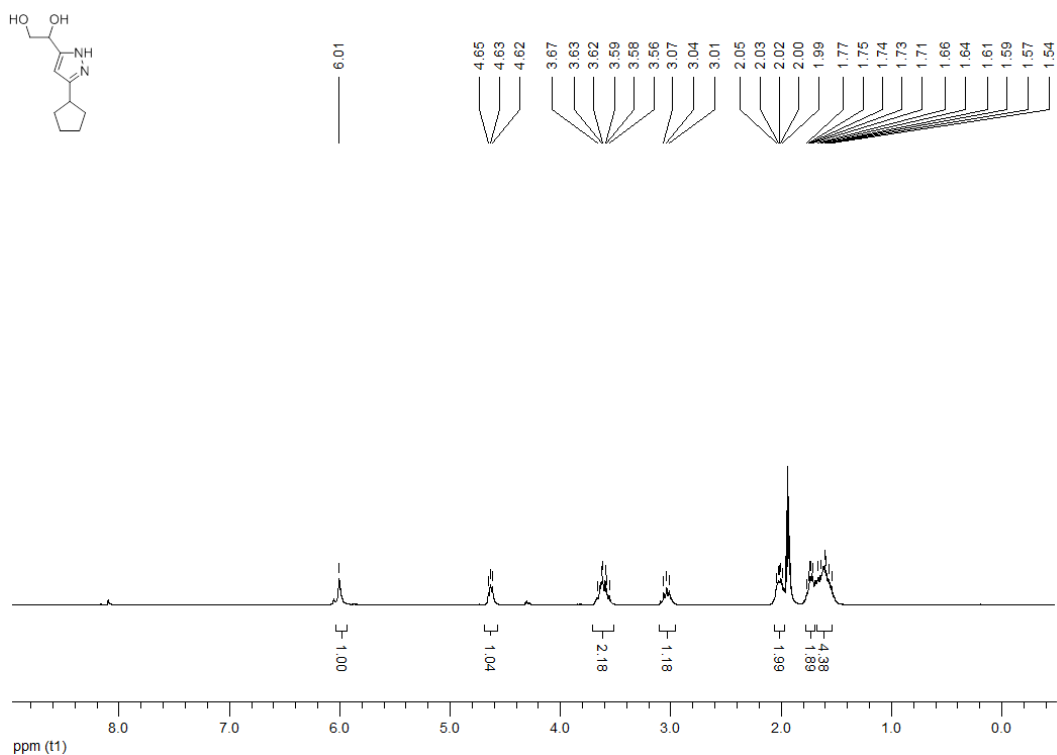
¹³C NMR (100 MHz, CD₃CN) 1-(3-cyclopentyl-1*H*-pyrazol-5-yl)ethane-1,2-diol (183f)

263
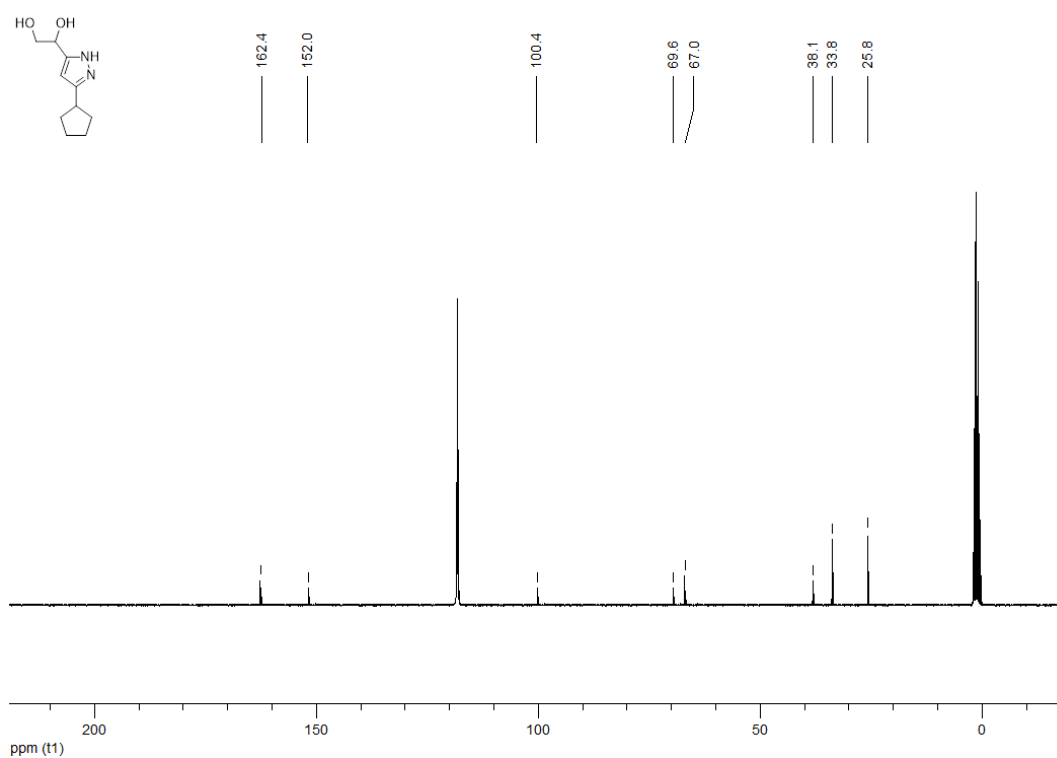
¹H NMR (300 MHz, MeOD) 1-[3-(adamantan-1-yl)-1H-pyrazol-5-yl]ethane-1,2-diol (183g)
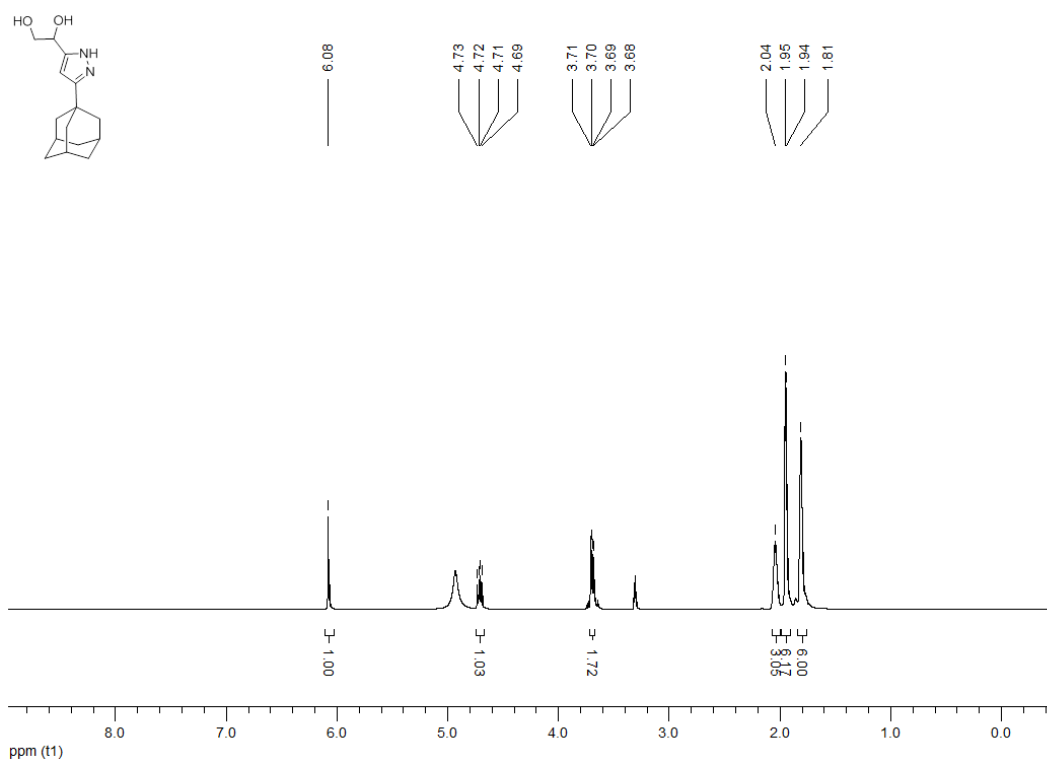
¹³C NMR (100 MHz, MeOD) 1-[3-(adamantan-1-yl)-1H-pyrazol-5-yl]ethane-1,2-diol (183g)
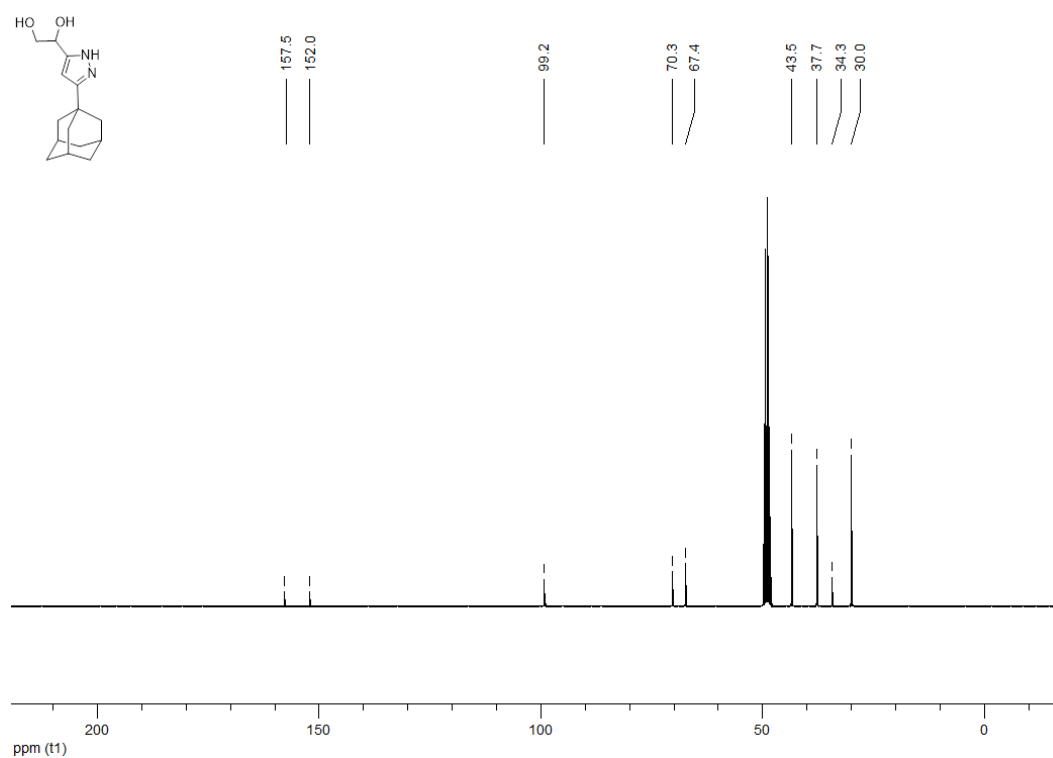
¹H NMR (300 MHz, MeOD) 1-(1-methyl-3-phenyl-1*H*-pyrazol-5-yl)ethane-1,2-diol (184a)
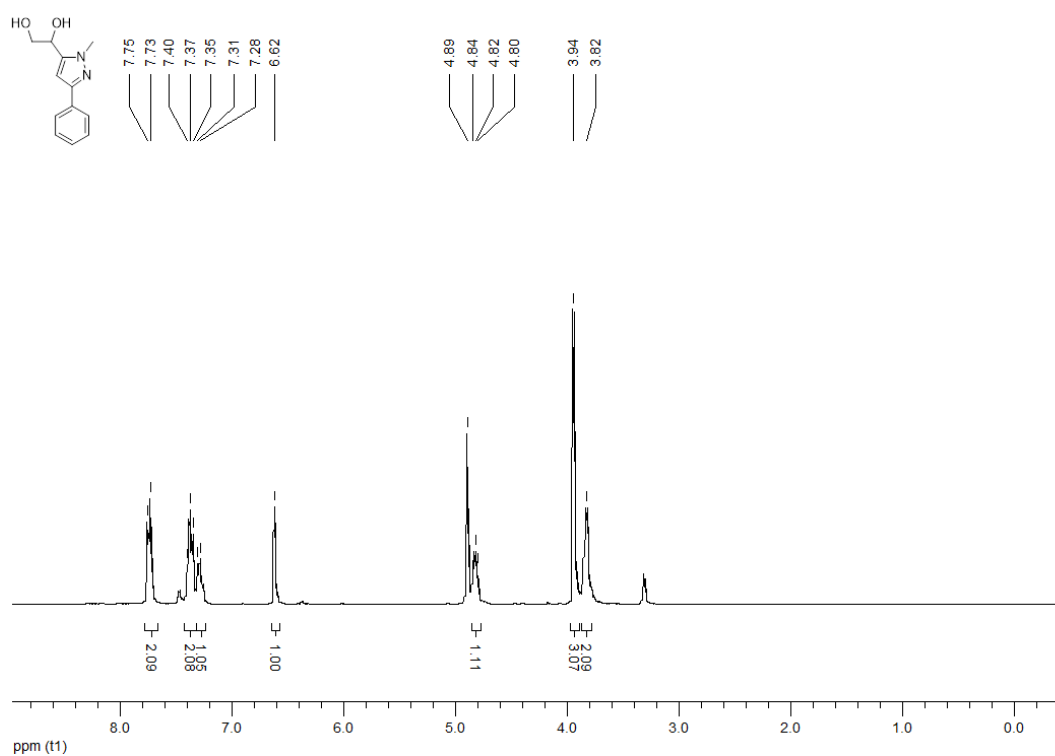
¹³C NMR (100 MHz, MeOD) 1-(1-methyl-3-phenyl-1*H*-pyrazol-5-yl)ethane-1,2-diol (184a)

^{1}H NMR (300 MHz, MeOD) 1-[3-(furan-2-yl)-1-methyl-1H-pyrazol-5-yl]ethane-1,2-diol (184b)
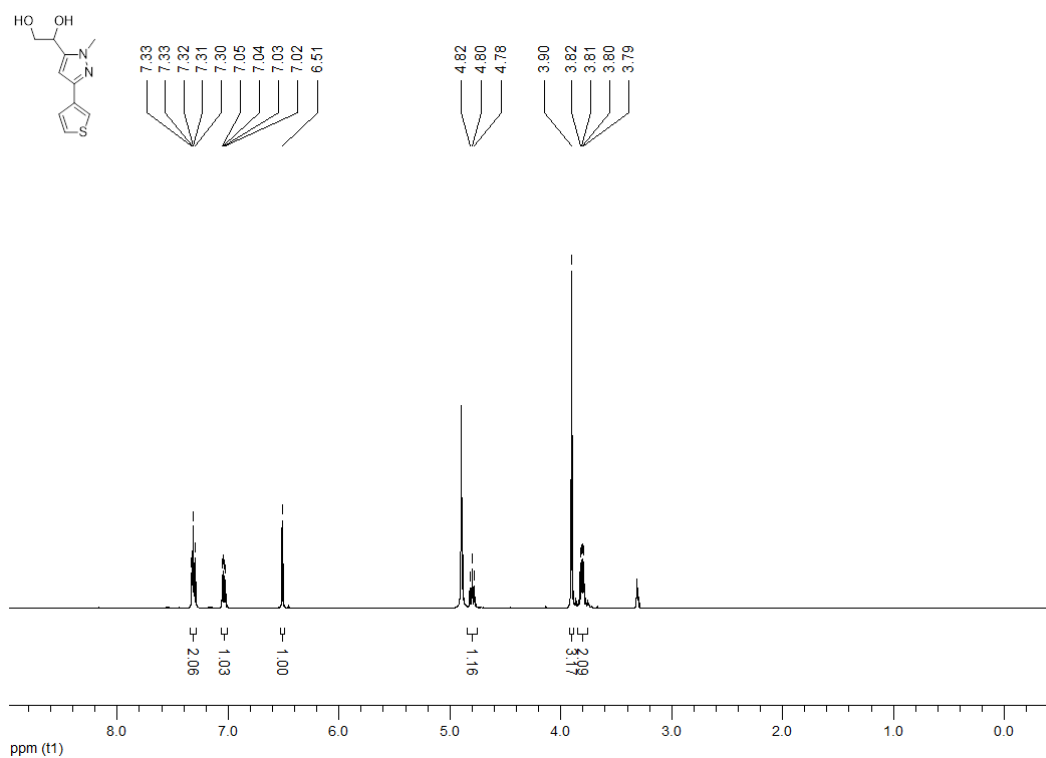
^{13}C NMR (100 MHz, MeOD) 1-[3-(furan-2-yl)-1-methyl-1H-pyrazol-5-yl]ethane-1,2-diol (184b)

¹H NMR (300 MHz, MeOD) 1-[1-methyl-3-(thiophen-2-yl)-1H-pyrazol-5-yl]ethane-1,2-diol (184c)

¹³C NMR (100 MHz, MeOD) 1-[1-methyl-3-(thiophen-2-yl)-1H-pyrazol-5-yl]ethane-1,2-diol (184c)

267
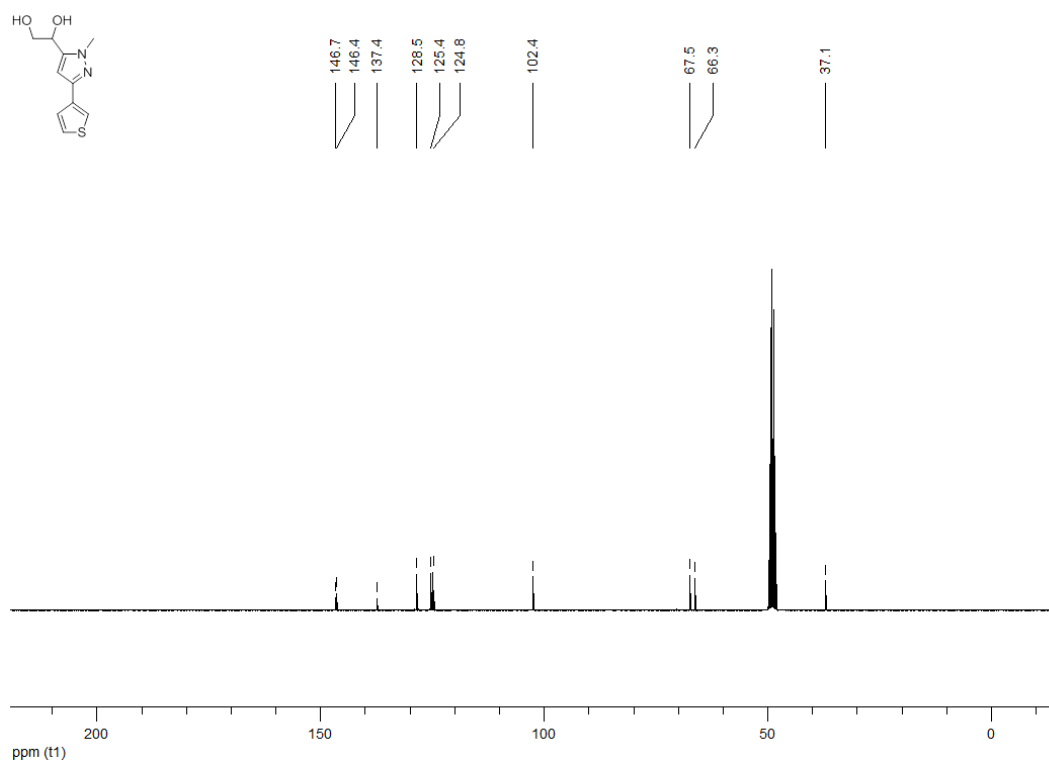
¹H NMR (300 MHz, MeOD) 1-[1-methyl-3-(propan-2-yl)-1*H*-pyrazol-5-yl]ethane-1,2-diol (184d)
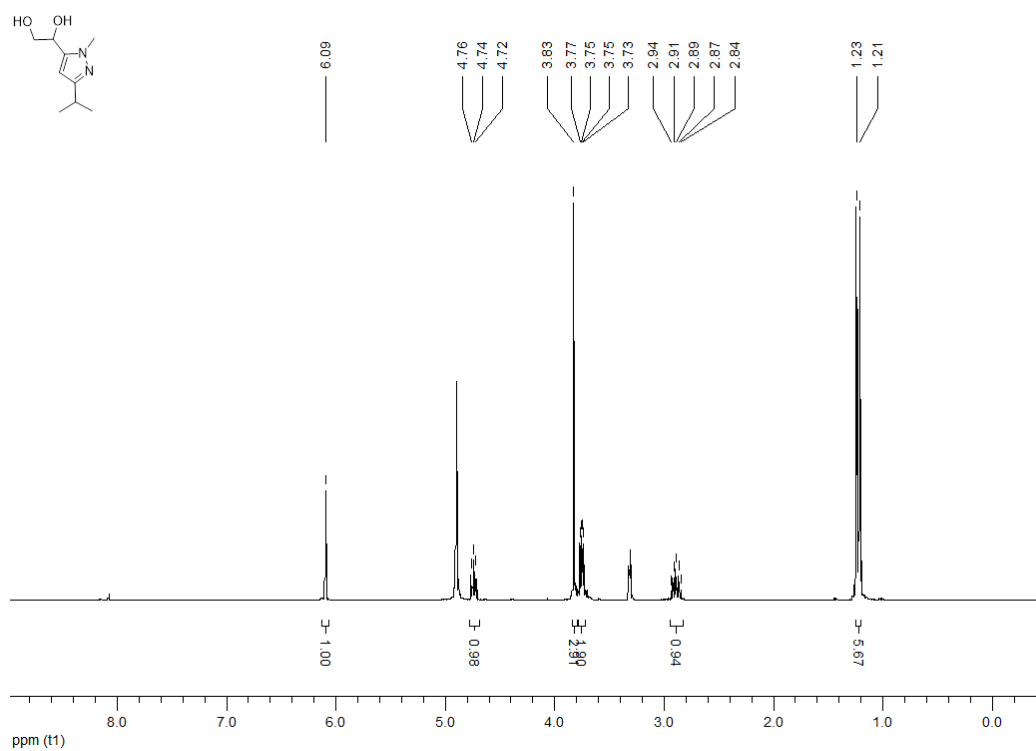
¹³C NMR (100 MHz, MeOD) 1-[1-methyl-3-(propan-2-yl)-1*H*-pyrazol-5-yl]ethane-1,2-diol (184d)
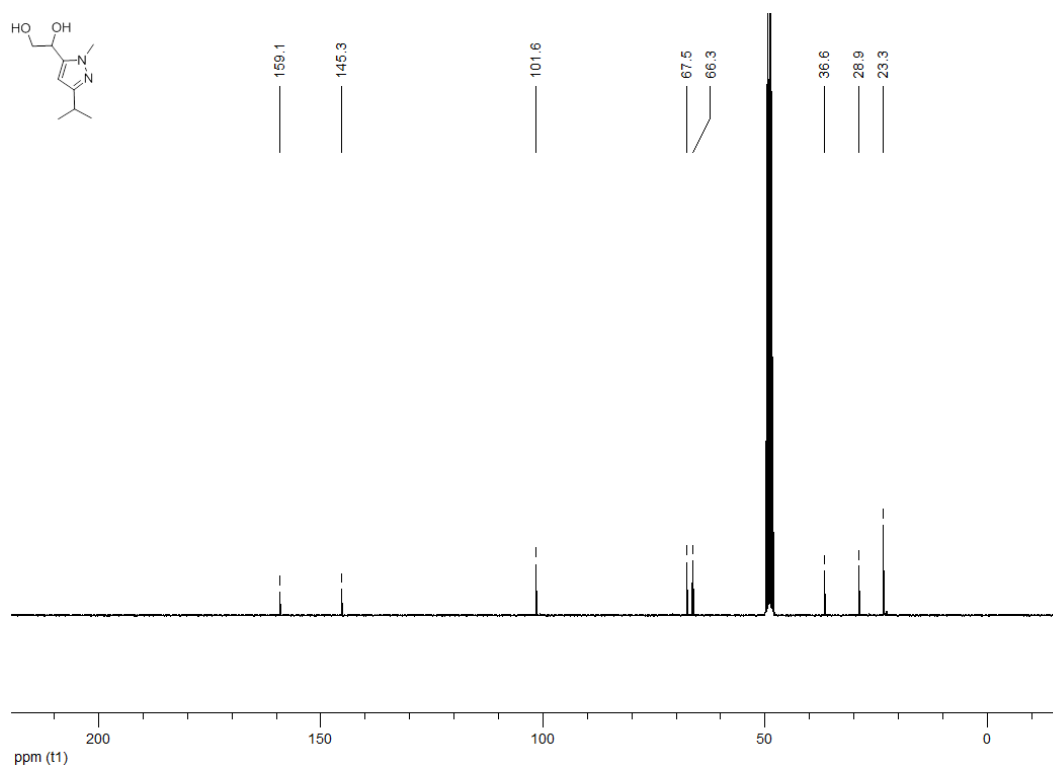
¹H NMR (300 MHz, MeOD) 1-(3-cyclopropyl-1-methyl-1*H*-pyrazol-5-yl)ethane-1,2-diol (184e)
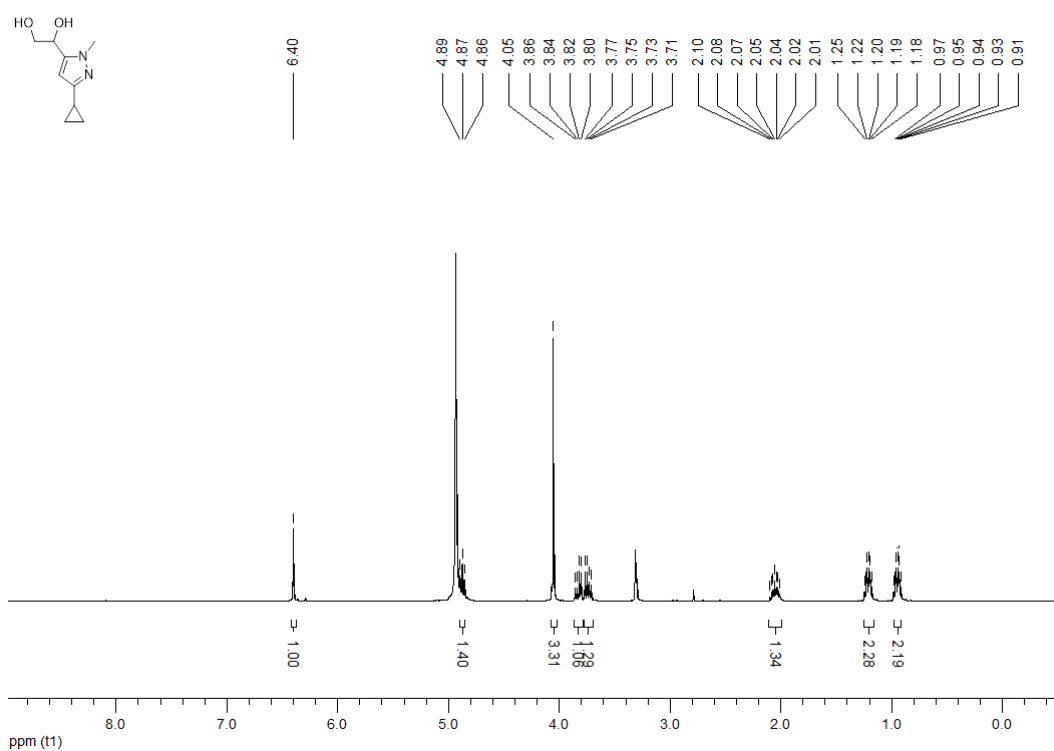
¹³C NMR (100 MHz, MeOD) 1-(3-cyclopropyl-1-methyl-1*H*-pyrazol-5-yl)ethane-1,2-diol (184e)
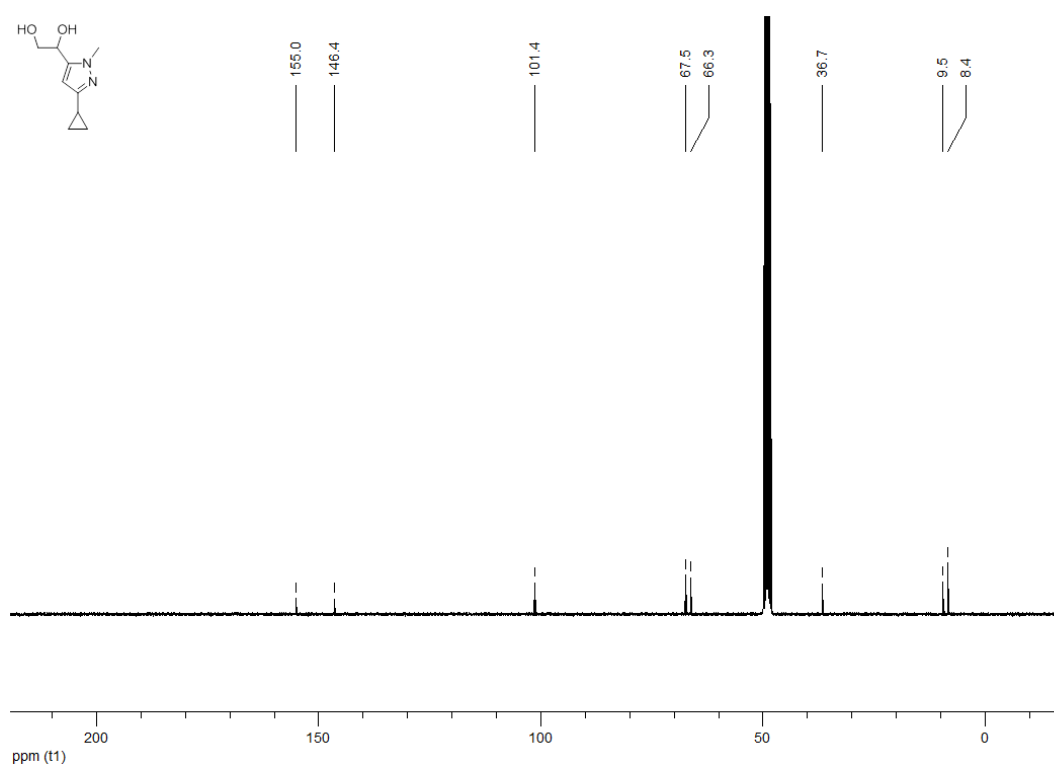
¹H NMR (300 MHz, MeOD) 1-(3-cyclopentyl-1-methyl-1*H*-pyrazol-5-yl)ethane-1,2-diol (184f)
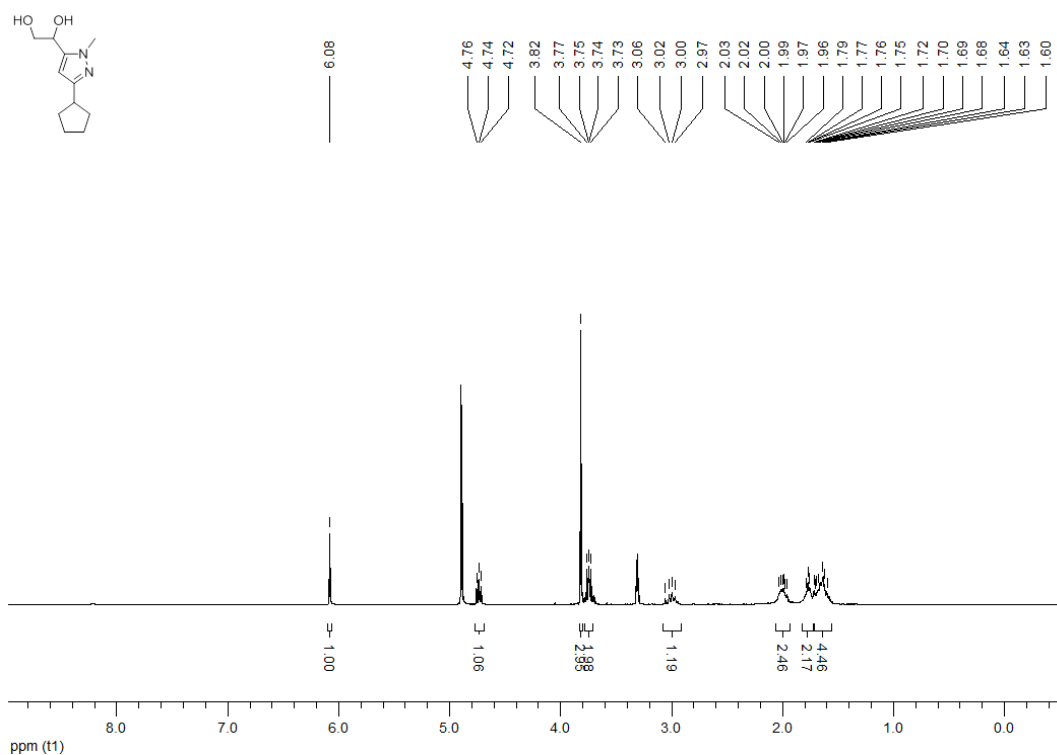
¹³C NMR (100 MHz, MeOD) 1-(3-cyclopentyl-1-methyl-1*H*-pyrazol-5-yl)ethane-1,2-diol (184f)
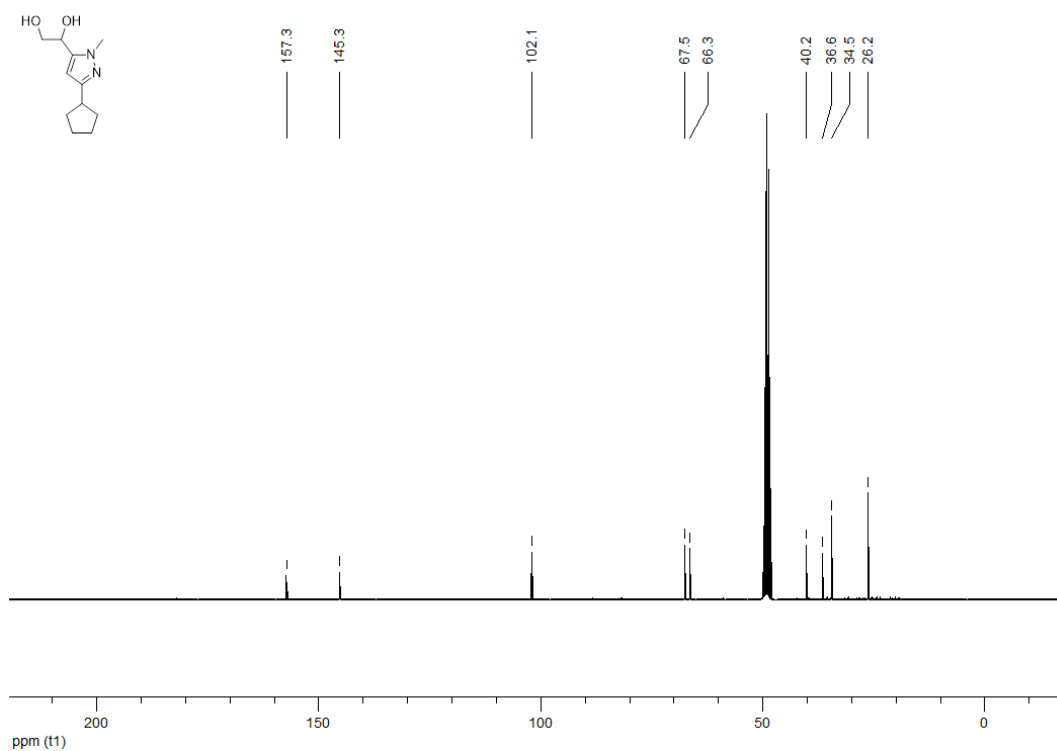
¹H NMR (300 MHz, MeOD) 1-[3-(adamantan-1-yl)-1-methyl-1*H*-pyrazol-5-yl]ethane-1,2-diol (184g)
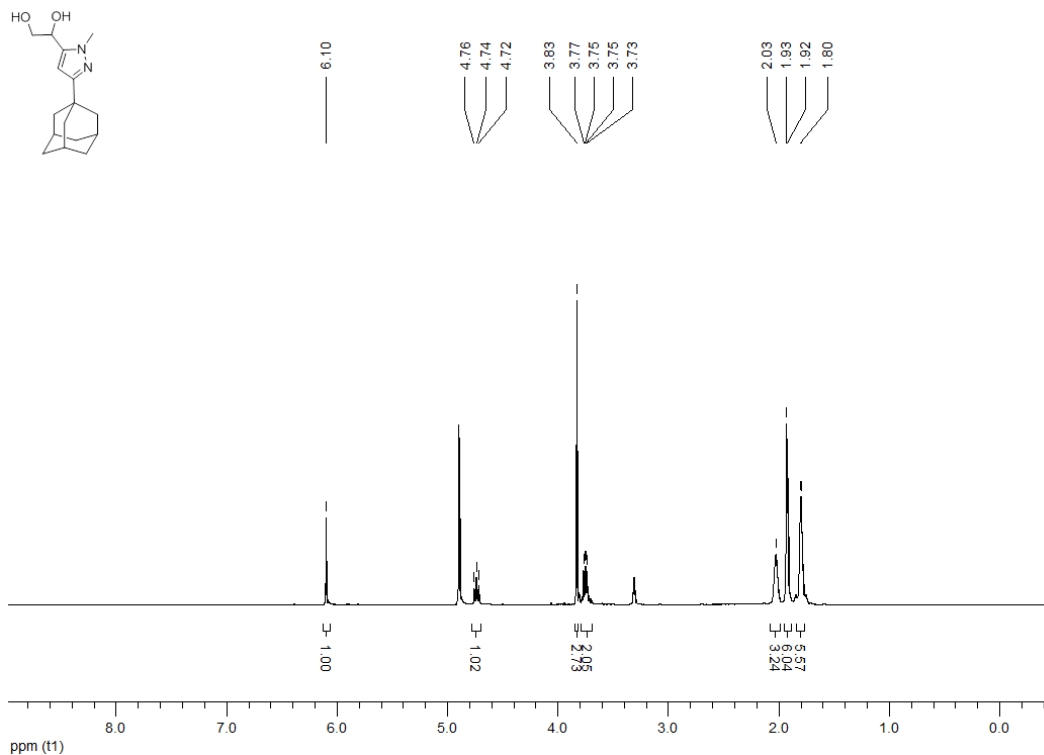
¹³C NMR (100 MHz, MeOD) 1-[3-(adamantan-1-yl)-1-methyl-1*H*-pyrazol-5-yl]ethane-1,2-diol (184g)
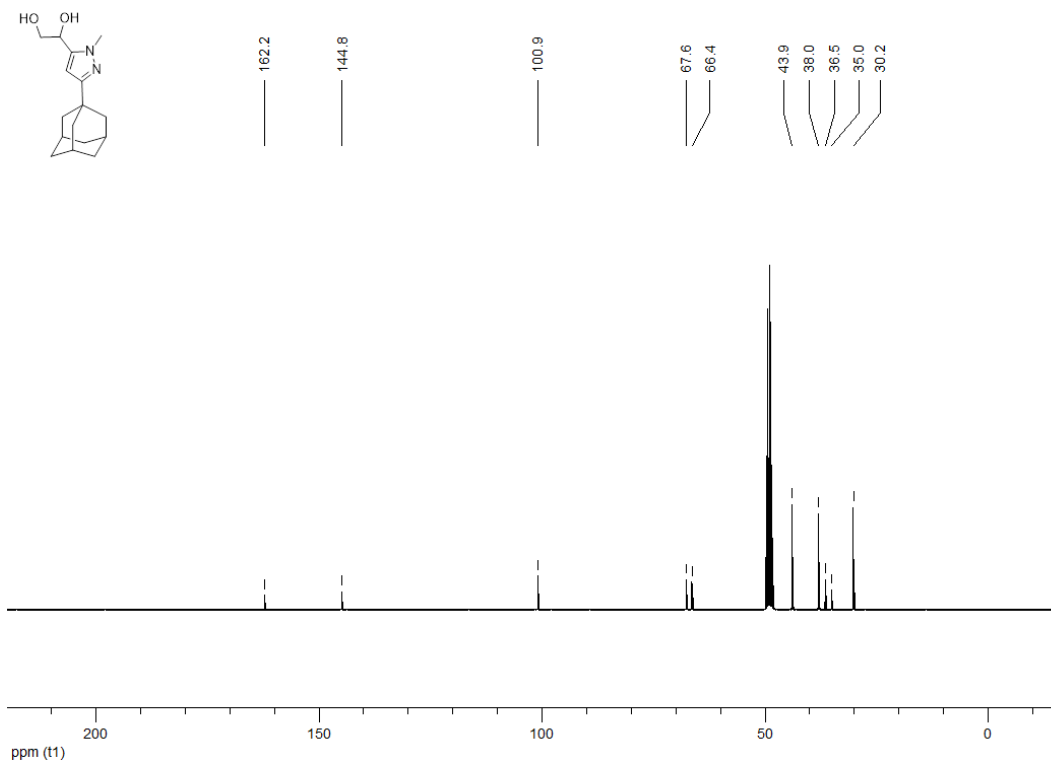
¹H NMR (300 MHz, CDCl₃) 5-{1,4-dioxaspiro[4.5]decan-2-yl}-1-ethyl-3-phenyl-1H-pyrazole (185a)
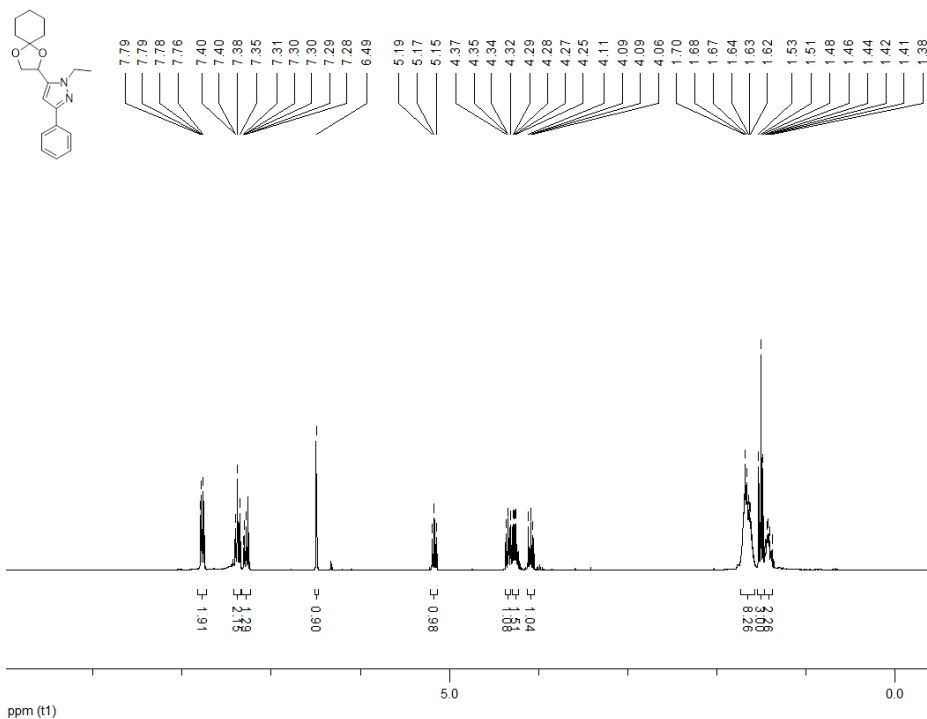
¹³C NMR (100 MHz, CDCl₃) 5-{1,4-dioxaspiro[4.5]decan-2-yl}-1-ethyl-3-phenyl-1H-pyrazole (185a)
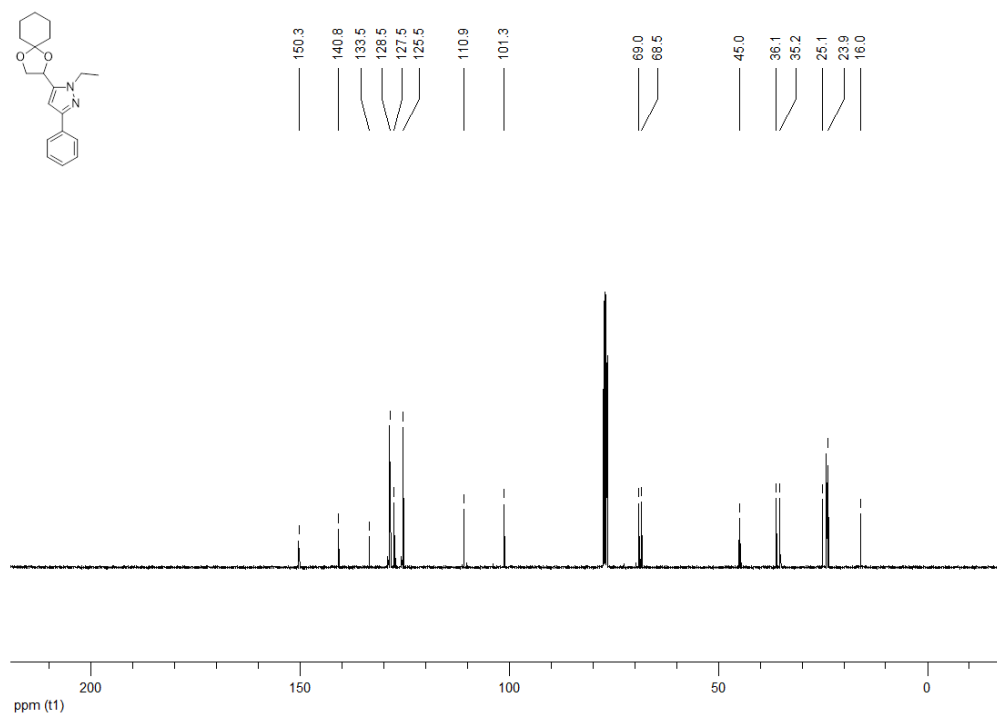
1H NMR (300 MHz, CDCl₃) 5-{1,4-dioxaspiro[4.5]decan-2-yl}-3-phenyl-1-(propan-2-yl)-1H-pyrazole (185b)
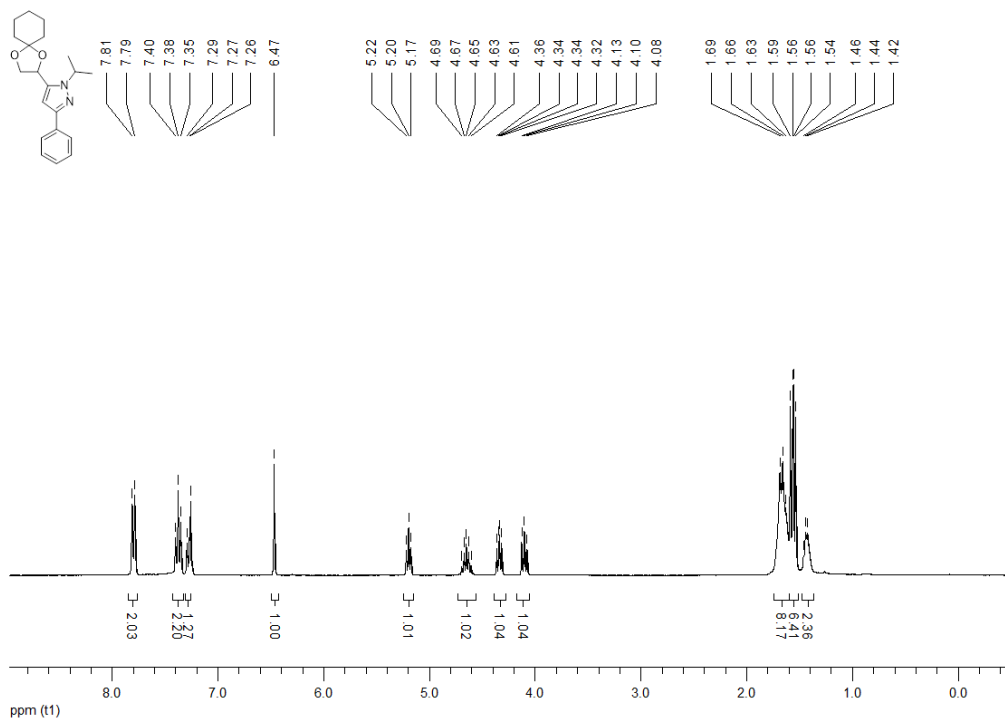
13C NMR (100 MHz, CDCl₃) 5-{1,4-dioxaspiro[4.5]decan-2-yl}-3-phenyl-1-(propan-2-yl)-1H-pyrazole (185b)
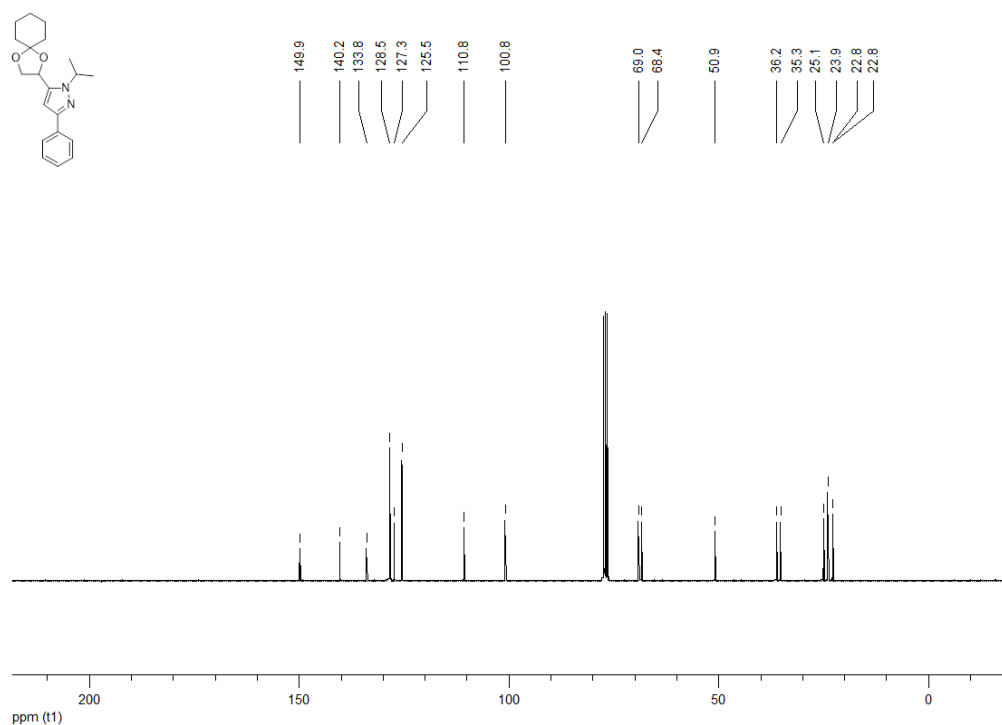
¹H NMR (300 MHz, CDCl₃) 1-cyclopropyl-5-{1,4-dioxaspiro[4.5]decan-2-yl}-3-phenyl-1H-pyrazole (185c)
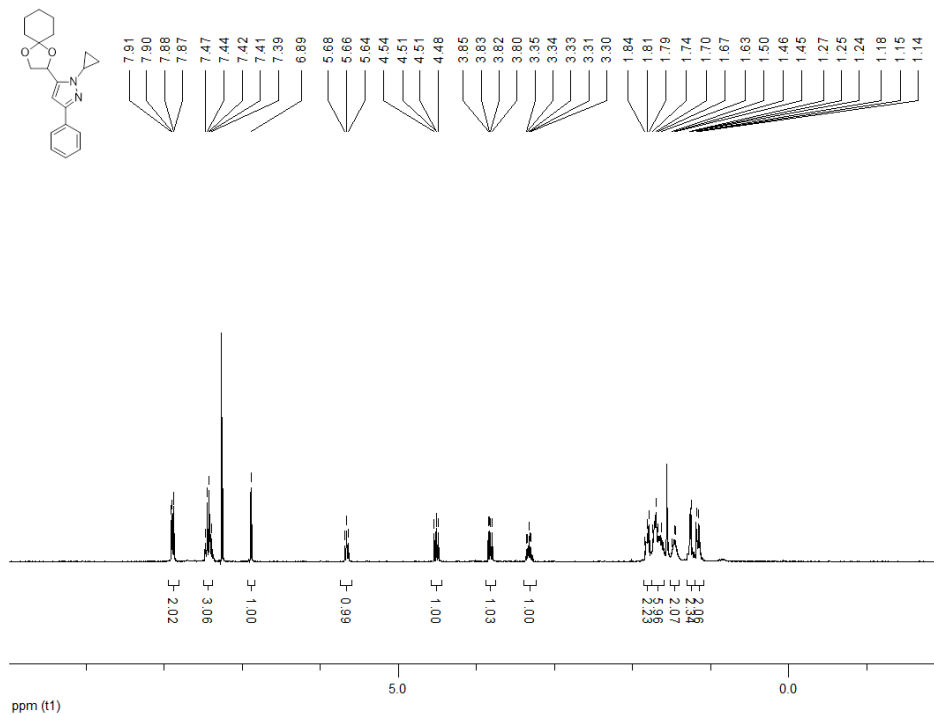
¹³C NMR (100 MHz, CDCl₃) 1-cyclopropyl-5-{1,4-dioxaspiro[4.5]decan-2-yl}-3-phenyl-1H-pyrazole (185c)
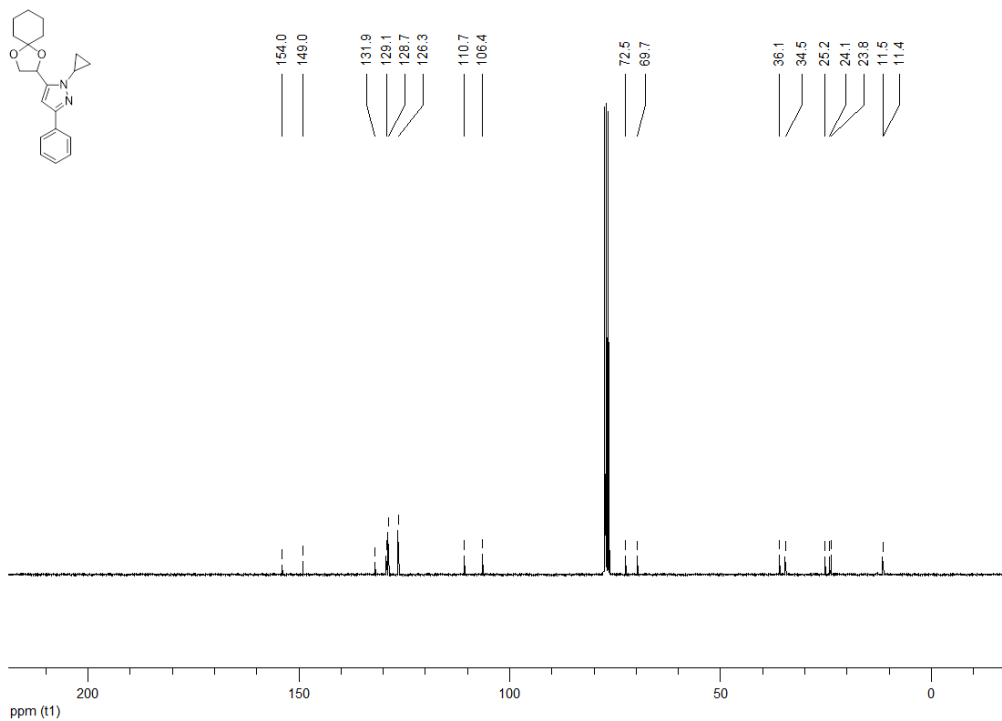
1H NMR (300 MHz, CDCl3) 3-(5-{1,4-dioxaspiro[4.5]decan-2-yl}-3-phenyl-1H-pyrazol-1-yl)propanenitrile (185d)
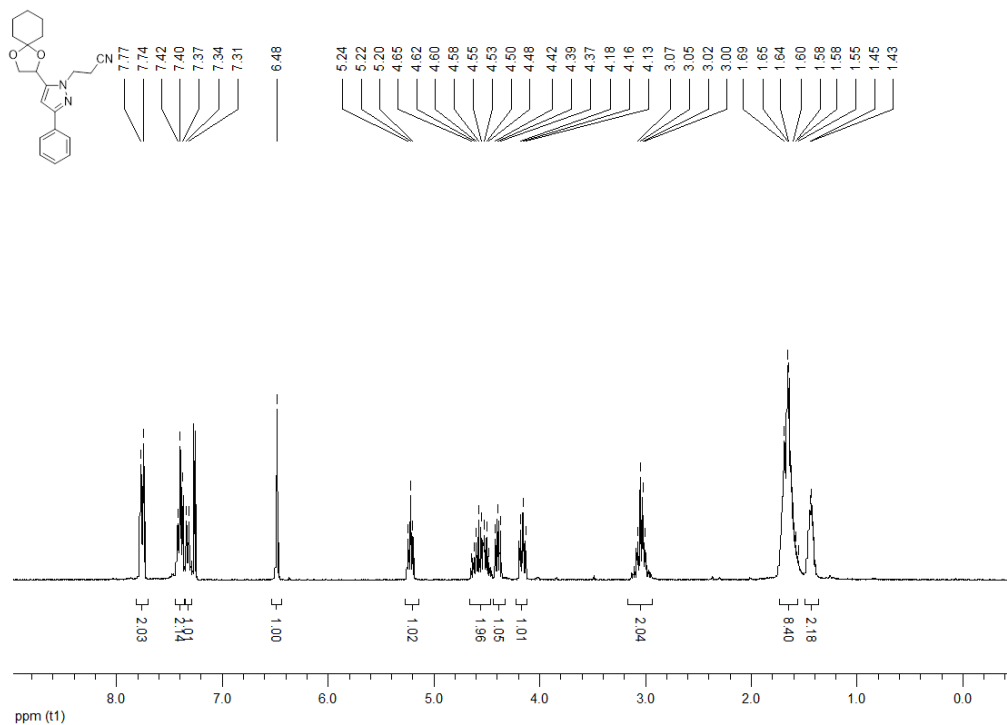
13C NMR (100 MHz, CDCl3) 3-(5-{1,4-dioxaspiro[4.5]decan-2-yl}-3-phenyl-1H-pyrazol-1-yl)propanenitrile (185d)
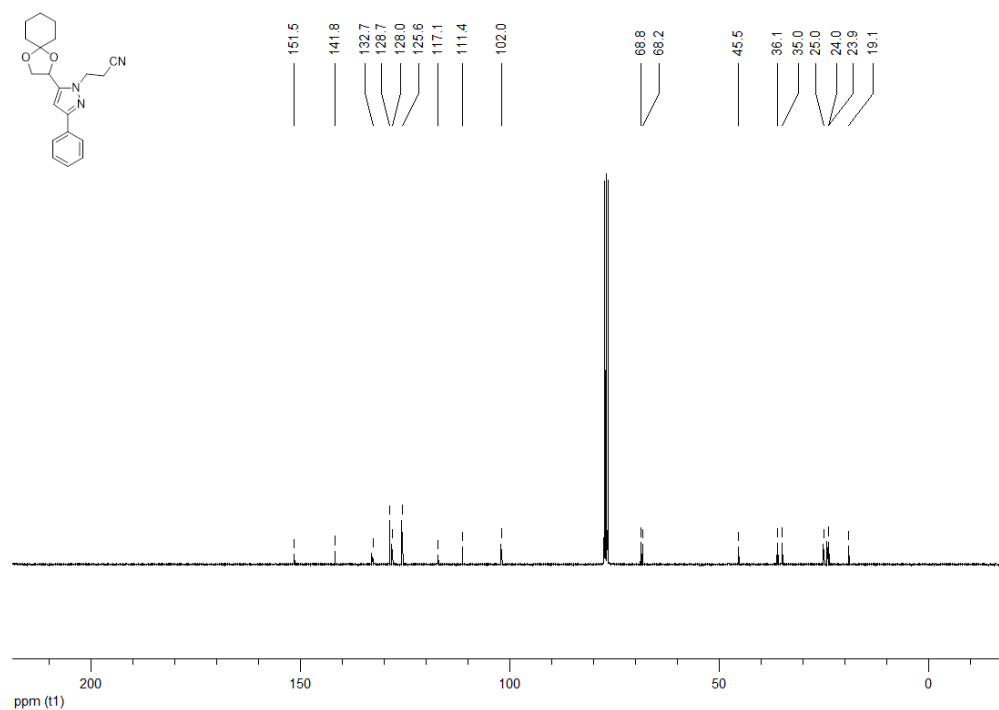
¹H NMR (300 MHz, CDCl₃) 1-cyclopentyl-5-{1,4-dioxaspiro[4.5]decan-2-yl}-3-phenyl-1H-pyrazole (185e)
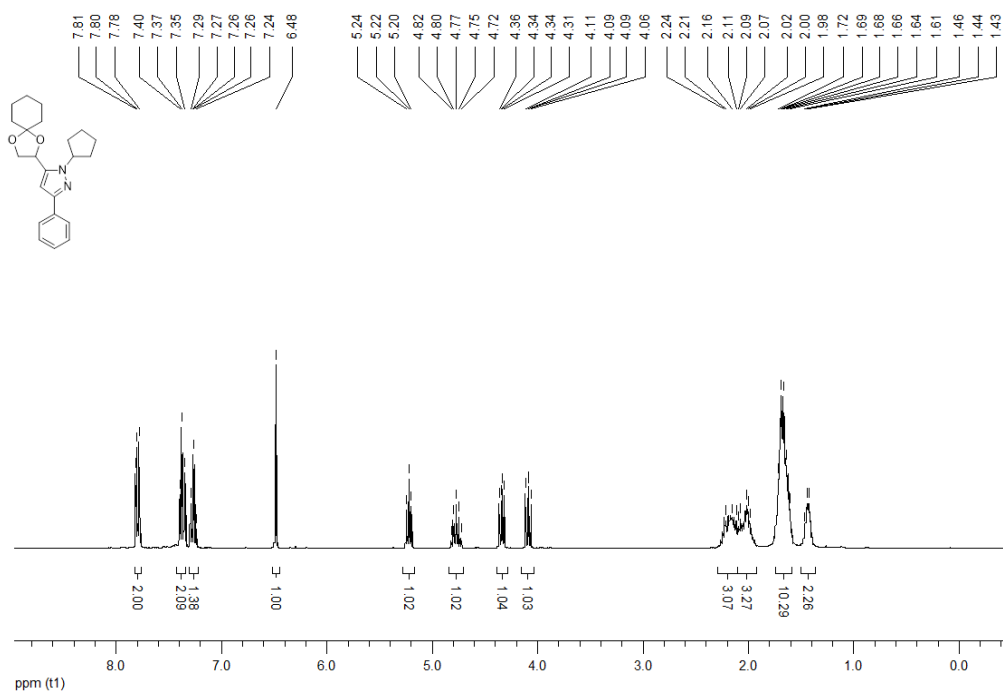
¹³C NMR (100 MHz, CDCl₃) 1-cyclopentyl-5-{1,4-dioxaspiro[4.5]decan-2-yl}-3-phenyl-1H-pyrazole (185e)

¹H NMR (300 MHz, CDCl₃) 5-{1,4-dioxaspiro[4.5]decan-2-yl}-1,3-diphenyl-1H-pyrazole (185f)
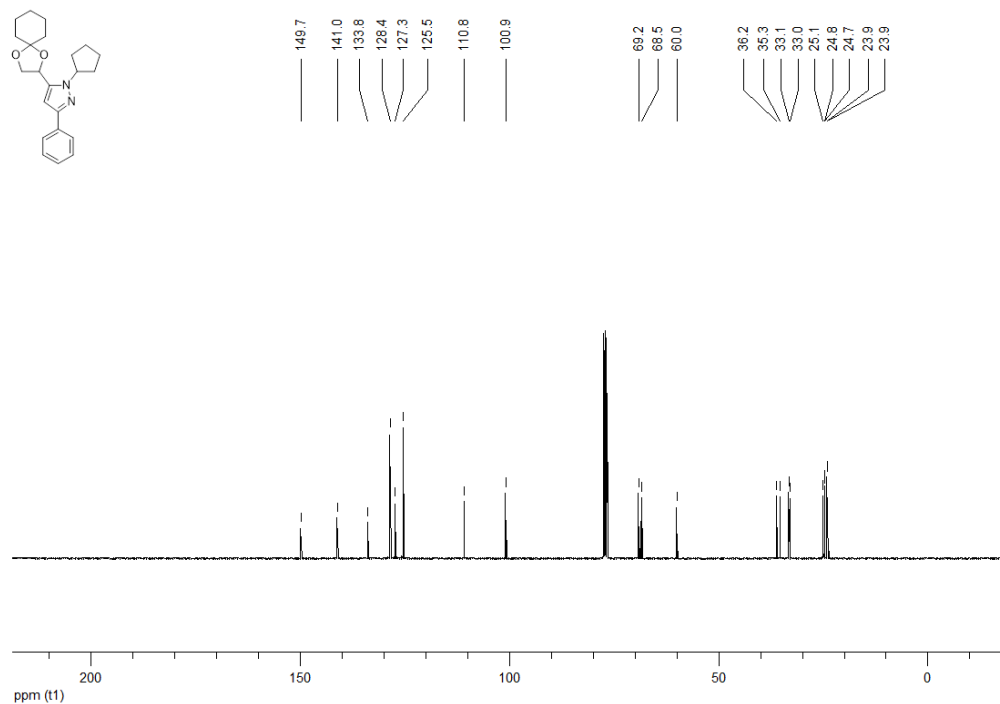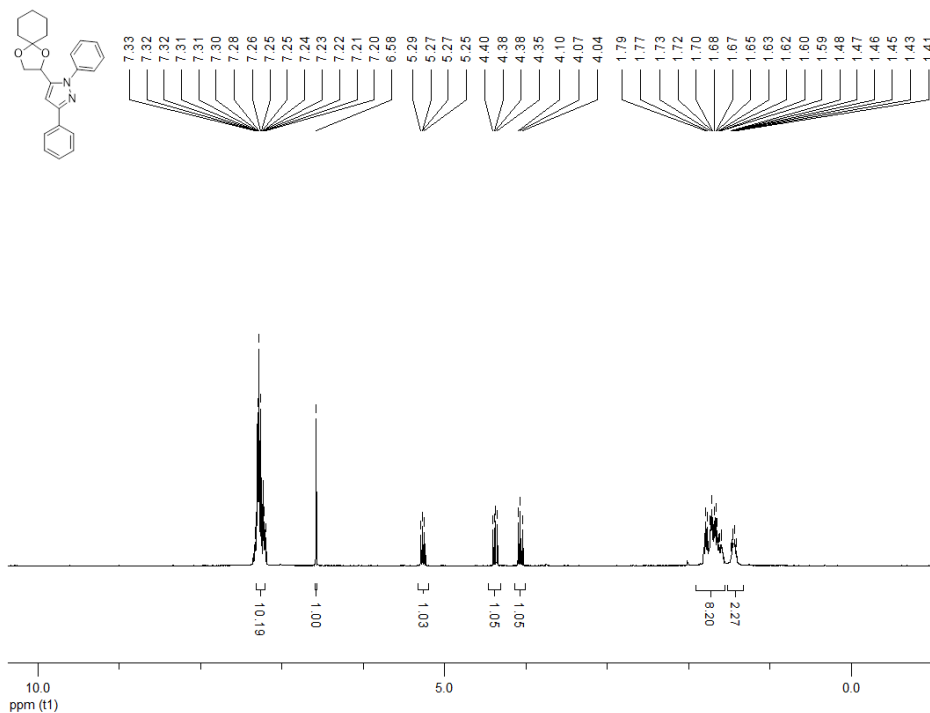
¹H NMR (300 MHz, CDCl₃) 5-{1,4-dioxaspiro[4.5]decan-2-yl}-1,3-diphenyl-1H-pyrazole (185f)

¹³C NMR (100 MHz, CDCl₃) 5-{1,4-dioxaspiro[4.5]decan-2-yl}-1,3-diphenyl-1H-pyrazole (185f)

^{1}H NMR (300 MHz, CDCl$_3$) 1,5-dimethyl-3-phenyl-1H-pyrazole (186)
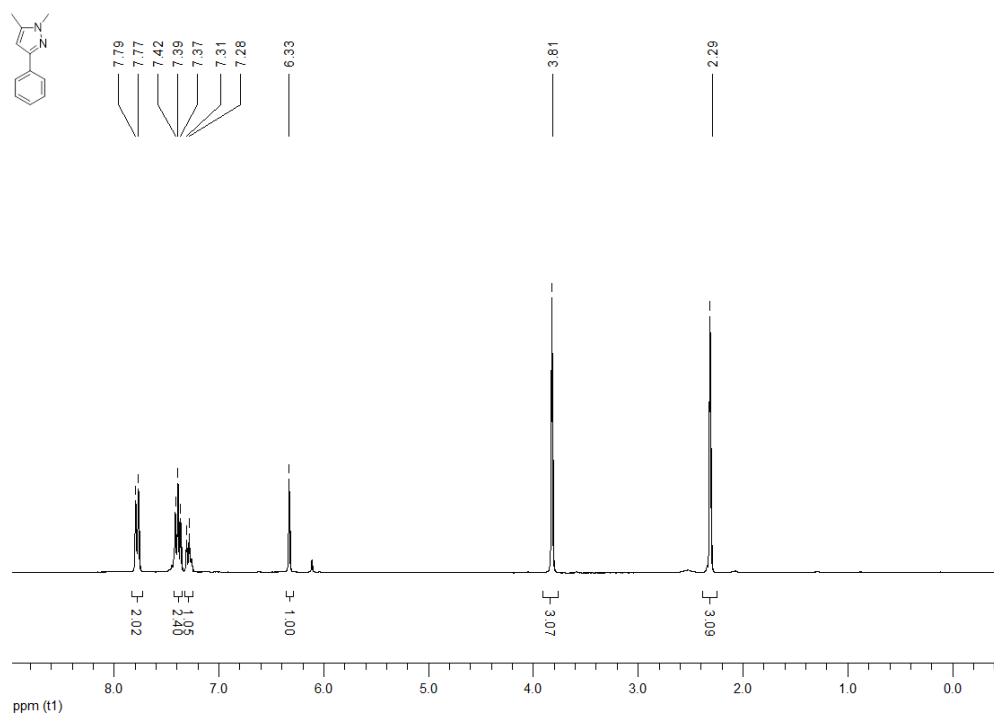
7.79
7.77
7.42
7.39
7.37
7.31
7.28
6.33
3.81
2.29

2.02
1.05
2.46
1.00
3.07
3.09

ppm (t1)

^{13}C NMR (100 MHz, CDCl$_3$) 1,5-dimethyl-3-phenyl-1H-pyrazole (186)

149.8
139.6
133.6
128.4
127.2
125.3
102.4
36.0
11.1

ppm (t1)
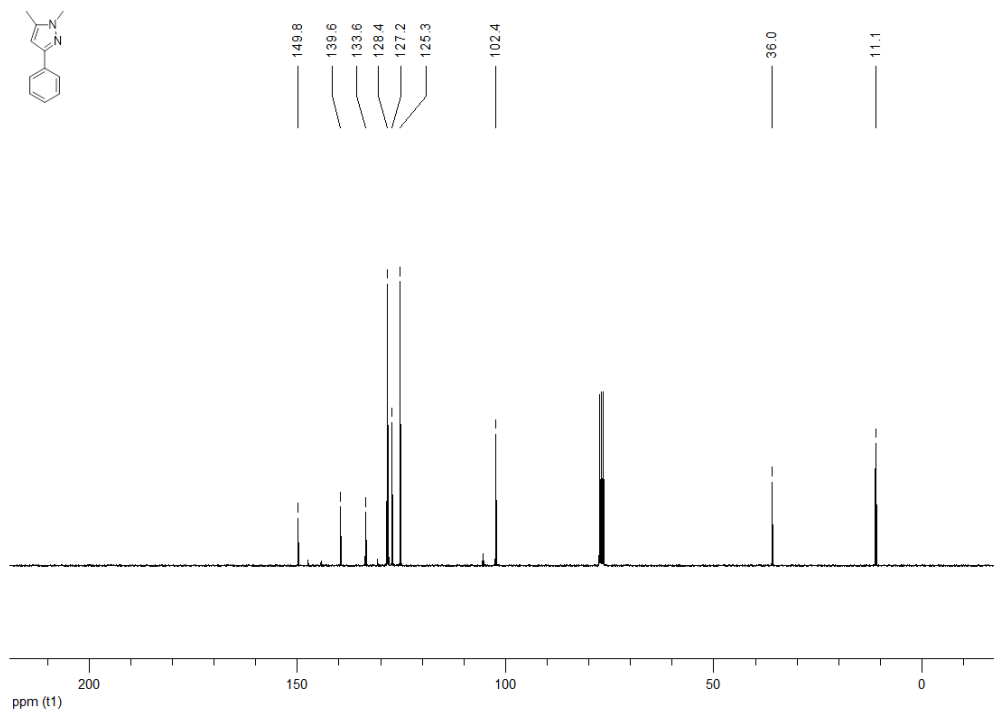
¹H NMR (300 MHz, CDCl₃) 5-{1,4-dioxaspiro[4.4]nonan-2-yl}-1-methyl-3-phenyl-1H-pyrazole (189a)
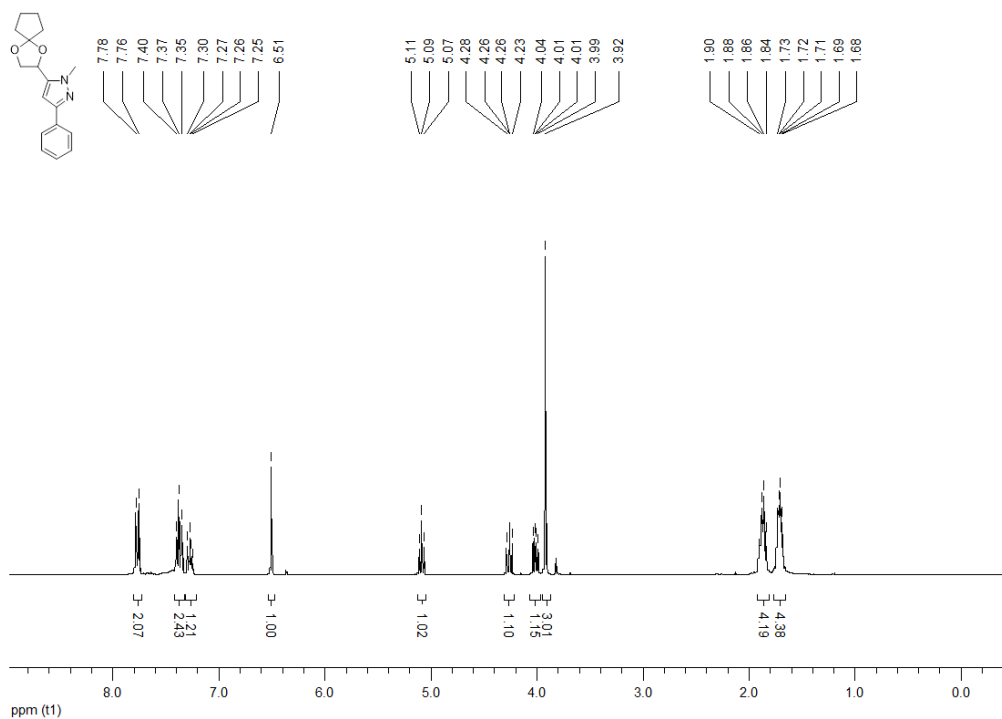
¹³C NMR (100 MHz, CDCl₃) 5-{1,4-dioxaspiro[4.4]nonan-2-yl}-1-methyl-3-phenyl-1H-pyrazole (189a)

¹H NMR (300 MHz, CDCl₃) 5-{1,4-dioxaspiro[4.6]undecan-2-yl}-1-methyl-3-phenyl-1H-pyrazole (189b)
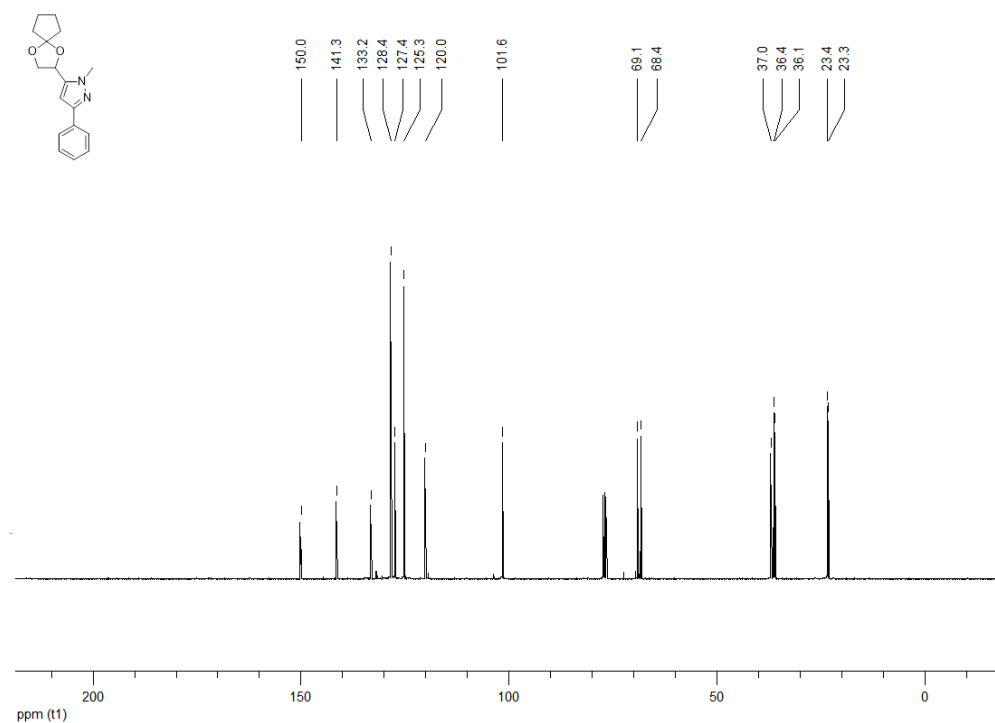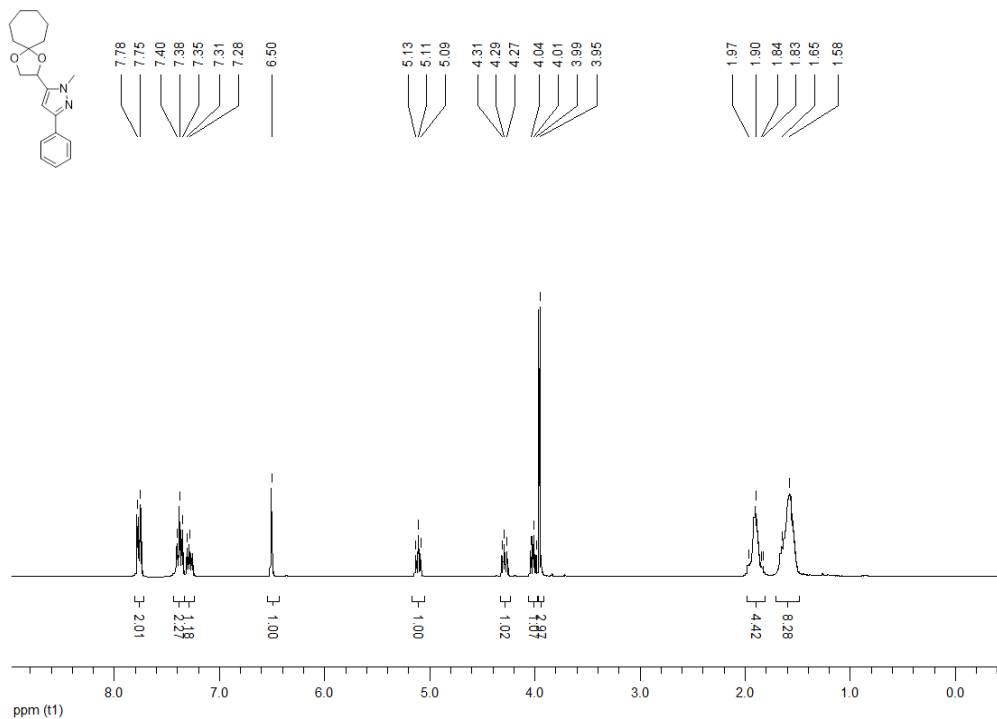
¹H NMR (300 MHz, CDCl₃) 5-{1,4-dioxaspiro[4.6]undecan-2-yl}-1-methyl-3-phenyl-1H-pyrazole (189b)

¹³C NMR (100 MHz, CDCl₃) 5-{1,4-dioxaspiro[4.6]undecan-2-yl}-1-methyl-3-phenyl-1H-pyrazole (189b)
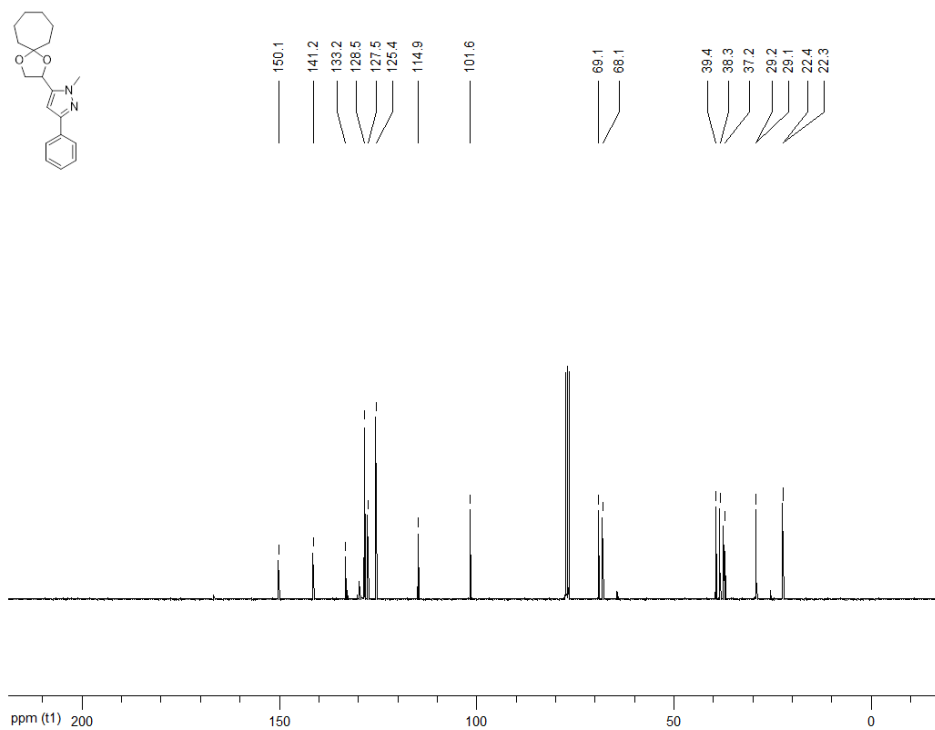
¹H NMR (300 MHz, CDCl₃) 1-methyl-3-phenyl-5-{1,4,8-trioxaspiro[4.5]decan-2-yl}-1H-pyrazole (189c)
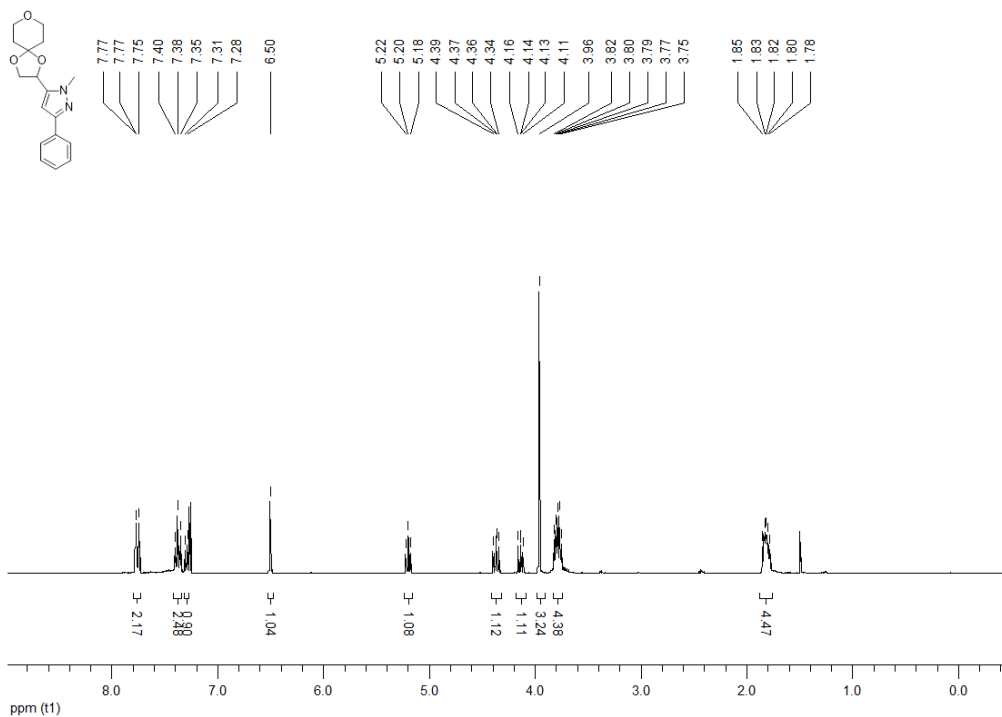
¹³C NMR (100 MHz, CDCl₃) 1-methyl-3-phenyl-5-{1,4,8-trioxaspiro[4.5]decan-2-yl}-1H-pyrazole (189c)
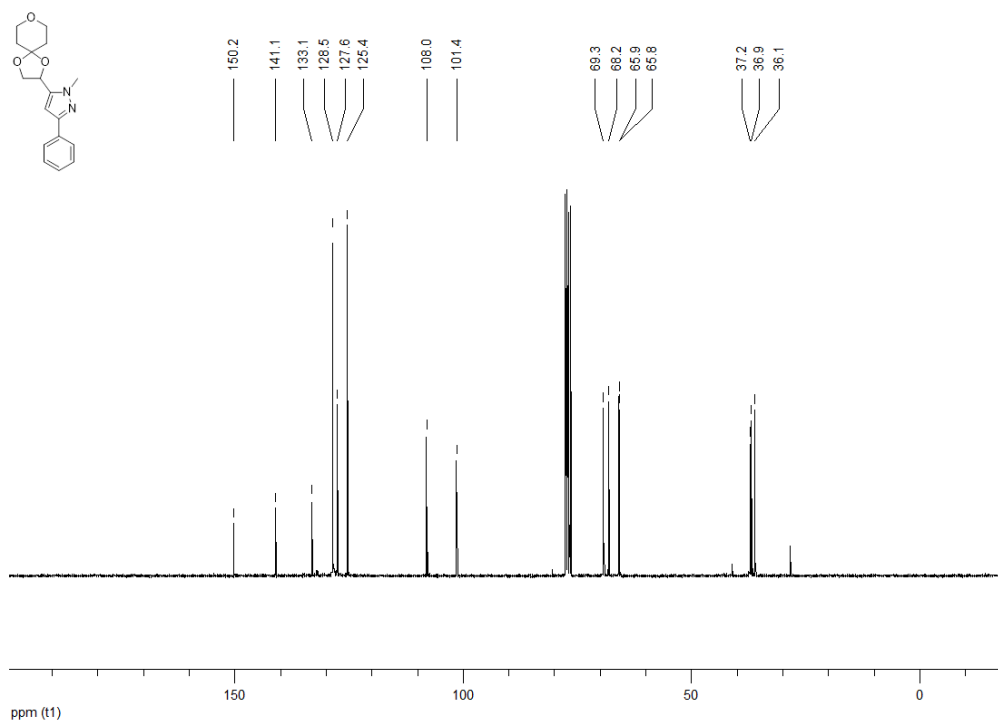
¹H NMR (300 MHz, CDCl₃) 1-[2-(1-methyl-3-phenyl-1H-pyrazol-5-yl)-1,4-dioxa-8-azaspiro[4.5]decan-8-yl]ethan-1-one (189d)
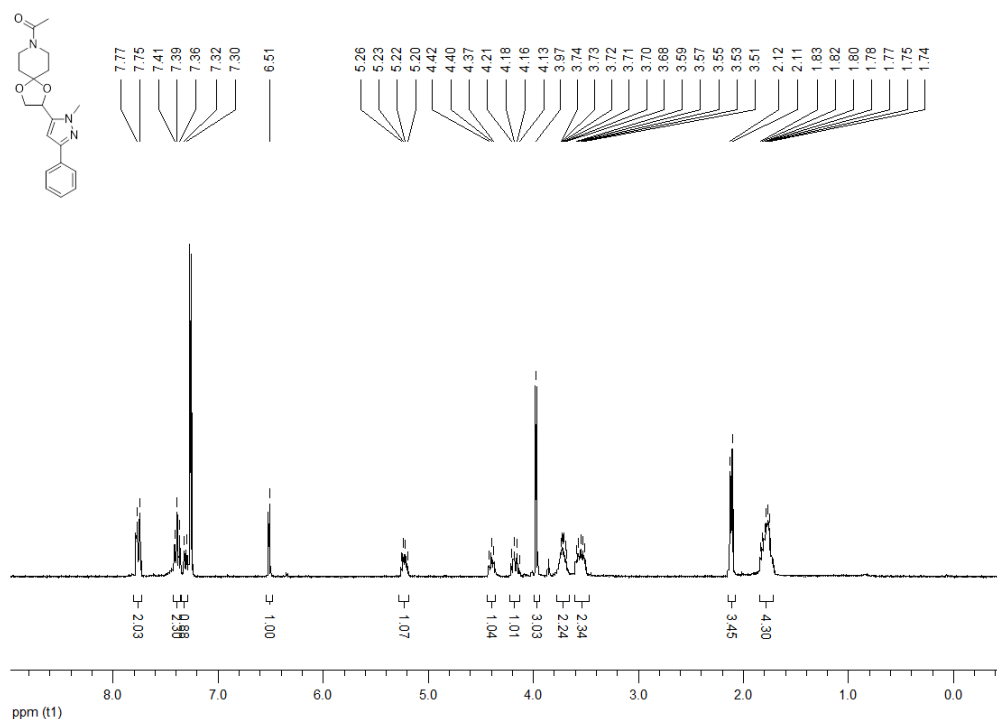
¹³C NMR (100 MHz, CDCl₃) 1-[2-(1-methyl-3-phenyl-1H-pyrazol-5-yl)-1,4-dioxa-8-azaspiro[4.5]decan-8-yl]ethan-1-one (189d)
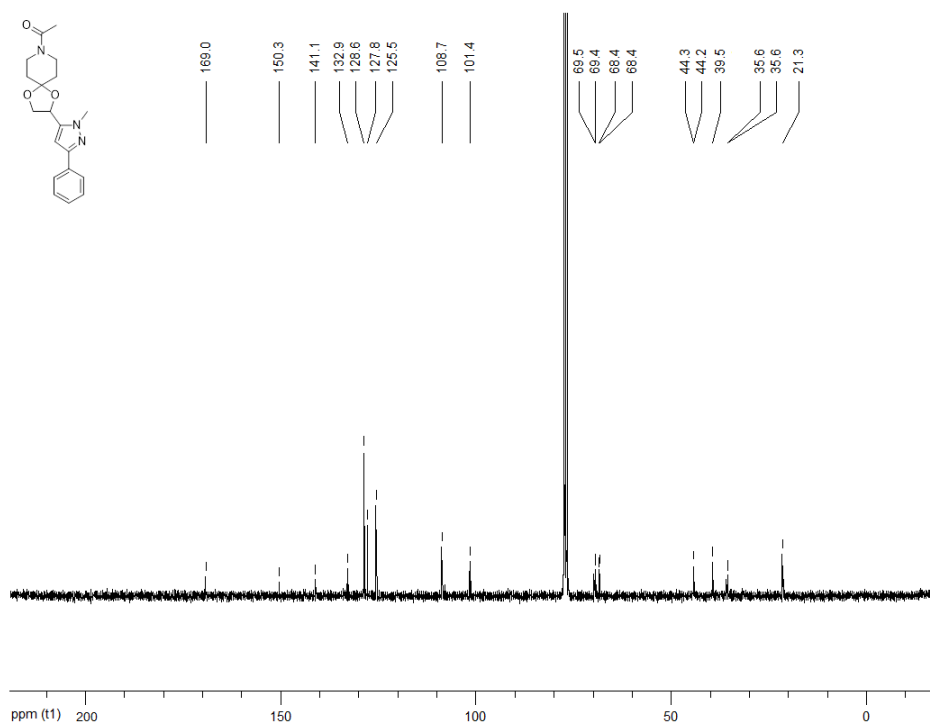
8.1.10 Synthesis, ^{1}H and ^{13}C NMR of disubstituted indoles and derivatives

Synthesis of 190c-h: a stirred solution of the corresponding 2-bromoanline (1.0 eq) and Et$_3$N (1.4 eq) in DCM was cooled to 0 °C using an ice bath. Trifluoroacetic anhydride (1.2 eq) was added dropwise. The mixture was stirred at room temperature overnight. The mixture was diluted with DCM and washed three times with water. The organic layer was dried over MgSO$_4$, filtered and concentrated *in vacuo* to yield the corresponding 2-bromotrifluoroacetanilide. The resulting compounds were used in the next step without being purified.[343]

Synthesis of 191b-g: a stirred solution of **40** (1.0 eq), the corresponding 2-bromotrifluoroacetanilide (1.1 eq), CuI (2% mol), L-proline (6% mol) and K$_2$CO$_3$ (2.0 eq) in DMF was heated at 80 °C for 1 − 6 days. The mixture was diluted with EtOAc and extracted three times with water. The organic layer was dried over MgSO$_4$, filtered and concentrated *in vacuo* to yield the corresponding indole. The crude was redissolved in ACN (1 mL), filtered and purified by preparative HPLC.[344]
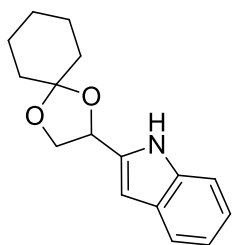
2-{1,4-dioxaspiro[4.5]decan-2-yl}-1*H*-indole (191b): orange oil, 50%, R_f = 0.34 (CyH/EtOAc 9:1), UHPLC-ESI-MS: R_t = 3.19, *m/z* = 258.2 [M + H] $^+$. ^{1}H NMR (300 MHz, CDCl$_3$) δ 8.33 (s br, 1H), 7.53 (d, *J* = 7.7 Hz, 1H), 7.27 (d, *J* = 8.0 Hz, 1H), 7.13 (t, *J* = 7.4 Hz, 1H), 7.06 (t, *J* = 7.3 Hz, 1H), 6.36 (s, 1H), 5.21 (t, *J* = 6.5 Hz, 1H), 4.24 (t, *J* = 7.2 Hz, 1H), 3.92 (t, *J* = 7.5 Hz, 1H), 1.73 − 1.62 (m, 8H), 1.40 − 1.37 (m, 2H) ppm; ^{13}C NMR (100 MHz, CDCl$_3$) δ 136.5, 136.0, 128.1, 122.0, 120.4, 119.8, 110.9, 110.5, 100.1, 71.6, 69.2, 36.1, 34.9, 25.0, 23.9, 23.7 ppm.
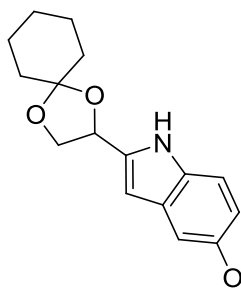
2-{1,4-dioxaspiro[4.5]decan-2-yl}-5-methoxy-1*H*-indole (191c): orange oil, 7%, R_f = 0.24 (CyH/EtOAc 9:1), UHPLC-ESI-MS: R_t = 3.09, *m/z* = 288.2 [M + H] $^+$. ^{1}H NMR (300 MHz, CDCl$_3$) δ 8.22 (s br, 1H), 7.25 (d, *J* = 8.4 Hz, 1H), 7.03 (s, 1H), 6.84 (dd, *J* = 2.1 Hz, *J* = 8.8 Hz, 1H), 6.34 (s, 1H), 5.27 (t, *J* = 6.5 Hz, 1H), 4.31 (t, *J* = 7.2 Hz, 1H), 3.96 (t, *J* = 7.5 Hz, 1H), 3.84 (s, 3H), 1.75

– 1.65 (m, 8H), 1.45 (d, J = 5.6 Hz, 2H) ppm; ^{13}C NMR (100 MHz, CDCl$_3$) δ 154.2, 137.3, 131.2, 128.7, 112.3, 111.6, 110.5, 102.3, 100.0, 71.8, 69.4, 55.8, 36.2, 35.0, 25.1, 24.0, 23.8 ppm.
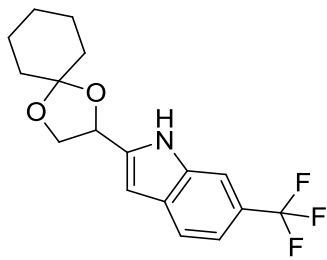
2-{1,4-dioxaspiro[4.5]decan-2-yl}-6-(trifluoromethyl)-1*H*-indole **(191d):** yellow oil, 14%, R_f = 0.28 (CyH/EtOAc 9:1), UHPLC-ESI-MS: R_t = 3.43, m/z = 326.2 [M + H] $^+$. ^{1}H NMR (300 MHz, CDCl$_3$) δ 8.55 (s br, 1H), 7.64 (d, J = 11.4 Hz, 2H), 7.33 (d, J = 8.3 Hz, 1H), 7.26 (s, 1H), 6.46 (s, 1H), 5.33 (t, J = 6.3 Hz, 1H), 4.36 (t, J = 7.2 Hz, 1H), 3.99 (t, J = 6.9 Hz, 1H), 1.73 – 1.66 (m, 8H), 1.47 – 1.41 (m, 2H) ppm; ^{13}C NMR (100 MHz, CDCl$_3$) δ 139.8, 134.7, 130.7, 126.9, 124.4, 120.8, 116.7 (q, J = 3.5 Hz), 110.9, 108.5 (q, J = 4.4 Hz), 100.0, 71.5, 69.4, 36.2, 34.9, 25.0, 24.0, 23.8 ppm.
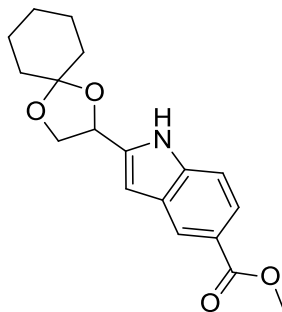
methyl 2-{1,4-dioxaspiro[4.5]decan-2-yl}-1*H*-indole-5-carboxylate **(191f):** yellow oil, 3%, R_f = 0.60 (CHCl$_3$/MeOH 9:1), UHPLC-ESI-MS: R_t = 3.07, m/z = 316.2 [M + H] $^+$. ^{1}H NMR (300 MHz, CDCl$_3$) δ 8.47 (s br, 1H), 8.33 (s, 1H), 7.89 (d, J = 8.6 Hz, 1H), 7.37 (d, J = 8.6 Hz, 1H), 6.49 (s, 1H), 5.31 (t, J = 6.3 Hz, 1H), 4.35 (dd, J = 6.9 Hz, J = 7.8 Hz, 1H), 3.99 (t, J = 7.2 Hz, 1H), 3.92 (s, 3H), 1.76 – 1.64 (m, 8H), 1.46 – 1.42 (m, 2H) ppm; ^{13}C NMR (100 MHz, CDCl$_3$) δ 168.1, 138.6, 138.2, 127.8, 123.6, 123.5, 122.1, 110.7, 110.6, 101.3, 71.5, 69.3, 51.8, 36.3, 34.8, 25.1, 24.0, 23.8 ppm.
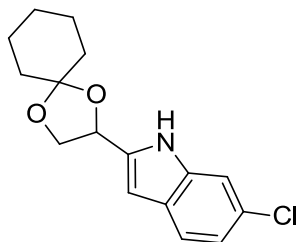
5-chloro-2-{1,4-dioxaspiro[4.5]decan-2-yl}-1*H*-indole (191e): brownish solid, 5%, R_f = 0.63 (CyH/EtOAc 3:1), UHPLC-ESI-MS: R_t = 3.38, m/z = 292.0 [M + H] $^+$. ^{1}H NMR (300 MHz, CDCl$_3$) δ 8.36 (s br, 1H), 7.53 (s, 1H), 7.27 (d, J = 8.3 Hz, 1H), 7.13 (dd, J = 0.9 Hz, J = 8.5 Hz, 1H),

6.35 (s, 1H), 5.29 (t, J = 6.4 Hz, 1H), 4.33 (t, J = 8.1 Hz, 1H), 3.96 (t, J = 7.2 Hz, 1H), 1.74 − 1.65 (m, 8H), 1.46 − 1.43 (m, 2H) ppm; ^{13}C NMR (100 MHz, CDCl$_3$) δ 138.2, 134.3, 129.3, 125.5, 122.4, 119.9, 111.9, 110.7, 99.7, 71.5, 69.4, 36.2, 34.9, 25.0, 24.0, 23.8 ppm.
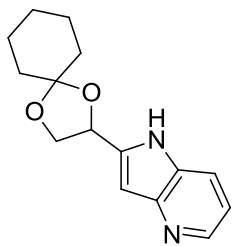
2-{1,4-dioxaspiro[4.5]decan-2-yl}-1*H*-pyrrolo[3,2-b]pyridine (191g): brown oil, 9%, R_f = 0.50 (CHCl$_3$/MeOH 9:1), UHPLC-ESI-MS: R_t = 1.76, m/z = 259.2 [M + H]$^+$. ^{1}H NMR (300 MHz, CDCl$_3$) δ 9.13 (s, 1H), 8.43 (s br, 1H), 7.66 (d, J = 7.5 Hz, 1H), 7.11 (s, 1H), 6.61 (s, 1H), 5.35 (t, J = 6.2 Hz, 1H), 4.36 (t, J = 7.2 Hz, 1H), 3.97 (t, J = 7.2 Hz, 1H), 1.71 − 1.64 (m, 8H), 1.44 − 1.39 (m, 2H) ppm; ^{13}C NMR (100 MHz, CDCl$_3$) δ 146.4, 140.9, 139.1, 131.7, 119.3, 118.3, 110.8, 100.5, 71.6, 69.5, 36.1, 34.9, 25.0, 24.0, 23.8 ppm.

¹H NMR (300 MHz, CDCl₃) 2-{1,4-dioxaspiro[4.5]decan-2-yl}-1*H*-indole (191b)
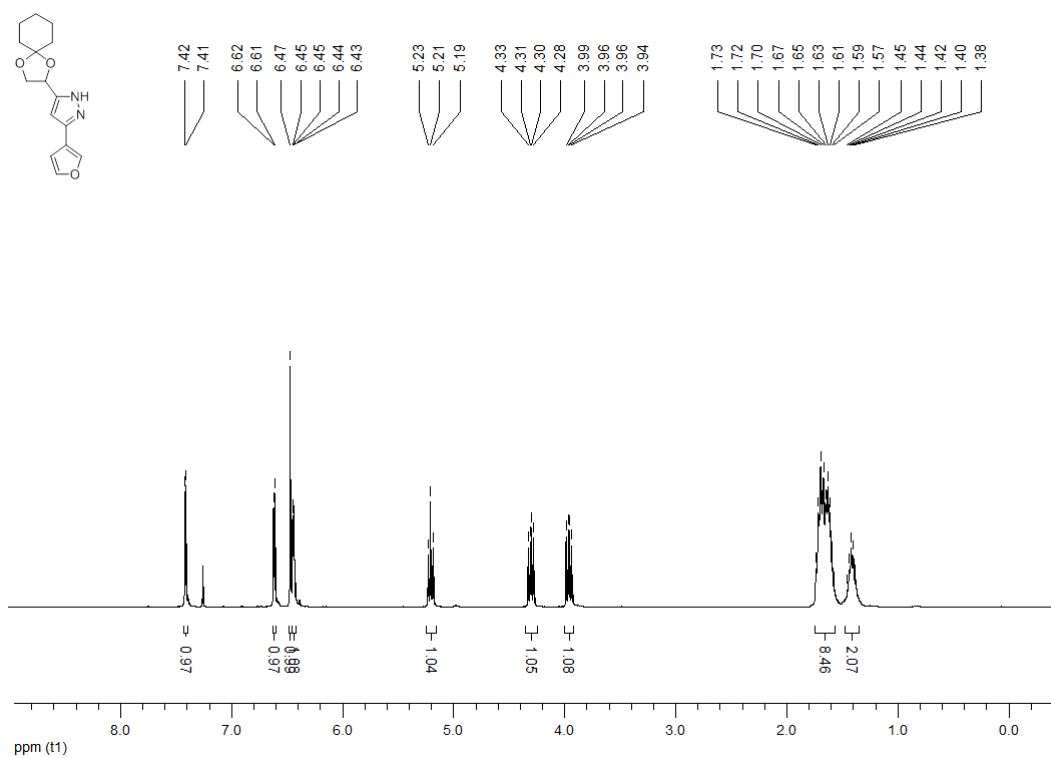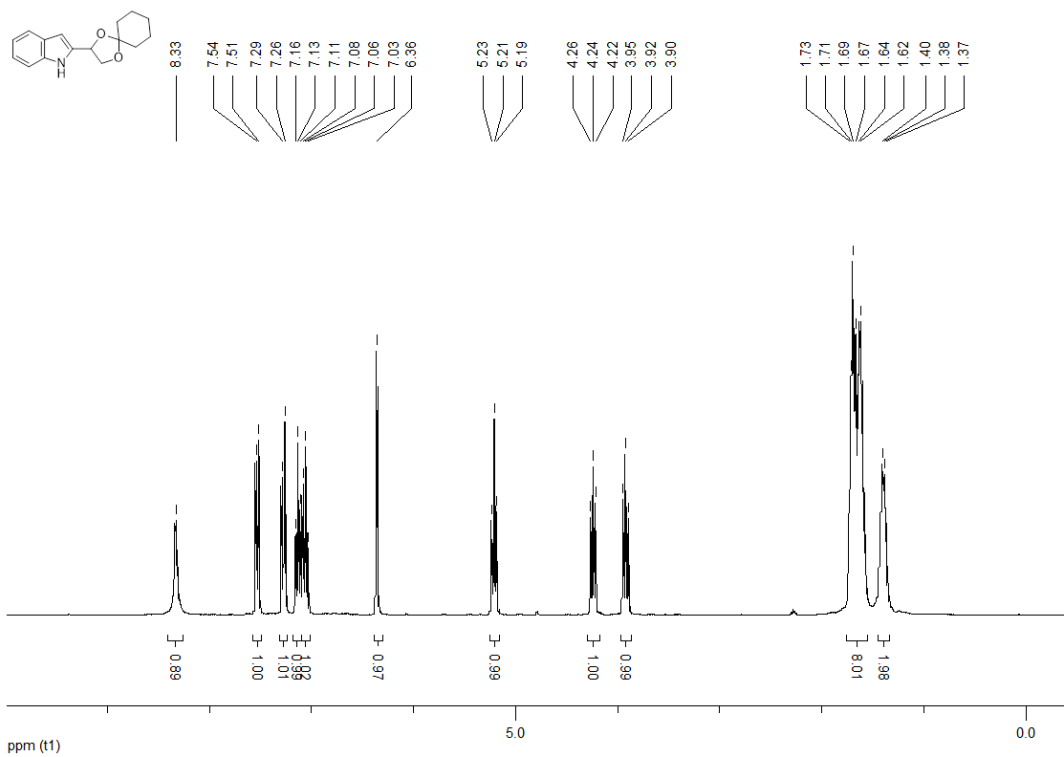
¹H NMR (300 MHz, CDCl₃) 2-{1,4-dioxaspiro[4.5]decan-2-yl}-1*H*-indole (191b)

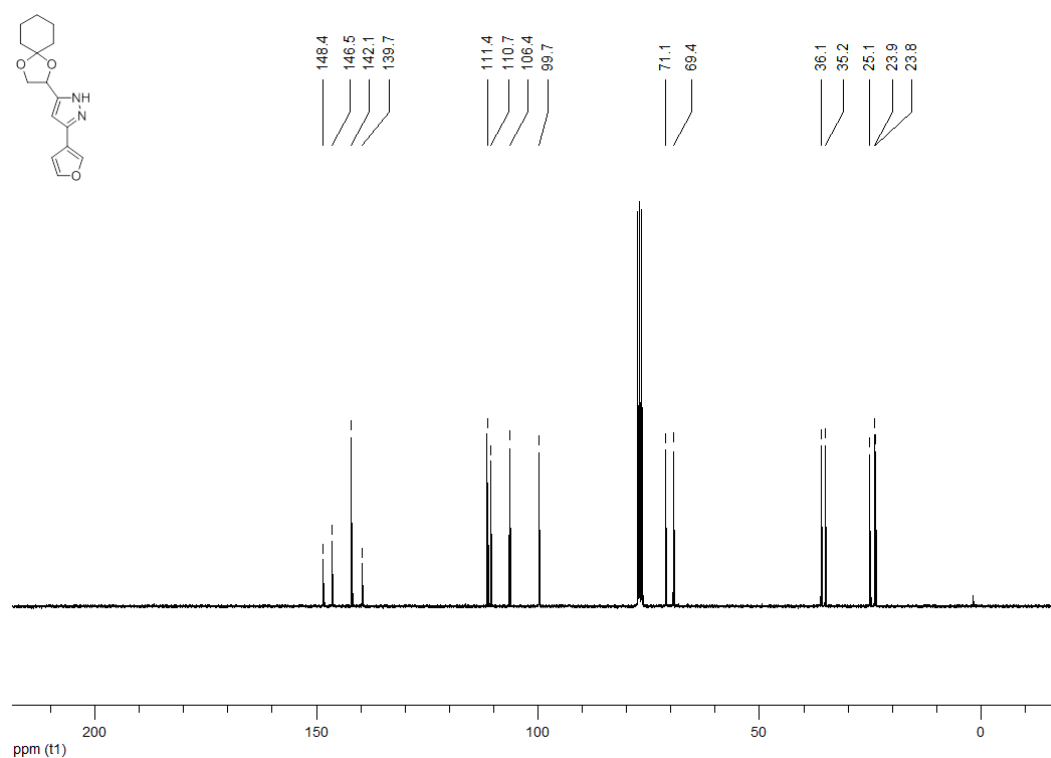## ¹³C NMR (100 MHz, CDCl₃) 2-{1,4-dioxaspiro[4.5]decan-2-yl}-1*H*-indole (191b)

¹³C NMR (100 MHz, CDCl₃) 2-{1,4-dioxaspiro[4.5]decan-2-yl}-1*H*-indole (191b)
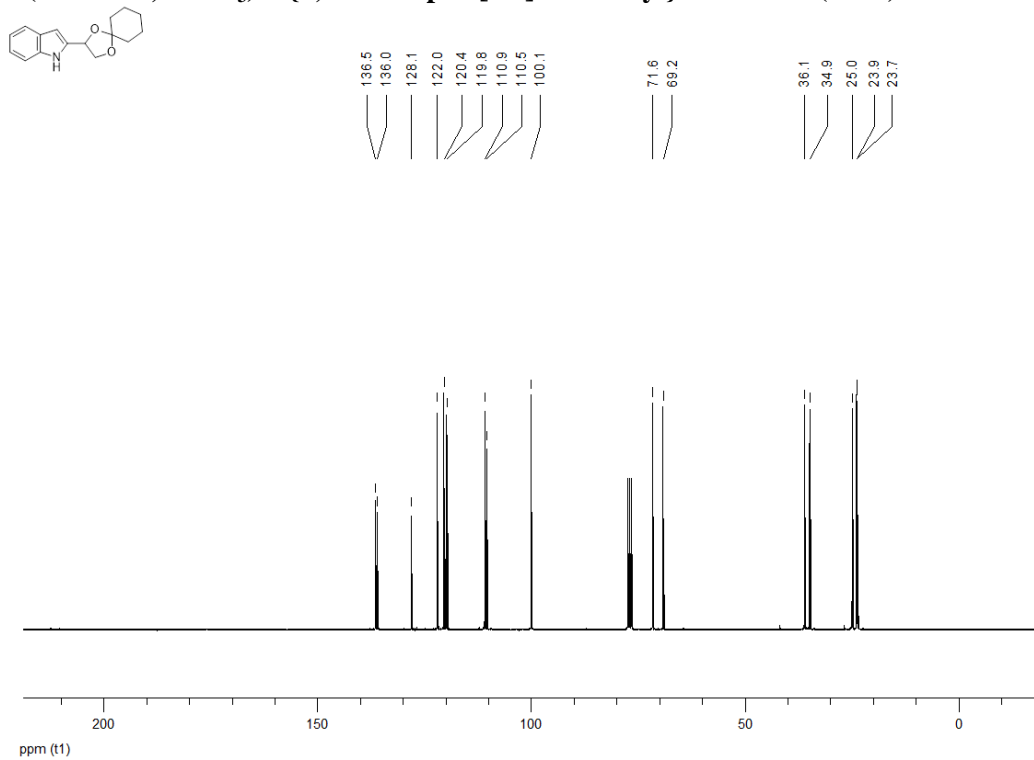
¹H NMR (300 MHz, CDCl₃) 2-{1,4-dioxaspiro[4.5]decan-2-yl}-5-methoxy-1*H*-indole (191c)
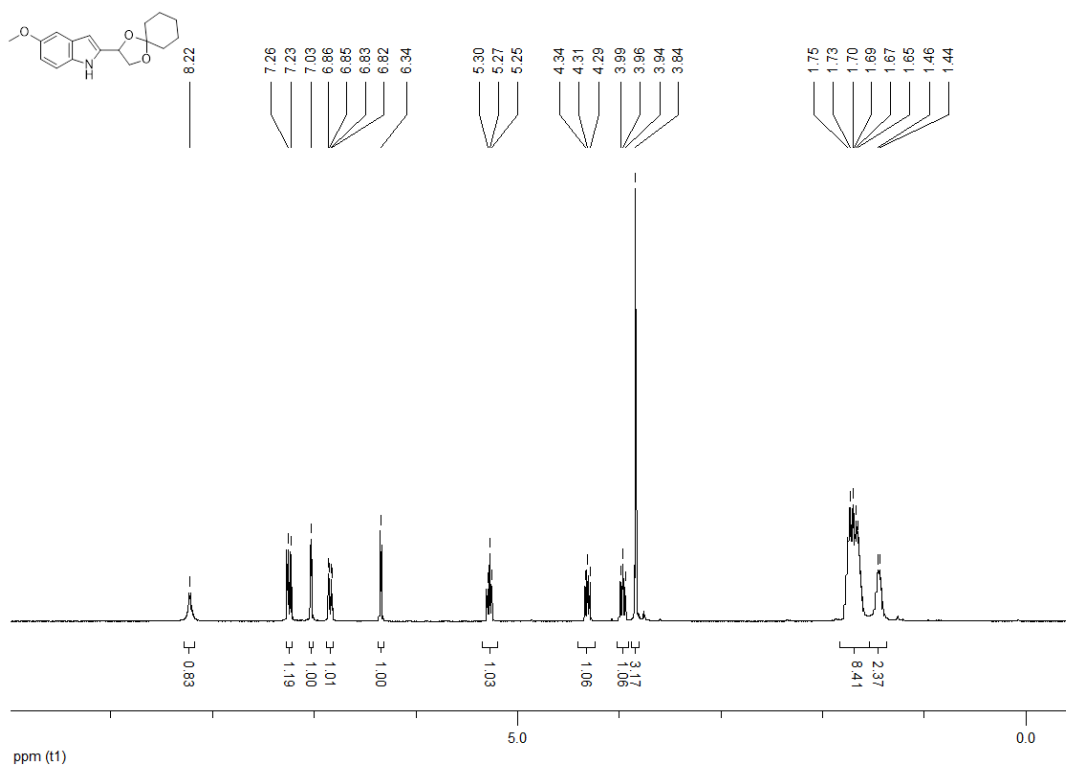
¹³C NMR (100 MHz, CDCl₃) 2-{1,4-dioxaspiro[4.5]decan-2-yl}-5-methoxy-1*H*-indole (191c)
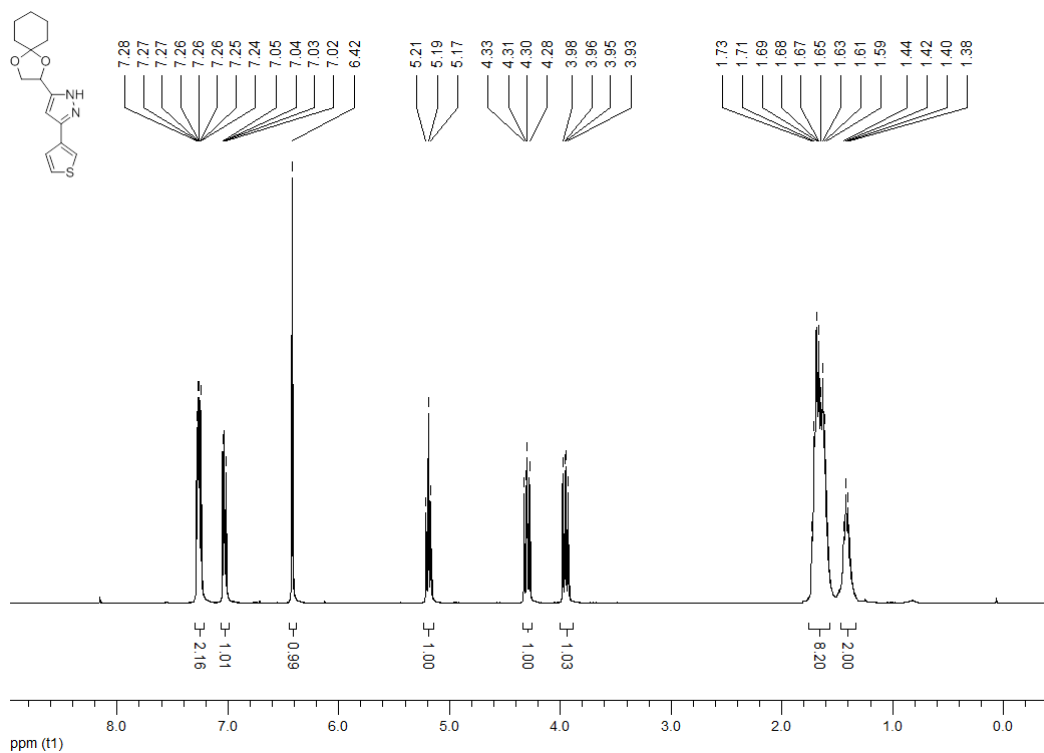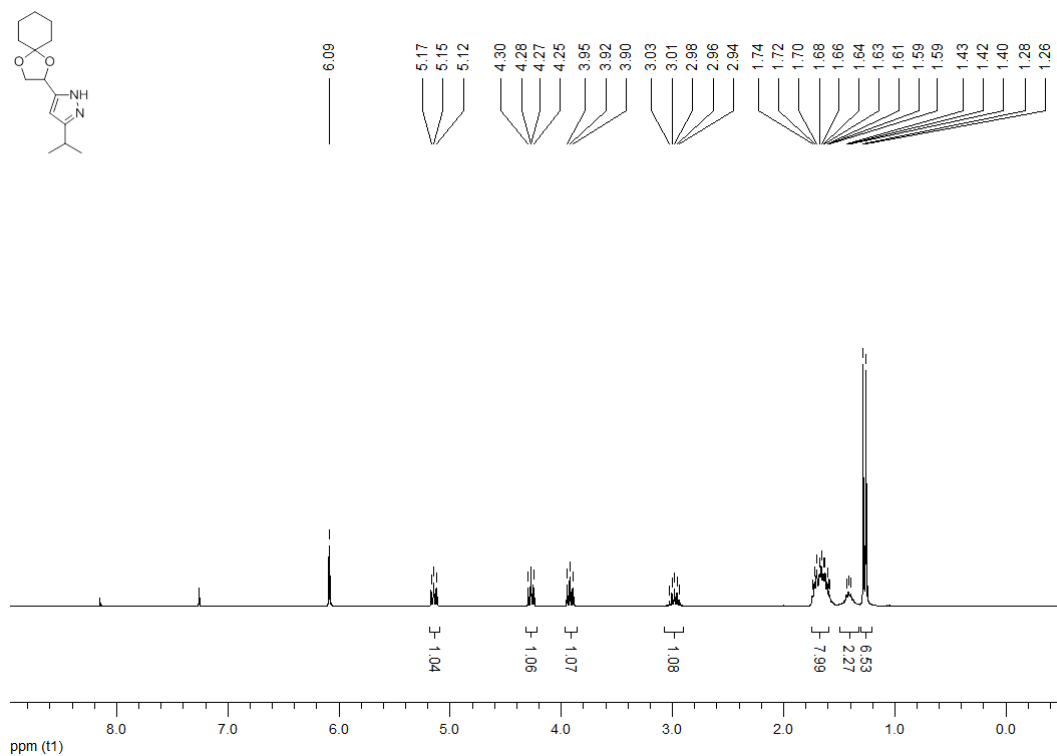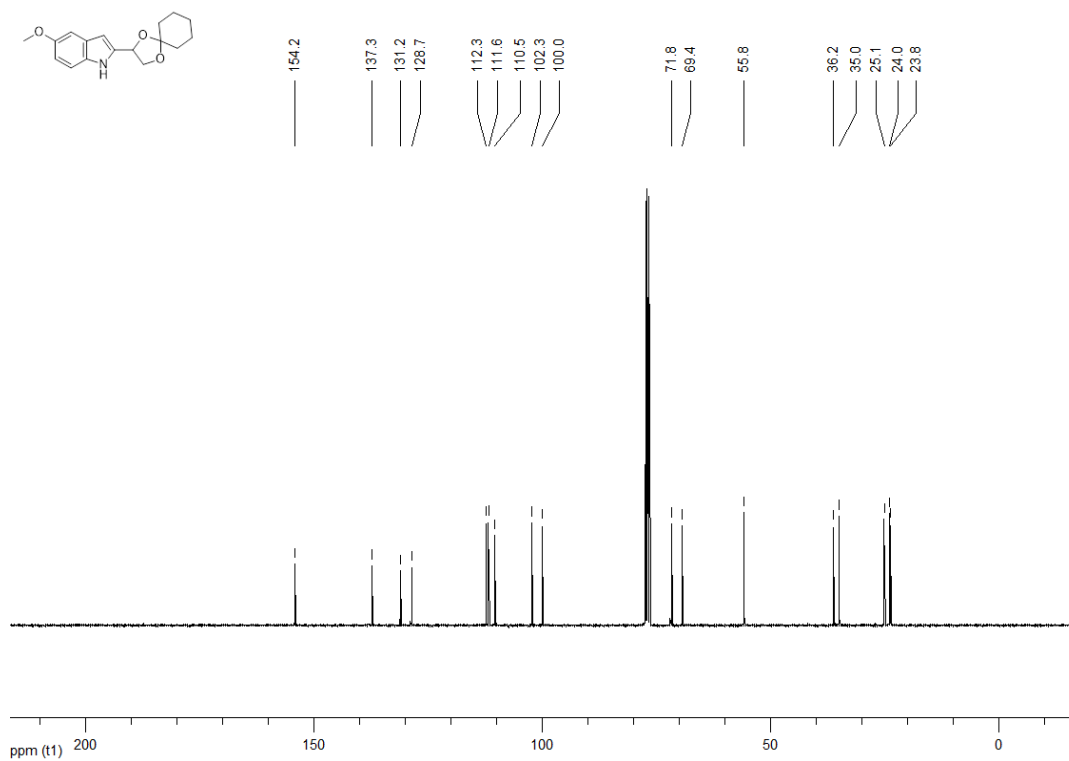
¹H NMR (300 MHz, CDCl₃) 2-{1,4-dioxaspiro[4.5]decan-2-yl}-6-(trifluoromethyl)-1*H*-indole (191d)
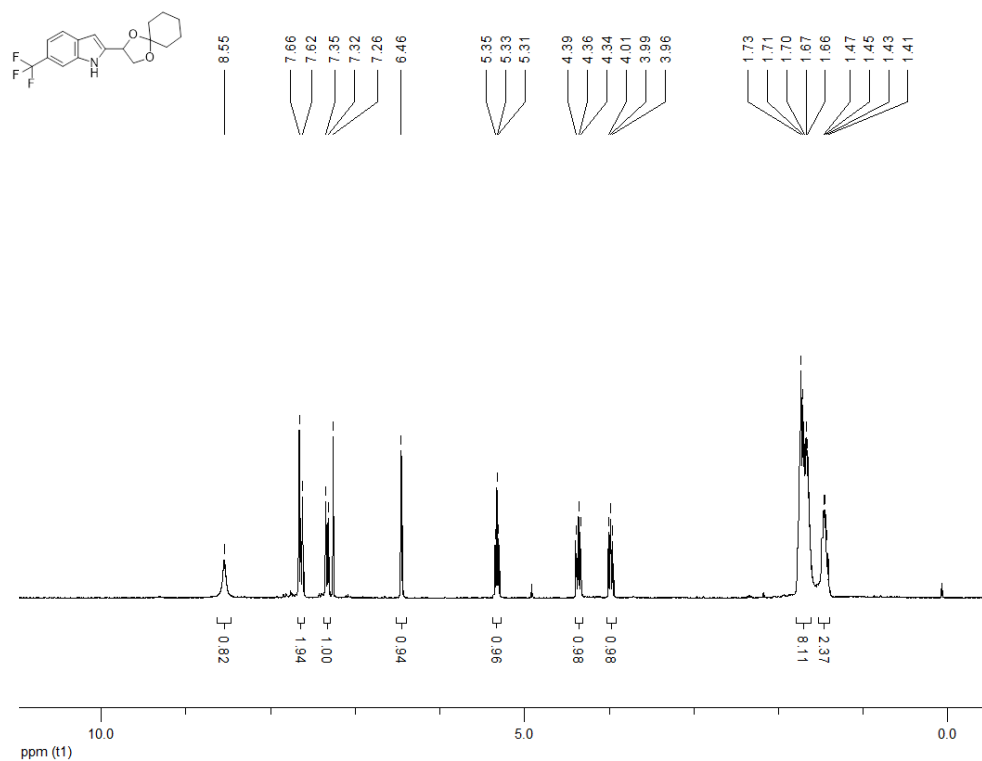
¹³C NMR (100 MHz, CDCl₃) 2-{1,4-dioxaspiro[4.5]decan-2-yl}-6-(trifluoromethyl)-1*H*-indole (191d)
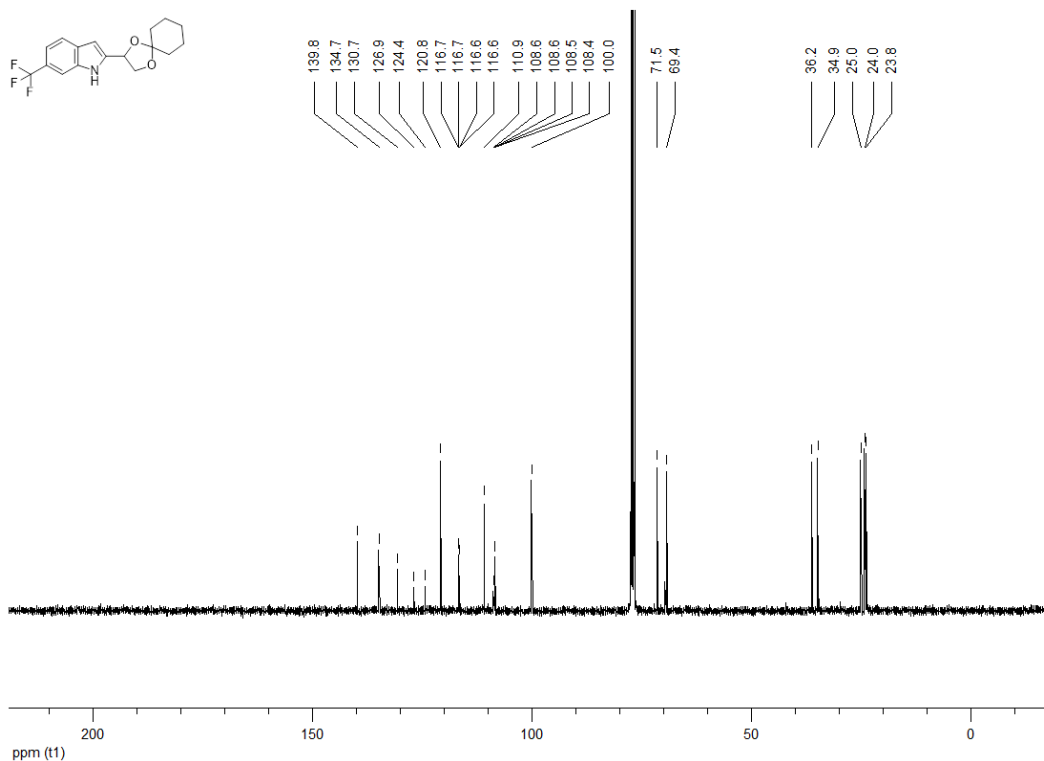
¹H NMR (300 MHz, CDCl₃) methyl 2-{1,4-dioxaspiro[4.5]decan-2-yl}-1*H*-indole-5-carboxylate (191e)
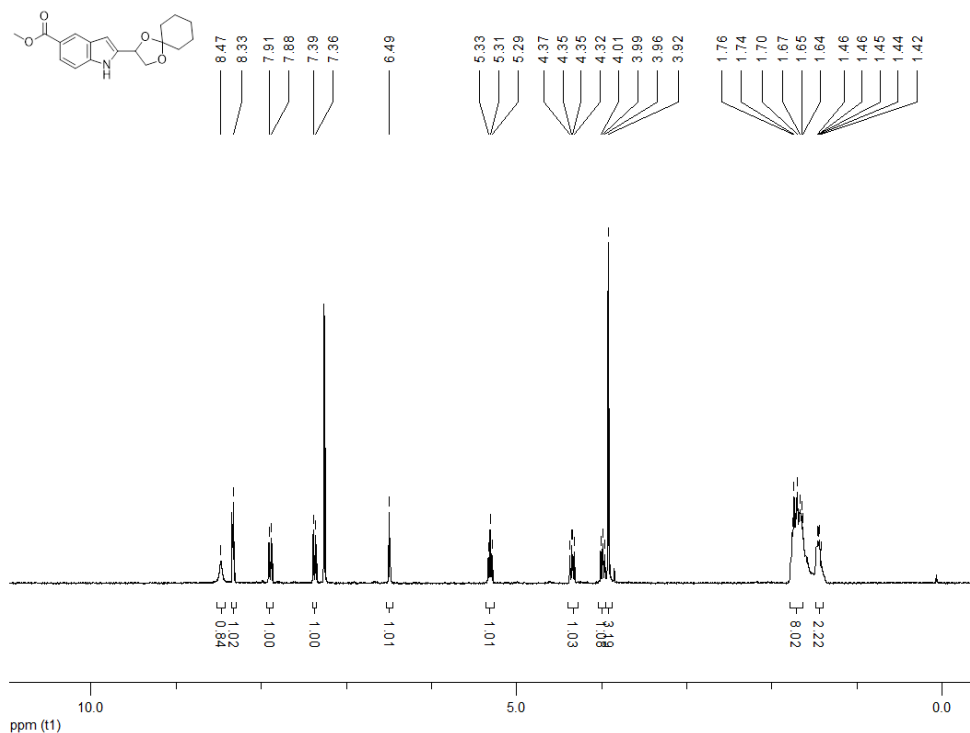
¹³C NMR (100 MHz, CDCl₃) methyl 2-{1,4-dioxaspiro[4.5]decan-2-yl}-1*H*-indole-5-carboxylate (191e)
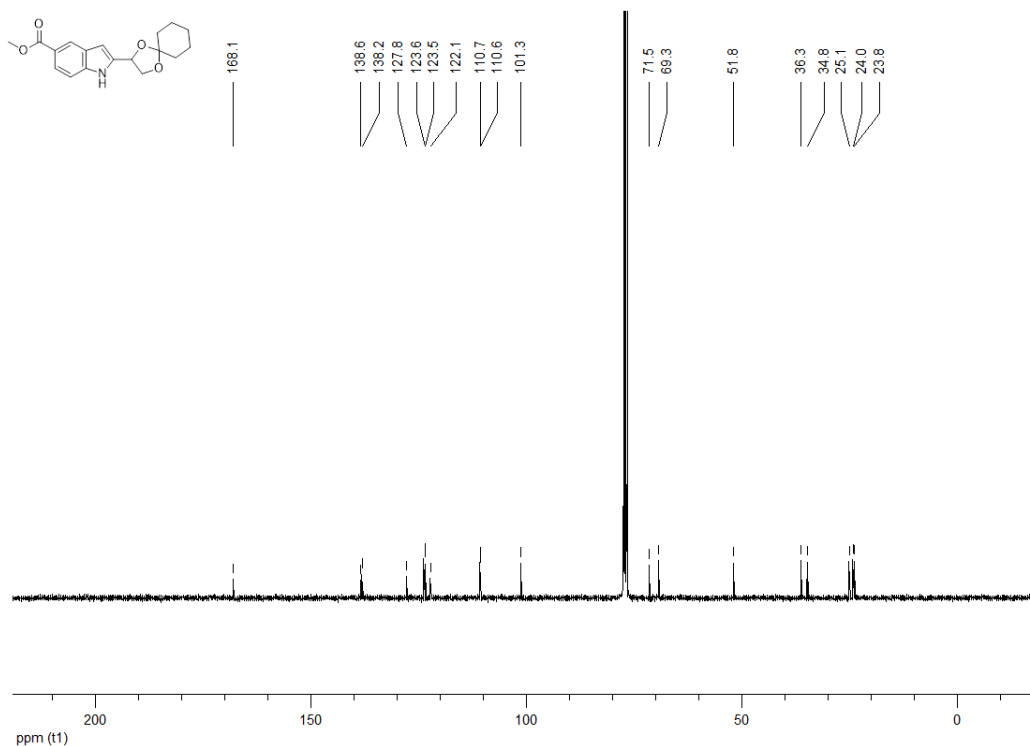
¹H NMR (300 MHz, CDCl₃) 5-chloro-2-{1,4-dioxaspiro[4.5]decan-2-yl}-1*H*-indole (191f)
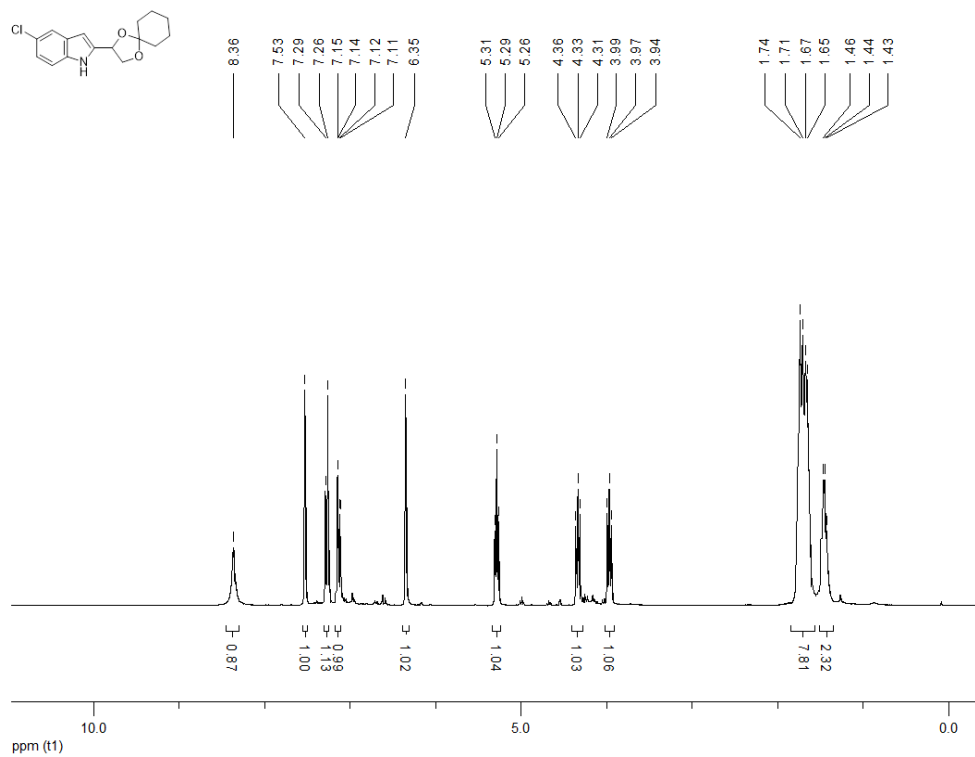
¹³C NMR (100 MHz, CDCl₃) 5-chloro-2-{1,4-dioxaspiro[4.5]decan-2-yl}-1*H*-indole (191f)

^{1}H NMR (300 MHz, CDCl$_3$) 2-{1,4-dioxaspiro[4.5]decan-2-yl}-1H-pyrrolo[3,2-b]pyridine (191g)
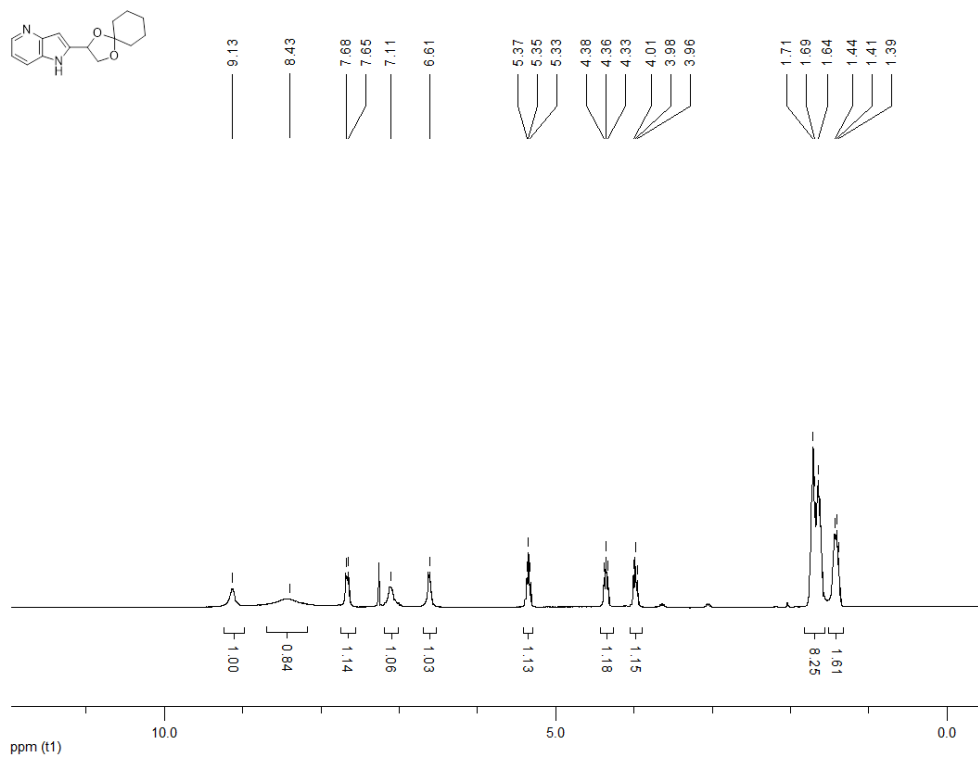
9.13
8.43
7.68
7.65
7.11
6.61
5.37
5.35
5.33
4.38
4.36
4.33
4.01
3.98
3.96
1.71
1.69
1.64
1.44
1.41
1.39

1.00
0.84
1.14
1.06
1.03
1.13
1.18
1.15
8.25
1.61

ppm (t1) 10.0 5.0 0.0

^{13}C NMR (100 MHz, CDCl$_3$) 2-{1,4-dioxaspiro[4.5]decan-2-yl}-1H-pyrrolo[3,2-b]pyridine (191g)

146.4
140.9
139.1
131.7
119.3
118.3
110.8
100.5
71.6
69.5
36.1
34.9
25.0
24.0
23.8

ppm (t1) 200 150 100 50 0

291
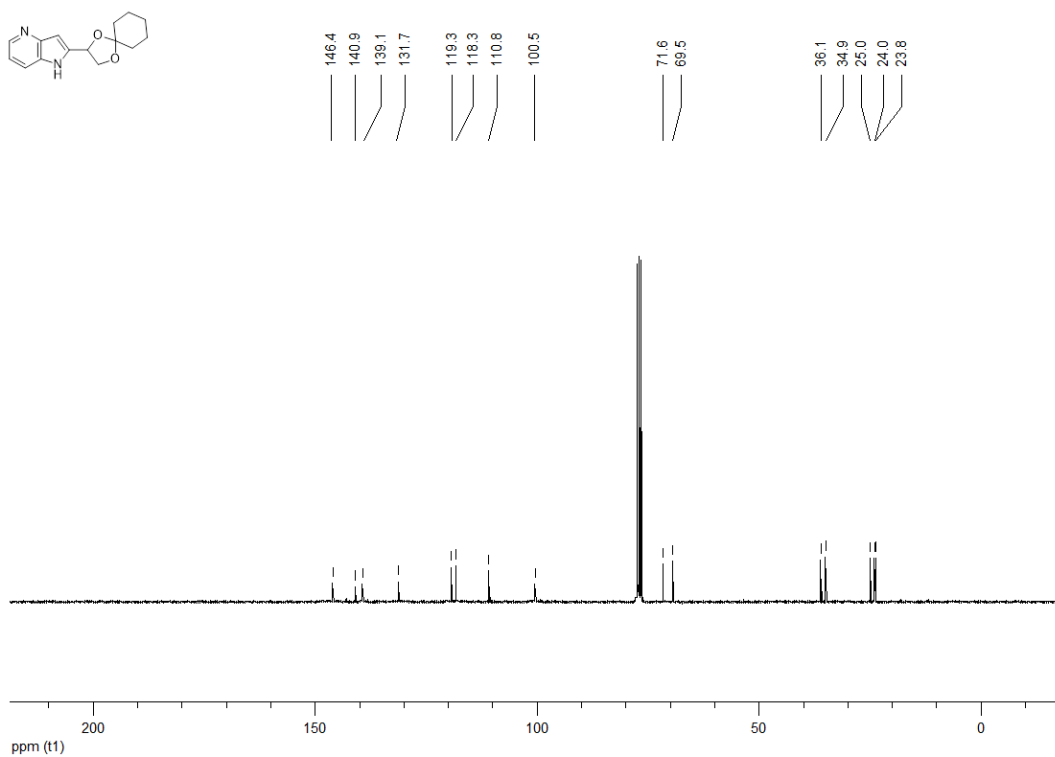
8.2 Computational

8.2.1 LsrK amino acid sequence

The three-dimensional structure of the following target sequence has been predicted by YASARA's homology modeling experiment, Version 16.4.6.L.32:

MARLFTLSESKYYLMALDAGTGSIRAVIFDLEGNQIAVGQAEWRHLAVPDVPGSMEFDLNKNWQL
ACECMRQALHNAGIAPEYIAAVSACSMREGIVLYNNEGAPIWACANVDARAAREVSELKELHNNT
FENEVYRATGQTLALSAIPRLLWLAHHRSDIYRQASTITMISDWLAYMLSGELAVDPSNAGTTGLLD
LTTRDWKPALLDMAGLRADILSPVKETGTLLGVVSSQAAELCGLKAGTPVVVGGGDVQLGCLGLG
VVRPAQTAVLGGTFWQQVVNLAAPVTDPEMNVRVNPHVIPGMVQAESISFFTGLTMRWFRDAFCA
EEKLIAERLGIDTYTLLEEMASRVPPGSWGVMPIFSDRMRFKTWYHAAPSFINLSIDPDKCNKATLFR
ALEENAAIVSACNLQQIADFSNIHPSSLVFAGGGSKGKLWSQILADVSGLPVNIPVVKEATALGCAIA
AGVGAGIFSSMAETGERLVRWERTHTPDPEKHELYQDSRDKWQAVYQDQLGLVDHGLTTSLWKA
PGL

Uniprot code: **Q8ZKQ6** (LsrK from *S. thyphimurium*, strain LT2). The target sequence contains 530 residues in one molecule.

8.2.2 Homology modeling parameters

The following parameters have been chosen for this target:

- Modeling speed (slow = best): **Slow**

- Number of PSI-BLAST iterations in template search (PSI-BLASTs): **3**

- Maximum allowed (PSI-)BLAST E-value to consider template (EValue Max): **0.5**

- Maximum number of templates to be used (Templates Total): **5**

- Maximum number of templates with same sequence (Templates SameSeq): **1**

- Maximum oligomerization state (OligoState): **4** (tetrameric)

- Maximum number of alignment variations per template: (Alignments): **5**

- Maximum number of conformations tried per loop (LoopSamples): **50**

- Maximum number of residues added to the termini (TermExtension): **10**

8.2.3 Homology modeling templates

Since the target sequence was the only available information, possible templates were identified by running 3 PSI-BLAST iterations to extract a position specific scoring matrix (PSSM) from UniRef90, and then searching the PDB for a match (i.e. hits with an E-value below the homology modeling cutoff 0.5).

The following 47 hits were found:

Entry	Total score**	BLAST E-value	Align score	Cover	ID	Res (Å)	Header
1	135.33	0	305.0	90%	3EZW-A	2.00	Crystal Structure Of A Hyperactive *E. coli* Glycerol Kinase Mutant Gly230 -> Asp Obtained Using Microfluidic Crystallization Devices (498 residues with quality score 0.493), released 2008-11-04
2	132.43	2e-115	327.0	90%	3IFR-B	2.30	The Crystal Structure Of Xylulose Kinase From *R. rubrum* (480 residues with quality score 0.450), released 2009-08-25
3	121.28	0	263.0	91%	3G25-B	1.90	1.9 Angstrom Crystal Structure Of Glycerol Kinase (Glpk) From *S. aureus* In Complex With Glycerol. (499 residues with quality score 0.506), released 2009-02-17
4	119.75	0	321.0	89%	2ZF5-Y	2.40	Crystal Structure Of Highly Thermostable Glycerol Kinase From A Hyperthermophilic Archaeon (494 residues with quality score 0.418), released 2008-05-06
5	119.63	6e-154	264.0	89%	3WXL-A	1.90	C (513 residues with quality score 0.511), released 2014-12-24
-	115.72	0	241.0	91%	3H3N-O	-	Glycerol Kinase H232r With Glycerol (501 residues with quality score 0.528), released 2009-06-02.*
-	115.64	6e-168	291.0	88%	2ITM-B	-	Crystal Structure Of The *E. coli* Xylulose Kinase Complexed With Xylulose (475 residues with quality score 0.451)*
-	114.93	0	259.0	90%	2D4W-B	-	Crystal Structure Of Glycerol Kinase From Cellulomonas Sp. Nt3060 (503 residues with quality score 0.491)*
-	111.37	0	243.0	91%	3H46-O	-	Glycerol Kinase H232e With Glycerol (500 residues with quality score 0.505), released 2009-06-02.*
-	111.13	0	252.0	90%	3D7E-O	-	*E. casseliflavus* Glycerol Kinase Mutant His232ala Complexed With Glycerol (495 residues with quality score 0.491), released 2009-04-28.*

Entry	Total score	BLAST E-value	Align score	Cover	ID	Res (Å)	Header
-	110.17	7e-78	266.0	92%	3QDK-D	-	Structural Insight On Mechanism And Diverse Substrate Selection Strategy Of Ribulokinase (554 residues with quality score 0.448), released 2011-02-09.*
-	109.54	1e-72	242.0	90%	3L0Q-A	-	The Crystal Structure Of Xlylulose Kinase From *Y. pseudotuberculosis* (541 residues with quality score 0.504), released 2010-01-05.*
-	106.63	2e-131	250.0	85%	3LL3-B	-	The Crystal Structure Of Ligand Bound Xylulose Kinase From *L. Acidophilus* (490 residues with quality score 0.499), released 2010-03-23.*
-	105.10	1e-80	217.0	89%	3HZ6-A	-	Crystal Structure Of Xylulokinase From *C. violaceum* (497 residues with quality score 0.545), released 2009-07-21.*
-	101.49	0	259.0	89%	4E1J-B	-	Crystal Structure Of Glycerol Kinase In Complex With Glycerol From *S. meliloti* 1021 (484 residues with quality score 0.440), released 2012-03-21.*
-	97.62	0	299.0	90%	1BU6-Y	-	Crystal Structures Of *E. coli* Glycerol Kinase And The Mutant A65t In An Inactive Tetramer: Conformational Changes And Implications For Allosteric Regulation (499 residues with quality score 0.362), released 1998-09-16.*
-	96.95	1e-133	191.0	91%	2W40-D	-	Crystal Structure Of *P. falciparum* Glycerol Kinase With Bound Glycerol (503 residues with quality score 0.557), released 2008-12-02.*
-	95.22	0	269.0	88%	2DPN-A	-	Crystal Structure Of The Glycerol Kinase From *T. thermophilus* Hb8 (492 residues with quality score 0.400), released 2006-11-12.*

Entry	Total score	BLAST E-value	Align score	Cover	ID	Res (Å)	Header
-	91.96	0	299.0	90%	1GLA-G	-	Structure Of The Regulatory Complex Of *E. coli* IIIglc With Glycerol Kinase (489 residues with quality score 0.341), released 1993-10-31.*
-	77.99	0	296.0	90%	1GLJ-Y	-	*E. coli* Glycerol Kinase Mutant With Bound Atp Analog Showing Substantial Domain Motion (494 residues with quality score 0.294), released 1999-05-18.*
-	66.25	5e-37	161.0	88%	4C23-B	-	L-fuculose Kinase (468 residues with quality score 0.469), released 2013-12-11.*
-	53.68	2e-67	129.0	83%	3I8B-A	-	The Crystal Structure Of Xylulose Kinase From *B. adolescentis* (506 residues with quality score 0.499), released 2009-08-04.*
-	48.82	1e-27	105.0	88%	2UYT-A	-	Structure Of L-Rhamnulose Kinase In Complex With Adp And Beta-L-Rhamnulose (479 residues with quality score 0.530), released 2007-06-26.*
-	46.36	2e-24	105.0	88%	2CGL-A	-	Crystal Structure Of L-Rhamnulose Kinase From *E. coli* In Complex With L-Fructose, Adp And A Modeled Atp Gamma Phosphate (479 residues with quality score 0.500), released 2006-05-31.*
-	42.88	3e-32	104.0	79%	5HUX-A	-	Putative Sugar Kinases From *S. elongatus* Pcc7942 In Complex With Adp (429 residues with quality score 0.524), released 2016-06-08.*
-	42.05	3e-30	103.0	77%	5HTJ-A	-	Putative Sugar Kinases From *S. elongatus* Pcc7942-d8a (419 residues with quality score 0.529), released 2016-06-08.*
-	41.01	3e-38	96.0	79%	5HTV-A	-	Putative Sugar Kinases From *A. thaliana* In Complex With Amppnp (424 residues with quality score 0.543), released 2016-06-08.*

Entry	Total score	BLAST E-value	Align score	Cover	ID	Res (Å)	Header
-	40.69	2e-30	105.0	77%	5HU2-A	-	Sugar Kinases From *S. elongatus* Pcc7942-t11a (420 residues with quality score 0.501), released 2016-06-08.*
-	36.77	2e-30	102.0	77%	5HTY-A	-	Sugar Kinases From *S. elongatus* Pcc7942-d221a (420 residues with quality score 0.466), released 2016-06-08.*
-	33.86	3e-46	72.0	91%	4BC5-A	-	Crystal Structure Of Human D-xylulokinase In Complex With Inhibitor 5-deoxy-5-fluoro-d-xylulose (524 residues with quality score 0.515), released 2012-11-28.*
-	28.63	3e-42	62.0	90%	4BC4-C	-	Crystal Structure Of Human D-xylulokinase In Complex With D-Xylulose (524 residues with quality score 0.513), released 2012-11-28.*
-	22.77	0	248.0	88%	1XUP-X	-	*E. casseliflavus* Glycerol Kinase Complexed With Glycerol (487 residues with quality score 0.104), released 2004-12-14.*
-	9.15	9e-07	25.0	82%	3H6E-B	-	The Crystal Structure Of A Carbohydrate Kinase From *N. aromaticivorans* (467 residues with quality score 0.445), released 2009-06-02.*
-	8.17	0.088	37.0	40%	3VGM-A	-	Crystal Structure Of A Rok Family Glucokinase From *S. griseus* In Complex With Glucose (312 residues with quality score 0.547), released 2011-12-07.*
-	2.05	0.037	7.0	53%	2YHY-A	-	Structure Of N-Acetylmannosamine Kinase In Complex With N-Acetylmannosamine And Adp (308 residues with quality score 0.550), released 2012-02-29.*
-	1.97	0.32	10.0	34%	5FPD-B	-	Structure Of Heat Shock-related 70kda Protein 2 With Small-molecule Ligand Pyrazine-2-carboxamide (at513) In An Alternate Binding Site. (377 residues with quality score 0.587), released 2015-12-16.*

Entry	Total score	BLAST E-value	Align score	Cover	ID	Res (Å)	Header
-	0.98	0.032	12.0	18%	4KBO-A	-	Crystal Structure Of The Human Mortalin (grp75) Atpase Domain In The Apo Form (374 residues with quality score 0.454), released 2014-04-02.*.
-	0.77	0.29	10.0	13%	4EHU-A	-	Activator Of The 2-Hydroxyisocaproyl-Coa Dehydratase From *C. difficile* With Bound Adpnp (268 residues with quality score 0.583), released 2012-08-08.*
-	0.56	0.09	8.0	12%	3WT0-D	-	Crystal Structure Analysis Of Cell Division Protein (378 residues with quality score 0.570), released 2015-04-29.*
-	0.39	0.047	8.0	9%	3BZK-A	-	Crystal Structure Of The Tex Protein From *P. aeruginosa*, Crystal Form 2 (728 residues with quality score 0.546), released 2008-04-08.*.
-	0.37	0.17	15.0	5%	3ZYY-X	-	Reductive Activator For Corrinoid, Iron-Sulfur Protein (628 residues with quality score 0.478), released 2012-04-04.*
-	0.29	0.42	9.0	6%	3CQY-B	-	Crystal Structure Of A Functionally Unknown Protein (So_1313) From *S. oneidensis* Mr-1 (369 residues with quality score 0.506), released 2008-04-22.*
-	0.21	0.48	6.0	6%	2E2O-A	-	Crystal Structure Of *S. tokodaii* Hexokinase In Complex With Glucose (299 residues with quality score 0.608), released 2007-01-16.*
-	0.06	0.28	11.0	1%	4FSV-A	-	Crystal Structure Of A Heat Shock 70kda Protein 2 (hspa2) From Homo Sapiens At 1.80 A Resolution (380 residues with quality score 0.580), released 2012-07-18.*.
-	0.05	0.12	7.0	2%	4J8F-A	-	Crystal Structure Of A Fusion Protein Containing The Nbd Of Hsp70 And The Middle Domain Of Hip (551 residues with quality score 0.486), released 2013-07-03.*

Entry	Total score	BLAST E-value	Align score	Cover	ID	Res (Å)	Header
-	0.05	0.31	7.0	1%	1I36-A	-	Structure Of Conserved Protein Mth1747 Of Unknown Function Reveals Structural Similarity With 3-Hydroxyacid Dehydrogenases (258 residues with quality score 0.575), released 2002-05-15.*
-	0.01	0.43	5.0	1%	1HUX-A	-	Crystal Structure Of The *A. fermentans* (R)-2- Hydroxyglutaryl-Coa Dehydratase Component A (259 residues with quality score 0.447), released 2001-03-21.*

Table 8.1: Homology modeling templates

***NOTE**: Starting from entry 6, each template was deliberately discarded as the maximum number of templates to use was selected as 5 (see Chapter 8.2.2).

**The "Total score" in the second column is the product of the BLAST alignment score, the "WHAT_CHECK"[345] quality score in the PDBFinder2 database and the target coverage. This makes sure that good template structures are used even if the alignment score is lower. The quality score ranges from 0.000 (terrible) to 1.000 (perfect). The target coverage can be artificially low if the alignment scores so badly, that unaligned overhangs on both sides are more favorable.

8.2.4 The secondary structure prediction

To aid alignment correction and loop modeling, a secondary structure prediction for the target sequence had to be obtained. This was achieved by running PSI-BLAST to create a target sequence profile and feeding it to the PSI-Pred secondary structure prediction algorithm.[346]

The resulting prediction is listed below :'PreHel', 'PreStr' and 'PreCoi' indicate the estimated probability for the three secondary structure classes helix, strand and coil.

SecStr

CCCCCCCCCCCCEEEEECCCCCEEEEECCCCCEEEEEECCCCCCCCCCCCCCCCCCHHHHHHHH
HHHHHHHHHHHHCCCCCCCEEEEEECCCCCEEEEECCCCCEEEHHCCCCCCHHHHHHHHHHHCC
CCHHHHHHHHHHCCCCCCCHHHHHHHHHHCCCHHHHHHCCCCCCHHHHHHHHHCCCCCCCHHH
HCCCCCCCCCCCCCHHHHHHHCCCCCCCCCCCCCCCCCCEECCHHHHHHCCCCCCCCEEEEHH
HHHHHHHCCCCCCCCCEEEEECCCEEEEEECCCCCCCCCCCEEEEEEECCCEEEEECHHHHHHHH
HHHHHHHHCHHHHHHHHHCCCCHHHHHHHHHHHCCCCCCCCCCCCCCCCCCCCCCCCCEEE
ECCCCCCCCCHHHHHHHHHHHHHHHHHHHHHHHHHHCCCCEEEEECCCCCHHHHHHHH
HHCCCEEEEECCCCCHHHHHHHHHHHHCCCCCCHHHHHHHCCCCCCEEECCCCCHHHHHHHH
HHHHHHHHHHHHHHHHCCCCCCCCCCCCCC

PreHel

011110000000000000002222342100000000000000000010000000010008899999999999999830001000000
021100000000000000023455234329999999998731036899999970000000588999987610468988744300357 7
88785100000015444432221000000158999983000000000000000011100188888820000001000045899988733
21012100000000111111110000000000000000000000000134444567899988875358999999950005899999988
52000000001221100000000000000100000000000000089999999999999999999999998750000000000012233778
99987662000000000001458999999976530000098898864321000000021199999999999999999888744322
21100000

PreStr

011111000023899996200023577883000188999654443331000001222000000000000000000000000017688
88310024788730000456325510000000000000000000000000121000000000000000000000001100000
00110110344200000111112100000000000000000000012101233564200000000000014988620000000000
11210138888662024676441001210002666654540069984311110000000000000000000000000000000000
00000002222211110000010000147886121000000000000000000000000000000000189997211000000
000000000069865322100000000000000011000000000011048851000000000000000000000000000013
22210000

PreCoi :
98777889887610000378665420000689981100034555666899999766791100000000000000000069998992400
106788742012689994422211366670000000001158863100000029988889311000012389531001245579531111
1111478864554444555666678899741000016999989898765775554467111111169999995000233100011266
67777676110226644211337887679999833334545992001234444322000011014641000000005999410000011
478988655555655667887799998421148889999991100000000000000000000001249999810003777666221
0001233899511446776542000000023458889901000135677962148987800000000000000000000000110255554
56679999

8.2.5 The target sequence profile

To help align target and templates, a target sequence profile has been created from the multiple sequence alignment of the UniRef90 sequences listed below:

UniRef90	Protein	Taxonomy
D8BSF2	Carbohydrate kinase	Enterobacteriaceae
A7ZLW9	Autoinducer 2 kinase LsrK	Enterobacteriaceae
D3V6E2	Putative sugar kinase, actin-like ATPase domain	Xenorhabdus
Q7N2E1	Autoinducer 2 kinase LsrK	Photorhabdus
A7FMJ5	Autoinducer 2 kinase LsrK	Yersinia
A8GBJ6	Carbohydrate kinase FGGY	Serratia
D4E993	Autoinducer-2 (AI-2) kinase	Serratia odorifera
E8XTU1	Carbohydrate kinase, FGGY-like protein	Rahnella sp Y9602
E6W8E5	Carbohydrate kinase, FGGY-like protein	Pantoea sp. At-9b
A6TEC0:	Autoinducer 2 kinase LsrK	Enterobacteriaceae
Q9CLG3	Putative uncharacterized protein	Pasteurella multocida subsp. multocida str. Pm70
9R4P4	Autoinducer-2 (AI-2) kinase	Aggregatibacter actinomycetemcomitans
C4EXE3	Autoinducer-2 (AI-2) kinase	Haemophilus influenzae

UniRef90	Protein	Taxonomy
B0UX03	Carbohydrate kinase FGGY	Histophilus somni
Q30QH7	Carbohydrate kinase, FGGY	Sulfurimonas denitrificans DSM 1251
A6Q6H0	Sugar kinase	Sulfurovum sp. NBC37-1
B6BKL0	Carbohydrate kinase, fggy	Campylobacterales bacterium GD 1
E0UUR0	Carbohydrate kinase, FGGY	Sulfurimonas autotrophica DSM 16294
D5V4S3	Carbohydrate kinase, FGGY	Arcobacter nitrofigilis DSM 7299
B1KE02	Carbohydrate kinase FGGY	Shewanella woodyi ATCC 51908
D4ZBQ5	Sugar kinase, putative	Shewanella violacea DSS12
C2W951	Carbohydrate kinase FGGY	Bacillus cereus Rock3-44
D5APP4	Carbohydrate kinase, FGGY	Rhodobacter capsulatus SB 1003
A9VJG5	Carbohydrate kinase, FGGY	Bacillus cereus group
C3BLJ1	Carbohydrate kinase FGGY	Bacillus
E0K6T9	Carbohydrate kinase, FGGY-like protein	Sinorhizobium meliloti
A0RFF4	Carbohydrate kinase, FGGY family	Bacillus cereus group
C8S4J3	Carbohydrate kinase FGGY	Rhodobacter sp. SW2
E4U7P3	Carbohydrate kinase, FGGY	Oceanithermus profundus DSM 14977
E4TXQ1	Carbohydrate kinase, FGGY	Sulfuricurvum kujiense DSM 16994
B0P8Y8	Putative uncharacterized protein	Anaerotruncus colihominis DSM 17241
C5EKU1	Autoinducer-2 kinase	Clostridiales bacterium 1_7_47FAA
A3PPI5	Carbohydrate kinase, FGGY	Rhodobacter sphaeroides
C0BWT0	Putative uncharacterized protein	Clostridium hylemonae DSM 15053

UniRef90	Protein	Taxonomy
C9CTR1	Carbohydrate kinase domain protein, fggy family	Silicibacter sp. TrichCH4B
Q92VV3	Probable sugar kinase, probably EGGY family protein	Sinorhizobium meliloti
UPI00020	FGGY domain-containing protein	Treponema primitia ZAS-2 R
E1R7F9	Carbohydrate kinase, FGGY	Spirochaeta smaragdinae DSM 11293
C8NF98	FGGY family carbohydrate kinase	Granulicatella adiacens ATCC 49175

Table 8.2: UniRef90 sequences used to create the target sequence profile

8.2.6 The homology models

For each of the templates listed above, models were built. Either a single model if the alignment was certain, or a number of alternative models if the alignment was ambiguous. 25 models were generated and sorted by their overall quality Z-scores.***

Rank	Z-score	State	Model ID	Original number	Residues	Comment
1	-1.603	Monomer	3IFR-B01	6	14-518	Satisfactory
2	-1.626	Monomer	3IFR-B04	9	14-518	Satisfactory
3	-1.695	Monomer	3IFR-B05	10	14-518	Satisfactory
4	-1.745	Monomer	3IFR-B03	8	14-518	Satisfactory
5	-1.765	Monomer	3IFR-B02	7	14-518	Satisfactory
6	-2.137	Homodimer	3WXL-~03	23	12-509	Poor
7	-2.155	Homodimer	3WXL-~01	21	12-509	Poor
8	-2.171	Homodimer	3WXL-~04	24	12-509	Poor
9	-2.225	Homodimer	3WXL-~05	25	12-509	Poor
10	-2.258	Homodimer	3WXL-~02	22	12-509	Poor
11	-2.298	Homodimer	2ZF5-~01	16	13-510	Poor
12	-2.340	Homodimer	2ZF5-~02	17	13-510	Poor
13	-2.368	Homodimer	2ZF5-~04	19	13-510	Poor
14	-2.414	Homodimer	2ZF5-~05	20	13-514	Poor
15	-2.488	Homodimer	2ZF5-~03	18	13-510	Poor
16	-2.504	Homotetramer	3EZW-~02	2	12-510	Poor

Rank	Z-score	State	Model ID	Original number	Residues	Comment
17	-2.527	Homotetramer	3EZW-~03	3	12-510	Poor
18	-2.545	Homotetramer	3G25-~05	15	12-513	Poor
19	-2.548	Homotetramer	3EZW-~04	4	12-510	Poor
20	-2.557	Homotetramer	3EZW-~01	1	12-510	Poor
21	-2.576	Homotetramer	3G25-~01	11	12-513	Poor
22	-2.585	Homotetramer	3G25-~03	13	12-513	Poor
23	-2.599	Homotetramer	3EZW-~05	5	12-510	Poor
24	-2.632	Homotetramer	3G25-~02	12	12-513	Poor
25	-2.667	Homotetramer	3G25-~04	14	12-517	Poor

Table 8.3: Homology models generated by YASARA

***NOTE: A Z-score describes how many standard deviations the model quality is away from the average high-resolution X-ray structure. Higher values are better, negative values indicate that the homology model looks worse than a high-resolution X-ray structure. The overall Z-scores for all models have been calculated as the weighted averages of the individual Z-scores using the formula Overall = 0.145*Dihedrals + 0.390*Packing1D + 0.465*Packing3D. The overall score thus captures the correctness of backbone- (Ramachandran plot) and side-chain dihedrals, as well as packing interactions. It applies to globular proteins only, and can be mislead by artificial structures like long single alpha helices (which have perfect dihedrals and are free of packing errors, since there is no packing).

8.2.7 Molecular modeling

In June 2018, three crystal structures of LsrK/HPr (a phosphocarrier protein) alone or in complex with ATP and ADP (PDB ID: 5YA0, 5YA1, 5YA2, respectively) were published.[199] All the synthesized compounds were docked into LsrK kinase binding site (PDB ID: 5YA1) and the resulting docking poses were analyzed for the interactions and geometry. Compound **181a** interacts with D 253, T 275 and K 453 (Figure 8.1); compound **182a** has a similar binding pose and the higher activity (IC_{50} **181a** = 475 (±11) µM, IC_{50} **182a** = 119 (±3) µM) 13a can be attributed to the methyl stabilization energy and the electrostatic potential of N-CH₃. The higher activity of compound **182a** in comparison to **181b** (**182a** = 119 (±3) µM, IC_{50} **181b** = 384 (±15) µM) can be attributed to the negative electrostatic potential near the oxygen of the furan ring (i.e., compound **181b**) and the local binding site environment (i.e., electrostatic repulsion of Thr 456).
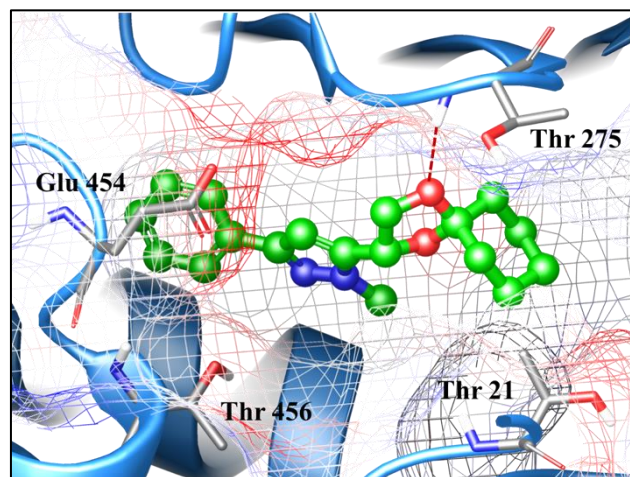
Figure 8.1: Binding pose of compound **182a** in the binding site of LsrK kinase. Hydrogen bonds are shown in red dashed lines. Electrostatic potential surfaces are shown as mesh (blue-positive potential and red-negative potential)

8.3 Microbiology

8.3.1 General

The following strains and plasmids were used in this work:

Strain or plasmid	Description	Source or reference
Strains		
Rosetta DE3	*E. coli* BL21 derivative, pRare2, Cm[r]	Tegel *et al.*[347]
E. coli MG 1655	MG 1655 derivative of *E. coli* K-12	Soupene *et al.* [348]
E. coli DH5α	DH5α derivative of *E. coli* K-12	Woodcock *et al.*[349]
Plasmids		
MBP-pMAL-c2X	MBP fusion cloning vector, Ap[r]	New England Biolabs
pET-19m	His$_6$- fusion cloning vector, Ap[r] (modified pET-19b, Novagen)	Dolan *et al.*[350]
MBP-pMAL-c2X-LsrK	MBP-pMAL containing LsrK from *E. coli*; Ap[r]	This study
pET-19m-LsrK	pET-19m containing LsrK from *E. coli*; Ap[r]	This study

The following primers were used in this work:

Primer	Sequence	Source
LsrK EcorI forward	GATCGAATTCATGGCTCGACTCTTTACCCTTTCAGAATC	Sigma-Aldrich
LsrK SalI reverse	GATCGTCGACCTATAACCCAGGCGCTTTCCATAACG	Sigma-Aldrich
MBP-pMAL-c2X forward	GGTCTGACCTTCCTGGTTGA	Sigma-Aldrich
MBP-pMAL-c2X reverse	ACGGCGTTTCACTTCTGAGT	Sigma-Aldrich
pET-19m forward	ACCATGGGCCATCATCATCA	Sigma-Aldrich
pET-19m reverse	CCAACTCAGCTTCCTTTCGG	Sigma-Aldrich
LsrK NdeI forward	CATGCATATGGCTCGACTCTTTACCCTTTCAGAATC	Sigma-Aldrich
LsrK XhoI reverse	CATGCTCGAGCTATAACCCAGGCGCTTTCCATAACG	Sigma-Aldrich
LuxS NdeI forward	ATAAAAAACATATGCCGTTGTTAGATAGCTTCAC	Sigma-Aldrich
LuxS XhoI reverse	AAAACTCGAGTAGATGTGCAGTTCCTGCAACT	Sigma-Aldrich
Mtn NdeI forward	ATAAAAAACATATGATGAAAATCGGCATCATTGGTGC	Sigma-Aldrich
Mtn XhoI reverse	AAAACTCGAGTTAGCCATGTGCAAGTTTCTGCA	Sigma-Aldrich

The following media were used in this work:

LB Broth (Lennox)

Tryptone (1% w/v), yeast extract (0.5% w/v) and sodium chloride (1% w/v) in water; adjusted to pH 7.0 with 1M NaOH and sterilized.

LB Agar

Tryptone (1% w/v), yeast extract (0.5% w/v), agar (1.5% w/v g) and sodium chloride (1% w/v) in water; adjusted to pH 7.0 with 1M NaOH and sterilized.

Carbenicillin stock

Carbenicillin disodium salt (50 mg/mL) in 50% aqueous EtOH (5 mL); filtered (0.22 μm); stored at – 20 °C.

Chloramphenicol stock

Chloramphenicol (34 mg/mL) in 50% aqueous EtOH (5 mL); filtered (0.22 μm); stored at – 20 °C.

IPTG stock

Isopropyl-β-D-1-thiogalactopyranoside (1 mM) in water; filtered (0.22 µm); stored at 4 °C.

1xTAE electrophoresis buffer

Tris (free base, 10 mM), acetic acid (20 mM) and EDTA (1mM) in water; adjusted to pH 7.6; stored at room temperature.

6xDNA loading dye

Gel loading dye purple (6x) purchased from BioLabs; stored at – 20 °C.

1Kb DNA ladder

HyperLadder^{TM} 1 Kb purchased from Bioline; stored at – 20 °C.

5xlower buffer (SDS-PAGE)

Tris*HCl (1.25 M) and sodium dodecyl sulfate (0.5% w/v) in water; adjusted to pH 8.8; stored at room temperature.

5xupper buffer (SDS-PAGE)

Tris*HCl (0.5 M) and sodium dodecyl sulfate (0.5% w/v) in water; adjusted to pH 6.8; stored at room temperature.

1x running buffer (SDS-PAGE)

Tris*HCl (25 mM), glycine (250 mM), sodium dodecyl sulfate (0.1% w/v) in water; adjusted to pH 7.5; stored at room temperature.

4xloading buffer (SDS-PAGE)

Tris*HCl (200 mM), DTT (400 mM), glycerol (40% v/v), sodium dodecyl sulfate (8% w/v) and bromophenol blue (0.4% w/v) in water; adjusted to pH 6.8; stored at – 20 °C.

Ladder (SDS-PAGE)

Precision Plus Protein^{TM} purchased from Bio-Rad; stored at – 20 °C.

Coomassie brilliant blue G-250 staining solution (SDS-PAGE)

Coomassie brilliant blue G-250 (0.1% w/v), methanol (50% v/v), acetic acid (10% v/v) in water; filtered through cotton; stored at room temperature.

Destain solution I (SDS-PAGE)

Methanol (50% v/v) and acetic acid (7% v/v) in water; stored at room temperature.

Destain solution II (SDS-PAGE)

Methanol (10% v/v) and acetic acid (7% v/v) in water; stored at room temperature.

Ammonium persulfate (APS, SDS-PAGE)

Ammonium persulfate (10% w/v) in water; stored at 4 °C.

Ni-NTA lysis buffer

Sodium phosphate (50 mM), NaCl (200 mM), glycerol (10% v/v) in water; adjusted to pH 8.0; stored at 4 °C.

Ni-NTA equilibration buffer

Tris*HCl (50 mM), NaCl (200 mM), imidazole (10 mM) and glycerol (10% v/v) in water; adjusted to pH 7.8; stored at 4 °C.

Ni-NTA elution buffer

Tris*HCl (50 mM), NaCl (200 mM), imidazole (250 mM) and glycerol (10% v/v) in water; adjusted to pH 7.4; stored at 4 °C.

Ni-NTA dialysis buffer

Tris*HCl (50 mM), NaCl (100 mM) and glycerol (5% v/v) in water; adjusted to pH 7.4; stored at 4 °C.

8.3.2 General procedures

General

LB refers to Luria Bertani Broth (Lennox); LBA refers to Luria Bertani Broth (Lennox) supplemented with 1.5% w/v agar. All growth media were sterilized prior to use. All reagents (analytical or molecular biology grade) were purchased from commercial vendors and used as received in accordance with the manufacturer's instructions where applicable. Spectrophotometry was performed at 280 nm or 600 nm using a Model 6715 UV-Vis spectrophotometer (Jenway) or nanodrop ND-1000 spectrophotometer (ThermoFisher). Centrifugation at 3.200x *g* was performed using an Avanti J-5810 R centrifuge (Eppendorf); centrifugation at 14.000x *g* was performed using an Avanti J-26 XPI centrifuge (Beckman Coulter). Sanger sequencing was performed by GATC Biotech.

Growth

Bacteria were grown at 37 °C on LBA plates. LB media (10 mL) was inoculated with a single colony and then grown as a planktonic culture (37 °C). Carbenicillin disodium salt selection (50 mg/mL) and/or chloramphenicol (34 mg/mL) were used to maintain transformed *E. coli*.

Polymerase Chain Reaction (PCR)

PCR was performed using a Veriti 96-well thermocycler (Applied Biosystems). *E. coli* genomic DNA (gDNA) was purified using a GeneJET Genomic DNA Purification kit (ThermoScientific) in accordance with the manufacturer's instructions. Oligonucleotides were purchased from Sigma-Aldrich and diluted according to the manufacturer's instructions. dNTP mixes, Phusion HF DNA polymerase and *Taq* DNA polymerase kits were purchased from New England Biolabs.

Pulsed-Field Gel Electrophoresis

DNA samples were separated by pulsed-field gel electrophoresis (10 V/cm) using a 1% w/v agarose gel in 1x TAE buffer. HyperLadder™ 1 Kb (Bioline) was used as a molecular weight marker. Gels were visualized by fluorescence using a Gene Genius Bio-Imaging system (Syngene). DNA was excised from the gel and purified using a GeneJET Gel Extraction kit (ThermoScientific) in accordance with the manufacturer's instructions.

Enzymatic Digestion

NdeI, XhoI, SalI, EcoRI enzymes were purchased from New England Biolabs and used in accordance with the manufacturer's instructions.

Enzymatic Ligation

T4 DNA ligase enzyme kit was purchased from New England Biolabs and used in accordance with the manufacturer's instructions.

Transformation of *E. coli* by heat shock

To 60 µL of chemically competent *E. coli* DH5α were added 10 µL of ligation mixture. The mixture was incubated on ice for 30 minutes, at 42 °C for 90 seconds and on ice for 2 minutes. After addition of 1 mL of LB, the mixture was incubated at 37 °C while shaking. The mixture was centrifuged (3.200x *g*, 5 minutes), part of the supernatant (800 µL) was removed and three aliquots (30 µL, 60 µL and 100 µL) of the resuspended mixture were spread onto LBA plates with carbenicillin disodium salt (50 mg/mL) and/or chloramphenicol (34 mg/mL) selection and grown overnight at 37 °C. Transformants were screened by colony PCR. The plasmid from a positive transformant was purified using a GeneJET Plasmid Miniprep kit (ThermoScientific) in accordance with the manufacturer's instructions; its identity was confirmed by Sanger sequencing.

Transformation of *E. coli* by electroporation

Electrocompetent Rosetta DE3 (BL21) were grown to stationary phase in LB (10 mL) at 37 °C. The cells were harvested by centrifugation at 4 °C (3.200x *g*, 5 minutes). The pellet was washed with ice-cold aqueous glycerol (10% v/v, 1 mL) and sedimented again at 4 °C (3.200x *g*, 5 minutes). This process was repeated three times in total. The ice-cold electroporation mixture containing the bacterial suspension (200 µL) and the ligation mixture (2 µL) was transformed by electroporation at 2.500 V using an Electroporator 2510 (Eppendorf). The parent plasmids were used as negative control. After electroporation, the mixture was allowed to regenerated for one hour in LB (1 mL) with gentle mixing. Aliquots (30 µL, 60 µL and 100 µL) of the mixture were spread onto LBA plates with carbenicillin disodium salt (50 mg/mL) and chloramphenicol (34 mg/mL) selection and grown overnight at 37 °C. Transformant were screened by colony PCR. The plasmid from a positive transformant was purified using a GeneJET Plasmid Miniprep kit (ThermoScientific) in accordance with the manufacturer's instructions; its identity was confirmed by Sanger sequencing.

Sanger sequencing

The samples were sent to GATC Biotech as 10 µL solutions containing 5 µL of 5mM primer (reverse or forward) and 80 – 100 ng/µL of DNA.

Recombinant protein expression

The growth medium, supplemented with carbenicillin disodium salt (50 mg/mL) and/or chloramphenicol (34 mg/mL) was inoculated with 0.1% v/v of a 10 mL overnight culture of the *E. coli* expression strain grown in LB supplemented with carbenicillin disodium salt (50 mg/mL) and/or chloramphenicol (34 mg/mL). The expression strain was grown to an OD_{600} of 0.5 – 0.6 at 37 °C with shaking (200 rpm) using an Innova 43 Incubator (New Brunswick). The *lac* promoter was induced with isopropyl-β-D-1-thiogalactopyranoside (0.42 mM – 1.0 mM). The cultures were left to grown at 22 °C – 37 °C. The cells were harvested by centrifugation at 4 °C (3.200x *g*, 10 – 30 minutes). The pellets were resuspended in ice-cold lysis buffer containing cOmplete EDTA-free protease inhibitor cocktail tablet (Roche).

The bacterial suspension was lysed by sonication with continuous cooling on ice-water using a Soniprep fitted with an exponential microprobe (Measuring and Scientific equipment). Cellular debris was removed by centrifugation at 4°C (3.200x g, 10 – 30 minutes). The clarified supernatants were filtered with a 0.22 µm filter and purified either manually or using ÄKTA Avant FPLC system (GE Healthcare). After purification, the mixtures were concentrated using Vivaspin columns (Sartorius) of the appropriate MWCO size.

SDS-PAGE

The separating and stacking gels were prepared as follow:

<u>Separating gel (12% acrylamide)</u>: acrylamide (4 mL), 5xlower buffer (2 mL), APS 10% w/v (200 µL), water (3.8 mL) and tetramethylethylenediamine (TMEDA, 5 µL).

<u>Stacking gel (5% acrylamide)</u>: acrylamide (1.7 mL), 5xupper buffer (2 mL), APS 10% w/v (200 µL), water (6.1 mL) and tetramethylethylenediamine (TMEDA, 5 µL).

40 µL of protein sample were diluted with 4x loading buffer and denatured by heating at 95 °C for 10 mins. Precision Plus Protein™ (Bio-Rad) was used as a molecular weight marker. Gels were developed by staining with Coomassie brilliant blue G-250 staining solution.

8.3.3 Cloning of LsrK (MBP-pMAL-c2X plasmid)

Amplification of LsrK

PCR was performed on *E. coli* gDNA using the following conditions:

Component	Per reaction / μL
LsrK NdeI forward	2.5 (10 mM)
LsrK XhoI reverse	2.5 (10 mM)
dNTP mix	1 (10 mM)
DMSO	1.5
5X Phusion HF Buffer	10
Taq DNA polymerase (40.000 units/mL)	0.5
E. coli MG 1655 gDNA (61.9 ng/μL)	2

Each PCR tube was loaded with 50 μL of reaction mixture. The following conditions were then used:

Stage 1: 98 °C (3 minutes);

Stage 2: 35 cycles of: 98 °C (5 sec); 58 °C (30 sec); 72 °C (25 sec);

Stage 3: 72 °C (5 minutes)

The samples were combined and separated by pulse-field gel electrophoresis. The band corresponding to the amplicon size (1593 bp, Figure 8.2) was excised from the gel and purified with GeneJET PCR Purification kit (ThermoScientific) in accordance with the manufacturer's instructions.
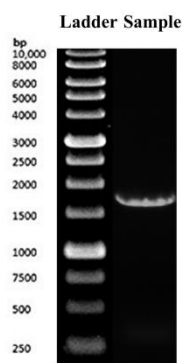
Figure 8.2: DNA agarose gel for LsrK

Restriction and ligation of LsrK into MBP-pMAL-c2X

gDNA and MBP-pMAL-c2X were each restricted as follow:

Reagent	Amount (µL)
Plasmid	
MBP-pMAL-c2X (79.6 ng/µL)	31
EcoRI	2
SalI	2
CutSmart	5
Water	10
Gene	
LsrK gene (173.5 ng/µL)	41
EcoRI	2
SalI	2
CutSmart	5
Water	—

The mixtures were incubated for 3 hours at 37 °C and purified with GeneJET PCR Purification kit (ThermoScientific) in accordance with the manufacturer's instructions.

5:1 w/w mixture of the LsrK insert and the linear vector (50 ng) were ligated with T4 DNA ligase (1 µL) in 10xT4 DNA ligase buffer (2 µL) and water (up to 20 µL in total) and incubated for one hour on ice and one hour at room temperature.

Transformation

The MBP-pMAL-c2X-LsrK plasmid (10 µL) was transformed into *E. coli* DH5α (60 µL) in accordance with the above instructions (Chapter 6.3.2). The resulting mixture was transformed into three LBA plates (30 µL, 60 µL and 100 µL) with carbenicillin disodium salt (50 mg/mL) selection and grown overnight at 37 °C.

Positive transformants were identified by colony PCR using the following conditions:

Component	Per reaction / µL
MBP-pMAL-c2X forward	2.5 (10 mM)
MBP-pMAL-c2X reverse	2.5 (10 mM)
dNTP mix	1 (10 mM)
DMSO	1.5
5X Phusion HF Buffer	10
Taq DNA polymerase (40.000 units/mL)	0.5
Colony suspension	2

Each colony was picked and suspended in water (50 µL), of which 2 µL was used as source of DNA. Each PCR tube was loaded with 50 µL of reaction mixture and the same conditions as for in Chapter 8.3.3.1 were used. Two positive hits were identified (shown in red in Figure 8.3). Each of the positive colony was grown overnight in 10 mL of LB containing carbenicillin disodium salt (50 mg/mL). After concentrating (3.200x *g*, 5 minutes), the supernatant was removed and the pellet was purified with GeneJET Plasmid Miniprep kit (ThermoScientific) in accordance with the manufacturer's instructions. The two samples were sent for Sanger sequencing but the results were not matching with positive transformants therefore a different construct (pET-19m) was employed.
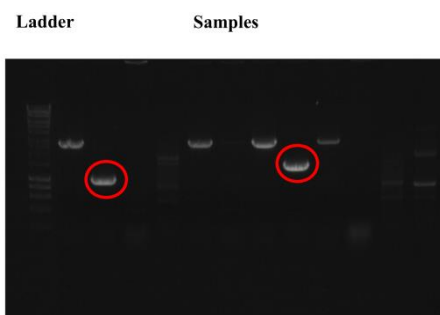
Figure 8.3: Transformants from pMAL-c2X-LsrK colony PCR

8.3.4 Cloning of LsrK (pET-19m plasmid)

Amplification of LsrK

PCR was performed on *E. coli* gDNA using the following conditions:

Component	Per reaction / µL
LsrK EcoRI forward	2.5 (10 mM)
LsrK SalI reverse	2.5 (10 mM)
dNTP mix	1 (10 mM)
DMSO	1.5
5X Phusion HF Buffer	10
Taq DNA polymerase (40.000 units/mL)	0.5
E. coli MG 1655 gDNA (61.9 ng/µL)	2

Each PCR tube was loaded with 50 µL of reaction mixture. The following conditions were then used:

Stage 1: 98 °C (3 minutes);

Stage 2: 35 cycles of: 98 °C (5 sec); 58 °C (30 sec); 72 °C (25 sec);

Stage 3: 72 °C (5 minutes)

The samples were combined and separated by pulse-field gel electrophoresis. The band corresponding to the amplicon size was excised from the gel and purified with GeneJET PCR Purification kit (ThermoScientific) in accordance with the manufacturer's instructions.

Restriction and ligation of LsrK into pET-19m

gDNA and pET-19m were each restricted as follow:

Reagent	Amount (µL)
Plasmid	
pET-19m (113.7 ng/µL)	36
NdeI	2
XhoI	2
CutSmart	5
Water	5
Gene	
LsrK gene (89.4 ng/µL)	41
NdeI	2
XhoI	2
CutSmart	5
Water	---

The mixtures were incubated for 3 hours at 37 °C and purified with GeneJET PCR Purification kit (ThermoScientific) in accordance with the manufacturer's instructions.

5:1 w/w mixture of the LsrK insert and the linear vector (50 ng) were ligated with T4 DNA ligase (1 µL) in 10xT4 DNA ligase buffer (2 µL) and water (up to 20 µL in total) and incubated for one hour on ice and one hour at room temperature.

Transformation by heat shock

The pET19m-LsrK plasmid (10 μL) was transformed into *E. coli* DH5α (60 μL) in accordance with the above instructions (Chapter 8.3.2). The resulting mixture was transformed into three LBA plates (30 μL, 60 μL and 100 μL) with carbenicillin disodium salt (50 mg/mL) sand chloramphenicol (34 mg/mL) selection and grown overnight at 37 °C. No viable colonies were observed, therefore, transformation was repeated by electroporation.

Transformation by electroporation

The pET19m-LsrK plasmid was electroporated into electrocompetent Rosetta DE3 (BL21) in accordance with the above instructions (Chapter 8.3.2). Positive transformants were identified by colony PCR using the following conditions:

Component	Per reaction / μL
pET-19m forward	2.5 (10 mM)
pET-19m reverse	2.5 (10 mM)
dNTP mix	1 (10 mM)
DMSO	1.5
5X Phusion HF Buffer	10
Taq DNA polymerase (40.000 units/mL)	0.5
Colony suspension	2

Each colony was picked and suspended in water (50 μL), of which 2 μL was used as source of DNA. Each PCR tube was loaded with 50 μL of reaction mixture and the same conditions as for in Chapter 6.2.4.1 were used. Three positive hits were identified (shown in red in Figure 8.4). Each of the positive colony was grown overnight in 10 mL of LB containing carbenicillin disodium salt (50 mg/mL) and chloramphenicol (34 mg/mL). After concentrating (3.200x *g*, 5 minutes), the supernatant was removed and the pellet was purified with GeneJET Plasmid Miniprep kit (ThermoScientific) in accordance with the manufacturer's instructions. A positive transformant was confirmed by Sanger sequencing.

Figure 8.4: Transformants from pET-19m-LsrK colony PCR

Optimization of the expression conditions of His$_6$-pET-19m-LsrK

Rosetta DE3 (BL21) containing the *E. coli* LsrK (1593 bp) open reading frame (cloned into a His$_6$-pET-19m plasmid) was used for expression of pET-19m-LsrK fusion protein.

Four different temperatures and IPTG concentrations were screened as follow:

Conditions 1: LB medium (250 mL) supplemented with carbenicillin disodium salt (50 mg/mL) and chloramphenicol (34 mg/mL) was inoculated with 250 μL of a 10 mL overnight culture of the *E. coli* expression strain grown in LB supplemented with carbenicillin disodium salt (50 mg/mL) and chloramphenicol (34 mg/mL).

The *E. coli* culture was grown at 37 °C with shaking (200 rpm) to and approximate OD$_{600}$ of 0.5. The temperature was then lowered to 22 °C and when the OD$_{600}$ reached 0.9, the *lac* promoter was induced with 0.42 mM IPTG. The culture was left grown at 22 °C overnight.

The cells were harvested by centrifugation at 4 °C (3.200x *g*, 10 minutes) and the pellets were resuspended in 5 mL of ice-cold lysis buffer containing a cOmpete EDTA-free protease inhibitor cocktail tablet.

The bacterial suspension was lysed by sonication with continuous cooling on ice-water (3 x 5 secs, 13 A, 1 min. pause between pulses). The cell lysate was clarified by ultracentrifugation at 4 °C (3.200x *g*, 10 minutes) and the clarified supernatant was filtered through a 0.45 μm filter. Samples of the lysis mixtures and supernatants were analyzed by SDS-PAGE (Figure 8.5).[351]

Conditions 2: LB medium (250 mL) supplemented with carbenicillin disodium salt (50 mg/mL) and chloramphenicol (34 mg/mL) was inoculated with 250 μL of a 10 mL overnight culture of the *E. coli* expression strain grown in LB supplemented with carbenicillin disodium salt (50 mg/mL) and chloramphenicol (34 mg/mL).

The *E. coli* culture was grown at 37 °C with shaking (200 rpm) to and approximate OD$_{600}$ of 0.5. The *tac* promoter was induced with 1.0 mM IPTG. The culture was left grown at 37 °C overnight.

The cells were harvested by centrifugation at 4 °C (3.200x *g*, 10 minutes) and the pellets were resuspended in 5 mL of ice-cold lysis buffer containing a cOmpete EDTA-free protease inhibitor cocktail tablet.

The bacterial suspension was lysed by sonication with continuous cooling on ice-water (3 x 5 secs, 13 A, 1 min. pause between pulses). The cell lysate was clarified by ultracentrifugation at 4 °C (3.200x *g*, 10 minutes) and the clarified supernatant was filtered through a 0.45 μm filter. Samples of the lysis mixtures and supernatants were analyzed by SDS-PAGE (Figure 8.5).

Conditions 3: LB medium (250 mL) supplemented with carbenicillin disodium salt (50 mg/mL) and chloramphenicol (34 mg/mL) was inoculated with 250 μL of a 10 mL overnight culture of the *E. coli* expression strain grown in LB supplemented with carbenicillin disodium salt (50 mg/mL) and chloramphenicol (34 mg/mL).

The *E. coli* culture was grown at 37 °C with shaking (200 rpm) to and approximate OD$_{600}$ of 0.5. The *tac* promoter was induced with 0.5 mM IPTG. The culture was left grown at 22 °C overnight

The cells were harvested by centrifugation at 4 °C (3.200x *g*, 10 minutes) and the pellets were resuspended in 5 mL of ice-cold lysis buffer containing a cOmpete EDTA-free protease inhibitor cocktail tablet.

The bacterial suspension was lysed by sonication with continuous cooling on ice-water (3 x 5 secs, 13 A, 1 min. pause between pulses). The cell lysate was clarified by ultracentrifugation at 4 °C (3.200x g, 10 minutes) and the clarified supernatant was filtered through a 0.45 μm filter. Samples of the lysis mixtures and supernatants were analyzed by SDS-PAGE (Figure 8.5).

Conditions 4: LB medium (250 mL) supplemented with carbenicillin disodium salt (50 mg/mL) and chloramphenicol (34 mg/mL) was inoculated with 250 μL of a 10 mL overnight culture of the *E. coli* expression strain grown in LB supplemented with carbenicillin disodium salt (50 mg/mL) and chloramphenicol (34 mg/mL).

The *E. coli* culture was grown at 37 °C with shaking (200 rpm) to and approximate OD_{600} of 0.5. The *tac* promoter was induced with 1.0 mM IPTG. The culture was left grown at 16 °C overnight

The cells were harvested by centrifugation at 4 °C (3.200x g, 10 minutes) and the pellets were resuspended in 5 mL of ice-cold lysis buffer containing a cOmpete EDTA-free protease inhibitor cocktail tablet.

The bacterial suspension was lysed by sonication with continuous cooling on ice-water (3 x 5 secs, 13 A, 1 min. pause between pulses). The cell lysate was clarified by ultracentrifugation at 4 °C (3.200x g, 10 minutes) and the clarified supernatant was filtered through a 0.45 μm filter. Samples of the lysis mixtures and supernatants were analyzed by SDS-PAGE (Figure 8.5).
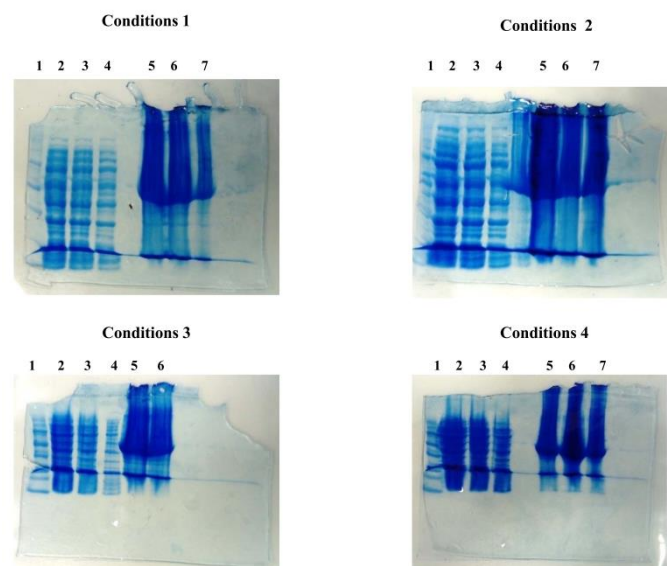
Figure 8.5: Screening of conditions for His_6-pET-19m-LsrK expression. The figure shows a Coomassie Brilliant Blue G250-stained 12% polyacrylamide gel run in SDS buffer. Lane 1: protein molecular marker; lane 2: crude cell-free lysate (20 μL); lane 3: crude cell-free lysate (10 μL); lane 4: crude cell-free lysate (5 μL); lane 5: supernatant (20 μL); lane 6: supernatant (10 μL); lane 7: supernatant (5 μL).

With all of the four conditions, the recombinant protein was well expressed but conditions 1 (already reported by Zhu *et al.*) were the ones where less material was lost as inclusion bodies (lanes 2 – 4). I therefore decided to apply such conditions for the expression of His_6-pET-19m-LsrK.

Expression of His$_6$-pET-19m-LsrK

LB medium (6 x 1000 mL) each supplemented with carbenicillin disodium salt (50 mg/mL) and chloramphenicol (34 mg/mL) was inoculated with 1 mL of a 10 mL overnight culture of the *E. coli* expression strain grown in LB supplemented with carbenicillin disodium salt (50 mg/mL) and chloramphenicol (34 mg/mL).

The *E. coli* culture was grown at 37 °C with shaking (200 rpm) to and approximate OD$_{600}$ of 0.5. The temperature was then lowered to 22 °C and when the OD$_{600}$ reached 0.9, the *tac* promoter was induced with 0.42 mM IPTG. The culture was left grown at 22 °C overnight.

The cells were harvested by centrifugation at 4 °C (14.000x *g*, 30 minutes) and the pellets were resuspended in a total volume of 100 mL of ice-cold lysis buffer containing a cOmpete EDTA-free protease inhibitor cocktail tablet.

The bacterial suspension was lysed by sonication with continuous cooling on ice-water (8 x 30 seconds, 13 A, 1 min. pause between pulses). The cell lysate was clarified by ultracentrifugation at 4 °C (11.000x *g*, 30 minutes) and the clarified supernatant was filtered through a 0.22 μm filter.[351]

Ni-NTA affinity chromatography of His$_6$-pET-19m-LsrK

Affinity chromatography was performed with Ni-NTA column (2 mL packed resin bed volume). The combined cell lysate was loaded onto the column and purified in accordance with the manufacturer's instruction. The column was washed overnight with equilibration buffer at 4 °C and afterward eluted with elution buffer. The protein was dialyzed overnight against two liters of dialysis buffer and the His$_6$-tag was removed using His$_6$-tagged TEV protease. The protein thus released was cleaned up by batch extraction in a slurry of Ni-NTA resin equilibrated in dialysis buffer and concentrated (Vivaspin MWCO 30.000, Sartorium) to 12 mg/mL (estimated by A$_{280}$ using $\varepsilon_{calc} \sim 93.390$ M^{-1} cm^{-1}). The mixture was snap-frozen in liquid nitrogen in aliquots of 1 mL and stored at -80 °C. SDS-PAGE confirmed the presence of a protein corresponding to the mass of the pET-19m-LsrK fusion protein (57.5 kDa) and some impurities (see Chapter 2, Figure 2.9).

8.3.5 LsrK overexpression and purification (University of Helsinki)

E. coli MET1158 [*E. coli*, amp resistance, BL21 (DE3) luxS-, with pMET1144 (lsrK-His in pET21b)], kindly donated by Prof. Karina Xavier (Instituto Gulbenkian de Ciência, Portugal)[352], was used for the overexpression of LsrK from *S. typhimurium*. Bacteria were grown overnight in 2xYPTG (yeast, tryptone, phosphate buffer and glucose) medium supplemented with 100 μg/ml ampicillin. At exponential phase, protein expression was induced by addition of 0.1 mM isopropyl β-D-1 thiogalactopyranoside for 9h at 22°C (250 rpm). Cells were harvested and frozen overnight before proceeding with lysis and purification, according to literature.[269]

8.3.6 DPD activity evaluation (University of Helsinki)

Phosphorylation of DPD by LsrK was evaluated with a bioluminescence-based assay,(ATP Bioluminescence kit CLSII (Roche) as previously described [352]. DPD was plated at 200 μM and 400 μM and a reaction mixture containing 200 nM Lsrk and 20 μM ATP in assay buffer (25 mM triethanolamine, pH 7.4, 200 μM MgCl$_2$). Commercially available DPD was tested for comparison at 200 μM. The level of ATP was monitored by ATP Bioluminescence kit CLSII following manufacturer´s instruction. Experiment was performed in kinetic-mode, monitoring luminescence every 2 minutes within a time window of 30 minutes at the Varioskan LUX plate reader (Thermo Fisher Scientific, Finland).

8.3.7 Screening of DPD-related compounds (University of Helsinki)

Activity of DPD-related compounds was evaluated in an LsrK inhibition assay. Compounds were plated in 384 well-plate to a final concentration of 200 μM in triplicate. 300 nM LsrK and 300 μM DPD diluted in assay buffer (25 mM triethanolamine, pH 7.4, 200 μM MgCl$_2$, 0.1 mg/ml BSA) were added to the plate followed by 100 μM ATP to start the reaction. After 15 minutes of reaction, Kinase Glo Luminescence assay reagent was added according to manufacturer´s instruction. Experiment was carried on in end-point mode and luminescence was recorded at the Varioskan LUX plate reader.

REFERENCES

(1)   O'Connell, K. M. G.; Hodgkinson, J. T.; Sore, H. F.; Welch, M.; Salmond, G. P. C.; Spring, D. R. Combating Multidrug-Resistant Bacteria: Current Strategies for the Discovery of Novel Antibacterials. *Angew. Chem. Int. Ed.* **2013**, *52* (41), 10706–10733.

(2)   Chain, E.; Florey, H. W.; Gardner, A. D.; Heatley, N. G.; Jennings, M. A.; Orr-Ewing, J.; Sanders, A. G. PENICILLIN AS A CHEMOTHERAPEUTIC AGENT. *The Lancet* **1940**, *236* (6104), 226–228.

(3)   Batchelor, F. R.; Doyle, F. P.; Nayler, J. H. C.; Rolinson, G. N. Synthesis of Penicillin: 6-Aminopenicillanic Acid in Penicillin Fermentations. *Nature* **1959**, *183* (4656), 257–258.

(4)   Hughes, D.; Karlén, A. Discovery and Preclinical Development of New Antibiotics. *Ups. J. Med. Sci.* **2014**, *119* (2), 162–169.

(5)   Donadio, S.; Maffioli, S.; Monciardini, P.; Sosio, M.; Jabes, D. Antibiotic Discovery in the Twenty-First Century: Current Trends and Future Perspectives. *J. Antibiot. (Tokyo)* **2010**, *63* (8), 423–430.

(6)   *Antibiotics: Challenges, Mechanisms, Opportunities*; American Society of Microbiology, 2016.

(7)   Projan, S. J. Why Is Big Pharma Getting out of Antibacterial Drug Discovery? *Curr. Opin. Microbiol.* **2003**, *6* (5), 427–430.

(8)   Wenzel, R. P. The Antibiotic Pipeline--Challenges, Costs, and Values. *N. Engl. J. Med.* **2004**, *351* (6), 523–526.

(9)   Overbye, K. M.; Barrett, J. F. Antibiotics: Where Did We Go Wrong? *Drug Discov. Today* **2005**, *10* (1), 45–52.

(10)   Nathan, C.; Goldberg, F. M. The Profit Problem in Antibiotic R&D. *Nat. Rev. Drug Discov.* **2005**, *4* (11), 887–891.

(11)   Klevens, R. M.; Edwards, J. R.; Richards, C. L.; Horan, T. C.; Gaynes, R. P.; Pollock, D. A.; Cardo, D. M. Estimating Health Care-Associated Infections and Deaths in U.S. Hospitals, 2002. *Public Health Rep. Wash. DC 1974* **2007**, *122* (2), 160–166.

(12)   Zimlichman, E.; Henderson, D.; Tamir, O.; Franz, C.; Song, P.; Yamin, C. K.; Keohane, C.; Denham, C. R.; Bates, D. W. Health Care-Associated Infections: A Meta-Analysis of Costs and Financial Impact on the US Health Care System. *JAMA Intern. Med.* **2013**, *173* (22), 2039–2046.

(13)   Smith, R.; Coast, J. The True Cost of Antimicrobial Resistance. *BMJ* **2013**, *346*, f1493.

(14)   Rex, J. H.; Goldberger, M.; Eisenstein, B. I.; Harney, C. The Evolution of the Regulatory Framework for Antibacterial Agents. *Ann. N. Y. Acad. Sci.* **2014**, *1323*, 11–21.

(15)   Fleischmann, R. D.; Adams, M. D.; White, O.; Clayton, R. A.; Kirkness, E. F.; Kerlavage, A. R.; Bult, C. J.; Tomb, J. F.; Dougherty, B. A.; Merrick, J. M. Whole-Genome Random Sequencing and Assembly of Haemophilus Influenzae Rd. *Science* **1995**, *269* (5223), 496–512.

(16)   Drews, J. Genomic Sciences and the Medicine of Tomorrow. *Nat. Biotechnol.* **1996**, *14* (11), 1516–1518.

(17) Lander, E. S.; Linton, L. M.; Birren, B.; Nusbaum, C.; Zody, M. C.; Baldwin, J.; Devon, K.; Dewar, K.; Doyle, M.; FitzHugh, W.; et al. Initial Sequencing and Analysis of the Human Genome. *Nature* **2001**, *409* (6822), 860–921.

(18) Macarron, R.; Banks, M. N.; Bojanic, D.; Burns, D. J.; Cirovic, D. A.; Garyantes, T.; Green, D. V. S.; Hertzberg, R. P.; Janzen, W. P.; Paslay, J. W.; et al. Impact of High-Throughput Screening in Biomedical Research. *Nat. Rev. Drug Discov.* **2011**, *10* (3), 188–195.

(19) Kinch, M. S.; Patridge, E.; Plummer, M.; Hoyer, D. An Analysis of FDA-Approved Drugs for Infectious Disease: Antibacterial Agents. *Drug Discov. Today* **2014**, *19* (9), 1283–1287.

(20) Liu, R.; Li, X.; Lam, K. S. Combinatorial Chemistry in Drug Discovery. *Curr. Opin. Chem. Biol.* **2017**, *38*, 117–126.

(21) Antibiotic Resistance Investments https://wwwn.cdc.gov/ARInvestments/

(22) £30 million of funding to tackle antimicrobial resistance https://www.gov.uk/government/news/30-million-of-funding-to-tackle-antimicrobial-resistance.

(23) unctad.org | Fighting the war on antibiotic resistance with new investment schemes -- Q&A with Christoph Spennemann. http://unctad.org/en/pages/newsdetails.aspx?OriginalVersionID=1585&Sitemap_x0020_Taxonomy=Intellectual%20Property.

(24) Chu, D. T.; Plattner, J. J.; Katz, L. New Directions in Antibacterial Research. *J. Med. Chem.* **1996**, *39* (20), 3853–3874.

(25) Conly, J.; Johnston, B. Where Are All the New Antibiotics? The New Antibiotic Paradox. *Can. J. Infect. Dis. Med. Microbiol.* **2005**, *16* (3), 159–160.

(26) Alanis, A. J. Resistance to Antibiotics: Are We in the Post-Antibiotic Era? *Arch. Med. Res.* **2005**, *36* (6), 697–705.

(27) Payne, D. J.; Gwynn, M. N.; Holmes, D. J.; Pompliano, D. L. Drugs for Bad Bugs: Confronting the Challenges of Antibacterial Discovery. *Nat. Rev. Drug Discov.* **2007**, *6* (1), 29–40.

(28) Aminov, R. I. A Brief History of the Antibiotic Era: Lessons Learned and Challenges for the Future. *Front. Microbiol.* **2010**, *1*.

(29) Coates, A. R.; Halls, G.; Hu, Y. Novel Classes of Antibiotics or More of the Same? *Br. J. Pharmacol.* **2011**, *163* (1), 184–194.

(30) Lewis, K. Platforms for Antibiotic Discovery. *Nat. Rev. Drug Discov.* **2013**, *12* (5), 371–387.

(31) Singh, S. B. Confronting the Challenges of Discovery of Novel Antibacterial Agents. *Bioorg. Med. Chem. Lett.* **2014**, *24* (16), 3683–3689.

(32) Butler, M. S.; Blaskovich, M. A.; Cooper, M. A. Antibiotics in the Clinical Pipeline at the End of 2015. *J. Antibiot. (Tokyo)* **2017**, *70* (1), 3–24.

(33) Fernandes, P.; Martens, E. Antibiotics in Late Clinical Development. *Biochem. Pharmacol.* **2017**, *133*, 152–163.

(34) Walsh, F. Superbugs to Kill "More than Cancer." *BBC News*. December 11, 2014.

(35) Spellberg, B.; Guidos, R.; Gilbert, D.; Bradley, J.; Boucher, H. W.; Scheld, W. M.; Bartlett, J. G.; Edwards, J.; Infectious Diseases Society of America. The Epidemic of Antibiotic-Resistant Infections: A Call to Action for the Medical Community from the Infectious Diseases Society of America. *Clin. Infect. Dis. Off. Publ. Infect. Dis. Soc. Am.* **2008**, *46* (2), 155–164.

(36) Gould, I. M. Antibiotic Resistance: The Perfect Storm. *Int. J. Antimicrob. Agents* **2009**, *34*, S2–S5.

(37) Hersh, A. L.; Newland, J. G.; Beekmann, S. E.; Polgreen, P. M.; Gilbert, D. N. Unmet Medical Need in Infectious Diseases. *Clin. Infect. Dis. Off. Publ. Infect. Dis. Soc. Am.* **2012**, *54* (11), 1677–1678.

(38) Reardon, S. Antibiotic Resistance Sweeping Developing World. *Nat. News* **2014**, *509* (7499), 141.

(39) Spellberg, B.; Bartlett, J. G.; Gilbert, D. N. The Future of Antibiotics and Resistance. *N. Engl. J. Med.* **2013**, *368* (4), 299–302.

(40) Holmes, A. H.; Moore, L. S. P.; Sundsfjord, A.; Steinbakk, M.; Regmi, S.; Karkey, A.; Guerin, P. J.; Piddock, L. J. V. Understanding the Mechanisms and Drivers of Antimicrobial Resistance. *Lancet Lond. Engl.* **2016**, *387* (10014), 176–187.

(41) Kapoor, G.; Saigal, S.; Elongavan, A. Action and Resistance Mechanisms of Antibiotics: A Guide for Clinicians. *J. Anaesthesiol. Clin. Pharmacol.* **2017**, *33* (3), 300–305.

(42) CDC Global Health - Infographics - Antibiotic Resistance The Global Threat https://www.cdc.gov/globalhealth/infographics/antibiotic-resistance/antibiotic_resistance_global_threat.htm.

(43) Hoelzer, K.; Wong, N.; Thomas, J.; Talkington, K.; Jungman, E.; Coukell, A. Antimicrobial Drug Use in Food-Producing Animals and Associated Human Health Risks: What, and How Strong, Is the Evidence? *BMC Vet. Res.* **2017**, *13*.

(44) Boeckel, T. P. V.; Glennon, E. E.; Chen, D.; Gilbert, M.; Robinson, T. P.; Grenfell, B. T.; Levin, S. A.; Bonhoeffer, S.; Laxminarayan, R. Reducing Antimicrobial Use in Food Animals. *Science* **2017**, *357* (6358), 1350–1352.

(45) Wellington, E. M. H.; Boxall, A. B.; Cross, P.; Feil, E. J.; Gaze, W. H.; Hawkey, P. M.; Johnson-Rollings, A. S.; Jones, D. L.; Lee, N. M.; Otten, W.; et al. The Role of the Natural Environment in the Emergence of Antibiotic Resistance in Gram-Negative Bacteria. *Lancet Infect. Dis.* **2013**, *13* (2), 155–165.

(46) Brooks, B. D.; Brooks, A. E. Therapeutic Strategies to Combat Antibiotic Resistance. *Adv. Drug Deliv. Rev.* **2014**, *78*, 14–27.

(47) Viale, P.; Giannella, M.; Tedeschi, S.; Lewis, R. Treatment of MDR-Gram Negative Infections in the 21st Century: A Never Ending Threat for Clinicians. *Curr. Opin. Pharmacol.* **2015**, *24*, 30–37.

(48) Chellat, M. F.; Raguž, L.; Riedl, R. Targeting Antibiotic Resistance. *Angew. Chem. Int. Ed. 55* (23), 6600–6626.

(49) Schillaci, D.; Spanò, V.; Parrino, B.; Carbone, A.; Montalbano, A.; Barraja, P.; Diana, P.; Cirrincione, G.; Cascioferro, S. Pharmaceutical Approaches to Target Antibiotic Resistance Mechanisms. *J. Med. Chem.* **2017**, *60* (20), 8268–8297.

(50) D'Costa, V. M.; King, C. E.; Kalan, L.; Morar, M.; Sung, W. W. L.; Schwarz, C.; Froese, D.; Zazula, G.; Calmels, F.; Debruyne, R.; et al. Antibiotic Resistance Is Ancient. *Nature* **2011**, *477* (7365), 457–461.

(51) Allen, H. K.; Donato, J.; Wang, H. H.; Cloud-Hansen, K. A.; Davies, J.; Handelsman, J. Call of the Wild: Antibiotic Resistance Genes in Natural Environments. *Nat. Rev. Microbiol.* **2010**, *8* (4), 251–259.

(52) Wright, G. D. The Antibiotic Resistome: The Nexus of Chemical and Genetic Diversity. *Nat. Rev. Microbiol.* **2007**, *5* (3), 175–186.

(53) Woodford, N.; Ellington, M. J. The Emergence of Antibiotic Resistance by Mutation. *Clin. Microbiol. Infect. Off. Publ. Eur. Soc. Clin. Microbiol. Infect. Dis.* **2007**, *13* (1), 5–18.

(54) Davies, J.; Davies, D. Origins and Evolution of Antibiotic Resistance. *Microbiol. Mol. Biol. Rev. MMBR* **2010**, *74* (3), 417–433.

(55) Cox, G.; Wright, G. D. Intrinsic Antibiotic Resistance: Mechanisms, Origins, Challenges and Solutions. *Int. J. Med. Microbiol. IJMM* **2013**, *303* (6–7), 287–292.

(56) van Hoek, A. H. A. M.; Mevius, D.; Guerra, B.; Mullany, P.; Roberts, A. P.; Aarts, H. J. M. Acquired Antibiotic Resistance Genes: An Overview. *Front. Microbiol.* **2011**, *2*.

(57) Blair, J. M. A.; Webber, M. A.; Baylay, A. J.; Ogbolu, D. O.; Piddock, L. J. V. Molecular Mechanisms of Antibiotic Resistance. *Nat. Rev. Microbiol.* **2015**, *13* (1), 42–51.

(58) Brauner, A.; Fridman, O.; Gefen, O.; Balaban, N. Q. Distinguishing between Resistance, Tolerance and Persistence to Antibiotic Treatment. *Nat. Rev. Microbiol.* **2016**, *14* (5), 320–330.

(59) von Wintersdorff, C. J. H.; Penders, J.; van Niekerk, J. M.; Mills, N. D.; Majumder, S.; van Alphen, L. B.; Savelkoul, P. H. M.; Wolffs, P. F. G. Dissemination of Antimicrobial Resistance in Microbial Ecosystems through Horizontal Gene Transfer. *Front. Microbiol.* **2016**, *7*.

(60) Kumar, A.; Schweizer, H. P. Bacterial Resistance to Antibiotics: Active Efflux and Reduced Uptake. *Adv. Drug Deliv. Rev.* **2005**, *57* (10), 1486–1513.

(61) Nikaido, H.; Pagès, J.-M. Broad-Specificity Efflux Pumps and Their Role in Multidrug Resistance of Gram-Negative Bacteria. *FEMS Microbiol. Rev.* **2012**, *36* (2), 340–363.

(62) Masi, M.; Réfregiers, M.; Pos, K. M.; Pagès, J.-M. Mechanisms of Envelope Permeability and Antibiotic Influx and Efflux in Gram-Negative Bacteria. *Nat. Microbiol.* **2017**, *2* (3), 17001.

(63) McPhee, J. B.; Tamber, S.; Brazas, M. D.; Lewenza, S.; Hancock, R. E. W. Antibiotic Resistance Due to Reduced Uptake. In *Antimicrobial Drug Resistance*; Infectious Disease; Humana Press, 2009; pp 97–110.

(64) WHO | Global action plan on AMR http://www.who.int/antimicrobial-resistance/global-action-plan/en/.

(65) Lohner, K.; Prenner, E. J. Differential Scanning Calorimetry and X-Ray Diffraction Studies of the Specificity of the Interaction of Antimicrobial Peptides with Membrane-Mimetic Systems. *Biochim. Biophys. Acta BBA - Biomembr.* **1999**, *1462* (1), 141–156.

(66) Brogden, K. A.; Ackermann, M.; McCray, P. B.; Tack, B. F. Antimicrobial Peptides in Animals and Their Role in Host Defences. *Int. J. Antimicrob. Agents* **2003**, *22* (5), 465–478.

(67) Fritz, J. H.; Brunner, S.; Birnstiel, M. L.; Buschle, M.; Gabain, A. v; Mattner, F.; Zauner, W. The Artificial Antimicrobial Peptide KLKLLLLLKLK Induces Predominantly a TH2-Type Immune Response to Co-Injected Antigens. *Vaccine* **2004**, *22* (25–26), 3274–3284.

(68) Reddy, K. V. R.; Yedery, R. D.; Aranha, C. Antimicrobial Peptides: Premises and Promises. *Int. J. Antimicrob. Agents* **2004**, *24* (6), 536–547.

(69) Peschel, A.; Sahl, H.-G. The Co-Evolution of Host Cationic Antimicrobial Peptides and Microbial Resistance. *Nat. Rev. Microbiol.* **2006**, *4* (7), 529–536.

(70) Hancock, R. E. W.; Sahl, H.-G. Antimicrobial and Host-Defense Peptides as New Anti-Infective Therapeutic Strategies. *Nat. Biotechnol.* **2006**, *24* (12), 1551–1557.

(71) Guilhelmelli, F.; Vilela, N.; Albuquerque, P.; Derengowski, L. da S.; Silva-Pereira, I.; Kyaw, C. M. Antibiotic Development Challenges: The Various Mechanisms of Action of Antimicrobial Peptides and of Bacterial Resistance. *Front. Microbiol.* **2013**, *4*, 353.

(72) Alves, D.; Olívia Pereira, M. Mini-Review: Antimicrobial Peptides and Enzymes as Promising Candidates to Functionalize Biomaterial Surfaces. *Biofouling* **2014**, *30* (4), 483–499.

(73) Bradbury, J. "My Enemy's Enemy Is My Friend." Using Phages to Fight Bacteria. *Lancet Lond. Engl.* **2004**, *363* (9409), 624–625.

(74) Levin, B. R.; Bull, J. J. Population and Evolutionary Dynamics of Phage Therapy. *Nat. Rev. Microbiol.* **2004**, *2* (2), 166–173.

(75) Burrowes, B.; Harper, D. R.; Anderson, J.; McConville, M.; Enright, M. C. Bacteriophage Therapy: Potential Uses in the Control of Antibiotic-Resistant Pathogens. *Expert Rev. Anti Infect. Ther.* **2011**, *9* (9), 775–785.

(76) Ghannad, M. S.; Mohammadi, A. Bacteriophage: Time to Re-Evaluate the Potential of Phage Therapy as a Promising Agent to Control Multidrug-Resistant Bacteria. *Iran. J. Basic Med. Sci.* **2012**, *15* (2), 693.

(77) Lin, D. M.; Koskella, B.; Lin, H. C. Phage Therapy: An Alternative to Antibiotics in the Age of Multi-Drug Resistance. *World J. Gastrointest. Pharmacol. Ther.* **2017**, *8* (3), 162–173.

(78) Kuroda, K.; Caputo, G. A. Antimicrobial Polymers as Synthetic Mimics of Host-Defense Peptides. *Wiley Interdiscip. Rev. Nanomed. Nanobiotechnol.* **2013**, *5* (1), 49–66.

(79) Timofeeva, L.; Kleshcheva, N. Antimicrobial Polymers: Mechanism of Action, Factors of Activity, and Applications. *Appl. Microbiol. Biotechnol.* **2011**, *89* (3), 475–492.

(80) Zhang, L.; Pornpattananangku, D.; Hu, C.-M. J.; Huang, C.-M. Development of Nanoparticles for Antimicrobial Drug Delivery. *Curr. Med. Chem.* **2010**, *17* (6), 585–594.

(81) Taylor, E.; Webster, T. J. Reducing Infections through Nanotechnology and Nanoparticles. *Int. J. Nanomedicine* **2011**, *6*, 1463–1473.

(82) Andrade, F.; Rafael, D.; Videira, M.; Ferreira, D.; Sosnik, A.; Sarmento, B. Nanotechnology and Pulmonary Delivery to Overcome Resistance in Infectious Diseases. *Adv. Drug Deliv. Rev.* **2013**, *65* (13–14), 1816–1827.

(83) Sharma, A.; Sharma, U. S. Liposomes in Drug Delivery: Progress and Limitations. *Int. J. Pharm.* **1997**, *154* (2), 123–140.

(84) Pinto-Alphandary, H.; Andremont, A.; Couvreur, P. Targeted Delivery of Antibiotics Using Liposomes and Nanoparticles: Research and Applications. *Int. J. Antimicrob. Agents* **2000**, *13* (3), 155–168.

(85) Drulis-Kawa, Z.; Dorotkiewicz-Jach, A. Liposomes as Delivery Systems for Antibiotics. *Int. J. Pharm.* **2010**, *387* (1), 187–198.

(86) Alhariri, M.; Azghani, A.; Omri, A. Liposomal Antibiotics for the Treatment of Infectious Diseases. *Expert Opin. Drug Deliv.* **2013**, *10* (11), 1515–1532.

(87) McDonnell, G.; Russell, A. D. Antiseptics and Disinfectants: Activity, Action, and Resistance. *Clin. Microbiol. Rev.* **1999**, *12* (1), 147–179.

(88) Sampath, L. A.; Tambe, S. M.; Modak, S. M. In Vitro and in Vivo Efficacy of Catheters Impregnated with Antiseptics or Antibiotics: Evaluation of the Risk of Bacterial Resistance to the Antimicrobials in the Catheters. *Infect. Control Hosp. Epidemiol.* **2001**, *22* (10), 640–646.

(89) Ejim, L.; Farha, M. A.; Falconer, S. B.; Wildenhain, J.; Coombes, B. K.; Tyers, M.; Brown, E. D.; Wright, G. D. Combinations of Antibiotics and Nonantibiotic Drugs Enhance Antimicrobial Efficacy. *Nat. Chem. Biol.* **2011**, *7* (6), 348–350.

(90) Fischbach, M. A. Combination Therapies for Combating Antimicrobial Resistance. *Curr. Opin. Microbiol.* **2011**, *14* (5), 519–523.

(91) Tamma, P. D.; Cosgrove, S. E.; Maragakis, L. L. Combination Therapy for Treatment of Infections with Gram-Negative Bacteria. *Clin. Microbiol. Rev.* **2012**, *25* (3), 450–470.

(92) Hamoud, R.; Zimmermann, S.; Reichling, J.; Wink, M. Synergistic Interactions in Two-Drug and Three-Drug Combinations (Thymol, EDTA and Vancomycin) against Multi Drug Resistant Bacteria Including E. Coli. *Phytomedicine Int. J. Phytother. Phytopharm.* **2014**, *21* (4), 443–447.

(93) Phougat, N.; Khatri, S.; Singh, A.; Dangi, M.; Kumar, M.; Dabur, R.; Chhillar, A. K. Combination Therapy: The Propitious Rationale for Drug Development. *Comb. Chem. High Throughput Screen.* **2014**, *17* (1), 53–67.

(94) Surette, M. G.; Miller, M. B.; Bassler, B. L. Quorum Sensing in Escherichia Coli, Salmonella Typhimurium, and Vibrio Harveyi: A New Family of Genes Responsible for Autoinducer Production. *Proc. Natl. Acad. Sci. U. S. A.* **1999**, *96* (4), 1639–1644.

(95) Waters, C. M.; Bassler, B. L. Quorum Sensing: Cell-to-Cell Communication in Bacteria. *Annu. Rev. Cell Dev. Biol.* **2005**, *21*, 319–346.

(96) Bassler, B. L.; Losick, R. Bacterially Speaking. *Cell* **2006**, *125* (2), 237–246.

(97) Lowery, C. A.; Dickerson, T. J.; Janda, K. D. Interspecies and Interkingdom Communication Mediated by Bacterial Quorum Sensing. *Chem. Soc. Rev.* **2008**, *37* (7), 1337–1346.

(98) Ng, W.-L.; Bassler, B. L. Bacterial Quorum-Sensing Network Architectures. *Annu. Rev. Genet.* **2009**, *43* (1), 197–222.

(99) Zhu, J.; Miller, M. B.; Vance, R. E.; Dziejman, M.; Bassler, B. L.; Mekalanos, J. J. Quorum-Sensing Regulators Control Virulence Gene Expression in Vibrio Cholerae. *Proc. Natl. Acad. Sci.* **2002**, *99* (5), 3129–3134.

(100) Antunes, L. C. M.; Ferreira, R. B. R.; Buckner, M. M. C.; Finlay, B. B. Quorum Sensing in Bacterial Virulence. *Microbiology* **2010**, *156* (8), 2271–2282.

(101) Ahmed, N. A. A. M.; Petersen, F. C.; Scheie, A. A. AI-2 Quorum Sensing Affects Antibiotic Susceptibility in Streptococcus Anginosus. *J. Antimicrob. Chemother.* **2007**, *60* (1), 49–53.

(102) Davies, D. G.; Parsek, M. R.; Pearson, J. P.; Iglewski, B. H.; Costerton, J. W.; Greenberg, E. P. The Involvement of Cell-to-Cell Signals in the Development of a Bacterial Biofilm. *Science* **1998**, *280* (5361), 295–298.

(103) Rickard, A. H.; Palmer, R. J.; Blehert, D. S.; Campagna, S. R.; Semmelhack, M. F.; Egland, P. G.; Bassler, B. L.; Kolenbrander, P. E. Autoinducer 2: A Concentration-Dependent Signal for Mutualistic Bacterial Biofilm Growth. *Mol. Microbiol.* **2006**, *60* (6), 1446–1456.

(104) Irie, Y.; Parsek, M. R. Quorum Sensing and Microbial Biofilms. *Curr. Top. Microbiol. Immunol.* **2008**, *322*, 67–84.

(105) Suga, H.; Smith, K. M. Molecular Mechanisms of Bacterial Quorum Sensing as a New Drug Target. *Curr. Opin. Chem. Biol.* **2003**, *7* (5), 586–591.

(106) Geske, G. D.; Wezeman, R. J.; Siegel, A. P.; Blackwell, H. E. Small Molecule Inhibitors of Bacterial Quorum Sensing and Biofilm Formation. *J. Am. Chem. Soc.* **2005**, *127* (37), 12762–12763.

(107) Rasmussen, T. B.; Givskov, M. Quorum-Sensing Inhibitors as Anti-Pathogenic Drugs. *Int. J. Med. Microbiol.* **2006**, *296* (2–3), 149–161.

(108) Clatworthy, A. E.; Pierson, E.; Hung, D. T. Targeting Virulence: A New Paradigm for Antimicrobial Therapy. *Nat. Chem. Biol.* **2007**, *3* (9), 541–548.

(109) Parsek, M. R.; Val, D. L.; Hanzelka, B. L.; Cronan, J. E.; Greenberg, E. P. Acyl Homoserine-Lactone Quorum-Sensing Signal Generation. *Proc. Natl. Acad. Sci.* **1999**, *96* (8), 4360–4365.

(110) Geske, G. D.; Wezeman, R. J.; Siegel, A. P.; Blackwell, H. E. Small Molecule Inhibitors of Bacterial Quorum Sensing and Biofilm Formation. *J. Am. Chem. Soc.* **2005**, *127* (37), 12762–12763.

(111) Pesci, E. C.; Milbank, J. B.; Pearson, J. P.; McKnight, S.; Kende, A. S.; Greenberg, E. P.; Iglewski, B. H. Quinolone Signaling in the Cell-to-Cell Communication System of Pseudomonas Aeruginosa. *Proc. Natl. Acad. Sci. U. S. A.* **1999**, *96* (20), 11229–11234.

(112) Dubern, J.-F.; Diggle, S. P. Quorum Sensing by 2-Alkyl-4-Quinolones in Pseudomonas Aeruginosa and Other Bacterial Species. *Mol. Biosyst.* **2008**, *4* (9), 882.

(113) Jimenez, P. N.; Koch, G.; Thompson, J. A.; Xavier, K. B.; Cool, R. H.; Quax, W. J. The Multiple Signaling Systems Regulating Virulence in Pseudomonas Aeruginosa. *Microbiol. Mol. Biol. Rev. MMBR* **2012**, *76* (1), 46–65.

(114) Barber, C. E.; Tang, J. L.; Feng, J. X.; Pan, M. Q.; Wilson, T. J.; Slater, H.; Dow, J. M.; Williams, P.; Daniels, M. J. A Novel Regulatory System Required for Pathogenicity of Xanthomonas Campestris Is Mediated by a Small Diffusible Signal Molecule. *Mol. Microbiol.* **1997**, *24* (3), 555–566.

(115) Deng, Y.; Wu, J.; Tao, F.; Zhang, L.-H. Listening to a New Language: DSF-Based Quorum Sensing in Gram-Negative Bacteria. *Chem. Rev.* **2011**, *111* (1), 160–173.

(116) Takano, E. Gamma-Butyrolactones: Streptomyces Signalling Molecules Regulating Antibiotic Production and Differentiation. *Curr. Opin. Microbiol.* **2006**, *9* (3), 287–294.

(117) Kesarwani, M.; Hazan, R.; He, J.; Que, Y.; Apidianakis, Y.; Lesic, B.; Xiao, G.; Dekimpe, V.; Milot, S.; Deziel, E.; et al. A Quorum Sensing Regulated Small Volatile Molecule Reduces Acute Virulence and Promotes Chronic Infection Phenotypes. *PLOS Pathog.* **2011**, *7* (8), e1002192.

(118) Loh, J.; Carlson, R. W.; York, W. S.; Stacey, G. Bradyoxetin, a Unique Chemical Signal Involved in Symbiotic Gene Regulation. *Proc. Natl. Acad. Sci. U. S. A.* **2002**, *99* (22), 14446–14451.

(119) Bassler, B. L.; Wright, M.; Showalter, R. E.; Silverman, M. R. Intercellular Signalling in Vibrio Harveyi: Sequence and Function of Genes Regulating Expression of Luminescence. *Mol. Microbiol.* **1993**, *9* (4), 773–786.

(120) Dubois, T.; Faegri, K.; Perchat, S.; Lemy, C.; Buisson, C.; Nielsen-LeRoux, C.; Gohar, M.; Jacques, P.; Ramarao, N.; Kolstø, A.-B.; et al. Necrotrophism Is a Quorum-Sensing-Regulated Lifestyle in Bacillus Thuringiensis. *PLOS Pathog.* **2012**, *8* (4), e1002629.

(121) Rocha-Estrada, J.; Aceves-Diez, A. E.; Guarneros, G.; de la Torre, M. The RNPP Family of Quorum-Sensing Proteins in Gram-Positive Bacteria. *Appl. Microbiol. Biotechnol.* **2010**, *87* (3), 913–923.

(122) Bassler, B. L.; Wright, M.; Silverman, M. R. Multiple Signalling Systems Controlling Expression of Luminescence in Vibrio Harveyi: Sequence and Function of Genes Encoding a Second Sensory Pathway. *Mol. Microbiol.* **1994**, *13* (2), 273–286.

(123) Bassler, B. L. How Bacteria Talk to Each Other: Regulation of Gene Expression by Quorum Sensing. *Curr. Opin. Microbiol.* **1999**, *2* (6), 582–587.

(124) Schauder, S.; Bassler, B. L. The Languages of Bacteria. *Genes Dev.* **2001**, *15* (12), 1468–1480.

(125) Schauder, S.; Shokat, K.; Surette, M. G.; Bassler, B. L. The LuxS Family of Bacterial Autoinducers: Biosynthesis of a Novel Quorum-Sensing Signal Molecule. *Mol. Microbiol.* **2001**, *41* (2), 463–476.

(126) Pereira, C. S.; McAuley, J. R.; Taga, M. E.; Xavier, K. B.; Miller, S. T. Sinorhizobium Meliloti, a Bacterium Lacking the Autoinducer-2 (AI-2) Synthase, Responds to AI-2 Supplied by Other Bacteria. *Mol. Microbiol.* **2008**, *70* (5), 1223–1235.

(127) Miller, S. T.; Xavier, K. B.; Campagna, S. R.; Taga, M. E.; Semmelhack, M. F.; Bassler, B. L.; Hughson, F. M. Salmonella Typhimurium Recognizes a Chemically Distinct Form of the Bacterial Quorum-Sensing Signal AI-2. *Mol. Cell* **2004**, *15* (5), 677–687.

(128) Kavanaugh, J. S.; Gakhar, L.; Horswill, A. R. The Structure of LsrB from Yersinia Pestis Complexed with Autoinducer-2. *Acta Crystallograph. Sect. F Struct. Biol. Cryst. Commun.* **2011**, *67* (12), 1501–1505.

(129) Chen, X.; Schauder, S.; Potier, N.; Van Dorsselaer, A.; Pelczer, I.; Bassler, B. L.; Hughson, F. M. Structural Identification of a Bacterial Quorum-Sensing Signal Containing Boron. *Nature* **2002**, *415* (6871), 545–549.

(130) Hauck, T.; Hübner, Y.; Brühlmann, F.; Schwab, W. Alternative Pathway for the Formation of 4,5-Dihydroxy-2,3-Pentanedione, the Proposed Precursor of 4-Hydroxy-5-Methyl-3(2H)-Furanone as Well as Autoinducer-2, and Its Detection as Natural Constituent of Tomato Fruit. *Biochim. Biophys. Acta BBA - Gen. Subj.* **2003**, *1623* (2–3), 109–119.

(131) Herzberg, M.; Kaye, I. K.; Peti, W.; Wood, T. K. YdgG (TqsA) Controls Biofilm Formation in Escherichia Coli K-12 through Autoinducer 2 Transport. *J. Bacteriol.* **2006**, *188* (2), 587–598.

(132) Kamaraju, K.; Smith, J.; Wang, J.; Roy, V.; Sintim, H. O.; Bentley, W. E.; Sukharev, S. Effects on Membrane Lateral Pressure Suggest Permeation Mechanisms for Bacterial Quorum Signaling Molecules. *Biochemistry* **2011**, *50* (32), 6983–6993.

(133) Ha, J.-H.; Eo, Y.; Grishaev, A.; Guo, M.; Smith, J. A. I.; Sintim, H. O.; Kim, E.-H.; Cheong, H.-K.; Bentley, W. E.; Ryu, K.-S. Crystal Structures of the LsrR Proteins Complexed with Phospho-AI-2 and Two Signal-Interrupting Analogues Reveal Distinct Mechanisms for Ligand Recognition. *J. Am. Chem. Soc.* **2013**, *135* (41), 15526–15535.

(134) Zhu, J.; Hixon, M. S.; Globisch, D.; Kaufmann, G. F.; Janda, K. D. Mechanistic Insights into the LsrK Kinase Required for Autoinducer-2 Quorum Sensing Activation. *J. Am. Chem. Soc.* **2013**, *135* (21), 7827–7830.

(135) Marques, J. C.; Lamosa, P.; Russell, C.; Ventura, R.; Maycock, C.; Semmelhack, M. F.; Miller, S. T.; Xavier, K. B. Processing the Interspecies Quorum-Sensing Signal Autoinducer-2 (AI-2): Characterization of Phospho-(S)-4,5-Dihydroxy-2,3-Pentanedione Isomerization by LsrG Protein. *J. Biol. Chem.* **2011**, *286* (20), 18331–18343.

(136) Marques, J. C.; Oh, I. K.; Ly, D. C.; Lamosa, P.; Ventura, M. R.; Miller, S. T.; Xavier, K. B. LsrF, a Coenzyme A-Dependent Thiolase, Catalyzes the Terminal Step in Processing the Quorum Sensing Signal Autoinducer-2. *Proc. Natl. Acad. Sci. U. S. A.* **2014**, *111* (39), 14235–14240.

(137) Penesyan, A.; Gillings, M.; Paulsen, I. T. Antibiotic Discovery: Combatting Bacterial Resistance in Cells and in Biofilm Communities. *Mol. Basel Switz.* **2015**, *20* (4), 5286–5298.

(138) Whitchurch, C. B.; Tolker-Nielsen, T.; Ragas, P. C.; Mattick, J. S. Extracellular DNA Required for Bacterial Biofilm Formation. *Science* **2002**, *295* (5559), 1487.

(139) Flemming, H.-C.; Wingender, J. The Biofilm Matrix. *Nat. Rev. Microbiol.* **2010**, *8* (9), 623–633.

(140) Mulcahy, H.; Charron-Mazenod, L.; Lewenza, S. Extracellular DNA Chelates Cations and Induces Antibiotic Resistance in Pseudomonas Aeruginosa Biofilms. *PLOS Pathog.* **2008**, *4* (11), e1000213.

(141) Lewis, K. Multidrug Tolerance of Biofilms and Persister Cells. *Curr. Top. Microbiol. Immunol.* **2008**, *322*, 107–131.

(142) Sun, F.; Qu, F.; Ling, Y.; Mao, P.; Xia, P.; Chen, H.; Zhou, D. Biofilm-Associated Infections: Antibiotic Resistance and Novel Therapeutic Strategies. *Future Microbiol.* **2013**, *8* (7), 877–886.

(143) Mulcahy, L. R.; Burns, J. L.; Lory, S.; Lewis, K. Emergence of Pseudomonas Aeruginosa Strains Producing High Levels of Persister Cells in Patients with Cystic Fibrosis. *J. Bacteriol.* **2010**, *192* (23), 6191–6199.

(144) Townsend, J. P.; Nielsen, K. M.; Fisher, D. S.; Hartl, D. L. Horizontal Acquisition of Divergent Chromosomal DNA in Bacteria: Effects of Mutator Phenotypes. *Genetics* **2003**, *164* (1), 13–21.

(145) Blázquez, J. Hypermutation as a Factor Contributing to the Acquisition of Antimicrobial Resistance. *Clin. Infect. Dis. Off. Publ. Infect. Dis. Soc. Am.* **2003**, *37* (9), 1201–1209.

(146) Conibear, T. C. R.; Collins, S. L.; Webb, J. S. Role of Mutation in Pseudomonas Aeruginosa Biofilm Development. *PLOS ONE* **2009**, *4* (7), e6289.

(147) Gonzalez Barrios, A. F.; Zuo, R.; Hashimoto, Y.; Yang, L.; Bentley, W. E.; Wood, T. K. Autoinducer 2 Controls Biofilm Formation in Escherichia Coli through a Novel Motility Quorum-Sensing Regulator (MqsR, B3022). *J. Bacteriol.* **2006**, *188* (1), 305–316.

(148) Roy, V.; Meyer, M. T.; Smith, J. A. I.; Gamby, S.; Sintim, H. O.; Ghodssi, R.; Bentley, W. E. AI-2 Analogs and Antibiotics: A Synergistic Approach to Reduce Bacterial Biofilms. *Appl. Microbiol. Biotechnol.* **2013**, *97* (6), 2627–2638.

(149) Kociolek, M. Quorum-Sensing Inhibitors and Biofilms. *Anti-Infect. Agents Med. Chem.* **2009**, *8* (4), 315–326.

(150) Brackman, G.; Coenye, T. Quorum Sensing Inhibitors as Anti-Biofilm Agents. *Curr. Pharm. Des.* **2015**, *21* (1), 5–11.

(151) Zhang, L.-H.; Dong, Y.-H. Quorum Sensing and Signal Interference: Diverse Implications. *Mol. Microbiol.* **2004**, *53* (6), 1563–1571.

(152) Persson, T.; Givskov, M.; Nielsen, J. Quorum Sensing Inhibition: Targeting Chemical Communication in Gram-Negative Bacteria. *Curr. Med. Chem.* **2005**, *12* (26), 3103–3115.

(153) Hoang, T. T.; Schweizer, H. P. Characterization of Pseudomonas Aeruginosa Enoyl-Acyl Carrier Protein Reductase (FabI): A Target for the Antimicrobial Triclosan and Its Role in Acylated Homoserine Lactone Synthesis. *J. Bacteriol.* **1999**, *181* (17), 5489–5497.

(154) Heath, R. J.; Yu, Y.-T.; Shapiro, M. A.; Olson, E.; Rock, C. O. Broad Spectrum Antimicrobial Biocides Target the FabI Component of Fatty Acid Synthesis. *J. Biol. Chem.* **1998**, *273* (46), 30316–30320.

(155) Nakayama, J.; Uemura, Y.; Nishiguchi, K.; Yoshimura, N.; Igarashi, Y.; Sonomoto, K. Ambuic Acid Inhibits the Biosynthesis of Cyclic Peptide Quormones in Gram-Positive Bacteria. *Antimicrob. Agents Chemother.* **2009**, *53* (2), 580–586.

(156) Cornell, K. A.; Swarts, W. E.; Barry, R. D.; Riscoe, M. K. Characterization of Recombinant Eschericha Coli 5'-Methylthioadenosine/S-Adenosylhomocysteine Nucleosidase: Analysis of Enzymatic Activity and Substrate Specificity. *Biochem. Biophys. Res. Commun.* **1996**, *228* (3), 724– 732.

(157) Lee, J. E.; Cornell, K. A.; Riscoe, M. K.; Howell, P. L. Structure of Escherichia Coli 5'- Methylthioadenosine/ S-Adenosylhomocysteine Nucleosidase Inhibitor Complexes Provide Insight into the Conformational Changes Required for Substrate Binding and Catalysis. *J. Biol. Chem.* **2003**, *278* (10), 8761–8770.

(158) Singh, V.; Lee, J. E.; Núñez, S.; Howell, P. L.; Schramm, V. L. Transition State Structure of 5'- Methylthioadenosine/ *S* -Adenosylhomocysteine Nucleosidase from *Escherichia Coli* and Its Similarity to Transition State Analogues [†]. *Biochemistry* **2005**, *44* (35), 11647–11659.

(159) Singh, V.; Schramm, V. L. Transition-State Analysis of S. Pneumoniae 5'-Methylthioadenosine Nucleosidase. *J. Am. Chem. Soc.* **2007**, *129* (10), 2783–2795.

(160) Siu, K. K. W.; Lee, J. E.; Smith, G. D.; Horvatin-Mrakovcic, C.; Howell, P. L. Structure of Staphylococcus Aureus 5'-Methylthioadenosine/S-Adenosylhomocysteine Nucleosidase. *Acta Crystallograph. Sect. F Struct. Biol. Cryst. Commun.* **2008**, *64* (Pt 5), 343–350.

(161) Parveen, N.; Cornell, K. A. Methylthioadenosine/S-Adenosylhomocysteine Nucleosidase, a Critical Enzyme for Bacterial Metabolism: Involvement of MTA/SAH Nucleosidase in Bacterial Metabolism. *Mol. Microbiol.* **2011**, *79* (1), 7–20.

(162) Singh, V.; Shi, W.; Evans, G. B.; Tyler, P. C.; Furneaux, R. H.; Almo, S. C.; Schramm, V. L. Picomolar Transition State Analogue Inhibitors of Human 5'-Methylthioadenosine Phosphorylase and X-Ray Structure with MT-Immucillin-A. *Biochemistry* **2004**, *43* (1), 9–18.

(163) Singh, V.; Evans, G. B.; Lenz, D. H.; Mason, J. M.; Clinch, K.; Mee, S.; Painter, G. F.; Tyler, P. C.; Furneaux, R. H.; Lee, J. E.; et al. Femtomolar Transition State Analogue Inhibitors of 5'- Methylthioadenosine/S-Adenosylhomocysteine Nucleosidase from Escherichia Coli. *J. Biol. Chem.* **2005**, *280* (18), 18265–18273.

(164) Schramm, V. L.; Gutierrez, J. A.; Cordovano, G.; Basu, I.; Guha, C.; Belbin, T. J.; Evans, G. B.; Tyler, P. C.; Furneaux, R. H. Transition State Analogues in Quorum Sensing and SAM Recycling. *Nucleic Acids Symp. Ser. 2004* **2008**, No. 52, 75–76.

(165) Gutierrez, J. A.; Crowder, T.; Rinaldo-Matthis, A.; Ho, M.-C.; Almo, S. C.; Schramm, V. L. Transition State Analogs of 5'-Methylthioadenosine Nucleosidase Disrupt Quorum Sensing. *Nat. Chem. Biol.* **2009**, *5* (4), 251–257.

(166) Guillerm, G.; Varkados, M.; Auvin, S.; Le Goffic, F. Synthesis of Hydroxylated Pyrrolidines Derivatives as Potential Inhibitors of SAH/MTA Nucleosidase. *Tetrahedron Lett.* **1987**, *28* (5), 535– 538.

(167) Li, X.; Chu, S.; Feher, V. A.; Khalili, M.; Nie, Z.; Margosiak, S.; Nikulin, V.; Levin, J.; Sprankle, K. G.; Tedder, M. E.; et al. Structure-Based Design, Synthesis, and Antimicrobial Activity of Indazole-Derived SAH/MTA Nucleosidase Inhibitors. *J. Med. Chem.* **2003**, *46* (26), 5663–5673.

(168) Tedder, M. E.; Nie, Z.; Margosiak, S.; Chu, S.; Feher, V. A.; Almassy, R.; Appelt, K.; Yager, K. M. Structure-Based Design, Synthesis, and Antimicrobial Activity of Purine Derived SAH/MTA Nucleosidase Inhibitors. *Bioorg. Med. Chem. Lett.* **2004**, *14* (12), 3165–3168.

(169) Lee, J. E.; Singh, V.; Evans, G. B.; Tyler, P. C.; Furneaux, R. H.; Cornell, K. A.; Riscoe, M. K.; Schramm, V. L.; Howell, P. L. Structural Rationale for the Affinity of Pico- and Femtomolar Transition State Analogues of Escherichia Coli 5′-Methylthioadenosine/S-Adenosylhomocysteine Nucleosidase. *J. Biol. Chem.* **2005**, *280* (18), 18274–18282.

(170) Gutierrez, J. A.; Luo, M.; Singh, V.; Li, L.; Brown, R. L.; Norris, G. E.; Evans, G. B.; Furneaux, R. H.; Tyler, P. C.; Painter, G. F.; et al. Picomolar Inhibitors as Transition-State Probes of 5′-Methylthioadenosine Nucleosidases. *ACS Chem. Biol.* **2007**, *2* (11), 725–734.

(171) Winzer, K.; Hardie, K. R.; Williams, P. LuxS and Autoinducer-2: Their Contribution to Quorum Sensing and Metabolism in Bacteria. *Adv. Appl. Microbiol.* **2003**, *53*, 291–396.

(172) Vendeville, A.; Winzer, K.; Heurlier, K.; Tang, C. M.; Hardie, K. R. Making "sense" of Metabolism: Autoinducer-2, LuxS and Pathogenic Bacteria. *Nat. Rev. Microbiol.* **2005**, *3* (5), 383–396.

(173) Alfaro, J. F.; Zhang, T.; Wynn, D. P.; Karschner, E. L.; Zhou, Z. S. Synthesis of LuxS Inhibitors Targeting Bacterial Cell−Cell Communication. *Org. Lett.* **2004**, *6* (18), 3043–3046.

(174) Wnuk, S. F.; Robert, J.; Sobczak, A. J.; Meyers, B. P.; Malladi, V. L. A.; Zhu, J.; Gopishetty, B.; Pei, D. Inhibition of S-Ribosylhomocysteinase (LuxS) by Substrate Analogues Modified at the Ribosyl C-3 Position. *Bioorg. Med. Chem.* **2009**, *17* (18), 6699–6706.

(175) Malladi, V. L. A.; Sobczak, A. J.; Meyer, T. M.; Pei, D.; Wnuk, S. F. Inhibition of LuxS by S-Ribosylhomocysteine Analogues Containing a [4-Aza]Ribose Ring. *Bioorg. Med. Chem.* **2011**, *19* (18), 5507–5519.

(176) Leadbetter, J. R.; Greenberg, E. P. Metabolism of Acyl-Homoserine Lactone Quorum-Sensing Signals by Variovorax Paradoxus. *J. Bacteriol.* **2000**, *182* (24), 6921–6926.

(177) Lin, Y.-H.; Xu, J.-L.; Hu, J.; Wang, L.-H.; Ong, S. L.; Leadbetter, J. R.; Zhang, L.-H. Acyl-Homoserine Lactone Acylase from Ralstonia Strain XJ12B Represents a Novel and Potent Class of Quorum-Quenching Enzymes. *Mol. Microbiol.* **2003**, *47* (3), 849–860.

(178) Bokhove, M.; Nadal Jimenez, P.; Quax, W. J.; Dijkstra, B. W. The Quorum-Quenching N-Acyl Homoserine Lactone Acylase PvdQ Is an Ntn-Hydrolase with an Unusual Substrate-Binding Pocket. *Proc. Natl. Acad. Sci. U. S. A.* **2010**, *107* (2), 686–691.

(179) Dong, Y.-H.; Xu, J.-L.; Li, X.-Z.; Zhang, L.-H. AiiA, an Enzyme That Inactivates the Acylhomoserine Lactone Quorum-Sensing Signal and Attenuates the Virulence of Erwinia Carotovora. *Proc. Natl. Acad. Sci.* **2000**, *97* (7), 3526–3531.

(180) Yates, E. A.; Philipp, B.; Buckley, C.; Atkinson, S.; Chhabra, S. R.; Sockett, R. E.; Goldner, M.; Dessaux, Y.; Cámara, M.; Smith, H.; et al. N-Acylhomoserine Lactones Undergo Lactonolysis in a PH-, Temperature-, and Acyl Chain Length-Dependent Manner during Growth of Yersinia Pseudotuberculosis and Pseudomonas Aeruginosa. *Infect. Immun.* **2002**, *70* (10), 5635–5646.

(181) Liu, D.; Momb, J.; Thomas, P. W.; Moulin, A.; Petsko, G. A.; Fast, W.; Ringe, D. Mechanism of the Quorum-Quenching Lactonase (AiiA) from Bacillus Thuringiensis. 1. Product-Bound Structures. *Biochemistry* **2008**, *47* (29), 7706–7714.

(182) Uroz, S.; Chhabra, S. R.; Cámara, M.; Williams, P.; Oger, P.; Dessaux, Y. N-Acylhomoserine Lactone Quorum-Sensing Molecules Are Modified and Degraded by Rhodococcus Erythropolis W2 by Both Amidolytic and Novel Oxidoreductase Activities. *Microbiol. Read. Engl.* **2005**, *151* (Pt 10), 3313–3322.

(183) Chowdhary, P. K.; Keshavan, N.; Nguyen, H. Q.; Peterson, J. A.; González, J. E.; Haines, D. C. Bacillus Megaterium CYP102A1 Oxidation of Acyl Homoserine Lactones and Acyl Homoserines. *Biochemistry* **2007**, *46* (50), 14429–14437.

(184) Bijtenhoorn, P.; Mayerhofer, H.; Müller-Dieckmann, J.; Utpatel, C.; Schipper, C.; Hornung, C.; Szesny, M.; Grond, S.; Thürmer, A.; Brzuszkiewicz, E.; et al. A Novel Metagenomic Short-Chain Dehydrogenase/Reductase Attenuates Pseudomonas Aeruginosa Biofilm Formation and Virulence on Caenorhabditis Elegans. *PloS One* **2011**, *6* (10), e26278.

(185) McInnis, C. E.; Blackwell, H. E. Thiolactone Modulators of Quorum Sensing Revealed through Library Design and Screening. *Bioorg. Med. Chem.* **2011**, *19* (16), 4820–4828.

(186) Brackman, G.; Risseeuw, M.; Celen, S.; Cos, P.; Maes, L.; Nelis, H. J.; Van Calenbergh, S.; Coenye, T. Synthesis and Evaluation of the Quorum Sensing Inhibitory Effect of Substituted Triazolyldihydrofuranones. *Bioorg. Med. Chem.* **2012**, *20* (15), 4737–4743.

(187) Frezza, M.; Castang, S.; Estephane, J.; Soulère, L.; Deshayes, C.; Chantegrel, B.; Nasser, W.; Queneau, Y.; Reverchon, S.; Doutheau, A. Synthesis and Biological Evaluation of Homoserine Lactone Derived Ureas as Antagonists of Bacterial Quorum Sensing. *Bioorg. Med. Chem.* **2006**, *14* (14), 4781–4791.

(188) Vannini, A.; Volpari, C.; Gargioli, C.; Muraglia, E.; Cortese, R.; De Francesco, R.; Neddermann, P.; Marco, S. D. The Crystal Structure of the Quorum Sensing Protein TraR Bound to Its Autoinducer and Target DNA. *EMBO J.* **2002**, *21* (17), 4393–4401.

(189) Zhang, R.; Pappas, K. M.; Pappas, T.; Brace, J. L.; Miller, P. C.; Oulmassov, T.; Molyneaux, J. M.; Anderson, J. C.; Bashkin, J. K.; Winans, S. C.; et al. Structure of a Bacterial Quorum-Sensing Transcription Factor Complexed with Pheromone and DNA. *Nature* **2002**, *417* (6892), 971–974.

(190) Yao, Y.; Martinez-Yamout, M. A.; Dickerson, T. J.; Brogan, A. P.; Wright, P. E.; Dyson, H. J. Structure of the Escherichia Coli Quorum Sensing Protein SdiA: Activation of the Folding Switch by Acyl Homoserine Lactones. *J. Mol. Biol.* **2006**, *355* (2), 262–273.

(191) Bottomley, M. J.; Muraglia, E.; Bazzo, R.; Carfì, A. Molecular Insights into Quorum Sensing in the Human Pathogen Pseudomonas Aeruginosa from the Structure of the Virulence Regulator LasR Bound to Its Autoinducer. *J. Biol. Chem.* **2007**, *282* (18), 13592–13600.

(192) Zou, Y.; Nair, S. K. Molecular Basis for the Recognition of Structurally Distinct Autoinducer Mimics by the Pseudomonas Aeruginosa LasR Quorum-Sensing Signaling Receptor. *Chem. Biol.* **2009**, *16* (9), 961–970.

(193) Thoendel, M.; Kavanaugh, J. S.; Flack, C. E.; Horswill, A. R. Peptide Signaling in the Staphylococci. *Chem. Rev.* **2011**, *111* (1), 117–151.

(194) Mayville, P.; Ji, G.; Beavis, R.; Yang, H.; Goger, M.; Novick, R. P.; Muir, T. W. Structure-Activity Analysis of Synthetic Autoinducing Thiolactone Peptides from Staphylococcus Aureus Responsible for Virulence. *Proc. Natl. Acad. Sci. U. S. A.* **1999**, *96* (4), 1218–1223.

(195) MDowell, P.; Affas, Z.; Reynolds, C.; Holden, M. T.; Wood, S. J.; Saint, S.; Cockayne, A.; Hill, P. J.; Dodd, C. E.; Bycroft, B. W.; et al. Structure, Activity and Evolution of the Group I Thiolactone Peptide Quorum-Sensing System of Staphylococcus Aureus. *Mol. Microbiol.* **2001**, *41* (2), 503–512.

(196) Lyon, G. J.; Wright, J. S.; Muir, T. W.; Novick, R. P. Key Determinants of Receptor Activation in the Agr Autoinducing Peptides of Staphylococcus Aureus. *Biochemistry* **2002**, *41* (31), 10095–10104.

(197) Fowler, S. A.; Stacy, D. M.; Blackwell, H. E. Design and Synthesis of Macrocyclic Peptomers as Mimics of a Quorum Sensing Signal from Staphylococcus Aureus. *Org. Lett.* **2008**, *10* (12), 2329–2332.

(198) Ni, N.; Choudhary, G.; Li, M.; Wang, B. Pyrogallol and Its Analogs Can Antagonize Bacterial Quorum Sensing in Vibrio Harveyi. *Bioorg. Med. Chem. Lett.* **2008**, *18* (5), 1567–1572.

(199) Ha, J.-H.; Hauk, P.; Cho, K.; Eo, Y.; Ma, X.; Stephens, K.; Cha, S.; Jeong, M.; Suh, J.-Y.; Sintim, H. O.; et al. Evidence of Link between Quorum Sensing and Sugar Metabolism in Escherichia Coli Revealed via Cocrystal Structures of LsrK and HPr. *Sci. Adv.* **2018**, *4* (6), eaar7063.

(200) Gray, N. S.; Wodicka, L.; Thunnissen, A.-M. W. H.; Norman, T. C.; Kwon, S.; Espinoza, F. H.; Morgan, D. O.; Barnes, G.; LeClerc, S.; Meijer, L.; et al. Exploiting Chemical Libraries, Structure, and Genomics in the Search for Kinase Inhibitors. *Science* **1998**, *281* (5376), 533–538.

(201) Cohen, P. Protein Kinases — the Major Drug Targets of the Twenty-First Century? *Nat. Rev. Drug Discov.* **2002**, *1* (4), 309–315.

(202) Manning, G.; Whyte, D. B.; Martinez, R.; Hunter, T.; Sudarsanam, S. The Protein Kinase Complement of the Human Genome. *Science* **2002**, *298* (5600), 1912–1934.

(203) Weinmann, H.; Metternich, R. Editorial: Drug Discovery Process for Kinease Inhibitors. *ChemBioChem 6* (3), 455–459.

(204) Noble, M. E. M.; Endicott, J. A.; Johnson, L. N. Protein Kinase Inhibitors: Insights into Drug Design from Structure. *Science* **2004**, *303* (5665), 1800–1805.

(205) Altman, A.; Kong, K.-F. Protein Kinase C Inhibitors for Immune Disorders. *Drug Discov. Today* **2014**, *19* (8), 1217–1221.

(206) Doles, J. D.; Olwin, B. B. The Impact of JAK-STAT Signaling on Muscle Regeneration. *Nat. Med.* **2014**, *20* (10), 1094–1095.

(207) Lee, B. Y.; Timpson, P.; Horvath, L. G.; Daly, R. J. FAK Signaling in Human Cancer as a Target for Therapeutics. *Pharmacol. Ther.* **2015**, *146*, 132–149.

(208) Kurosu, M.; Begari, E. Bacterial Protein Kinase Inhibitors. *Drug Dev. Res. 71* (3), 168–187.

(209) Xing, L.; Klug-Mcleod, J.; Rai, B.; Lunney, E. A. Kinase Hinge Binding Scaffolds and Their Hydrogen Bond Patterns. *Bioorg. Med. Chem.* **2015**, *23* (19), 6520–6527.

(210) Mondal, J.; Tiwary, P.; Berne, B. J. How a Kinase Inhibitor Withstands Gatekeeper Residue Mutations. *J. Am. Chem. Soc.* **2016**, *138* (13), 4608–4615.

(211) Zuccotto, F.; Ardini, E.; Casale, E.; Angiolini, M. Through the "Gatekeeper Door": Exploiting the Active Kinase Conformation. *J. Med. Chem.* **2010**, *53* (7), 2681–2694.

(212) Treiber, D. K.; Shah, N. P. Ins and Outs of Kinase DFG Motifs. *Chem. Biol.* **2013**, *20* (6), 745–746.

(213) Kinase Inhibitors | Cambridge MedChem Consulting https://www.cambridgemedchemconsulting.com/resources/hit_identification/focus/kinaseinhib.html.

(214) Tong, M.; Seeliger, M. A. Targeting Conformational Plasticity of Protein Kinases. *ACS Chem. Biol.* **2015**, *10* (1), 190–200.

(215) Davies, S. P.; Reddy, H.; Caivano, M.; Cohen, P. Specificity and Mechanism of Action of Some Commonly Used Protein Kinase Inhibitors. *Biochem. J.* **2000**, *351* (1), 95–105.

(216) Liao, J. J.-L. Molecular Recognition of Protein Kinase Binding Pockets for Design of Potent and Selective Kinase Inhibitors. *J. Med. Chem.* **2007**, *50* (3), 409–424.

(217) Norman, R. A.; Toader, D.; Ferguson, A. D. Structural Approaches to Obtain Kinase Selectivity. *Trends Pharmacol. Sci.* **2012**, *33* (5), 273–278.

(218) Rettenmaier, T. J.; Sadowsky, J. D.; Thomsen, N. D.; Chen, S. C.; Doak, A. K.; Arkin, M. R.; Wells, J. A. A Small-Molecule Mimic of a Peptide Docking Motif Inhibits the Protein Kinase PDK1. *Proc. Natl. Acad. Sci. U. S. A.* **2014**, *111* (52), 18590–18595.

(219) YASARA - Yet Another Scientific Artificial Reality Application http://yasara.org/.

(220) National Center for Biotechnology Information https://www.ncbi.nlm.nih.gov.

(221) Zhang, Y.; Zagnitko, O.; Rodionova, I.; Osterman, A.; Godzik, A. The FGGY Carbohydrate Kinase Family: Insights into the Evolution of Functional Specificities. *PLoS Comput Biol* **2011**, *7* (12), e1002318.

(222) Xavier, K. B.; Miller, S. T.; Lu, W.; Kim, J. H.; Rabinowitz, J.; Pelczer, I.; Semmelhack, M. F.; Bassler, B. L. Phosphorylation and Processing of the Quorum-Sensing Molecule Autoinducer-2 in Enteric Bacteria. *ACS Chem. Biol.* **2007**, *2* (2), 128–136.

(223) Xavier, K. B.; Bassler, B. L. Regulation of Uptake and Processing of the Quorum-Sensing Autoinducer AI-2 in Escherichia Coli. *J. Bacteriol.* **2005**, *187* (1), 238–248.

(224) Roy, V.; Fernandes, R.; Tsao, C.-Y.; Bentley, W. E. Cross Species Quorum Quenching Using a Native AI-2 Processing Enzyme. *ACS Chem. Biol.* **2010**, *5* (2), 223–232.

(225) Zhang, Z., Burley, S.K., Swaminathan, S. The Crystal Structure of Xylulose Kinase from Rhodospirillum Rubrum.

(226) Minasov, G., Skarina, T., Onopriyenko, O., Savchenko, A., Anderson, W.F. 1.9 Angstrom Crystal Structure of Glycerol Kinase (GlpK) from Staphylococcus Aureus in Complex with Glycerol.

(227) Feese, M. D.; Faber, H. R.; Bystrom, C. E.; Pettigrew, D. W.; Remington, S. J. Glycerol Kinase from Escherichia Coli and an Ala65-->Thr Mutant: The Crystal Structures Reveal Conformational Changes with Implications for Allosteric Regulation. *Structure* **1998**, *6*, 1407–1418.

(228) Grueninger, D.; Schulz, G. E. Substrate Spectrum of L-Rhamnulose Kinase Related to Models Derived from Two Ternary Complex Structures. *FEBS Lett.* **2007**, *581* (16), 3127–3130.

(229) INTEGRATE ETN Project http://www.integrate.fi/home/integrate-etn-project.

(230) Zhu, J.; Hixon, M. S.; Globisch, D.; Kaufmann, G. F.; Janda, K. D. Mechanistic Insights into the LsrK Kinase Required for Autoinducer-2 Quorum Sensing Activation. *J. Am. Chem. Soc.* **2013**, *135* (21), 7827–7830.

(231) Meijler, M. M.; Hom, L. G.; Kaufmann, G. F.; McKenzie, K. M.; Sun, C.; Moss, J. A.; Matsushita, M.; Janda, K. D. Synthesis and Biological Validation of a Ubiquitous Quorum-Sensing Molecule. *Angew. Chem. Int. Ed.* **2004**, *43* (16), 2106–2108.

(232) Semmelhack, M. F.; Campagna, S. R.; Federle, M. J.; Bassler, B. L. An Expeditious Synthesis of DPD and Boron Binding Studies. *Org. Lett.* **2005**, *7* (4), 569–572.

(233) Globisch, D.; Lowery, C. A.; McCague, K. C.; Janda, K. D. Uncharacterized 4,5-Dihydroxy-2,3-Pentanedione (DPD) Molecules Revealed Through NMR Spectroscopy: Implications for a Greater Signaling Diversity in Bacterial Species. *Angew. Chem. Int. Ed.* **2012**, *51* (17), 4204–4208.

(234) Kaufmann, G. F.; Sartorio, R.; Lee, S.-H.; Rogers, C. J.; Meijler, M. M.; Moss, J. A.; Clapham, B.; Brogan, A. P.; Dickerson, T. J.; Janda, K. D. Revisiting Quorum Sensing: Discovery of Additional Chemical and Biological Functions for 3-Oxo-N-Acylhomoserine Lactones. *Proc. Natl. Acad. Sci.* **2005**, *102* (2), 309–314.

(235) Horswill, A. R.; Stoodley, P.; Stewart, P. S.; Parsek, M. R. The Effect of the Chemical, Biological, and Physical Environment on Quorum Sensing in Structured Microbial Communities. *Anal. Bioanal. Chem.* **2007**, *387* (2), 371–380.

(236) Park, J.; Jagasia, R.; Kaufmann, G. F.; Mathison, J. C.; Ruiz, D. I.; Moss, J. A.; Meijler, M. M.; Ulevitch, R. J.; Janda, K. D. Infection Control by Antibody Disruption of Bacterial Quorum Sensing Signaling. *Chem. Biol.* **2007**, *14* (10), 1119–1127.

(237) Semmelhack, M. F.; Campagna, S. R.; Hwa, C.; Federle, M. J.; Bassler, B. L. Boron Binding with the Quorum Sensing Signal AI-2 and Analogues. *Org. Lett.* **2004**, *6* (15), 2635–2637.

(238) Chang, J.; Warren, T. K.; Zhao, X.; Gill, T.; Guo, F.; Wang, L.; Comunale, M. A.; Du, Y.; Alonzi, D. S.; Yu, W.; et al. Small Molecule Inhibitors of ER α-Glucosidases Are Active against Multiple Hemorrhagic Fever Viruses. *Antiviral Res.* **2013**, *98* (3), 432–440.

(239) DeKeersmaecker, S. C. J.; Vanderleyden, J. Constraints on Detection of Autoinducer-2 (AI-2) Signalling Molecules Using Vibrio Harveyi as a Reporter. *Microbiol. Read. Engl.* **2003**, *149* (Pt 8), 1953–1956.

(240) Turovskiy, Y.; Chikindas, M. L. Autoinducer-2 Bioassay Is a Qualitative, Not Quantitative Method Influenced by Glucose. *J. Microbiol. Methods* **2006**, *66* (3), 497–503.

(241) Vilchez, R.; Lemme, A.; Thiel, V.; Schulz, S.; Sztajer, H.; Wagner-Döbler, I. Analysing Traces of Autoinducer-2 Requires Standardization of the Vibrio Harveyi Bioassay. *Anal. Bioanal. Chem.* **2007**, *387* (2), 489–496.

(242) Rajamani, S.; Zhu, J.; Pei, D.; Sayre, R. A LuxP-FRET-Based Reporter for the Detection and Quantification of AI-2 Bacterial Quorum-Sensing Signal Compounds. *Biochemistry* **2007**, *46* (13), 3990–3997.

(243) Zhu, J.; Pei, D. A LuxP-Based Fluorescent Sensor for Bacterial Autoinducer II. *ACS Chem. Biol.* **2008**, *3* (2), 110–119.

(244) Thiel, V.; Vilchez, R.; Sztajer, H.; Wagner-Döbler, I.; Schulz, S. Identification, Quantification, and Determination of the Absolute Configuration of the Bacterial Quorum-Sensing Signal Autoinducer-2 by Gas Chromatography–Mass Spectrometry. *ChemBioChem* **2009**, *10* (3), 479–485.

(245) Campagna, S. R.; Gooding, J. R.; May, A. L. Direct Quantitation of the Quorum Sensing Signal, Autoinducer-2, in Clinically Relevant Samples by Liquid Chromatography-Tandem Mass Spectrometry. *Anal. Chem.* **2009**, *81* (15), 6374–6381.

(246) Zibuck, R.; Seebach, D. Note on the Preparation of 1,2-Diketones from Acetylenes. *Helv. Chim. Acta* **1988**, *71* (1), 237–240.

(247) Frezza, M.; Soulère, L.; Queneau, Y.; Doutheau, A. A Baylis–Hillman/Ozonolysis Route towards (±) 4,5-Dihydroxy-2,3-Pentanedione (DPD) and Analogues. *Tetrahedron Lett.* **2005**, *46* (38), 6495–6498.

(248) De Keersmaecker, S. C. J.; Varszegi, C.; van Boxel, N.; Habel, L. W.; Metzger, K.; Daniels, R.; Marchal, K.; De Vos, D.; Vanderleyden, J. Chemical Synthesis of (S)-4,5-Dihydroxy-2,3-Pentanedione, a Bacterial Signal Molecule Precursor, and Validation of Its Activity in Salmonella Typhimurium. *J. Biol. Chem.* **2005**, *280* (20), 19563–19568.

(249) Lowery, C. A.; Park, J.; Kaufmann, G. F.; Janda, K. D. An Unexpected Switch in the Modulation of AI-2-Based Quorum Sensing Discovered through Synthetic 4,5-Dihydroxy-2,3-Pentanedione Analogues. *J. Am. Chem. Soc.* **2008**, *130* (29), 9200–9201.

(250) Smith, J. A. I.; Wang, J.; Nguyen-Mau, S.-M.; Lee, V.; Sintim, H. O. Biological Screening of a Diverse Set of AI-2 Analogues in Vibrio Harveyi Suggests That Receptors Which Are Involved in Synergistic Agonism of AI-2 and Analogues Are Promiscuous. *Chem. Commun. Camb. Engl.* **2009**, No. 45, 7033–7035.

(251) Kadirvel, M.; Stimpson, W. T.; Moumene-Afifi, S.; Arsic, B.; Glynn, N.; Halliday, N.; Williams, P.; Gilbert, P.; McBain, A. J.; Freeman, S.; et al. Synthesis and Bioluminescence-Inducing Properties of

Autoinducer (S)-4,5-Dihydroxypentane-2,3-Dione and Its Enantiomer. *Bioorg. Med. Chem. Lett.* **2010**, *20* (8), 2625–2628.

(252) Ascenso, O. S.; Marques, J. C.; Santos, A. R.; Xavier, K. B.; Rita Ventura, M.; Maycock, C. D. An Efficient Synthesis of the Precursor of AI-2, the Signalling Molecule for Inter-Species Quorum Sensing. *Bioorg. Med. Chem.* **2011**, *19* (3), 1236–1241.

(253) Stotani, S.; Gatta, V.; Medda, F.; Padmanaban, M.; Karawajczyk, A.; Tammela, P.; Giordanetto, F.; Tzalis, D.; Collina, S.; Stotani, S.; et al. A Versatile Strategy for the Synthesis of 4,5-Dihydroxy-2,3-Pentanedione (DPD) and Related Compounds as Potential Modulators of Bacterial Quorum Sensing. *Molecules* **2018**, *23* (10), 2545.

(254) Winzer, K.; Hardie, K. R.; Burgess, N.; Doherty, N.; Kirke, D.; Holden, M. T. G.; Linforth, R.; Cornell, K. A.; Taylor, A. J.; Hill, P. J.; et al. LuxS: Its Role in Central Metabolism and the in Vitro Synthesis of 4-Hydroxy-5-Methyl-3(2H)-Furanone. *Microbiol. Read. Engl.* **2002**, *148* (Pt 4), 909–922.

(255) Lowery, C. A.; McKenzie, K. M.; Qi, L.; Meijler, M. M.; Janda, K. D. Quorum Sensing in Vibrio Harveyi: Probing the Specificity of the LuxP Binding Site. *Bioorg. Med. Chem. Lett.* **2005**, *15* (9), 2395–2398.

(256) Chen, X.; Schauder, S.; Potier, N.; Van Dorsselaer, A.; Pelczer, I.; Bassler, B. L.; Hughson, F. M. Structural Identification of a Bacterial Quorum-Sensing Signal Containing Boron. *Nature* **2002**, *415* (6871), 545–549.

(257) Semmelhack, M. F.; Campagna, S. R.; Hwa, C.; Federle, M. J.; Bassler, B. L. Boron Binding with the Quorum Sensing Signal AI-2 and Analogues. *Org. Lett.* **2004**, *6* (15), 2635–2637.

(258) Ganin, H.; Tang, X.; Meijler, M. M. Inhibition of Pseudomonas Aeruginosa Quorum Sensing by AI-2 Analogs. *Bioorg. Med. Chem. Lett.* **2009**, *19* (14), 3941–3944.

(259) Shintani, R.; Duan, W.-L.; Park, S.; Hayashi, T. Rhodium-Catalyzed Isomerization of Unactivated Alkynes to 1,3-Dienes. *Chem. Commun.* **2006**, *0* (34), 3646–3647.

(260) Mandabi, A.; Ganin, H.; Meijler, M. M. Synergistic Activation of Quorum Sensing in Vibrio Harveyi. *Bioorg. Med. Chem. Lett.* **2015**, *25* (18), 3966–3969.

(261) Smith, J. A. I.; Wang, J.; Nguyen-Mau, S.-M.; Lee, V.; Sintim, H. O. Biological Screening of a Diverse Set of AI-2 Analogues in Vibrio Harveyi Suggests That Receptors Which Are Involved in Synergistic Agonism of AI-2 and Analogues Are Promiscuous. *Chem. Commun.* **2009**, No. 45, 7033.

(262) Roy, V.; Smith, J. A. I.; Wang, J.; Stewart, J. E.; Bentley, W. E.; Sintim, H. O. Synthetic Analogs Tailor Native AI-2 Signaling across Bacterial Species. *J. Am. Chem. Soc.* **2010**, *132* (32), 11141–11150.

(263) Gamby, S.; Roy, V.; Guo, M.; Smith, J. A. I.; Wang, J.; Stewart, J. E.; Wang, X.; Bentley, W. E.; Sintim, H. O. Altering the Communication Networks of Multispecies Microbial Systems Using a Diverse Toolbox of AI-2 Analogues. *ACS Chem. Biol.* **2012**, *7* (6), 1023–1030.

(264) Ho, G.-J.; Mathre, D. J. Lithium-Initiated Imide Formation. A Simple Method for N-Acylation of 2-Oxazolidinones and Bornane-2,10-Sultam. *J. Org. Chem.* **1995**, *60* (7), 2271–2273.

(265) Frezza, M.; Balestrino, D.; Soulère, L.; Reverchon, S.; Queneau, Y.; Forestier, C.; Doutheau, A. Synthesis and Biological Evaluation of the Trifluoromethyl Analog of (4S)-4,5-Dihydroxy-2,3-Pentanedione (DPD). *Eur. J. Org. Chem.* **2006**, *2006* (20), 4731–4736.

(266) Guo, M.; Zheng, Y.; Terell, J. L.; Ad, M.; Opoku-Temeng, C.; Bentley, W. E.; Sintim, H. O. Geminal Dihalogen Isosteric Replacement in Hydrated AI-2 Affords Potent Quorum Sensing Modulators. *Chem. Commun.* **2015**, *51* (13), 2617–2620.

(267) Roy, V.; Smith, J. A. I.; Wang, J.; Stewart, J. E.; Bentley, W. E.; Sintim, H. O. Synthetic Analogs Tailor Native AI-2 Signaling across Bacterial Species. *J. Am. Chem. Soc.* **2010**, *132* (32), 11141–11150.

(268) Kadirvel, M.; Fanimarvasti, F.; Forbes, S.; McBain, A.; Gardiner, J. M.; Brown, G. D.; Freeman, S. Inhibition of Quorum Sensing and Biofilm Formation in Vibrio Harveyi by 4-Fluoro-DPD; a Novel Potent Inhibitor of Signalling. *Chem. Commun. Camb. Engl.* **2014**, *50* (39), 5000–5002.

(269) Tsuchikama, K.; Zhu, J.; Lowery, C. A.; Kaufmann, G. F.; Janda, K. D. C4-Alkoxy-HPD: A Potent Class of Synthetic Modulators Surpassing Nature in AI-2 Quorum Sensing. *J. Am. Chem. Soc.* **2012**, *134* (33), 13562–13564.

(270) Mohamed, Y. A. M.; Inagaki, F.; Takahashi, R.; Mukai, C. A New Procedure for the Preparation of 2-Vinylindoles and Their [4+2] Cycloaddition Reaction. *Tetrahedron* **2011**, *67* (29), 5133–5141.

(271) Frezza, M.; Soulère, L.; Balestrino, D.; Gohar, M.; Deshayes, C.; Queneau, Y.; Forestier, C.; Doutheau, A. Ac2-DPD, the Bis-(O)-Acetylated Derivative of 4,5-Dihydroxy-2,3-Pentanedione (DPD) Is a Convenient Stable Precursor of Bacterial Quorum Sensing Autoinducer AI-2. *Bioorg. Med. Chem. Lett.* **2007**, *17* (5), 1428–1431.

(272) Guo, M.; Gamby, S.; Nakayama, S.; Smith, J.; Sintim, H. O. A Pro-Drug Approach for Selective Modulation of AI-2-Mediated Bacterial Cell-to-Cell Communication. *Sensors* **2012**, *12* (12), 3762–3772.

(273) Rui, F.; Marques, J. C.; Miller, S. T.; Maycock, C. D.; Xavier, K. B.; Ventura, M. R. Stereochemical Diversity of AI-2 Analogs Modulates Quorum Sensing in Vibrio Harveyi and Escherichia Coli. *Bioorg. Med. Chem.* **2012**, *20* (1), 249–256.

(274) Collins, K. C.; Tsuchikama, K.; Lowery, C. A.; Zhu, J.; Janda, K. D. Dissecting AI-2-Mediated Quorum Sensing through C5-Analogue Synthesis and Biochemical Analysis. *Tetrahedron* **2015**, *72* (25), 3593–3598.

(275) Tsuchikama, K.; Lowery, C. A.; Janda, K. D. Probing Autoinducer-2 Based Quorum Sensing: The Biological Consequences of Molecules Unable To Traverse Equilibrium States. *J. Org. Chem.* **2011**, *76* (17), 6981–6989.

(276) 1,1-, 1,2-, and 1,4-Eliminations from the Corresponding Dihalogenated Compounds Using Bu3SnSiMe3-F−. *Tetrahedron* **1996**, *52* (24), 8143–8158.

(277) Frezza, M.; Balestrino, D.; Soulère, L.; Reverchon, S.; Queneau, Y.; Forestier, C.; Doutheau, A. Synthesis and Biological Evaluation of the Trifluoromethyl Analog of (4S)-4,5-Dihydroxy-2,3-Pentanedione (DPD). *Eur. J. Org. Chem.* **2006**, *2006* (20), 4731–4736.

(278) Phosphorylated and Branched Dihydroxy-Pentane-Dione (DPD) Analogs as Quorum Sensing Inhibitors in Bacteria.

(279) Guo, M.; Zheng, Y.; Terell, J. L.; Ad, M.; Opoku-Temeng, C.; Bentley, W. E.; Sintim, H. O. Geminal Dihalogen Isosteric Replacement in Hydrated AI-2 Affords Potent Quorum Sensing Modulators. *Chem. Commun. Camb. Engl.* **2015**, *51* (13), 2617–2620.

(280) Tsuchikama, K.; Zhu, J.; Lowery, C. A.; Kaufmann, G. F.; Janda, K. D. C4-Alkoxy-HPD: A Potent Class of Synthetic Modulators Surpassing Nature in AI-2 Quorum Sensing. *J. Am. Chem. Soc.* **2012**, *134* (33), 13562–13564.

(281) Peyton, L. R.; Gallagher, S.; Hashemzadeh, M. Triazole Antifungals: A Review. *Drugs Today Barc. Spain 1998* **2015**, *51* (12), 705–718.

(282) Kartsev, V. G. NATURAL COMPOUNDS IN DRUG DISCOVERY. BIOLOGICAL ACTIVITY AND NEW TRENDS IN THE CHEMISTRY OF ISOQUINOLINE ALKALOIDS. *Med. Chem. Res.* **2004**, *13* (6–7), 325–336.

(283) Galán, A.; Moreno, L.; Párraga, J.; Serrano, Á.; Sanz, M. J.; Cortes, D.; Cabedo, N. Novel Isoquinoline Derivatives as Antimicrobial Agents. *Bioorg. Med. Chem.* **2013**, *21* (11), 3221–3230.

(284) Iranshahy, M.; Quinn, R. J.; Iranshahi, M. Biologically Active Isoquinoline Alkaloids with Drug-like Properties from the Genus Corydalis. *RSC Adv.* **2014**, *4* (31), 15900–15913.

(285) Dembitsky, V. M.; Gloriozova, T. A.; Poroikov, V. V. Naturally Occurring Plant Isoquinoline N-Oxide Alkaloids: Their Pharmacological and SAR Activities. *Phytomedicine* **2015**, *22* (1), 183–202.

(286) Altaf, A. A.; Shahzad, A.; Gul, Z.; Rasool, N.; Badshah, A.; Lal, B.; Khan, E. A Review on the Medicinal Importance of Pyridine Derivatives. *J. Drug Des. Med. Chem.* **2015**, *1* (1), 1.

(287) Renuka, S.; Kota, R. K. Medicinal and Biological Significance of Isoxazole A Highly Important Scaffold for Drug Discovery. *Asian J. Res. Chem.* **2011**, *4* (7), 1038–1042.

(288) Selvam, T. P.; James, C. R.; Dniandev, P. V.; Valzita, S. K. A Mini Review of Pyrimidine and Fused Pyrimidine Marketed Drugs. *Res. Pharm.* **2012**, *2* (4).

(289) Yerragunta, V.; Patil, P.; Anusha, V.; KumaraSwamy, T.; Suman, D.; Samhitha, T. Pyrimidine and Its Biological Activity: A Review. *PharmaTutor* **2013**, *1* (2), 39–44.

(290) Naim, M. J.; Alam, O.; Nawaz, F.; Alam, M. J.; Alam, P. Current Status of Pyrazole and Its Biological Activities. *J. Pharm. Bioallied Sci.* **2016**, *8* (1), 2–17.

(291) Faria, J. V.; Vegi, P. F.; Miguita, A. G. C.; dos Santos, M. S.; Boechat, N.; Bernardino, A. M. R. Recently Reported Biological Activities of Pyrazole Compounds. *Bioorg. Med. Chem.* **2017**, *25* (21), 5891–5903.

(292) Paterson, I.; Delgado, O.; Florence, G. J.; Lyothier, I.; O'Brien, M.; Scott, J. P.; Sereinig, N. A Second-Generation Total Synthesis of (+)-Discodermolide: The Development of a Practical Route Using Solely Substrate-Based Stereocontrol. *J. Org. Chem.* **2005**, *70* (1), 150–160.

(293) Rostovtsev Vsevolod V.; Green Luke G.; Fokin Valery V.; Sharpless K. Barry. A Stepwise Huisgen Cycloaddition Process: Copper(I)-Catalyzed Regioselective "Ligation" of Azides and Terminal Alkynes. *Angew. Chem. Int. Ed.* **2002**, *41* (14), 2596–2599.

(294) Rodionov Valentin O.; Fokin Valery V.; Finn M. G. Mechanism of the Ligand-Free CuI-Catalyzed Azide–Alkyne Cycloaddition Reaction. *Angew. Chem. Int. Ed.* **2005**, *44* (15), 2210–2215.

(295) Rodionov, V. O.; Presolski, S. I.; Díaz Díaz, D.; Fokin, V. V.; Finn, M. G. Ligand-Accelerated Cu-Catalyzed Azide−Alkyne Cycloaddition: A Mechanistic Report. *J. Am. Chem. Soc.* **2007**, *129* (42), 12705–12712.

(296) Worrell, B. T.; Malik, J. A.; Fokin, V. V. Direct Evidence of a Dinuclear Copper Intermediate in Cu(I)-Catalyzed Azide-Alkyne Cycloadditions. *Science* **2013**, *340* (6131), 457–460.

(297) Iacobucci Claudio; Reale Samantha; Gal Jean-François; De Angelis Francesco. Dinuclear Copper Intermediates in Copper(I)-Catalyzed Azide–Alkyne Cycloaddition Directly Observed by Electrospray Ionization Mass Spectrometry. *Angew. Chem. Int. Ed.* **2015**, *54* (10), 3065–3068.

(298) Jin, L.; Tolentino, D. R.; Melaimi, M.; Bertrand, G. Isolation of Bis(Copper) Key Intermediates in Cu-Catalyzed Azide-Alkyne "Click Reaction." *Sci. Adv.* **2015**, *1* (5), e1500304.

(299) Özkılıç, Y.; Tüzün, N. Ş. A DFT Study on the Binuclear CuAAC Reaction: Mechanism in Light of New Experiments. *Organometallics* **2016**, *35* (16), 2589–2599.

(300) MacDonald, J. P.; Badillo, J. J.; Arevalo, G. E.; Silva-García, A.; Franz, A. K. Catalytic Stereoselective Synthesis of Diverse Oxindoles and Spirooxindoles from Isatins. *ACS Comb. Sci.* **2012**, *14* (4), 285–293.

(301) Nolte, C.; Mayer, P.; Straub, B. F. Isolation of a Copper(I) Triazolide: A "Click" Intermediate. *Angew. Chem. Int. Ed Engl.* **2007**, *46* (12), 2101–2103.

(302) Shao, C.; Wang, X.; Xu, J.; Zhao, J.; Zhang, Q.; Hu, Y. Carboxylic Acid-Promoted Copper(I)-Catalyzed Azide−Alkyne Cycloaddition. *J. Org. Chem.* **2010**, *75* (20), 7002–7005.

(303) Shao Changwei; Cheng Guolin; Su Deyong; Xu Jimin; Wang Xinyan; Hu Yuefei. Copper(I) Acetate: A Structurally Simple but Highly Efficient Dinuclear Catalyst for Copper-Catalyzed Azide-Alkyne Cycloaddition. *Adv. Synth. Catal.* **2010**, *352* (10), 1587–1592.

(304) Shao, C.; Wang, X.; Zhang, Q.; Luo, S.; Zhao, J.; Hu, Y. Acid–Base Jointly Promoted Copper(I)-Catalyzed Azide–Alkyne Cycloaddition. *J. Org. Chem.* **2011**, *76* (16), 6832–6836.

(305) Himo, F.; Lovell, T.; Hilgraf, R.; Rostovtsev, V. V.; Noodleman, L.; Sharpless, K. B.; Fokin, V. V. Copper(I)-Catalyzed Synthesis of Azoles. DFT Study Predicts Unprecedented Reactivity and Intermediates. *J. Am. Chem. Soc.* **2005**, *127* (1), 210–216.

(306) Zhang, L.; Chen, X.; Xue, P.; Sun, H. H. Y.; Williams, I. D.; Sharpless, K. B.; Fokin, V. V.; Jia, G. Ruthenium-Catalyzed Cycloaddition of Alkynes and Organic Azides. *J. Am. Chem. Soc.* **2005**, *127* (46), 15998–15999.

(307) Boren, B. C.; Narayan, S.; Rasmussen, L. K.; Zhang, L.; Zhao, H.; Lin, Z.; Jia, G.; Fokin, V. V. Ruthenium-Catalyzed Azide-Alkyne Cycloaddition: Scope and Mechanism. *J. Am. Chem. Soc.* **2008**, *130* (28), 8923–8930.

(308) Cecchi, L.; De Sarlo, F.; Machetti, F. 1,4-Diazabicyclo[2.2.2]Octane (DABCO) as an Efficient Reagent for the Synthesis of Isoxazole Derivatives from Primary Nitro Compounds and Dipolarophiles: The Role of the Base. *Eur. J. Org. Chem.* **2006**, *2006* (21), 4852–4860.

(309) Chand, P.; Kotian, P. L.; Dehghani, A.; El-Kattan, Y.; Lin, T.-H.; Hutchison, T. L.; Babu, Y. S.; Bantia, S.; Elliott, A. J.; Montgomery, J. A. Systematic Structure-Based Design and Stereoselective Synthesis of Novel Multisubstituted Cyclopentane Derivatives with Potent Antiinfluenza Activity. *J. Med. Chem.* **2001**, *44* (25), 4379–4392.

(310) Jones, P.; Atack, J. R.; Braun, M. P.; Cato, B. P.; Chambers, M. S.; O'Connor, D.; Cook, S. M.; Hobbs, S. C.; Maxey, R.; Szekeres, H. J.; et al. Pharmacokinetics and Metabolism Studies on (3-Tert-Butyl-7-(5-Methylisoxazol-3-Yl)-2-(1-Methyl-1H-1,2,4-Triazol-5-Ylmethoxy) Pyrazolo[1,5-d][1,2,4]Triazine, a Functionally Selective GABAA A5 Inverse Agonist for Cognitive Dysfunction. *Bioorg. Med. Chem. Lett.* **2006**, *16* (4), 872–875.

(311) Quan, M. L.; Liauw, A. Y.; Ellis, C. D.; Pruitt, J. R.; Carini, D. J.; Bostrom, L. L.; Huang, P. P.; Harrison, K.; Knabb, R. M.; Thoolen, M. J.; et al. Design and Synthesis of Isoxazoline Derivatives as Factor Xa Inhibitors. 1. *J. Med. Chem.* **1999**, *42* (15), 2752–2759.

(312) Pomeranz, C. Über eine neue Isochinolinsynthese. *Monatshefte Für Chem. Verwandte Teile Anderer Wiss.* **1893**, *14* (1), 116–119.

(313) Bischler, A.; Napieralski, B. Zur Kenntniss Einer Neuen Isochinolinsynthese. *Berichte Dtsch. Chem. Ges.* **1893**, *26* (2), 1903–1908.

(314) Pictet, A.; Spengler, T. Über Die Bildung von Isochinolin-Derivaten Durch Einwirkung von Methylal Auf Phenyl-Äthylamin, Phenyl-Alanin Und Tyrosin. *Berichte Dtsch. Chem. Ges.* **1911**, *44* (3), 2030–2036.

(315) ChemInform Abstract: An Efficient Method for the Preparation of New Analogues of Leucettamine B under Solvent-Free Microwave Irradiation (PDF Download Available) http://www.researchgate.net/publication/244780799_ChemInform_Abstract_An_Efficient_Method_for_the_Preparation_of_New_Analogues_of_Leucettamine_B_under_Solvent-Free_Microwave_Irradiation.

(316) *Chemistry of Heterocyclic Compounds: The Pyrimidines*; Brown, D. J., Mason, S. F., Eds.; Chemistry of Heterocyclic Compounds: A Series Of Monographs; John Wiley & Sons, Inc.: Hoboken, NJ, USA, 1962.

(317) DeRosa, T. F. Pyrimidines. In *Advances in Synthetic Organic Chemistry and Methods Reported in US Patents*; Elsevier: Oxford, 2006; pp 545–547.

(318) Karpov, A. S.; Müller, T. J. J. Straightforward Novel One-Pot Enaminone and Pyrimidine Syntheses by Coupling-Addition-Cyclocondensation Sequences. *Synthesis* **2003**, *2003* (18), 2815–2826.

(319) Palimkar, S. S.; Kumar, P. H.; Jogdand, N. R.; Daniel, T.; Lahoti, R. J.; Srinivasan, K. V. Copper-, Ligand- and Solvent-Free Synthesis of Ynones by Coupling Acid Chlorides with Terminal Alkynes. *Tetrahedron Lett.* **2006**, *47* (31), 5527–5530.

(320) Cox, R. J.; Ritson, D. J.; Dane, T. A.; Berge, J.; Charmant, J. P. H.; Kantacha, A. Room Temperature Palladium Catalysed Coupling of Acyl Chlorides with Terminal Alkynes. *Chem. Commun.* **2005**, *8*, 1037–1039.

(321) Bohlmann, F.; Rahtz, D. Über eine neue Pyridinsynthese. *Chem. Ber.* **1957**, *90* (10), 2265–2272.

(322) Bagley, M. C.; Dale, J. W.; Bower, J. A New Modification of the Bohlmann-Rahtz Pyridine Synthesis. *Synlett* **2001**, *2001* (07), 1149–1151.

(323) Bagley, M. C.; Lunn, R.; Xiong, X. A New One-Step Synthesis of Pyridines under Microwave-Assisted Conditions. *Tetrahedron Lett.* **2002**, *43* (46), 8331–8334.

(324) Xiong, X.; Bagley, M. C.; Chapaneri, K. A New Mild Method for the One-Pot Synthesis of Pyridines. *Tetrahedron Lett.* **2004**, *45* (32), 6121–6124.

(325) Worley, J. D. Heterocyclic Chemistry, Second Edition (Gilchrist, T.L.). *J. Chem. Educ.* **1993**, *70* (3), A89.

(326) Knorr, L.; Laubmann, H. Ueber Das Verhalten Der Pyrazole Und Pyrazoline. *Berichte Dtsch. Chem. Ges.* **1888**, *21* (1), 1205–1212.

(327) Pechmann, H. v. Pyrazol Aus Acetylen Und Diazomethan. *Berichte Dtsch. Chem. Ges.* **1898**, *31* (3), 2950–2951.

(328) Fustero, S.; Simón-Fuentes, A.; Sanz-Cervera, J. F. Recent Advances in the Synthesis of Pyrazoles. A Review. *Org. Prep. Proced. Int.* **2009**, *41* (4), 253–290.

(329) Fustero, S.; Sánchez-Roselló, M.; Barrio, P.; Simón-Fuentes, A. From 2000 to Mid-2010: A Fruitful Decade for the Synthesis of Pyrazoles. *Chem. Rev.* **2011**, *111* (11), 6984–7034.

(330) Zora, M.; Kivrak, A.; Yazici, C. Synthesis of Pyrazoles via Electrophilic Cyclization. *J. Org. Chem.* **2011**, *76* (16), 6726–6742.

(331) Gerstenberger, B. S.; Rauckhorst, M. R.; Starr, J. T. One-Pot Synthesis of N-Arylpyrazoles from Arylhalides. *Org. Lett.* **2009**, *11* (10), 2097–2100.

(332) Jiang, N.; Li, C.-J. Novel 1,3-Dipolar Cycloaddition of Diazocarbonyl Compounds to Alkynes Catalyzed by InCl3 in Water. *Chem. Commun.* **2004**, *0* (4), 394–395.

(333) Cabrele, C.; Reiser, O. The Modern Face of Synthetic Heterocyclic Chemistry. *J. Org. Chem.* **2016**, *81* (21), 10109–10125.

(334) Kaspar, L. T.; Ackermann, L. Three-Component Indole Synthesis Using Ortho-Dihaloarenes. *Tetrahedron* **2005**, *61* (48), 11311–11316.

(335) Lu, B. Z.; Zhao, W.; Wei, H.-X.; Dufour, M.; Farina, V.; Senanayake, C. H. A Practical Mild, One-Pot, Regiospecific Synthesis of 2,3-Disubstituted Indoles via Consecutive Sonogashira and Cacchi Reactions. *Org. Lett.* **2006**, *8* (15), 3271–3274.

(336) Lu, B. Z.; Wei, H.-X.; Zhang, Y.; Zhao, W.; Dufour, M.; Li, G.; Farina, V.; Senanayake, C. H. One-Pot and Regiospecific Synthesis of 2,3-Disubstituted Indoles from 2-Bromoanilides via Consecutive Palladium-Catalyzed Sonogashira Coupling, Amidopalladation, and Reductive Elimination. *J. Org. Chem.* **2013**, *78* (9), 4558–4562.

(337) Liu, F.; Ma, D. Assembly of Conjugated Enynes and Substituted Indoles via CuI/Amino Acid-Catalyzed Coupling of 1-Alkynes with Vinyl Iodides and 2-Bromotrifluoroacetanilides. *J. Org. Chem.* **2007**, *72* (13), 4844–4850.

(338) Henke, J. M.; Bassler, B. L. Three Parallel Quorum-Sensing Systems Regulate Gene Expression in Vibrio Harveyi. *J. Bacteriol.* **2004**, *186* (20), 6902–6914.

(339) Taga, M. E.; Miller, S. T.; Bassler, B. L. Lsr-Mediated Transport and Processing of AI-2 in Salmonella Typhimurium: Transport and Processing of AI-2. *Mol. Microbiol.* **2003**, *50* (4), 1411–1427.

(340) Yang, D.; Burugupalli, S.; Daniel, D.; Chen, Y. Microwave-Assisted One-Pot Synthesis of Isoquinolines, Furopyridines, and Thienopyridines by Palladium-Catalyzed Sequential Coupling–Imination–Annulation of 2-Bromoarylaldehydes with Terminal Acetylenes and Ammonium Acetate. *J. Org. Chem.* **2012**, *77* (9), 4466–4472.

(341) Karpov, A. S.; Müller, T. J. J. Straightforward Novel One-Pot Enaminone and Pyrimidine Syntheses by Coupling-Addition-Cyclocondensation Sequences. *Synthesis* **2003**, *2003* (18), 2815–2826.

(342) Trost, B. M.; Hung, C.-I. (Joey). Broad Spectrum Enolate Equivalent for Catalytic Chemo-, Diastereo-, and Enantioselective Addition to N-Boc Imines. *J. Am. Chem. Soc.* **2015**, *137* (50), 15940–15946.

(343) VAN LOEVEZIJN, A.; LANGE, J. H. M.; BARF, G. A.; DEN HARTOG, A. P. EP2011051100 SYNTHESIS OF SUBSTITUTED PYRAZOLINE CARBOXAMIDINE DERIVATIVES https://patentscope.wipo.int/search/en/detail.jsf?docId=WO2011092226&recNum=1&tab=PCTClaims&maxRec=&office=&prevFilter=&sortOption=&queryString= (accessed Mar 13, 2018).

(344) Liu, F.; Ma, D. Assembly of Conjugated Enynes and Substituted Indoles via CuI/Amino Acid-Catalyzed Coupling of 1-Alkynes with Vinyl Iodides and 2-Bromotrifluoroacetanilides. *J. Org. Chem.* **2007**, *72* (13), 4844–4850.

(345) Hooft, R. W.; Vriend, G.; Sander, C.; Abola, E. E. Errors in Protein Structures. *Nature* **1996**, *381* (6580), 272.

(346) Jones, D. T. Protein Secondary Structure Prediction Based on Position-Specific Scoring Matrices. *J. Mol. Biol.* **1999**, *292* (2), 195–202.

(347) Tegel, H.; Tourle, S.; Ottosson, J.; Persson, A. Increased Levels of Recombinant Human Proteins with the Escherichia Coli Strain Rosetta(DE3). *Protein Expr. Purif.* **2010**, *69* (2), 159–167.

(348) Soupene, E.; Heeswijk, W. C. van; Plumbridge, J.; Stewart, V.; Bertenthal, D.; Lee, H.; Prasad, G.; Paliy, O.; Charernnoppakul, P.; Kustu, S. Physiological Studies of Escherichia Coli Strain MG1655: Growth Defects and Apparent Cross-Regulation of Gene Expression. *J. Bacteriol.* **2003**, *185* (18), 5611–5626.

(349) Woodcock, D. M.; Crowther, P. J.; Doherty, J.; Jefferson, S.; DeCruz, E.; Noyer-Weidner, M.; Smith, S. S.; Michael, M. Z.; Graham, M. W. Quantitative Evaluation of Escherichia Coli Host Strains for Tolerance to Cytosine Methylation in Plasmid and Phage Recombinants. *Nucleic Acids Res.* **1989**, *17* (9), 3469–3478.

(350) Dolan, S. K.; Bock, T.; Hering, V.; Owens, R. A.; Jones, G. W.; Blankenfeldt, W.; Doyle, S. Structural, Mechanistic and Functional Insight into Gliotoxin Bis-Thiomethylation in Aspergillus Fumigatus. *Open Biol.* **2017**, *7* (2).

(351) Zhu, J.; Hixon, M. S.; Globisch, D.; Kaufmann, G. F.; Janda, K. D. Mechanistic Insights into the LsrK Kinase Required for Autoinducer-2 Quorum Sensing Activation. *J. Am. Chem. Soc.* **2013**, *135* (21), 7827–7830.

(352) Xavier, K. B.; Miller, S. T.; Lu, W.; Kim, J. H.; Rabinowitz, J.; Pelczer, I.; Semmelhack, M. F.; Bassler, B. L. Phosphorylation and Processing of the Quorum-Sensing Molecule Autoinducer-2 in Enteric Bacteria. *ACS Chem. Biol.* **2007**, *2* (2), 128–136.

Article

A Versatile Strategy for the Synthesis of 4,5-Dihydroxy-2,3-Pentanedione (DPD) and Related Compounds as Potential Modulators of Bacterial Quorum Sensing

Silvia Stotani [1,2], Viviana Gatta [3], Federico Medda [1,†], Mohan Padmanaban [1],
Anna Karawajczyk [1,‡], Päivi Tammela [3], Fabrizio Giordanetto [1,§], Dimitrios Tzalis [1] and Simona Collina [2,*

[1] Medicinal Chemistry, Taros Chemicals GmbH & Co. KG, Emil-Figge-Straße 76a, 44227 Dortmund, Germany; silviastotani@hotmail.it (S.S.); fmedda@centurionbiopharma.com (F.M.); mpadmanaban@taros.de (M.P.); akarawajczyk@gmail.com (A.K.); Fabrizio.Giordanetto@deshawresearch.com (F.G.); dtzalis@taros.de (D.T.)

[2] Department of Drug Sciences, Medicinal Chemistry and Pharmaceutical Technology Section, University of Pavia, Viale Taramelli 12, 27100 Pavia, Italy

[3] Drug Research Program, Division of Pharmaceutical Biosciences, Faculty of Pharmacy, University of Helsinki, FI-00014 Helsinki, Finland; viviana.gatta@helsinki.fi (V.G.); paivi.tammela@helsinki.fi (P.T.)

† Current address: Centurion Biopharma Corporation, Engesserstraße 4, 79108 Freiburg im Breisgau, Germany

‡ Current address: Selvita S.A., Park Life Science, Bobrzyňskiego 14, 30-348 Krakow, Poland

§ Current address: DE Shaw Research, 120W 45th Street, New York, NY 10036, USA

* Correspondence: simona.collina@unipv.it; Tel.: +39-0382-987379

Abstract: Resistance to antibiotics is an increasingly serious threat to global public health and its management translates to significant health care costs. The validation of new Gram-negative antibacterial targets as sources for potential new antibiotics remains a challenge for all the scientists working in this field. The interference with bacterial Quorum Sensing (QS) mechanisms represents a potentially interesting approach to control bacterial growth and pursue the next generation of antimicrobials. In this context, our research is focused on the discovery of novel compounds structurally related to (*S*)-4,5-dihydroxy-2,3-pentanedione, commonly known as (*S*)-DPD, a small signaling molecule able to modulate bacterial QS in both Gram-negative and Gram-positive bacteria. In this study, a practical and versatile synthesis of racemic DPD is presented. Compared to previously reported syntheses, the proposed strategy is short and robust: it requires only one purification step and avoids the use of expensive or hazardous starting materials as well as the use of specific equipment. It is therefore well suited to the synthesis of derivatives for pharmaceutical research, as demonstrated by four series of novel DPD-related compounds described herein.

---

1. Introduction

Bacterial chemical communication (i.e., quorum sensing, QS) allows bacteria to coordinate their gene expression and act as a population [1–5]. This phenomenon is detrimental for humans as QS regulates pathogenic processes such as the virulence factor production [6,7], susceptibility to antibiotics [8] and biofilm formation [9–11]. In recent decades, the modulation of QS has therefore emerged as a potential therapeutic approach to fight bacterial infections [12–17].

QS is mediated by production and release of and response to small molecules called autoinducers (AIs). Among these AIs, Autoinducer-2 (AI-2) is responsible for intra- and interspecies bacterial communication and, as a consequence, it has been termed the "universal autoinducer". The development of small molecules able to modulate the AI-2-mediated signaling would possibly result in broad-spectrum antimicrobial

activity. However, targeting the AI-2-based QS remains challenging mostly because of the rapid interconversion of the AI-2 precursor (*S*)-DPD (Figure 1) to several linear and cyclic forms recognized by different bacteria [18] (Figure 1). In aqueous solutions, (*S*)-DPD is in equilibrium with its two cyclic stereoisomers (*S*-DHMF and *R*-DHMF; Figure 1) [19]. Hydration of the C_3 carbonyl group of both the cyclic and linear structures was confirmed by X-ray crystallography. In the presence of boric acid, *S*-THMF (Figure 1) forms a borate ester (*S*-THMF-borate; Figure 1) which is recognized by LuxP in *V. harveyi* (PDB ID: 1JX6) [20]. *R*-THMF instead (Figure 1) does not coordinate boron and binds to the transporter LsrB which is responsible for its internalization and acts as the active species in *S. thyphimurium* AI-2-mediated QS (PDB ID: 1TJY) [21]. The hydrated form of linear (*S*)-DPD (*S*-THP, Figure1) is phosphorylated by LsrK, resulting in phospho-DPD (P-DPD, Figure 1) [22] recognized by the transcriptional repressor LsrR (PDB ID: 4L4Z) [23] and responsible for *E coli* and *S. typhimurium* AI-2-mediated signaling.
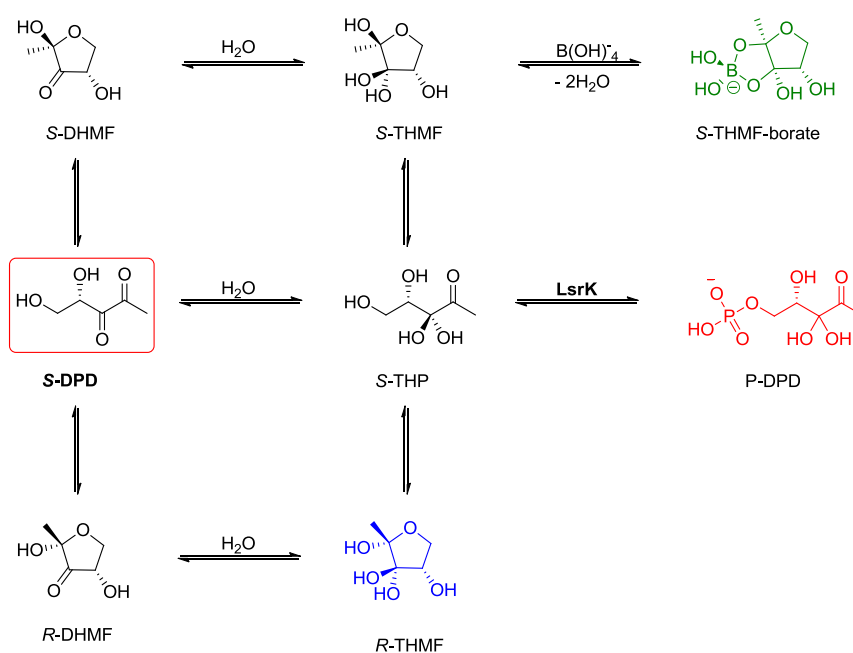
Figure 1. (*S*)-DPD in an aqueous medium: all species in equilibrium. (2*S*,4*S*)-2,4-dihydroxy-2-methyldihydrofuran-3-one (**S**-DHMF); (*S*)-4,5-dihydroxy-2,3-pentanedione (DPD); (2*R*,4*S*)-2,4-dihydroxy-2-methyldihydrofuran-3-one (**R**-DHMF); (2*S*,4*S*)-2-methyl-2,3,3,4-tetrahydroxytetrahydrofuran (*S* THMF); (*S*)-3,3,4,5-tetrahydroxy-2-pentanone (**S**-THP); (2*R*,4*S*)-2-methyl-2,3,3,4-tetrahydroxytetrahydrofuran (*R*-THMF); (2*S*,4*S*)-2-methyl-2,3,3,4-tetrahydroxytetrahydrofuranborate (*S*-THMF-borate); (*S*)-3,3,4,5-tetrahydroxy-2-pentanone-5-phosphate (P-DPD).

Modulation/inhibition of QS can control several bacterial virulence factors (e.g., biofilm formation) that facilitate human infections and reduce their negative effects, including mortality [24]. Quorum Sensing Inhibitors (QSI) therefore represent interesting tools to use in combination with "conventional" antibiotic therapies against antimicrobial resistance (AMR) [25,26].

In this work, we describe the set-up of a new protocol for the synthesis of racemic DPD and its application to the synthesis of four novel small libraries of DPD-related compounds (Figure 2), designed to target LsrK kinase, a key mediator in AI-2-mediated QS in enteric bacteria. The essential role of the enzyme has been demonstrated by LsrK gene deletion in *E. coli*, generating a mutant strain unable to activate AI-2-mediated QS [27]. Therefore, we believe that the generation of DPD-related compounds for the inhibition of LsrK may be the starting point for the development of new QSI that will serve as potential tools for overcoming antimicrobial resistance.
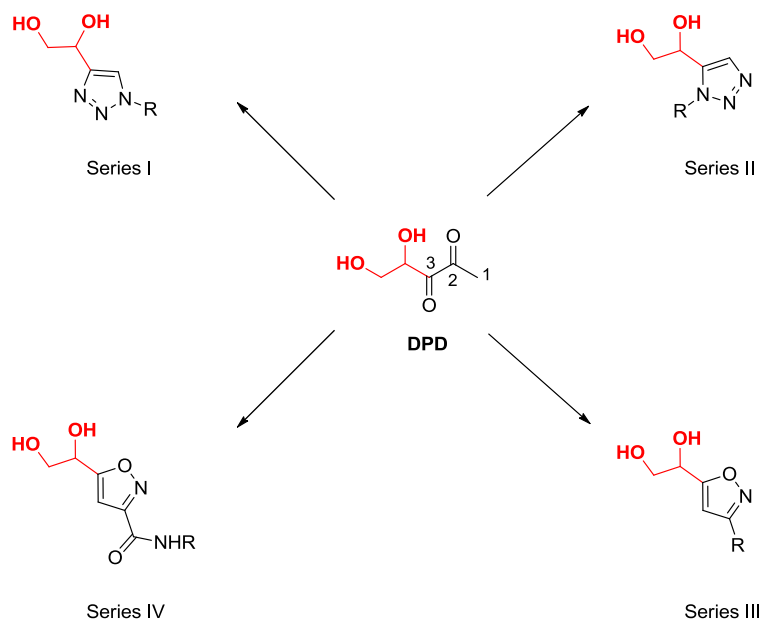
Figure 2. The DPD-related compounds presented in this work.

2. Results and discussion

Since 2004, much effort has been devoted to the study of synthetic pathways for the preparation of DPD and analogs in both racemic and enantiomeric forms. Literature analysis revealed that the synthesis of homochiral DPD requires the use of expensive (i.e., (*S*)-1,4-dioxaspiro[4.5]decane-2-carboxaldehyde) or unstable (i.e., (*S*)-glyceraldehyde acetonide) chiral starting materials and of further time-consuming purification steps [18,28–33]. Conversely, the synthetic procedures published so far to obtain racemic DPD proceed smoothly but suffer from hazardous chemical steps (i.e., reductive ozonolysis or the use of diazomethane) [34,35].

Starting from these considerations and keeping in mind that in the initial phase of the drug discovery process racemic compounds are usually evaluated and only once the most active ones have been identified both enantiomers must be prepared for biological testing [36], herein we studied a novel versatile strategy for the synthesis of racemic DPD suitable for readily supporting practical chemical diversification. The proposed synthetic strategy leading to DPD could be useful for the preparation of C_1 DPD-analogs and for the synthesis of DPD structurally related compounds, where the two carbonyl groups of DPD at C_2 and C_3 are embedded in heteroaromatic rings (Figure 2). To the best of our knowledge, no modification at C_2 have been reported and position C_3 has been barely explored and no heteroaromatic substituents (except for a furan at C_1) were previously described.

9.2 Synthesis of DPD and Ph-DPD

The synthetic strategies originally evaluated are outlined in Scheme 1.

Scheme 1.
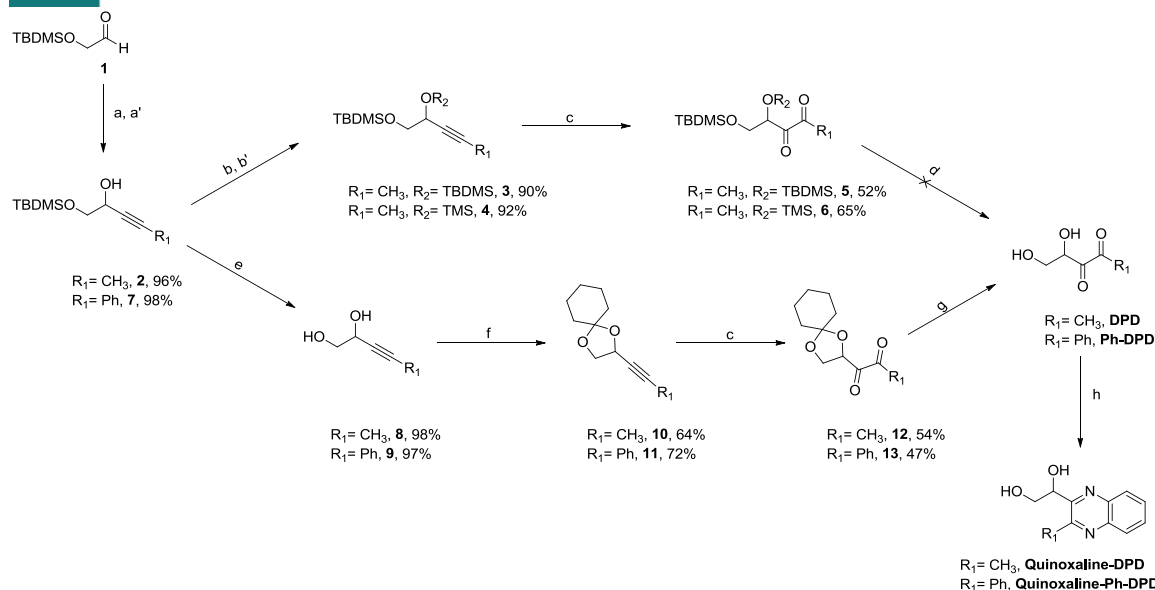
The synthesis of racemic DPD, Ph-DPD, quinoxaline-DPD and quinoxaline-Ph-DPD. Reagents and conditions: (**a**) 1-propynylmagnesium bromide (0.5 M in THF, 1.3 eq), THF, 0 °C to rt, 3 h; (**a'**) phenylethynylmagnesium bromide (1.0 M in THF, 1.3 eq), THF, 0 °C to rt, 3 h; (**b**) TBDMSCl (1.2 eq), NaH (2.0 eq), THF, rt, 3 h; (**b'**) TMSCl (1.2 eq), NaH (2.0 eq), THF, rt, 3 h; (**c**) NaIO$_4$ (4.4 eq), Ru$_2$O·H$_2$O (2.5% mol), CHCl$_3$/ACN/H$_2$O (1:1:1), rt, 1 h; (**d**) see Table S1; (**e**) Dowex50WX8 100–200 mesh, MeOH, rt, overnight; (**f**) cyclohexanone dimethyl ketal (3.0 eq), *p*-TSA (cat.), rt, overnight; (**g**) Dowex50WX8 100–200 mesh, D$_2$O (10 mM), rt, overnight; (**h**) *o*-phenylendiamine (2.0 eq), rt, overnight.

Briefly, the addition of 1-propynylmagnesium bromide to (*t*-butyldimethylsilyloxy)acetaldehyde [37] (**1**, Scheme 1), followed by the protection of the resulting secondary alcohol with TBDMSCl or TMSCl afforded compounds **3** or **4**, respectively (Scheme 1). The subsequent oxidation of the internal alkyne to yield diketone **5** or **6** was performed under optimized RuO$_2$*H$_2$O/NaIO$_4$-catalyzed conditions (Table 1, entry 5) using CHCl$_3$/ACN/H$_2$O (1:1:1) as the solvent.

Table 1. The optimization of the conditions for the oxidation of compound **3**. All the reactions were performed at room temperature.

Entry	Solvent	Oxidant and eq	Time	Yield (%)
1	Acetone	KMnO$_4$/NaHCO$_3$/MgSO$_4$ 3.8/0.6/2.0	Overnight	No reaction
2	Acetone	KMnO$_4$/NaHCO$_3$/MgSO$_4$ 3.9/0.6/4.2	Overnight	Traces
3	CCl$_4$/ACN (1:1)	NaIO$_4$/RuO$_2$·H$_2$O 2.2 eq/2.5% mol	3 h	Traces
4	CCl$_4$/ACN (1:1)	NaIO$_4$/RuO$_2$·H$_2$O 4.4 eq/2.5% mol	3 h	23
5	CHCl$_3$/ACN/H$_2$O (1:1:1)	NaIO$_4$/RuO$_2$·H$_2$O 4.4 eq/2.5% mol	3 h	52

The final acidic removal of the two TBDMS groups of compound **5** was performed under different conditions, but resulted in being unsuccessful (Table S1). Particularly, decomposition was observed when H$_2$SO$_4$ (or D$_2$SO$_4$) and TBAF were employed (Table S1). The partial removal of the two protecting groups (up to a maximum of 30% in total) was achieved with the use of acetic acid or Dowex50WX8 (Table S1). When the bulky protecting TBDMS group was replaced with TMS, (Scheme 1), similar results were obtained and a maximum of 40% cleavage was achieved using Dowex50WX8 in ACN-d_3.

A different approach was then investigated: compound **2** and the analogous **7** were deprotected in acidic conditions (Dowex50WX8), affording diols **8** and **9**, respectively. These intermediates were then

protected with a cyclohexyliden group and oxidized under the previously described conditions (Table 1). The oxidation of **10** and **11** was followed by the Dowex50WX8-mediated removal of the protecting group. ^{1}H-NMR analysis of the crude products was consistent with the literature-reported data and revealed the presence of a mixture of structures in equilibrium with each other (see SI for additional details). To further confirm the success of our procedure, the mixtures were treated with *o*-phenilendiamine to form, respectively, quinoxaline-DPD and quinoxaline-Ph-DPD (Scheme 1), which were isolated and fully characterized.

To sum up, the approach described above allows for the rapid production of racemic DPD in five steps and it does not require the use of dangerous or expensive reagents nor of particular equipment (i.e. ozonolysator); furthermore, only one purification step via column chromatography is necessary. Not less important, this procedure is suitable for the synthesis of C_1-DPD analogs (as long as the corresponding Grignard reagent can be purchased or produced) as the synthesis of Ph-DPD demonstrated. Additionally, the ethyne function introduced in the first step is a practical synthetic handle for further chemical derivatization, as demonstrated by the four small series of derivatives described below.

2.2 Synthesis of DPD-Related Compounds

As anticipated, we designed novel DPD-related compounds in which the carbonyl groups at C_2 and C_3 are embedded in heteroaromatic moiety to obtain compounds stable in solution, thus avoiding the open/closed equilibrium typical of the majority of the DPD-analogs reported so far (Figure 1). As heteroaromatic rings, we selected 1,2,3-triazole and isoxazole, two scaffolds common in medicinal chemistry present in several natural and synthetic drugs including antimicrobial, anticancer, anti-inflammatory and antireumatic drugs [38–43].

The newly designed compounds can be obtained starting from the two common intermediates **15** and **16** (Scheme 2) strictly related to **2** and **7** (Scheme 1). In details, as in the case of DPD, the first of the two building blocks necessary to start the synthesis of all the analogs presented in this work was produced by the Grignard addition of ethynylmagnesium bromide to aldehyde **1**, followed by acidic removal of the TBDMS protecting group. Further protection of the resulting diol **15** as acetal, using cyclohexanone dimethyl ketal, afforded the second building block compound **16** (Scheme 2).
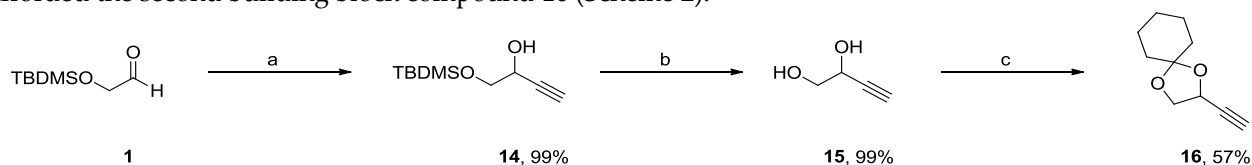
Scheme 2. The synthesis of intermediates **15** and **16**. Reagents and conditions: (**a**) ethynylmagnesium bromide (0.5 M in THF, 1.3 eq), THF, 0 °C to rt, 3h; (**b**) Dowex50WX8 100–200 mesh, MeOH, rt, overnight; (**c**) cyclohexanone dimethyl ketal (3.0 eq), *p*-TSA (cat.), rt, overnight.

2.2.1. 1,4- and 1,5-Disubstituted 1,2,3-Triazoles DPD-Derivatives (Series I and II)

1,2,3-triazoles (both 1,4- and 1,5-disubstituted) can be synthesized applying azide-alkyne Huisgen cycloaddition conditions where an azide is reacted with an alkyne in a 1,3-dipolar cycloaddition reaction. At first, we tested three different Copper-Catalyzed Azide-Alkyne Cycloaddition (CuAAC) conditions to select the best procedure for the synthesis of the planned compounds. For this purpose, (2-azidoethyl)benzene (**17a**) was chosen as the reference azide (Table 2). First, we used CuI (10% mol) and DIPEA (15% mol) in nonaqueous, nonprotic THF to afford the desired product with 58% isolated yield (Table 2, entry 1) [44]. As the addition of AcOH was found to accelerate the protonation of the Cu-C bond [45–47] (thus facilitating the formation of the product), a catalytic amount of AcOH was added to the mixture (containing 2% mol CuI and 4% mol DIPEA). This acid-base system jointly promoted CuAAC and resulted in a 14% increase of the isolated yield (Table 2, entry 2) when compared to the previous conditions (Table 2, entry 1) [48]. It is known that the use of ligands is beneficial for the reaction as it prevents Cu(I) oxidation and avoids the use of a base. Therefore, it is not surprising that the in situ generation of Cu(I) by the reduction of $CuSO_4 \cdot 5H_2O$ from

sodium ascorbate together with the formation of L-ascorbic acid (that acts both as a ligand and as acidic source) raised the yield up to 89% (Table 2, entry 3) [49]. The 1,4-disubstitution was confirmed by the HMBC of compound **18a** (see Supporting Information).

Table 2. The reaction conditions to obtain **18a–f** and **19a**. All reactions were performed overnight at room temperature except for entry 4 where the mixture was heated at 60 °C.
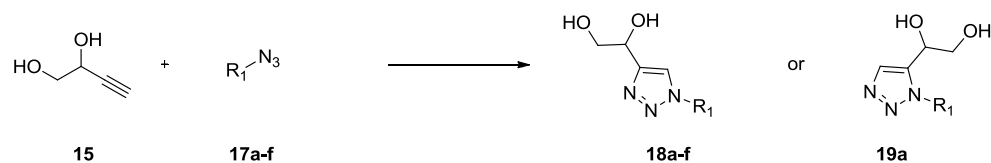
Entry	R_1	Azide, eq	Solvent	Catalyst	Product	Yield (%) [a]	Ref.
1	(CH$_2$)$_2$-Ph	**17a**, 1.1	THF	CuI (10% mol) DIPEA (15% mol)	**18a**	58	[44]
2	(CH$_2$)$_2$-Ph	**17a**, 1.05	DCM	CuI (2% mol) DIPEA (4% mol) AcOH (cat)	**18a**	72	[48]
3	(CH$_2$)$_2$-Ph	**17a**, 1.0	*t*-BuOH/H$_2$O (1:1)	CuSO$_4$·5H$_2$O (5% mol) Na Ascorbate (0.5 eq)	**18a**	89	[49]
4	(CH$_2$)$_2$-Ph	**17a**, 1.0	1,4-dioxane	(Cp*RuCl(PPh$_3$)$_2$) (2% mol)	**19a**	87	[50]
5	(CH$_2$)-Ph	**17b**, 1.0	*t*-BuOH/H$_2$O (1:1)	CuSO$_4$·5H$_2$O (5% mol) Na Ascorbate (0.5 eq)	**18b**	60	[49]
6	(CH$_2$)$_2$-*o*-F-Ph	**17c**, 1.0	*t*-BuOH/H$_2$O (1:1)	CuSO$_4$·5H$_2$O (5% mol) Na Ascorbate (0.5 eq)	**18c**	62	[49]
7	(CH$_2$)$_2$-*m*-Pyr	**17d**, 1.0	*t*-BuOH/H$_2$O (1:1)	CuSO$_4$·5H$_2$O (5% mol) Na Ascorbate (0.5 eq)	**18d**	88	[49]
8	(CH$_2$)$_5$-CN	**17e**, 1.0	*t*-BuOH/H$_2$O (1:1)	CuSO$_4$·5H$_2$O (5% mol) Na Ascorbate (0.5 eq)	**18e**	72	[49]
9	(CH$_2$)$_2$-CyH	**17f**, 1.0	*t*-BuOH/H$_2$O (1:1)	CuSO$_4$·5H$_2$O (5% mol) Na Ascorbate (0.5 eq)	**18f**	73	[49]

[a] Isolated yield.

The corresponding 1,5-disubstituted 1,2,3-triazole **19a** was also synthesized by varying the experimental conditions: the regioselective synthesis was achieved with the use of Ruthenium-catalyzed Azide-Alkyne Cycloaddition (RuAAC) conditions. Azide **17a** was reacted with terminal alkyne **15** in the presence of 2% mol pentamethylcyclopentadienylbis (triphenylphosphine)ruthenium(II) chloride (Cp*RuCl(PPh$_3$)$_2$) regioselectively yielding, after stirring overnight the mixture in refluxing 1,4-dioxane, the corresponding 1,5-disubstituted 1,2,3-triazole **19a** (Table 2, entry 4). ^{1}H, ^{13}C, TLC, UHPLC, and HMBC unambiguously confirmed the different nature of the two compounds (see Supporting Information) [50].

Once optimal conditions for the regioselective synthesis of 1,4-disubstituted 1,2,3-triazoles were established, we synthesized five azides of different chemical nature including aromatic, heteroaromatic and aliphatic elements (**17b–f**). This was achieved by stirring overnight at room temperature the corresponding bromo compounds with an excess (1.5 eq) of sodium azide. The five azides were reacted with alkyne **15** applying the previously found conditions and products **18b–f** were isolated in good to excellent yields (60–88%, Table 2, entry 5–9).

As the synthesis of triazoles substituted with short alkyl chains (e.g., methyl, butyl) was unattainable by this route because of safety issues related to the explosive and unstable nature of the required azides, we installed the desired substituents on the triazole scaffold via alkylation. We elected to use a single, small and dangerous azide (i.e., TMSN$_3$) over the use of four different ones. The acetal protected terminal alkyne **16** was carefully reacted with an excess (10.0 eq) of TMSN$_3$ under previously established CuAAC conditions. The resulting unsubstituted triazole (**20**, Scheme 3) was both deprotected under acidic conditions (**18g,**

Scheme 3) and, to install the desired substituents, alkylated with four different (i.e., methyl, cyclopropylmethyl, butyl, ethoxyethyl) bromides (Scheme 3).
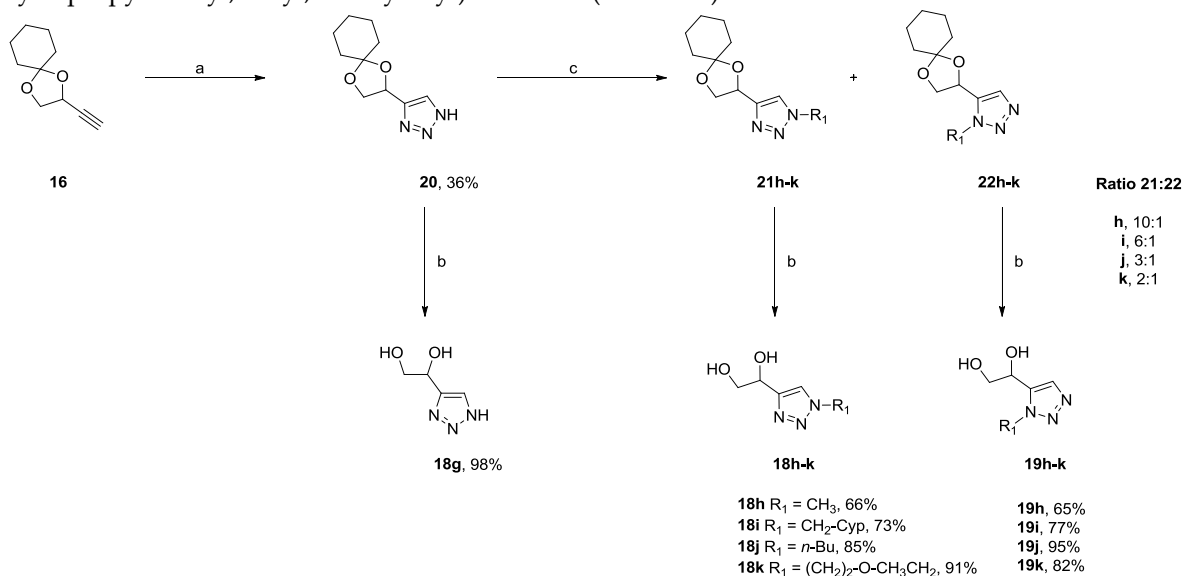
Scheme 3. The synthesis of 1,4-disubstituted 1,2,3-triazoles **18g–k** and 1,5-disubstituted 1,2,3-triazoles **19h–k**. Reagents and conditions: (a) TMSN$_3$ (10.0 eq), CuSO$_4$·5H$_2$O (5% mol), Na ascorbate (0.5 eq), t-BuOH/H$_2$O (1:1), rt, overnight; (b) 12M HCl (cat.), 1,4-dioxane, 0 °C to rt, 1–3 h; (c) R$_1$Br (1.5 eq), K$_2$CO$_3$ (2.0 eq), THF, 40 °C, overnight; preparative HPLC.

As expected, no regioselectivity was observed and both the 1,4- and the 1,5-disubstituted 1,2,3-triazoles formed. Experimenting with base (i.e, 1.1 eq, 1.3 eq and 1.5 eq of K$_2$CO$_3$) and/or the alkylbromides (i.e., 0.8 eq and 0.9 eq of R$_1$Br) stoichiometry did not consistently changed the ratio of the two regioisomers (data not shown). For each substituent, the two corresponding regioisomers were isolated by preparative HPLC. The resulting eight products (**21h–k** and **22h–k**, Scheme 3) were lastly deprotected with a catalytic amount of concentrated hydrochloric acid. The ratio of the two regioisomers was determined by crude NMR. For all of the four regioisomeric pairs, the 1,4-dibustituted 1,2,3-triazoles formed in excess when compared to the respective 1,5-regioisomers and, as predictable, the ratio decreased as the sterical hindrance of the R$_1$ substituent increased (Scheme 3). Concentrated HCl was preferred over Dowex 50WX8 for the removal of the acetal protecting group due to the shorter reaction time (1–3 h vs overnight) and shorter workup (no filtration to remove the acidic resin required).

2.2.2. 3,5-Disubstituted Isoxazoles DPD-Derivatives (Series III and IV)

Compound **15** (Scheme 2) is also the key intermediate for the synthesis of 3,5-disubstituded DPD related compounds **26l–r** (Scheme 4). Briefly, aldehydes **23l–r** were converted into their corresponding oximes **24l–r** using NH$_2$OH·HCl. The resulting crude compounds were directly chlorinated by a reaction with N-chlorosuccinimide (NCS). According to Himo et al. [49], the addition of CuSO$_4$·5H$_2$O, Na ascorbate, and KHCO$_3$ in t-BuOH/H$_2$O (1:1) to the isolated chloro-oximes allowed them to form the nitrile oxide which reacted by 1,3-dipolar cycloaddition with **15**. After preparative HPLC purification, the targeted isoxazoles **26l–r** were, therefore, obtained in good to excellent yields (i.e., 63–89%, Scheme 4).
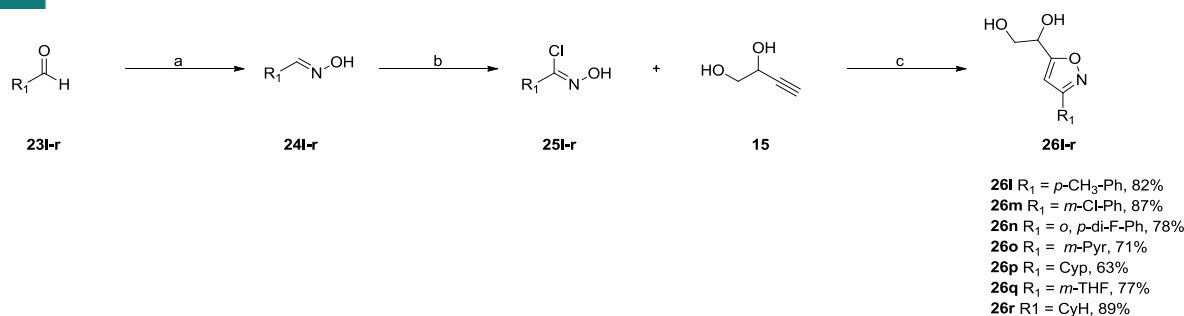
Scheme 4. The synthesis of 3,5-disubstituted isoxazoles **26l–r**. Reagents and conditions: (a) NH$_2$OH·HCl (3.0 eq), Et$_3$N (1.5 eq), H$_2$O/EtOH (1:1), rt, 1–3 h; (b) NCS (1.0 eq), DMF, rt, 1–2 h; (c) 15 (1.0 eq), CuSO$_4$·5H$_2$O (5% mol), Na ascorbate (0.5 eq), KHCO$_3$, t-BuOH/H$_2$O (1:1), rt, overnight.

The same procedure was attempted to obtain 3,5-disubstituted isoxazoles of DPD-analogs bearing an amide moiety at position 3, but starting from the protected precursor **16** instead of **15** due to the cross-reactivity between the 1,3-diol and the reagents necessary in the following steps (e.g., NaOH, DIPEA, Scheme 5). Formation of the nitrile oxide for the cycloaddition was attempted using the dehydration of ethyl nitroacetate with several bases (i.e., DABCO, DMAP, DBU, NMI, Scheme S1, conditions a) and also with a combination of PhNCO/Et$_3$N (Scheme S1, conditions b), commonly used to activate nitro groups. All of the aforementioned methods resulted in a mixture of unreacted starting materials [51,52].

The 1,3-dipole species was then changed to the chloro-oxime of ethyl glyoxalate (50% solution in toluene) but the employment of the same conditions as above (CuSO$_4$·5H$_2$O (5% mol), Na ascorbate (0.5 eq), KHCO$_3$, t-BuOH/H$_2$O (1:1), Scheme 4) did not yield the desired product while the simple use of an equimolar amount of Et$_3$N gave only traces of **28** (Scheme 5) [49,53].

We then change our strategy and employed the oxime of ethyl glyoxalate **27** together with an excess (40.0 eq) of sodium hypochlorite, both as a chlorinating agent and as a base to form the corresponding nitrile oxide, following the procedure already described by Quan et al. [54]. Compound **28** was successfully obtained, even if with a low yield (16%). Different reaction times, as well as ratios of dipolarophile **16** and 1,3-dipole **28**, were then tested (Table S2) in order to improve the initially poor yield (i.e., 16%, Table S2). Increasing the concentration of 1,3-dipole **27** enhanced the formation of intermediate **28** up to a maximum of 36% isolated yield (Table S2) with the complete consumption of the dipolarophile **16**, followed by removal of the excess of **27** by column chromatography.

Once a solution for the key 1,3-dipolar cycloaddition step was found, the rest of the synthetic pathway proceeded smoothly (Scheme 5). Saponification of the ethylic ester was followed by the amidification of the resulting carboxylic acid moiety using HOBt as the coupling agent and employing both primary and secondary amines (aromatic, heteroaromatic, aliphatic). The final acidic removal of the acetal protecting group afforded six 3,5-disubstituted isoxazoles (with an amide moiety at position 3) **33b**, **33s–z** in moderate to excellent yields (i.e., 37–79%, Scheme 5). Two more products were isolated after the acidic deprotection of intermediates **28** and **30** (i.e., **29** and **31**, respectively, Scheme 5).
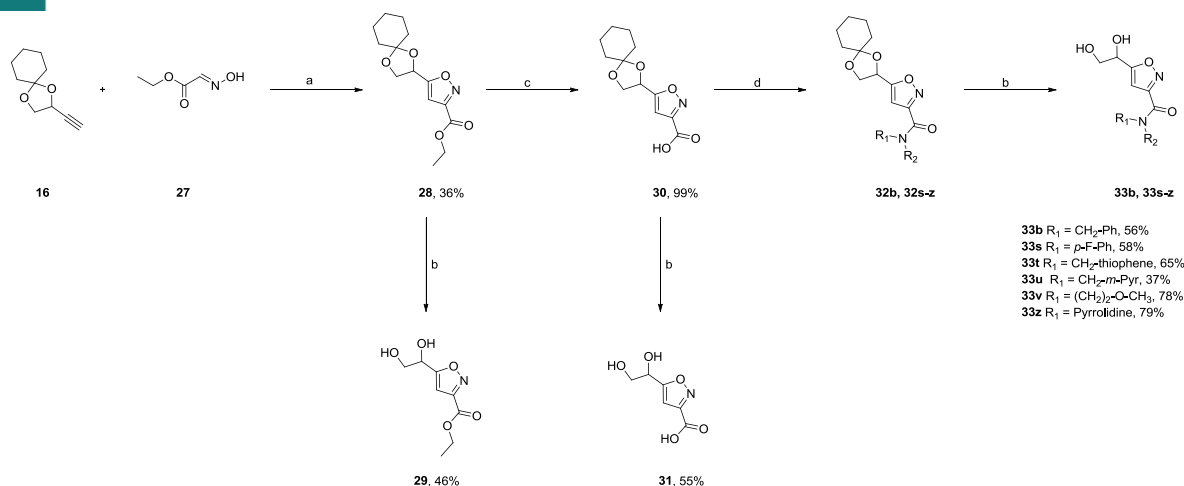
Scheme 5. The synthesis of 3,5-disubstituted isoxazoles (with an amide moiety at position 3) **33b**, **33s–z**. Reagents and conditions: (a) 27 (2.0 eq), NaOCl (40.0 eq), THF, rt, 12 h; (b) 12M HCl (cat.), 1,4-dioxane, 0 °C to rt, 1–3 h; (c) NaOH 1M (3.0 eq), THF, rt, overnight; (d) amine (2.0 eq), HOBt (2.0 eq), EDC*HCl (2.0 eq), Et₃N, DCM, rt, overnight.

2. Biological Evaluation of Synthesized Compounds

The activity of the synthetized compounds was evaluated with a bioluminescence-based assay against the target enzyme. Our results clearly highlight that racemic DPD prepared using our procedure is efficiently phosphorylated by LsrK (see Supporting Information, Figure S1). In fact, the level of ATP is significantly reduced by the addition of racemic DPD, resulting in a light emission lower than the sample including only LsrK and ATP.

These results confirmed the validity of the approach adopted. Indeed, in this initial phase of the drug discovery process, we prepared racemic DPD and studied a versatile synthesis suitable for readily supporting practical chemical diversification racemic compounds. Only once the most active ones have been identified will both enantiomers be prepared for biological testing. Accordingly, the activity of racemic DPD is essential for demonstrating that our approach has a valid basis. Regarding the DPD-derivatives, unfortunately, they did not show any activity (the data are reported in Supporting Information, Table S3).

3. Experimental

3.1 Chemistry

Chemicals and solvents were obtained from commercial suppliers and were used without further purification. All dry reactions were performed under a nitrogen atmosphere using commercial dry solvents. Flash column chromatography was performed on a silica column using 230-400 mesh silica gel or the Grace Reveleris X2 flash chromatography system using silica gel packed Macherey Nagel Chromabond Flash BT cartridges (60 Å, 45 μm) and Grace Reveleris flash Cartridges (60 Å, 40 μm). Thin layer chromatography was performed on Macherey Nagel precoated TLC aluminum sheets with silica gel 60 UV254 (5–17 μm). TLC visualization was accomplished by irradiation with a UV lamp (254 nm) and/or staining with KMnO₄ solutions. ¹H-NMR spectra were recorded at room temperature on a Bruker Avance spectrometer operating at 300 MHz (Hamburg, Germany). Chemical shifts are given in ppm (δ) from tetramethylsilane as an internal standard or residual solvent peak. Significant ¹H-NMR data are tabulated in the following order: multiplicity (s, singlet; d, doublet; t, triplet; q, quartet; m, multiplet; dd, doublet of doublets; dt, doublet of triplets; td, triplet of doublets; br, broad), coupling constant(s) in hertz, number of protons. Proton decoupled ¹³C-NMR data were acquired at 100 MHz. ¹³C chemical shifts are reported in parts per million (δ, ppm). All NMR data were collected at room temperature (25 °C). Analytical, preparative HPLC and Electron Spray Ionization (ESI) mass spectra were performed on an Agilent UHPLC (1290 Infinity, Santa Clara, CA, USA) and an

Agilent Prep-HPLC (1260 Infinity), both equipped with a Diode Array Detector and a Quadrupole MS using mixture gradients of formic acid/water/acetonitrile as solvents. High-resolution electrospray ionization mass spectra (ESI-FTMS) were recorded on a Thermo LTQ Orbitrap (Thermo Electron, Dreieich, Germany) coupled to an 'Accela' HPLC system supplied with a 'Hypersil GOLD' column (Termo Electron).

3.2 Synthesis of DPD and Ph-DPD

Synthesis of 2 and 7: to a stirred solution of (*t*-butyldimethylsilyloxy)acetaldehyde (1.0 eq) in dry THF, 1-propynylmagnesium bromide was added (over 15 min; 0.5 M in THF, 1.3 eq) (or phenylethynylmagnesium bromide (1.0 M in THF, 1.3 eq) at 0° C). After the addition, the reaction was allowed to reach room temperature and stirred for 3 h. The solvent was removed under reduced pressure, the residue was poured into a cold saturated solution of NH_4Cl and extracted three times with Et_2O. The organic layer was washed twice with water and once with brine, dried over $MgSO_4$, filtered and concentrated in vacuo to yield **2** as a yellowish oil (96%) or **7** as a yellow oil (98%).

1-[(t-Butyldimethylsilyl)oxy]pent-3-yn-2-ol (**2**): yellowish oil, 96%, R_f = 0.20 (CyH/EtOAc 9:1). ^{1}H-NMR (300 MHz, CDCl$_3$) δ 4.36–4.34 (m, 1H), 3.73 (dd, *J* = 3.6 Hz, *J* = 10.0 Hz, 1H), 3.59 (dd, *J* = 7.7 Hz, *J* = 10.0 Hz,1H), 2.57 (s br, 1H), 1.83 (d, *J* = 1.9 Hz, 3H), 0.91 (s, 9H), 0.08 (d, *J* = 1.3 Hz, 6H) ppm; ^{13}C-NMR (100 MHz, CDCl$_3$) δ 81.8, 79.6, 67.3, 66.3, 25.8, 18.3, 3.5, −5.4 ppm [55]

1-[(t-Butyldimethylsilyl)oxy]-4-phenylbut-3-yn-2-ol (**7**): yellow oil, 98%, R_f = 0.72 (CyH/EtOAc 9:1). ^{1}H-NMR (300 MHz, CDCl$_3$) δ 7.45–7.42 (m, 2H), 7.32–7.29 (m, 3H), 4.65–4.60 (m, 1H), 3.87 (dd, *J* = 3.8 Hz, *J* = 10.0 Hz, 1H), 3.75 (dd, *J* = 6.9 Hz, *J* = 10.0 Hz, 1H), 2.71 (d, *J* = 4.9 Hz, 1H), 0.93 (s, 9H), 0.13 (d, *J* = 3.1 Hz, 6H) ppm; ^{13}C-NMR (100 MHz, CDCl$_3$) δ 131.8, 128.4, 128.2, 122.5, 87.0, 85.3, 67.0, 63.6, 25.9, 18.4, 5.3 ppm [56]

Synthesis of 8 and 9: to a stirred solution of **2** (or **7**) (1.0 eq) in MeOH, Dowex50WX8 100–200 mesh (100 mg/1 mL) was added. The reaction was stirred at room temperature overnight. The mixture was filtered through paper and the solvent was evaporated under reduced pressure to yield **8** as an orange oil (98%) or **9** as an orange oil (97%).

Pent-3-yne-1,2-diol (**8**): orange oil, 98%, R_f = 0.38 (CHCl$_3$/MeOH 9:1). ^{1}H-NMR (300 MHz, CDCl$_3$) δ 4.44–4.39 (m, 1H), 3.70 (dd, *J* = 3.8 Hz, *J* = 11.3 Hz, 1H), 3.62 (dd, *J* = 6.6 Hz, *J* = 11.3 Hz, 1H), 2.41 (s br, 2H), 1.85 (d, *J* = 2.1 Hz, 3H) ppm; ^{13}C-NMR (100 MHz, CDCl$_3$) δ 82.8, 79.7, 66.8, 63.4, 3.5 ppm [32].

4-Phenylbut-3-yne-1,2-diol (**9**): orange oil, 97%, R_f = 0.44 (CHCl$_3$/MeOH 9:1). ^{1}H-NMR (300 MHz, CDCl$_3$) δ 7.46–7.42 (m, 2H), 7.36–7.29 (m, 3H), 4.69 (dd, *J* = 3.9 Hz, *J* = 6.5 Hz, 1H), 3.87–3.74 (m, 2H), 2.23 (s br, 2H) ppm; ^{13}C-NMR (100 MHz, CDCl$_3$) δ 131.8, 128.7, 128.3, 122.0, 86.5, 86.3, 66.6, 63.7 ppm [56]

Synthesis of 10 and 11: to **8** (or **9**) (1.0 eq) cyclohexanone dimethyl ketal (3.0 eq) and a catalytic amount of *p*-TSA was added. The reaction was stirred at room temperature overnight. The solvent was removed under reduced pressure and the crude was re-dissolved in Et_2O and washed three times with $NaHCO_3$. The organic layer was dried over $MgSO_4$, filtered and concentrated in vacuo to yield **10** as a yellow oil (64%) or **11** as a yellow oil (72%).

2-(Prop-1-yn-1-yl)-1,4-dioxaspiro[4.5]decane (**10**): yellow oil, 64%, R_f = 0.50 (CyH/EtOAc 9:1). ^{1}H-NMR (300 MHz, CDCl$_3$) δ 4.70–4.64 (m, 1H), 4.11 (dd, *J* = 6.2 Hz, *J* = 7.9 Hz, 1H), 3.81 (t, *J* = 7.5 Hz, 1H), 1.85 (d, *J* = 2.1 Hz, 3H), 1.74–1.70 (m, 2H), 1.65–1.57 (m, 6H), 1.43–1.38 (m, 2H) ppm; ^{13}C-NMR (100 MHz, CDCl$_3$) δ 110.5, 85.8, 82.3, 69.7, 65.5, 35.8, 25.1, 23.9, 3.7 ppm [32].

2-(2-Phenylethynyl)-1,4-dioxaspiro[4.5]decane (**11**): yellow oil, 72%, R_f = 0.60 (CyH/EtOAc 9:1). ^{1}H-NMR (300 MHz, CDCl$_3$) δ 7.46–7.42 (m, 2H), 7.33–7.28 (m, 3H), 4.95 (t, *J* = 6.4 Hz, 1H), 4.23 (dd, *J* = 6.3 Hz, *J* = 7.9 Hz,

1H), 4.01 (dd, J = 6.5 Hz, J = 7.9 Hz, 1H), 1.81–1.77 (m, 2H), 1.68–1.56 (m, 6H), 1.44–1.41 (m, 2H), ppm; ^{13}C-NMR (100 MHz, CDCl$_3$) δ 131.8, 128.5, 128.2, 122.4, 111.0, 86.6, 85.6, 69.7, 65.7, 35.5, 25.1, 23.9 ppm.

Synthesis of 12 and 13: to a stirred solution of **10** (or **11**) (1.0 eq) in a 1:1:1 mixture of CHCl$_3$/ACN/H$_2$O, NaIO$_4$ (4.4 eq) and RuO$_2$·H$_2$O (2.5% mol) were added. The mixture was vigorously stirred at room temperature overnight. The solvent was evaporated under reduced pressure and the crude was re-dissolved in CHCl$_3$ and filtered through a silica pad. The eluate was washed three times with water, dried over MgSO$_4$, filtered and concentrated in vacuo to yield **12** as a yellow oil (54%) or **13** as yellow oil (47%).

1-{1,4-Dioxaspiro[4.5]decan-2-yl}propane-1,2-dione (**12**): yellow oil, 54%, R_f = 0.42 (CyH/EtOAc 3:1). ^{1}H-NMR (300 MHz, CDCl$_3$) δ 5.14 (dd, J = 5.3 Hz, J = 7.9 Hz, 1H), 4.35 (dd, J = 8.0 Hz, J = 8.9 Hz, 1H), 3.99 (dd, J = 5.3 Hz, J = 8.9 Hz, 1H), 2.39 (s, 3H), 1.66–1.57 (m, 8H), 1.45–1.42 (m, 2H) ppm; ^{13}C-NMR (100 MHz, CDCl$_3$) δ 197.5, 190.0, 109.2, 75.9, 66.9, 36.4, 35.6, 25.9, 24.8, 24.0 ppm [28].

1-{1,4-Dioxaspiro[4.5]decan-2-yl}-2-phenylethane-1,2-dione (**13**): yellow oil, 47%, R_f = 0.46 (CyH/EtOAc 9:1). ^{1}H-NMR (300 MHz, CDCl$_3$), δ 7.98 (d, J = 7.1 Hz, 2H), 7.66 (d, J = 7.4 Hz, 1H), 7.51 (t, J = 7.7 Hz, 2H), 5.12 (t, J = 6.2 Hz, 1H), 4.34 (d, J = 6.4 Hz, 2H), 1.65–1.49 (m, 8H), 1.39–1.32 (m, 2H) ppm; ^{13}C-NMR (100 MHz, CDCl$_3$) δ 200.5, 193.0, 134.9, 132.2, 129.9, 128.9, 112.2, 77.9, 65.9, 35.4, 34.6, 24.9, 23.8, 23.0 ppm.

Synthesis of DPD and Ph-DPD: to a stirred solution of **12** (or **13**) (10 mM) in D$_2$O, Dowex 50WX8 resin was added (100 mg/1 mL). The mixture was stirred at room temperature overnight. The mixture was filtered to remove the resin and extracted with CDCl$_3$ to remove the released cyclohexanone.

4,5-Dihydroxy-2,3-pentanedione (**DPD**): ^{1}H-NMR (300 MHz, D$_2$O) δ 4.41–4.37 (m, 1H), 4.21–4.14 (m, 2H), 4.07 (dd, J = 3.2 Hz, J = 6.0 Hz, 1H), 3.99 (dd, J = 3.8 Hz, J = 7.4 Hz, 1H), 3.86–3.78 (m, 2H), 3.69–3.65 (m, 1H), 3.59 (dd, J = 5.6 Hz, J = 9.4 Hz, 1H), 2.39 (s, 3H), 1.46 (s, 3H), 1.43 (s, 3H) ppm [34]. The NMR shows that some cyclohexanone is left as two multiplets at 1.88–1.86 and 1.75–1.74 ppm.

3,4-Dihydroxy-1-phenylbutane-1,2-dione (**Ph-DPD**): ^{1}H-NMR (300 MHz, D$_2$O) δ 8.25–8.15 (m, 2H), 8.07–7.92 (m, 2H), 7.73–7.68 (m, 1H), 7.62–7.59 (m, 5H), 7.48–7.46 (m, 5H), 4.49–4.42 (m, 1H), 4.40–4.36 (m, 1H), 4.13 (dd, J = 2.7 Hz, J = 5.6 Hz, 1H), 4.09 (d, J = 2.8 Hz, 1H), 4.06 (d, J = 2.6 Hz, 1H), 3.88 (d, J = 4.0 Hz, 1H), 3.85–3.79 (m, 1H), 3.73–3.66 (m, 1H) ppm [30].

Synthesis of quinoxaline-DPD and quinoxaline-Ph-DPD: to a stirred solution of **DPD** (or **Ph-DPD**) in D$_2$O, *o*-phenylendiamine (2.0 eq) was added. The reaction was stirred at room temperature overnight. The solvent was evaporated under reduced pressure, the crude was re-dissolved in ACN (1 mL), filtered and purified by preparative HPLC.

1-(3-Methylquinoxalin-2-yl)ethane-1,2-diol (**Quinoxaline-DPD**): orange solid, R_f = 0.52 (CHCl$_3$/MeOH 9:1). ^{1}H-NMR (700 MHz, MeOD) δ 8.09–8.07 (m, 1H), 7.98–7.97 (m, 1H), 7.76 (pd, J = 7.0 Hz, J = 1.6 Hz, 2H), 5.15–5.13 (m, 1H), 4.02 (dd, J = 11.4 Hz, J = 5.4 Hz, 1H), 3.96 (dd, J = 11.4 Hz, J = 6.3 Hz, 1H), 2.84 (s, 3H) ppm; ^{13}C-NMR (176 MHz, MeOD) δ 156.6, 154.7, 142.3, 141. 8, 131.2, 130.5, 129.9, 128.8, 72.9, 66.3, 22.3 ppm; HRMS (ESI-MS) calcd. for C$_{11}$H$_{12}$N$_2$O$_2$ [M + H]$^+$ = 205.0899. Found: 205.0972. The NMR was consistent with previously reported data [18]. The NMR was measured with a Bruker DRX700 (700 MHz).

1-(3-Phenylquinoxalin-2-yl)ethane-1,2-diol (**Quinoxaline-Ph-DPD**): orange solid, R_f = 0.48 (CHCl$_3$/MeOH 9:1). ^{1}H-NMR (700 MHz, CDCl$_3$) δ 8.18 (dd, J = 6.4 Hz, J = 3.3 Hz, 1H), 8.13 (dd, J = 6.1 Hz, J = 3.6 Hz, 1H), 7.82 (dd, J = 6.4 Hz, J = 3.4 Hz, 2H), 7.68 (dd, J = 7.8 Hz, J = 1.3 Hz, 2H), 7.57–7.53 (m, 3H), 5.30 (dd, J = 4.9 Hz, J = 3.6 Hz, 1H), 3.74 (dd, J = 11.7 Hz, J = 3.4 Hz, 1H), 3.54 (dd, J = 11.7 Hz, 5.1 Hz, 1H) ppm; ^{13}C-NMR (176 MHz, CDCl$_3$) δ 153.7, 152.5, 141.8, 139.6, 137.6, 130.5, 130.4, 129.6, 129.4, 129.0, 128.8, 128.4, 70.6, 65.7 ppm. HRMS (ESI-MS) calcd. for C16H14N2O2 [M + H]$^+$ = 267.1055. Found: 267.1129. The NMR was consistent with previously reported data [57]. The NMR was measured with a Bruker DRX700 (700 MHz).

3.3 General Procedures for the Synthesis of 1,4- and 1,5-Disubstituted Triazoles DPD-Derivatives (Series I and II)

Synthesis of 1-[(*t*-butyldimethylsilyl)oxy]but-3-yn-2-ol (14): to a stirred solution of (*t*-butyldimethylsilyloxy)acetaldehyde (1.0 eq) in dry THF, ethynylmagnesium bromide (0.50 M in THF, 1.3 eq) was added over 15 minutes at 0 °C. After the addition, the reaction was allowed to reach room temperature and stirred for 3 hours. The solvent was removed under reduced pressure, the residue was poured into a cold saturated solution of NH_4Cl and extracted three times with Et_2O. The organic layer was washed twice with water and once with brine, dried over $MgSO_4$, filtered and concentrated in vacuo to yield **14** as a yellow oil, 99%, R_f = 0.55 (CyH/EtOAc 3:1). ^{1}H-NMR (300 MHz, CDCl₃) δ 4.40–4.37 (m, 1H), 3.79 (dd, *J* = 3.8 Hz, *J* = 10.1 Hz, 1H), 3.66 (dd, *J* = 6.8 Hz, *J* = 10.0 Hz, 1H), 2.62 (d, *J* = 5.1 Hz, 1H), 2.42 (d, *J* = 2.2 Hz, 1H), 0.91 (s, 9H), 0.10 (d, *J* = 1.5 Hz, 6H) ppm; ^{13}C-NMR (100 MHz, CDCl₃) δ 81.9, 73.4, 66.8, 62.9, 25.8, 18.3, −5.4 ppm [58].

Synthesis of but-3-yne-1,2-diol (15): to a stirred solution of **14** in MeOH, a Dowex50WX8 100–200 mesh (100 mg/1 mL) was added. The reaction was stirred at room temperature overnight. The mixture was filtered through paper and the solvent was evaporated under reduced pressure to yield **15** as an orange oil, 99%, R_f = 0.50 (CHCl₃/MeOH 9:1). ^{1}H-NMR (300 MHz, CDCl₃) δ 4.49–4.45 (m, 1H), 3.80–3.68 (m, 1H), 2.51 (d, *J* = 2.2 Hz, 1H), 2.31 (s, 2H) ppm; ^{13}C-NMR (100 MHz, CDCl₃) δ 81.5, 74.3, 66.3, 63.0 ppm [59].

Synthesis of 2-ethynyl-1,4-dioxaspiro[4.5]decane (16): to **15** (1.0 eq) cyclohexanone dimethyl ketal (10.0 eq) and a catalytic amount of *p*-TSA were added. The reaction was stirred at room temperature overnight. The solvent was removed under reduced pressure and the crude was re-dissolved in Et_2O and washed three times with $NaHCO_3$. The organic layer was dried over $MgSO_4$, filtered and concentrated in vacuo to yield **16** as a yellow oil, 57%, R_f = 0.42 (CyH/EtOAc 9:1). ^{1}H-NMR (300 MHz, CDCl₃) δ 4.71 (dt, *J* = 2.0 Hz, *J* = 6.3 Hz, 1H), 4.16 (dd, *J* = 6.4 Hz, *J* = 8.0 Hz, 1H), 3.94 (dd, *J* = 6.3 Hz, *J* = 8.0 Hz, 1H), 2.48 (d, *J* = 2.0 Hz, 1H), 1.77–1.72 (m, 2H), 1.65–1.59 (m, 6H), 1.42–1.39 (m, 2H) ppm; ^{13}C-NMR (100 MHz, CDCl₃) δ 111.2, 81.6, 73.7, 69.5, 64.9, 35.6, 25.0, 23.8 ppm [30]

General procedure for the synthesis of 17a–f: to a stirred suspension of NaN_3 (1.5 eq) in DMSO (5 mL), the corresponding bromo compound (1.0 eq) was added. The reaction was stirred at room temperature overnight. The mixture was diluted with diethyl ether and extracted five times with water and once with brine, dried over $MgSO_4$, filtered and concentrated in vacuo to yield the desired azide as a colorless/yellowish oil.

General procedure for the synthesis of 18a–f: to a stirred solution of **15** (1.0 eq) in a 1:1 mixture of H_2O/*t*-BuOH, the corresponding azide (1.0 eq), sodium ascorbate (0.5 eq) and $CuSO_4·5H_2O$ (5% mol) were added. The reaction was stirred at room temperature overnight. The solvent was evaporated under reduced pressure, the crude was redissolved in ACN (1 mL), filtered and purified by preparative HPLC [49].

1-[1-(2-Phenylethyl)-1H-1,2,3-triazol-4-yl]ethane-1,2-diol (**18a**): orange oil, 89%, R_f = 0.24 (CHCl₃/MeOH 9:1), UHPLC-ESI-MS: R_t = 1.80, *m/z* = 234.2 [M + H]⁺. ^{1}H-NMR (300 MHz, CD₃CN) δ 7.56 (s, 1H), 7.31–7.20 (m, 3H), 7.15 (d, *J* = 6.7 Hz, 2H), 4.75 (dd, *J* = 4.3 Hz, *J* = 6.7 Hz, 1H), 4.57 (t, *J* = 7.3 Hz, 2H), 3.72 (dd, *J* = 4.2 Hz, *J* = 11.2 Hz, 1H), 3.60 (dd, *J* = 6.9 Hz, *J* = 11.2 Hz, 1H), 3.17 (t, *J* = 7.2 Hz, 2H), 2.23 (s br, 1H) ppm; ^{13}C-NMR (100 MHz, CD₃CN) δ 149.4, 138.8, 129.7, 129.4, 127.6, 122.8, 68.5, 66.8, 51.9, 36.9 ppm.

1-(1-Benzyl-1H-1,2,3-triazol-4-yl)ethane-1,2-diol (**18b**): yellowish oil, 60%, R_f = 0.24 (CHCl₃/MeOH 9:1), UHPLC-ESI-MS: R_t = 1.70, *m/z* = 220.2 [M + H]⁺. ^{1}H-NMR (300 MHz, CD₃CN) δ 7.72 (s, 1H), 7.38–7.29 (m, 5H), 5.51 (s, 2H), 4.79 (dd, *J* = 4.4 Hz, *J* = 6.3 Hz, 1H), 3.75 (dd, *J* = 4.2 Hz, *J* = 11.2 Hz, 1H), 3.64 (dd, *J* = 6.7 Hz, *J* = 11.2 Hz, 1H) ppm; ^{13}C-NMR (100 MHz, CD₃CN) δ 150.1, 136.9, 129.8, 129.3, 128.9, 123.0, 68.5, 66.7, 54.4 ppm.

1-{1-[.2-(2-Fluorophenyl)ethyl]-1H-1,2,3-triazol-4-yl}ethane-1,2-diol (**18c**): colorless oil, 62%, R_f = 0.49 (CHCl₃/MeOH 9:1), UHPLC-ESI-MS: R_t = 1.82, *m/z* = 252.2 [M + H]⁺. ^{1}H-NMR (300 MHz, CD₃CN) δ 7.58 (s, 1H), 7.30–7.23 (m, 1H), 7.14–7.04(m, 3H), 4.75(dd, *J* = 4.3 Hz, *J* = 6.8 Hz, 1H), 4.58 (t, *J* = 7.1 Hz, 2H), 3.71 (dd, *J* = 4.2 Hz, *J* = 11.2 Hz, 1H), 3.59 (dd, *J* = 6.9 Hz, *J* = 11.2 Hz, 1H), 3.21 (t, *J* = 7.1 Hz, 2H), 2.23 (s br, 1H) ppm; ^{13}C-NMR (100 MHz, CD₃CN) δ 162.8 (d, *J* = 243.8 Hz), 150.2, 132.9 (d, *J* = 4.6 Hz), 130.6 (d, *J* = 8.2 Hz), 126.2, 126.0 (d, *J* = 3.5 Hz), 123.6, 116.8 (d, *J* = 22.0 Hz), 69.2, 67.5, 51.2, 31.3 (d, *J* = 2.4 Hz) ppm.

1-{1-[2-(Pyridin-2-yl)ethyl]-1H-1,2,3-triazol-4-yl}ethane-1,2-diol (**18d**): yellow oil, 88%, R_f = 0.28 (CHCl₃/MeOH 9:1), UHPLC-ESI-MS: R_t = 0.38, *m/z* = 232.2 [M + H]⁺. ¹H-NMR (300 MHz, CD₃CN) δ 8.51 (s, 1H), 7.66–7.59 (m, 2H), 7.21–7.12 (m, 2H), 4.75 (t, *J* = 7.1 Hz, 3H), 3.71 (dd, *J* = 4.1 Hz, *J* = 11.2 Hz, 1H), 3.59 (dd, *J* = 6.8 Hz, *J* = 11.1 Hz, 1H), 3.33 (t, *J* = 7.1 Hz, 2H) ppm; ¹³C-NMR (100 MHz, CD₃CN) δ 158.5, 150.3, 143.3, 137.5, 124.4, 123.2, 122.8, 68.5, 66.8, 50.0, 38.8 ppm.

6-[4-(1,2-Dihydroxyethyl)-1H-1,2,3-triazol-1-yl]hexanenitrile (**18e**): orange oil, 72%, R_f = 0.54 (CHCl₃/MeOH 9:1), UHPLC-ESI-MS: R_t = 1.39, *m/z* = 225.2 [M + H]⁺. ¹H-NMR (300 MHz, CD₃CN) δ 7.68 (s, 1H), 4.78 (s, 1H), 4.34 (dt, *J* = 1.9 Hz, *J* = 7.1 Hz, 2H), 3.76–3.73 (m, 1H), 3.66–3.57 (m, 1H), 3.08 (s br, 1H), 2.37 (dt, *J* = 1.9 Hz, *J* = 7.1 Hz, 2H), 1.88–1.83 (m, 2H), 1.68–1.58 (m, 2H), 1.44–1.34 (m, 2H) ppm; ¹³C-NMR (100 MHz, CD₃CN) δ 148.4, 121.5, 119.8, 67.3, 65.6, 49.2, 28.8, 24.9, 24.2, 16.0 ppm.

1-[1-(2-Cyclohexylethyl)-1H-1,2,3-triazol-4-yl]ethane-1,2-diol (**18f**): orange oil, 73%, R_f = 0.43 (CHCl₃/MeOH 9:1), UHPLC-ESI-MS: R_t = 2.20, *m/z* = 240.2 [M + H]⁺. ¹H-NMR (300 MHz, CD₃CN) δ 7.69 (s, 1H), 4.78 (t, *J* = 5.3 Hz, 1H), 4.35 (t, *J* = 7.5 Hz, 2H), 3.74 (s, 1H), 3.67–3.62 (m, 1H), 2.21 (s br, 1H), 1.78–1.63 (m, 7H), 1.24–1.17 (m, 4H), 1.0–0.94 (m, 2H) ppm; ¹³C-NMR (100 MHz, CD₃CN) δ 150.4, 123.5, 69.2, 67.5, 49.4, 39.0, 36.4, 34.2, 27.8, 27.5 ppm.

Synthesis of 1-[1-(2-phenylethyl)-1*H*-1,2,3-triazol-5-yl]ethane-1,2-diol (19a): to a stirred solution of **15** (1.0 eq) in 1,4-dioxane, (2-azidoethyl)benzene (**17a**) (1.0 eq) and Cp*RuCl(PPh₃)₂ (2% mol) were added. The reaction was stirred at reflux overnight. The solvent was evaporated under reduced pressure, the crude was re-dissolved in ACN (1 mL), filtered and purified by preparative HPLC to yield **19a** as a yellow solid, 87%, R_f = 0.17 (CHCl₃/MeOH 9:1), UHPLC-ESI-MS: R_t = 1.75, *m/z* = 234.2 [M + H] ⁺. ¹H-NMR (300 MHz, CD₃CN) δ 7.51 (s, 1H), 7.28 (t, *J* = 7.3 Hz, 2H), 7.23 (t, *J* = 7.3 Hz, 1H), 7.15 (d, *J* = 7.1 Hz, 2H), 4.62 (d, *J* = 6.3 Hz, 1H), 4.61–4.58 (m, 2H), 3.70 (s br, 1H), 3.62 (dd, *J* = 6.6 Hz, *J* = 11.3 Hz, 1H), 3.56 (dd, *J* = 4.9 Hz, *J* = 11.3 Hz, 1H), 3.21 (t, *J* = 7.4 Hz, 2H), 2.21 (s, 1H) ppm; ¹³C-NMR (100 MHz, CD₃CN) δ 139.0, 138.5, 132.1, 129.7, 129.4, 127.6, 65.5 (d, *J* = 7.6 Hz), 50.4, 37.0 ppm.

Synthesis of 4-{1,4-dioxaspiro[4.5]decan-2-yl}-1*H*-1,2,3-triazole (20): to a stirred solution of **16** (1.0 eq) in a 1:1 mixture of H₂O/*t*-BuOH, trimethylsilyl azide (10.0 eq), sodium ascorbate (0.5 eq) and CuSO₄·5H₂O (5% mol) were added. The reaction was stirred at room temperature overnight. The solvent was evaporated under reduced pressure, the crude was re-dissolved in EtOAc and extracted three times with water. The organic layer was dried over MgSO₄, filtered and concentrated in vacuo. The crude was purified using CyH/TBME (3:1) as an eluent to yield 20 as a yellowish oil, 36%, R_f = 0.61 (CHCl₃/MeOH 9:1), UHPLC-ESI-MS: R_t = 2.13, *m/z* = 210.2 [M + H] ⁺. ¹H-NMR (300 MHz, CD₃CN) δ 7.72 (s, 1H), 5.25 (t, *J* = 6.6 Hz, 1H), 4.31–4.26 (m, 1H), 4.00–3.95 (m, 1H), 2.37 (s br, 1–1.58 (m, 8H), 1.43–1.40 (m, 2H) ppm; ¹³C-NMR (100 MHz, CD₃CN) δ 147.4, 130.0, 111.1, 70.9, 69.8, 36.8, 35.9, 25.8, 24.7, 24.6 ppm.

General procedure for the synthesis of 21h–k and 22h–k: to a stirred solution of **20** (1.0 eq) in dry THF, K₂CO₃ (2.0 eq) and the corresponding alkyl halide (bromide or iodide) were added. The reaction was stirred at reflux overnight. The solvent was evaporated under reduced pressure, the crude was re-dissolved in ACN (1 mL), filtered and purified by preparative HPLC.

For each compound, two different fractions were isolated corresponding to the 1,4- and 1,5-disubstitued products. The different substitution was determined by HMBC of two representative samples (**21i, 22i**).

General procedure for the synthesis of 18g–k and 19h–k: a stirred solution of **20** (or **21h–k**, or **22h–k**) in 1,4-dioxane was cooled to 0 °C using an ice bath. A catalytic amount of 12M HCl was added. The reaction was stirred at room temperature overnight. The solvent was evaporated under reduced pressure; the crude was re-dissolved in Et₂O and extracted with water. The aqueous layer was extracted three times with Et₂O and dried in vacuo to yield the corresponding products **18g–k** and **19h–k**.

1-(1H-1,2,3-Triazol-4-yl)ethane-1,2-diol (**18g**): yellowish oil, 98%, R_f = 0.13 (CHCl₃/MeOH 9:1), UHPLC-ESI-MS: R_t = 0.32, *m/z* = 130.3 [M + H]⁺. ¹H-NMR (300 MHz, MeOD) δ 8.38 (s, 1H), 5.05 (t, *J* = 5.5 Hz, 1H), 3.86–3.74 (m, 2H) ppm; ¹³C-NMR (100 MHz, MeOD) δ 146.0, 126.4, 67.0, 66.2 ppm.

1-(1-Methyl-1H-1,2,3-triazol-4-yl)ethane-1,2-diol (**18h**): colorless oil, 66%, R_f = 0.29 (CHCl₃/MeOH 9:1), UHPLC-ESI-MS: R_t = 0.45, m/z = 144.2 [M + H]⁺. ¹H-NMR (300 MHz, MeOD) δ 8.40 (s, 1H), 5.04 (t, *J* = 5.5 Hz, 1H), 4.35 (s, 3H), 3.94–3.80 (m, 2H) ppm; ¹³C-NMR (100 MHz, MeOD) δ 151.9, 133.5, 70.0, 68.2, 42.9 ppm.

1-(1-Methyl-1H-1,2,3-triazol-5-yl)ethane-1,2-diol (**19h**): colorless oil, 65%, R_f = 0.32 (CHCl₃/MeOH 9:1), UHPLC-ESI-MS: R_t = 0.65, m/z = 144.1 [M + H]⁺. ¹H-NMR (300 MHz, MeOD) δ 7.60 (s, 1H), 4.81 (dd, *J* = 4.8 Hz, *J* = 6.8 Hz, 1H), 4.13 (s, 3H), 3.81–3.68 (m, 2H) ppm; ¹³C-NMR (100 MHz, MeOD) δ 150.6, 133.4, 68.7, 67.0, 41.7 ppm.

1-[1-(Cyclopropylmethyl)-1H-1,2,3-triazol-4-yl]ethane-1,2-diol (**18i**): colorless oil, 73%, R_f = 0.32 (CHCl₃/MeOH 9:1), UHPLC-ESI-MS: R_t = 1.25, m/z = 184.2 [M + H]⁺. ¹H-NMR (300 MHz, CD₃CN) δ 8.29 (d, *J* = 9.1 Hz, 1H), 6.21 (s br, 2H), 5.02 (dd, *J* = 3.9 Hz, *J* = 6.4 Hz, 1H), 4.36 (dd, *J* = 2.5 Hz, *J* = 7.4 Hz, 2H), 3.80 (d, *J* = 5.3 Hz, 2H), 1.40–1.35 (m, 1H), 0.70–0.64 (m, 2H), 0.52–0.47 (m, 2H) ppm; ¹³C-NMR (100 MHz, CD₃CN) δ 146.8, 125.8, 66.9, 65.7, 57.8, 11.1, 4.5 ppm.

1-[1-(Cyclopropylmethyl)-1H-1,2,3-triazol-5-yl]ethane-1,2-diol (**19i**): colorless oil, 77%, R_f = 0.35 (CHCl₃/MeOH 9:1), UHPLC-ESI-MS: R_t = 1.31, m/z = 184.2 [M + H]⁺. ¹H-NMR (300 MHz, CD₃CN) δ 7.87 (s, 1H), 4.91 (t, *J* = 5.5 Hz, 1H), 4.34 (d, *J* = 7.3 Hz, 2H), 3.76 (d, *J* = 5.5 Hz, 2H), 1.43–1.38 (m, 1H), 0.64–0.58 (m, 2H), 0.49–0.46 (m, 2H) ppm; ¹³C-NMR (100 MHz, CD₃CN) δ 140.3, 130.7, 65.5, 65.4, 55.2, 11.7, 4.6 ppm.

1-(1-Butyl-1H-1,2,3-triazol-4-yl)ethane-1,2-diol (**18j**): colorless oil, 85%, R_f = 0.37 (CHCl₃/MeOH 9:1), UHPLC-ESI-MS: R_t = 1.45, m/z = 186.2 [M + H]⁺. ¹H-NMR (300 MHz, MeOD) δ 8.28 (s, 1H), 4.77 (t, *J* = 5.5 Hz, 1H), 4.39 (t, *J* = 7.2 Hz, 2H), 3.63–3.49 (m, 2H), 1.81–1.71(m, 2H), 1.23–1.11 (m, 2H), 0.76 (t, *J* = 7.4 Hz, 3H) ppm; ¹³C-NMR (100 MHz, MeOD) δ 147.5, 126.7, 67.2, 66.1, 53.8, 32.6, 20.5, 13.7 ppm.

1-(1-Butyl-1H-1,2,3-triazol-5-yl)ethane-1,2-diol (**19j**): colorless oil, 95%, R_f = 0.39 (CHCl₃/MeOH 9:1), UHPLC-ESI-MS: R_t = 1.50, m/z = 186.2 [M + H]⁺. ¹H-NMR (300 MHz, MeOD) δ 8.21 (s, 1H), 4.98 (t, *J* = 5.7 Hz, 1H), 4.62 (dd, *J* = 6.5 Hz, *J* = 8.4 Hz, 2H), 3.91–3.78 (m, 2H), 2.04–1.94 (m, 2H), 1.49–1.37 (m, 2H), 1.00 (t, *J* = 7.3 Hz, 3H) ppm; ¹³C-NMR (100 MHz, MeOD) δ 142.7, 130.1, 65.9, 65.8, 51.5, 32.8, 20.7, 13.8 ppm.

1-[1-(2-Ethoxyethyl)-1H-1,2,3-triazol-4-yl]ethane-1,2-diol (**18k**): colorless oil, 91%, R_f = 0.31 (CHCl₃/MeOH 9:1), UHPLC-ESI-MS: R_t = 1.21, m/z = 202.2 [M + H]⁺. ¹H-NMR (300 MHz, CD₃CN) δ 7.92 (s, 1H), 4.89 (t, *J* = 5.1 Hz, 1H), 4.54 (t, *J* = 5.1 Hz, 2H), 3.83–3.68 (m, 4H), 3.47 (q, *J* = 7.0 Hz, 2H), 1.10 (t, *J* = 7.0 Hz, 3H) ppm; ¹³C-NMR (100 MHz, CD₃CN) δ 148.3, 124.9, 68.8, 67.7, 66.9, 66.3, 52.1, 15.2 ppm.

1-[1-(2-Ethoxyethyl)-1H-1,2,3-triazol-4-yl]ethane-1,2-diol (**19k**): colorless oil, 82%, R_f = 0.37 (CHCl₃/MeOH 9:1), UHPLC-ESI-MS: R_t = 1.23, m/z = 202.2 [M + H]⁺. ¹H-NMR (300 MHz, MeOD) δ 8.10 (s, 1H), 5.00 (t, *J* = 5.5 Hz, 1H), 4.74 (dd, *J* = 3.7 Hz, *J* = 5.3 Hz, 2H), 3.84 (t, *J* = 5.2 Hz, 2H), 3.77 (t, *J* = 5.8 Hz, 2H), 3.46–3.38 (m, 2H), 1.05 (t, *J* = 7.0 Hz, 3H) ppm; ¹³C-NMR (100 MHz, MeOD) δ 143.4, 130.3, 69.6, 67.7, 66.0, 65.9, 51.7, 15.3 ppm.

3.4 General Procedures for the Synthesis of 3,5-Disubstituted Isoxazoles DPD Derivatives (Series III and IV)

General procedure for the synthesis of 24l–r: to a stirred solution of the corresponding aldehyde (1.0 eq) in EtOH (10 mL), Et₃N (1.5 eq) and NH₂OH*HCl (1.5 eq) dissolved in water (10 mL) were added. The reaction was stirred at room temperature for 1–3 hours (monitored by TLC). The solvent was evaporated under reduced pressure; the crude was re-dissolved in EtOAc and extracted three times with water. The organic layer was dried over MgSO₄, filtered and concentrated in vacuo to yield the corresponding oxime. All the resulting compounds were used in the next step without being purified.

General procedure for the synthesis of 25l–r: to a stirred solution of the corresponding oxime (1.0 eq) in DMF, *N*-chlorosuccinimide (1.0 eq) was added in two portions. The reaction was stirred at room temperature for 1–2 h (monitored by TLC). The crude was diluted with Et₂O and extracted five times with water and once with brine. The organic layer was dried over MgSO₄, filtered and concentrated in vacuo to

yield the corresponding chloro-oxime. All the resulting compounds were used in the next step without being purified.

General procedure for the synthesis of 26l–r: to a stirred solution of **15** (1.0 eq) in a 1:1 mixture of H_2O/*t*-BuOH, the corresponding chloro-oxime (1.0 eq), sodium ascorbate (0.5 eq), $CuSO_4 \cdot 5H_2O$ (5% mol) and $KHCO_3$ (4.3 eq) were added. The mixture was stirred at room temperature overnight. The solvent was evaporated under reduced pressure; the crude was redissolved in ACN (1 mL), filtered and purified by preparative HPLC [49].

1-[3-(4-Methylphenyl)-1,2-oxazol-5-yl]ethane-1,2-diol (**26l**): white solid, 82%, R_f = 0.38 (CHCl$_3$/MeOH 9:1), UHPLC-ESI-MS: R_t = 2.15, *m/z* = 220.1 [M + H]$^+$. ^{1}H-NMR (300 MHz, CD$_3$CN) δ 7.73 (d, *J* = 8.0 Hz, 2H), 7.31 (d, *J* = 7.9 Hz, 2H), 6.67 (s, 1H), 4.82 (d, *J* = 5.2 Hz, 1H), 3.92 (s br, 1H), 3.83–3.71 (m, 2H), 3.14 (s br, 1H), 2.38 (s, 3H) ppm; ^{13}C-NMR (100 MHz, CD$_3$CN) δ 175.3, 163.7, 142.0, 131.3, 128.2, 127.9, 101.2, 69.2, 66.0, 22.0 ppm.

1-[3-(3-Chlorophenyl)-1,2-oxazol-5-yl]ethane-1,2-diol (**26m**): white solid, 87%, R_f = 0.51 (CHCl$_3$/MeOH 9:1), UHPLC-ESI-MS: R_t = 2.24, *m/z* = 240.0 [M + H]$^+$. ^{1}H-NMR (300 MHz, CD$_3$CN) δ 7.87 (s, 1H), 7.77 (dd, *J* = 5.4 Hz, *J* = 6.8 Hz, 1H), 7.48 (d, *J* = 5.8 Hz, 2H), 6.74 (s, 1H), 4.84 (t, *J* = 5.3 Hz, 1H), 3.78 (dq, *J* = 5.3 Hz, *J* = 11.4 Hz, 2H) ppm; ^{13}C-NMR (100 MHz, CD$_3$CN) δ 175.2, 162.0, 135.4, 132.0, 131.6, 130.9, 127.5, 126.1, 100.8, 68.5, 65.2 ppm.

1-[3-(2,4-Difluorophenyl)-1,2-oxazol-5-yl]ethane-1,2-diol (**26n**): white solid, 78%, R_f = 0.49 (CHCl$_3$/MeOH 9:1), UHPLC-ESI-MS: R_t = 2.06, *m/z* = 242.2 [M + H]$^+$. ^{1}H-NMR (300 MHz, CD$_3$CN) δ 7.97–7.89 (m, 1H), 7.14–7.06 (m, 2H), 6.69 (d, *J* = 3.3 Hz, 1H), 4.86 (t, *J* = 5.3 Hz, 1H), 3.85–3.73 (m, 2H) ppm; ^{13}C-NMR (100 MHz, CD$_3$CN) δ 174.8, 164.9 (dd, *J* = 8.5 Hz, *J* = 246.4 Hz), 161.4 (dd, *J* = 8.5 Hz, *J* = 249.4 Hz), 157.9, 131.6 (dd, *J* = 4.6 Hz, *J* = 10.1 Hz), 114.7 (dd, *J* = 3.9 Hz, *J* = 12.6 Hz), 113.2 (dd, *J* = 3.6 Hz, *J* = 21.9 Hz), 105.6 (t, *J* = 26.1 Hz), 102.7 (d, *J* = 7.4 Hz), 68.5, 65.3 ppm.

1-[3-(Pyridin-3-yl)-1,2-oxazol-5-yl]ethane-1,2-diol (**26o**): orange solid, 71%, R_f = 0.22 (CHCl$_3$/MeOH 9:1), UHPLC-ESI-MS: R_t = 1.14, *m/z* = 207.2 [M + H]$^+$. ^{1}H-NMR (300 MHz, CD$_3$CN) δ 9.04 (s, 1H), 8.67 (s, 1H), 8.18 (d, *J* = 7.9 Hz, 1H), 7.46 (dd, *J* = 5.3 Hz, *J* = 7.2 Hz, 1H), 6.79 (s, 1H), 4.87 (t, *J* = 5.3 Hz, 1H), 3.85–3.73 (m, 2H) ppm; ^{13}C-NMR (100 MHz, CD$_3$CN) δ 175.4, 160.9, 151.9, 148.7, 135.0, 126.2, 124.9, 100.7, 68.5, 65.3 ppm.

1-(3-Cyclopropyl-1,2-oxazol-5-yl)ethane-1,2-diol (**26p**): yellow oil, 63%, R_f = 0.12 (CHCl$_3$/MeOH 9:1), UHPLC-ESI-MS: R_t = 1.91, *m/z* = 170.2 [M + H]$^+$. ^{1}H-NMR (300 MHz, CD$_3$CN) δ 5.98 (s, 1H), 4.71 (ddd, *J* = 0.6 Hz, *J* = 4.6 Hz, *J* = 6.1 Hz, 1H), 3.74–3.62 (m, 2H), 2.00–1.91 (m, 1H), 1.03–0.97 (m, 2H), 0.78–0.72 (m, 2H) ppm; ^{13}C-NMR (100 MHz, CD$_3$CN) δ 173.5, 167.3, 99.7, 68.3, 65.2, 8.3, 7.8 ppm.

1-[3-(Oxolan-3-yl)-1,2-oxazol-5-yl]ethane-1,2-diol (**26q**): yellow oil, 77%, R_f = 0.50 (CHCl$_3$/MeOH 9:1), UHPLC-ESI-MS: R_t = 1.53, *m/z* = 200.2 [M + H]$^+$. ^{1}H-NMR (300 MHz, CD$_3$CN) δ 6.22 (s, 1H), 4.77–4.73 (m, 1H), 4.03–3.98 (m, 1H), 3.94–3.85 (m, 1H), 3.82–3.76 (m, 1H), 3.74–3.65 (m, 2H), 3.55–3.47 (m, 1H), 2.37–2.25 (m, 2H), 2.09–2.00 (m, 1H) ppm; ^{13}C-NMR (100 MHz, CD$_3$CN) δ 174.1, 166.1, 101.2, 72.7, 68.5, 65.3, 63.7, 37.4, 32.5 ppm.

1-(3-Cyclohexyl-1,2-oxazol-5-yl)ethane-1,2-diol (**26r**): yellow oil, 89%, R_f = 0.31 (CHCl$_3$/MeOH 9:1), UHPLC-ESI-MS: R_t = 2.13, *m/z* = 212.2 [M + H]$^+$. ^{1}H-NMR (300 MHz, CD$_3$CN) δ 6.18 (s, 1H), 4.73 (t, *J* = 5.4 Hz, 1H), 3.71 (dq, *J* = 5.4 Hz, *J* = 11.3 Hz, 2H), 2.70 (dt, *J* = 3.3 Hz, *J* = 10.7 Hz, 1H), 2.21 (s br, 2H), 1.90–1.69 (m, 5H), 1.50–1.25 (m, 5H) ppm; ^{13}C-NMR (100 MHz, CD$_3$CN) δ 173.9, 169.8, 101.5, 69.2, 66.0, 37.3, 33.4, 27.3, 27.2 ppm.

Synthesis of ethyl (2*E*)-2-(hydroxyimino)acetate (27): to a stirred solution of ethyl glyoxalate (50% solution in toluene, 1.0 eq) in EtOH, Et$_3$N (1.5 eq) and NH$_2$OH·HCl (1.5 eq) dissolved in water (10 mL) were added. The reaction was stirred at room temperature for 2 hours (monitored by TLC). The solvent was evaporated under reduced pressure; the crude was re-dissolved in Et$_2$O and extracted three times with water. The organic layer was dried over MgSO$_4$, filtered and concentrated in vacuo to yield **27** as a colorless

oil, 84%, R_f = 0.64 (CHCl$_3$/MeOH 9:1). ^{1}H-NMR (300 MHz, CDCl$_3$) δ 9.83 (s br, 1H), 7.56 (s, 1H), 4.32 (q, J = 7.1 Hz, 2H), 1.34 (t, J = 7.1 Hz, 3H) ppm; ^{13}C-NMR (100 MHz, CDCl$_3$) δ 162.4, 141.6, 61.8, 13.8 ppm [60].

Synthesis of ethyl 5-{1,4-dioxaspiro[4.5]decan-2-yl}-1,2-oxazole-3-carboxylate (28): to a stirred solution of **16** (1.0 eq) in THF, **27** (2.0 eq) and NaOCl (40.0 eq portion wise over 12 hours) were added. The reaction was stirred at room temperature for 12 hours. The solvent was evaporated under reduced pressure, the crude was re-dissolved in DCM and washed three times with water. The organic layer was dried over MgSO$_4$, filtered and concentrated in vacuo. The crude was re-dissolved in ACN (1 mL), filtered and purified by preparative HPLC to yield **28** as a yellowish oil, 36%, R_f = 0.57 (CyH/EtOAC 3:1), UHPLC-ESI-MS: R_t = 3.04, m/z = 282.2 [M + H]$^+$. ^{1}H-NMR (300 MHz, CDCl$_3$) δ 6.67 (s, 1H), 5.23 (t, J = 6.0 Hz, 1H), 4.43 (q, J = 7.2 Hz, 2H), 4.35 (dd, J = 6.7 Hz, J = 8.6 Hz, 1H), 4.09 (dd, J = 5.4 Hz, J = 8.6 Hz, 1H), 1.71–1.62 (m, 9H), 1.41 (t, J = 7.1 Hz, 4H) ppm; ^{13}C-NMR (100 MHz, CDCl$_3$) δ 173.5, 159.8, 156.3, 111.9, 102.5, 69.8, 68.1, 62.2, 35.8, 34.9, 25.0, 23.9, 23.8, 14.1 ppm.

Synthesis of 5-{1,4-dioxaspiro[4.5]decan-2-yl}-1,2-oxazole-3-carboxylic acid (30): a stirred solution of **28** in THF was cooled to 0 °C using an ice bath. A solution of 10 M NaOH (5.0 eq) was added dropwise and the reaction was stirred at room temperature overnight. The solvent was evaporated under reduced pressure; the crude was re-dissolved in DCM and extracted with water. The aqueous layer was acidified with 1M HCl until pH = 1 and extracted three times with CHCl$_3$/*i*-PrOH (7:3). The organic layer was dried over MgSO$_4$, filtered and concentrated in vacuo to yield **30** as a white solid, 99%, R_f = 0.17(CHCl$_3$/MeOH 5:1), UHPLC-ESI-MS: R_t = 2.37, m/z = 254.2 [M + H]$^+$. ^{1}H-NMR (300 MHz, CDCl$_3$) δ 6.74 (s, 1H), 5.26 (t, J = 5.9 Hz, 1H), 4.38 (dd, J = 6.6 Hz, J = 8.7 Hz, 1H), 4.12 (dd, J = 5.3 Hz, J = 8.7 Hz, 1H), 1.73–1.60 (m, 8H), 1.47–1.43 (m, 2H) ppm; ^{13}C-NMR (100 MHz, CDCl$_3$) δ 174.2, 162.4, 155.6, 112.1, 102.8, 69.8, 68.1, 35.9, 34.9, 24.9, 23.9, 23.8 ppm.

General procedure for the synthesis of 32b, 32s–z: the reactions were performed in parallel in 15 ml reaction tubes in a 24 position Mettler-Toledo Miniblock® equipped with a heat transfer block and inert gas manifold. Each reaction tube was loaded with a previously prepared solution of 30 mg of **28** (1.0 eq) in 2 mL of DMF, DIPEA (5.0 eq), HOBt (2.0 eq), EDC·HCl (2.5 eq). Then the corresponding amine was added (2.0 eq). The reaction mixtures were stirred at room temperature overnight. The reaction conversion was confirmed through a UHPLC check of some representative samples. The mixtures were evaporated until dryness. The crudes were re-dissolved in 1.0 mL of ACN, filtered and purified with preparative HPLC (gradient acetonitrile/water with 0.1% formic acid, 2–98%).

General procedure for the synthesis of 29, 31, 33b, 33s–z: a stirred solution of **28** (or **30**, or **32b**, or **32s–z**) was cooled to 0 °C using an ice bath. A catalytic amount of concentrated HCl was added. The reactions were stirred at room temperature overnight. The solvent was evaporated under reduced pressure, the crudes were re-dissolved in ACN (1 mL), filtered and purified by preparative HPLC.

Ethyl 5-(1,2-dihydroxyethyl)-1,2-oxazole-3-carboxylate (**29**): colorless oil, 46%, R_f = 0.44 (CHCl$_3$/MeOH 9:1), UHPLC-ESI-MS: R_t = 1.51, m/z = 202.2 [M + H]$^+$. ^{1}H-NMR (300 MHz, CD$_3$CN) δ 6.65 (s, 1H), 4.84 (t, J = 5.3 Hz, 1H), 4.37 (q, J = 7.1 Hz, 2H), 3.76 (dd, J = 4.2 Hz, J = 5.2 Hz, 2H), 2.18 (s br, 1H), 1.35 (t, J = 7.1 Hz, 3H) ppm; ^{13}C-NMR (100 MHz, CD$_3$CN) δ 176.2, 160.8, 157.4, 103.0, 68.3, 65.1, 62.9, 14.3 ppm.

5-(1,2-Dihydroxyethyl)-1,2-oxazole-3-carboxylic acid (**31**): colorless oil, 55%, R_f = 0.11 (CHCl$_3$/MeOH 9:1), UHPLC-ESI-MS: R_t = 0.42, m/z = 174.2 [M + H]$^+$. ^{1}H-NMR (300 MHz, CD$_3$CN) δ 6.65 (s, 1H), 4.84 (t, J = 5.1 Hz, 1H), 3.81–3.70 (m, 2H) ppm; ^{13}C-NMR (100 MHz, CD$_3$CN) δ 176.2, 161.0, 157.2, 103.2, 68.3, 65.1 ppm.

N-Benzyl-5-(1,2-dihydroxyethyl)-1,2-oxazole-3-carboxamide (**33b**): white solid, 58%, R_f = 0.25 (CHCl$_3$/MeOH 9:1), UHPLC-ESI-MS: R_t = 1.89, m/z = 263.2 [M + H]$^+$. ^{1}H-NMR (300 MHz, Acetone-d_6) δ 7.40–7.27 (m, 4H), 7.26–7.22 (m, 1H), 6.68 (s, 1H), 4.91 (t, J = 5.4 Hz, 1H), 4.59 (s, 2H), 3.89–3.78 (m, 2H) ppm; ^{13}C-NMR (100 MHz, Acetone-d_6) δ 177.2, 160.6, 141.0, 137.3, 130.2, 129.4, 128.9, 102.9, 69.5, 66.4, 44.4 ppm.

5-(1,2-Dihydroxyethyl)-N-(4-fluorophenyl)-1,2-oxazole-3-carboxamide (**33s**): white solid, 58%, R_f = 0.25 (CHCl$_3$/MeOH 9:1), UHPLC-ESI-MS: R_t = 1.97, m/z = 267.2 [M + H]$^+$. ^{1}H-NMR (300 MHz, Acetone-d_6) δ 7.92–7.88 (m, 2H), 7.16 (t, J = 8.8 Hz, 2H), 6.76 (s, 1H), 4.95 (t, J = 5.4 Hz, 1H), 3.92–3.81 (m, 2H) ppm; ^{13}C-NMR (100

MHz, Acetone-*d₆*) δ 177.6, 162.8, 159.8 (d, *J* = 133.8 Hz), 159.6, 136.3 (d, *J* = 2.7 Hz), 124.1 (d, *J* = 7.7 Hz), 117.2 (d, *J* = 22.6 Hz), 103.1, 69.5, 66.4 ppm.

5-(1,2-Dihydroxyethyl)-N-[(thiophen-2-yl)methyl]-1,2-oxazole-3-carboxamide (**33t**): white solid, 65%, R_f = 0.34 (CHCl₃/MeOH 9:1), UHPLC-ESI-MS: R_t = 1.79, *m/z* = 269.2 [M + H]⁺. ¹H-NMR (300 MHz, Acetone-*d₆*) δ 8.43 (s br, 0.5H), 7.32 (dd, *J* = 1.3 Hz, *J* = 5.1 Hz, 1H), 7.06 (dd, *J* = 1.1 Hz, *J* = 3.4 Hz, 1H), 6.95 (dd, *J* = 3.5 Hz, *J* = 5.1 Hz, 1H), 6.68 (s, 1H), 4.99 (s br, 0.5H), 4.90 (t, *J* = 5.1 Hz, 1H), 4.77–4.75 (m, 2H), 4.15 (s br, 0.5H), 3.84–3.81 (m, 2H), 2.87 (s br, 0.5H) ppm; ¹³C-NMR (100 MHz, Acetone-*d₆*) δ 177.3, 160.4, 143.6, 141.4, 128.5, 127.8, 126.8, 102.9, 69.6, 66.5, 39.3 ppm.

5-(1,2-Dihydroxyethyl)-N-[(pyridin-3-yl)methyl]-1,2-oxazole-3-carboxamide (**33u**): yellow oil, 37%, R_f = 0.33 (CHCl₃/MeOH 9:1), UHPLC-ESI-MS: R_t = 0.38, *m/z* = 264.2 [M + H]⁺. ¹H-NMR (300 MHz, MeOD) δ 8.56 (s, 1H), 8.44 (s br, 1H), 7.86 (d, *J* = 7.9 Hz, 1H), 7.43 (dd, *J* = 4.9 Hz, *J* = 7.8 Hz, 1H), 6.70 (s, 1H), 4.84 (d, *J* = 5.8 Hz, 1H), 4.59 (s, 1H), 3.80 (dd, *J* = 3.3 Hz, *J* = 5.6 Hz, 2H) ppm; ¹³C-NMR (100 MHz, MeOD) δ 176.6, 161.6, 159.6, 149.6, 149.0, 137.8, 136.5, 125.3, 102.1, 68.8, 65.6, 41.6 ppm.

5-(1,2-Dihydroxyethyl)-N-(2-methoxyethyl)-1,2-oxazole-3-carboxamide (**33v**): yellow oil, 78%, R_f = 0.38 (CHCl₃/MeOH 9:1), UHPLC-ESI-MS: R_t = 1.23, *m/z* = 231.2 [M + H]⁺. ¹H-NMR (300 MHz, Acetone-*d₆*) δ 6.64 (s, 1H), 4.90 (t, *J* = 5.4 Hz, 1H), 3.83 (dd, *J* = 3.6 Hz, *J* = 5.4 Hz, 2H), 3.58–3.50 (m, 4H), 3.32 (s, 3H), 2.85 (s br, 2H) ppm; ¹³C-NMR (100 MHz, Acetone-*d₆*) δ 177.3, 160.5, 147.7, 102.8, 72.4, 69.6, 66.5, 59.6, 40.5 ppm.

1-[3-(Pyrrolidine-1-carbonyl)-1,2-oxazol-5-yl]ethane-1,2-diol (**33z**): yellow oil, 79%, R_f = 0.30 (CHCl₃/MeOH 9:1), UHPLC-ESI-MS: R_t = 1.51, *m/z* = 227.2 [M + H] ⁺. ¹H-NMR (300 MHz, Acetone-*d₆*) δ 6.58 (s, 1H), 4.90 (t, *J* = 5.3 Hz, 1H), 3.83 (t, *J* = 5.1 Hz, 2H), 3.76 (t, *J* = 6.6 Hz, 2H), 3.54 (t, *J* = 6.6 Hz, 2H), 2.84 (s br, 2H), 1.99–1.89 (m, 4H) ppm; ¹³C-NMR (100 MHz, Acetone-*d₆*) δ 175.8, 161.7, 149.6, 104.2, 69.6, 66.6, 50.0, 48.2, 27.8, 25.5 ppm.

3.5 Biology

All chemicals were purchased from Sigma (Hamburg, Germany) if not otherwise stated. (*S*)-DPD was purchased from OMM Scientific (Dallas, TX, USA). The ATP Bioluminescence kit CLS II and Kinase Glo Luminescence assay kit were respectively purchased from Roche Scientific (Manheim, Germany) and Promega (Madison, WI, USA)

3.5.1 LsrK Overexpression and Purification

E. coli MET1158 (*E. coli*, amp resistance, BL21 (DE3) luxS-, with pMET1144 (lsrK-His in pET21b)), kindly donated by Prof. Karina Xavier (Instituto Gulbenkian de Ciência, Portugal) [61], was used for the overexpression of LsrK from *S. typhimurium*. The bacteria were grown overnight in 2 × YPTG (yeast, tryptone, phosphate buffer and glucose) mediums supplemented with 100 μg/ml ampicillin. At the exponential phase, protein expression was induced by the addition of 0.1 mM isopropyl β-D-1 thiogalactopyranoside for 9h at 22 °C (250 rpm). Cells were harvested and frozen overnight before proceeding with lysis and purification, according to the literature [62].

3.5.2 DPD Activity Evaluation

Phosphorylation of DPD by LsrK was evaluated with a bioluminescence-based assay, ATP Bioluminescence kit CLSII (Roche) as previously described in Reference [61]. DPD was plated at 200 μM and 400 μM and a reaction mixture containing 200 nM Lsrk and 20 μM ATP in assay buffer (25 mM triethanolamine, pH 7.4, 200 μM MgCl₂). Commercially available DPD was tested for comparison at 200 μM. The level of ATP was monitored by the ATP Bioluminescence kit CLSII following the manufacturer´s instructions. The experiment was performed in the kinetic-mode, monitoring the luminescence every 2 min

within a time window of 30 min at the Varioskan LUX plate reader (Thermo Fisher Scientific, Vantaa, Finland).

3.5.3 Screening of DPD-Related Compounds

The activity of DPD-related compounds was evaluated in an LsrK inhibition assay. Compounds were plated in a 384 well-plate to a final concentration of 200 μM in triplicate. A 300 nM LsrK and 300 μM DPD diluted in an assay buffer (25 mM triethanolamine, pH 7.4, 200 μM MgCl$_2$, 0.1 mg/mL BSA) were added to the plate followed by 100 μM ATP to start the reaction. After 15 minutes of reaction, the Kinase Glo Luminescence assay reagent was added according to the manufacturer´s instructions. The experiment was carried on in end-point mode and the luminescence was recorded at the Varioskan LUX plate reader.

4. Conclusions

Resistance to antibiotics poses a continuous threat to public health. In the last few decades, receptors able to modulate QS started to be considered interesting targets for anti-infective therapy and the modulation/inhibition of QS has become an appealing strategy against bacterial resistance. Several studies have already shown that interference with QS affects biofilm formation and biofilm properties (e.g., thickness, mass). Particularly, DPD, the key compound in the biosynthesis of AI-2, is able to modulate QS in both Gram-negative and Gram-positive bacteria. Accordingly, DPD-analogs may have great potential as QSI and, therefore, as antimicrobial drugs. Of note, two different DPD-related compounds (i.e. isobutyl-DPD and phenyl-DPD) in combination with gentamicin have almost completely cleared the pre-existing biofilms in *E. coli* and *P. aeruginosa*, respectively [63].

In this work, we successfully developed a new short and robust strategy for the synthesis of DPD which requires only one purification step. Ph-DPD was also synthesized to show the applicability of our protocol to the production of different C$_1$-DPD analogs. The new strategy inspired the synthesis of 30 novel DPD-related compounds: the cycloaddition to two common precursors was employed to produce (in maximum four steps) four different small libraries where the diketo moiety of DPD was embedded in heteroaromatic rings. All the designed compounds were purified and characterized by ^{1}H-NMR, ^{13}C-NMR, and UHPLC-MS (purity > 90%). It is worth noting that in these compounds the open/closed equilibrium (typical of the majority of the DPD-analogs reported so far, Figure 1) is not possible. The so-obtained more stable compounds were easily purify by column chromatography. Moreover, the presence of heteroaromatic groups increases the UV absorbance and MW, rendering the compound detection by the classical analytical method (e.g., LC-MS) easier compared to previously reported analogs (e.g., ethyl-DPD).

Our new synthetic approach allowed us to synthetize a small set of racemic DPD-related compounds in a relatively easy and fast way. We demonstrated that racemic DPD is efficiently phosphorylated by LsrK, corroborating the validity of our approach. On the other hand, all compounds of our library of DPD-related did not show any activity on LsrK. Nevertheless, the synthetic procedure herein proposed might lead to the preparation of a wider compound library, thus, allowing for the discovery of a new class of LsrK inhibitors as potential antivirulence agents. Moreover, we decided to add these products to the library of MuTaLig, an innovative ligand identification platform for the drug-discovery process.

Supplementary Materials: Supplementary materials are available online.

Author Contributions:

Conceptualization, S.S., F.G and S.C.; Methodology, S.S., F.G.; Formal Analysis, F.M., M.P.; Investigation, S.S., V.G., M.P., F.G., S.C., P.T.; Resources, D.T., P.T.; Writing-Original Draft Preparation, S.S., V.G., P.T.; Writing-Review & Editing, S.S., F.G., P.T., S.C.; Supervision, S.C.; Project Administration, A.K., D.T.; Funding Acquisition, F.G., D.T.

References

1. Surette, M. G.; Miller, M. B.; Bassler, B. L. Quorum sensing in Escherichia coli, Salmonella typhimurium, and Vibrio harveyi: a new family of genes responsible for autoinducer production. *Proc. Natl. Acad. Sci. U.S.A.* **1999**, *96*, 1639–1644.
2. Waters, C. M.; Bassler, B. L. Quorum sensing: cell-to-cell communication in bacteria. *Annu. Rev. Cell Dev. Biol.* **2005**, *21*, 319–346, doi:10.1146/annurev.cellbio.21.012704.131001.
3. Bassler, B. L.; Losick, R. Bacterially speaking. *Cell* **2006**, *125*, 237–246, doi:10.1016/j.cell.2006.04.001.
4. Lowery, C. A.; Dickerson, T. J.; Janda, K. D. Interspecies and interkingdom communication mediated by bacterial quorum sensing. *Chem Soc Rev* **2008**, *37*, 1337–1346, doi:10.1039/b702781h.
5. Ng, W.-L.; Bassler, B. L. Bacterial Quorum-Sensing Network Architectures. *Annual Review of Genetics* **2009**, *43*, 197–222, doi:10.1146/annurev-genet-102108-134304.
6. Zhu, J.; Miller, M. B.; Vance, R. E.; Dziejman, M.; Bassler, B. L.; Mekalanos, J. J. Quorum-sensing regulators control virulence gene expression in Vibrio cholerae. *PNAS* **2002**, *99*, 3129–3134, doi:10.1073/pnas.052694299.
7. Antunes, L. C. M.; Ferreira, R. B. R.; Buckner, M. M. C.; Finlay, B. B. Quorum sensing in bacterial virulence. *Microbiology* **2010**, *156*, 2271–2282, doi:10.1099/mic.0.038794-0.
8. Ahmed, N. A. A. M.; Petersen, F. C.; Scheie, A. A. AI-2 quorum sensing affects antibiotic susceptibility in Streptococcus anginosus. *J Antimicrob Chemother* **2007**, *60*, 49–53, doi:10.1093/jac/dkm124.
9. Davies, D. G.; Parsek, M. R.; Pearson, J. P.; Iglewski, B. H.; Costerton, J. W.; Greenberg, E. P. The involvement of cell-to-cell signals in the development of a bacterial biofilm. *Science* **1998**, *280*, 295–298.
10. Rickard, A. H.; Palmer, R. J.; Blehert, D. S.; Campagna, S. R.; Semmelhack, M. F.; Egland, P. G.; Bassler, B. L.; Kolenbrander, P. E. Autoinducer 2: a concentration-dependent signal for mutualistic bacterial biofilm growth. *Mol. Microbiol.* **2006**, *60*, 1446–1456, doi:10.1111/j.1365-2958.2006.05202.x.
11. Irie, Y.; Parsek, M. R. Quorum sensing and microbial biofilms. *Curr. Top. Microbiol. Immunol.* **2008**, *322*, 67–84.
12. Smith, K. M.; Bu, Y.; Suga, H. Library screening for synthetic agonists and antagonists of a Pseudomonas aeruginosa autoinducer. *Chem. Biol.* **2003**, *10*, 563–571.
13. Suga, H.; Smith, K. M. Molecular mechanisms of bacterial quorum sensing as a new drug target. *Current Opinion in Chemical Biology* **2003**, *7*, 586–591, doi:10.1016/j.cbpa.2003.08.001.
14. Geske, G. D.; Wezeman, R. J.; Siegel, A. P.; Blackwell, H. E. Small Molecule Inhibitors of Bacterial Quorum Sensing and Biofilm Formation. *J. Am. Chem. Soc.* **2005**, *127*, 12762–12763, doi:10.1021/ja0530321.
15. Rasmussen, T. B.; Givskov, M. Quorum-sensing inhibitors as anti-pathogenic drugs. *International Journal of Medical Microbiology* **2006**, *296*, 149–161, doi:10.1016/j.ijmm.2006.02.005.
16. Geske, G. D.; O'Neill, J. C.; Miller, D. M.; Mattmann, M. E.; Blackwell, H. E. Modulation of Bacterial Quorum Sensing with Synthetic Ligands: Systematic Evaluation of *N* -Acylated Homoserine Lactones in Multiple Species and New Insights into Their Mechanisms of Action. *Journal of the American Chemical Society* **2007**, *129*, 13613–13625, doi:10.1021/ja074135h.
17. Clatworthy, A. E.; Pierson, E.; Hung, D. T. Targeting virulence: a new paradigm for antimicrobial therapy. *Nat. Chem. Biol.* **2007**, *3*, 541–548, doi:10.1038/nchembio.2007.24.
18. Meijler, M. M.; Hom, L. G.; Kaufmann, G. F.; McKenzie, K. M.; Sun, C.; Moss, J. A.; Matsushita, M.; Janda, K. D. Synthesis and Biological Validation of a Ubiquitous Quorum-Sensing Molecule. *Angewandte Chemie International Edition* **2004**, *43*, 2106–2108, doi:10.1002/anie.200353150.
19. Globisch, D.; Lowery, C. A.; McCague, K. C.; Janda, K. D. Uncharacterized 4,5-Dihydroxy-2,3-Pentanedione (DPD) Molecules Revealed Through NMR Spectroscopy: Implications for a Greater

Signaling Diversity in Bacterial Species. *Angewandte Chemie International Edition* **2012**, *51*, 4204–4208, doi:10.1002/anie.201109149.

20. Chen, X.; Schauder, S.; Potier, N.; Van Dorsselaer, A.; Pelczer, I.; Bassler, B. L.; Hughson, F. M. Structural identification of a bacterial quorum-sensing signal containing boron. *Nature* **2002**, *415*, 545–549, doi:10.1038/415545a.

21. Miller, S. T.; Xavier, K. B.; Campagna, S. R.; Taga, M. E.; Semmelhack, M. F.; Bassler, B. L.; Hughson, F. M. Salmonella typhimurium recognizes a chemically distinct form of the bacterial quorum-sensing signal AI-2. *Mol. Cell* **2004**, *15*, 677–687, doi:10.1016/j.molcel.2004.07.020.

22. Zhu, J.; Hixon, M. S.; Globisch, D.; Kaufmann, G. F.; Janda, K. D. Mechanistic Insights into the LsrK Kinase Required for Autoinducer-2 Quorum Sensing Activation. *J. Am. Chem. Soc.* **2013**, *135*, 7827–7830, doi:10.1021/ja4024989.

23. Ha, J.-H.; Eo, Y.; Grishaev, A.; Guo, M.; Smith, J. A. I.; Sintim, H. O.; Kim, E.-H.; Cheong, H.-K.; Bentley, W. E.; Ryu, K.-S. Crystal Structures of the LsrR Proteins Complexed with Phospho-AI-2 and Two Signal-Interrupting Analogues Reveal Distinct Mechanisms for Ligand Recognition. *Journal of the American Chemical Society* **2013**, *135*, 15526–15535, doi:10.1021/ja407068v.

24. Penesyan, A.; Gillings, M.; Paulsen, I. T. Antibiotic discovery: combatting bacterial resistance in cells and in biofilm communities. *Molecules* **2015**, *20*, 5286–5298, doi:10.3390/molecules20045286.

25. Kociolek, M. Quorum-Sensing Inhibitors and Biofilms. *Anti-Infective Agents in Medicinal Chemistry* **2009**, *8*, 315–326, doi:10.2174/187152109789760117.

26. Brackman, G.; Coenye, T. Quorum sensing inhibitors as anti-biofilm agents. *Curr. Pharm. Des.* **2015**, *21*, 5–11.

27. Xavier, K. B.; Bassler, B. L. Regulation of uptake and processing of the quorum-sensing autoinducer AI-2 in Escherichia coli. *J. Bacteriol.* **2005**, *187*, 238–248, doi:10.1128/JB.187.1.238-248.2005.

28. Semmelhack, M. F.; Campagna, S. R.; Federle, M. J.; Bassler, B. L. An Expeditious Synthesis of DPD and Boron Binding Studies. *Organic Letters* **2005**, *7*, 569–572, doi:10.1021/ol047695j.

29. De Keersmaecker, S. C. J.; Varszegi, C.; van Boxel, N.; Habel, L. W.; Metzger, K.; Daniels, R.; Marchal, K.; De Vos, D.; Vanderleyden, J. Chemical synthesis of (S)-4,5-dihydroxy-2,3-pentanedione, a bacterial signal molecule precursor, and validation of its activity in Salmonella typhimurium. *J. Biol. Chem.* **2005**, *280*, 19563–19568, doi:10.1074/jbc.M412660200.

30. Lowery, C. A.; Park, J.; Kaufmann, G. F.; Janda, K. D. An Unexpected Switch in the Modulation of AI-2-Based Quorum Sensing Discovered through Synthetic 4,5-Dihydroxy-2,3-pentanedione Analogues. *Journal of the American Chemical Society* **2008**, *130*, 9200–9201, doi:10.1021/ja802353j.

31. Kadirvel, M.; Stimpson, W. T.; Moumene-Afifi, S.; Arsic, B.; Glynn, N.; Halliday, N.; Williams, P.; Gilbert, P.; McBain, A. J.; Freeman, S.; Gardiner, J. M. Synthesis and bioluminescence-inducing properties of autoinducer (S)-4,5-dihydroxypentane-2,3-dione and its enantiomer. *Bioorganic & Medicinal Chemistry Letters* **2010**, *20*, 2625–2628, doi:10.1016/j.bmcl.2010.02.064.

32. Ascenso, O. S.; Marques, J. C.; Santos, A. R.; Xavier, K. B.; Rita Ventura, M.; Maycock, C. D. An efficient synthesis of the precursor of AI-2, the signalling molecule for inter-species quorum sensing. *Bioorganic & Medicinal Chemistry* **2011**, *19*, 1236–1241, doi:10.1016/j.bmc.2010.12.036.

33. Guo, M.; Gamby, S.; Zheng, Y.; Sintim, H. Small Molecule Inhibitors of AI-2 Signaling in Bacteria: State-of-the-Art and Future Perspectives for Anti-Quorum Sensing Agents. *International Journal of Molecular Sciences* **2013**, *14*, 17694–17728, doi:10.3390/ijms140917694.

34. Frezza, M.; Soulère, L.; Queneau, Y.; Doutheau, A. A Baylis–Hillman/ozonolysis route towards (±) 4,5-dihydroxy-2,3-pentanedione (DPD) and analogues. *Tetrahedron Letters* **2005**, *46*, 6495–6498, doi:10.1016/j.tetlet.2005.07.102.

35. Smith, J. A. I.; Wang, J.; Nguyen-Mau, S.-M.; Lee, V.; Sintim, H. O. Biological screening of a diverse set of AI-2 analogues in Vibrio harveyi suggests that receptors which are involved in synergistic agonism of AI-2 and analogues are promiscuous. *Chemical Communications* **2009**, 7033, doi:10.1039/b909666c.

36. Rossi, D.; Tarantino, M.; Rossino, G.; Rui, M.; Juza, M.; Collina, S. Approaches for multi-gram scale isolation of enantiomers for drug discovery. *Expert Opin Drug Discov* **2017**, *12*, 1253–1269, doi:10.1080/17460441.2017.1383981.

37. Paterson, I.; Delgado, O.; Florence, G. J.; Lyothier, I.; O'Brien, M.; Scott, J. P.; Sereinig, N. A second-generation total synthesis of (+)-discodermolide: the development of a practical route using solely substrate-based stereocontrol. *J. Org. Chem.* **2005**, *70*, 150–160, doi:10.1021/jo048534w.

38. Peyton, L. R.; Gallagher, S.; Hashemzadeh, M. Triazole antifungals: a review. *Drugs Today* **2015**, *51*, 705–718, doi:10.1358/dot.2015.51.12.2421058.

39. Lal, K.; Yadav, P. Recent Advancements in 1,4-Disubstituted 1H-1,2,3-Triazoles as Potential Anticancer Agents. *Anticancer Agents Med Chem* **2018**, *18*, 21–37, doi:10.2174/1871520616666160811113531.

40. -H. Zhou, C.; Zhou, C.-H.; Wang, Y. Recent Researches in Triazole Compounds as Medicinal Drugs. *Current Medicinal Chemistry 19*, 239–280.

41. Haider, S.; Alam, M. S.; Hamid, H. 1,2,3-Triazoles: scaffold with medicinal significance. *Inflammation and Cell Signaling* **2014**, *1*, doi:10.14800/ics.95.

42. Keri, R. S.; Patil, S. A.; Budagumpi, S.; Nagaraja, B. M. Triazole: A Promising Antitubercular Agent. *Chemical Biology & Drug Design* **2015**, *86*, 410–423, doi:10.1111/cbdd.12527.

43. Kharb, R.; Shahar Yar, M.; Sharma, P. C. Recent advances and future perspectives of triazole analogs as promising antiviral agents. *Mini Rev Med Chem* **2011**, *11*, 84–96.

44. MacDonald, J. P.; Badillo, J. J.; Arevalo, G. E.; Silva-García, A.; Franz, A. K. Catalytic Stereoselective Synthesis of Diverse Oxindoles and Spirooxindoles from Isatins. *ACS Combinatorial Science* **2012**, *14*, 285–293, doi:10.1021/co300003c.

45. Nolte, C.; Mayer, P.; Straub, B. F. Isolation of a copper(I) triazolide: a "click" intermediate. *Angew. Chem. Int. Ed. Engl.* **2007**, *46*, 2101–2103, doi:10.1002/anie.200604444.

46. Shao, C.; Wang, X.; Xu, J.; Zhao, J.; Zhang, Q.; Hu, Y. Carboxylic Acid-Promoted Copper(I)-Catalyzed Azide–Alkyne Cycloaddition. *J. Org. Chem.* **2010**, *75*, 7002–7005, doi:10.1021/jo101495k.

47. Shao Changwei; Cheng Guolin; Su Deyong; Xu Jimin; Wang Xinyan; Hu Yuefei Copper(I) Acetate: A Structurally Simple but Highly Efficient Dinuclear Catalyst for Copper-Catalyzed Azide-Alkyne Cycloaddition. *Advanced Synthesis & Catalysis* **2010**, *352*, 1587–1592, doi:10.1002/adsc.200900768.

48. Shao, C.; Wang, X.; Zhang, Q.; Luo, S.; Zhao, J.; Hu, Y. Acid–Base Jointly Promoted Copper(I)-Catalyzed Azide–Alkyne Cycloaddition. *J. Org. Chem.* **2011**, *76*, 6832–6836, doi:10.1021/jo200869a.

49. Himo, F.; Lovell, T.; Hilgraf, R.; Rostovtsev, V. V.; Noodleman, L.; Sharpless, K. B.; Fokin, V. V. Copper(I)-Catalyzed Synthesis of Azoles. DFT Study Predicts Unprecedented Reactivity and Intermediates. *J. Am. Chem. Soc.* **2005**, *127*, 210–216, doi:10.1021/ja0471525.

50. Boren, B. C.; Narayan, S.; Rasmussen, L. K.; Zhang, L.; Zhao, H.; Lin, Z.; Jia, G.; Fokin, V. V. Ruthenium-catalyzed azide-alkyne cycloaddition: scope and mechanism. *J. Am. Chem. Soc.* **2008**, *130*, 8923–8930, doi:10.1021/ja0749993.

51. Cecchi, L.; De Sarlo, F.; Machetti, F. 1,4-Diazabicyclo[2.2.2]octane (DABCO) as an Efficient Reagent for the Synthesis of Isoxazole Derivatives from Primary Nitro Compounds and Dipolarophiles: The Role of the Base. *Eur. J. Org. Chem.* **2006**, *2006*, 4852–4860, doi:10.1002/ejoc.200600475.

52. Chand, P.; Kotian, P. L.; Dehghani, A.; El-Kattan, Y.; Lin, T.-H.; Hutchison, T. L.; Babu, Y. S.; Bantia, S.; Elliott, A. J.; Montgomery, J. A. Systematic Structure-Based Design and Stereoselective Synthesis of Novel Multisubstituted Cyclopentane Derivatives with Potent Antiinfluenza Activity. *J. Med. Chem.* **2001**, *44*, 4379–4392, doi:10.1021/jm010277p.

53. Jones, P.; Atack, J. R.; Braun, M. P.; Cato, B. P.; Chambers, M. S.; O'Connor, D.; Cook, S. M.; Hobbs, S. C.; Maxey, R.; Szekeres, H. J.; Szeto, N.; Wafford, K. A.; MacLeod, A. M. Pharmacokinetics and metabolism studies on (3-tert-butyl-7-(5-methylisoxazol-3-yl)-2-(1-methyl-1H-1,2,4-triazol-5-ylmethoxy) pyrazolo[1,5-d][1,2,4]triazine, a functionally selective GABAA α5 inverse agonist for cognitive dysfunction. *Bioorganic & Medicinal Chemistry Letters* **2006**, *16*, 872–875, doi:10.1016/j.bmcl.2005.11.012.

54. Quan, M. L.; Liauw, A. Y.; Ellis, C. D.; Pruitt, J. R.; Carini, D. J.; Bostrom, L. L.; Huang, P. P.; Harrison, K.; Knabb, R. M.; Thoolen, M. J.; Wong, P. C.; Wexler, R. R. Design and Synthesis of Isoxazoline Derivatives as Factor Xa Inhibitors. 1. *J. Med. Chem.* **1999**, *42*, 2752–2759, doi:10.1021/jm980405i.

55. Mohamed, Y. A. M.; Inagaki, F.; Takahashi, R.; Mukai, C. A new procedure for the preparation of 2-vinylindoles and their [4+2] cycloaddition reaction. *Tetrahedron* **2011**, *67*, 5133–5141, doi:10.1016/j.tet.2011.05.064.

56. Aponick, A.; Li, C.-Y.; Malinge, J.; Marques, E. F. An Extremely Facile Synthesis of Furans, Pyrroles, and Thiophenes by the Dehydrative Cyclization of Propargyl Alcohols. *Org. Lett.* **2009**, *11*, 4624–4627, doi:10.1021/ol901901m.

57. Gamby, S.; Roy, V.; Guo, M.; Smith, J. A. I.; Wang, J.; Stewart, J. E.; Wang, X.; Bentley, W. E.; Sintim, H. O. Altering the communication networks of multispecies microbial systems using a diverse toolbox of AI-2 analogues. *ACS Chem. Biol.* **2012**, *7*, 1023–1030, doi:10.1021/cb200524y.

58. Morriello, G.; Devita, R.; Mills, S.; Moyes, C.; Lin, P. Anti-Hypercholesterolemic Compounds 2010.

59. Mames, A.; Stecko, S.; Mikołajczyk, P.; Soluch, M.; Furman, B.; Chmielewski, M. Direct, Catalytic Synthesis of Carbapenams via Cycloaddition/Rearrangement Cascade Reaction: Unexpected Acetylenes' Structure Effect. *J. Org. Chem.* **2010**, *75*, 7580–7587, doi:10.1021/jo101355h.

60. Jen, T.; Mendelsohn, B. A.; Ciufolini, M. A. Oxidation of α-Oxo-Oximes to Nitrile Oxides with Hypervalent Iodine Reagents. *J. Org. Chem.* **2011**, *76*, 728–731, doi:10.1021/jo102241s.

61. Xavier, K. B.; Miller, S. T.; Lu, W.; Kim, J. H.; Rabinowitz, J.; Pelczer, I.; Semmelhack, M. F.; Bassler, B. L. Phosphorylation and Processing of the Quorum-Sensing Molecule Autoinducer-2 in Enteric Bacteria. *ACS Chemical Biology* **2007**, *2*, 128–136, doi:10.1021/cb600444h.

62. Tsuchikama, K.; Zhu, J.; Lowery, C. A.; Kaufmann, G. F.; Janda, K. D. C4-Alkoxy-HPD: A Potent Class of Synthetic Modulators Surpassing Nature in AI-2 Quorum Sensing. *Journal of the American Chemical Society* **2012**, *134*, 13562–13564, doi:10.1021/ja305532y.

63. Roy, V.; Meyer, M. T.; Smith, J. A. I.; Gamby, S.; Sintim, H. O.; Ghodssi, R.; Bentley, W. E. AI-2 analogs and antibiotics: a synergistic approach to reduce bacterial biofilms. *Applied Microbiology and Biotechnology* **2013**, *97*, 2627–2638, doi:10.1007/s00253-012-4404-6.

Sample Availability: Samples of the compounds are all available from the authors.

Supplementary data

Along the road for overcoming antimicrobial resistance: set up of a versatile strategy for the synthesis of 4,5-dihydroxy-2,3-pentanedione (DPD) and its related compounds

Silvia Stotani[1,2], Viviana Gatta[3], Federico Medda[1,#], Mohan Padmanaban[1], Anna Karawajczyk[1,†], Païvi Tammela[3], Fabrizio Giordanetto[1,§], Dimitrios Tzalis[1] and Simona Collina[2,*]

[1] Medicinal Chemistry, Taros Chemicals GmbH & Co. KG, Emil-Figge-Straße 76a, 44227 Dortmund, Germany

[2] Department of Drug Sciences, Medicinal Chemistry and Pharmaceutical Technology Section, University of Pavia, Viale Taramelli 6 and 12, 27100, Pavia, Italy

³ Centre for Drug Research, Division of Pharmaceutical Biosciences, University of Helsinki, Helsinki, Finland

#Current address: Centurion Biopharma Corporation, Engesserstraße 4, 79108 Freiburg im Breisgau, Germany

† Current address: Selvita S.A., Park Life Science, Bobrzyňskiego 14, 30-348 Krakow, Poland

§ Current address: DE Shaw Research, 120W 45th Street, New York, NY

* Correspondence: simona.collina@unipv.it; Tel.: +39 0382-987379

![molecules logo] **Table of contents** ![MDPI logo]

General information

Chemicals and solvents were obtained from commercial suppliers and were used without further purification. All dry reactions were performed under nitrogen atmosphere using commercial dry solvents. Flash column chromatography was performed on a silica column using 230400 mesh silica gel or Grace Reveleris X2 flash chromatography system using silica gel packed Macherey Nagel Chromabond Flash BT cartridges (60 Å, 45 μm) and Grace Reveleris flash Cartridges (60 Å, 40 μm). Thin layer chromatography was performed on Macherey Nagel precoated TLC aluminum sheets with silica gel 60 UV254 (5 μm – 17 μm). TLC visualization was accomplished by irradiation with a UV lamp (254 nm) and/or staining with $KMnO_4$ solutions. ^{1}H NMR spectra were recorded at room temperature on a Bruker Avance spectrometer operating at 300 MHz. Chemical shifts are given in ppm (δ) from tetramethylsilane as an internal standard or residual solvent peak. Significant ^{1}H NMR data are tabulated in the following order: multiplicity (s, singlet; d, doublet; t, triplet; q, quartet; m, multiplet; dd, doublet of doublets; dt, doublet of triplets; td, triplet of doublets; br, broad), coupling constant(s) in hertz, number of protons. Proton decoupled ^{13}C NMR data were acquired at 100 MHz. [13]C chemical shifts are reported in parts per million (δ, ppm). All NMR data were collected at room temperature (25 °C). Analytical, preparative HPLC and Electron Spray Ionization (ESI) mass spectra were performed on an Agilent UHPLC (1290 Infinity) and an Agilent Prep-HPLC (1260 Infinity) both equipped with a Diode Array Detector and a Quadrupole MS using mixture gradients of formic acid/water/acetonitrile as solvents. High-resolution electrospray ionization mass spectra (ESI-FTMS) were recorded on a Thermo LTQ Orbitrap (high-resolution mass spectrometer from Thermo Electron) coupled to an 'Accela' HPLC system supplied with a 'Hypersil GOLD' column (Termo Electron).

Tables
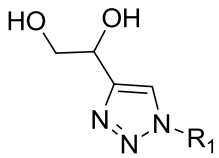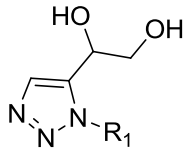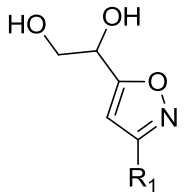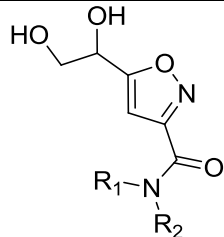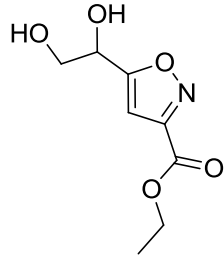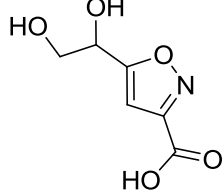
Entry	Solvent	Deprotecting agent	Temp (° C)	Time	Result
1	D_2O/DMSO-d_6 (4:1) (10 mM)	D_2SO_4 (Final 5 mM)	rt	Overnight	Decomposition
2	D_2O/DMSO-d_6 (4:1) (10 mM)	D_2SO_4 (Final 5 m)	0	Overnight	Decomposition
3	D_2O/DMSO-d_6 (4:1) (10 mM)	H_2SO_4 (cat.)	0→100	2 days	Decomposition
4	MeOD (10 mM)	D_2SO_4 (Final 5 mM)	rt	Overnight	Decomposition
5	THF	TBAF (1.1 eq)	rt	Overnight	Decomposition
6	ACN-d_3 (10 mM)	NH_4F (4.0 eq)	rt	Overnight	SM
7	ACN-d_3/D_2O (1:1) (10 mM)	ACOD-d_3 (3.0 eq)	rt	Overnight	~10 % deprotection
8	MeOD (10 mM)	Dowex 50WX8 100-200 mesh	rt	Overnight	~30 % deprotection
9	ACN-d_3 (10 mM)	Dowex 50WX8 100-200 mesh	rt	Overnight	~30 % deprotection
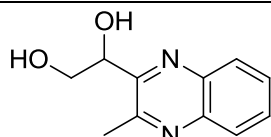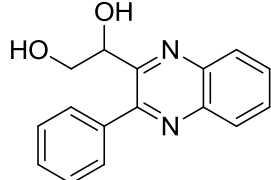
Table S1: Screening of the conditions for the acidic removal of the two TBDMS groups of compound **5**.
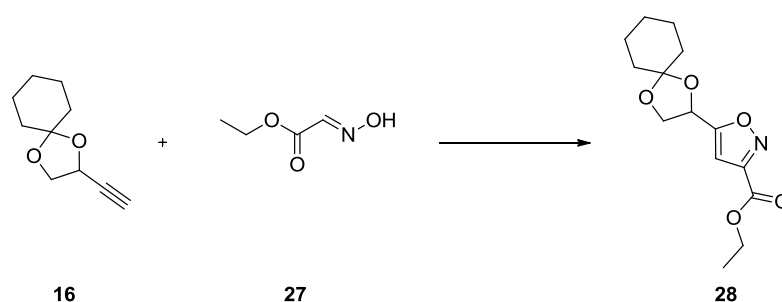
Entry	16 (Eq)	27 (Eq)	Time (h)	Yield (%)[a]
1	1.2	1	96	16
2	1	1.2	72	18
3	1	1.5	24	21
4	1	2.0	12	36

Table S2: Different ratios of dipolarophile **16** and 1,3-dipole **27** tested for the synthesis of intermediate **28**.
[a] Isolated yield

373

Series	Structure	Compound	R¹	Inhibition (%)
Series I *1,4-disubstituted 1,2,3-triazoles DPD-derivatives*		**18a**	$(CH_2)_2$-Ph	0
		18b	(CH_2)-Ph	1.9
		18c	$(CH_2)_2$-*o*-F-Ph	3.3
		18d	$(CH_2)_2$-*m*-Pyr	0.1
		18e	$(CH_2)_5$-CN	2.2
		18f	$(CH_2)_2$-CyH	2.7
		18g	H	2.3
		18h	CH_3	2.0
		18i	CH_2-Cyp	2.5
		18j	*n*-Bu	5.5
		18k	$(CH_2)_2$-O-CH_3CH_2	2.2
Series II *1,5-disubstituted 1,2,3-triazoles DPD-derivatives*		**19a**	$(CH_2)_2$-Ph	2.0
		19h	CH_3	2.5
		19i	CH_2-Cyp	1.6
		19j	*n*-Bu	2.4
		19k	$(CH_2)_2$-O-CH_3CH_2	2.0
Series III *3,5-disubstituted isoxazoles DPD-derivatives*		**26l**	*p*-CH_3-Ph	1.9
		26m	*m*-Cl-Ph	0.1
		26n	*o, p*-di-F-Ph	0.2
		26o	*m*-Pyr	4.8
		26p	Cyp	8.4
		26q	*m*-THF	0.8
		26r	CyH	5.5
Series IV *3,5-disubstituted isoxazoles DPD-derivatives*		**33b**	CH_2-Ph	2.5
		33s	*p*-F-Ph	2.5
		33t	CH_2-thiophene	2.5
		33u	CH_2-*m*-Pyr	1.2
		33v	$(CH_2)_2$-O-CH_3	1.0
		33z	Pyrrolidine	2.5
Other		**29**	—	3.1
Other		**31**	—	2.1

Other		Quinoxaline-DPD	—	10.9
Other		Quinoxaline-Ph-DPD	—	0

Table S3: Biological activity of the synthesized compounds measured at 200 μM

NOTE: No positive control was used in the present study as there was no known inhibitor of LsrK kinase at the time the study started.

Schemes

16

EthylInitro acetate

28
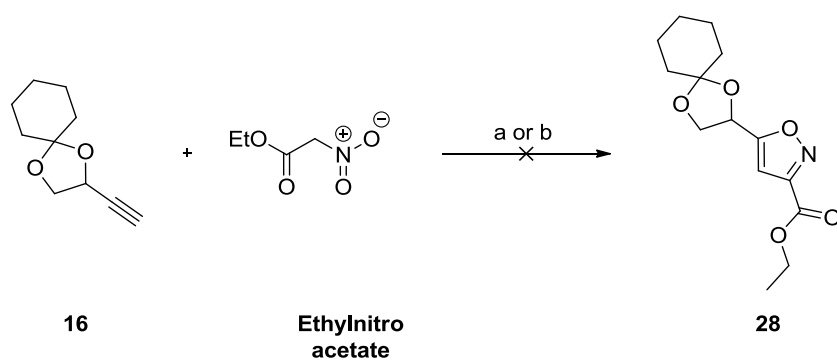
Scheme S1: Attempts for the synthesis of intermediate **28**. Reagents and conditions: (a) **16** (1.0 eq), base (1.5 eq), CHCl$_3$, 60 °C, 3 days; (b) **16** (1.0 eq), PhNCO (2.0 eq), Et$_3$N (1.5 eq), PhMe, 100 °C, 3 days.

Synthesis of 3 and 4: To a stirred suspension of NaH (2.0 eq) in THF was added **2** (1.0 eq). The suspension was stirred at room temperature for 45 min and afterwards it was cooled to 0 °C using an ice bath. TBDMSCl (or TMSCl) (1.3 eq) in THF was added dropwise. The reaction was vigorously stirred at room temperature for 2 hours. The mixture was poured **slowly** onto a cold solution of aqueous K_2CO_3 (10%) and extracted three times with Et_2O. The organic layer was dried over $MgSO_4$, filtered and concentrated *in vacuo* to yield **3** as a yellowish oil (90%) or 4 as a colorless oil (92%).

2,2,3,3,8,8,9,9-octamethyl-5-(prop-1-yn-1-yl)-4,7-dioxa-3,8-disiladecane (3): yellowish oil, 90%, R_f = 0.65 (CyH/EtOAc 9:1). ^{1}H NMR (300 MHz, CDCl$_3$) δ 4.37 – 4.33 (m, 1H), 3.63 (s, 1H), 3.61 (s, 1H), 1.81 (d, *J* = 2.1 Hz, 3H), 0.90 (d, *J* = 4.3 Hz, 18H), 0.11 (d, *J* = 5.9 Hz, 6H), 0.07 (d, *J* = 2.2 Hz, 6H) ppm.

2,2,7,7,8,8-hexamethyl-4-(prop-1-yn-1-yl)-3,6-dioxa-2,7-disilanonane (4): colorless oil, 92%, R_f = 0.73 (CyH/EtOAc 9:1). ^{1}H NMR (300 MHz, CDCl$_3$) δ 4.39 – 4.31 (m, 1H), 3.64 – 3.62 (m, 1H), 3.60 – 3.56 (m, 1H), 1.85 – 1.81 (m, 3H), 0.91 (d, *J* = 3.3 Hz, 9H), 0.17 (s, 6H), 0.12 – 0.07 (m, 9H) ppm.

Synthesis of 5 and 6: To a stirred solution of **3** (or **4**) (1.0 eq) in a 1:1:1 mixture of CHCl$_3$/ACN/H$_2$O was added NaIO$_4$ (4.4 eq) and RuO$_2$*H$_2$O (2.5% mol). The mixture was vigorously stirred for 3 hours. Solvent was evaporated under reduced pressure, the residue was redissolved in EtOAc and filtered through a silica pad. The eluate was extracted three times with water, dried over MgSO$_4$, filtered and concentrated *in vacuo*. Flash chromatography using CyH/EtOAc (3:1) afforded **5** as a yellow oil (52%) and **6** as a yellow oil (65%).

4,5-bis[(*t*-butyldimethylsilyl)oxy]pentane-2,3-dione (5): yellow oil, 52%, R_f = 0.25 (CyH/EtOAc 9:1). ^{1}H NMR (300 MHz, CDCl$_3$) δ 4.96 (t, *J* = 4.9 Hz, 1H), 4.00 (dd, *J* = 5.0 Hz, *J* = 10.3 Hz, 1H), 3.76 (dd, *J* = 4.7 Hz, *J* = 10.3 Hz, 1H), 2.32 (s, 3H), 0.89 (s, 10H), 0.85 (s, 8H), 0.09 – 0.07 (m, 4H), 0.04 – 0.03 (m, 8H) ppm.

5-[(*t*-butyldimethylsilyl)oxy]-4-[(trimethylsilyl)oxy]pentane-2,3-dione (6): yellow oil, 65%, R_f = 0.75 (CHCl$_3$/MeOH 5:1). ^{1}H NMR (300 MHz, CDCl$_3$) δ 4.90 (s, 1H), 4.14 (dd, *J* = 3.0 Hz, *J* = 10.8 Hz, 1H), 3.86 (dd, *J* = 2.8 Hz, *J* = 10.8 Hz, 1H), 2.39 (s, 3H), 0.91 (s, 9H), 0.83 (s, 9H), 0.01 (d, *J* = 8.3 Hz, 6H) ppm.

Characterization of compounds 17a-f

(2-azidoethyl)benzene (17a): yellow oil, 85%. ^{1}H NMR (300 MHz, CDCl$_3$) δ 7.31 – 7.28 (m, 2H), 7.23 – 7.17 (m, 3H), 3.46 (dt, J = 2.8 Hz, J = 7.2 Hz, 2H), 2.85 (t, J = 7.3 Hz, 2H) ppm; ^{13}C NMR (100 MHz, CDCl$_3$) δ 138.0, 128.7, 128.6, 126.7, 52.4, 35.3 ppm [1].

(azidomethyl)benzene (17b): colorless oil, 70%. ^{1}H NMR (300 MHz, CDCl$_3$) δ 7.44 – 7.32 (m, 5H), 4.35 (s, 2H) ppm; ^{13}C NMR (100 MHz, CDCl$_3$) δ 135.4, 128.8, 128.3, 128.2, 54.8 ppm [2].

1-(2-azidoethyl)-2-fluorobenzene (17c) colorless oil, 86%. ^{1}H NMR (300 MHz, CDCl$_3$) δ 7.26 (t, J = 7.2 Hz, 2H), 7.15 – 7.04 (m, 2H), 3.54 (t, J = 7.1 Hz, 2H), 2.97 (t, J = 7.2 Hz, 2H) ppm; ^{13}C NMR (100 MHz, CDCl$_3$) δ 161.2 (d, J = 245.5 Hz), 131.1 (d, J = 4.8 Hz), 128.7 (d, J = 8.2 Hz), 124.9 (d, J = 15.8 Hz), 124.2 (d, J = 3.5 Hz), 115.5 (d, J = 22.0 Hz), 51.1 (d, J = 1.5 Hz), 29.0 (d, J = 2.2 Hz) ppm [3]

2-(2-azidoethyl)pyridine (17d): yellowish oil, 30%. ^{1}H NMR (300 MHz, CDCl$_3$) δ 8.55 (d, J = 4.4 Hz, 1H), 7.62 (dt, J = 1.8 Hz, J = 7.7 Hz, 1H), 7.21 – 7.14 (m, 2H), 3.71 (t, J = 6.9 Hz, 2H), 3.05 (t, J = 6.9 Hz, 2H) ppm; ^{13}C NMR (100 MHz, CDCl$_3$) δ 158.0, 149.5, 136.5, 123.5, 121.8, 50.6, 37.5 ppm [4].

6-azidohexanenitrile (17e): colorless oil, 48%. ^{1}H NMR (300 MHz, CDCl$_3$) δ 3.30 (t, J = 6.5 Hz, 2H), 2.36 (t, J = 6.9 Hz, 2H), 1.74 – 1.50 (m, 6H) ppm; ^{13}C NMR (100 MHz, CDCl$_3$) δ 119.4, 51.0, 28.1, 25.8, 25.0, 17.1 ppm [5].

(2-azidoethyl)cyclohexane (17f): colorless oil, 64%. ^{1}H NMR (300 MHz, CDCl$_3$) δ 3.28 (t, J = 7.2 Hz, 2H), 1.72 – 1.64 (m, 5H), 1.49 (dd, J = 7.0 Hz, J = 14.1 Hz, 2H), 1.40 – 1.30 (m, 1H), 1.26 – 1.12 (m, 3H), 0.91 (q, J = 11.5 Hz, 2H) ppm; ^{13}C NMR (100 MHz, CDCl$_3$) δ 49.2, 36.0, 35.0, 33.0, 26.4, 26.1 ppm [6].

Different conditions tested for the synthesis of triazole 18a

A) To a stirred solution of **15** (1.0 eq) in THF was added CuI (10% mol), DIPEA (15% mol) and (2-azidoethyl)benzene (**17a**) (1.1 eq). The mixture was stirred at room temperature overnight. Solvent was evaporated under reduced pressure, the crude was redissolved in ACN (1 mL), filtered and purified by preparative HPLC to yield **18a** as an orange oil (58%) [7].

B) To a stirred solution of **15** (1.0 eq), CuI (2%mol), DIPEA (15%mol) and AcOH (cat.) in DCM was added (2-azidoethyl)benzene (**17a**) (1.05 eq). The mixture was stirred at room temperature overnight. Solvent was evaporated under reduced pressure, the crude was redissolved in ACN (1 mL), filtered and purified by preparative HPLC to yield **18a** as an orange oil (72%) [8].

C) To a stirred solution of **15** (1.0 eq) in a 1:1 mixture of H_2O/t-BuOH were added (2-azidoethyl)benzene (**17a**) (1.0 eq), sodium ascorbate (0.5 eq) and $CuSO_4$*$5H_2O$ (5% mol). The reaction was stirred at room temperature overnight. Solvent was evaporated under reduced pressure, the crude was redissolved in ACN (1 mL), filtered and purified by preparative HPLC to yield **18a** as an orange oil (89%) [9].

Characterization of compounds 21h-k and 22h-k

4-{1,4-dioxaspiro[4.5]decan-2-yl}-1-methyl-1H-1,2,3-triazole (21h): yellowish oil, 53%, R_f = 0.48 (CyH/EtOAC 3:1), UHPLC-ESI-MS: R_t = 2.30, m/z = 224.2 [M + H] $^+$. ^{1}H NMR (300 MHz, CDCl$_3$) δ 7.59 (s, 1H), 5.20 (t, J = 6.4 Hz, 1H), 4.35 (dd, J = 6.4 Hz, J = 8.5 Hz, 1H), 4.11 (s, 3H), 4.06 (dd, J = 6.5 Hz, J = 8.5 Hz, 1H), – 1.56 (m, 8H), 1.42 – 1.41 (m, 2H) ppm; ^{13}C NMR (100 MHz, CDCl$_3$) δ 135.3, 131.9, 111.5, 67.9, 67.5, 35.9, 35.4, 34.9, 24.9, 23.9, 23.8 ppm.

5-{1,4-dioxaspiro[4.5]decan-2-yl}-1-methyl-1H-1,2,3-triazole (22h): yellowish oil, 62%, R_f = 0.50 (CyH/EtOAC 3:1), UHPLC-ESI-MS: R_t = 2.54, m/z = 224.0 [M + H] $^+$. ^{1}H NMR (300 MHz, CDCl$_3$) δ 7.57 (s, 1H), 5.22 (t, J = 6.6 Hz, 1H), 4.32 (dd, J = 6.3 Hz, J = 8.3 Hz, 1H), 4.16 (s, 3H), 3.99 (dd, J = 7.0 Hz, J = 8.3 Hz, 1H), – 1.60 (m, 8H), 1.44 – 1.41 (m, 2H) ppm; ^{13}C NMR (100 MHz, CDCl$_3$) δ 147.5, 132.4, 110.7, 70.2, 69.3, 41.6, 36.0, 35.2, 25.1, 23.9, 23.8 ppm.

1-(cyclopropylmethyl)-4-{1,4-dioxaspiro[4.5]decan-2-yl}-1H-1,2,3-triazole (21i): colorless oil, 47%, R_f = 0.29 (CHCl$_3$/MeOH 9:1), UHPLC-ESI-MS: R_t = 2.61, m/z = 264.2 [M + H] $^+$. ^{1}H NMR (300 MHz, CDCl$_3$) δ 7.63 (s, 1H), 5.29 (t, J = 6.6 Hz, 1H), 4.36 (t, J = 7.3 Hz, 1H), 4.18 (d, J = 7.2 Hz, 2H), 4.03 (t, J = 7.6 Hz, 1H), 1.69 – 1.62 (m, 8H), 1.41 – 1.39 (m, 2H), 1.28 – 1.25 (m, 1H), 0.68 (d, J = 7.3 Hz, 2H), 0.42 (d, J = 4.3 Hz, 2H) ppm; ^{13}C NMR (100 MHz, CDCl$_3$) δ 147.5, 120.9, 110.4, 70.6, 69.4, 54.9, 36.1, 35.1, 25.0, 23.9, 23.8, 10.9, 4.2 (d, J = 4.1 Hz) ppm.

1-(cyclopropylmethyl)-5-{1,4-dioxaspiro[4.5]decan-2-yl}-1H-1,2,3-triazole (22i): colorless oil, 42%, R_f = 0.31 (CHCl$_3$/MeOH 9:1), UHPLC-ESI-MS: R_t = 2.72, m/z = 264.2 [M + H] $^+$. ^{1}H NMR (300 MHz, CDCl$_3$) δ 7.59 (s, 1H), 5.21 (t, J = 6.4 Hz, 1H), 4.36 (dd, J = 6.3 Hz, J = 8.4 Hz, 1H), 4.28 (d, J = 7.2 Hz, 2H), 4.07 (dd, J = 6.6 Hz, J = 8.4 Hz, 1H), 1.65 – 1.60 (m, 8H), 1.42 – 1.38 (m, 3H), 0.63 (d, J = 8.1 Hz, 2H), 0.48 (d, J = 4.8 Hz, 2H) ppm; ^{13}C NMR (100 MHz, CDCl$_3$) δ 134.8, 131.6, 111.4, 68.2, 67.4, 53.3, 35.9, 35.0, 24.9, 23.8, 11.3, 4.5, 4.0 ppm.

1-butyl-4-{1,4-dioxaspiro[4.5]decan-2-yl}-1H-1,2,3-triazole (21j): colorless oil, 37%, R_f = 0.23 (CyH/EtOAC 3:1), UHPLC-ESI-MS: R_t = 2.77, m/z = 266.2 [M + H] $^+$. ^{1}H NMR (300 MHz, CDCl$_3$) δ 7.51 (s, 1H), 5.29 (t, J = 6.6 Hz, 1H), 4.39 – 4.31 (m, 3H), 4.02 (dd, J = 7.0 Hz, J = 8.2 Hz, 1H), 1.88 (td, J = 7.4 Hz, J = 14.9 Hz, 2H), 1.70 – 1.62 (m, 8H), 1.44 – 1.32 (m, 4H), 0.95 (t, J = 7.3 Hz, 3H) ppm; ^{13}C NMR (100 MHz, CDCl$_3$) δ 147.7, 121.2, 110.4, 70.7, 69.5, 50.1, 36.2, 35.2, 32.2, 25.1, 24.0, 23.8, 19.7, 13.4 ppm.

1-butyl-4-{1,4-dioxaspiro[4.5]decan-2-yl}-1H-1,2,3-triazole (22j): colorless oil, 31%, R_f = 0.26 (CyH/EtOAC 3:1), UHPLC-ESI-MS: R_t = 2.89, m/z = 266.2 [M + H] $^+$. ^{1}H NMR (300 MHz, CDCl$_3$) δ 7.59 (s, 1H), 5.17 (t, J = 6.5 Hz, 1H), 4.43 – 4.33 (m, 3H), 4.06 (dd, J = 6.6 Hz, J = 8.4 Hz, 1H), 1.93 (td, J = 7.4 Hz, J = 15.1 Hz, 2H), 1.69 – 1.58 (m, 8H), 1.43 – 1.36 (m, 4H), 0.97 (t, J = 7.3 Hz, 3H) ppm; ^{13}C NMR (100 MHz, CDCl$_3$) δ 144.8, 135.1, 111.5, 68.2, 67.5, 48.6, 36.0, 35.1, 32.2, 25.0, 23.9, 19.8, 13.6 ppm.

4-{1,4-dioxaspiro[4.5]decan-2-yl}-1-(2-ethoxyethyl)-1H-1,2,3-triazole (21k): colorless oil, 38%, R_f = 0.21 (CyH/EtOAC 3:1), UHPLC-ESI-MS: R_t = 2.51, m/z = 282.2 [M + H] $^+$. ^{1}H NMR (300 MHz, CDCl$_3$) δ 7.69 (s, 1H), 5.30 (t, J = 6.6 Hz, 1H), 4.51 (t, J = 5.1 Hz, 2H), 4.37 (dd, J = 6.3 Hz, J = 8.3 Hz, 1H), 4.06 (dd, J = 6.9 Hz, J = 8.3 Hz, 1H), 3.78 (t, J = 5.4 Hz, 2H), 3.48 (t, J = 7.0 Hz, 2H), 1.72 – 1.62 (m, 8H), 1.45 – 1.41 (m, 2H), 1.17 (t, J = 7.0 Hz, 3H) ppm; ^{13}C NMR (100 MHz, CDCl$_3$) δ 147.6, 122.7, 110.5, 70.7, 69.5, 68.7, 66.8, 50.5, 36.2, 35.3, 25.1, 24.0, 23.9, 15.0 ppm.

4-{1,4-dioxaspiro[4.5]decan-2-yl}-1-(2-ethoxyethyl)-1H-1,2,3-triazole (22k): colorless oil, 29%, R_f = 0.23 (CyH/EtOAC 3:1), UHPLC-ESI-MS: R_t = 2.64, m/z = 282.2 [M + H] $^+$. ^{1}H NMR (300 MHz, CDCl$_3$) δ 7.61 (s, 1H), 5.31 (t, J = 6.3 Hz, 1H), 4.59 – 4.55 (m, 2H), 4.35 (dd, J = 6.3 Hz, J = 8.4 Hz, 1H), 4.03 (dd, J = 6.5 Hz, J = 8.4 Hz, 1H), 3.85 – 3.80 (m, 2H), 3.46 – 3.41 (m, 2H), 1.66 – 1.57 (m, 8H), 1.43 – 1.41 (m, 2H), 1.12 (t, J = 7.0 Hz, 3H) ppm; ^{13}C NMR (100 MHz, CDCl$_3$) δ 146.0, 122.1, 111.2, 69.2, 68.7, 67.8, 66.8, 48.7, 36.0, 35.1, 25.0, 23.9, 15.0 ppm.
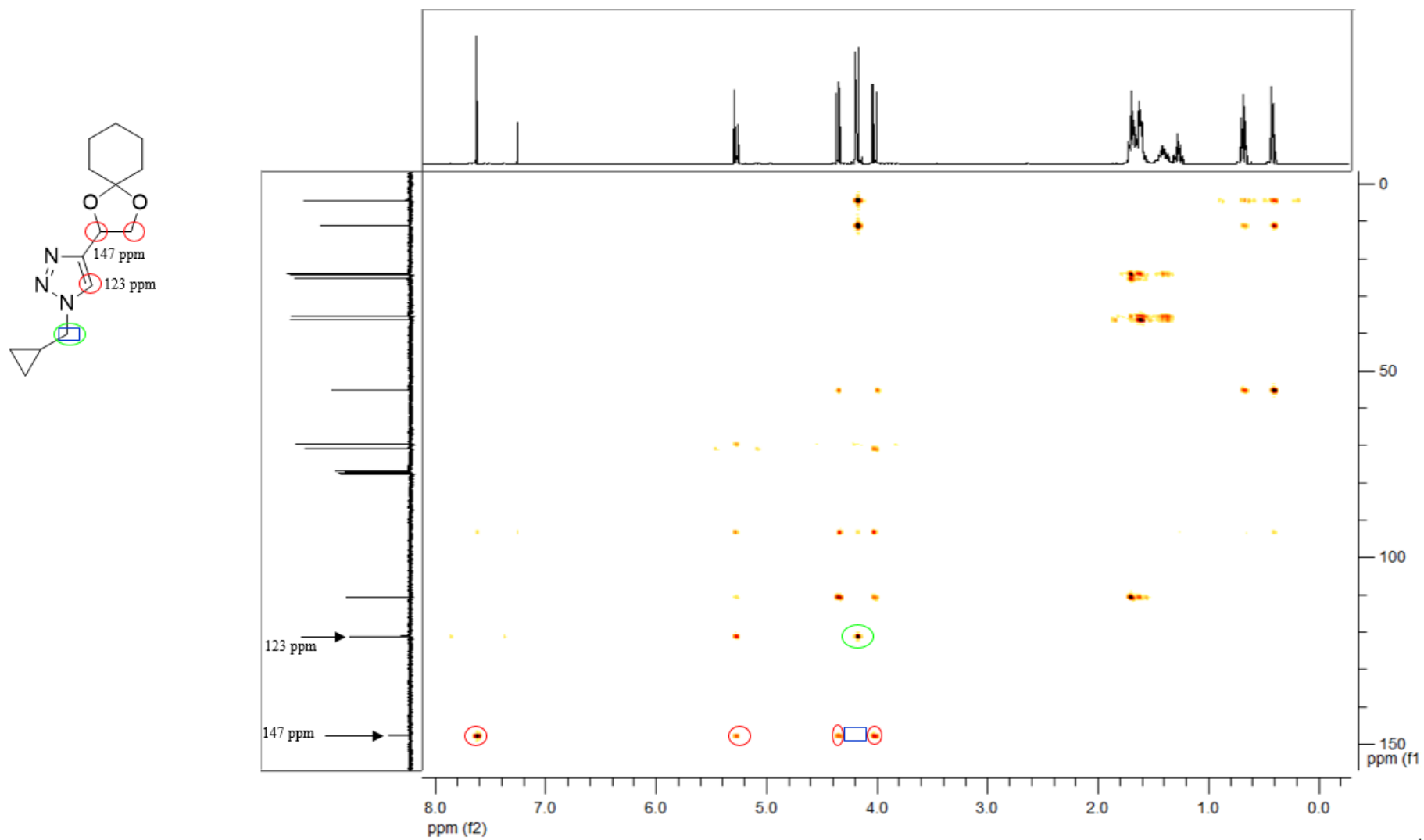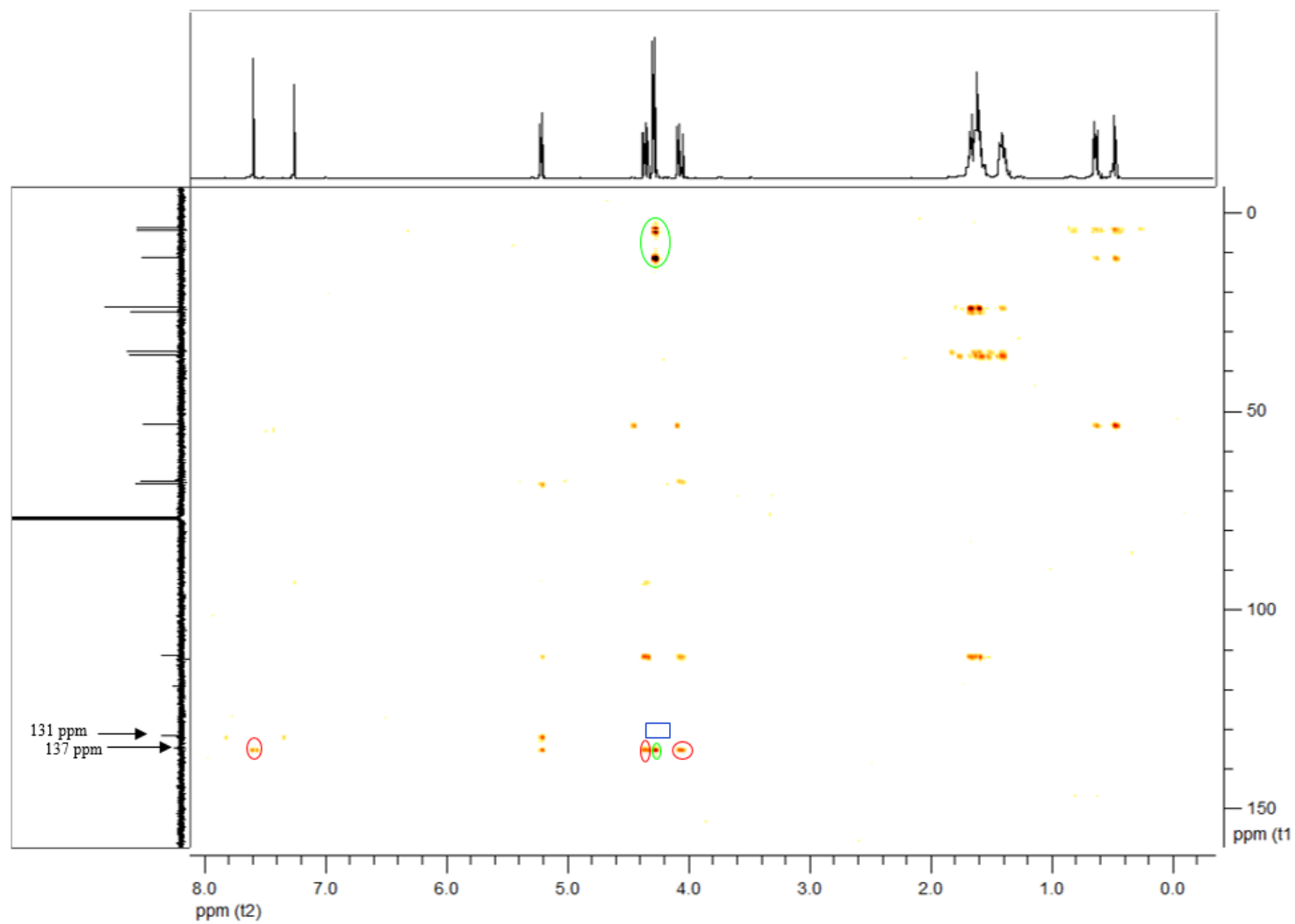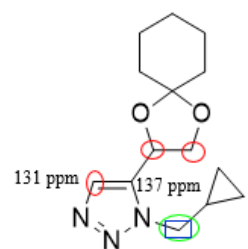
HMBC of compound 18a
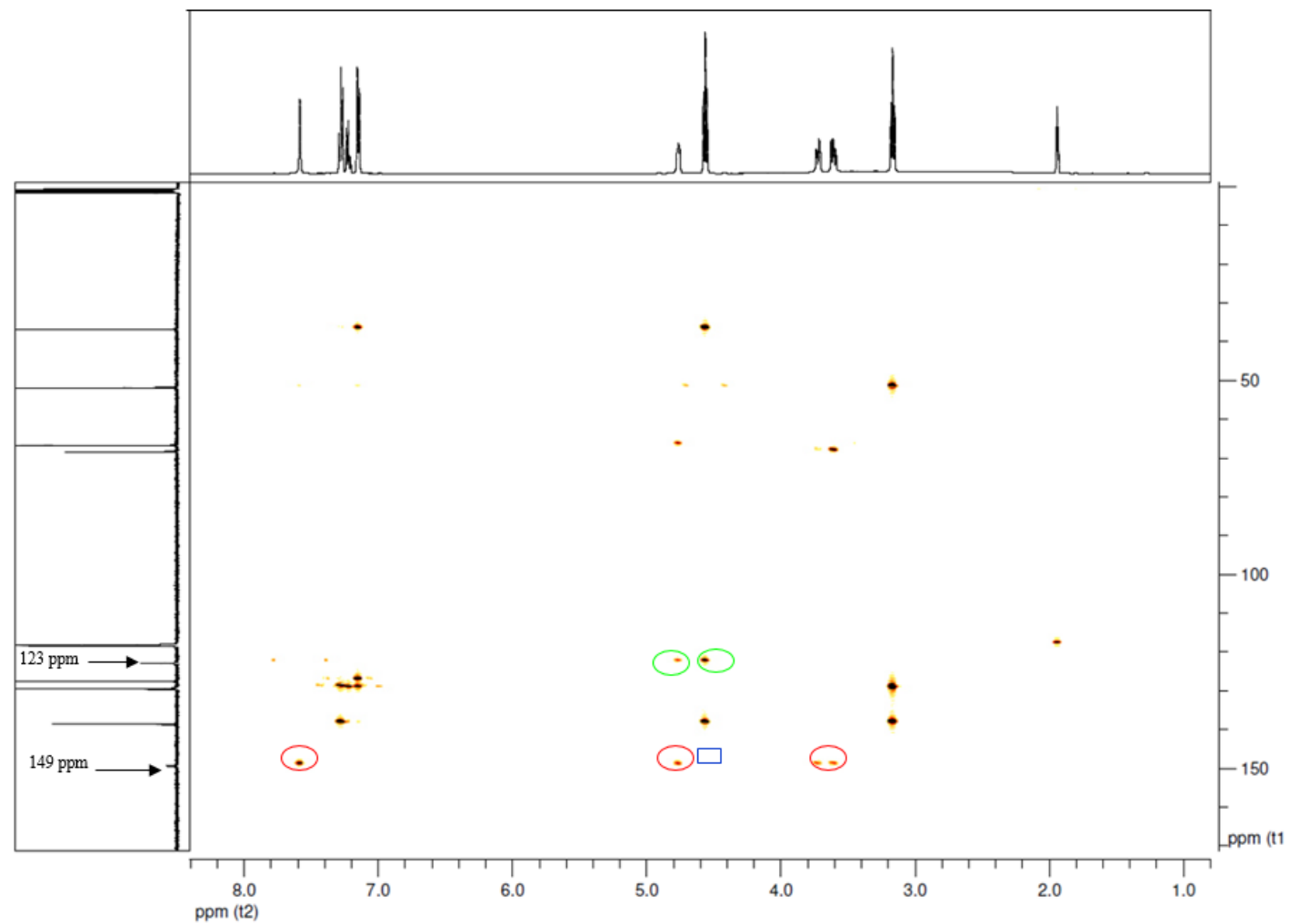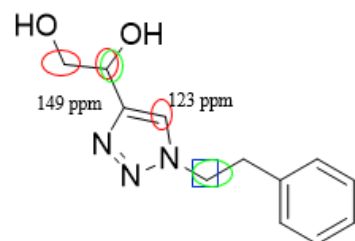
HMBC of compound 19a
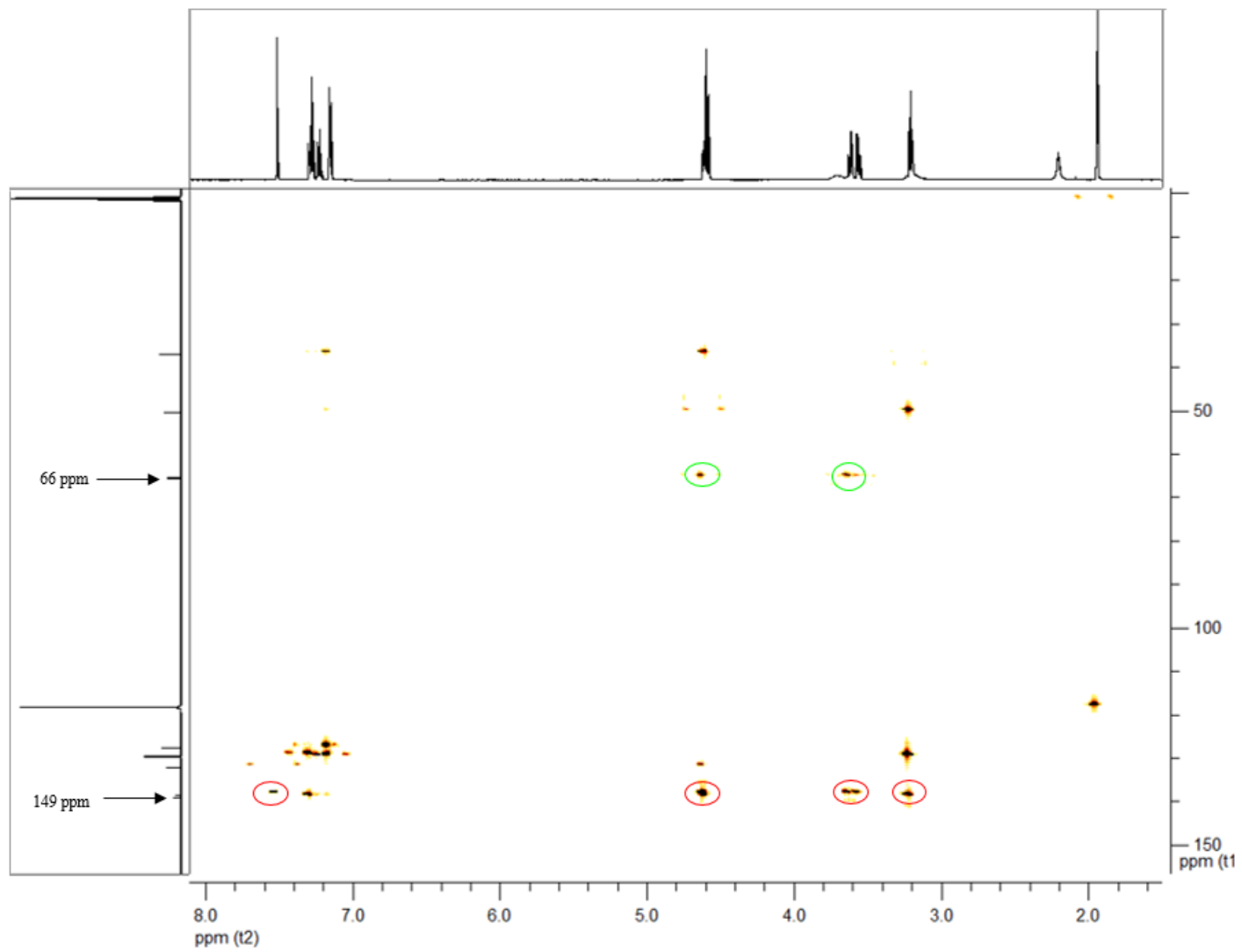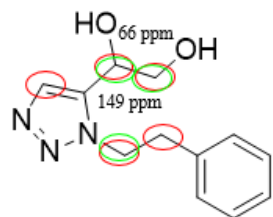
HMBC of compound 21i

HMBC of compound 22i

131 ppm

137 ppm

131 ppm

137 ppm

(E)-N-[(4-methylphenyl)methylidene]hydroxylamine (24l): brownish solid, 90%, R_f = 0.68 (CHCl$_3$/MeOH 9:1). ^{1}H NMR (300 MHz, CDCl$_3$) δ 8.67 (s br, 1H), 8.14 (s, 1H), 7.48 (d, J = 8.1 Hz, 2H), 7.20 (d, J = 7.9 Hz, 2H), 2.38 (s, 3H) ppm; ^{13}C NMR (100 MHz, CDCl$_3$) δ 150.3, 140.3, 129.5, 129.2, 127.0, 21.4 ppm [10].

(E)-N-[(3-chlorophenyl)methylidene]hydroxylamine (24m): white solid, 98%, R_f = 0.70 (CHCl$_3$/MeOH 9:1). ^{1}H NMR (300 MHz, CDCl$_3$) δ 8.10 (s, 1H), 7.59 (d, J = 1.8 Hz, 1H), 7.44 (td, J = 1.6 Hz, J = 7.0 Hz, 1H), 7.39 – 7.29 (m, 2H) ppm; ^{13}C NMR (100 MHz, CDCl$_3$) δ 149.1, 134.9, 133.8, 130.0, 126.8, 125.2 ppm [10].

(E)-N-[(2,4-difluorophenyl)methylidene]hydroxylamine (24n): white solid, 90%, R_f = 0.74 (CHCl$_3$/MeOH 9:1). ^{1}H NMR (300 MHz, CDCl$_3$) δ 8.31 (s, 1H), 7.73 (dt, J = 6.5 Hz, J = 8.4 Hz, 1H), 6.94 – 6.82 (m, 2H) ppm; ^{13}C NMR (100 MHz, CDCl$_3$) δ 164.2 (dd, J = 12.1 Hz, J = 217.2 Hz), 160.8 (dd, J = 12.0 Hz, J = 219.3 Hz), 143.6, 128.3 (dd, J = 4.4 Hz, J = 9.8 Hz), 116.3 (dd, J = 4.0 Hz, J = 11.0 Hz), 112.2 (dd, J = 3.6 Hz, J = 21.9 Hz), 104.4 (t, J = 25.3 Hz) ppm [11].

(E)-N-[(pyridin-3-yl)methylidene]hydroxylamine (24o): white solid, 83%, R_f = 0.47 (CHCl$_3$/MeOH 9:1). ^{1}H NMR (300 MHz, DMSO-d_6) δ 11.56 (s, 1H), 8.75 (d, J = 1.8 Hz, 1H), 8.55 (dd, J = 1.6 Hz, J = 4.8 Hz, 1H), 8.20 (s, 1H), 7.99 (td, J = 1.8 Hz, J = 7.9 Hz, 1H), 7.42 (dd, J = 4.8 Hz, J = 7.9 Hz, 1H) ppm; ^{13}C NMR (100 MHz, DMSO-d_6) δ 149.9, 147.7, 145.6, 133.0, 128.9, 123.8 ppm [12].

(E)-N-(cyclopropylmethylidene)hydroxylamine (24p): white solid, 77%, R_f = 0.66 (CHCl$_3$/MeOH 9:1). The compound was obtained as a mixture of *syn* and *anti* oximes. The mixture was not separated and the compound was used for further reaction without purification. Only the **major** isomer is reported. ^{1}H NMR (300 MHz, CDCl$_3$) δ 6.02 (d, J = 8.8 Hz, 1H), 2.34 – 2.23 (m, 1H), 0.98 – 0.91 (m, 2H), 0.65 – 0.60 (m, 2H) ppm; ^{13}C NMR (100 MHz, CDCl$_3$) δ 155.4, 10.8, 6.0, 5.5 ppm [13].

(E)-N-[(oxolan-3-yl)methylidene]hydroxylamine (24q): yellowish oil, 76%, R_f = 0.64 (CHCl$_3$/MeOH 9:1). The compound was obtained as a mixture of *syn* and *anti* oximes. The mixture was not separated and the compound was used for further reaction without purification. Only the **major** isomer is reported (not all the peaks are integrated and peaked in order to make the NMR picture easier to understand). ^{1}H NMR (300 MHz, CDCl$_3$) δ 8.68 (s br), 7.38 (d, J = 7.2 Hz, 1H), 3.96 – 3.93 (m, 1H), 3.84 – 3.75 (m, 2H), 3.70 – 3.67 (m, 1H), 3.11 – 2.99 (m, 1H), 2.17 – 2.10 (m, 1H), 1.95 – 1.87 (m, 1H) ppm; ^{13}C NMR (100 MHz, CDCl$_3$) δ 152.1, 70.6, 68.0, 39.5, 30.5 ppm [14].

(E)-N-(cyclohexylmethylidene)hydroxylamine (24r): yellowish oil, 98%, R_f = 0.58 (CHCl$_3$/MeOH 9:1). The compound was obtained as a mixture of *syn* and *anti* oximes. The mixture was not separated and the compound was used for further reaction without purification. Only the **major** isomer is reported. ^{1}H NMR (300 MHz, CDCl$_3$) δ 7.32 (d, J = 6.1 Hz, 1H), 2.25 – 2.16 (m, 1H), 1.81 – 1.15 (m, 15 H, major and minor) ppm; ^{13}C NMR (100 MHz, CDCl$_3$) δ 155.9, 38.4, 30.1, 25.8, 25.4 ppm [15].

(Z)-N-hydroxy-4-methylbenzene-1-carbonimidoyl chloride (25l): whitish solid, 75%, R_f = 0.64 (CyH/EtOAc 3:1). ^{1}H NMR (300 MHz, CDCl$_3$) δ 8.74 (s br, 1H), 7.73 (d, J = 8.3 Hz, 2H), 7.21 (d, J = 8.0 Hz, 2H), 2.39 (s, 3H) ppm; ^{13}C NMR (100 MHz, CDCl$_3$) δ 150.7, 141.1, 140.4, 129.2, 127.1, 21.3 ppm [16].

(Z)-3-chloro-N-hydroxybenzene-1-carbonimidoyl chloride (25m): white solid, 80%, R_f = 0.66 (CyH/EtOAc 3:1). ^{1}H NMR (300 MHz, CDCl$_3$) δ 8.61 (s, 1H), 7.83 (t, J = 1.7 Hz, 1H), 7.72 (ddd, J = 1.3 Hz, J = 1.8 Hz, J = 7.8 Hz, 1H), 7.42 (ddd, J = 1.2 Hz, J = 1.9 Hz, J = 8.0 Hz, 1H), 7.34 (t, J = 7.9 Hz, 1H) ppm; ^{13}C NMR (100 MHz, CDCl$_3$) δ 138.8, 134.6, 134.1, 130.7, 129.7, 127.2, 125.3 ppm [17].

(Z)-2,4-difluoro-N-hydroxybenzene-1-carbonimidoyl chloride (25n): white solid, 73%, R_f = 0.66 (CyH/EtOAc 3:1). ^{1}H NMR (300 MHz, CDCl$_3$) δ 8.81 (s, 1H), 7.67 (dt, J = 6.3 Hz, J = 8.4 Hz 1H), 7.00 – 6.88 (m, 2H) ppm; ^{13}C NMR (100 MHz, CDCl$_3$) δ 164.0 (dd, J = 11.9 Hz, J = 254.4 Hz), 160.4 (dd, J = 12.3 Hz, J = 258.6 Hz), 134.5 (d, J = 5.5 Hz), 132.1 (dd, J = 2.8 Hz, J = 10.1 Hz), 117.6 (dd, J = 4.1 Hz, J = 11.3 Hz), 111.8 (dd, J = 3.8 Hz, J = 21.8 Hz), 105.1 (t, J = 25.8 Hz) ppm [11].

(Z)-N-hydroxypyridine-3-carbonimidoyl chloride (25o): orange solid, 38%, R_f = 0.38 (CyH/EtOAc 3:1). ^{1}H NMR (300 MHz, MeOD) δ 8.95 (s, 1H), 8.56 (d, J = 4.6 Hz, 1H), 8.25 – 8.21 (m, 1H), 7.48 (dd, J = 4.9 Hz, J = 8.1 Hz, 1H) ppm; ^{13}C NMR (100 MHz, MeOD) δ 152.8, 150.9, 147.8, 136.5, 130.1, 125.2 ppm [18].

(Z)-N-hydroxycyclopropanecarbonimidoyl chloride (25p): colorless oil, 66%, R_f = 0.52 (CyH/EtOAc 3:1). ^{1}H NMR (300 MHz, CDCl$_3$) δ 8.50 (s, 1H), 1.95 – 1.86 (m, 1H), 0.99 – 0.92 (m, 2H), 0.90 – 0.81 (m, 2H) ppm; ^{13}C NMR (100 MHz, CDCl$_3$) δ 144.4, 15.9, 5.9 ppm [19].

(Z)-N-hydroxyoxolane-3-carbonimidoyl chloride (25q): colorless oil, 52%, R_f = 0.52 (CyH/EtOAc 3:1). ^{1}H NMR (300 MHz, CDCl$_3$) δ 9.17 (s, 1H), 4.02 – 3.82 (m, 4H), 3.39 – 3.29 (m, 1H), 2.22 – 2.15 (m, 2H) ppm; ^{13}C NMR (100 MHz, CDCl$_3$) δ 141.5, 70.3, 68.2, 45.7, 30.1 ppm [20].

(Z)-N-hydroxycyclohexanecarbonimidoyl chloride (25r): colorless oil, 85%, R_f = 0.36 (CyH/EtOAc 3:1). ^{1}H NMR (300 MHz, CDCl$_3$) δ 8.56 (s, 1H), 2.46 (tt, J = 3.4 Hz, J = 11.4, 1H), 1.96 – 1.92 (m, 2H), 1.83 – 1.78 (m, 2H), 1.71 – 1.66 (m, 1H), 1.50 – 1.35 (m, 2H), 1.35 – 1.23 (m, 3H) ppm; ^{13}C NMR (100 MHz, CDCl$_3$) δ 146.5, 45.4, 30.2, 25.6, 25.5 ppm [21].

N-benzyl-5-{1,4-dioxaspiro[4.5]decan-2-yl}-1,2-oxazole-3-carboxamide (32b): yellowish solid, 68%, R_f = 0.39 (CyH/EtOAc 3:1), UHPLC-ESI-MS: R_t = 3.04, *m/z* = 343.2 [M + H] $^+$. ^{1}H NMR (300 MHz, CDCl$_3$) δ 7.36 – 7.29 (m, 5H), 7.09 (s br, 1H), 6.75 (s, 1H), 5.22 (t, *J* = 6.0 Hz, 1H), 4.62 (d, *J* = 6.0 Hz, 2H), 4.34 (dd, *J* = 6.6 Hz, *J* = 8.6 Hz, 1H), 4.09 (dd, *J* = 5.4 Hz, *J* = 8.6 Hz, 1H), 1.71 – 1.60 (m, 8H), 1.46 – 1.42 (m, 2H) ppm; ^{13}C NMR (100 MHz, CDCl$_3$) δ 173.3, 158.5, 140.4, 137.2, 128.8, 127.9, 127.8, 111.9, 101.9, 69.8, 68.1, 43.5, 35.8, 34.9, 25.0, 23.9, 23.8 ppm.

5-{1,4-dioxaspiro[4.5]decan-2-yl}-*N*-(4-fluorophenyl)- 1,2-oxazole-3-carboxamide (32s): yellowish solid, 58%, R_f = 0.53 (CyH/EtOAc 3:1), UHPLC-ESI-MS: R_t = 3.14, *m/z* = 347.2 [M + H] $^+$. ^{1}H NMR (300 MHz, CDCl$_3$) δ 8.48 (s, 1H), 7.64 – 7.59 (m, 2H), 7.10 – 7.04 (m, 2H), 6.80 (s, 1H), 5.26 (t, *J* = 6.0 Hz, 1H), 4.37 (dd, *J* = 6.6 Hz, *J* = 8.7 Hz, 1H), 4.12 (dd, *J* = 5.4 Hz, *J* = 8.7 Hz, 1H), 1.74 – 1.62 (m, 8H), 1.47 – 1.43 (m, 2H) ppm; ^{13}C NMR (100 MHz, CDCl$_3$) δ 173.9, 161.4, 157.5 (d, *J* = 171.1 Hz), 156.3, 132.9 (d, *J* = 2.8 Hz), 121.8 (d, *J* = 7.9 Hz), 115.9 (d, *J* = 22.6 Hz), 112.0, 101.9, 69.8, 68.1, 35.9, 34.9, 25.0, 23.9, 23.8 ppm.

5-{1,4-dioxaspiro[4.5]decan-2-yl}-*N*-[(thiophen-2-yl)methyl]-1,2-oxazole-3-carboxamide (32t): yellowish solid, 53%, R_f = 0.39 (CyH/EtOAc 3:1), UHPLC-ESI-MS: R_t = 3.00, *m/z* = 349.2 [M + H] $^+$. ^{1}H NMR (300 MHz, CDCl$_3$) δ 7.25 (dd, *J* = 1.2 Hz, *J* = 3.9 Hz, 1H), 7.12 (s br, 1H), 7.04 (dd, *J* = 1.0 Hz, *J* = 3.4 Hz, 1H), 6.97 (dd, *J* = 3.5 Hz, *J* = 5.1 Hz, 1H), 6.74 (s, 1H), 5.22 (t, *J* = 5.8 Hz, 1H), 4.79 (d, *J* = 5.9 Hz, 2H), 4.34 (dd, *J* = 6.6 Hz, *J* = 8.6 Hz, 1H), 4.09 (dd, *J* = 5.4 Hz, *J* = 8.6 Hz, 1H), 1.71 – 1.61 (m, 8H), 1.46 – 1.42 (m, 2H) ppm; ^{13}C NMR (100 MHz, CDCl$_3$) δ 173.4, 158.3, 143.3, 139.6, 127.0, 126.5, 125.6, 111.9, 101.8, 69.8, 68.1, 38.1, 35.8, 34.9, 25.0, 23.9, 23.8 ppm.

5-{1,4-dioxaspiro[4.5]decan-2-yl}-*N*-[(pyridin-3-yl)methyl]-1,2-oxazole-3-carboxamide (32u): yellow oil, 57%, R_f = 0.38 (CHCl$_3$/MeOH 5:1), UHPLC-ESI-MS: R_t = 2.00, *m/z* = 344.2 [M + H] $^+$. ^{1}H NMR (300 MHz, CDCl$_3$) δ 8.61 (d, *J* = 1.7 Hz, 1H), 8.56 (dd, *J* = 1.4 Hz, *J* = 4.8 Hz, 1H), 7.75 – 7.71 (m, 1H), 7.32 (dd, *J* = 4.9 Hz, *J* = 7.8 Hz, 1H), 7.21 (s br, 1H), 6.74 (s, 1H), 5.23 (t, *J* = 5.7 Hz, 1H), 4.65 (d, *J* = 6.2 Hz, 2H), 4.35 (dd, *J* = 6.6 Hz, *J* = 8.6 Hz, 1H), 4.09 (dd, *J* = 5.4 Hz, *J* = 8.7 Hz, 1H), 1.71 – 1.62 (m, 8H), 1.46 – 1.42 (m, 2H) ppm; ^{13}C NMR (100 MHz, CDCl$_3$) δ 173.6, 163.3, 158.8, 158.1, 148.8, 136.0, 133.3, 123.8, 111.9, 101.8, 69.8, 68.1, 40.9, 35.8, 34.9, 24.9, 23.9, 23.8 ppm.

5-{1,4-dioxaspiro[4.5]decan-2-yl}-*N*-(2-methoxyethyl)-1,2-oxazole-3-carboxamide (32v): yellow oil, 52%, R_f = 0.25 (CyH/EtOAc 3:1), UHPLC-ESI-MS: R_t = 2.57, *m/z* = 311.2 [M + H] $^+$. ^{1}H NMR (300 MHz, CDCl$_3$) δ 6.70 (s, 1H), 5.22 (t, *J* = 6.0 Hz, 1H), 4.34 (dd, *J* = 6.6 Hz, *J* = 8.6 Hz, 1H), 4.08 (dd, *J* = 5.5 Hz, *J* = 8.6 Hz, 1H), 3.64 – 3.59 (m, 2H), 3.52 (dd, *J* = 2.8 Hz, *J* = 7.5 Hz, 2H), 3.37 (s, 3H), 1.70 – 1.61 (m, 8H), 1.45 – 1.41 (m, 2H), ppm; ^{13}C NMR (100 MHz, CDCl$_3$) δ 173.1, 158.7, 158.4, 111.8, 101.8, 70.7, 69.8, 68.1, 58.8, 39.2, 35.8, 34.9, 24.9, 23.8 (d, *J* = 4.2 Hz) ppm.

5-{1,4-dioxaspiro[4.5]decan-2-yl}-3-(pyrrolidine-1-carbonyl)-1,2-oxazole (32z): brown oil, 18%, R_f = 0.25 (CyH/EtOAc 3:1), UHPLC-ESI-MS: R_t = 2.79, *m/z* = 307.2 [M + H] $^+$. ^{1}H NMR (300 MHz, CDCl$_3$) δ 6.67 (s, 1H), 5.22 (t, *J* = 6.1 Hz, 1H), 4.34 (dd, *J* = 6.6 Hz, *J* = 8.6 Hz, 1H), 4.09 (dd, *J* = 5.7 Hz, *J* = 8.6 Hz, 1H), 3.85 (t, *J* = 6.5 Hz, 2H), 3.65 (t, *J* = 6.6 Hz, 2H), 1.99 – 1.91 (m, 4H), 1.74– 1.62 (m, 8H), 1.45 – 1.41 (m, 2H) ppm; ^{13}C NMR (100 MHz, CDCl$_3$) δ 171.4, 159.7, 158.4, 111.8, 103.4, 69.8, 68.2, 48.7, 46.9, 35.8, 35.0, 26.2, 25.0, 23.9, 23.8 ppm.

Biological activity of LsrK
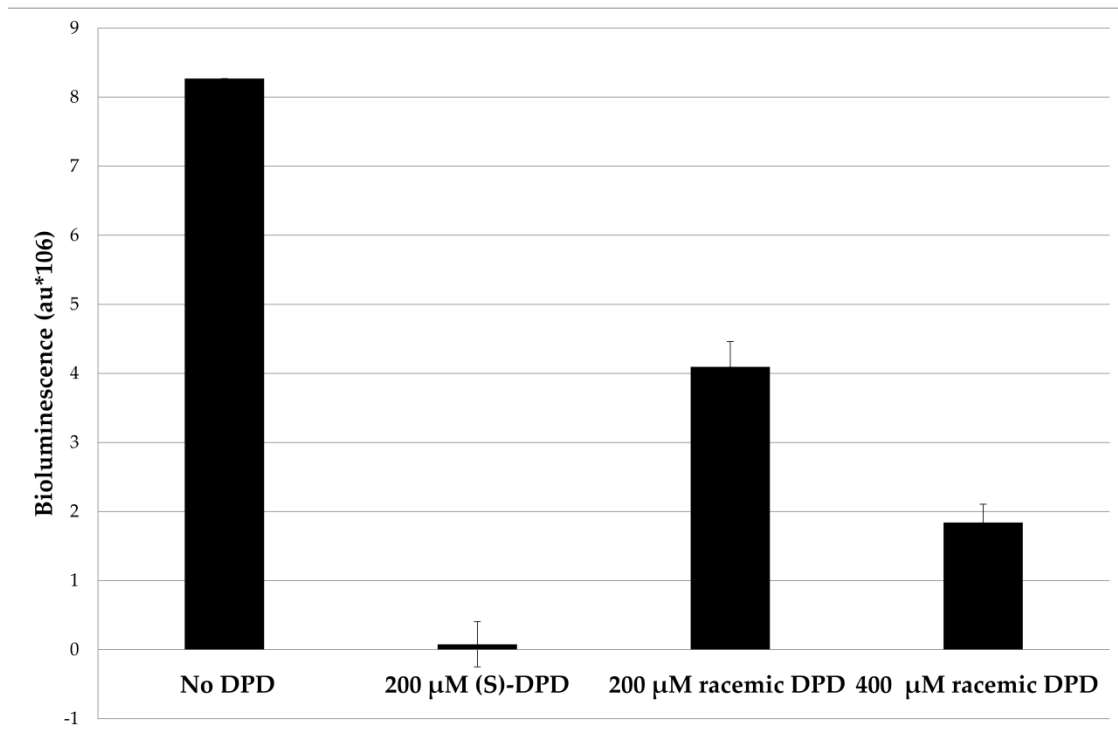
Figure S1: Activity of LsrK in the presence of racemic DPD and (*S*)-DPD (from OMM Scientific) detected by measuring ATP depletion.

References

1. Colombano, G.; Travelli, C.; Galli, U.; Caldarelli, A.; Chini, M. G.; Canonico, P. L.; Sorba, G.; Bifulco, G.; Tron, G. C.; Genazzani, A. A. A Novel Potent Nicotinamide Phosphoribosyltransferase Inhibitor Synthesized via Click Chemistry. *J. Med. Chem.* **2010**, *53*, 616–623, doi:10.1021/jm9010669.

2. Campbell-Verduyn, L. S.; Mirfeizi, L.; Dierckx, R. A.; Elsinga, P. H.; Feringa, B. L. Phosphoramidite accelerated copper(I)-catalyzed [3 + 2] cycloadditions of azides and alkynes. *Chem. Commun.* **2009**, 2139–2141, doi:10.1039/B822994E.

3. Suzuki, T.; Ota, Y.; Ri, M.; Bando, M.; Gotoh, A.; Itoh, Y.; Tsumoto, H.; Tatum, P. R.; Mizukami, T.; Nakagawa, H.; Iida, S.; Ueda, R.; Shirahige, K.; Miyata, N. Rapid Discovery of Highly Potent and Selective Inhibitors of Histone Deacetylase 8 Using Click Chemistry to Generate Candidate Libraries. *J. Med. Chem.* **2012**, *55*, 9562–9575, doi:10.1021/jm300837y.

4. Bevilacqua, V.; King, M.; Chaumontet, M.; Nothisen, M.; Gabillet, S.; Buisson, D.; Puente, C.; Wagner, A.; Taran, F. Copper-Chelating Azides for Efficient Click Conjugation Reactions in Complex Media. *Angew. Chem. Int. Ed.* **2014**, *53*, 5872–5876, doi:10.1002/anie.201310671.

5. Luo, L.; Wilhelm, C.; Sun, A.; Grey, C. P.; Lauher, J. W.; Goroff, N. S. Poly(diiododiacetylene): Preparation, Isolation, and Full Characterization of a Very Simple Poly(diacetylene). *J. Am. Chem. Soc.* **2008**, *130*, 7702–7709, doi:10.1021/ja8011403.

6. Wijtmans, M.; de Graaf, C.; de Kloe, G.; Istyastono, E. P.; Smit, J.; Lim, H.; Boonnak, R.; Nijmeijer, S.; Smits, R. A.; Jongejan, A.; Zuiderveld, O.; de Esch, I. J. P.; Leurs, R. Triazole Ligands Reveal Distinct Molecular Features That Induce Histamine H4 Receptor Affinity and Subtly Govern H4/H3 Subtype Selectivity. *J. Med. Chem.* **2011**, *54*, 1693–1703, doi:10.1021/jm1013488.

7. MacDonald, J. P.; Badillo, J. J.; Arevalo, G. E.; Silva-García, A.; Franz, A. K. Catalytic Stereoselective Synthesis of Diverse Oxindoles and Spirooxindoles from Isatins. *ACS Comb. Sci.* **2012**, *14*, 285–293, doi:10.1021/co300003c.

8. Shao, C.; Wang, X.; Zhang, Q.; Luo, S.; Zhao, J.; Hu, Y. Acid–Base Jointly Promoted Copper(I)-Catalyzed Azide–Alkyne Cycloaddition. *J. Org. Chem.* **2011**, *76*, 6832–6836, doi:10.1021/jo200869a.

9. Himo, F.; Lovell, T.; Hilgraf, R.; Rostovtsev, V. V.; Noodleman, L.; Sharpless, K. B.; Fokin, V. V. Copper(I)-Catalyzed Synthesis of Azoles. DFT Study Predicts Unprecedented Reactivity and Intermediates. *J. Am. Chem. Soc.* **2005**, *127*, 210–216, doi:10.1021/ja0471525.

10. Allen, C. L.; Davulcu, S.; Williams, J. M. J. Catalytic Acylation of Amines with Aldehydes or Aldoximes. *Org. Lett.* **2010**, *12*, 5096–5099, doi:10.1021/ol101978h.

11. Bonjouklian, R.; Johnson, D. W.; Lander, P. A.; Lohman, M. C.; Patel, V. F.; Vepachedu, S.; Xie, Y. Compounds and method for inhibiting MRP1 2003.

12. Erenler, R. Synthesis and Characterization of Pyridyl Propargyloximes. *Asian J. Chem.* **2011**, *23*, 3546–3548.

13. Wu, P.-L.; Wang, W.-S. Thermal Ring-Expansion of N-Acyl Cyclopropyl Imines. *J. Org. Chem.* **1994**, *59*, 622–627, doi:10.1021/jo00082a020.

14. Metzner, R.; Okazaki, S.; Asano, Y.; Gröger, H. Cyanide-free Enantioselective Synthesis of Nitriles: Synthetic Proof of a Biocatalytic Concept and Mechanistic Insights. *ChemCatChem* **2014**, *6*, 3105–3109, doi:10.1002/cctc.201402612.

15. Minakata, S.; Okumura, S.; Nagamachi, T.; Takeda, Y. Generation of Nitrile Oxides from Oximes Using *t*-BuOI and Their Cycloaddition. *Org. Lett.* **2011**, *13*, 2966–2969, doi:10.1021/ol2010616.

16. Tóth, M.; Kun, S.; Bokor, É.; Benltifa, M.; Tallec, G.; Vidal, S.; Docsa, T.; Gergely, P.; Somsák, L.; Praly, J.-P. Synthesis and structure–activity relationships of C-glycosylated oxadiazoles as inhibitors of glycogen phosphorylase. *Bioorg. Med. Chem.* **2009**, *17*, 4773–4785, doi:10.1016/j.bmc.2009.04.036.

17. Hanan, E. J.; van Abbema, A.; Barrett, K.; Blair, W. S.; Blaney, J.; Chang, C.; Eigenbrot, C.; Flynn, S.; Gibbons, P.; Hurley, C. A.; Kenny, J. R.; Kulagowski, J.; Lee, L.; Magnuson, S. R.; Morris, C.; Murray, J.; Pastor, R. M.; Rawson, T.; Siu, M.; Ultsch, M.; Zhou, A.; Sampath, D.; Lyssikatos, J. P. Discovery of Potent and Selective Pyrazolopyrimidine Janus Kinase 2 Inhibitors. *J. Med. Chem.* **2012**, *55*, 10090–10107, doi:10.1021/jm3012239.

18.   Zhu, J.; Ye, Y.; Ning, M.; Mándi, A.; Feng, Y.; Zou, Q.; Kurtán, T.; Leng, Y.; Shen, J. Design, Synthesis, and Structure–Activity Relationships of 3,4,5-Trisubstituted 4,5-Dihydro-1,2,4-oxadiazoles as TGR5 Agonists. *ChemMedChem* **2013**, *8*, 1210–1223, doi:10.1002/cmdc.201300144.

19.   Samajdar, S.; ABBINENI, C.; SASMAL, S.; Hosahalli, S. Bicyclic heterocyclic derivatives as bromodomain inhibitors 2015.

20.   US20090156603A1 - 2-aminopyridine analogs as glucokinase activators - Google Patents Available online: https://patents.google.com/patent/US20090156603/ko

21.   WO2006090234A1 - Heterocyclic derivatives as cell adhesion inhibitors - Google Patents Available online: https://patents.google.com/patent/WO2006090234A1/zh:

ACKNOWLEDGEMENTS

A huge thank to all my Italian friends in Cambridge, it wouldn't have been the same without them! Federico (Cippo)…well…because is Cippo! So annoying and chatterer that you can either hate him or love him…And at the end we all loved him! I had a really nice time with him, he taught me a lot and is always good to have a chat with him (unless he starts to send stupid selfie!); Mauro (Manlio) for his accent and his jokes (le pileeee!), parklife, his Italian bike and "il divanesimo"; Agnese, for her dark humor, her horror stories, her "dead lipstick" and her acute voice; Fab(b)io, the "pussy rocket" guy, for the trips together, his car, "driving safe in UK", the surf and "asticella alta"; Luca (bon!), for the funny moments together, for organizing amazing trips in every detail, for his wise advices; Flavio, for his contagious laugh; Ursula (Burzy) for her wisdom; Benedetta (Betta) for hosting me in her house like a sister, for the long talks and the experiences shared; Marco, who made the Cambridge 2.0 experience amazing! For the beautiful moments together, for having me for dinner sooo many times! For the bike's tour in the middle of the night, with the helmet and "I Ratti della Sabina" playing out loud….Rocco, the health and safety guy, for the nice moments together despite all the "caciottina" issues; Debbie and Lily, it has been so nice to live in such a dusty but comfy home; Sarka, Jacopo, Giorgia, Francesco and Rosanna even if for a short time, it has been pleasant to meet them.

Many thanks to my Groningen friends: Gabriele (Gallo), for his humor and jokes; Giulia, Fede (Fonty), Francesco M. (il Mec), Marco & Silvia (i "Dal lago"), Stefano F (il presidont), Eva (Stormy) and Michela for their hospitality, the nights at &Zo, Pakhuis (zio Pak), Twister, Het Feest and all the "best" places in Groningen; Francesco L. (Ciccio Lanza) for the Grey's Anatomy marathon, for his couch, for being always there for me; Elena (Kaps), the queen of Groningen, it's a shame we haven't hanged out much when I was there, but luckily we had the chance to meet afterwards and start a very good friendship. Thanks to my Greek friends Dino, Nick and Tryf, they've always helped me since my first day in the lab and I really miss our breakfasts on Saturday morning! I will always be Σιλβια πολύ τρελη for you guys!

Last but not the least, I would like to thank my family for supporting me in all the crazy things I do. It has been very hard to be far away for such a long time! I've missed my parents, my brother and my little nephew a lot!!!

Thanks to all the people I've met during this journey, each of you has contributed to this work, with a word, a hug, a smile, a laugh. I've lost the count of how many person I've encountered but I know that some of them will be part of my life for a very long time.

One last thank to all the people that manage to attend to my defence. I really appreciate you effort and I know that the ones that were not fisically there were thinking about me.

THANK YOU